



A National Center of Excellence in Multiscale Technology Applications

ISSN 1520-295X

Development and Evaluation of Simplified Procedures for Analysis and Design of Buildings with Passive Energy Dissipation Systems

by

Oscar M. Ramirez, Michael C. Constantinou,
Charles A. Kircher, Andrew S. Whittaker,
Martin W. Johnson, Juan D. Gomez and
Christis Z. Chrysostomou

University at Buffalo, State University of New York
Department of Civil, Structural and Environmental Engineering
Ketter Hall
Buffalo, NY 14260

Technical Report MCEER-00-0010
Revision 1

November 16, 2001

This research was conducted at the University at Buffalo, State University of New York and was supported primarily by the Earthquake Engineering Research Centers Program of the National Science Foundation under award number EEC-9701471.



Development and Evaluation of Simplified Procedures for Analysis and Design of Buildings with Passive Energy Dissipation Systems

by

Oscar M. Ramirez¹, Michael C. Constantinou², Charles A. Kircher³,
Andrew S. Whittaker⁴, Martin W. Johnson⁵, Juan D. Gomez⁶
and Christis Z. Chrysostomou⁷

Revision Date: November 16, 2001
Publication Date: December 8, 2000
Submittal Date: December 7, 2000

Technical Report MCEER-00-0010
Revision 1

Task Numbers 98-2403, 99-2403, 00-2042 and 01-2043c

NSF Master Contract Number EEC 9701471

- 1 Professor, Department of Civil Engineering, Technological University of Panama; former Graduate Student, Department of Civil, Structural and Environmental Engineering, University at Buffalo, State University of New York
- 2 Professor and Chairman, Department of Civil, Structural and Environmental Engineering, University at Buffalo, State University of New York
- 3 Principal, C.A. Kircher Associates, Palo Alto, California
- 4 Associate Professor, Department of Civil, Structural and Environmental Engineering, University at Buffalo, State University of New York
- 5 Group Manager, EQE International, Irvine, California
- 6 Graduate Student, Department of Civil, Structural and Environmental Engineering, University at Buffalo, State University of New York
- 7 Lecturer, Department of Civil Engineering, Higher Technical Institute, Cyprus

MULTIDISCIPLINARY CENTER FOR EARTHQUAKE ENGINEERING RESEARCH
University at Buffalo, State University of New York
Red Jacket Quadrangle, Buffalo, NY 14261

Preface

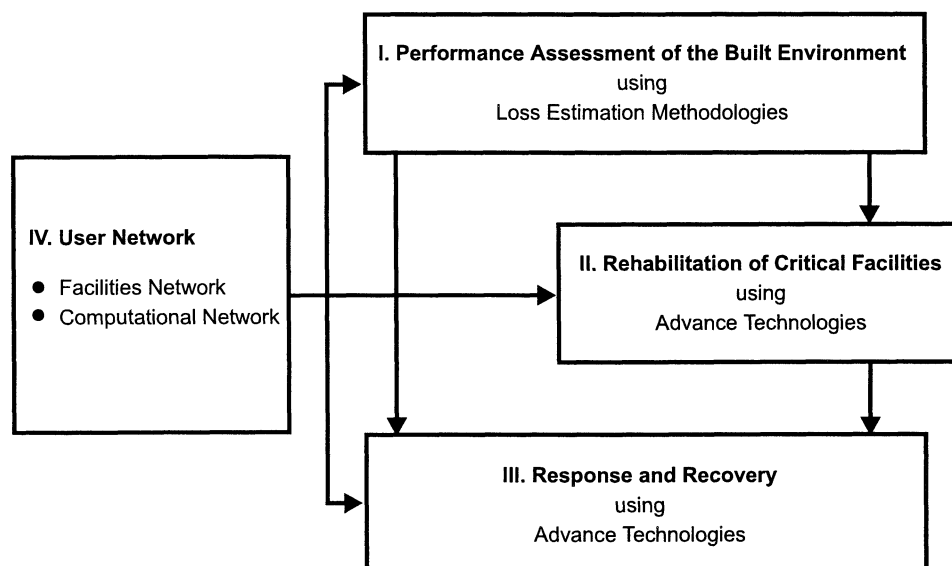
The Multidisciplinary Center for Earthquake Engineering Research (MCEER) is a national center of excellence in advanced technology applications that is dedicated to the reduction of earthquake losses nationwide. Headquartered at the University at Buffalo, State University of New York, the Center was originally established by the National Science Foundation in 1986, as the National Center for Earthquake Engineering Research (NCEER).

Comprising a consortium of researchers from numerous disciplines and institutions throughout the United States, the Center's mission is to reduce earthquake losses through research and the application of advanced technologies that improve engineering, pre-earthquake planning and post-earthquake recovery strategies. Toward this end, the Center coordinates a nationwide program of multidisciplinary team research, education and outreach activities.

MCEER's research is conducted under the sponsorship of two major federal agencies: the National Science Foundation (NSF) and the Federal Highway Administration (FHWA), and the State of New York. Significant support is derived from the Federal Emergency Management Agency (FEMA), other state governments, academic institutions, foreign governments and private industry.

The Center's NSF-sponsored research is focused around four major thrusts, as shown in the figure below:

- quantifying building and lifeline performance in future earthquake through the estimation of expected losses;
- developing cost-effective, performance based, rehabilitation technologies for critical facilities;
- improving response and recovery through strategic planning and crisis management;
- establishing two user networks, one in experimental facilities and computing environments and the other in computational and analytical resources.



This report presents the development and evaluation of simplified methods of analysis and design for buildings with passive energy dissipation systems. The work was conducted under the auspices of the Building Seismic Safety Council, Technical Subcommittee 12, Base Isolation and Energy Dissipation, for the year 2000 update of the “NEHRP Recommended Provisions for Seismic Regulations for New Buildings and Other Structures.” Topics presented in the report include development of extended damping coefficients for modification of response spectra for damping in excess of 5% of critical; development of relationships between elastic and inelastic displacement of yielding systems with energy dissipating devices; a study of displacement ductility demand in yielding structures with viscous damping systems; development of equivalent lateral force and modal analysis procedures for buildings with damping systems; and validation studies of the developed analysis procedures using 3- and 6-story structures with linear viscous, nonlinear viscous, solid viscoelastic and yielding damping systems.

Technical Report MCEER-00-0010 was first published on December 8, 2000. Since then, the report has been rigorously reviewed by Dr. Christis Chrysostomou, who independently re-worked the examples and checked the validity of the presented results. This resulted in a substantial volume of changes and corrections that are included in the current version of the report, which is published as Revision 1. The changes are identified with lines on the border of each page.

ABSTRACT

This report presents the development and evaluation of simplified methods of analysis and design for buildings with passive energy dissipation systems. The work described in this report was conducted under the auspices of the Buildings Seismic Safety Council Technical Subcommittee 12, Base Isolation and Energy Dissipation, for the year 2000 update of the *NEHRP Recommended Provisions for Seismic Regulations for New Buildings and Other Structures*.

The work presented in this report includes:

- (a) Development of extended damping coefficients for modification of response spectra for damping in excess of 5-percent of critical.
- (b) Development of relationships between elastic and inelastic displacement of yielding systems with energy dissipating devices.
- (c) A study of displacement ductility demand in yielding structures with viscous damping systems.
- (d) Development of equivalent lateral force and modal analysis procedures for buildings with damping systems.
- (e) Validation studies of the developed analysis procedures using 3- and 6-story structures with linear viscous, nonlinear viscous, solid viscoelastic and yielding damping systems.

ACKNOWLEDGEMENTS

Financial support for this project was provided by the Multidisciplinary Center for Earthquake Engineering Research, task on Rehabilitation Strategies for Buildings (Projects No. 982403, No. 992403, and No. 00-2042). The work was performed under the auspices of Technical Subcommittee 12, Base isolation and Energy Dissipation, of the Building Seismic Safety Council which was charged with the task of developing analysis and design procedures for inclusion in the year 2000 NEHRP Recommended Provisions for Seismic Regulations for New Buildings and Other Structures. The work of Technical Subcommittee 12 was supported by the Federal Emergency Management Agency.

Technical Report MCEER-00-0010 was first published on December 8, 2000. Since then the report has been rigorously reviewed by Dr. Christis Chrysostomou who independently re-worked the examples and checked the validity of the presented results. This resulted in a substantial volume of changes and corrections that are included in the current revision of the report, which is published as Revision 1. Financial support for the work of Dr. Chrysostomou has been provided by the Multidisciplinary Center for Earthquake Engineering Research, task on Facilitating Technologies, Project 01-2043c. Dr. Chrysostomou is also indebted to the Higher Technical Institute of Cyprus for approving a leave of absence for the period September to December 2001.

TABLE OF CONTENTS

SECTION	TITLE	PAGE
1	INTRODUCTION	1
1.1	Passive Energy Dissipation Systems	1
1.2	Procedures for Implementation of Passive Energy Dissipators	2
1.2.1	General	2
1.2.2	1992 SEAONC Energy Dissipation Working Group	2
1.2.3	1994 NEHRP Recommended Provisions for Seismic Regulations for New Buildings	3
1.2.4	1997 NEHRP Guidelines for the Seismic Rehabilitation of Buildings	4
1.2.5	1999 SEAOC Recommended Lateral Force Requirements	5
1.2.6	2000 NEHRP Recommended Provisions for Seismic Regulations for New buildings and Other Structures	6
1.3	Report Organization	6
2	DESCRIPTION OF NONLINEAR STATIC ANALYSIS PROCEDURES OF FEMA	7
2.1	Introduction	
2.2	Nonlinear Static Procedure, Method 2	7
2.2.1	General Description	7
2.2.2	Pushover Curve	9
2.2.3	Design Demand Curve	10
2.2.4	Calculation of Velocity Dependent Forces	11
2.2.5	Calculation of Maximum Actions	12
2.3	Nonlinear Static Procedure, Method 1	12
2.4	Calculation of Effective Damping	13
2	MODIFICATION OF RESPONSE SPECTRUM FOR HIGHER DAMPING	19
3.1	Introduction	19
3.2	Procedure to Establish Values of the Damping Coefficient	21
3.3	Conclusions	23
4	EVALUATION OF SIMPLIFIED METHODS OF ANALYSIS OF YIELDING SINGLE-DEGREE-OF-FREEDOM SYSTEMS WITH ENERGY DISSIPATION DEVICES	31
4.1	Introduction	31
4.2	Non-Linear Time History Analysis	32
4.2.1	General Description	32
4.2.2	Description of Structural System Behavior	33
4.2.3	Description of Viscous Damping System	34
4.2.4	Description of Yielding Damping System	34

TABLE OF CONTENTS (cont'd)

SECTION	TITLE	PAGE
4.2.5	Ground Motions used in the Time History Analysis	35
4.3	Analyzed Systems	35
4.3.1	Bilinear Hysteretic System with Linear Viscous Damping Devices	36
4.3.2	Bilinear Hysteretic System with Nonlinear Viscous Damping Devices	36
4.3.3	Bilinear Elastic System with Linear Viscous Damping Devices	37
4.3.4	Bilinear Hysteretic System with Yielding Damping Devices	37
4.4	Application of Simplified Method of Analysis for Bilinear Hysteretic System with Linear Viscous Damping Devices	38
4.5	Application of Simplified Method of Analysis for Bilinear Hysteretic System with Nonlinear Viscous Damping Devices	39
4.6	Application of Simplified Method of Analysis for Bilinear Elastic System with Linear Viscous Damping Devices	40
4.7	Application of Simplified Method of Analysis for Bilinear Hysteretic System with Yielding Damping Devices	40
4.8	Calculation of Maximum Velocity and Acceleration in Systems with Viscous Damping Devices	41
4.9	Results of Simplified Method of Analysis and Comparison to Results of Nonlinear Time History Analysis	44
4.10	Correction Factors for Velocity	45
4.11	Conclusions	47
5.	RATIO OF INELASTIC DISPLACEMENT TO DISPLACEMENT CALCULATED ASSUMING ELASTIC BEHAVIOR	69
5.1	Introduction	69
5.2	Coefficient C_I and Review of Past Studies	69
5.2.1	Study of Mander et al. (1984)	70
5.2.2	Study of Riddell et al.(1989)	71
5.2.3	Study of Nassar and Krawinkler (1991)	71
5.2.4	Study of Vidic et al. (1992)	72
5.2.5	Study of Miranda (1993)	72
5.2.6	Summary	72
5.3	Procedure for Development of Coefficient C_I and Results	73
5.4	Summary	74
6.	DISPLACEMENT DUCTILITY DEMAND IN STRUCTURES WITH VISCOUS DAMPING SYSTEMS	79
6.1	Introduction	79
6.2	Procedure for Evaluation of Displacement Ductility Demand	80
6.3	Results	82
6.4	Conclusions	82

TABLE OF CONTENTS (cont'd)

SECTION	TITLE	PAGE
7	DEVELOPMENT OF EQUIVALENT LATERAL FORCE AND AND MODAL ANALYSIS PROCEDURES FOR NEW BUILDINGS WITH DAMPING SYSTEMS	87
7.1	Introduction	87
7.2	$R, R_{\mu}, \Omega_0, C_d$ Factors and Maximum Effective Ductility	88
7.3	Elements of Structural Dynamics	90
7.4	Viscous Damping Ratio of Elastic Building	93
7.5	Effective Period and Effective Damping of Yielding Buildings with Damping Systems	96
7.5.1	Buildings with Linear Viscous Damping Systems	96
7.5.2	Buildings with Nonlinear Viscous Damping Systems	97
7.5.3	Buildings with Viscoelastic Damping Systems	98
7.5.4	Building with Yielding Damping Systems	101
7.6	Quality Factor, q_H	103
7.7	Minimum Allowable Base Shear	106
7.8	NEHRP (2000), Appendix to Chapter 13, Structures with Damping Systems	108
7.9	Conclusions	109
8	EVALUATION OF METHODS OF ANALYSIS AND DESIGN OF BUILDINGS WITH DAMPING SYSTEMS	117
8.1	Introduction	117
8.2	Design of 3-Story and 6-Story Reference Frames	118
8.3	Design of 3-Story and 6-Story Frames with Damping Systems	119
8.4	Nonlinear Time History Analysis	122
8.5	Comparison of Results of Simplified Methods of Analysis to Results of Nonlinear Time History Analysis	123
8.6	Implications of Errors in the Calculation of Base Shear Strength	126
8.7	Effect of Viscous Damping Forces on Pushover Curve	127
8.8	Comparison of Pattern and Extend Damage in Frames without and with Damping Systems	127
8.9	Conclusions	129
9	SUMMARY, CONCLUSIONS AN RECOMMENDATIONS	167
9.1	Summary	167
9.2	Conclusions	168
9.3	Recommendations for Future Research	170
10	REFERENCES	173
Appendix A	NEHRP 2000 – Appendix to Chapter 13: Structures with Damping Systems	179

TABLE OF CONTENTS (cont'd)		
SECTION	TITLE	PAGE
Appendix B	Description of Example Buildings without Damping Systems and Design of Lateral Force Resisting Systems per NEHRP (1997)	215
Appendix C	Approximate Construction of Pushover Curve of Buildings without and with Damping Systems on the Basis of Plastic Analysis	229
Appendix D	Considerations in the Design of Metallic Yielding and Viscoelastic Solid Damping Devices	265
Appendix E	Detailed Calculations for the Simplified Analysis of 3-story and 6-story Frames with Linear Viscous Damping System	275
Appendix F	Detailed Calculations for the Simplified Analysis of 3-story Frames with Nonlinear Viscous Damping System	323
Appendix G	Detailed Calculations for the Simplified Analysis of 3-story Frames with Viscoelastic Damping System	345
Appendix H	Detailed Calculations for the Simplified Analysis of 3-story Frames with Yielding Damping System	373
Appendix I	Detailed Calculations for the Simplified Analysis of 3-story Frames with Linear Viscous Damping System Using Nonlinear Static Procedure Method 2 (FEMA, 1997)	387
Appendix J	Input Files for Eigenvalue and Pushover Analysis of Frames With Damping Systems in Program SAP-2000NL	409
Appendix K	Input files for Nonlinear Time-History and Pushover Analysis of Frames with Damping Systems in Program IDARCD2D	441

LIST OF FIGURES

FIGURE	TITLE	PAGE
2-1	Illustration of Nonlinear Static Procedure, Method 2	15
2-2	Example of Design Demand Curves	16
2-3	Damping Coefficient B as Function of Period and Damping	17
2-4	Acceleration Response Spectra for Various Levels of Effective Damping Established with the use of the Damping Coefficient Developed in this Study (conservative values in Table 3-3). 5%-Damped Spectrum Representative of NEHRP (2000) Design Spectrum with $S_{DS} = 1.0$, $S_{D1} = 0.6$ and $T_s = 0.6$ sec	18
3-1	Maximum, Average and Minimum Spectral Acceleration Values of Scaled Motions	27
3-2	Average Spectra of Acceleration for Damping in the Range of 2% to 100-Percent of Critical	28
3-3	Calculated Damping Coefficient as Function of Period	29
3-4	Proposed Relation of Damping Coefficient vs. Period	29
3-5	Comparison of Calculated Damping Coefficient to Proposed Model (Best Fit)	30
4-1	Structural System Behavior Considered in this Study	51
4-2	Illustration of Behavior of Analyzed Systems	52
4-3	Behavior of Bilinear Hysteretic System with Yielding Damping Devices	53
4-4	Harmonic Motion of Structure with Nonlinear Viscous Damping Devices and Force-Displacement Relation	54
4-5	Comparison of Time History Analysis Results (Average of 20 Values) to Results of Simplified Method of Analysis for Bilinear Hysteretic System without Damping Devices	55
4-6	Comparison of Time History Analysis Results (Average of 20 Values) to Results of Simplified Method of Analysis for Bilinear Hysteretic System with Linear Viscous Damping Devices, $\beta_v = 0.15$	56
4-7	Comparison of Time History Analysis Results (Average of 20 Values) to Results of Simplified Method of Analysis for Bilinear Hysteretic System with Linear Viscous Damping Devices, $\beta_v = 0.25$	57
4-8	Comparison of Time History Analysis Results (Average of 20 Values) to Results of Simplified Method of Analysis for Bilinear Hysteretic System with Non-Linear Viscous Damping Devices, $\beta_v = 0.15$	58
4-9	Comparison of Time History Analysis Results (Average of 20 Values) to Results of Simplified Method of Analysis for Bilinear Hysteretic System with Non-Linear Viscous Damping Devices, $\beta_v = 0.25$	59
4-10	Comparison of Time History Analysis Results (Average of 20 Values) to Results of Simplified Method of Analysis for Bilinear Elastic System without Damping Devices	60

LIST OF FIGURES (cont'd)

FIGURE	TITLE	PAGE
4-11	Comparison of Time History Analysis Results (Average of 20 Values) to Results of Simplified Method of Analysis for Bilinear Elastic System with Linear Viscous Damping Devices, $\beta_v = 0.15$	61
4-12	Comparison of Time History Analysis Results (Average of 20 Values) to Results of Simplified Method of Analysis for Bilinear Elastic System with Linear Viscous Damping Devices, $\beta_v = 0.25$	62
4-13	Comparison of Time History Analysis Results (Average of 20 Values) to Results of Simplified Method of Analysis for Bilinear Hysteretic System with Yielding Damping Devices	63
4-14	Comparison of Velocity Predictions without and with Correction Factors for Bilinear Hysteretic System with Linear Viscous Damping Devices, $\beta_v = 0.15$	64
4-15	Comparison of Velocity Predictions without and with Correction Factors for Bilinear Hysteretic System with Linear Viscous Damping Devices, $\beta_v = 0.25$	65
4-16	Comparison of Velocity Predictions without and with Correction Factors for Bilinear Hysteretic System with Non-Linear Viscous Damping Devices, $\beta_v = 0.15$	66
4-17	Comparison of Velocity Predictions without and with Correction Factors for Bilinear Hysteretic System with Non-Linear Viscous Damping Devices, $\beta_v = 0.25$	67
4-18	Comparison of Velocity Predictions without and with Correction Factors for Bilinear Elastic System with Linear Viscous Damping Devices	68
5-1	Elastic and Idealized Inelastic Behavior of Structure	75
5-2	Comparison of Values of Coefficient C_1 Established by Nonlinear Time History Analysis to Predictions of Eq. 5-10 for Viscous Damping Ratio of 0.05	76
5-3	Comparison of Values of Coefficient C_1 Established by Nonlinear Time History Analysis to Predictions of Eq. 5-10 for Viscous Damping Ratio of 0.20	77
5-4	Comparison of Values of Coefficient C_1 Established by Nonlinear Time History Analysis to Predictions of Eq. 5-10 for Viscous Damping Ratio of 0.30	78
6-1	Comparison of Average Displacement Ductility Ratio for 5% and 20%-Damped Systems	84
6-2	Comparison of Average Displacement Ductility Ratio for 5% and 30%-Damped Systems	85
6-3	Comparison of Maximum, Average and Minimum Displacement Ductility Ratios of 5% and 20%-Damped Systems with $\alpha = 0.05$	86

LIST OF FIGURES (cont'd)

FIGURE	TITLE	PAGE
7-1	Structural Response and Relation Between Response Quantities	112
7-2	Displacement Amplification Factors for Various Damping System Configurations	113
7-3	Effective Damping Constant of Nonlinear Viscous Damping Device for Higher Mode Response Calculation	114
7-4	Idealized Spectral Capacity Curves of Building Without and With a Viscoelastic Damping System	115
7-5	Idealized Trilinear and Equivalent Elastoplastic Spectral Capacity Curves of Building with a Yielding Damping System	116
8-1	Example No.1: Frame 3S-60 with Linear Viscous Damping System to Provide 10% Viscous Damping Ratio when Assuming Elastic Frame Behavior	152
8-2	Example No.2: Frame 3S-75 with Linear Viscous Damping System to Provide 10% Viscous Damping Ratio when Assuming Elastic Frame Behavior	152
8-3	Example No.3: Frame 3S-90 with Linear Viscous Damping System to Provide 10% Viscous Damping Ratio when Assuming Elastic Frame Behavior	153
8-4	Example No.4: Frame 3S-100 with Linear Viscous Damping System to Provide 20% Viscous Damping Ratio when Assuming Elastic Frame Behavior	153
8-5	Example No.5: Frame 6S-75 with Linear Viscous Damping System to Provide 10% Viscous Damping Ratio when Assuming Elastic Frame Behavior	154
8-6	Example No.6: Frame 3S-80 with Nonlinear Viscous Damping System to Provide 10% Viscous Damping Ratio when Assuming Elastic Frame Behavior in the DBE	154
8-7	Example No.7: Frame 3S-80 with Nonlinear Viscous Damping System to Provide 20% Viscous Damping Ratio when Assuming Elastic Frame Behavior in the MCE	155
8-8	Example No.8: Frame 3S-75 with Viscoelastic Damping System to Provide 8.5% Viscous Damping Ratio when Assuming Elastic Frame Behavior	155
8-9	Example No.9: Frame 3S-75 with Metallic Yielding Damping System	156
8-10	Modeling of Viscoelastic Solid Damping Device in Program IDARC2D	157
8-11	Modeling of Metallic Yielding Damping Device in Program IDARC2D	158
8-12	Base-Shear-First Story Drift Loops of Frame of Example No.1: 3-story ($0.60V_y$) with Linear Viscous Damping System in Scaled San Fernando, Station 458, Component S00W (see Table 3-2)	159
8-13	Base-Shear-First Story Drift Loops of Frame of Example No.2: 3-story ($0.75V_y$) with Linear Viscous Damping System in Scaled San Fernando, Station 458, Component S00W (see Table 3-2)	160

LIST OF FIGURES (cont'd)

FIGURE	TITLE	PAGE
8-14	Plastic Hinge Formation and Key Response Quantities of Frame without Damping System in DBE and MCE	161
8-15	Plastic Hinge Formation and Key Response Quantities of Frame 3S-75 with Linear Viscous Damping System (damping ratio of 10%) in DBE and MCE	162
8-16	Plastic Hinge Formation and Key Response Quantities of Frame 3S-100 with Linear Viscous Damping System (damping ratio of 20%) in DBE and MCE	163
8-17	Plastic Hinge Formation and Key Response Quantities of Frame without Damping System in Near-Fault Seismic Excitation	164
8-18	Plastic Hinge Formation and Key Response Quantities of Frame 3S-75 with Linear Viscous Damping System (damping ratio of 10%) in Near-Fault Seismic Excitation	165
8-19	Plastic Hinge Formation and Key Response Quantities of Frame 3S-100 with Linear Viscous Damping System (damping ratio of 20%) in Near-Fault Seismic Excitation	166

LIST OF TABLES

TABLE	TITLE	PAGE
1-1	1994 NEHRP Reduction Factors for Increased Damping (NEHRP,1994)	4
2-1	Values of Damping Coefficient B	14
3-1	Damping Coefficient from Various Sources	24
3-2	Motions used in Analysis and Scale Factors	25
3-3	Values of Parameters B_S and B_I in Proposed Model of Damping Coefficient	26
4-1	Values of Parameters in Study of Bilinear Hysteretic System with Viscous Damping Devices	48
4-2	Values of Parameter λ	48
4-3	Values of Parameters in Study of Bilinear Elastic System with Linear Viscous Damping Devices	49
4-4	Values of Parameters in Study of Bilinear Hysteretic System with Yielding Damping Devices	49
4-5	Correction Factor for Velocity (from Sadek et al., 1999)	50
4-6	Revised Correction Factors	50
5-1	Values of Parameter a_o	75
7-1	Values of Quality Factor q_H predicted by Equations 7-68 and 7-69	111
8-1	Characteristics of Example Frames Exclusive of the Damping System	130
8-2	Comparison of Results of Simplified Methods of Analysis to Results of Nonlinear Time History Analysis. Case of Example No.1: 3-Story ($0.60V_y$) with Linear Viscous Damping System. Analysis for the DBE	131
8-3	Comparison of Results of Simplified Methods of Analysis to Results of Nonlinear Time History Analysis. Case of Example No.1: 3-Story ($0.60V_y$) with Linear Viscous Damping System. Analysis for the MCE	132
8-4	Comparison of Results of Simplified Methods of Analysis to Results of Nonlinear Time History Analysis. Case of Example No.2: 3-Story ($0.75V_y$) with Linear Viscous Damping System. Analysis for the DBE	133
8-5	Comparison of Results of Simplified Methods of Analysis to Results of Nonlinear Time History Analysis. Case of Example No.2: 3-Story ($0.75V_y$) with Linear Viscous Damping System. Analysis for the MCE	134
8-6	Comparison of Results of Simplified Methods of Analysis to Results of Nonlinear Time History Analysis. Case of Example No.3: 3-Story ($0.90V_y$) with Linear Viscous Damping System. Analysis for the DBE	135

LIST OF TABLES (cont'd)

TABLE	TITLE	PAGE
8-7	Comparison of Results of Simplified Methods of Analysis to Results of Nonlinear Time History Analysis. Case of Example No.3: 3-Story (0.90V _y) with Linear Viscous Damping System. Analysis for the MCE	136
8-8	Comparison of Results of Simplified Methods of Analysis to Results of Nonlinear Time History Analysis. Case of Example No.5: 6-Story (0.75V _y) with Linear Viscous Damping System. Analysis for the DBE	137
8-9	Comparison of Results of Simplified Methods of Analysis to Results of Nonlinear Time History Analysis. Case of Example No.5: 6-Story (0.75V _y) with Linear Viscous Damping System. Analysis for the MCE	139
8-10	Comparison of Results of Simplified Methods of Analysis to Results of Nonlinear Time History Analysis. Case of Example No.6: 3-Story (0.80V _y) with Nonlinear Viscous Damping System Designed for 10% Damping Ratio in the DBE. Analysis for the DBE	141
8-11	Comparison of Results of Simplified Methods of Analysis to Results of Nonlinear Time History Analysis. Case of Example No.6: 3-Story (0.80V _y) with Nonlinear Viscous Damping System Designed for 10% Damping Ratio in the DBE. Analysis for the MCE	142
8-12	Comparison of Results of Simplified Methods of Analysis to Results of Nonlinear Time History Analysis. Case of Example No.7: 3-Story (0.80V _y) with Nonlinear Viscous Damping System Designed for 20% Damping Ratio in the MCE. Analysis for the MCE	143
8-13	Comparison of Results of Simplified Methods of Analysis to Results of Nonlinear Time History Analysis. Case of Example No.8: 3-Story (0.75V _y) with Viscoelastic Damping System. Analysis for the DBE	144
8-14	Comparison of Results of Simplified Methods of Analysis to Results of Nonlinear Time History Analysis. Case of Example No.8: 3-Story (0.75V _y) with Viscoelastic Damping System. Analysis for the MCE	145
8-15	Comparison of Results of Simplified Methods of Analysis to Results of Nonlinear Time History Analysis. Case of Example No.9: 3-Story (0.75V _y) with Metallic Yielding Damping System. Analysis for the DBE	146
8-16	Comparison of Results of Simplified Methods of Analysis to Results of Nonlinear Time History Analysis. Case of Example No.9: 3-Story (0.75V _y) with Metallic Yielding Damping System. Analysis for the MCE	147
8-17	Summary of Results that are useful in Design Produced by Various Methods of Analysis	148

LIST OF TABLES (cont'd)

TABLE	TITLE	PAGE
8-18	Comparison of Results of Simplified Methods of Analysis to Results of Nonlinear Time History Analysis. Case of Example No.2: 3-Story ($0.75V_y$) with Linear Viscous Damping System Designed for 10% Damping Ratio. Analysis for Near-Fault Ground Motions	149
8-19	Comparison of Results of Simplified Methods of Analysis to Results of Nonlinear Time History Analysis. Case of Example No.4: 3-Story ($1.0V_y$) with Linear Viscous Damping System Designed for 20% Damping Ratio. Analysis for Near-Fault Ground Motions	150
8-20	Results of Analysis of Example No.1 and No.3 Using Assumed and Actual Base Shear Strengths for the DBE	151

SECTION 1

INTRODUCTION

1.1 Passive Energy Dissipation Systems

Conventionally designed and constructed earthquake-resistant buildings rely on significant inelastic action (energy dissipation) in selected components of the framing system in the design earthquake. For the commonly used moment-resisting frame, inelastic action should occur in the beams near the columns and in the beam-column panel zones: both zones form part of the gravity-load-resisting system. Inelastic action results in damage, which is often substantial in scope and difficult to repair. Damage to the gravity-load-resisting system can result in significant direct and indirect (business interruption) losses.

The desire to avoid damage to components of gravity-load-resisting frames in buildings following the 1989 Loma Prieta and 1994 Northridge earthquakes has spurred the development of passive energy dissipation systems. The primary objective of adding energy dissipation systems to building frames has been to focus the energy dissipation during an earthquake into disposable elements specifically designed for this purpose, and to substantially reduce (or eliminate) energy dissipation in the gravity-load-resisting frame. Because energy dissipators do not form part of the gravity frame and can be replaced after an earthquake without compromising the structural integrity of the frame.

Passive metallic yielding, viscoelastic, and viscous energy dissipators (also termed dampers in this report) are now available in the marketplace, both in the United States and overseas. Soong and Dargush (1997) and Constantinou et al. (1998) describe these passive dampers and other types of dampers under development at the time of this writing.

One impediment to the widespread use of passive energy dissipation systems has been the lack of robust and validated guidelines for the modeling, analysis, design, and testing of the dampers. The following section presents sample information on the procedures developed in the 1990s to aid in the implementation of passive energy dissipation systems.

1.2 Procedures for Implementation of Passive Energy Dissipators

1.2.1 General

Up to the time of this writing, five code-oriented procedures have been published related to the implementation of passive energy dissipation devices in buildings. The first procedures were published in 1992 by the Structural Engineers Association of Northern California (SEAONC). The Federal Emergency Management Agency (FEMA) included draft guidelines for the implementation of passive energy dissipation devices in new buildings in the 1994 edition of the *NEHRP Recommended Guidelines for Seismic Regulations for New Buildings* (NEHRP, 1994). Guidelines for the implementation of passive energy dissipation devices in retrofit construction were published in 1997 in the *NEHRP Guidelines for the Seismic Rehabilitation of Buildings* (FEMA, 1997). In 1999, the SEAOC Ad-Hoc Committee on Energy Dissipation published guidelines for implementing energy dissipation devices in new buildings in the SEAOC Blue Book (SEAOC, 1999) in a format consistent with that of the 1997 Uniform Building Code.

This year (2000), FEMA is to publish the 2000 edition of the *NEHRP Recommended Guidelines for Seismic Regulations for New Building*. Summary remarks on each of these documents follow.

1.2.2 1992 SEAONC Energy Dissipation Working Group

The first draft code requirements in the United States for the design and implementation of passive energy dissipation systems were prepared by the Energy Dissipation Working Group of the Base Isolation Subcommittee of SEAONC (Whittaker, et al. 1993). The philosophy adopted in this draft document was to confine inelastic activity in the structure to the energy dissipators and keep the gravity-load-resisting system elastic in the design-basis earthquake. Because the energy dissipation devices did not form part of the gravity-load-resisting system, they were considered to be replaceable following strong earthquake shaking. The SEAONC document required that the framing system *exclusive* of the energy dissipation system comply with all requirements of the 1988 Uniform Building Code, including those of base shear strength and maximum interstory drift.

The document provided general design requirements applicable to a wide range of systems, and, as such, relied on testing of system hardware to confirm the engineering parameters used in the

design, and to verify the overall adequacy of the energy dissipation system. Two types of dampers were recognized in the document: rate-independent (or displacement-dependent) dampers and rate-dependent (or velocity-dependent) dampers. Maximum responses in the energy dissipation system were computed using dynamic analysis, including response-spectrum analysis, and linear and non-linear response-history analysis. Seismic demands were described by the spectral demands of the design-basis earthquake. Design actions and deformations in the energy dissipation system were based on the design-basis earthquake analysis. All components of the energy dissipation system exclusive of the dampers were designed for forces corresponding to 120 percent of the design-basis earthquake damper displacement. Stability of the dampers had to be verified by testing for displacements and velocities corresponding to the maximum level of earthquake shaking that was expected at the building site. Whittaker et al. note that the SEAONC document "...was prepared in keeping with the most current information and the present state-of-the-practice of energy dissipation" and that because "...seismic energy dissipation is a relatively new technology and there are many design-related issues that require additional research..." that a conservative approach was taken to develop the design guidelines.

1.2.3 1994 NEHRP Recommended Provisions for Seismic Regulations for New Buildings

Whereas the 1992 SEAONC guidelines required that the lateral-force-resisting system exclusive of the dampers comply in full with the strength and interstory drift requirements of the Uniform Building Code, the 1994 *NEHRP Recommended Provisions for Seismic Regulations for New Buildings* (NEHRP, 1994) permitted the engineer to use the dampers to reduce the base shear strength of the building. The underlying assumption of these Provisions was that the damped building would suffer no more damage in a design earthquake than the corresponding conventionally framed building. The minimum design forces in the building frame could be calculated as the product of the forces associated with the framing system exclusive of the dampers and the reduction factors listed in Table 1-1 below, which were based on the work of Wu and Hanson (1989). The Provisions noted "Structural members that transmit the forces from the energy dissipation devices to the foundation [including all damper framing members] should be designed to remain elastic for 1.2 times the maximum devices forces associated with the design basis earthquake." Two types of dampers were identified in the provisions: linear viscous devices, and *other* energy dissipation devices. Linear analysis procedures were presented for

each type of damper. The Provisions recommended that the building design be verified by nonlinear response-history analysis.

Table 1-1 1994 NEHRP Reduction Factors for Increased Damping (NEHRP, 1994)

<i>Fraction of Critical Damping</i>	<i>Reduction Factor</i>
0.05	1.00
0.10	0.84
0.15	0.72
0.20	0.64
0.25	0.58
0.30	0.53

1.2.4 1997 NEHRP Guidelines for the Seismic Rehabilitation of Building

The 1997 *NEHRP Guidelines for the Seismic Rehabilitation of Building* (FEMA, 1997), widely known as FEMA 273, presented unified procedures for the implementation of energy dissipation devices in retrofit building construction. Consistent with the remainder of the guidelines, four analysis procedures were presented for analyzing buildings incorporating energy dissipation devices: linear static, linear dynamic, nonlinear static, and nonlinear dynamic. All four procedures were displacement (damage)-based methods rather than the traditional force-based methods such as the 1992 SEAONC and 1994 *NEHRP Recommended Provisions*. Because the products of any of these procedures were displacements and deformations, the procedures represented a paradigm shift in the practice of earthquake engineering, and have been used for performance-based earthquake engineering. FEMA 273 permitted the engineer to select performance levels and objectives, so no limits on minimum base shear strength and maximum

interstory drift were established in the *Guidelines*. Two types of dampers were identified in the *Guidelines*: displacement-dependent dampers; and velocity-dependent dampers.

The linear procedures of FEMA 273 could only be used if it could be demonstrated that the framing system exclusive of the dampers remained essentially elastic for the level of earthquake shaking under consideration. Further, the effective damping provided by the energy dissipation system could not exceed 30 percent of critical. The linear methods accounted for energy dissipation (damping) in the elastic frame and the dampers. FEMA 273 promoted the use of nonlinear analysis for retrofit building construction using passive energy dissipation devices. Two methods of nonlinear static analysis were presented: Method 1, also known as the Coefficient Method; and Method 2, which was a variant of the well-known Capacity Spectrum Method. These nonlinear methods accounted for energy dissipation in both the yielding frame and the dampers.

1.2.5 1999 SEAOC Recommended Lateral Force Requirements

In 1999, the Structural Engineers Association of California (SEAOC) published guidelines for implementing passive energy dissipation devices in buildings as part of the *Recommended Lateral Force Requirements and Commentary*. The guidelines follow the same format as that of the 1997 Uniform Building Code, and use the same (linear) analysis procedures as those presented in the Code for design of conventional construction, namely, equivalent lateral force, response-spectrum, and response-history analysis. Nonlinear response-history analysis is also permitted but no guidance is offered. Two types of dampers were identified in the *Requirements*: displacement-dependent dampers and velocity-dependent dampers. The framing system exclusive of the dampers has to comply with the base shear strength requirements of the Uniform Building Code regardless of the type of analysis used. Metallic-yielding (displacement-dependent) dampers can be included as part of the lateral-force-resisting system to meet these strength requirements. If either the equivalent lateral force or response-spectrum procedures is used, or if linear response-history analysis is used and the resultant demand-capacity ratios exceed 2.0, the framing system exclusive of the dampers must meet the drift requirements of the Code. If nonlinear response-history analysis is used, or if linear response-history analysis is used

and the resultant demand-capacity ratios are less than 2.0, the energy dissipation provided by the damping system may be used to satisfy the drift requirements of the Code.

1.2.6 2000 NEHRP Recommended Provisions for Seismic Regulations for New Buildings

The 2000 *NEHRP Recommended Provisions for Seismic Regulations for New Buildings and Other Structures* present completely revised procedures for implementing passive energy dissipation devices in new buildings. The December 1999 ballot version of the energy dissipation provisions (Appendix to Chapter 13) is presented in Appendix A of this report. Robust linear procedures (equivalent lateral force and response-spectrum methods) are presented for use with displacement- and velocity-dependent dampers. These procedures were developed in part by the author as part of his doctoral studies at the University at Buffalo, in close co-operation with the members of BSSC Committee TS12, who were tasked with writing new energy dissipation procedures for the *Provisions*. The studies presented in this report served to validate these procedures, which will form the national standard for implementing passive energy dissipation devices in buildings. Much additional discussion on the procedures are presented in the following chapters.

1.3 Report Organization

This report is divided into nine sections, references, and eleven appendices. Section 2 provides a description of the FEMA 273 and 274 nonlinear static analysis procedures. Procedures for modifying response spectra to account for damping in excess of 5 percent of critical are presented in Section 3. Simplified methods of analysis of yielding systems are described in Section 4. Relationships between inelastic and elastic displacement responses are presented in Section 5. A method for estimating the displacement ductility demand in yielding systems including viscous energy dissipation devices is presented in Section 6. Information from Sections 2 through 6 are integrated in Section 7 in the form of new equivalent lateral force and modal analysis procedures for implementing energy dissipation devices in new buildings. Section 8 describes the results of validation studies of the methods of Section 7 using 3- and 6-story frames. A summary, conclusions and recommendations for future work are presented in Section 9. A list of references follows Section 10. The eleven appendices provide supplemental information and detailed calculations in support of Sections 2 through 9.

SECTION 2

DESCRIPTION OF NONLINEAR STATIC ANALYSIS PROCEDURES OF FEMA 273

2.1 Introduction

The intent of performance-based seismic design is to produce structures with predictable performance levels. To achieve this, nonlinear analysis procedures are used. The most realistic of the nonlinear procedures is response-history analysis. However, this method of analysis requires a complex description of the analyzed system and the response is strongly sensitive to the models and the characteristics of the ground motion used in the analysis. Simplified nonlinear analysis methods have been developed based on the use of equivalent linear representations of the structural system.

FEMA (1997) describes two simplified nonlinear static methods of analysis: Method 1 and Method 2. Both methods are briefly described herein and subsequently some clarifications and improvements of these methods are presented.

2.2 Nonlinear Static Procedure, Method 2

2.2.1 General Description

The seismic response of yielding systems may be estimated by simplified methods of analysis in which the yielding system is replaced by an equivalent linear elastic and viscous system. Chopra and Goel (1999) recently presented a brief historical review of these methods and Iwan and Gates (1979) presented a collection of such methods and a study of their accuracy.

Method 2 of FEMA (1997) is largely based on the capacity spectrum method (Freeman et al., 1975; Freeman, 1978) but extended to include structures with damping systems. Method 2 contains a number of steps as explained below for structures with damping systems and illustrated in Figure 2-1.

- (1) A mathematical model of the structure including all the characteristics of the framing system and energy dissipation devices is developed. A relation between the base shear force and

roof displacement is established. This relationship is commonly known as the pushover curve. Although the pushover curve should be a description of the capacity of a given structure, its shape varies as a function of the pattern of lateral loads used to monotonically push the structure.

- (2) A value of the roof displacement is assumed and the effective damping is determined from

$$\beta = \frac{W_D}{4\pi W_s} \quad (2-1)$$

where W_D is the energy dissipated in a cycle of harmonic motion to the assumed displacement and W_s is the strain energy at the assumed displacement. The value of W_D includes the damping effect of the supplemental damping devices, by yielding of the framing system, and due to the structural damping inherent in the frame. For the assumed value of the roof displacement, eigenvalue analysis is performed using the secant stiffness properties of the structural elements. Using the fundamental mode properties, the pushover curve is converted to the spectral capacity curve, that is, a plot of spectral acceleration versus spectral displacement. The spectral acceleration (S_a) for the first mode representation of the structure is given by

$$S_a = \frac{V}{\bar{W}_1} g \quad (2-2)$$

where V is the base shear, and \bar{W}_1 is the first modal weight given by

$$\bar{W}_1 = \frac{\sum_{i=1}^N (w_i \phi_{i1})^2}{\sum_{i=1}^N w_i \phi_{i1}^2} \quad (2-3)$$

and where ϕ_{i1} is the first mode shape vector, w_i is the reactive weight of the i^{th} degree of freedom, and N is the number of degrees of freedom.

In a similar way, the spectral displacement (S_d) for the first mode representation of the structure is given by

$$S_d = \frac{\delta_r}{\phi_{r1}\Gamma_1} \quad (2-4)$$

where δ_r is the roof displacement, Γ_1 is the first mode modal participation factor, and ϕ_{r1} is the ordinate of the first mode shape at the roof.

- (3) The capacity curve computed in step 2 is superimposed on the design demand curve, which is a plot of spectral acceleration versus spectral displacement after modification for the effective damping. The displacement demand is determined from the intersection point of the capacity curve and the design demand curve.
- (4) The assumed and computed values of the displacement are compared and the process is repeated until satisfactory convergence is achieved.
- (5) The contribution of higher modes to the total response is calculated by utilizing modal analysis procedures and assuming elastic behavior with properties based on the secant stiffnesses at the displacement calculated in step (4). For this calculation, Equations (2-1) to (2-4) are used but with \bar{W}_1 is replaced by \bar{W}_m , ϕ_{i1} is replaced by ϕ_{im} , ϕ_{r1} is replaced by ϕ_{rm} and Γ_1 is replaced by Γ_m , where the subscript m denotes the m^{th} mode of vibration. It should be noted that in this calculation, iteration is not required due to the assumption of elastic behavior. The total response is finally calculated through the use of an appropriate combination rule.

2.2.2 Pushover Curve

The pushover curve constitutes an important major step in the simplified method of analysis. In a practical sense it represents the capacity of the structure to resist lateral loads. The pushover curve is constructed by “pushing” a mathematical model of the structure by monotonically increasing lateral loads of constant proportions. As the magnitude of the load increases, progressive yielding of the model occurs, which is accompanied by a change in the dynamic properties of the structure. Recognizing that the structural capacity and, therefore, its

degradation pattern is not independent of the demand, it can be concluded that the ordinates of pushover curve are a function of the assumed pattern of lateral loads.

The pattern of loads should be consistent with the expected distribution of inertia forces in the yielding structure. Some studies have suggested that the most appropriate distribution is one in which the loads change as the structure is displaced. This approach is termed *adaptive load pattern*. Researchers have proposed the use of a lateral pattern consistent with the deflected shape of the structure (Fajfar and Fischinger, 1988), the use of load patterns based on mode shapes derived from secant stiffnesses (Eberhard and Sozen, 1993), and the use of patterns in which the lateral forces are related to story resistances at each increment of loading (Reinhorn et al., 1995; Bracci et al., 1997).

The simplified analysis procedure described in FEMA (1997) requires the use of at least two different patterns of lateral loads in order to produce bounds on the response. The first one, termed a *uniform pattern*, is based on the lateral forces being proportional to the total mass at each level. The second pattern, termed a *modal pattern*, is nearly proportional to the first modal shape. Furthermore, FEMA (1997) suggests that the load pattern be computed by combination of modal responses using response-spectrum analysis and considering as many modes as necessary to capture 90% of the total mass.

2.2.3 Design Demand Curve

The seismic hazard is typically represented by the 5%-damped pseudo-acceleration response spectrum, that is a plot of spectral acceleration (acceleration at the time of maximum displacement) of a single-degree-of-freedom elastic system with 5% equivalent viscous damping versus the structural period. The pseudo-acceleration S_a and the spectral displacement S_d (maximum drift) of the single-degree-of-freedom system are related through

$$S_d = \frac{T^2}{4\pi^2} S_a \quad (2-5)$$

where T is the period. A plot of spectral acceleration versus the spectral displacement is termed the design demand curve. In this figure, points of equal period are located along lines radiating

from the origin as shown in Figure 2-2. Plots for different levels of damping are also presented in the figure.

The design demand curves for levels of damping higher than 5% are constructed by dividing the 5%-damped curve by the damping coefficient B . Values of the damping coefficient have been presented in FEMA, 1997. As shown in Table 2-1, FEMA utilizes two factors, one for the constant acceleration region of the response spectrum (B_s) and the other for the constant velocity region of the spectrum (B_1). Interestingly, the values in the constant acceleration region are larger than those in the constant velocity region, which contradicts the fact that there is little or not reduction of displacement with increasing damping in very stiff structures. Also, the values of the damping coefficient are terminated at the damping ratio of 0.5 in an apparent exercise of conservatism due to lack of data for larger levels of damping.

New values of the damping coefficient, which correctly account for reduction of the damping coefficient with reducing period and extend to critically damped systems have been established in Section 3. The case of critically and over-critically damped systems may actually arise in the higher modes of structures with viscous damping devices. Presented in Figure 2-3, the values of this study may be seen as large for damping ratio larger than 0.5 by comparison to the values in FEMA (1997). However, the damping coefficient values of this study are realistic and their use is important in correctly assessing the benefits of energy dissipation systems. The values established in this study have been utilized, after some minor simplification, in the 2000 NEHRP Recommended Provisions for Seismic Regulations for New Buildings and Other Structures, Appendix to Chapter 13, Structures with Damping Systems (NEHRP, 2000). The values of the damping coefficient in NEHRP (2000) are presented in Table 2-1 and graphically compared to the FEMA (1997) and the values of this study in Figure 2-3. As an example, Figure 2-4 presents response spectra established by using damping coefficients developed in this study. The 5%-damped spectrum is that described in NEHRP (2000) for parameters $S_{DS} = 1.0$, $S_{DI} = 0.6$ and $T_s = 0.6$ sec.

2.2.4 Calculation of Velocity Dependent Forces

Velocity dependent forces are calculated in Method 2 by utilizing pseudo-velocities as estimates of maximum velocities. This simple approach introduces errors since it is known that pseudo-

velocity generally under-estimates the maximum velocity for long-period structures and it generally over-estimates the maximum velocity for short-period structures. Moreover, the degree of error depends on the amount of effective damping. Sadek et al. (1999) proposed the use of correction factors to multiply the pseudo-velocity in order to obtain a better estimate of maximum velocity. The Sadek approach has been investigated in this study and found promising. Results are presented in Section 4, where it is shown that correction factors established by the approach of Sadek et al. (1999) produce good estimates of drift velocities.

2.2.5 Calculation of Maximum Actions

The seismic design forces are calculated at three stages: (a) maximum drift, (b) maximum velocity, and (c) maximum acceleration. Stages (b) and (c) are important only for structures with velocity dependent damping systems because maximum actions in buildings incorporating displacement dependent damping systems will occur at the time of maximum displacement.

The design forces at the stage of maximum acceleration are calculated as a linear combination of the forces calculated at the stages of maximum drift and maximum velocity after multiplication by combination factors CF_1 and CF_2 , respectively. These factors have been developed on the basis of the assumption of linear-elastic and linear-viscous behavior (Tsopelas et al., 1997; Constantinou et al., 1998).

It is now recognized that the combination factors in FEMA (1997) are incorrect for yielding structures and for structures with nonlinear viscous damping systems. Section 4 herein presents the corrected combination factors, which have been implemented in NEHRP (2000).

2.3 Nonlinear Static Procedure, Method 1

Method 1 was developed as a simple one-step analysis method in which the roof (or target) displacement of structures exhibiting bilinear behavior is prescribed by an equation of the form

$$\delta_r = C_0 \cdot C_1 \cdot C_2 \cdot C_3 \cdot S_a \cdot \frac{T_e^2}{4\pi^2} \quad (2-6)$$

where T_e is the elastic period of the structure, S_a is the spectral acceleration for period T_e , C_o is a coefficient relating roof displacement to spectral displacement, C_I is a coefficient relating maximum inelastic displacements to displacements calculated assuming linear elastic response, and C_2 and C_3 are coefficients to represent the effects of stiffness and strength degradation, and dynamic P- Δ effects, respectively.

As originally conceived, Method 1 can bypass steps (2) to (5) of Method 2 and can obtain the design forces and member deformations by only performing pushover analysis until the target roof displacement is reached. However, the application of Method 1 is complicated when velocity-dependent damping systems are utilized. Specifically:

- (a) The effect of added damping must be considered in the evaluation of the spectral acceleration. This requires that step (2) of Method 2 is performed, however excluding the contribution from yielding of the building frame. For linear viscous and viscoelastic damping systems, this represents a simple calculation. For nonlinear viscous damping systems, an iterative procedure similar to that of Method 2 must be performed.
- (b) The effects of higher modes need to be considered. These effects are important in the calculation of velocity-dependent forces.
- (c) Coefficient C_I , as described in FEMA (1997), does not account for the effect of added viscous damping on the ratio of inelastic displacements to displacement calculated assuming elastic response. It will be shown in Section 5 that added viscous damping affects coefficient C_I . New expressions prescribing coefficient C_I are derived and presented in Section 5.

2.4 Calculation of Effective Damping

Equation (2-1) describes a general approach for calculating the effective damping of a structural system. The calculation requires that information on the properties and configuration of the damping system, and information on the properties of the structural frame (period, mode shape, reactive floor weights) are available. The details of calculation differ depending on the nature of the damping system. Details are presented in Section 4 where simplified methods of analysis of single-degree-of-freedom systems are evaluated and in Section 7.4 where the calculation of the effective damping in multiple-degree-of-freedom-systems is presented.

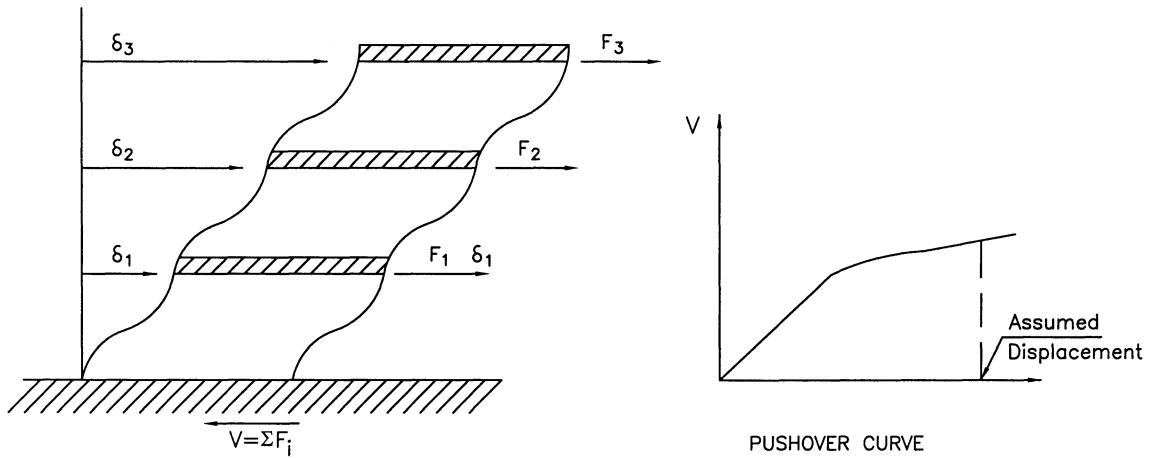
TABLE 2-1 Values of Damping Coefficient B

Effective Damping β	FEMA 273		This Study (Section 3)		NEHRP 2000
	B_s 1	B_1 2	B_s 3	B_1 4	B 5
<0.02	0.8	0.8	0.80	0.80	0.8
0.05	1.0	1.0	1.00	1.00	1.0
0.10	1.3	1.2	1.20	1.20	1.2
0.20	1.8	1.5	1.50	1.50	1.5
0.30	2.3	1.7	1.70	1.70	1.8
0.40	2.7	1.9	1.90	1.90	2.1
0.50	3.0	2.0	2.20	2.20	2.4
0.60	3.0	2.0	2.30	2.60	2.7
0.70	3.0	2.0	2.35	2.90	3.0
0.80	3.0	2.0	2.40	3.30	3.3
0.90	3.0	2.0	2.45	3.70	3.6
1.00	3.0	2.0	2.50	4.00	4.0

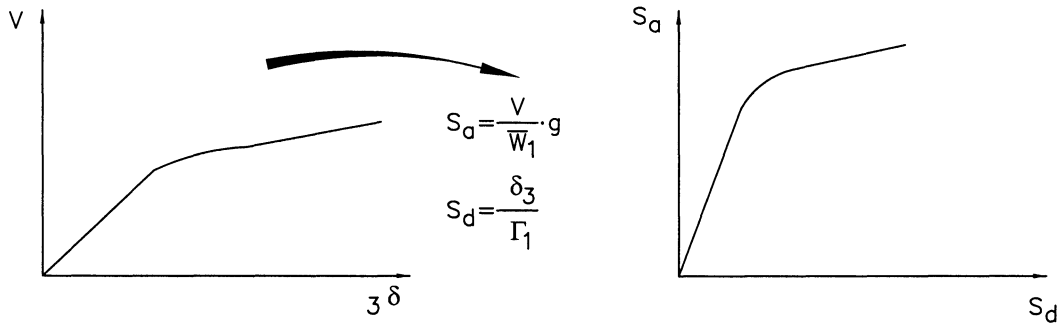
- 1 Valid for $T \leq T_s B_s / B_1$
- 2 Valid for $T \geq T_s B_s / B_1$
- 3 Valid at $T = T_s / 5$. For $T_s / 5 < T < T_s$, B is determined by linear interpolation between values B_s and B_1 . For $T < T_s / 5$, B is determined by linear interpolation between values of 1.0 (valid at $T=0.0$) and B_s (valid at $T = T_s / 5$).
- 4 Valid for $T \geq T_s$
- 5 Valid for $T \geq T_s / 5$. Also B = 1.0 for $T = 0.0$. Values of B for $0 < T < T_s / 5$ may be obtained by linear interpolation.

T = period, T_s = period at which the constant acceleration and constant velocity regions of the response spectrum intersect.

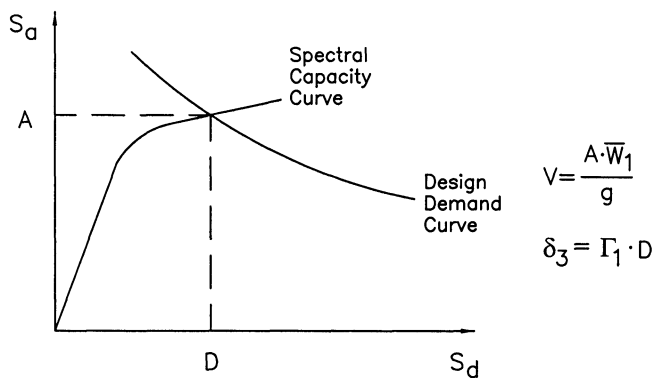
STEP 1 PUSHOVER ANALYSIS



STEP 2 PERFORM EINGENVALUE ANALYSIS USING EFFECTIVE MEMBER STIFFNESSES AT ASSUMED DISPLACEMENT
 CONVERT PUSHOVER CURVE TO SPECTRAL CAPACITY CURVE



STEP 3 ESTABLISH DESIGN DEMAND SPECTRUM USING EFFECTIVE DAMPING IN FUNDAMENTAL MODE
 OVERLIE SPECTRAL CAPACITY CURVE ON DESIGN DEMAND SPECTRUM AND CALCULATE RESPONSE



STEP 4 IF CALCULATED $\delta_3 \neq$ ASSUMED DISPLACEMENT, REPEAT STEPS 2 TO 5

STEP 5 OBTAIN HIGHER MODE RESPONSE

FIGURE 2-1 Illustration of Nonlinear Static Procedure, Method 2

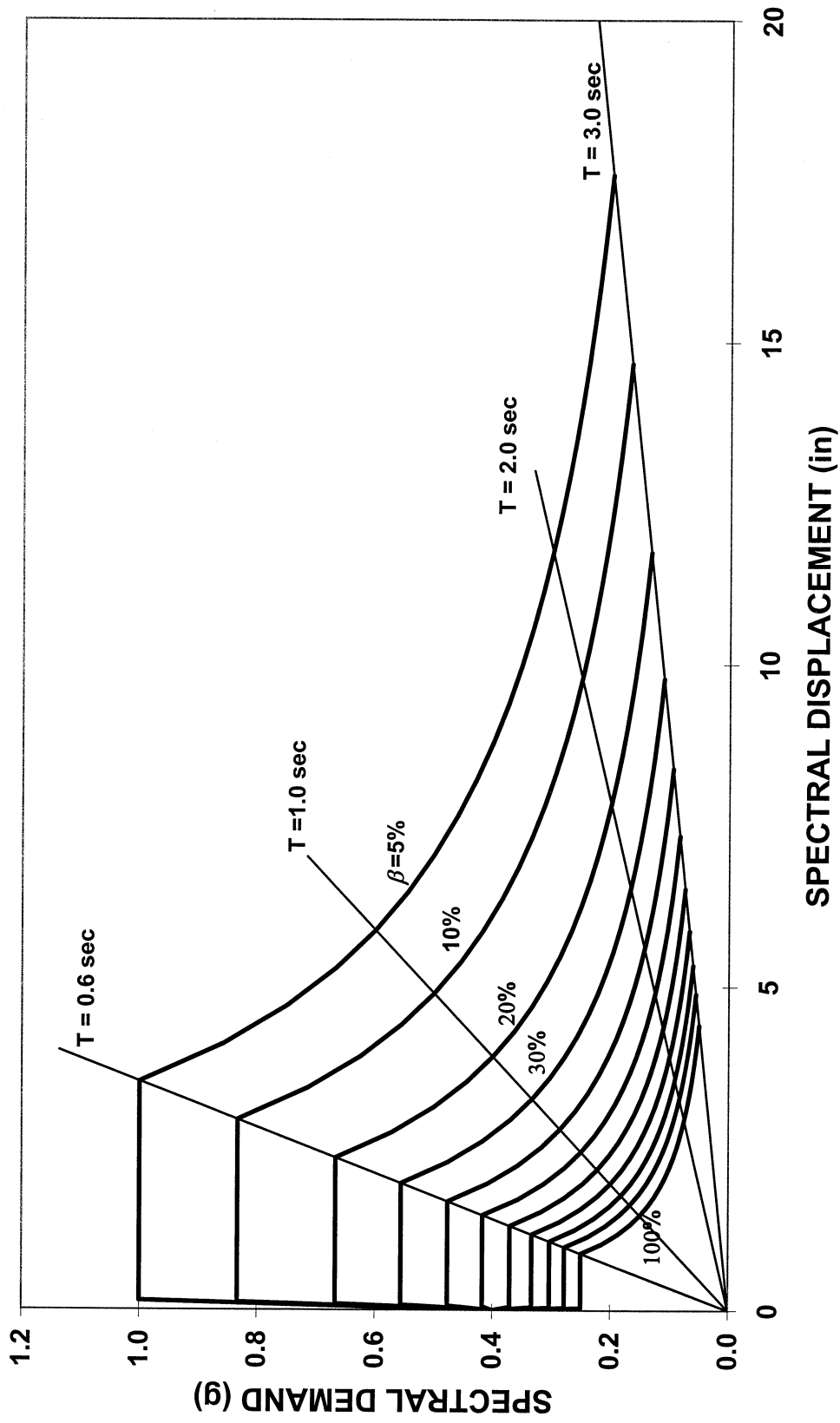


FIGURE 2-2 Example of Design Demand Curves

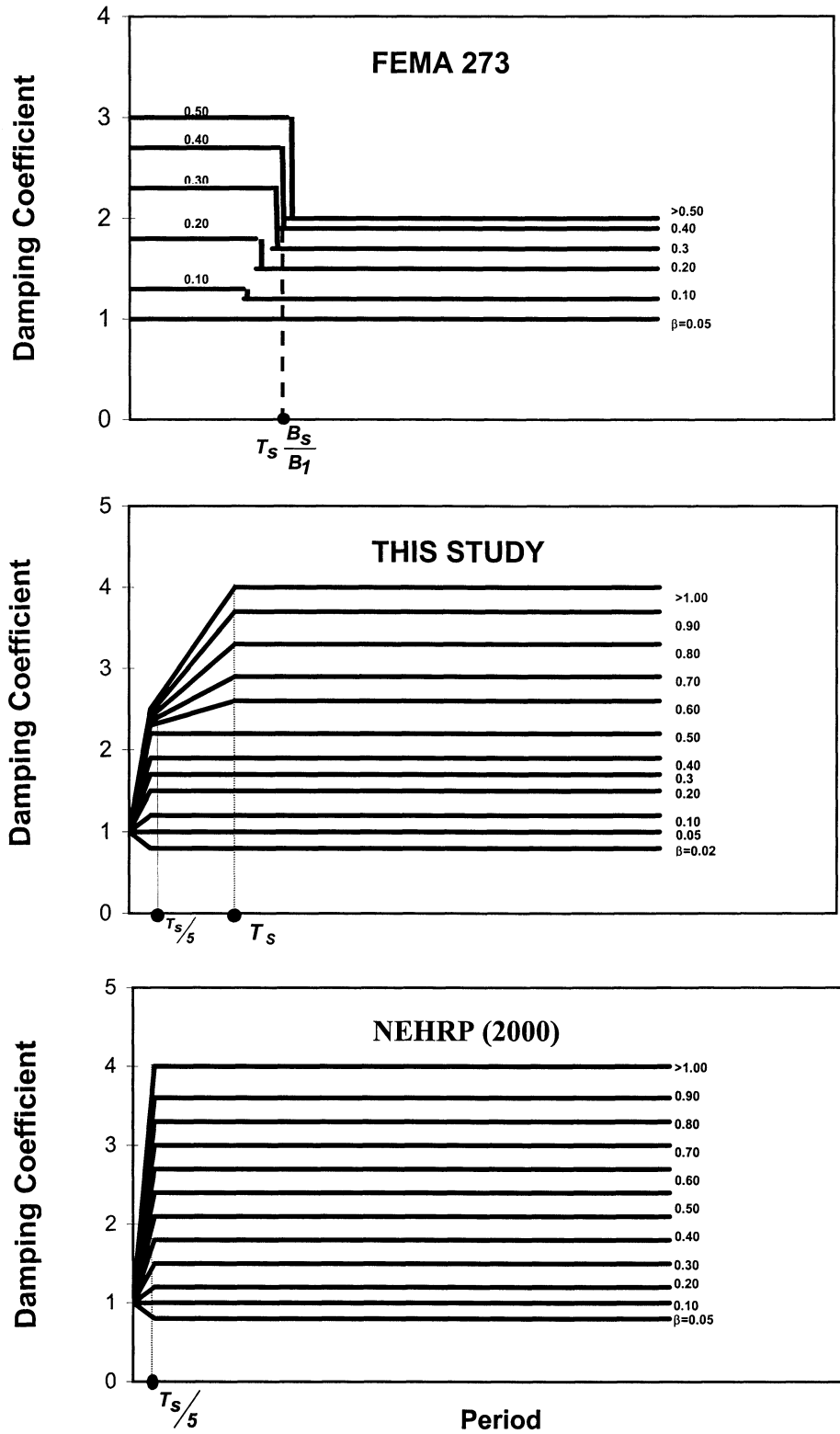


FIGURE 2-3 Damping Coefficient B as Function of Period and Damping

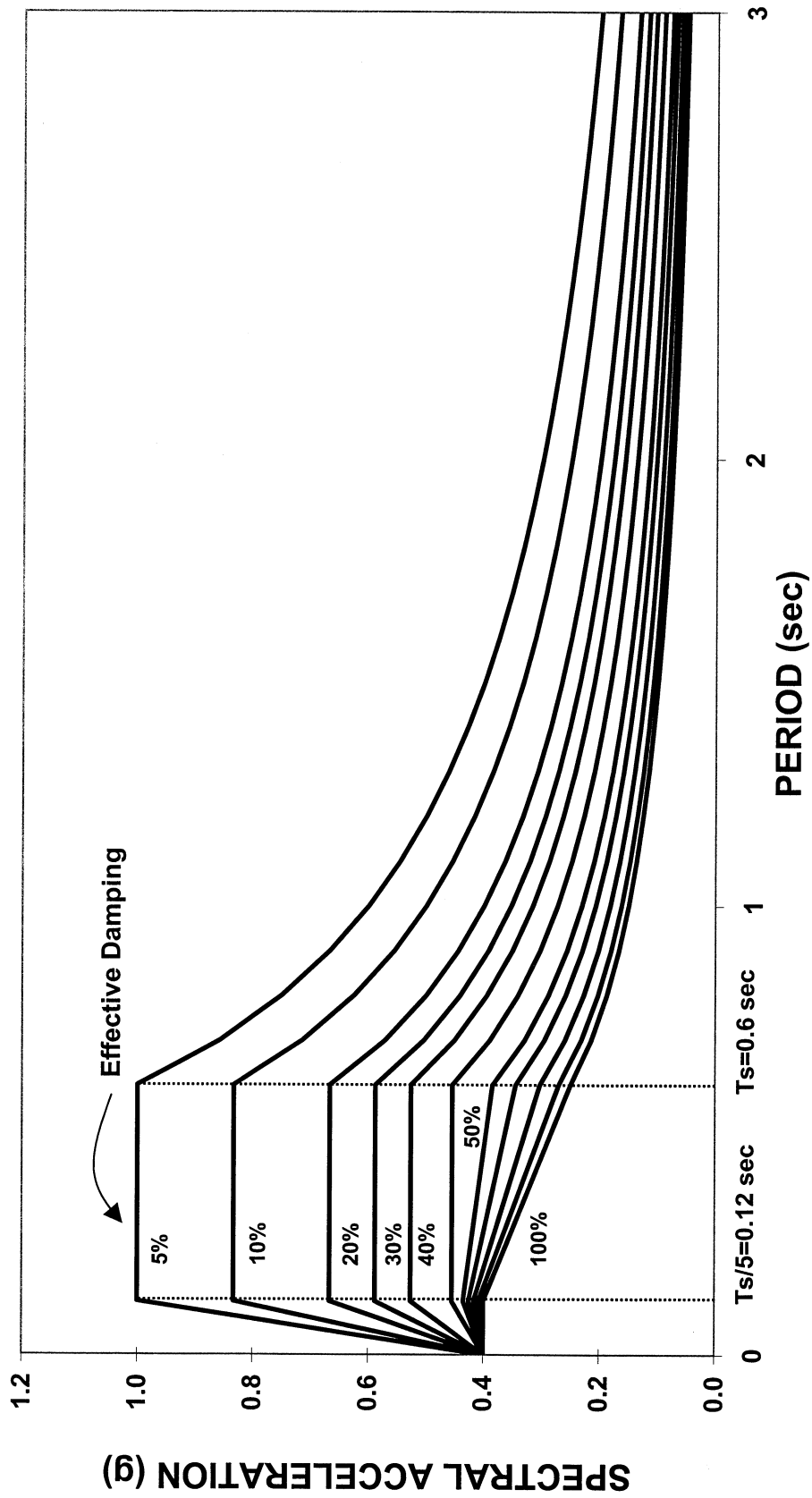


FIGURE 2-4 Acceleration Response Spectra for Various Levels of Effective Damping Established with the use of the Damping Coefficient Developed in this Study (conservative values in Table 3-3). 5%-Damped Spectrum Representative of NEHRP (2000) Design Spectrum with $S_{ds} = 1.0$, $S_{d1} = 0.6$ and $T_s = 0.6$ sec.

SECTION 3

MODIFICATION OF RESPONSE SPECTRUM FOR HIGHER DAMPING

3.1 Introduction

The 5%-damped elastic response spectrum represents the usual seismic loading specification. Spectra for higher damping need to be constructed for the application of simplified methods of analysis of structures with damping systems. Elastic spectra constructed for higher viscous damping are useful in the analysis of linear elastic structures with linear viscous damping systems. Moreover, they are used in the simplified analysis of yielding structures since simplified methods of analysis are based on the premise that yielding structures with damping systems may be analyzed by using equivalent linear and viscous representations. The validity and accuracy of such representations is the subject of the study reported in Section 4.

The typical approach of constructing an elastic spectrum for damping greater than 5-percent is to divide the 5%-damped spectral acceleration by a damping coefficient B :

$$S_a(T, \beta) = \frac{S_a(T, 5\%)}{B} \quad (3-1)$$

where $S_a(T, \beta)$ is the spectral acceleration at period T for damping ratio β . Note that the spectral acceleration is the acceleration at maximum displacement (it does not contain any contribution from the viscous force) and is therefore related directly to the spectral displacement through equation (2-5). The damping coefficient is a function of the damping ratio and may be a function of the period.

The derivation of damping coefficients or their inverse (which may be extracted from spectrum amplification factors) may be traced back nearly 30 years (e.g., see Newmark and Hall, 1982 and several of their references). Table 3-1 has been prepared to compare values of the damping coefficient from various sources. The values attributed to Newmark and Hall (1982) have been derived from the spectrum amplification factors, that is, factors used to multiply the peak ground motion to obtain the response spectrum. These factors likely originated from data on response spectra of earthquakes which occurred prior to 1973. It should also be noted that Newmark and

Rosenblueth (1971) and Newmark and Hall (1969) reported amplification factors, which have not been utilized herein. The data of Newmark and Hall (1982) are limited to damping ratio of 0.20. However, the equations presented by Newmark and Hall (1982) for the amplification factor in the constant velocity region of the spectrum were utilized herein to obtain values of the damping coefficient for damping ratios up to 1.0. These values are reported in Table 3-1. Specifically, Newmark and Hall (1982) proposed for the constant velocity region of the spectrum:

$$A_{\beta} = 2.31 - 0.41 \ln(100\beta) \quad (3-2)$$

where A_{β} = amplification factor for damping ratio β . Since the damping coefficient B is equal to

$$B = \frac{A_{0.05}}{A_{\beta}} \quad (3-3)$$

it follows that in the constant velocity region

$$B = \frac{1.65}{2.31 - 0.41 \ln(100\beta)} \quad (3-4)$$

The values for the damping coefficient of Newmark and Hall (1982) in the constant velocity region of the spectrum are basically the same as those of NEHRP (2000). This is surprising since the NEHRP (2000) values were based on the study reported herein, which used different earthquake records and a different analysis procedure than that of Newmark and Hall (1982). Nevertheless, this fact may enhance our confidence in the damping coefficient values in NEHRP (2000).

The values of the damping coefficient that appeared in the 1994 NEHRP (NEHRP, 1994) were based on a study of Wu and Hanson (1989). Later, the FEMA 273 Guidelines (FEMA, 1997) were developed in which the damping coefficients were based on the work of Newmark and Hall (1982) but were extended to higher values of the damping ratio. The extension to higher values of the damping ratio was necessary since simplified methods of analysis introduced in FEMA 273 could result in high effective damping due to the combined effects of yielding of the

building frame and added viscous damping. There are two drawbacks to the damping coefficients of FEMA 273:

- (a) The values for the constant acceleration region of the spectrum (region of low periods) are higher than those valid in the constant velocity region. This contradicts the fact that there is little or no reduction of displacement with increasing damping in very stiff structures. It also leads to the erroneous impression that damping systems are most effective when used on stiff structures.
- (b) The effect of damping in reducing displacement is ignored when the damping ratio exceeds 50% of critical leading to conservative estimates of displacement in highly damped buildings, which may be the case for frames having good hysteretic behavior, enhanced with viscous damping systems and undergoing significant inelastic action.

The study reported in this section resulted in values of the damping coefficient in the constant velocity region which are larger than those in FEMA 273 (see column of results labeled best fit in Table 3-1). For this reason, conservative values of the damping coefficient are proposed in this study. The proposed values of the damping coefficient have been utilized, after some simplification, in the NEHRP Recommended Provisions (NEHRP, 2000).

3.2 Procedure to Establish Values of the Damping Coefficient

Using (3-1), values of coefficient B may be obtained as

$$B = \frac{S_a(T, 5\%)}{S_a(T, \beta)} \quad (3-5)$$

Equation (3-5) may be used to obtain values of coefficient B for a range of values of period T and for selected earthquake motions. The results for the selected earthquake motions may then be statistically processed to obtain average or median values.

The procedure followed herein is based on the use of scaled earthquakes which on the average represent well a specific design response spectrum. The scaling process of these earthquakes has been presented in Tsopelas et al. (1997). Herein it is sufficient to mention that the scaling

process preserves the frequency content of the records and ensures an equal contribution of these records to the average response spectrum.

The selected 20 horizontal components of 10 earthquake motions are presented in Table 3-2 together with their scale factors. Each of these earthquakes was selected to have a magnitude larger than 6.5, epicentral distance between 10 and 20 km, and site conditions characterized by site class C to D in accordance with NEHRP (2000). That is, the selected records did not include motions recorded on soft soil sites and motions with near-fault characteristics. The applicable design response spectrum had parameters $S_{DS} = 1.0$, $S_{DI} = 0.6$ and $T_S = 0.6$ sec. Figure 3-1 presents the average response spectrum of the 20 scaled motions and compares that to the target NEHRP design response spectrum. The average of the 20 scaled motions represents well the target spectrum. Figure 3-1 presents also the maximum and minimum spectral acceleration values of the 20 scaled motions. These spectra demonstrate the variability in the characteristics of the scaled motions. This variability is implicit in the definition of seismic hazard.

The 20 scaled motions have been used in the construction of elastic response spectra for higher damping. Average spectra (average of spectral acceleration values of the 20 scaled motions) are presented in Figure 3-2 for damping ratio in the range of 2 to 100-percent. The damping coefficient for a particular period was determined as the ratio of the 5%-damped design spectral acceleration to the average spectral acceleration for higher damping, as described by (3-5). Representative plots of the damping coefficient are shown in Figure 3-3. On the basis of such plots, it is reasonable to propose a trilinear relation for the damping coefficient as shown in Figure 3-4. In this relation, the damping coefficient is constant in the constant velocity region of the spectrum and it gradually reduces towards unity at zero. The proposed model requires three parameters for each damping value, B_s , B_l and T_s , as shown in Figure 3-4.

Figure 3-5 presents graphs of the calculated damping coefficient for damping ratio in the range of 2 to 100-percent together with graphs of the coefficient produced by the calibrated trilinear model. The parameters of the model are presented in Table 3-3 and described as been based on best fit. The values of parameter B_1 based on the best fit of the calculated damping coefficient are generally higher than the values of the same parameter in the FEMA 273 Guidelines (FEMA,

1997). Accordingly, conservative values of parameters B_S and B_1 have been established to be consistent with the FEMA (1997) values. These values are listed in Table 3-3.

The proposed conservative trilinear model for the damping is utilized for all calculations described in this report. The data in Table 3-3 were made available at the time of writing of the 2000 NEHRP Recommended Provisions, and were used to establish the simpler two-parameter model for the damping coefficient that is presented in NEHRP (2000) and listed in Table 3-1.

3.3 Conclusions

This section established new values for the damping coefficient which is used in the calculation of spectral acceleration values for damping higher than 5-percent. The presented damping coefficient values are valid for viscous damping ratio in the range of 2 to 100-percent of critical. The derivation of these values was based on the analysis of response of structural systems to selected ground motions which did not include records on soft soil sites and records with near-fault characteristics. The presented values have been utilized, after some simplification, in the NEHRP (2000) Recommended Provisions.

TABLE 3-1 Damping Coefficient from Various Sources

Damping Ratio	Newmark & Hall (1982) (median values)		1994 NEHRP (all periods)	FEMA 273 (1997)		This Study* (conservative values)		2000 NEHRP (all periods > T _s /5)
	Accel. Region	Velocity Region		Accel. Region	Velocity Region	(best fit) Velocity Region	Velocity Region	
0.02	0.78	0.81		0.8	0.8	0.80	0.80	0.8
0.05	1.00	1.00	1.00	1.0	1.0	1.00	1.00	1.0
0.10	1.29	1.21	1.19	1.3	1.2	1.25	1.20	1.2
0.20	1.81	1.53	1.56	1.8	1.5	1.75	1.50	1.5
0.30		1.80	1.89	2.3	1.7	2.10	1.70	1.8
0.40		2.07		2.7	1.9	2.45	1.90	2.1
0.50		2.34		3.0	2.0	2.90	2.20	2.4
0.60		2.61		3.0	2.0	3.30	2.60	2.7
0.70		2.90		3.0	2.0	3.60	2.90	3.0
0.80		3.21		3.0	2.0	4.00	3.30	3.3
0.90		3.55		3.0	2.0	4.30	3.70	3.6
1.00		3.91		3.0	2.0	4.65	4.00	4.0

* For acceleration domain, B is less than the value in table.

T_s = Period at which the constant velocity and constant acceleration regions of spectrum intersect.

Table 3-2 Motions used in Analysis and Scale Factors

Year	Earthquake	Station	Components	Scale Factor
1949	Washington	325 (USGS)	N04W, N86E	2.74
1954	Eureka	022 (USGS)	N11W, N79E	1.74
1971	San Fernando	241 (USGS)	N00W, S90W	1.96
1971	San Fernando	458 (USGS)	S00W, S90W	2.22
1989	Loma Prieta	Gilroy 2 (CDMG)	90,0	1.46
1989	Loma Prieta	Hollister (CDMG)	90,0	1.07
1992	Landers	Yermo (CDMG)	360,270	1.28
1992	Landers	Joshua (CDMG)	90,0	1.48
1994	Northridge	Moorpark (CDMG)	180,90	2.61
1994	Northridge	Century (CDMG)	90,360	2.27

TABLE 3-3 Values of Parameters B_S and B_I in Proposed Model of Damping Coefficient

Damping Ratio	Values Based on Best Fit (as shown in Fig. 3-5)		Conservative Values (Consistent with FEMA 273)	
	B_S	B_I	B_S	B_I
0.02	0.80	0.80	0.80	0.80
0.05	1.00	1.00	1.00	1.00
0.10	1.25	1.25	1.20	1.20
0.20	1.75	1.75	1.50	1.50
0.30	2.10	2.10	1.70	1.70
0.40	2.20	2.45	1.90	1.90
0.50	2.30	2.90	2.20	2.20
0.60	2.40	3.30	2.30	2.60
0.70	2.50	3.60	2.35	2.90
0.80	2.60	4.00	2.40	3.30
0.90	2.70	4.30	2.45	3.70
1.00	2.75	4.65	2.50	4.00

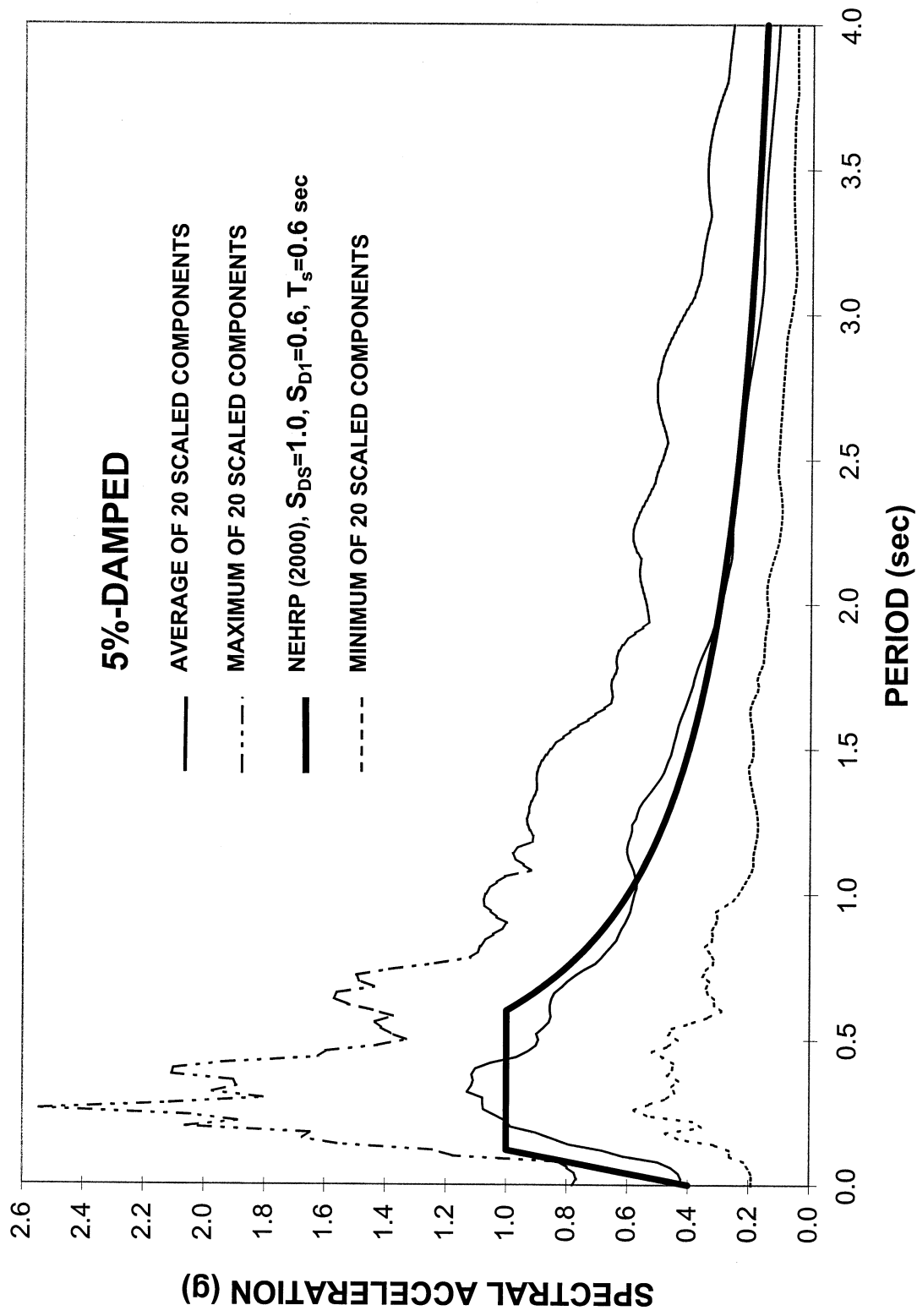


FIGURE 3-1 Maximum, Average and Minimum Spectral Acceleration Values of Scaled Motions

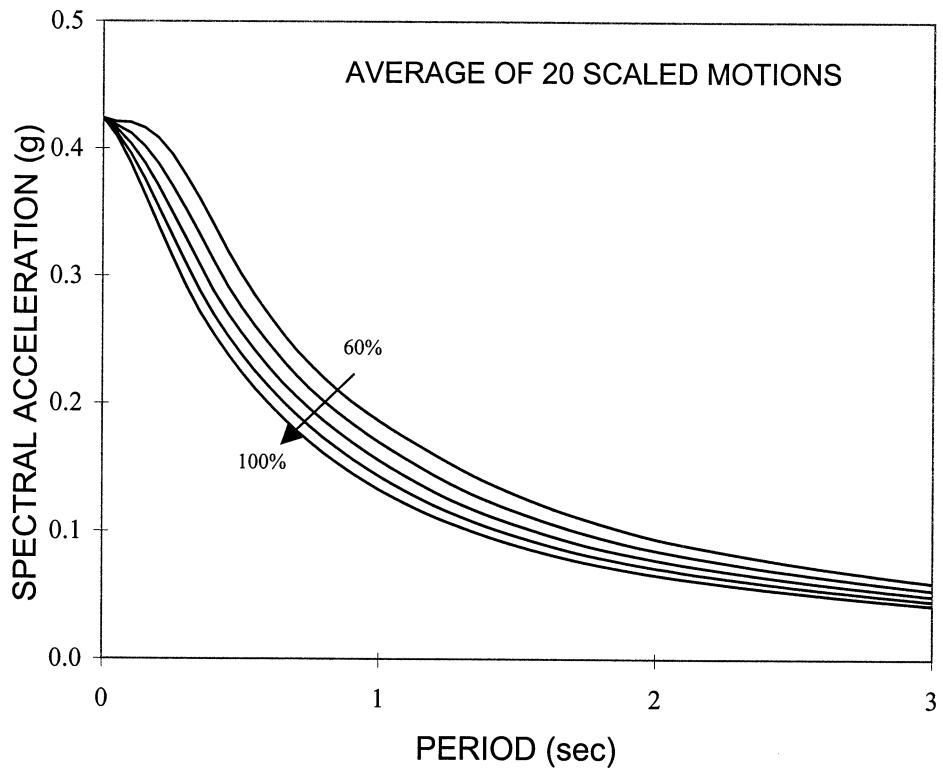
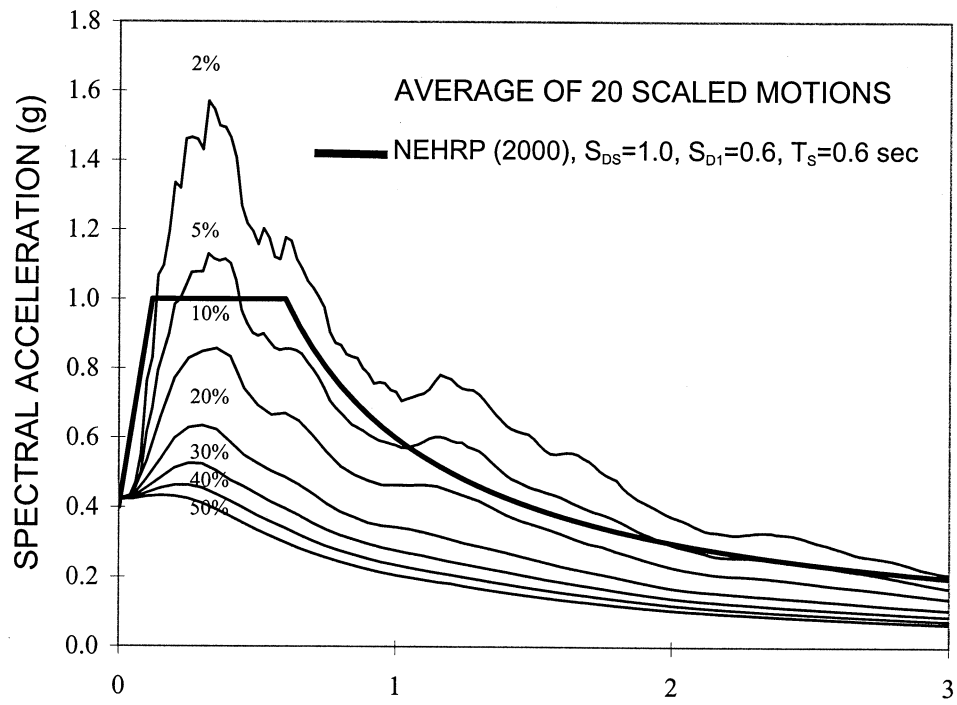


FIGURE 3-2 Average Spectra of Acceleration for Damping in the Range of 2 to 100-Percent of Critical

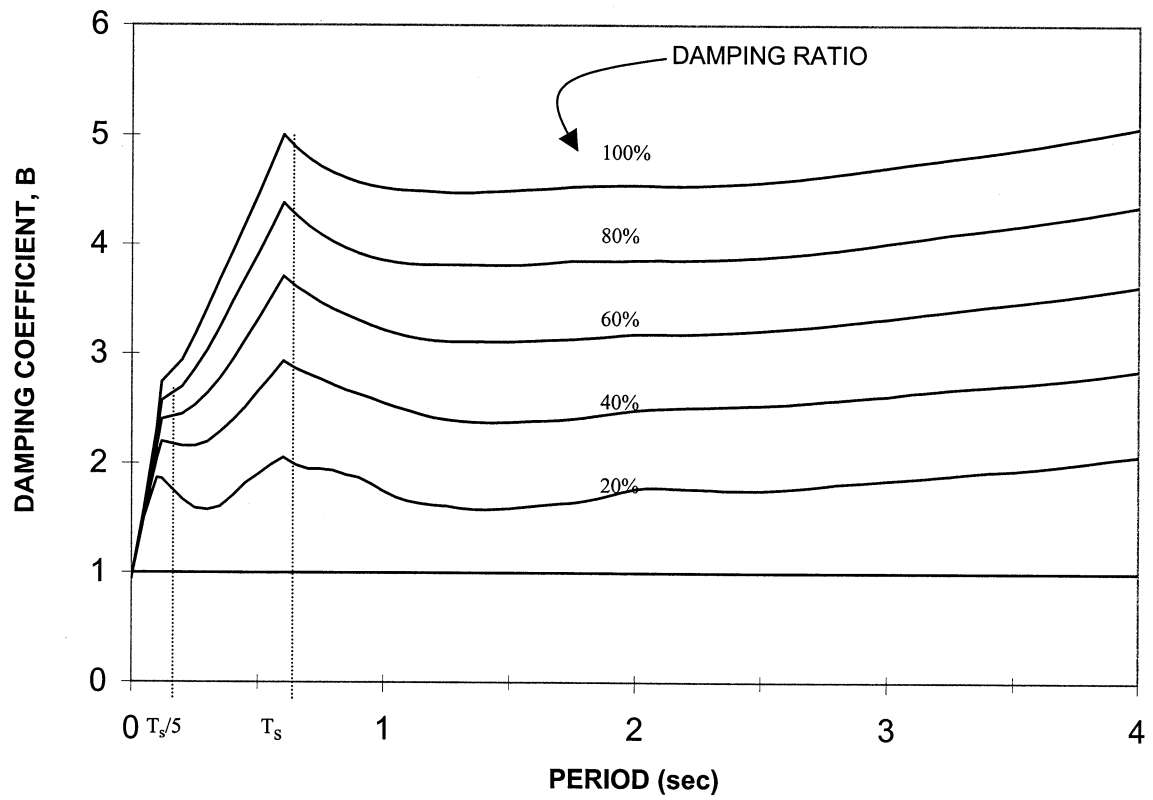


FIGURE 3-3 Calculated Damping Coefficient as Function of Period

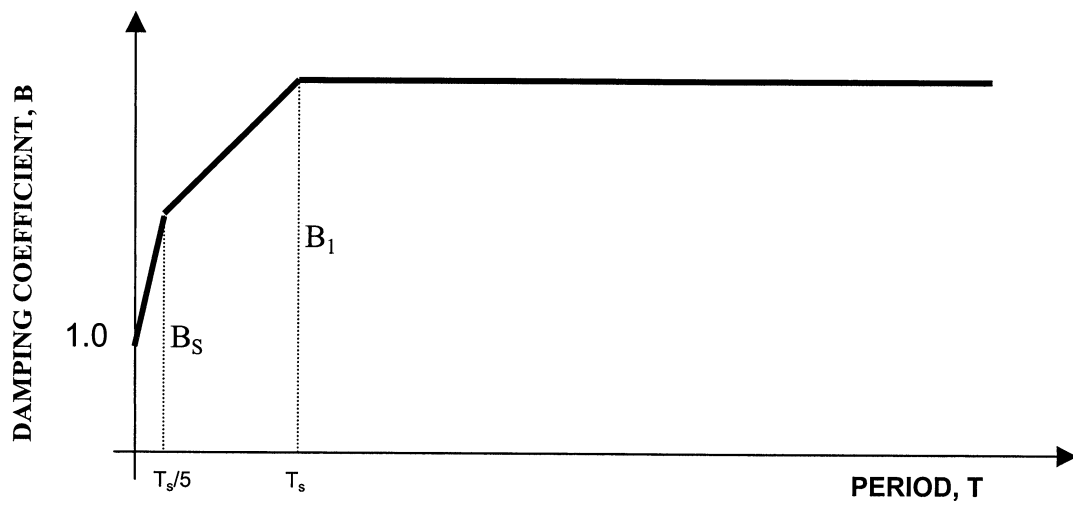


FIGURE 3-4 Proposed Relation of Damping Coefficient vs Period

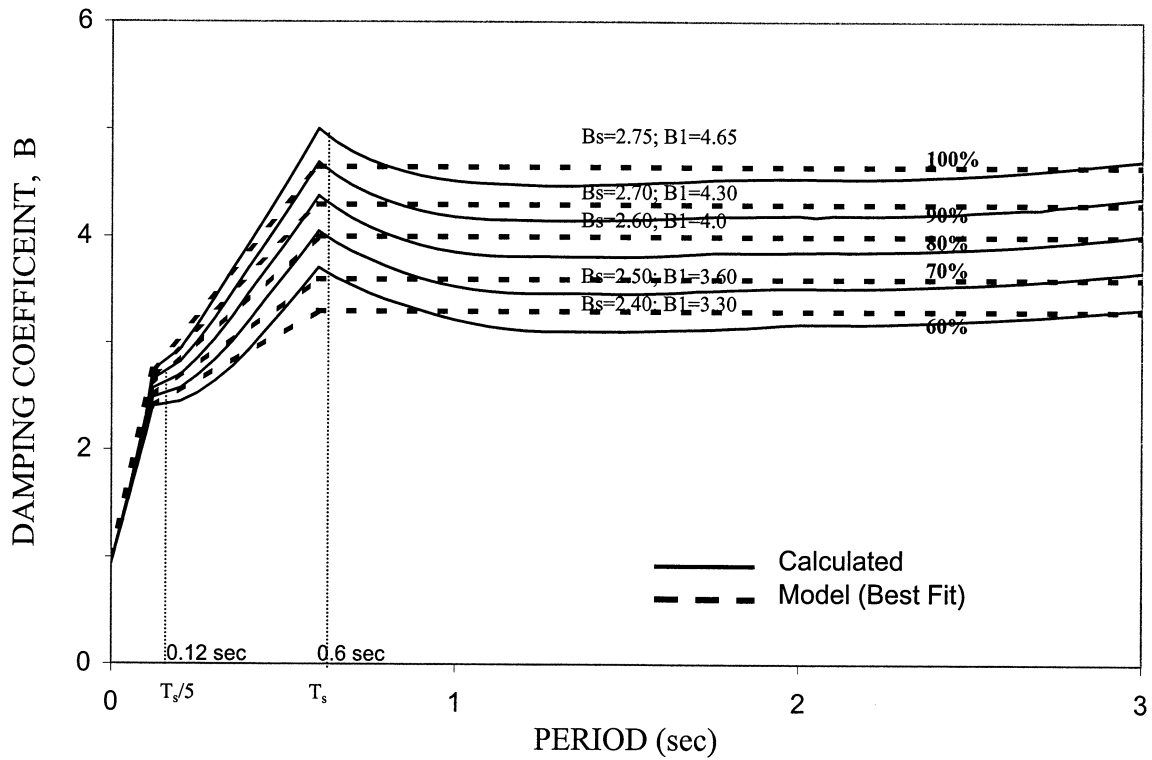
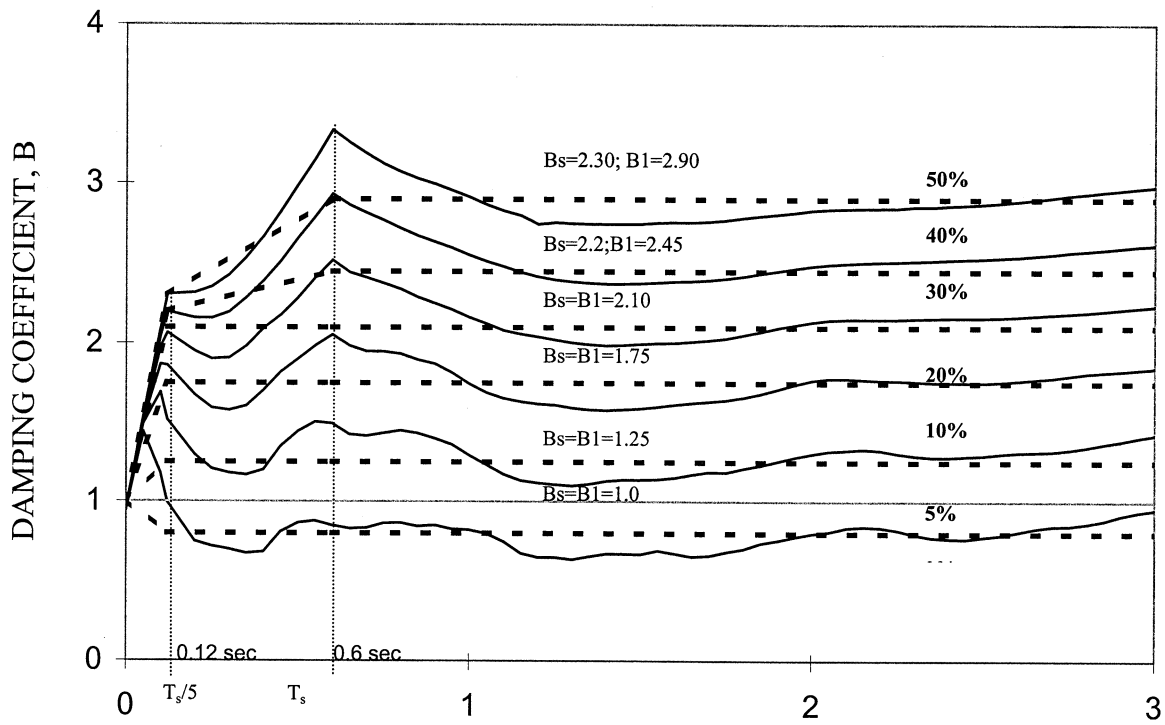


FIGURE 3-5 Comparison of Calculated Damping Coefficient to Proposed Model (Best Fit)

SECTION 4

EVALUATION OF SIMPLIFIED METHODS OF ANALYSIS OF YIELDING SINGLE-DEGREE-OF-FREEDOM SYSTEMS WITH ENERGY DISSIPATION DEVICES

4.1 Introduction

Simplified methods of analysis of structures with energy dissipation systems are based on several approximations. An important approximation is the representation of the yielding structure by an equivalent linear elastic, viscously damped single-degree-of-freedom system. The capability of such an approximation to produce realistic estimates of the peak dynamic response has been the subject of many studies (e.g, Iwan and Gates, 1979a and 1979b; Tsopelas et al., 1997; Chopra and Goel, 1999). These studies concentrated on yielding structures without damping systems and assessed the accuracy of various approximate methods in estimating the peak displacement response. Exception has been the study of Tsopelas et al.(1997) which included structures with linear viscous damping systems.

The study reported in this section extends the work of Tsopelas et al.(1997) to include nonlinear viscous and hysteretic damping systems and assesses the accuracy of Method 2 of FEMA (1997) in predicting the peak displacement, velocity and acceleration responses of single-degree-of-freedom systems. Note that by concentrating on single-degree-of-freedom systems, the application of Method 2 did not require to perform pushover analysis and to account for the contribution of higher modes to the dynamic response. These two steps may also be sources of significant errors. The contribution of these steps of the analysis to the total error is investigated in Section 8 where multi-story buildings with damping systems are analyzed.

Method 2 of FEMA (1997) requires, for single-degree-of-freedom systems, estimation of the peak displacement, calculation of the effective (secant) stiffness or equivalently the effective period, and the effective damping at the peak displacement, calculation of the peak displacement as the intersection of the capacity and demand curves, and iteration until convergence. Details of the calculation of the effective stiffness and effective damping are presented in Section 4.3 for

structures with damping systems consisting of linear viscous, nonlinear viscous and yielding damping devices. Further details are presented in Section 7 where the calculation of the effective properties is derived for multi-degree-of-freedom systems. Moreover, this section presents methodologies for improved prediction of the maximum velocity and presents the derivation of revised load combination factors (factors CF_1 and CF_2 in FEMA 1997) for calculating the maximum acceleration in viscously damped structures. The revised load combination factors account for inelastic action in the structural system and nonlinear viscous behavior.

Among the studies of evaluation of simplified methods of analysis the one of Chopra and Goel (1999) presented a bleak view of these simplified methods of analysis despite evidence to the contrary presented in the earlier study of Tsopelas et al. (1997). Herein the approach of Tsopelas et al. (1997) is utilized to extend the evaluation study to nonlinear viscous and hysteretic damping systems, and to assess the accuracy of improved methodologies for predicting peak velocities and peak accelerations. The results of this study are extensively presented in Gomez (2000), whereas herein only results in condensed form are presented.

4.2 Non-Linear Time History Analysis

4.2.1 General Description

Non-linear time history analysis of single-degree-of-freedom inelastic systems with damping devices were performed by numerically integrating the equation of motion:

$$m\ddot{u}(t) + F_D(t) + \frac{4\pi\beta_i m\dot{u}(t)}{T_{eff}} + F_F(t) = -ma_g(t) \quad (4-1)$$

where m is the mass, \dot{u} is the relative velocity, \ddot{u} is the relative acceleration, a_g is the ground acceleration, T_{eff} is the effective (or secant) period, β_i is the inherent damping ratio, F_D is the force from damping devices, and F_F is the force from inelastic structural system.

Equation (4-1) is basically identical to the one utilized by Tsopelas et al.(1997) except that the forms of the damping force F_D and structural system force F_F are different. Key to this equation is the description of inherent damping, which is described as linear viscous with

damping ratio equal to β_i . This ratio is defined with respect to the effective (or secant) stiffness K_{eff} of the structure (equal to the peak restoring force divided by the peak displacement). The effective (or secant) period in (4-1) is given by:

$$T_{eff} = 2\pi \sqrt{\frac{m}{K_{eff}}} \quad (4-2)$$

All analyses were performed with β_i equal to 0.05. Equation (4-1) was numerically integrated using an adaptive predictor-corrector integration scheme and a linear interpolation scheme for the ground acceleration input (Tsopelas et al., 1997).

4.2.2 Description of Structural System Behavior

Two types of structural system behavior were considered. The first was smooth perfect bilinear hysteretic behavior (without deterioration of any kind or P- Δ effects) as depicted in Figure 4-1 and described by (Tsopelas et al., 1997) using:

$$F_F = \alpha \frac{F_y}{D_y} u + (1 - \alpha) F_y Z_F \quad (4-3)$$

$$D_y \dot{Z}_F + 0.5 |\dot{u}| |Z_F| |Z_F|^{\eta-1} + 0.5 \dot{u} |Z_F|^\eta - \dot{u} = 0 \quad (4-4)$$

where $|\cdot|$ stands for the absolute value, Z_F is a dimensionless variable and η is a dimensionless parameter. In this study, η was set equal to 5.0.

The perfect bilinear hysteretic system represents the best possible behavior of a yielding system. The opposite to this (but still without deterioration of either strength or stiffness) is a system that lacks the ability to dissipate energy. Such a system was analyzed by modeling it as a bilinear elastic system having the force-displacement relation depicted in Figure 4-1. This relation is mathematically described by

$$F_F = \begin{cases} K_1 u, & |u| < D_1 \\ \frac{(K_2 - K_1)(u - D_1)^2}{2(D_2 - D_1)} \text{sgn}(u) + K_1 u, & D_1 \leq |u| \leq D_2 \\ \frac{(K_1 - K_2)(D_1 + D_2)}{2} \text{sgn}(u) + K_2 u, & |u| \geq D_2 \end{cases} \quad (4-5)$$

Note that this mathematical relation is smooth with transition points (from linear to nonlinear behavior) at displacements D_1 and D_2 , which were selected to be at $0.7D_y$ and $1.3D_y$, respectively. The smoothness of the force-displacement relation, as expressed by the fact that the derivative of F_F with respect to u is continuous, facilitates numerical integration.

4.2.3 Description of Viscous Damping System

Viscous damping systems were modeled as having either linear or non-linear behavior. That is, for linear viscous behavior

$$F_D = C\dot{u} \quad (4-6)$$

and

$$F_D = C_N |\dot{u}|^a \text{sgn}(\dot{u}) \quad (4-7)$$

for non-linear viscous behavior. In (4-6) and (4-7) C and C_N are coefficients, \dot{u} is the relative velocity and a is the damping exponent which was set equal to 0.5 in this study.

4.2.4 Description of Yielding Damping System

Yielding damping systems were modeled with smooth elasto-plastic behavior described by

$$F_D = F_d Z_D \quad (4-8)$$

$$D_{yd} \dot{Z}_D + 0.5 |\dot{u}| Z_D |Z_D|^{\eta-1} + 0.5 \dot{u} |Z_D|^\eta - \dot{u} = 0 \quad (4-9)$$

where Z_D is a dimensionless variable, η is equal to 5, and F_d and D_{yd} are the yield force and yield displacement of the damping system, respectively.

4.2.5 Ground Motions used in the Time History Analysis

The 20 scaled horizontal components of the ten earthquakes listed in Table 3-2 were used in this study. The selection and scaling of these motions is presented in Tsopelas et al. (1997).

4.3 Analyzed Systems

The formulations of the systems analyzed in this report were described in Section 4.2. Figure 4-2 illustrates the force-displacement relations of the analyzed systems and identifies the parameters in the description of these systems. Each of these systems is characterized by the force-displacement relation of the structural frame exclusive of the damping devices (shown on the left column of Figure 4-2). Note that A_y represents the acceleration at yield of the single-degree-of-freedom system. It is convenient to describe the behavior of the structural frame in terms of the following parameters:

- (a) Elastic period, T_e :

$$T_e = 2\pi \left(\frac{D_y}{A_y} \right)^{1/2} \quad (4-10)$$

- (b) Post-yielding to elastic stiffness ratio: α

- (c) Ductility-based portion of the R -factor

$$R_\mu = \frac{S_{ae}}{A_y} \quad (4-11)$$

where S_{ae} is the spectral acceleration at period T_e and damping ratio of 5% (elastic conditions).

Each system analyzed in this study had inherent viscous damping of 5-percent as described in Section 4.2.1.

4.3.1 Bilinear Hysteretic System with Linear Viscous Damping Devices

The bilinear hysteretic system with linear viscous damping devices was originally analyzed by Tsopelas et al. (1997). Additional analyses were performed in this study for a wider range of values of period T_e and for calculating velocities which were omitted in the earlier study. This system is described by the parameters presented in Section 4.3 and the added viscous damping ratio, β_v , under elastic conditions:

$$\beta_v = \frac{CT_e}{4\pi m} \quad (4-12)$$

The parameters used in the analysis of this system are presented in Table 4-1.

4.3.2 Bilinear Hysteretic System with Nonlinear Viscous Damping Devices

The bilinear hysteretic system with nonlinear viscous damping devices is characterized by the parameters presented in Section 4.3 and two additional parameters describing the nonlinear viscous damping devices: exponent a and coefficient C_N (see Section 4.2.3 and equation 4-7). It is inconvenient to use parameter C_N and a dimensionless parameter with a physical significance similar to that of the damping ratio for linear viscous damping systems (eq. 4-12) was used instead. This parameter is defined as the effective damping ratio under elastic conditions

$$\beta_v = \frac{C_N \lambda}{2\pi m} D^{a-1} \left(\frac{2\pi}{T_e} \right)^{a-2} \quad (4-13)$$

$$\lambda = 4 \cdot 2^a \frac{\Gamma^2(1+a/2)}{\Gamma(2+a)} \quad (4-14)$$

where D is the maximum displacement (drift) and Γ is the gamma function. Equation (4-13) is based on the effective damping ratio being

$$\beta = \frac{W_D}{4\pi W_s} \quad (4-15)$$

where W_D is the energy dissipated per cycle at period T_e and displacement D , and W_s is the strain energy at amplitude D . An expression for W_D has been derived in Constantinou et al. (1998) and utilized in FEMA (1997):

$$W_D = \lambda C_N D^{1+a} \left(\frac{2\pi}{T_e} \right)^a \quad (4-16)$$

Values of parameter λ are presented in Table 4-2. It may be seen that for linear viscous devices for which a equals 1.0, λ equals 3.142 ($=\pi$) and (4-13) reduces to (4-12).

The effective damping in (4-13) depends on the amplitude of displacement D as a result of the nonlinear behavior of the viscous devices. In general, iteration is needed to obtain the value of the effective damping given the properties of the structural frame and damping devices, and the characteristics of the excitation. However, herein the value of β_v is selected (say 0.15) and used for the calculation of the corresponding value of C_N . Given the period T_e and total damping under elastic conditions ($\beta_v + \beta_i$), displacement D is calculated and then used in (4-13) and (4-14) to calculate C_N for the application of the simplified method of analysis and the time history analysis. The values of the parameters used for the studies described in this report are presented in Table 4-1.

4.3.3 Bilinear Elastic System with Linear Viscous Damping Devices

The bilinear elastic system with linear viscous damping devices is characterized by the elastic period T_e (eq. 4-10), the ductility-based R -factor R_μ (eq. 4-11), the viscous damping ratio β_v (eq. 4-12), the stiffness ratio α ($=0.05$) and the inherent damping ratio β_i ($=0.05$). The values of the parameters used for the studies described in this report are presented in Table 4-3.

4.3.4 Bilinear Hysteretic System with Yielding Damping Devices

The bilinear hysteretic system with yielding damping devices is characterized by the elastic period, T_e , in the absence of the yielding damping devices (eq. 4-10), the ductility-based portion

of the R -factor R_μ (eq. 4-11), the stiffness ratio α ($=0.05$), the inherent damping ratio β_i ($=0.05$) and the following two additional parameters:

- (1) Ratio of the elastic stiffness of the structure inclusive of the damping devices to the elastic stiffness of the structure exclusive of the damping devices (see Fig. 4-3)

$$\frac{K_t}{K_f} = \frac{\frac{F_d}{D_{yd}} + \frac{F_y}{D_y}}{\frac{F_y}{D_y}} = 1 + \frac{F_d D_y}{F_y D_{yd}} \quad (4-17)$$

where F_y and D_y are the yield strength and yield displacement of the structural frame exclusive of the damping system, respectively, K_f is the elastic stiffness of the structural frame exclusive of the damping system ($= F_y/D_y$), F_d and D_{yd} are the yield strength and yield displacement of the damping system, respectively, and K_t is the elastic stiffness of the frame inclusive of the damping system.

- (2) Ratio of the strength of the damping devices F_d to the strength of the structural frame F_y , F_d / F_y .

The values of the parameters used in this study are presented in Table 4-4.

4.4 Application of Simplified Method of Analysis for Bilinear Hysteretic System with Linear Viscous Damping Devices

Given values of the parameters T_e , R_μ , α , β_i , and β_v (see Section 4.3 and Table 4-1) and the response spectrum, the behavior of the system is completely defined. In the simplified method of analysis, the peak displacement D is assumed (and presumed larger than D_y) and the effective period, T_{eff} , and effective damping, β_{eff} , are calculated:

$$T_{eff} = 2\pi \left(\frac{D}{A} \right)^{1/2} \quad (4-18)$$

$$\beta_{eff} = \beta_i + \beta_v \frac{T_{eff}}{T_e} + \frac{2q_H(A_y D - AD_y)}{\pi AD} \quad (4-19)$$

where

$$D_y = \frac{S_{ae} T_e^2}{4\pi^2 R_\mu} \quad (4-20)$$

Note that (4-19) is based on (4-15) and includes the inherent damping, the component due to inelastic action (presumed perfectly hysteretic) and the viscous component. Moreover quantity A is defined in Figure 4-2 and represents the acceleration at maximum displacement:

$$A = A_y + \alpha \frac{A_y}{D_y} (D - D_y) \quad (4-21)$$

It should be noted that the component of the effective damping in (4-19) due to yielding of the structural frame includes the hysteretic loop adjustment factor q_H which is utilized to reduce the area under the perfect bilinear hysteretic loop to better represent the behavior of the real structural systems. However, the systems studied in this report have perfect bilinear hysteresis behavior a value of q_H equal to 1.0 has been used.

4.5 Application of Simplified Method of Analysis for Bilinear Hysteretic System with Nonlinear Viscous Damping Devices

The behavior of this system is defined by parameters T_e , R_μ , α , β_i , β_v and a (see Section 4.3 and Table 4-1) and the response spectrum. The peak displacement D is assumed and the effective period is calculated using (4-18), (4-20) and (4-21). The effective damping is calculated using (4-15):

$$\beta_{eff} = \beta_i + \beta_v \left(\frac{T_{eff}}{T_e} \right)^{2-a} + \frac{2q_H(A_y D - AD_y)}{\pi AD} \quad (4-22)$$

Note that for a equal to 1.0 (linear viscous damping devices), (4-22) reduces to (4-19).

4.6 Application of Simplified Method of Analysis for Bilinear Elastic System with Linear Viscous Damping Devices

This system exhibits all the characteristics of the bilinear hysteretic system with linear viscous damping devices except for the damping contribution due to inelastic action in the structure. Accordingly, (4-18), (4-20) and (4-21) hold but the effective damping is given by

$$\beta_{eff} = \beta_i + \beta_v \frac{T_{eff}}{T_e} \quad (4-23)$$

4.7 Application of Simplified Method of Analysis for Bilinear Hysteretic System with Yielding Damping Devices

The behavior of this system is described by parameters T_e , R_μ , α , β_i , K_t / K_f and F_d / F_y (see Section 4.3 and Table 4-4). The yield displacement of the structural frame, D_y , is determined from (4-20) and the yield displacement of the yielding damping devices (see Figure 4-2) is determined from:

$$D_{yd} = \frac{D_y}{\left(\frac{K_t}{K_f} - 1 \right)} \frac{F_d}{F_y} \quad (4-24)$$

It is assumed hereafter that $F_d \leq F_y$ and that $D_{yd} \leq D_y$ which are both reasonable assumptions for the implementation of yielding damping systems in flexible building frames. The combined structural frame and yielding damping device lateral force-displacement relation is tri-linear as depicted in Figure 4-3. Consider now that the peak displacement D is larger than D_y , as shown in Figure 4-3. The effective period is then given by

$$T_{eff} = 2\pi \left(\frac{D}{A + A_d} \right)^{1/2} \quad (4-25)$$

where A is given by (4-21). The effective damping is given by

$$\beta_{eff} = \beta_i \left(\frac{A}{A + A_d} \right)^{1/2} + \frac{2q_H (A_y D - A D_y) + 2A_d (D - D_{yd})}{\pi (A + A_d) D} \quad (4-26)$$

Note that in this formulation, the inherent damping of the combined system is reduced due to the increase in stiffness under elastic conditions. It is presumed in this case that the damping system does not dissipate any energy for displacements less than D_{yd} so that T_{eff} in (4-1) is calculated on the basis of the assumption that $A_d=0$. It is also presumed that the yielding damping system has perfect bilinear hysteretic behavior.

4.8 Calculation of Maximum Velocity and Acceleration in Systems with Viscous Damping Devices

The simplified analysis method described in Sections 4.4 to 4.7 is iterative since it is based on an assumed value of displacement D , calculation of the effective period and effective damping, calculation of the displacement using the response spectrum after modification for increased damping, and comparison of the calculated and assumed values of displacement. A limit on the calculated displacement, not being less than the displacement calculated for elastic conditions, is then enforced. The results of this analysis are values of the maximum displacement D and the acceleration A (or $A + A_d$) at maximum displacement. In addition, for systems with viscous damping devices the maximum velocity is needed for the calculation of the peak damping force. Moreover, the maximum acceleration, which is larger than A and occurs at some displacement less than D , must be calculated.

The maximum velocity is taken in this method as the pseudo-velocity, that is:

$$V = \left(\frac{2\pi}{T_{eff}} \right) D \quad (4-27)$$

The maximum acceleration can be determined by the procedure described by Tsopelas et al. (1997) and incorporated in FEMA (1997). A more general procedure for nonlinear viscous damping devices and yielding structures is presented below.

The procedure for a linear elastic structure with a nonlinear viscous damping device is described first. It is assumed that the structure of stiffness K and mass m undergoes harmonic vibration at its natural frequency ω_n and amplitude D :

$$u = D \cos \omega_n t \quad (4-28)$$

with velocity

$$\dot{u} = -D \omega_n \sin \omega_n t \quad (4-29)$$

The combined restoring and damping force is given by

$$F = ku + C_N |\dot{u}|^a \text{sgn}(\dot{u}) \quad (4-30)$$

Equation (4-30) may be written in the form

$$\frac{F}{m \omega_n^2 D} = -\frac{2\pi}{\lambda} \beta_V \sin^a \omega_n t + \cos \omega_n t \quad (4-31)$$

in which λ is given by (4-14), β_V is given by (4-13), and

$$\omega_n = \left(\frac{k}{m} \right)^{1/2} = \frac{2\pi}{T_e} \quad (4-32)$$

Equation (4-31) was derived using (4-28) and (4-29). The velocity is negative during the considered cycle of motion as shown in Figure 4-4.

The maximum value of F (and acceleration) occurs at a time t^* when the derivative of the right hand side of (4-31) with respect to time is zero. This results in the following

$$\frac{\sin^{2-a} \omega_n t^*}{\cos \omega_n t^*} = -\frac{2\pi a \beta_V}{\lambda} \quad (4-33)$$

This equation cannot be exactly solved for time t^* except for the case of linear viscous device ($a=1$). However, an approximate solution can be derived assuming that (see Fig. 4-4)

$$\omega_n t^* = \pi - \delta \quad (4-34)$$

in which δ is a small phase lag as shown in Figure 4-4. This assumption is good when a is small (e.g., $\delta = 0$ when $a = 0$) and the phase lag can be calculated as

$$\delta = \left(\frac{2\pi a \beta_v}{\lambda} \right)^{\frac{1}{2-a}} \quad (4-35)$$

For linear viscous damping devices, the phase lag δ may be calculated exactly as

$$\delta = \tan^{-1}(2\beta_v) \quad (4-36)$$

Note that (4-35) provides a good approximation even in the case of linear viscous damping devices. For such a case, $a=1$ and $\lambda = \pi$ so that (4-35) yields $\delta = 2\beta_v$. By comparison to (4-36), use of (4-35) results in an error of about 3% for $\beta_v = 0.15$ and an error of about 7% for $\beta_v = 0.25$.

The maximum acceleration is determined by substituting (4-34) and (4-35) into (4-31):

$$A_{\max} = A \left(CF_1 + \frac{2\pi\beta_v}{\lambda} CF_2 \right) \quad (4-37)$$

where

$$CF_1 = \cos \delta \quad (4-38)$$

and

$$CF_2 = (\sin \delta)^a \quad (4-39)$$

Parameters CF_1 and CF_2 are load combination factors used to calculate the response at the time of maximum acceleration by combining the effects at the instants of maximum drift and maximum velocity.

Equation (4-38) describes the contribution of the restoring force to the maximum acceleration. It is valid for elastic behavior, that is, for $D < D_y$. As inelastic action occurs, the value of CF_1 increases and eventually obtains the maximum value of unity. This is recognized when considering that the maximum acceleration occurs when $u = \cos \delta \cdot D$ as seen in Figure 4-4. Moreover, the effective viscous damping ratio increases with inelastic action. Accordingly, it can be shown that

$$A_{\max} = A \left(CF_1 + \frac{2\pi\beta_{\text{veff}}}{\lambda} CF_2 \right) \quad (4-40)$$

where

$$\left. \begin{array}{ll} \text{If } D < D_y, & CF_1 = \cos \delta \\ \text{If } D > D_y \quad \text{and } \mu \cdot \cos \delta < 1, & CF_1 = \mu \cdot \cos \delta \\ \text{If } D > D_y \quad \text{and } \mu \cdot \cos \delta \geq 1, & CF_1 = 1.0 \end{array} \right\} \quad (4-41)$$

$$\beta_{\text{veff}} = \beta_i + \beta_v \left(\frac{T_{\text{eff}}}{T_e} \right)^{2-a} \quad (4-42)$$

$$\mu = \frac{D}{D_y} \quad (4-43)$$

and CF_2 is still given by (4-39). Parameter δ is computed from (4-35) with β_v replaced by β_{veff} . Equations (4-39) and (4-41) have been used to calculate the values of the force coefficients that are tabulated in NEHRP (2000).

4.9 Results of Simplified Method of Analysis and Comparison to Results of Nonlinear Time History Analysis

The response of each analyzed system was determined using the simplified method of analysis described in Sections 4.4 to 4.8. The response spectrum with parameters $S_{DS} = 1.0$, $S_{D1} = 0.6$ and $T_s = 0.6$ sec was utilized together with the “conservative” values of the damping coefficient of Table 3-3. The spectra for these parameters and for damping ratio up to 100% are shown in

Figure 2-4. Figures 4-5 to 4-13 present a comparison of the results of time history analysis (average of 20 values) and the results of the simplified method of analysis. The graphs compare the calculated peak displacement, peak velocity and peak acceleration (including the viscous component) by plotting the results of the time history analysis on the vertical axis against the results of the simplified method of analysis on the horizontal axis. Points located below the diagonal “45-degree” line indicate conservatism in the prediction of the simplified method of analysis.

These figures clearly demonstrate that:

- (a) The simplified methods of analysis produce exact or conservative estimates of the peak displacement and peak acceleration.
- (b) The simplified method of analysis underpredicts the peak velocities for structures with a large effective period (say $T_{eff} > 1.5$ sec) but overpredicts the peak velocity for structures with a moderate-to-short effective period (say $T_{eff} < 1.0$ sec). The differences are as large as 50% for large effective period and as much as 100% for short effective period.

The results are consistent with the use of pseudo-velocity as a predictor of the maximum relative velocity (Chopra, 1995; Constantinou et al., 1998). The greatest errors occurred for framing systems with low ratio of post-elastic stiffness to elastic stiffness (α) and large ductility-based portion of the R -factor (R_{μ}). It will be demonstrated later herein that structures with damping systems designed on the basis of NEHRP (2000) typically exhibit nearly elastic behavior for the design basis earthquake. Under such conditions, the error in predicting the relative velocity by using the pseudo-velocity is relatively small and acceptable for design purposes.

4.10 Correction Factors for Velocity

It is worthy of investigating the likelihood that a simple method is developed for obtaining better estimates of the relative velocity. Sadek et al. (1999) and Pekcan et al. (1999) proposed that the relative velocity is determined as the product of pseudo-velocity and a correction factor. The correction factor was determined in these studies as the ratio of the exact relative velocity of single-degree-of-freedom to the pseudo-velocity, which was calculated as the exact displacement

times the natural frequency of the system. The two studies primarily differed in the selection of the earthquake records used with (a) Sadek et al. utilizing 72 horizontal components of Californian earthquakes including some with near-fault characteristics, and (b) Pekcan et al. utilizing 36 horizontal components of Californian, Japanese and other earthquakes, of which most had near-fault characteristics with peak ground velocities in the range of 1 to 1.8 m/s. Moreover, Pekcan et al. (1999) scaled the earthquake motions to have a peak ground velocity of 1 m/sec, which is somehow similar to the scaling employed by Tsopelas et al. (1997) and in our study. This scaling results in a more balanced contribution of the various earthquake components to the average response.

Values of the correction factor from the study of Sadek et al. (1999) are presented in Table 4-5. The study of Pekcan et al. (1999) utilized least square regression analysis to establish equations for the correction factor. The following equation describes the correction factor CFV for period, T , values in the range of $T_s/5$ to 3 sec. and damping ratio, β , values in the range of 5 to 40-percent, where T_s is the period value at the intersection of the constant acceleration and constant velocity regions of the response spectrum:

$$CFV = \left(\frac{T}{T_s} \right)^{0.455\beta + 0.132} \quad (4-44)$$

The availability of a significant number of response-history analysis results for a wide range of parameters for yielding systems in this study facilitated the calculation of improved velocity correction factors. Utilizing results on the exact relative velocity and the pseudo-velocity from the study reported in Section 4.9, revised velocity correction factors were derived and are presented in Table 4-6. Note that these correction factors differ from those of Sadek et al. and Pekcan et al. In the following: (a) the earthquake motions used in either derivation do not contain any with near-fault characteristics, (b) the analyzed systems are nonlinear, (c) the pseudo-velocity is calculated as the product of the peak displacement and the effective frequency, both of which were calculated by approximate means (use of 5-percent damped spectrum, damping coefficient B and the effective period and damping), and (d) the factors extend to values of effective period of 4.0 sec and effective damping of 100-percent.

The utility of the correction factors in Tables 4-5 and 4-6, and of equation (4-44) has been investigated by recalculating the velocity in all cases of the present study as the product of pseudo-velocity and the correction factor and interpreting the period in (4-44) and in Table 4-5 as the effective period and the viscous damping ratio in (4-44) and in Table 4-5 as the effective damping. Results are presented in Figures 4-14 to 4-18 where they are compared to results of the time history analysis. Each of these figures contains four graphs in which the vertical axis represents the average value of the results of nonlinear time history analysis on the velocity and the horizontal axis represents the velocity calculated by simplified methods and without and with the use of correction factors. It is apparent that the correction factors reduce the scatter in the data and produce either very conservative results (factors of Sadek et al., 1999) or results of acceptable accuracy (factors of Pekcan et al., 1999 and revised factors of Table 4-6).

4.11 Conclusions

The simplified method of analysis, as described herein including the correction for velocity prediction of either Pekcan et al. (1999) in (4-44) or the revised ones in Table 4-6, produces estimates of the peak displacement, peak velocity and peak acceleration (including the viscous component) which are either conservative or in good agreement with the average of results of nonlinear time history analysis. The simplified method of analysis is not error-free. However, it is simple to apply, it systematically converges and produces results of sufficient accuracy for design purposes.

It should be noted that the presented results were based on the use of damping coefficients (Table 3-3, “conservative” values), which were derived from analyses using earthquake motions that did not include records on very soft soil and records with near-field characteristics. Therefore, the results may not apply in these cases.

TABLE 4-1 Values of Parameters in Study of Bilinear Hysteretic System with Viscous Damping Devices

Elastic Period T_e (second)	0.3, 0.5, 0.7, 1.0, 1.5, 2.0
Ductility-based Portion of R-factor, R_μ	2, 3.33, 5
Post-Elastic to Elastic Stiffness Ratio, α	0.05, 0.10, 0.25, 0.50, 1.0 (elastic)
Inherent Damping Ratio, β_I	0.05
Added Viscous Damping Ratio Under Elastic Conditions, β_v	Linear Viscous 0, 0.15, 0.25
	Nonlinear Viscous ($a=0.5$) 0.15, 0.25

TABLE 4-2 Values of Parameter λ

<i>Exponent a</i>	<i>Parameter λ</i>
0.00	4.000
0.25	3.723
0.50	3.496
0.75	3.305
1.00	3.142 (= π)
1.25	3.000
1.50	2.876
1.75	2.765
2.00	2.667

**TABLE 4-3 Values of Parameters in Study of Bilinear Elastic System
with Linear Viscous Damping Devices**

Elastic Period T_e (second)	0.3, 0.5, 0.7, 1.0, 1.5, 2.0
Ductility-based Portion of R-factor, R_μ	2, 3.33, 5
Post-Elastic to Elastic Stiffness Ratio, α	0.05
Inherent Damping Ratio, β_i	0.05
Added Viscous Damping Ratio under Elastic Conditions, β_v	0, 0.15, 0.25

**TABLE 4-4 Values of Parameters in Study of Bilinear Hysteretic System
with Yielding Damping Devices**

Elastic Period T_e (second)	0.5, 0.7, 1.0, 1.5, 2.0
Ductility-based Portion of R-factor, R_μ	2, 3.33, 5
Post-Elastic to Elastic Stiffness Ratio, α	0.05
Inherent Damping Ratio, β_i	0.05
Stiffness Ratio K_i/K_f	2, 6, 10
Strength Ratio F_d/F_y	0.1, 0.2, 0.3, 0.4, 0.5

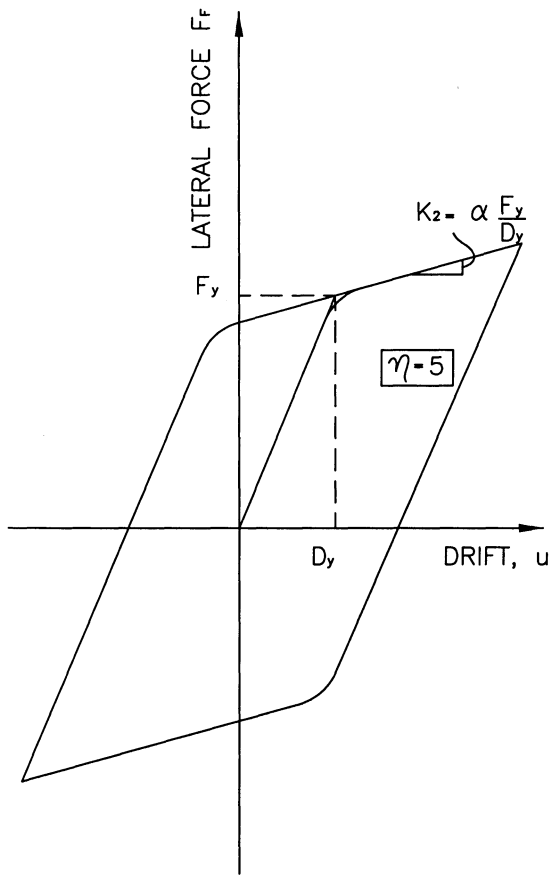
Table 4-5 Correction Factor for Velocity (from Sadek et al., 1999)

Period (sec)	Viscous Damping Ratio								
	0.02	0.05	0.10	0.15	0.20	0.30	0.40	0.50	0.60
0.1	0.70	0.63	0.57	0.53	0.51	0.47	0.45	0.43	0.41
0.3	0.96	0.94	0.91	0.88	0.86	0.82	0.79	0.78	0.77
0.5	0.99	0.99	0.99	0.99	0.99	1.00	1.00	1.00	1.00
1.0	1.06	1.08	1.11	1.13	1.15	1.22	1.28	1.32	1.36
1.5	1.13	1.20	1.27	1.31	1.36	1.46	1.54	1.61	1.65
2.0	1.20	1.28	1.39	1.47	1.53	1.63	1.73	1.82	1.90
2.5	1.23	1.33	1.47	1.55	1.64	1.78	1.89	1.99	2.09
3.0	1.39	1.47	1.56	1.64	1.72	1.88	2.02	2.10	2.26
3.5	1.51	1.60	1.70	1.79	1.87	2.01	2.16	2.29	2.42
4.0	1.61	1.74	1.88	2.00	2.09	2.23	2.36	2.50	2.62

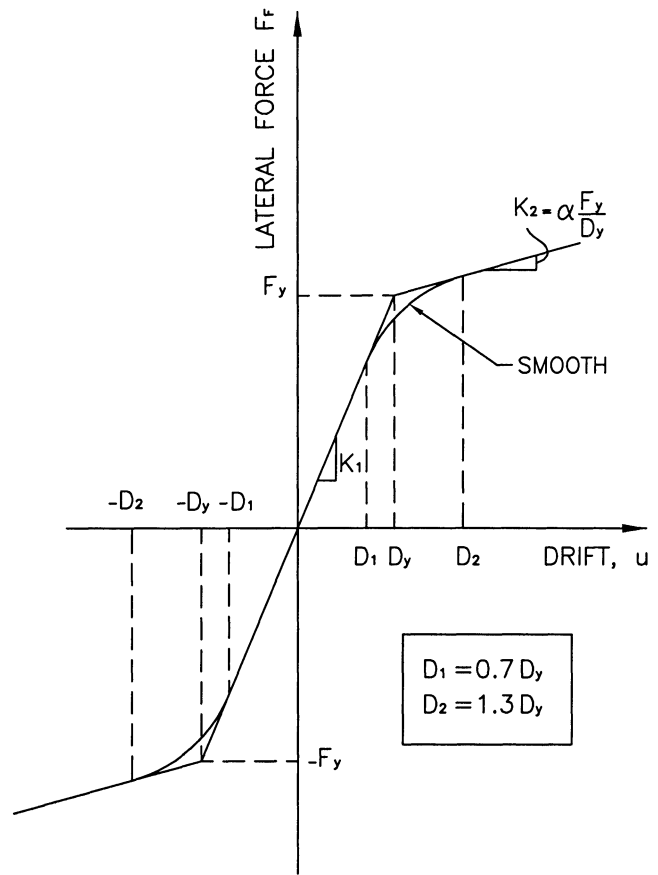
Period is interpreted as the effective period and viscous damping ratio is interpreted as the effective damping

TABLE 4-6 Revised Correction Factors

Effective Period (sec)	Effective Damping Ratio									
	0.10	0.20	0.30	0.40	0.50	0.60	0.70	0.80	0.90	1.00
0.3	0.72	0.70	0.69	0.67	0.63	0.60	0.58	0.58	0.54	0.49
0.5	0.75	0.73	0.73	0.70	0.69	0.67	0.65	0.64	0.62	0.61
1.0	0.82	0.83	0.86	0.86	0.88	0.89	0.90	0.92	0.93	0.95
1.5	0.95	0.98	1.00	1.04	1.05	1.09	1.12	1.14	1.17	1.20
2.0	1.08	1.12	1.16	1.19	1.23	1.27	1.30	1.34	1.38	1.41
2.5	1.05	1.11	1.17	1.24	1.30	1.36	1.42	1.48	1.54	1.59
3.0	1.00	1.08	1.17	1.25	1.33	1.42	1.50	1.58	1.67	1.75
3.5	1.09	1.15	1.22	1.30	1.37	1.45	1.52	1.60	1.67	1.75
4.0	0.95	1.05	1.15	1.24	1.38	1.49	1.60	1.70	1.81	1.81



SMOOTH PERFECT BILINEAR
HYSTERETIC SYSTEM



BILINEAR ELASTIC SYSTEM

FIGURE 4-1 Structural System Behavior Considered in this Study

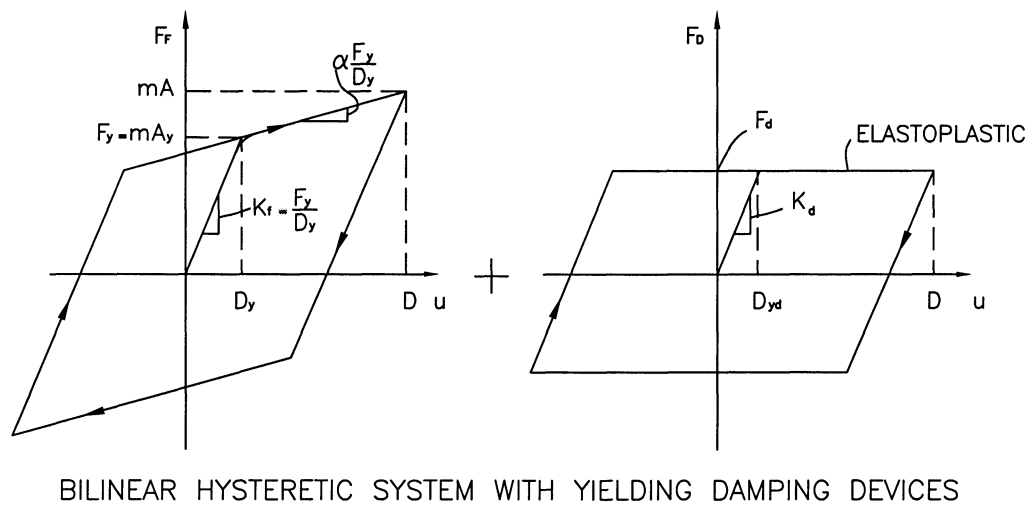
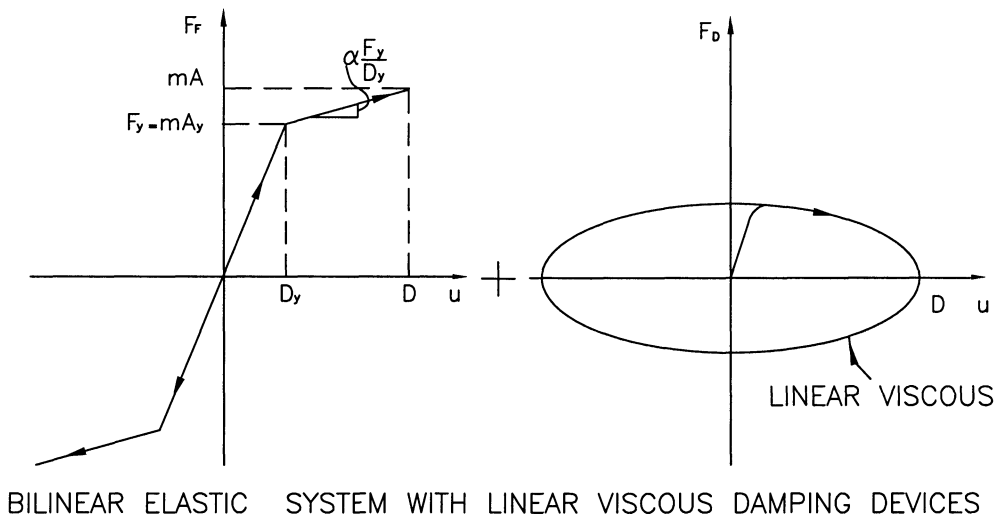
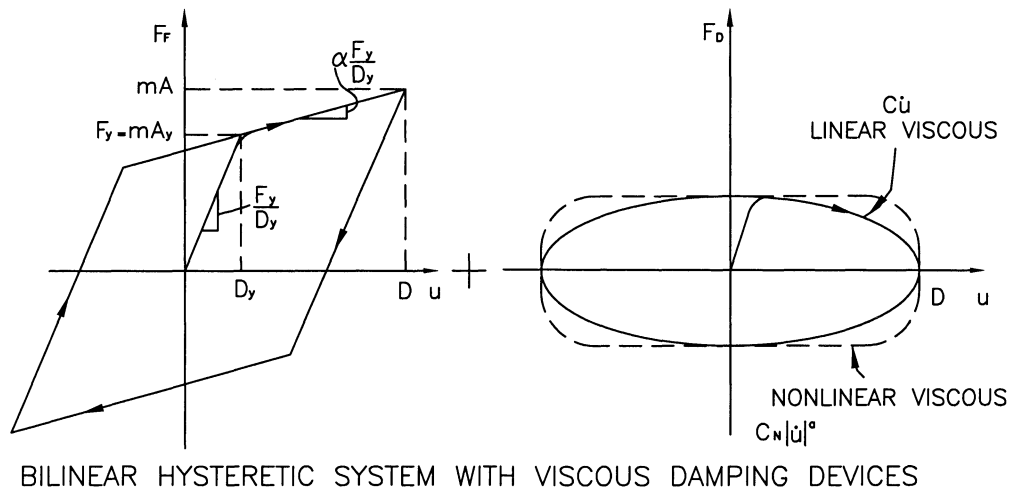
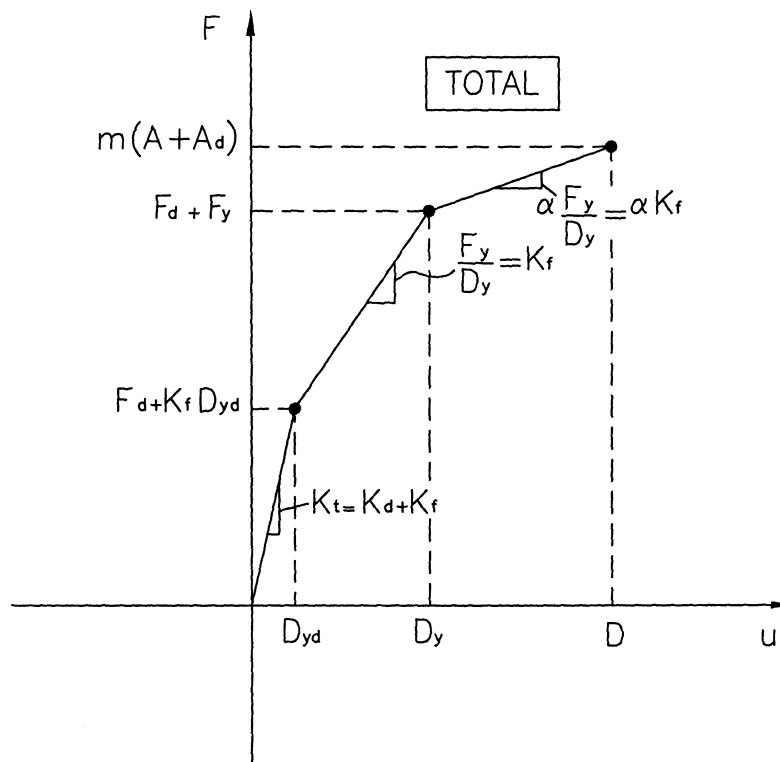
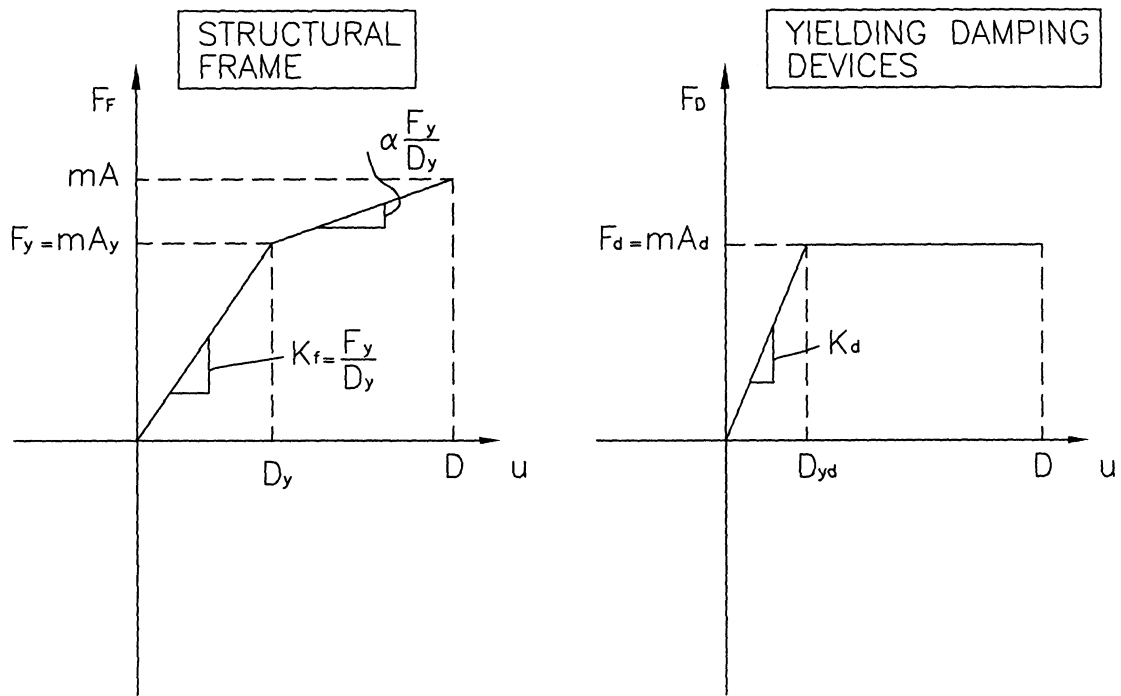


FIGURE 4-2 Illustration of Behavior of Analyzed Systems



VALID FOR $F_d \leq F_y$, $D_{yd} \leq D_y$

FIGURE 4-3 Behavior of Bilinear Hysteretic System with Yielding Damping Devices

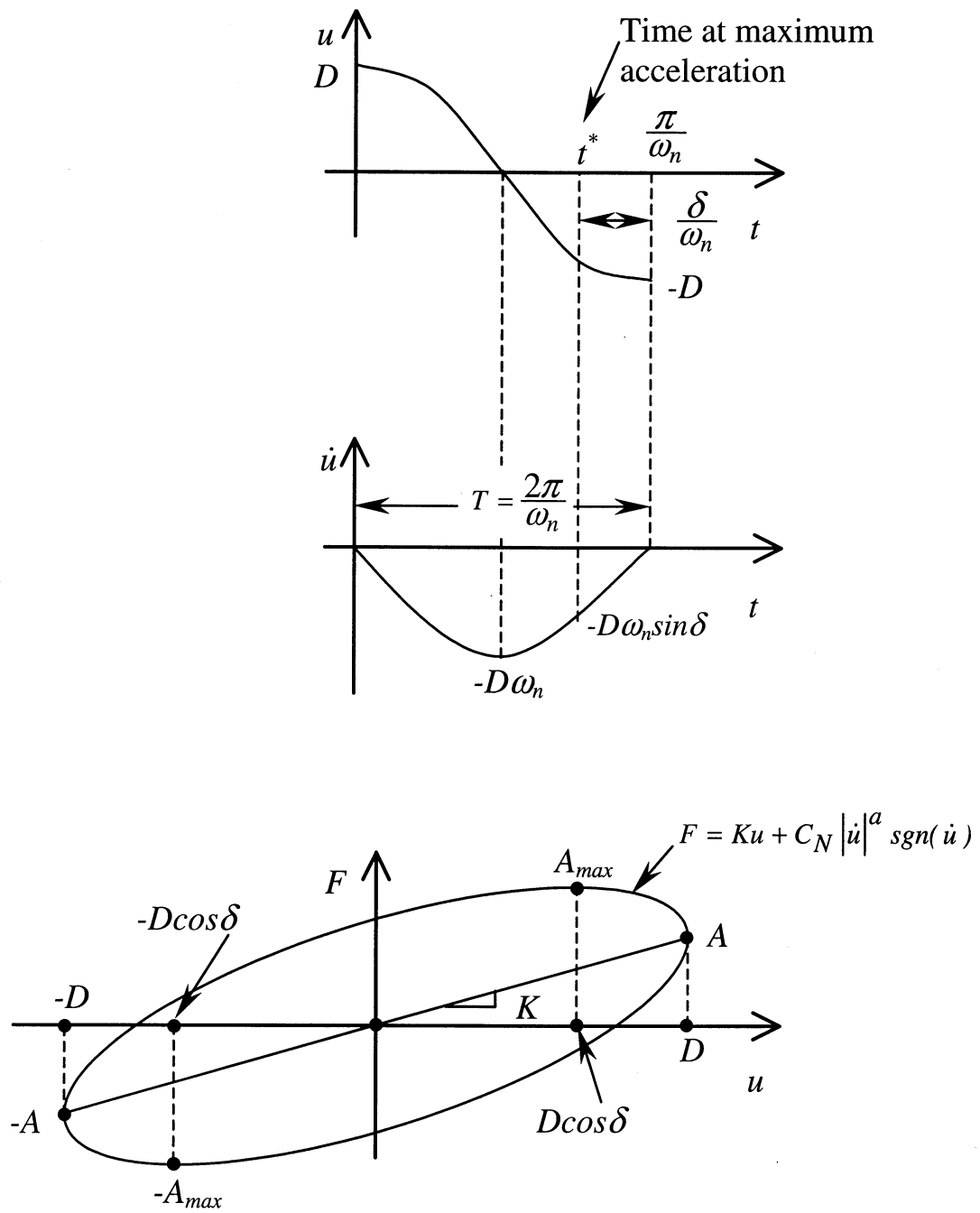


FIGURE 4-4 Harmonic Motion of Structure with Viscous Nonlinear Damping Device and Force-Displacement Relation

Perfect Bilinear Hysteretic System ($\alpha=0.05, 0.15, 0.25, 0.5, 1.0, \beta_i=0.05$)

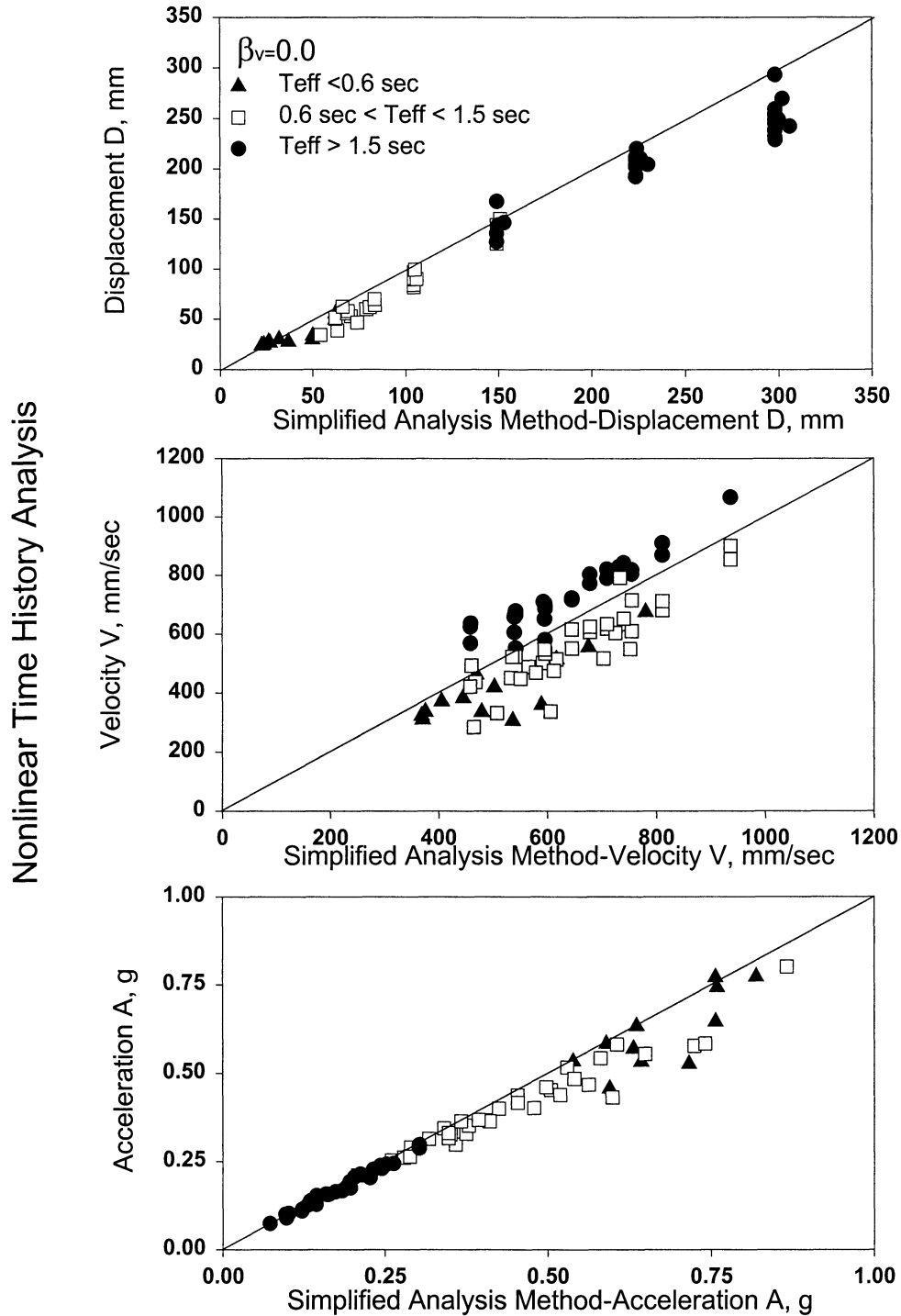


FIGURE 4-5 Comparison of Time History Analysis Results (Average of 20 values) to Results of Simplified Method of Analysis for Bilinear Hysteretic System without Damping Devices

Perfect Bilinear Hysteretic System ($\alpha=0.05, 0.15, 0.25, 0.5, 1.0, \beta_i=0.05$)
 With Linear Viscous Damping Devices

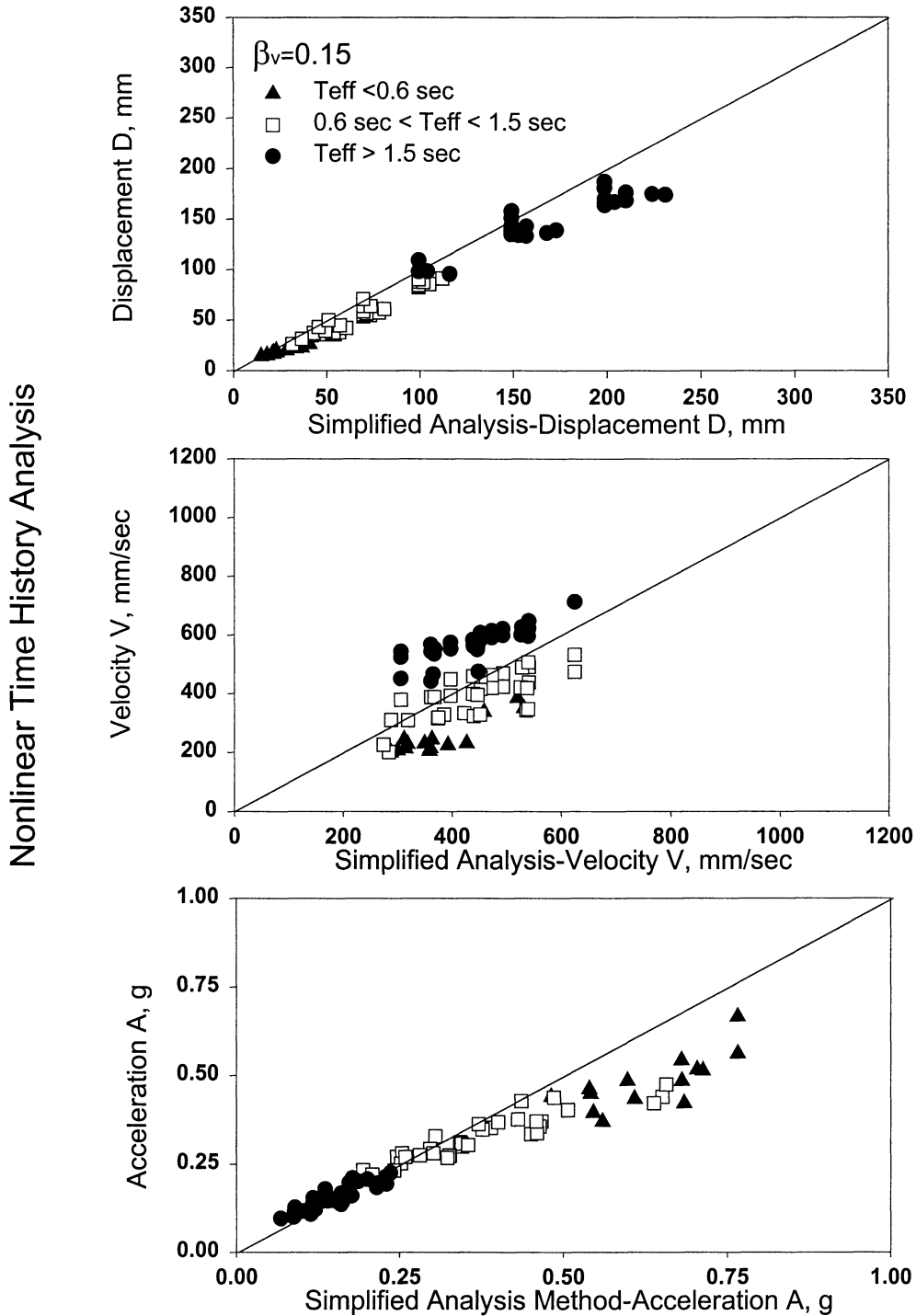


FIGURE 4-6 Comparison of Time History Analysis Results (Average of 20 values) to Results of Simplified Method of Analysis for Bilinear Hysteretic System with Linear Viscous Damping Devices, $\beta_v = 0.15$

Perfect Bilinear Hysteretic System ($\alpha=0.05, 0.15, 0.25, 0.5, 1.0, \beta_i=0.05$)
 With Linear Viscous Damping Devices

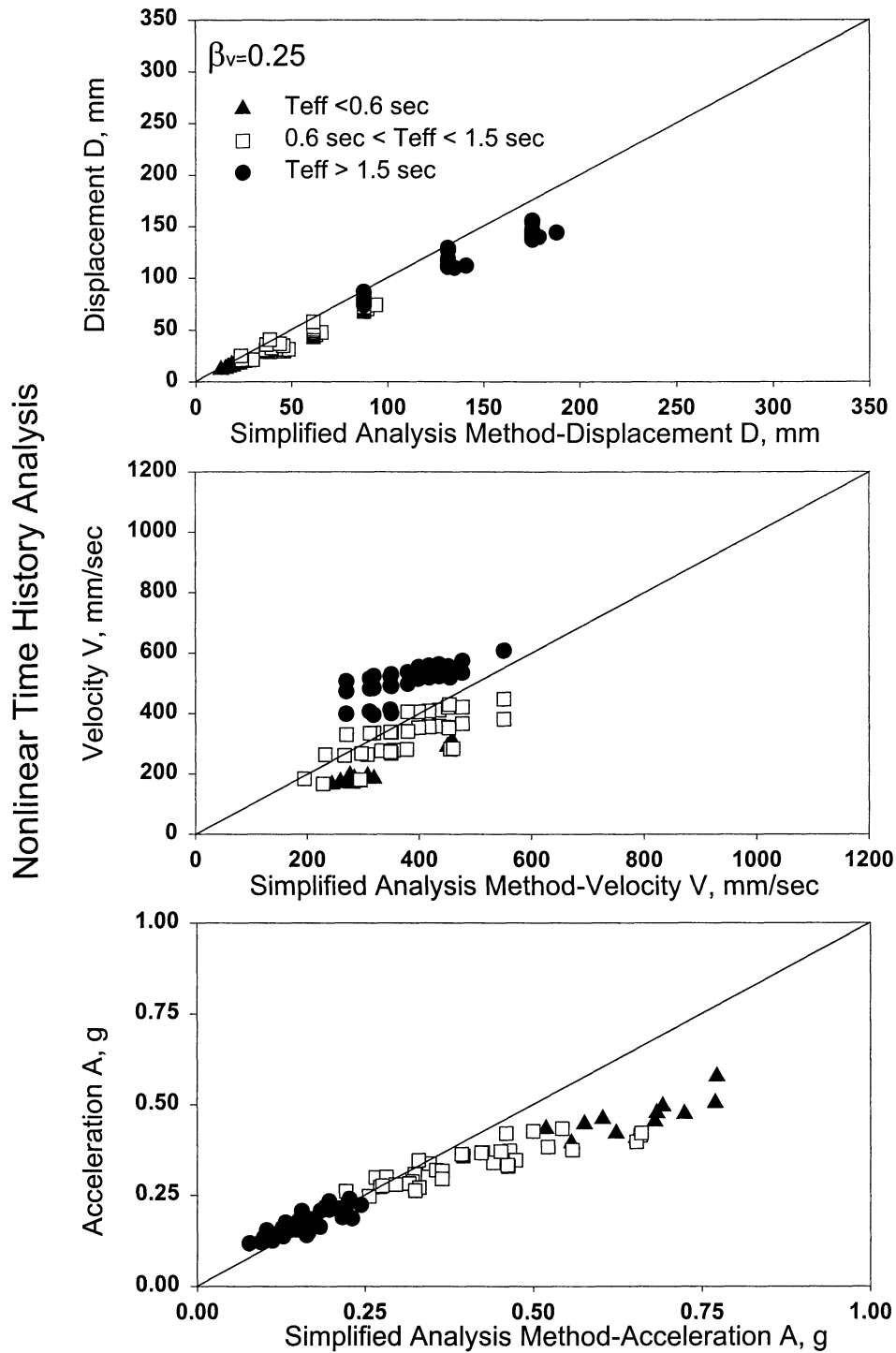


FIGURE 4-7 Comparison of Time History Analysis Results (Average of 20 values) to Results of Simplified Method of Analysis for Bilinear Hysteretic System with Linear Viscous Damping Devices, $\beta_v = 0.25$

Perfect Bilinear Hysteretic System ($\alpha=0.05, 0.15, 0.25, 1.0, \beta_i=0.05$)
 With Non-Linear Viscous Damping Devices ($a=0.5$)

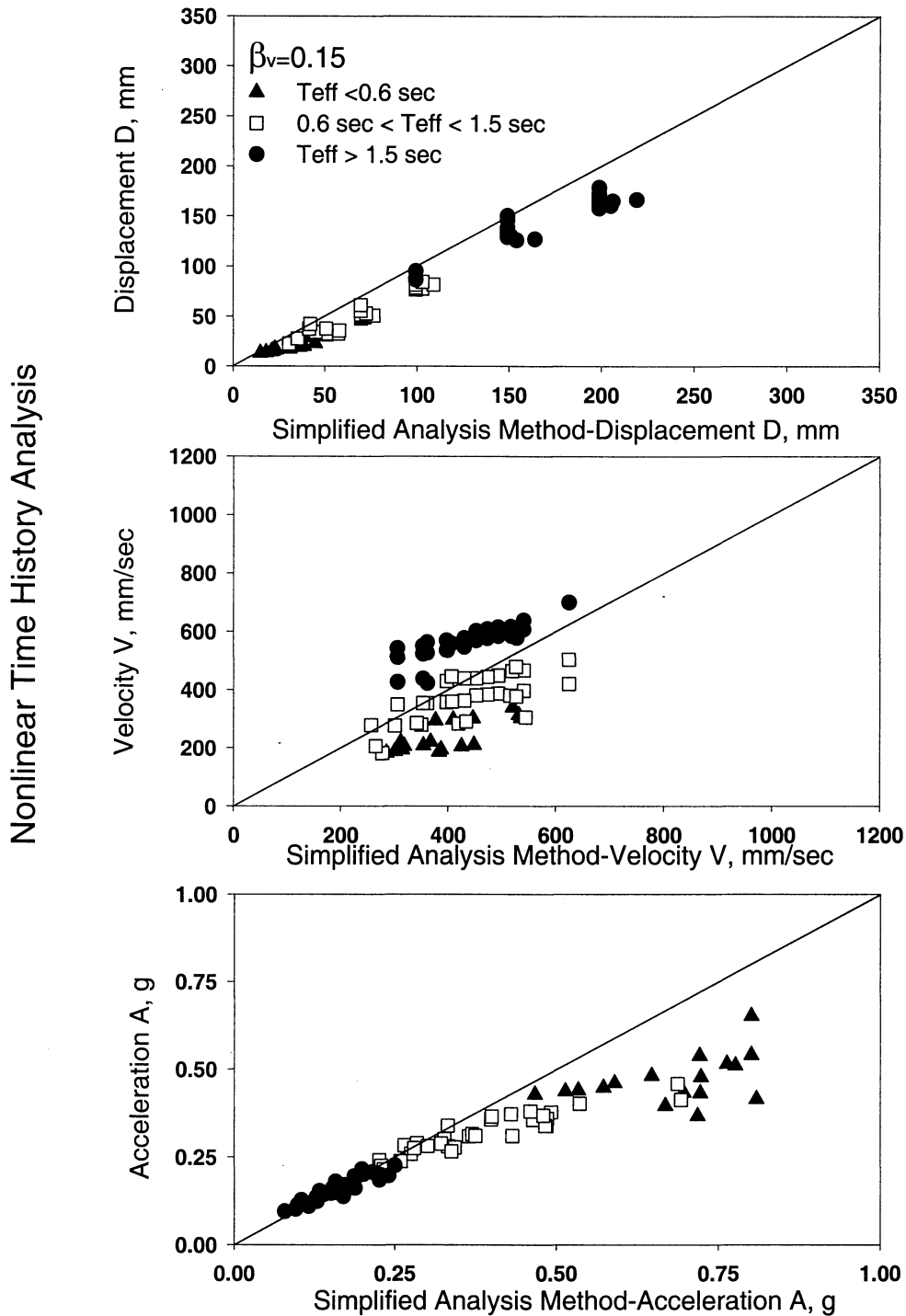


FIGURE 4-8 Comparison of Time History Analysis Results (Average of 20 values) to Results of Simplified Method of Analysis for Bilinear Hysteretic System with Non-Linear Viscous Damping Devices, $\beta_v = 0.15$

Perfect Bilinear Hysteretic System With ($\alpha=0.05, 0.15, 0.25, 1.0, \beta_i=0.05$)
 Non-Linear Viscous Damping Devices ($a=0.5$)

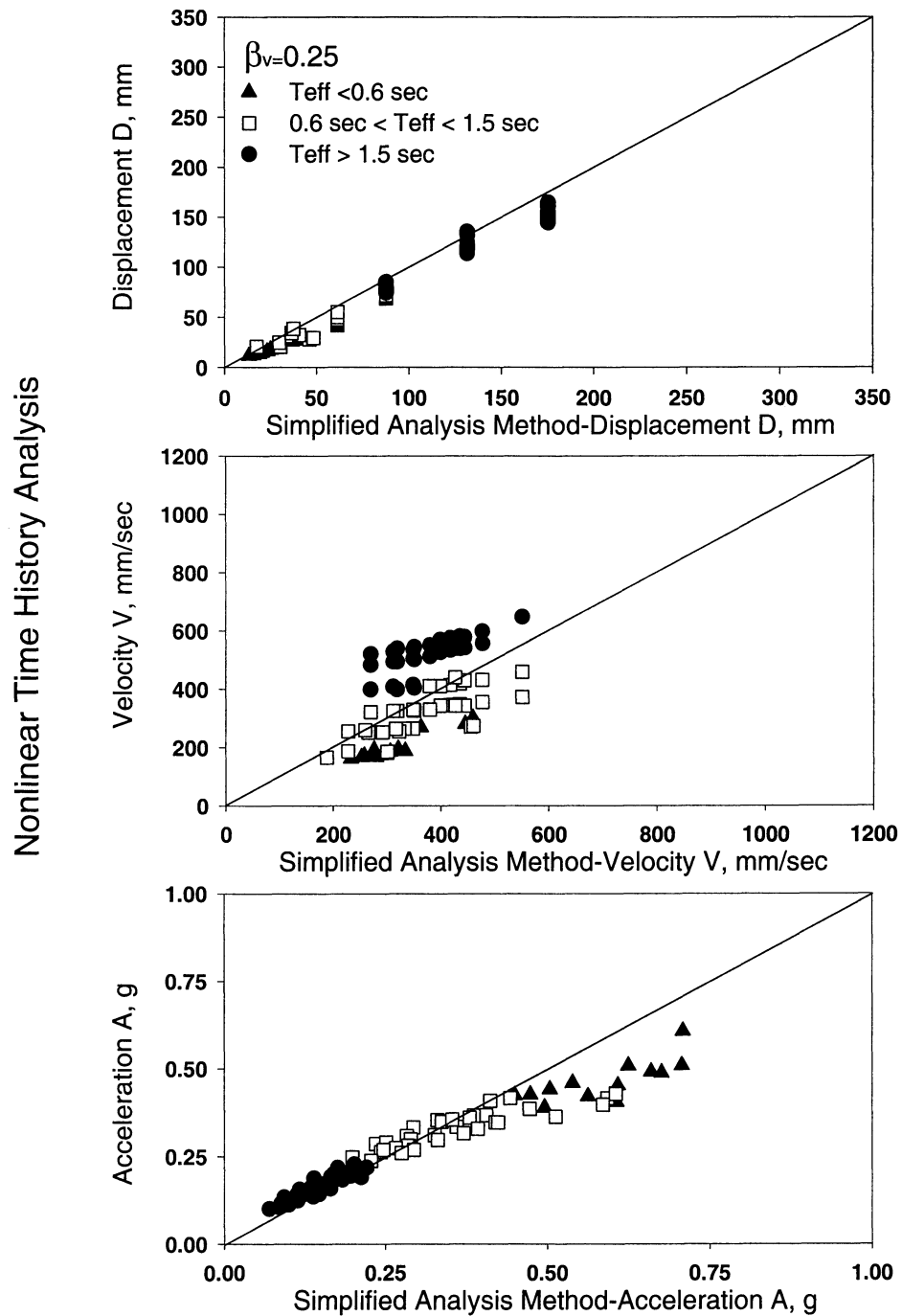


FIGURE 4-9 Comparison of Time History Analysis Results (Average of 20 values) to Results of Simplified Method of Analysis for Bilinear Hysteretic System with Non-Linear Viscous Damping Devices, $\beta_v = 0.25$

Bilinear Elastic System ($\alpha=0.05$, $\beta_i=0.05$)
Without Damping Devices

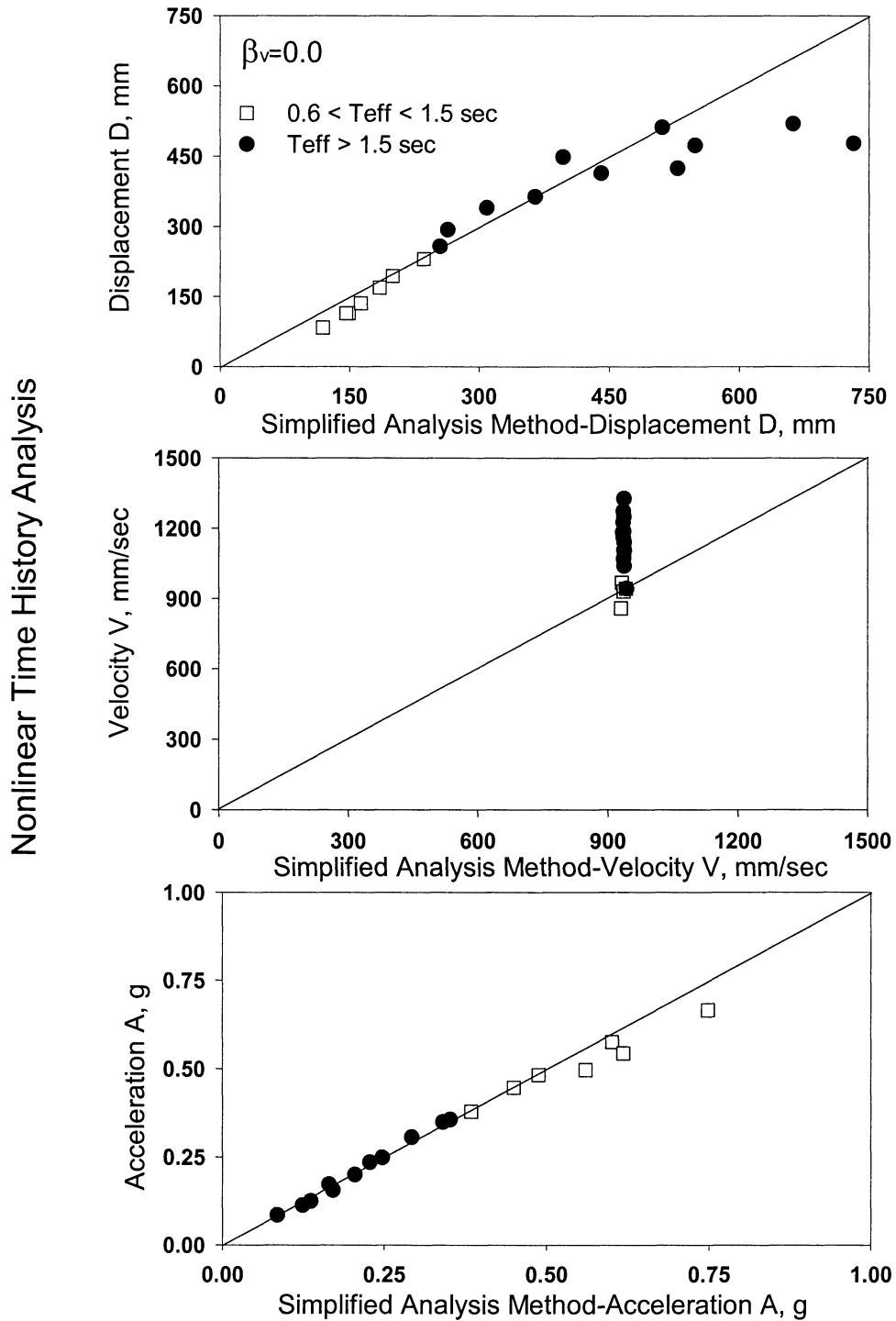


FIGURE 4-10 Comparison of Time History Analysis Results (Average of 20 values) to Results of Simplified Method of Analysis for Bilinear Elastic System without Damping Devices

Bilinear Elastic System ($\alpha=0.05, \beta_i=0.05$)
 With Linear Viscous Damping Devices

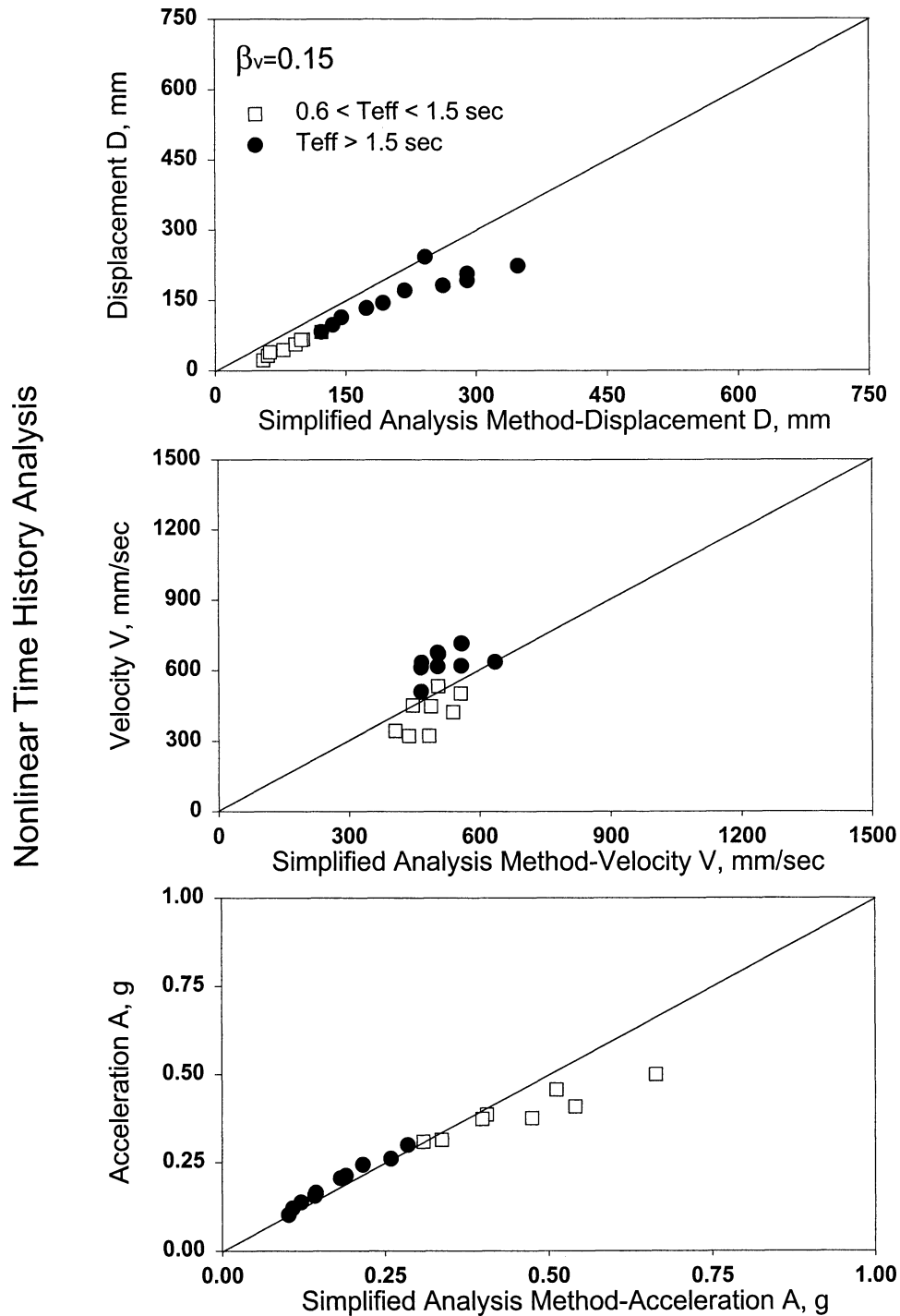


FIGURE 4-11 Comparison of Time History Analysis Results (Average of 20 values) to Results of Simplified Method of Analysis for Bilinear Elastic System with Linear Viscous Damping Devices, $\beta_v = 0.15$

Bilinear Elastic System ($\alpha=0.05$, $\beta_i=0.05$)
 With Linear Viscous Damping Devices

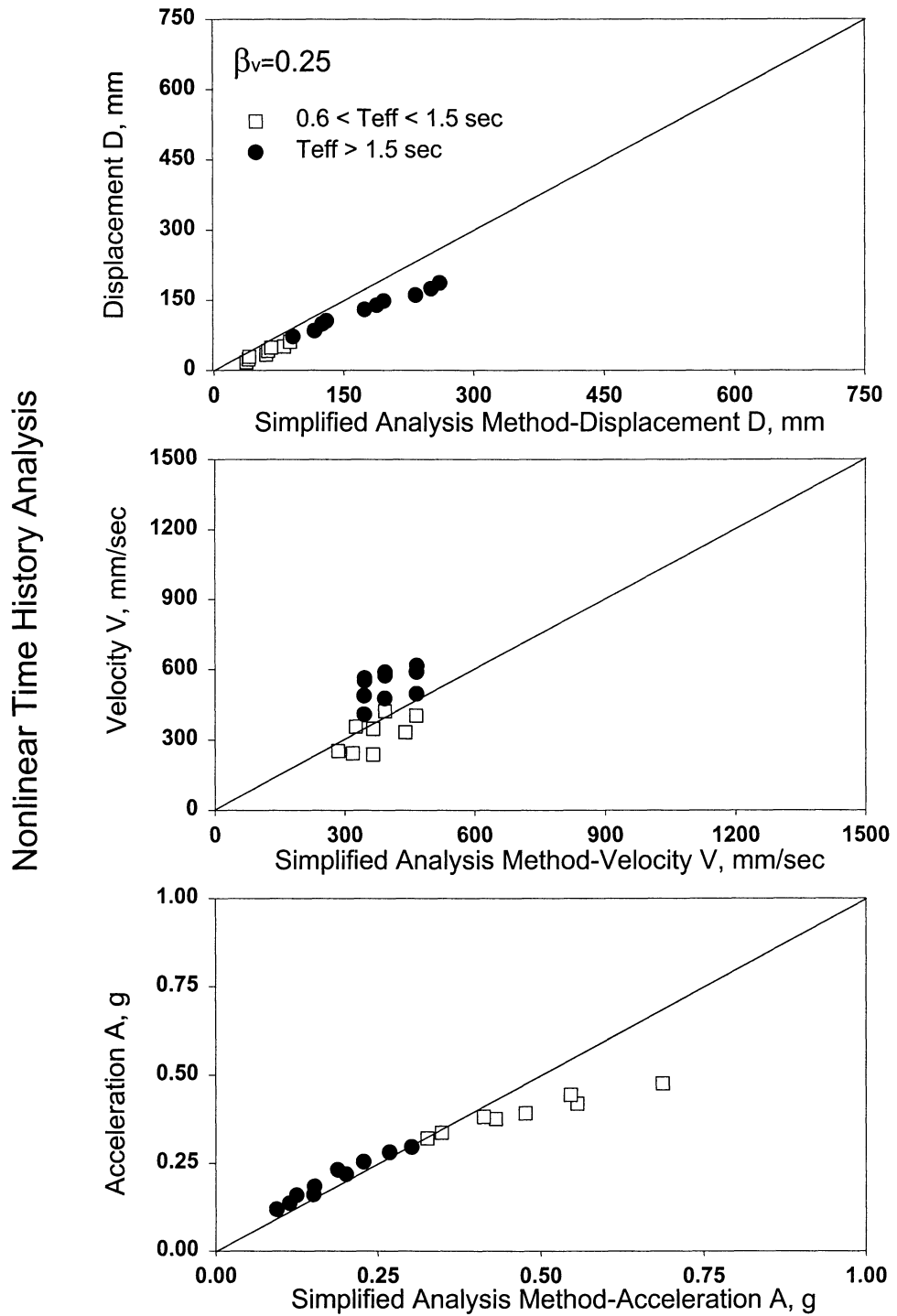


FIGURE 4-12 Comparison of Time History Analysis Results (Average of 20 values) to Results of Simplified Method of Analysis for Bilinear Elastic System with Linear Viscous Damping Devices, $\beta_v = 0.25$

Bilinear Hysteretic System ($\alpha=0.05, \beta_i=0.05$)
With Yielding Damping Devices

Nonlinear Time History Analysis

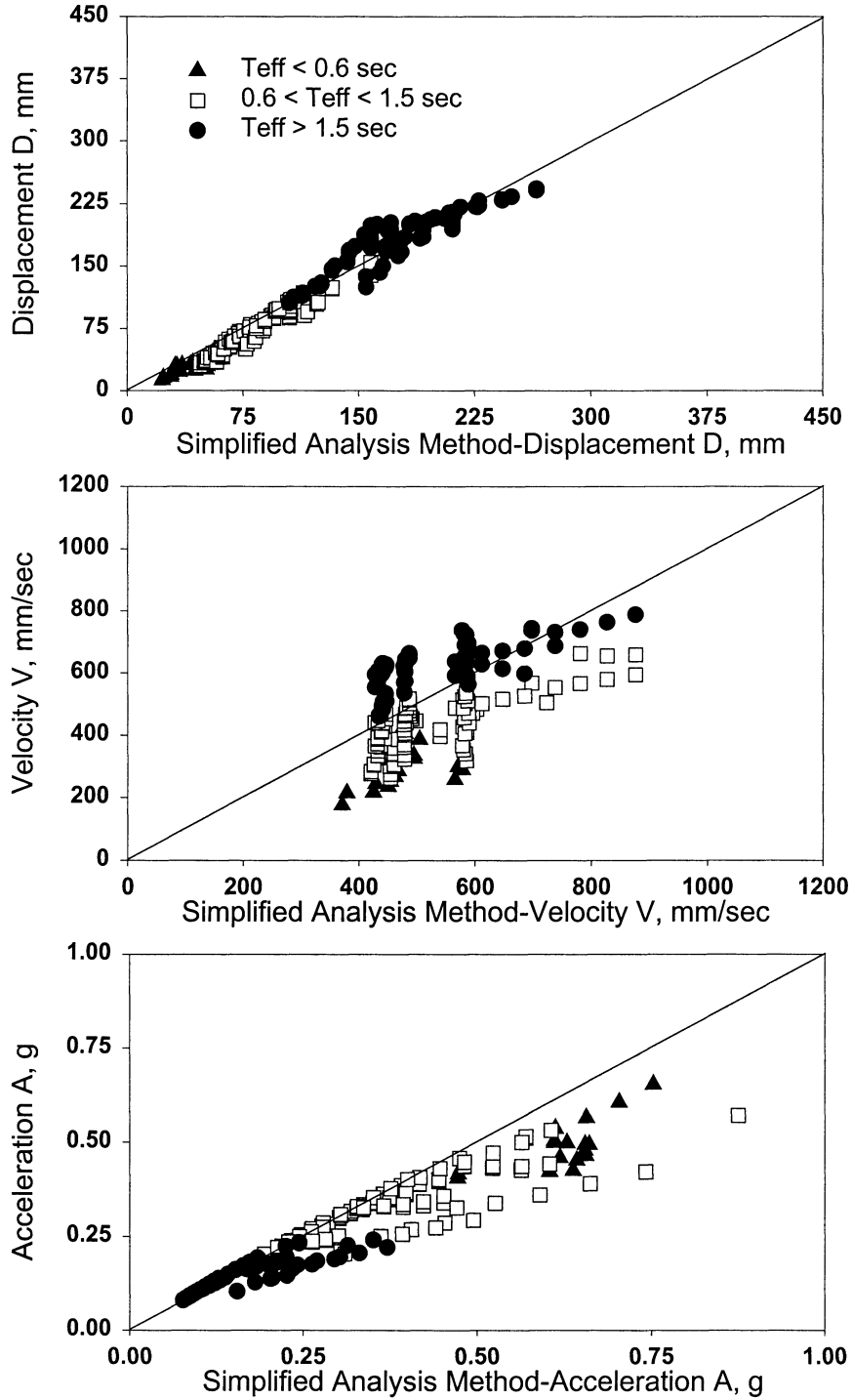


FIGURE 4-13 Comparison of Time History Analysis Results (Average of 20 values) to Results of Simplified Method of Analysis for Bilinear Hysteretic System with Yielding Damping Devices

Perfect Bilinear Hysteretic System ($\alpha=0.05, 0.15, 0.25, 1.0, \beta_i=0.05$)
 With Linear Viscous Damping Devices, $\beta_v=0.15$

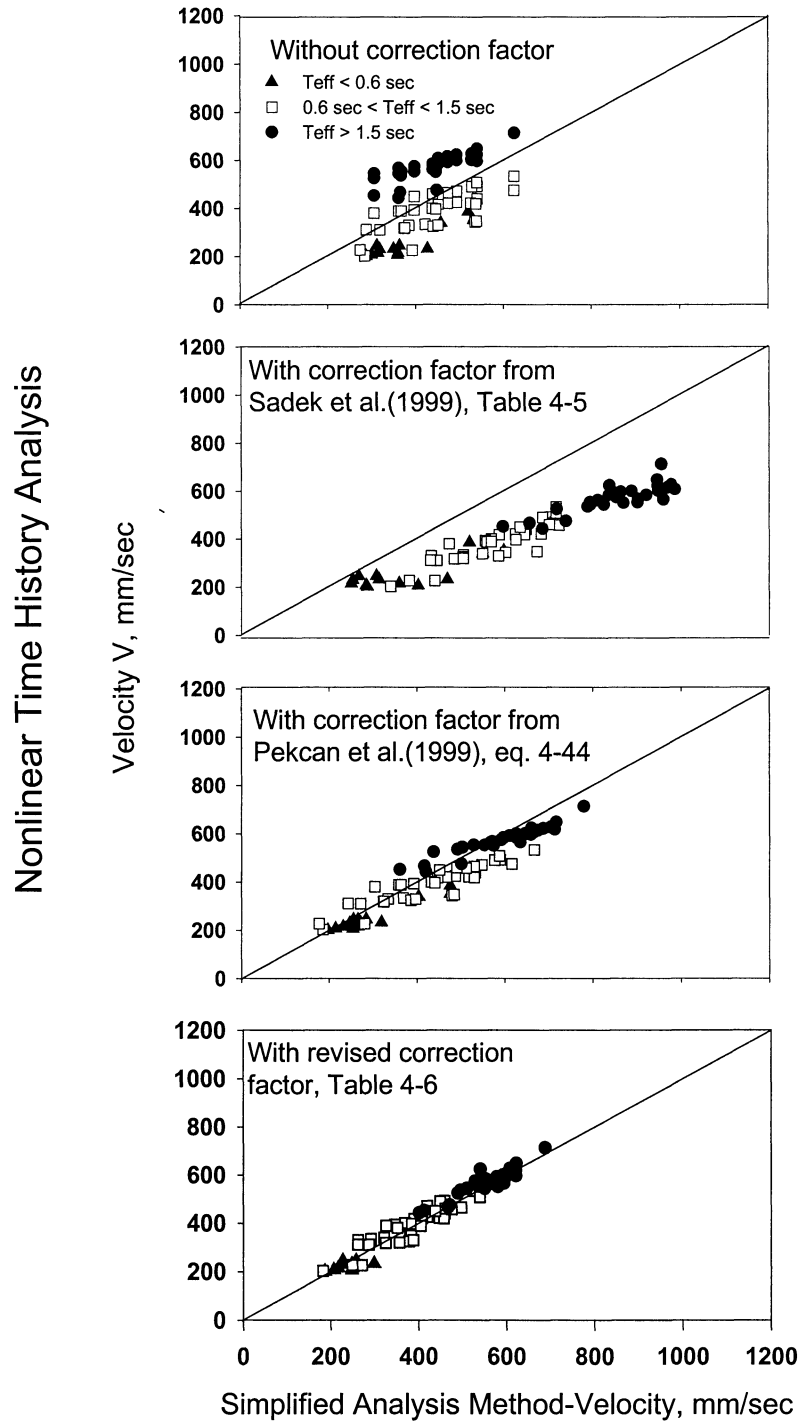


FIGURE 4-14 Comparison of Velocity Predictions without and with Correction Factors for Bilinear Hysteretic System with Linear Viscous Damping Devices, $\beta_v=0.15$

Perfect Bilinear Hysteretic System ($\alpha=0.05, 0.15, 0.25, 1.0, \beta_i=0.05$)
 With Linear Viscous Damping Devices, $\beta_v=0.25$

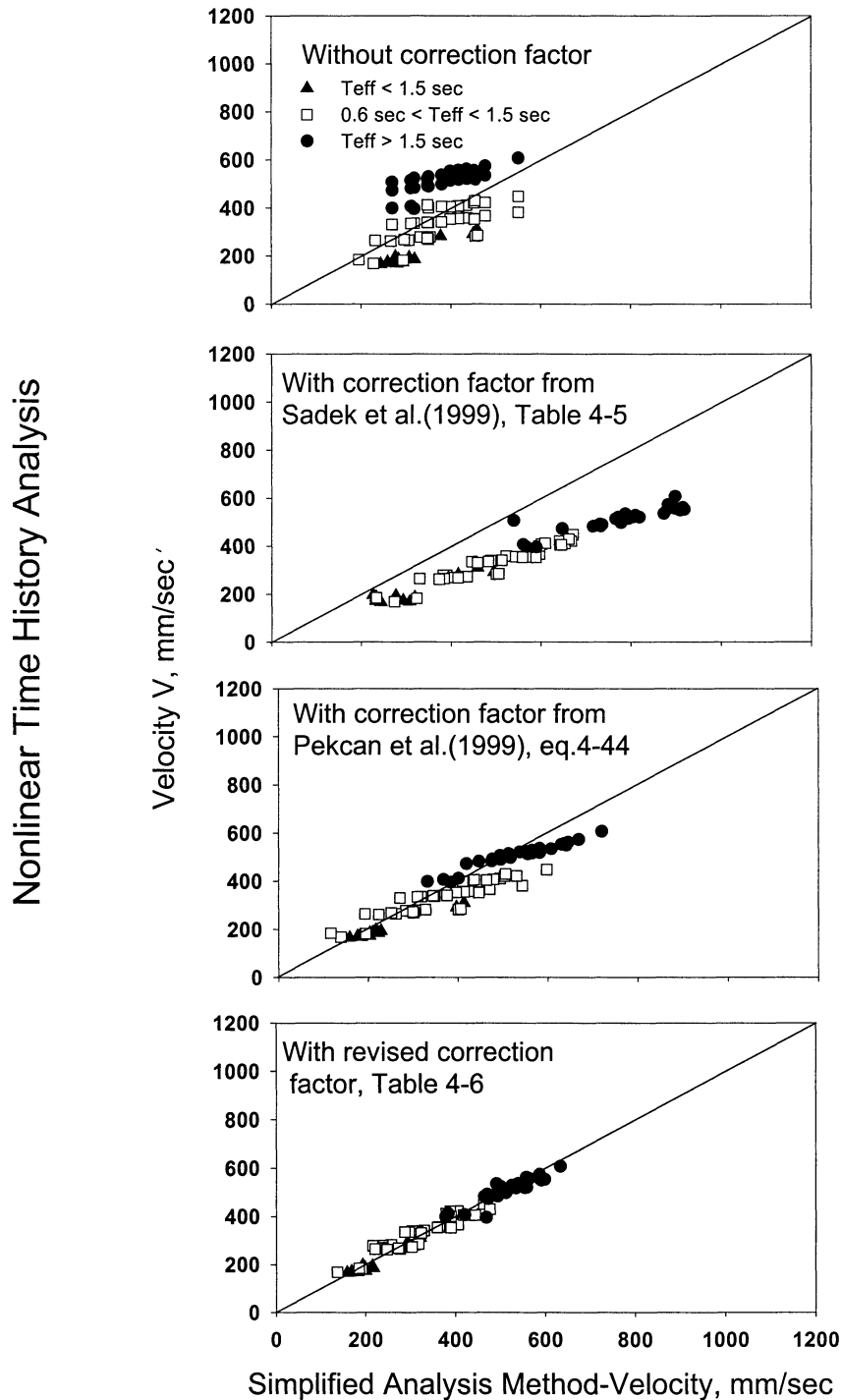


FIGURE 4-15 Comparison of Velocity Predictions without and with Correction Factors for Bilinear Hysteretic System with Linear Viscous Damping Devices, $\beta_v=0.25$

Perfect Bilinear Hysteretic System With ($\alpha=0.05, 0.15, 0.25, 1.0, \beta_i=0.05$)
 Non-Linear Viscous Damping Devices ($a=0.5$), $\beta_v=0.15$

Nonlinear Time History Analysis

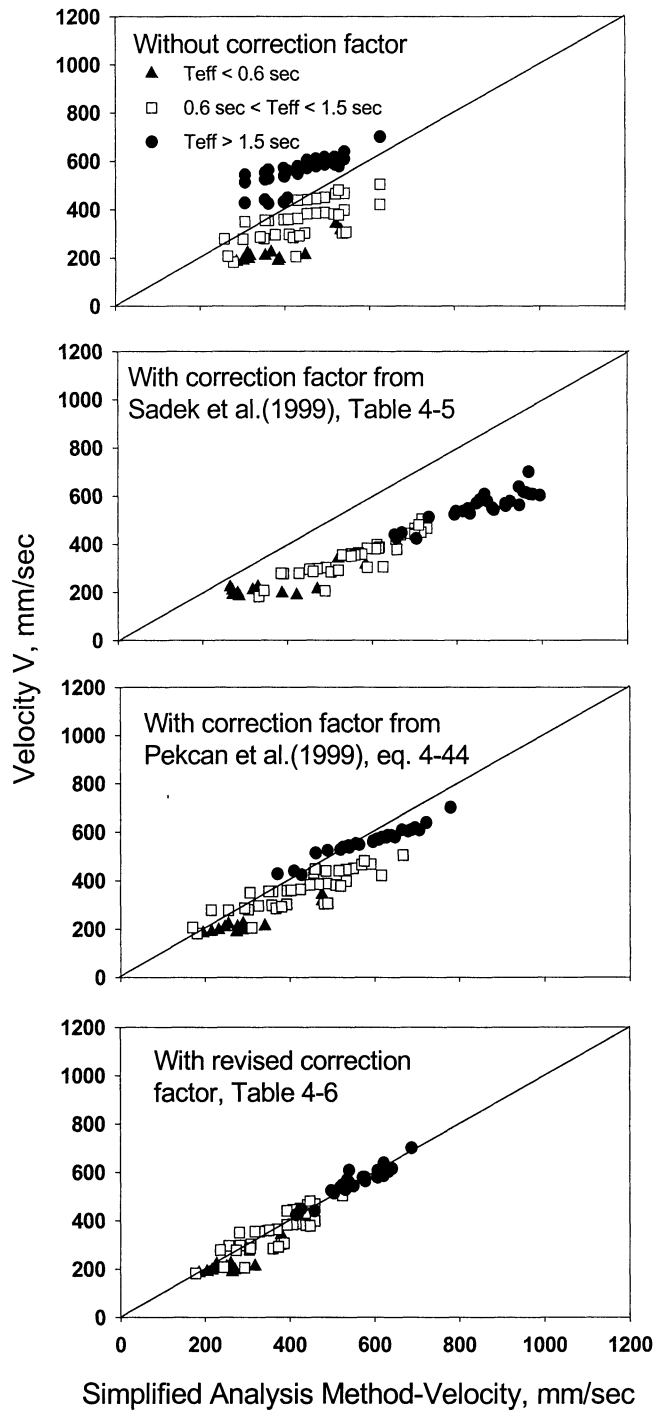


FIGURE 4-16 Comparison of Velocity Predictions without and with Correction Factors for Bilinear Hysteretic System with Non-Linear Viscous Damping Devices, $\beta_v=0.15$

Perfect Bilinear Hysteretic System With ($\alpha=0.05, 0.15, 0.25, 1.0, \beta_i=0.05$)
 Non-Linear Viscous Damping Devices ($a=0.5$), $\beta_v=0.25$

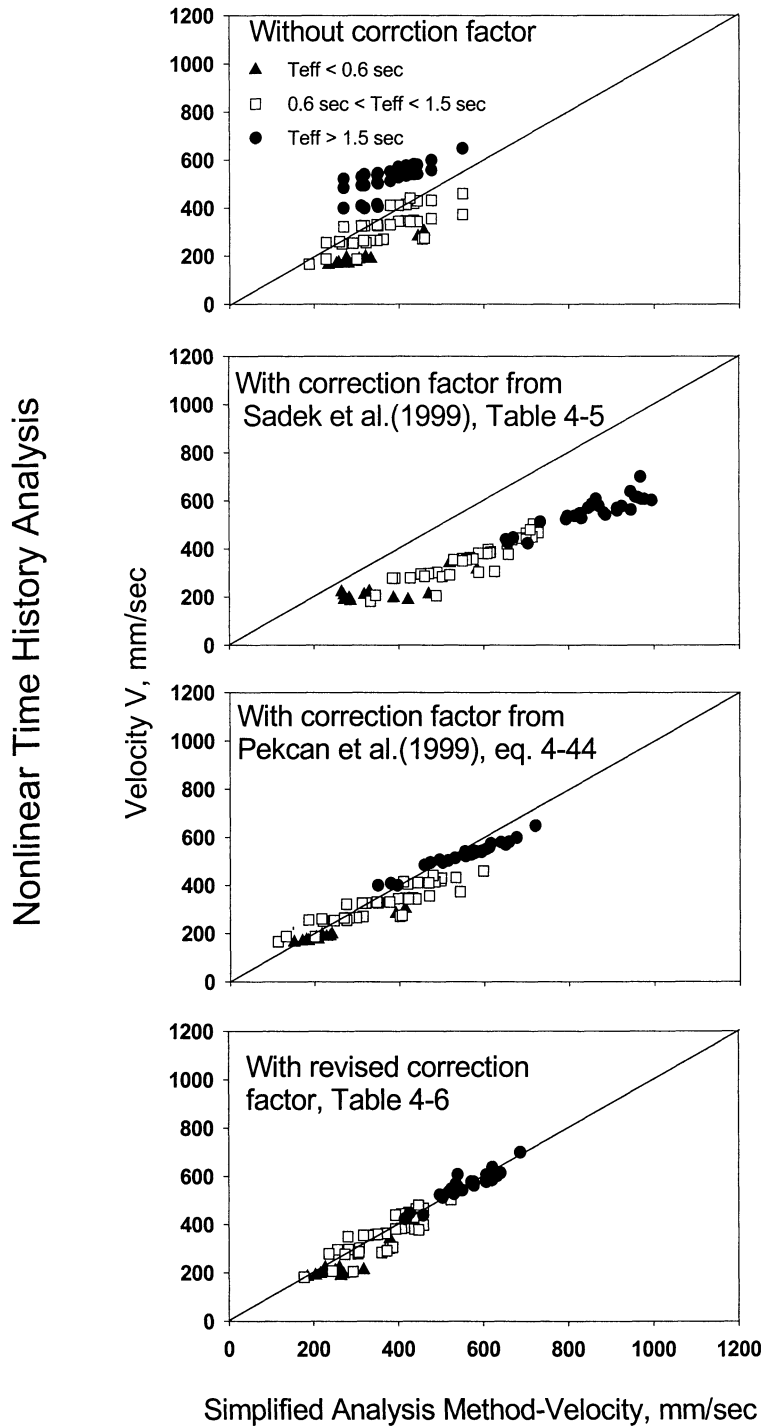


FIGURE 4-17 Comparison of Velocity Predictions without and with Correction Factors for Bilinear Hysteretic System with Non-Linear Viscous Damping Devices, $\beta_v=0.25$

Bilinear Elastic System ($\alpha=0.05, \beta_i=0.05$)
 With Linear Viscous Damping Devices, $\beta_v=0.0, 0.15, 0.25$

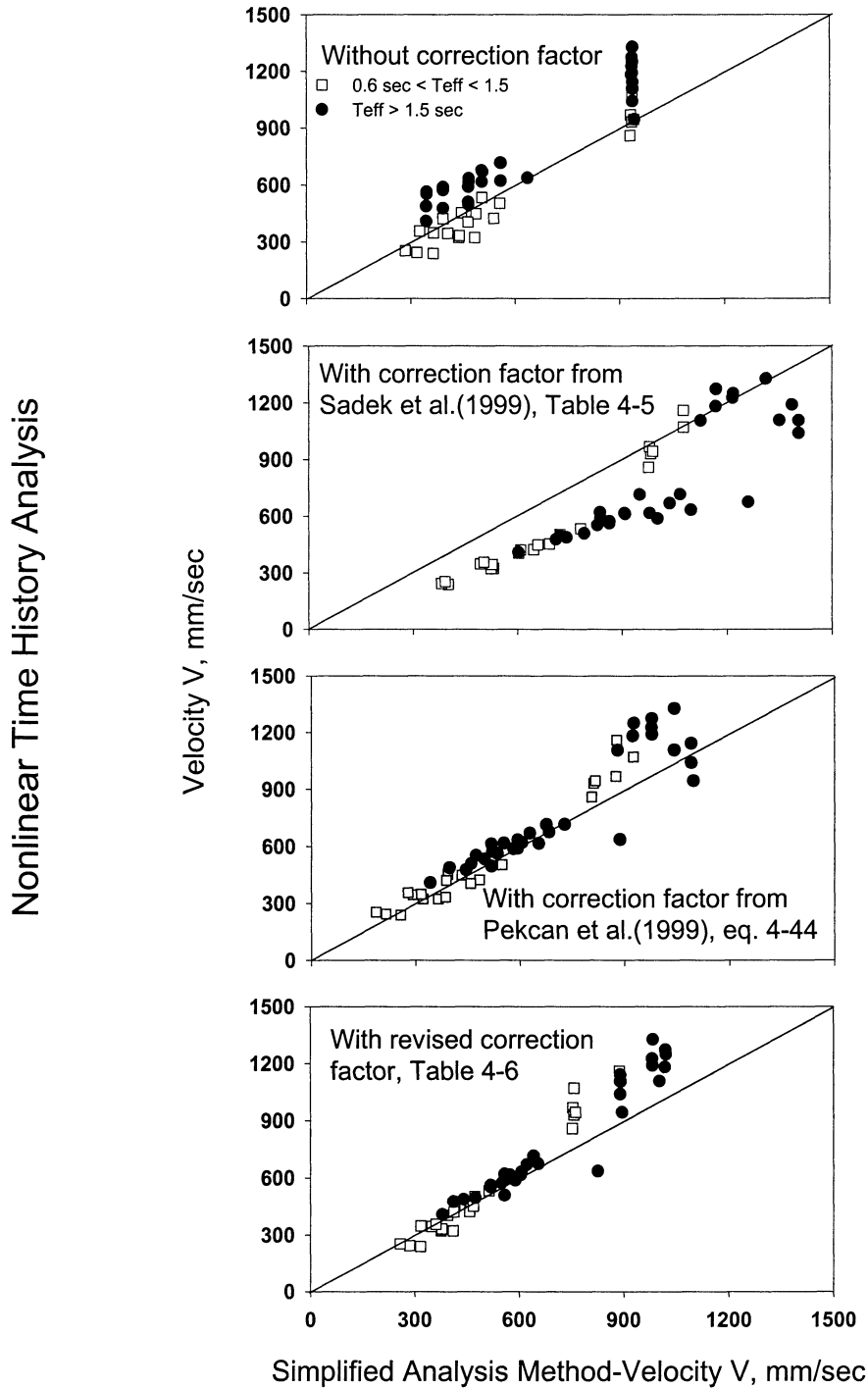


FIGURE 4-18 Comparison of Velocity Predictions without and with Correction Factors for Bilinear Elastic System with Linear Viscous Damping Devices

SECTION 5

RATIO OF INELASTIC DISPLACEMENT TO DISPLACEMENT CALCULATED ASSUMING ELASTIC BEHAVIOR

5.1 Introduction

The ratio of maximum inelastic displacement to maximum displacement calculated under elastic conditions was introduced in FEMA (1997) as coefficient C_I to facilitate the calculation of the displacements in yielding structures.

Several studies considered the problem of deriving simple expressions for the coefficient C_I . Typically, these studies proposed expressions that relate the coefficient C_I to structural parameters such as the elastic period, parameters related to the seismic excitation such as the value of period at the intersection of the constant velocity and constant acceleration regions of the design response spectrum, and parameters related to the response such as the ratio of elastic strength demand to yield strength. These studies did not consider the response of structures with added viscous damping.

The large nonlinear time history analysis dataset for yielding structures with damping systems permitted a re-evaluation of the C_I coefficient. The results presented in Section 4 were used to establish damping-dependent expressions for this coefficient.

5.2 Coefficient C_I and Review of Past Studies

Figure 5-1 illustrates the idealized behavior of a single-degree-of-freedom structure in terms of its base shear-drift relation. Under elastic conditions, the seismic demand consists of the peak force F_e and peak displacement D_{el} . Under inelastic conditions the peak displacement is D_{in} . By definition

$$C_I = \frac{D_{in}}{D_{el}} = \frac{\mu \cdot D_y}{D_{el}} = \frac{\mu}{R_\mu} \quad (5-1)$$

where

$$\mu = \frac{D_{in}}{D_y} \quad (5-2)$$

is the displacement ductility ratio and

$$R_\mu = \frac{F_e}{F_y} = \frac{D_e}{D_y} \quad (5-3)$$

is the ratio of the elastic strength demand to the yield strength. R_μ is the ductility-based portion of the R -factor. For the study below, the elastic period is T_e (based on stiffness K_e), the ratio of post-elastic stiffness to elastic stiffness is equal to α , D_y is the yield displacement and F_y is the yield strength.

Miranda and Bertero (1994) presented an evaluation of studies on the ductility-based portion of the R -factor. The data of Miranda and Bertero were used to establish values for coefficient C_I in FEMA 273. Some of the studies evaluated in Miranda and Bertero (1994) are reviewed below together with a review of other studies.

5.2.1 Study of Mander et al. (1984)

Mander et al. (1984) proposed the following relation

$$C_I = \begin{cases} \frac{1}{R_\mu} \left[1 + (R_\mu - 1) \left(\frac{T_o}{T} \right) \right] & \geq 1 \\ 1 & \text{for } T_e \geq T_o \end{cases} \quad (5-4)$$

where T_o is the period that separates long-period from medium-period structures. Mander et al. (1984) proposed a values of $T_o = 1$ sec.

More recently, Chang and Mander (1994) re-visited the 1984 work of Mander and modified equation (5-4) by replacing the term (T_o/T_e) with the term $(T_o/T_e)^\eta$ where η is an exponent dependent on R_μ with values in the range of 1.2 to about 1.35. Moreover, T_o has been interpreted

as the period at which the maximum spectral velocity response occurs. For a typical design spectrum such as the 5%-damped spectrum depicted in Figure 3-1, and utilizing the pseudo-velocity as a measure of the maximum velocity, period T_o coincides with period T_s , that is, the period at which the constant acceleration and constant velocity regions of the design spectrum intersect. Interestingly, (5-4) is used in FEMA (1997) with T_o being the aforementioned period T_s .

5.2.2 Study of Riddell et al. (1989)

Riddell et al. (1989) established a relationship between the ductility-based portion of the R -factor, ductility and period. Such relations are useful in selecting appropriate response modification factors that are dependent on the period of the structure. Riddell et al. (1989) proposed the relation

$$R_{\mu} = \begin{cases} 1 + (\mu - 1) \frac{T_e}{T_o} & , \quad T_e < T_o \\ \mu & , \quad T_e \geq T_o \end{cases} \quad (5-5)$$

where T_o ranges between 0.1 and 0.4 sec. Use of (5-1) and (5-5) results in equation (5-4).

5.2.3 Study of Nassar and Krawinkler (1991)

Nassar and Krawinkler (1991) developed a relation similar to that of Riddell et al. (1989). Their relationship was based on the results of analysis of systems with a wider range of structural parameters and different seismic excitations. The relationship is

$$R_{\mu} = [1 + (\mu - 1)c]^{1/c} \quad (5-6)$$

where c is a parameter dependent on the elastic period and the post-elastic to elastic stiffness ratio (α). Inverting (5-6) and using (5-1) results in an expression for C_I , namely:

$$C_I = \frac{1}{R_{\mu}} \left(1 + \frac{R_{\mu}^c - 1}{c} \right) \quad (5-7)$$

that has the same basic form as (5-4).

5.2.4 Study of Vidic et al. (1992)

Vidic et al. (1992) arrived at a relation identical to that of Riddell et al. (1989) but with parameter T_o being dependent on the ductility ratio μ and the characteristics of the seismic excitation.

5.2.5 Study of Miranda (1993)

Miranda (1993) proposed the relation of (5-8) using results of analyses with a large number (124) of recorded ground motion:

$$R_\mu = 1 + \frac{\mu - 1}{\Phi} \geq 1 \quad (5-8)$$

where Φ is a parameter dependent on μ , T_e and the predominant period of the ground motion.

5.2.6 Summary

It is evident that many investigators developed similar relations, relating either the coefficient C_I to the ductility-based portion of the R -factor and the elastic period or the ductility-based portion of the R -factor to the ductility ratio and the elastic period. The latter relation was studied as early as 1973 by Newmark and Hall (1973) and then later by Riddell and Newmark (1979) who considered, in addition to other parameters, the effect of viscous damping. Unfortunately, the proposed relations are too complex to be inverted so that expressions for the coefficient C_I can be obtained.

Of interest in the analysis of structures with viscous damping systems is a calibrated relation between coefficient C_I and the post-elastic to elastic stiffness ratio, α (range ≤ 0.5), the elastic period, T_e , the viscous damping ratio under elastic conditions, β_v (range of 0.05 to 0.30) and the period T_s , which characterizes the design response spectrum. Such a relation does not exist in the literature and was established in this study using the results of the nonlinear time history analysis presented in Section 4.

5.3 Procedure for Development of Coefficient C_I and Results

The bilinear hysteretic simple structural system with linear viscous devices described in Section 4 was prepared with the following parameters:

- (a) Elastic period T_e from 0.2 to 3.0 sec, and in steps of 0.1 sec.
- (b) Post-elastic to elastic stiffness ratio α equal to 0.05, 0.15, 0.25, 0.50 and 1.0 ($\alpha=1$ represents elastic behavior).
- (c) Ductility-based portion of the R -factor, R_μ equal to 2.0, 3.33 and 5.0.
- (d) Linear viscous damping ratio under elastic conditions β_v equal to 0.0, 0.15, and 0.25, plus inherent viscous damping of 0.05 for a total viscous damping ratio under elastic conditions of β_v equal to 0.05, 0.20, and 0.30.

Parameter R_μ (see eq. 5-3) can also be described by

$$R_\mu = \frac{m S_a(T_e, \beta = 0.05)}{F_y B} \quad (5-9)$$

where m is the mass, S_a is the spectral acceleration for damping of 5-percent and B is the damping coefficient for the total damping ratio. The damping coefficient presented in Section 3 and described as the “conservative” trilinear model has been utilized in the calculation of the yield strength of the analyzed systems. The seismic excitation consisted of the 20 scaled motions described in Section 3 and used in the analyses reported in Section 4. Note that for these motions, $T_S = 0.6$ sec.

The coefficient C_I was obtained as the ratio of the average peak inelastic displacement to the average peak elastic displacement. Plots of this coefficient versus period T_e revealed the basic nature of the relation. Moreover, since C_I should converge to unity when either R_μ or α are equal to unity, the following relation was considered:

$$C_I = 1 + \frac{(1-\alpha)(R_\mu - 1)}{R_\mu} \left(a \frac{T_S}{T_e} \right)^b \quad (5-10)$$

in which parameters a and b were obtained by calibration of the model on the basis of the results of dynamic analysis. The simplest form of these parameters was found to be

$$a = a_0 (2 + 0.45 R_\mu) \quad (5-11)$$

$$b = 3.24 - 0.10 R_\mu - 4.5 \beta_v \quad (5-12)$$

where a_0 is the parameter in Table 5-1.

Figures 5-2 to 5-4 compare values of coefficient C_I obtained by nonlinear time history analysis to the predictions of the model described by (5-10). Evidently, the proposed relation described by (5-10) describes well the calculated values of the coefficient and it follows the desired behavior for large values of period T_e . That is, (5-10) predicts a value of near unity for $T_e > T_S$.

5.4 Summary

In this section a new relation describing the ratio of peak inelastic displacement to the peak displacement assuming elastic behavior (coefficient C_I) has been presented. The new feature of this relation is the inclusion of the effect of added viscous damping. This relation may be used to obtain quick estimates of displacement demands in structures with damping systems without the need to use iterative analysis procedures. The results presented in Figures 5-2 to 5-4 illustrate effect of viscous damping on coefficient C_I . It may be noted that the effect of damping in the range of 5 to 30-percent is not significant.

TABLE 5-1 Values of Parameter a_0

Damping Ratio β_v	$\alpha=0.05$	$\alpha=0.15$	$\alpha=0.25$	$\alpha=0.50$
0.05	0.116	0.100	0.093	0.071
0.30	0.195	0.160	0.143	0.111

Linear Interpolation is Valid

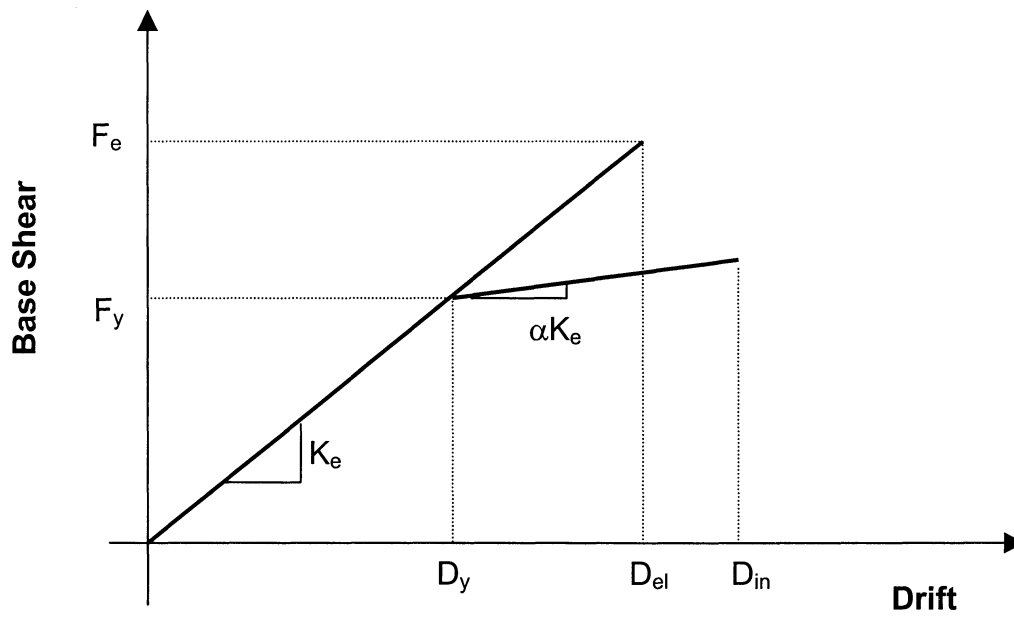


Figure 5-1 Elastic and Idealized Inelastic Behavior of Structure

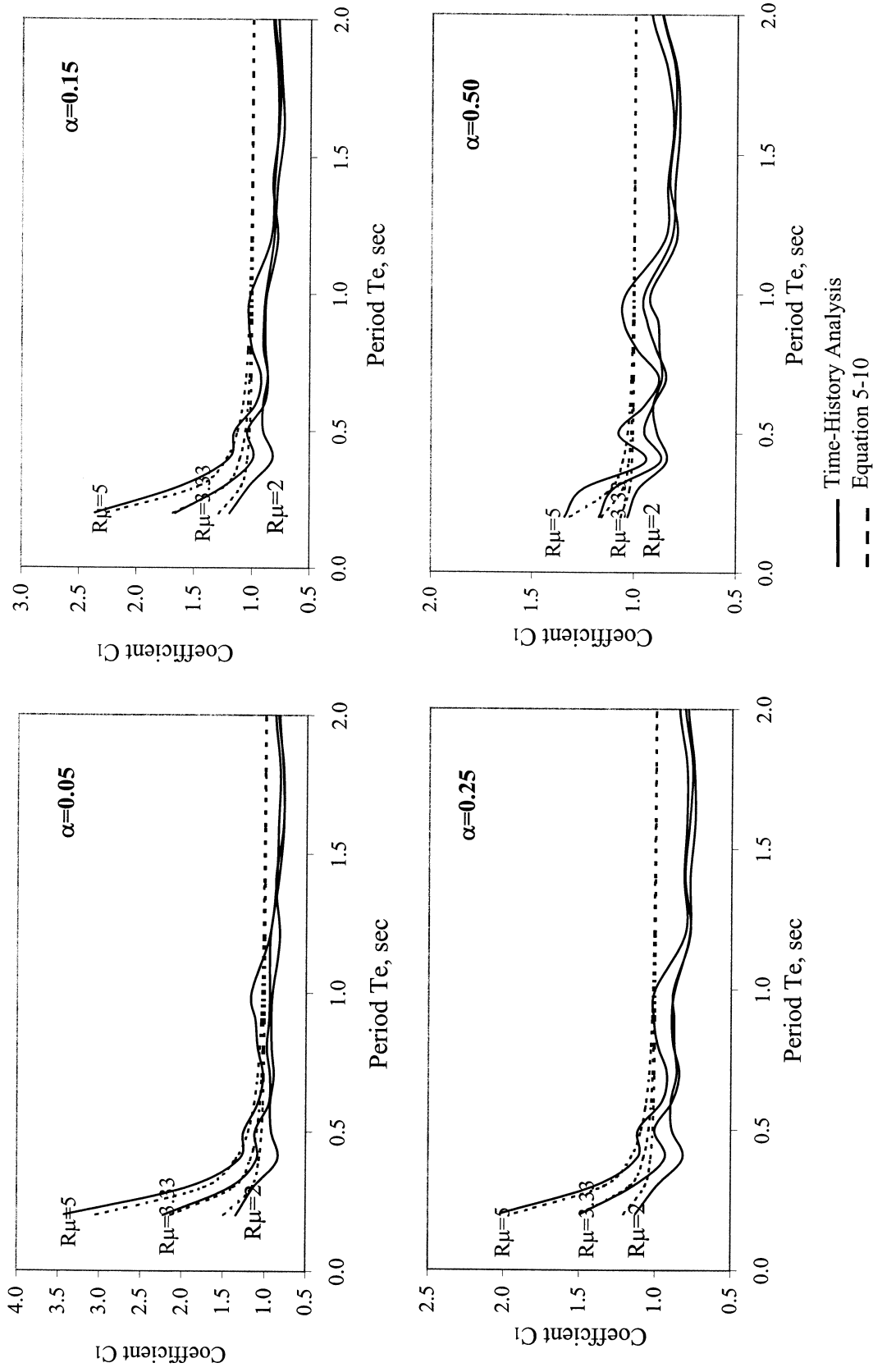


FIGURE 5-2 Comparison of Values of Coefficient C_1 Established by Nonlinear Time History Analysis to Predictions of Eq. 5-10 for Viscous Damping Ratio of 0.05

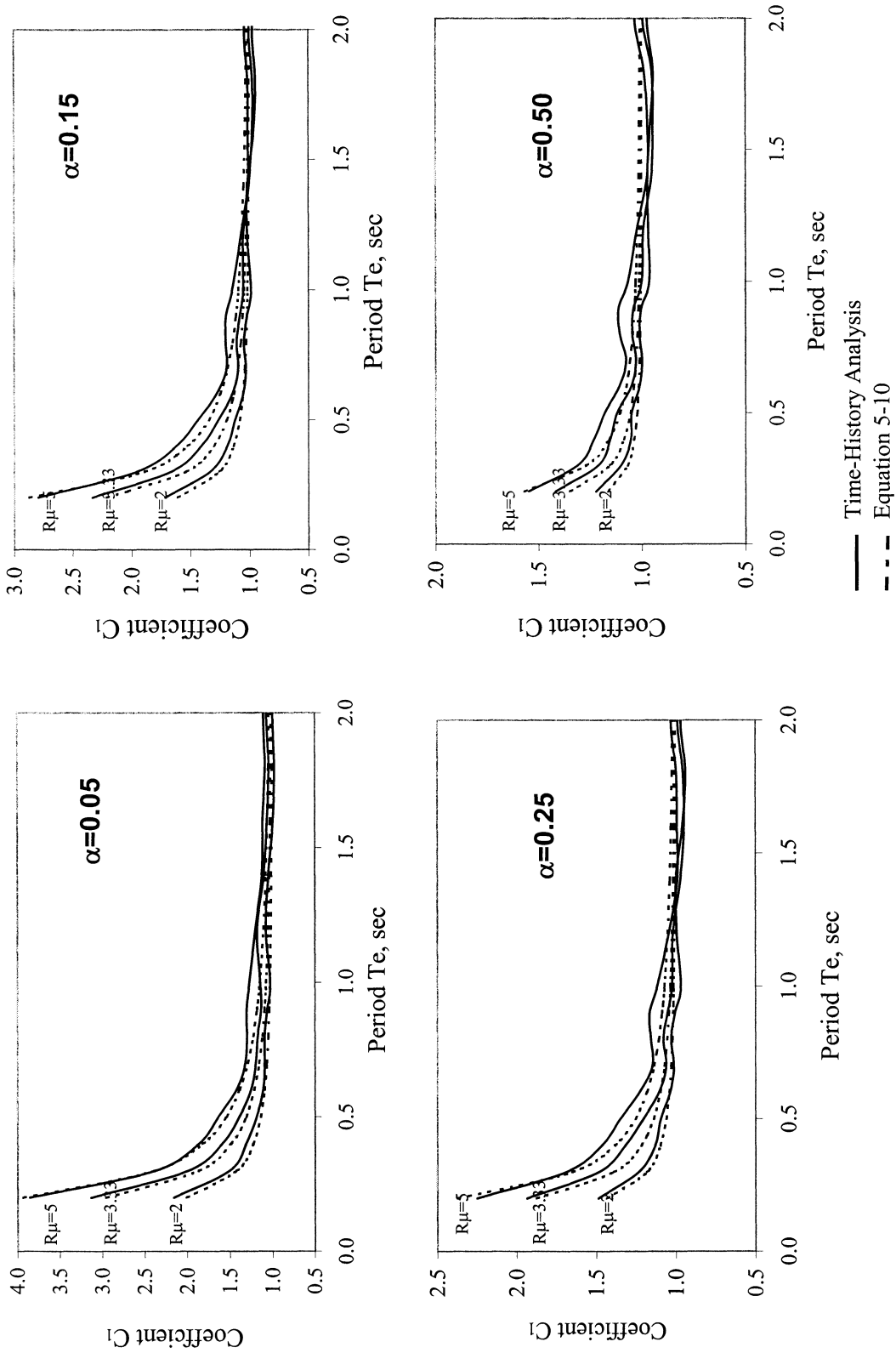


FIGURE 5-3 Comparison of Values of Coefficient C_1 Established by Nonlinear Time History Analysis to Predictions of Eq. 5-10 for Viscous Damping Ratio of 0.20

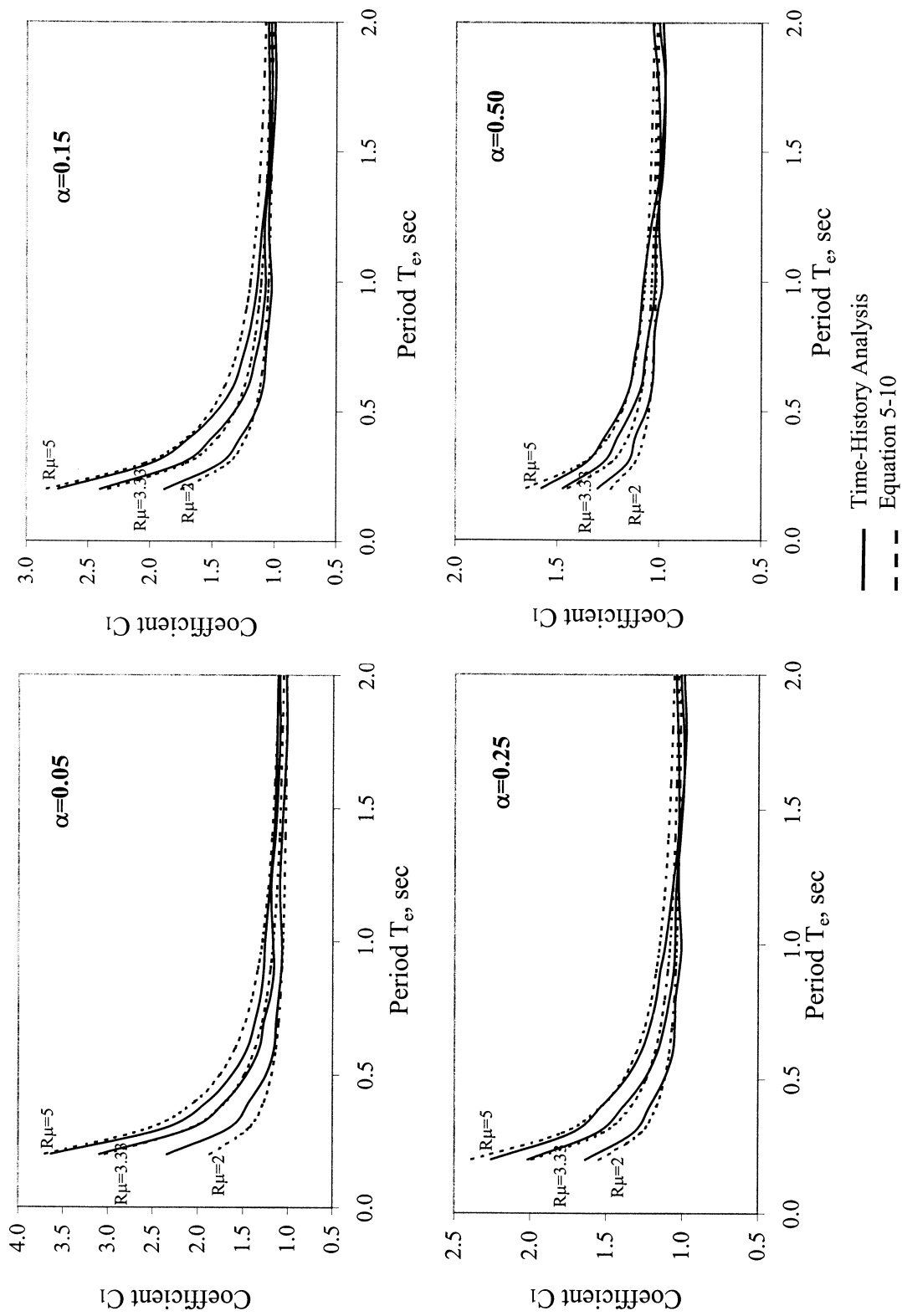


FIGURE 5-4 Comparison of Values of Coefficient C_1 Established by Nonlinear Time History Analysis to Predictions of Eq. 5-10 for Viscous Damping Ratio of 0.30

SECTION 6

DISPLACEMENT DUCTILITY DEMAND IN STRUCTURES WITH VISCOUS DAMPING SYSTEMS

6.1 Introduction

A structure without a damping system would typically be designed for code-prescribed lateral loads equal to the elastic inertia forces divided by a response modification factor (or R -factor). Such a structure will have an actual yield strength F_{yu} given by

$$F_{yu} = \frac{\text{Elastic Demand}}{R_{\mu}} \quad (6-1)$$

where R_{μ} is the ductility-based portion of the R -factor. In (6-1), elastic demand is the peak base shear calculated assuming that the structure is elastic with damping ratio equal to 5-percent. A structure designed on the basis of (6-1) will undergo inelastic deformations when subjected to the design earthquake.

Consider now that a structure with a viscous damping system is designed using a similar approach. The structure is designed to have an actual yield strength F_{yd} given by

$$F_{yd} = \frac{\text{Elastic Demand (for 5\% damping)}}{R_{\mu} \cdot B} \quad (6-2)$$

where B is the damping coefficient for the viscous damping ratio of the structure under elastic conditions (say β_v). The elastic demand in (6-2) is as defined (6-1), so that the ratio elastic demand/ B is the base shear of the damped structure calculated assuming that the structure is elastic with damping ratio equal to β_v . If we consider a value of $\beta_v = 0.20$ (0.05 inherent plus 0.15 added viscous damping) and a relatively flexible structure so that its elastic period T_e is larger than T_s , B is equal to 1.5 per Section 3. Accordingly for the same ductility-based portion

of the R -factor, the strength of the damped structure will be substantially less than that of the undamped structure, or for this example, $F_{yd} < 0.67 F_{yu}$.

A question then arises as to whether the two structures will have comparable displacement ductility demands. The issue is further complicated by the fact that the damped structure has also less stiffness than the undamped structure. This section presents a systematic study that answers the displacement ductility question. This section presents results that demonstrate that the two structures indeed have comparable displacement ductility demands

6.2 Procedure for Evaluation of Displacement Ductility Demand

Bilinear hysteretic single-degree-of-freedom systems without and with linear viscous damping devices were considered. Each system without damping devices was characterized by the elastic period T_e , ductility-based portion of R -factor, R_μ , ratio of post-elastic to elastic stiffness, α , and the inherent damping ratio, $\beta_i = 0.05$. Values of $T_e = 0.2$ to 2.0 sec, $\alpha = 0.05, 0.15, 0.25$ and 0.50 , and $R_\mu = 2.0, 3.33$ and 5.0 were selected.

Each system with damping devices was characterized by the same parameters β_i , α , and R_μ , a value of elastic period T_{ed} larger than T_e , and added linear viscous damping ratio $\beta_v = 0.15$ or 0.25 under elastic conditions. Accordingly, the total damping ratio under elastic conditions was either 0.20 or 0.30 . The damped system had a lower yield strength than the undamped system as indicated in equations (6-1) and (6-2).

The elastic period T_{ed} of the damped system was related to the period T_e of the corresponding undamped system (damped at 5%) on the basis of the following equation:

$$\frac{T_{ed}}{T_e} = B^\eta \quad (6-3)$$

where η is a parameter dependent on the fundamental period and the shape of the beam and column sections of the structure, which was calculated as follows. The elastic period of the structure is related to the moment of inertia, I , of the beam and column sections, that is, $T \sim 1/\sqrt{I}$. The yield strength of the structure is related to the plastic moments of the beam and

columns which are proportional to the plastic section modulus and the material yield stress. Assuming that the damped and the undamped structure are made of the same material, it follows that $F_{yu}/F_{yd} = Z_e/Z_d$ where Z_e and Z_d are the plastic section moduli of the sections of the undamped and the damped structures, respectively. Consider now that both structures have elastic periods that fall within the constant acceleration domain of the design spectrum. Use of (6-1) and (6-2) results in $F_{yu}/F_{yd} = B$. Thus,

$$\frac{T_{ed}}{T_e} = \left(\frac{I_e}{I_d} \right)^{1/2} \quad (6-4)$$

$$\frac{Z_e}{Z_d} = B \quad (6-5)$$

where I_e and I_d are representative moments of inertia of the beam and columns of the undamped and the damped structures, respectively. For a rectangular $b \times h$ section, $I \sim h^3$ and $Z \sim h^2$, so that $T \sim h^{-3/2}$. That is,

$$\frac{T_{ed}}{T_e} = \left(\frac{h_e}{h_d} \right)^{3/2} = \left(\frac{Z_e}{Z_d} \right)^{3/4} = B^{3/4} \quad (6-6)$$

where h_e and h_d are the heights of the sections of the undamped and the damped structures, respectively. A similar expression, but with an exponent equal to $2/3$ rather than $3/4$, is obtained for square sections. Similarly, for wide flange sections, equation (6-3) is valid with $\eta = 0.45$ to 0.65 .

Moreover, analysis considering that both T_e and T_{ed} are within the constant velocity region of the design spectrum, results again in (6-3) but with η of the order of or larger than unity. Accordingly, analysis were performed utilizing (6-3) with $\eta = 0.5$ when $T_e < T_s$ and $\eta = 1.0$ when $T_e \geq T_s$. Note that T_s is the period at the intersection of the constant acceleration and constant velocity regions of the design spectrum.

6.3 Results

Analyses were performed using the 20 scaled motions described in Section 3. In the calculation of the period and the yield strength of the damped structure, the “conservative values” of the damping coefficient B were used (see Section 3).

Figures 6-1 and 6-2 compare the calculated average displacement ductility ratio for the undamped and the damped structures (the average is that of the 20 calculated values for each combination of parameters). The ductility demand in the two structures is nearly the same. Moreover, Figure 6-3 presents a further comparison of the displacement ductility ratio of the undamped and the 20%-damped structures with $\alpha = 0.05$. In this figure, in addition to the average, the maximum, and the minimum displacement ductility ratios of the 20 calculated values are compared. Such a representation reveals the possible scatter in the ductility demand. Interestingly, the scatter in the ductility demand in the damped structures is similar as that in the undamped structure. This further justifies the use of the design approach described by (6-2).

6.4 Conclusions

In this section a comparison of ductility demands in damped and undamped structures has been presented. The structures have been designed to have a yield strength described by (6-1) to (6-3), so that

$$\frac{F_{yd}}{F_{yu}} = \begin{cases} \frac{1}{B} & \text{when } T_e, T_{ed} < T_s \\ \frac{1}{B^2} & \text{when } T_e, T_{ed} \geq T_s \end{cases} \quad (6-7)$$

That is, the yield strength of the damped systems was between 0.35 and 0.67 times the strength of the undamped structure. The calculated average, maximum and minimum displacement ductility ratios in the two structures were nearly the same for the same R_μ and α . On the basis of these results, as well as results on inelastic spectra of structures with added viscous damping presented by Wu and Hanson (1989), NEHRP (2000) allows the design of structures with

damping systems for a seismic base shear that is the greatest of V/B or $0.75V$, where V is the minimum seismic base shear for the design of the structure without a damping system and B is the damping coefficient for the combined inherent and viscous damping under elastic conditions.

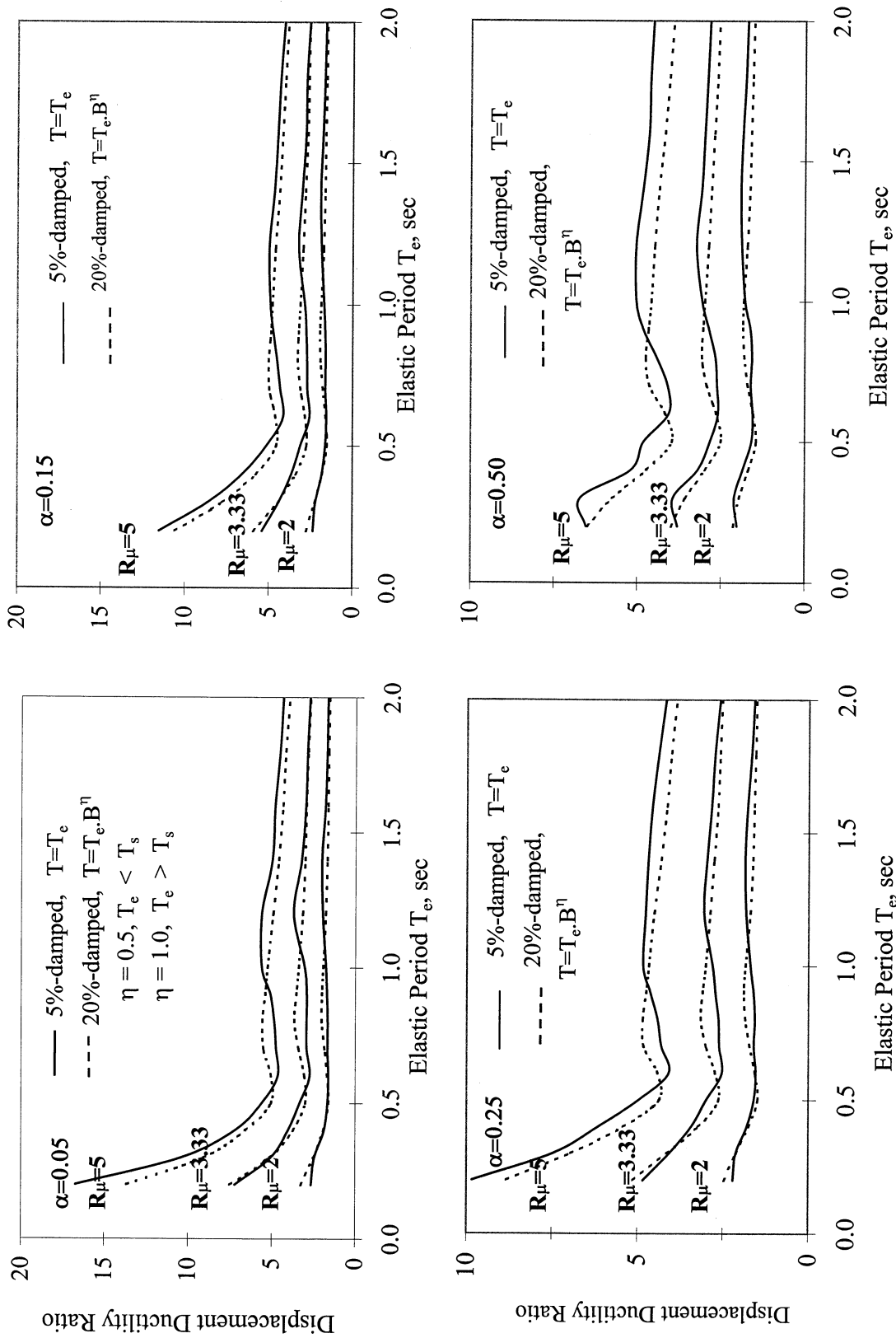


FIGURE 6-1 Comparison of Average Displacement Ductility Ratio for 5% and 20%-Damped Systems

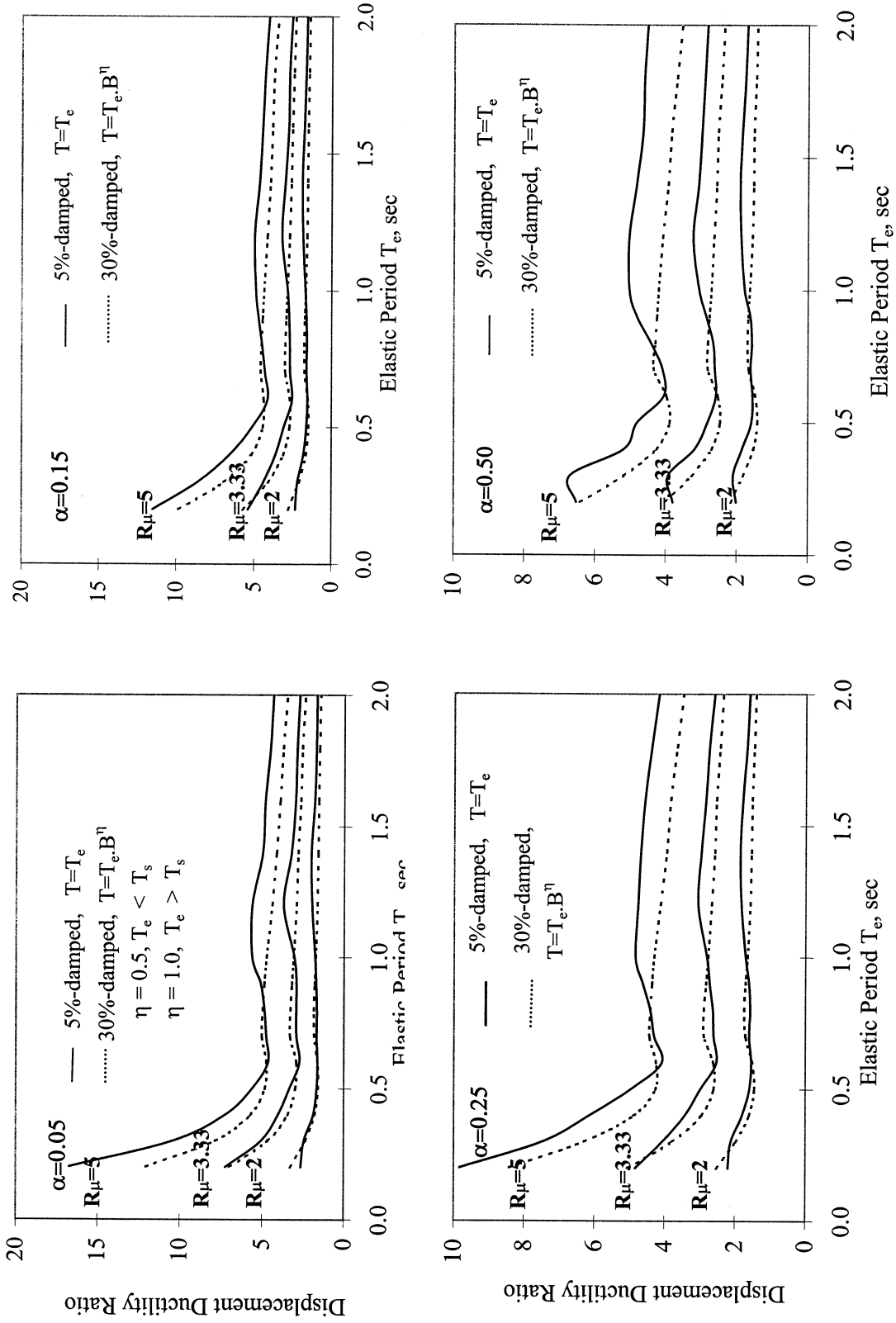


FIGURE 6-2 Comparison of Average Displacement Ductility Ratio for 5% and 30%-Damped Systems

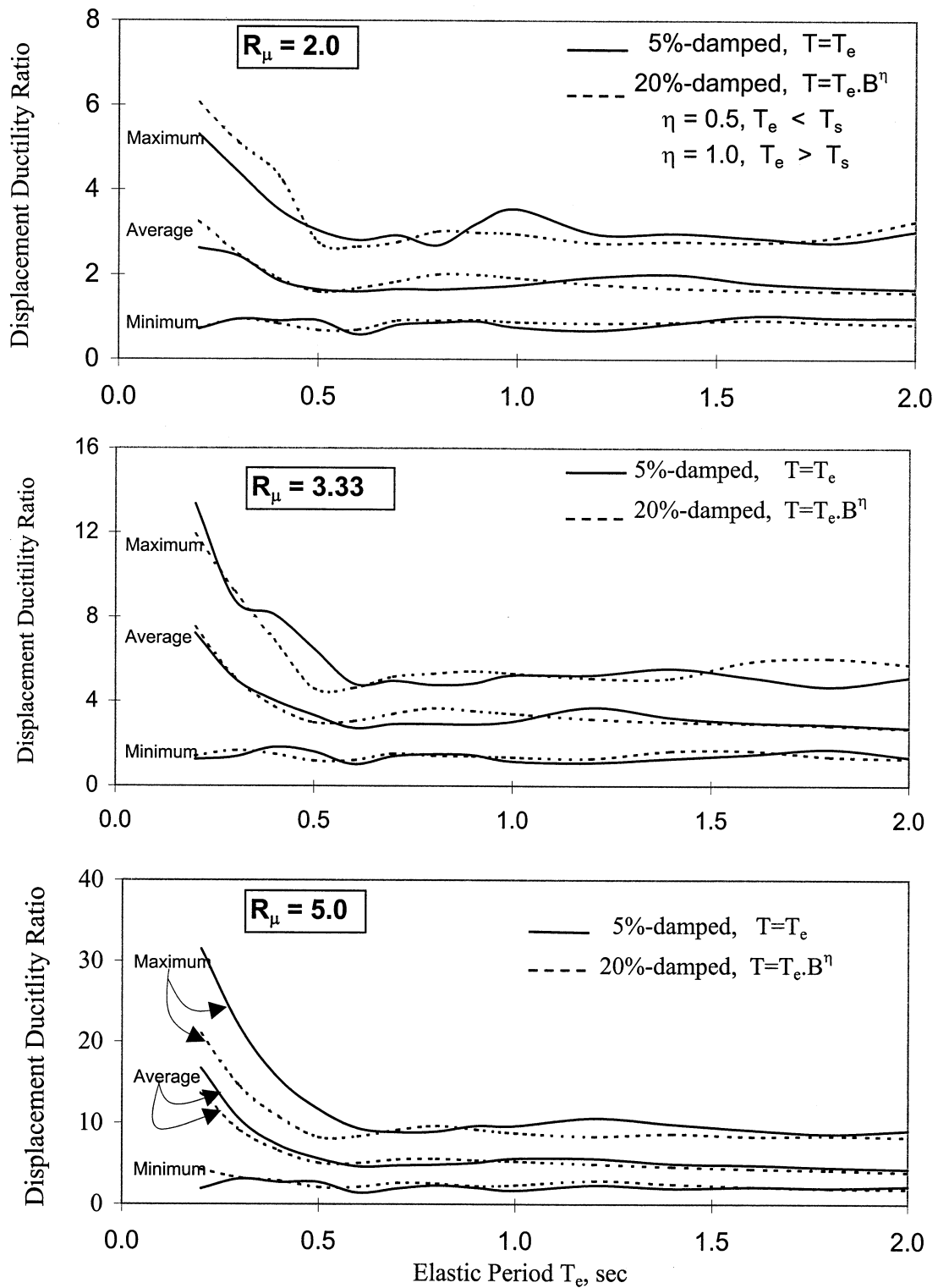


FIGURE 6-3 Comparison of Maximum, Average and Minimum Displacement Ductility Ratios of 5% and 20%-Damped Systems with $\alpha = 0.05$.

SECTION 7

DEVELOPMENT OF EQUIVALENT LATERAL FORCE AND MODAL ANALYSIS PROCEDURES FOR NEW BUILDINGS WITH DAMPING SYSTEMS

7.1 Introduction

The Nonlinear Static Procedure of FEMA 273 FEMA (1997) is the most comprehensive guideline for the evaluation of buildings with damping systems at the time of this writing. Specifically, Method 2 of FEMA (1997) is suitable for the analysis of buildings with velocity-dependent (i.e., viscous and viscoelastic) damping systems, whereas Method 1 of FEMA (1997) requires modifications along the lines of Method 2 for its application to velocity-dependent systems.

Method 2 of FEMA (1997) is somewhat cumbersome to apply because it requires to perform at least two pushover analyses, each with repeated eigenvalue analyses utilizing secant member stiffnesses. Moreover, the method is suitable for the analysis of existing buildings and does not provide guidance for preliminary sizing of members.

There is interest in the development of equivalent lateral force and modal analysis procedures for buildings with damping systems that parallel the corresponding procedures for buildings without damping systems, as in the NEHRP Recommended Provisions for Seismic Regulations for New Buildings and Other Structures (NEHRP, 1997). Such procedures could simplify the design of buildings with damping systems.

An equivalent lateral force procedure and a modal analysis procedure for damped buildings are presented in this section. They are largely based on Method 2 of FEMA (1997) but are simpler as a result of the following assumptions:

- (1) The building is designed to have a proper collapse mechanism so that the distribution of drift may be reasonably estimated on the basis of either eigenvalue analysis under elastic

conditions or on the basis of assumptions (e.g., the drift distribution has an inverted triangular shape).

- (2) The building is analyzed in each principal direction as a model with one degree-of-freedom per floor.
- (3) The behavior of the building can be represented by an elastoplastic model.
- (4) The yield strength of the building can be estimated by either a) plastic analysis since the collapse mechanism is known, or b) using the specified minimum seismic base shear and values of the response modification (R), system overstrength (Ω_0) and deflection amplification (C_d) factors presented in NEHRP (2000).

7.2 R , R_μ , Ω_0 , C_d Factors and Maximum Effective Ductility

The definitions of the response modification factor R , the ductility-based portion of R -factor R_μ (or R_d in NEHRP, 1997), the system overstrength factor Ω_0 , and the deflection amplification factor C_d may be found in NEHRP (1997). A review of the values of some of these factors may be found in Uang (1991). A brief description of these parameters is presented below.

Shown in Figure 7-1 is the structural response of a one-story building. The base shear-drift relations of this building are termed capacity curves. The “actual” capacity curve shown dashed in the figure is replaced by the idealized elastoplastic capacity curve that is shown as a solid line. The elastic and inelastic responses of this building are obtained as the intersection points of the capacity curves and the demand spectra (the latter multiplied by the reactive weight W to obtain force). The yield strength of the idealized building is V_y and the elastic demand (or required elastic strength) is F_e . The inelastic displacement is D_I and is shown in Figure 7-1 to be larger than the elastic displacement D_e . The effective yield displacement is D_y , and the force and displacement at the formation of the first plastic hinge are V_s and D_s , respectively. The displacement ductility ratio (or effective ductility demand) is $\mu = D_I/D_y$. The definitions of the various factors are:

$$R_\mu = \frac{F_e}{V_y} \quad (7-1)$$

$$\Omega_0 = \frac{V_y}{V_s} \quad (7-2)$$

$$R = \frac{F_e}{V_s} = R_\mu \cdot \Omega_0 \quad (7-3)$$

$$C_d = \frac{D_i}{D_s} = \mu \cdot \Omega_0 \quad (7-4)$$

Note that typical structural design criteria prescribe the seismic base shear V_s (or V in 1997 NEHRP Recommended Provisions) and its distribution over the height of the building. Analysis of the building for these forces assuming elastic behavior results in the elastic drift D_s . The design drift is calculated as $C_d D_s$, which is supposed to be an estimate of the actual inelastic displacement. However, relative values of C_d and R are inconsistent, so that the design drift $C_d D_s$ is less than displacement D_i , except for structural systems for which $R/C_d = 1.0$. This fact has implications in the use of specified allowable story drift limits when the analysis procedure predicts the actual displacement (as it is the case in Method 2 and the procedure presented in this section).

The displacement ductility ratio μ may be related to factors R and Ω_0 as follows. In the constant velocity region of the spectrum ($T_1 \geq T_s$), the equal displacement assumption may be used, so that $D_i = D_e$. It follows that

$$\mu = R_\mu, \quad T_1 \geq T_s \quad (7-5)$$

In the constant acceleration region of the spectrum ($T_1 < T_s$), the equal energy assumption may be used, so that

$$\mu = \frac{1}{2} (R_\mu^2 + 1), \quad T_1 < T_s \quad (7-6)$$

Utilizing (7-3) and introducing the importance factor I (NEHRP, 1997) the maximum effective ductility demand is

$$\mu_{max} = \frac{R}{\Omega_0 \cdot I} \quad , T_l \geq T_s \quad (7-7)$$

$$\mu_{max} = \frac{1}{2} \left[\left(\frac{R}{\Omega_0 \cdot I} \right)^2 + 1 \right] \quad , T_l < T_s \quad (7-8)$$

Note that in (7-7) and (7-8), T_l is the period of the fundamental mode of vibration of the structure in the direction of interest under elastic conditions. Equations (7-7) and (7-8) are utilized in NEHRP (2000), except that T_l is replaced by the effective period T_{eff} in (7-7) avoid a discontinuity in μ_{max} at period T_s .

7.3 Elements of Structural Dynamics

Certain results of the theory of structural dynamics are used in the development of the simplified analysis procedure. The results are derived from Clough and Penzien (1975).

Consider the earthquake response analysis of an elastic building. The building is modeled as a multi-degree-of-freedom two-dimensional system with one degree of freedom per floor. Reactive weights w_i are concentrated at the floor levels. The degrees of freedom are the horizontal displacements of each reactive weight with respect to the ground, u_i . The seismic excitation is described by the time history of the horizontal ground acceleration a_g . Neglecting damping, the equations of motion are

$$[M]\{\ddot{u}\} + [K]\{u\} = -[M]\{I\}a_g \quad (7-9)$$

where $[M]$ is the mass matrix (diagonal with elements w_i/g), $[K]$ is the stiffness matrix, $\{I\}$ is a unity vector, $\{u\}$ is a vector containing displacements u_i , and $\{\ddot{u}\}$ is a vector of accelerations, \ddot{u}_i .

The solution of the eigenvalue problem of (7-9) results in modal frequencies ω_m (the corresponding period, T_m is $2\pi/\omega_m$) and mode shapes $\{\phi\}_m$, where m varies between 1 and the number of degrees of freedom, N . The dynamic response of the building can be obtained by modal analysis as the superposition of modal responses by substituting in (7-9)

$$\{u\} = [\Phi]\{y\} \quad (7-10)$$

where $\{y\}$ = vector of modal displacements, $[\Phi]$ = matrix having vectors $\{\phi\}_m$ as columns. Note that in (7-10), $[\Phi]$ is defined to be dimensionless so that $\{y\}$ has dimensions of displacement. The use of the orthogonality condition results in decomposition of (7-9) into N uncoupled equations of the form

$$\ddot{y}_m + \omega_m^2 y_m = -\Gamma_m a_g \quad (7-11)$$

where Γ_m is the modal participation factor given by

$$\Gamma_m = \frac{\sum_{i=1}^N w_i \cdot \phi_{im}}{\sum_{i=1}^N w_i \cdot \phi_{im}^2} \quad (7-12)$$

where ϕ_{im} = element of mode shape m corresponding to degree of freedom u_i .

Equation (7-11) is used to calculate the peak values of y_m from the 5%-damped response spectrum of motion a_g (the issue of the validity of this approach for highly damped systems is discussed later on). Let the spectral displacement of motion a_g (5%-damped, frequency ω_m) be S_d and the corresponding spectral acceleration be S_a (note that $S_a = \omega_m^2 \cdot S_d$). It follows from (7-10) and (7-11) that the contribution to the displacement vector from mode m is

$$\{u\}_m = \Gamma_m \{\phi\}_m S_d = \Gamma_m \{\phi\}_m \frac{S_a}{\omega_m^2} \quad (7-13)$$

Moreover, the peak lateral inertia forces on the building contributed by mode m are given by

$$\{F\}_m = [M] \{\phi\}_m \Gamma_m S_a \quad (7-14)$$

and the resultant of these forces (the base shear) is given by

$$V_m = \frac{\overline{W}_m S_a}{g} \quad (7-15)$$

where \bar{W}_m is the m^{th} modal weight (or effective modal load)

$$\bar{W}_m = \frac{\left(\sum_{i=1}^N w_i \phi_{im} \right)^2}{\sum_{i=1}^N w_i \phi_{im}^2} = \Gamma_m \left(\sum_{i=1}^N w_i \phi_{im} \right) \quad (7-16)$$

It may be shown that

$$\sum_{m=1}^N \bar{W}_m = \sum_{i=1}^N w_i = W \quad (7-17)$$

That is, the sum of the modal weights equals the total weight W of the building. Moreover, it may be shown that for any $i = 1$ to N

$$\sum_{m=1}^N \phi_{im} \Gamma_m = 1 \quad (7-18)$$

Hereafter the mode shapes $\{\phi\}_m$ are normalized so that ϕ_{im} is equal to 1 at the roof level. Under this condition it can be shown that

$$\sum_{m=1}^N \Gamma_m = 1 \quad (7-19)$$

Equations (7-17) to (7-19) allow for a theoretically consistent simple definition of a residual mode that could approximately account for the contribution of the higher modes of vibration. Specifically, the equivalent lateral force procedure described herein will utilize the contribution from the first mode and a residual mode of which the associated frequency is arbitrarily selected but the modal weight, modal participation factor and mode shape are determined on the basis of (7-17) to (7-19):

$$\bar{W}_R = W - \bar{W}_1 \quad (7-20)$$

$$\Gamma_R = I - \Gamma_I \quad (7-21)$$

$$\{\phi\}_R = \frac{I}{\Gamma_R} \{I\} - \frac{\Gamma_I}{\Gamma_R} \{\phi\}_I \quad (7-22)$$

It may be easily shown that the residual mode shape $\{\phi\}_R$, as defined by (7-22), satisfies the orthogonality conditions.

7.4 Viscous Damping Ratio of Elastic Building

Consider an elastic building with linear viscous damping devices. The damped system is non-classically damped and its frequencies (eigenvalues) and mode shapes (eigenvectors) are not those determined by eigenvalue analysis of the undamped system. Nevertheless, the use of the undamped frequencies and mode shapes together with energy-based calculation of the damping ratios may provide good estimates of the seismic response of damped structures. This is particularly true for buildings with complete vertical distributions of viscous damping devices (Constantinou and Symans, 1992). It may also be valid for cases of incomplete vertical distributions or cases of concentration of damping devices. A case of validity of this approach is in the approximate analysis of soil-structure interaction effects (Veletsos and Meek, 1973; Novak and El Hifnawy, 1983), whereas Constantinou and Symans (1992) demonstrated the validity of the approach in some cases of incomplete vertical distribution of damping devices.

The force-velocity relation of each linear viscous damping device is described by

$$F_{Dj} = C_j \dot{u}_{Dj} \quad (7-23)$$

where C_j is the damper coefficient, u_{Dj} is the device relative displacement and \dot{u}_{Dj} is the relative velocity between the ends of the device along the axis of the device. Moreover, the relation between the device relative displacement and the interstory drift Δ_{rj} is

$$u_{Dj} = f_j \Delta_{rj} \quad (7-24)$$

where f_j is the displacement magnification factor. This factor equals unity for the chevron brace configuration and equals $\cos \theta_j$ for the diagonal configuration, where θ_j is the angle of inclination

of device j (FEMA, 1997; Constantinou et al., 1998). Figure 7-2 shows different installations of damping devices for which the displacement amplification factors can be larger than unity (Constantinou and Sigaher, 2000).

Modal damping ratios in a building can be calculated using (4-15). If it is assumed that a building undergoes harmonic vibration such that

$$\{u\} = D_{roof} \{\phi\}_m \sin\left(\frac{2\pi t}{T_m}\right) \quad (7-25)$$

where D_{roof} is the amplitude of roof displacement; T_m is the undamped m^{th} period of vibration; and $\{\phi\}_m$ is the m^{th} undamped mode shape (normalized so that $\phi_{im} = 1$ for i corresponding to the roof displacement), the energy dissipated by the damping system per cycle of motion in mode m is

$$W_D = \frac{2\pi^2}{T_m} \sum_j C_j f_j^2 D_{roof}^2 \phi_{rj}^2 \quad (7-26)$$

where

$$\phi_{rj} = \phi_{jm} - \phi_{(j-1)m} \quad (7-27)$$

is the difference between the m^{th} modal ordinates associated with degrees of freedom j and $(j-1)$. Note that (7-26) is based on $\Delta_{rj} = D_{roof} \phi_{rj}$. The maximum strain energy W_s is equal to the maximum kinetic energy,

$$W_s = \frac{2\pi^2}{T_m^2} \sum_i \left(\frac{w_i}{g}\right) D_{roof}^2 \phi_{im}^2 \quad (7-28)$$

and the viscous damping ratio in mode m is given by

$$\beta_{vm} = \left(\frac{T_m}{4\pi} \right) \frac{\sum_j C_j f_j^2 \phi_{rj}^2}{\sum_i \left(\frac{w_i}{g} \right) \phi_{im}^2} \quad (7-29)$$

where summation over i extends over all reactive weights and summation over j extends over all damping devices. Equation (7-29) is identical to that given in Constantinou et al. (1998) except that the displacement amplification factor f_j is used in lieu of $\cos \theta_j$.

Consider now the case of nonlinear viscous damping devices for which

$$F_{Dj} = C_{Nj} |\dot{u}_{Dj}|^{a_j} \text{sgn}(\dot{u}_{Dj}) \quad (7-30)$$

where C_{Nj} is the damper coefficient and a_j is the damper exponent. Equation (4-15) may still be used to calculate damping ratio, but the ratio will be amplitude-dependent. Assuming vibration in accordance with (7-25),

$$W_D = \sum_j \left(\frac{2\pi}{T_m} \right)^{a_j} C_{Nj} \lambda_j (D_{roof} f_j \phi_{rj})^{1+a_j} \quad (7-31)$$

where λ_j is given by (4-14) as function of the exponent a_j (see Table 4-2). Using (7-28) which is still valid, the damping ratio for mode m equal to 1 is given by

$$\beta_{v1} = \frac{\sum_j (2\pi)^{a_j} \cdot T_1^{2-a_j} \cdot \lambda_j C_{Nj} f_j^{1+a_j} D_{roof}^{a_j-1} \phi_{rj}^{1+a_j}}{8\pi^3 \sum_i \left(\frac{w_i}{g} \right) \phi_{i1}^2} \quad (7-32)$$

Equation (7-32) reduces to (7-29) when $a_j = 1$ (linear viscous damping devices, for which $\lambda_j = \pi$).

Equations (7-29) and (7-32) are utilized for the simplified analysis of yielding damped buildings by replacing period T_1 by the effective period T_{eff} . Details are presented in the next section.

7.5 Effective Period and Effective Damping of Yielding Buildings with Damping Systems

7.5.1 Buildings with Linear Viscous Damping Systems

For a multi-degree-of-freedom building, conversion of the pushover curve to an elastoplastic spectral capacity curve (see Fig. 2-1) results in:

$$A = A_y = \frac{V_y g}{W_1} \quad (7-33)$$

$$D_y = \frac{A_y T_1^2}{4\pi^2} = \frac{D_{yR}}{\Gamma_1} \quad (7-34)$$

where V_y is the yield strength established by pushover or plastic analysis using a pattern of lateral loads proportional to the first mode shape of the building for elastic conditions, D_y is the yield displacement in the elastoplastic spectral capacity curve, D_{yR} is the yield displacement in the elastoplastic pushover curve (the subscript R denotes roof displacement) and Γ_1 is the first mode participation factor. The effective period (in the first mode of vibration) is given by (4-18), which on the basis of (7-33) and (7-34) becomes

$$T_{eff} = T_1 \sqrt{\mu} \quad (7-35)$$

where T_1 is the first mode period for elastic conditions and μ is the displacement ductility ratio

$$\mu = \frac{D}{D_y} \quad (7-36)$$

Similarly, the effective damping is given by (4-19) but simplified to

$$\beta_{eff} = \beta_i + \beta_{v1} \sqrt{\mu} + \frac{2q_H}{\pi} \left(1 - \frac{1}{\mu} \right) \quad (7-37)$$

where β_{v1} is the damping ratio under elastic conditions given by (7-29) for m equal to 1. NEHRP (2000) utilizes (7-37) but replaces $(2/\pi)$ by $(0.64 - \beta_i)$ in order to avoid overestimation of the contribution of inherent damping.

Variables T_{eff} and β_{eff} are the effective period and damping in the first mode. Higher modes of the yielded building may be conservatively assumed to possess the properties of the higher modes of the elastic building. That is, the periods are equal to T_m and the damping ratios are given by

$$\beta_m = \beta_i + \beta_{vm} \quad (7-38)$$

where m ranges from 2 to N , and β_{vm} is given by (7-29). This is the approach followed in NEHRP (2000). Some improvement may be realized by approximately accounting for the softening of the building due to inelastic action through the use of $T_m\sqrt{\mu}$ as an estimate of the period of higher modes.

When a residual mode is used together with the first mode of vibration, the effective period of the residual mode may arbitrarily be assumed to be either T_2 , $T_2\sqrt{\mu}$ or some multiple of T_1 . In NEHRP (2000), T_R is set to be equal to $0.4T_1$. The effective damping in the residual mode may be conservatively assumed to be

$$\beta_R = \beta_i + \beta_{vR} \quad (7-39)$$

where β_{vR} is given by (7-29) with $m=R$.

7.5.2 Buildings with Nonlinear Viscous Damping Systems

Using information from Section 4.5, the effective period and effective damping of buildings with nonlinear viscous damping systems are described by equations (7-35) and (7-37), respectively, with β_{eff} equal to

$$\beta_{eff} = \beta_i + \beta_{v1}(\mu)^{1-\frac{a}{2}} + \frac{2q_H}{\pi} \left(1 - \frac{1}{\mu}\right) \quad (7-40)$$

where β_{v1} is the damping ratio determined from (7-32) for $m=1$ (note that calculation of β_{v1} requires knowledge of the roof displacement, D_{roof}) and all other terms were defined previously. Equation (7-40) also assumes that all devices have the same exponent $a_j = a$.

The calculation of the damping ratio in the higher modes or the residual mode is complicated by the fact that (7-32) is not applicable to higher modes. To circumvent this difficulty, Seleemah and Constantinou (1997) resorted to a physical interpretation of the higher mode response. They viewed higher mode response as small amplitude, high frequency motion centered around the first mode response. Accordingly, one could define an effective damping constant C_{eff} for each nonlinear viscous device as illustrated in Figure 7-3. This constant is taken as the slope of the force-velocity curve of the device at the calculated device velocity in the first mode, \dot{u}_1 :

$$C_{eff} = a_j C_{Nj} \dot{u}_1^{a_j-1} \quad (7-41)$$

Accordingly, the effective damping in the higher modes is given by

$$\beta_m = \beta_i + \beta_{vm} \quad \text{and} \quad \beta_R = \beta_i + \beta_{vR} \quad (7-42)$$

where β_{vm} and β_{vR} are calculated using (7-29) with C_{eff} in place of C_j .

7.5.3 Buildings with Viscoelastic Damping Systems

Viscoelastic damping systems exhibit stiffness and damping which are frequency-dependent (Soong and Dargush, 1997; Constantinou et al., 1998). Considering viscoelastic solid devices with bonded area A_b and total thickness h , the storage stiffness K_j and the damping constant C_j of a device are

$$K_j = \frac{G' A_b}{h} \quad , \quad C_j = \frac{G'' A_b}{\omega h} \quad (7-43)$$

where G' and G'' are the storage and loss shear moduli of the viscoelastic material, respectively, and ω is the excitation frequency. Both moduli are strongly frequency-dependent but their ratio η , the loss factor, is only mildly dependent on frequency:

$$\eta = \frac{G''}{G'} \quad (7-44)$$

Approximately, and for the purpose of simplified analysis calculations, η may be assumed to be equal to unity. A comprehensive database of material properties for a common viscoelastic material valid for a range of temperatures, shear strain and frequency may be found in Zimmer (1999).

Evidently, simplified analysis of buildings with viscoelastic damping systems requires that: (1) the frequency of vibration in each mode is known in order to calculate the storage stiffness and damping constant of each device, and (2) the storage stiffness of each device is included in the mathematical model of the building. The additional stiffness provided by the viscoelastic damping system alters the pushover curve of the building as shown schematically in Figure 7-4. Appendix D presents an example of the analysis of a building with a viscoelastic damping system in which a simple procedure for constructing the idealized pushover curve of the damped structure is presented.

The application of the simplified analysis procedure requires iterative analysis (even under elastic conditions) since the values of storage stiffness and damping constant are frequency-dependent. A reasonable estimate of the first mode period of the damped building under elastic conditions may be obtained as follows. Let the first-mode period of the building without the damping system be T'_1 , and the period with the damping system be T_1 . Let the first mode of vibration be $\{\phi\}_1$ and let assume that the mode remains the same after adding the damping system. This assumption would be approximately valid in damping systems with a complete vertical distribution of devices that have storage stiffness distributed approximately in proportion to the shear stiffness of the stories. It follows that

$$T'_1 = 2\pi \left(\frac{\sum_i w_i \phi_i^2}{g \sum_j K'_j \phi_{rj}^2} \right)^{1/2} \quad (7-45)$$

$$T_1 = 2\pi \left(\frac{\sum_i w_i \phi_i^2}{g \sum_j (K'_j + K_j \cos^2 \theta_j) \phi_{rj}^2} \right)^{1/2} \quad (7-46)$$

where w_i , ϕ_i are defined in Section 7.3 and ϕ_{rj} in Section 7.4, K'_j is the shear stiffness of story j , K_j is the storage stiffness of devices in story j , and θ_j is the angle of inclination of devices in story j . Stiffness K_j may be written on the basis of (7-43) as

$$K_j = \frac{2\pi C_j}{\eta T_1} \quad (7-47)$$

Use of (7-45), (7-46) and (7-47) results in

$$\frac{1}{T_1^2} = \frac{1}{T_1'^2} + \frac{2}{T_1'^2 \eta} \left\{ \frac{T_1 \sum_j C_j \cos^2 \theta_j \phi_{rj}^2}{4\pi \sum_i \left(\frac{w_i}{g} \right) \phi_i^2} \right\} \quad (7-48)$$

The quantity within the brackets in (7-48) is recognized to be damping ratio under elastic conditions, β_{v1} (see eq.7-29). Accordingly

$$T_1 = T_1' \left(1 - \frac{2\beta_{v1}}{\eta} \right)^{1/2} \quad (7-49)$$

Equation (7-49) is particularly useful in obtaining quick estimates of the period of viscoelastically damped structures (given that $\eta \approx 1$).

When the viscoelastically damped building undergoes inelastic action, the idealized spectral capacity curve is shown in Figure 7-4. The effective period is given by (4-18), which for the bilinear representation of the spectral capacity curve takes the form:

$$T_{eff} = T_1' \left(1 - \frac{2\beta_{v1}}{\eta} \right)^{1/2} \left(\frac{\mu}{1 + \alpha\mu - \alpha} \right)^{1/2} \quad (7-50)$$

where $\mu = D/D_y$ is the displacement ductility ratio, and α is the ratio of the post-elastic stiffness and the elastic stiffness of the viscoelastically damped building.

Similarly, the effective damping is given by (4-19), which now takes the form:

$$\beta_{eff} = \beta_i + \beta_{vl} \left(\frac{\mu}{1 + \alpha\mu - \alpha} \right)^{1/2} + \frac{2q_H}{\pi} \left(\frac{1}{1 + \alpha\mu - \alpha} - \frac{1}{\mu} \right) \quad (7-51)$$

Typically, μ will be less than 1.5 and α will be less than 0.2, and quantity $(1 + \alpha\mu - \alpha)$ can be replaced by unity with little error. This allows the use of equations that are valid for the elastoplastic representation of the pushover curve, as done for the viscous damping systems.

It is of interest to obtain an estimate for the stiffness ratio α . On the basis of Figure 7-4 (consider that the spectral capacity curves are obtained from pushover curves that are established by pushing over with loads proportional to the first mode shape)

$$\frac{T_1}{T_1'} = \left(\frac{K_e'}{K_e} \right)^{1/2} = \left(\frac{K_e - \alpha K_e}{K_e} \right)^{1/2} \quad (7-52)$$

Note that (7-52) was derived on the basis of the observation that the added stiffness by the damping system is αK_e . Use of (7-49) and (7-52) results in

$$\alpha = \frac{2\beta_{vl}}{\eta} \quad (7-53)$$

NEHRP (2000) does not contain specific procedures for viscoelastic damping systems. Rather, allows for the use of procedures which are valid for linear viscous damping systems. As explained in this section, and in more detail in Appendix G, the approach of NEHRP (2000) may be used for viscoelastic damping systems provided that the effect of the damping system on the stiffness and strength of the building is accounted for.

7.5.4 Building with Yielding Damping Systems

The pushover curve of a building with a yielding damping system is approximately trilinear as shown in Figure 4-3. The idealized spectral capacity curve of the building is illustrated in Figure 7-5. In this figure, V_y is the yield strength (or base shear strength) of the building excluding the yielding damping system, and V_d is the added yield strength due to the yielding damping system. The shape of the idealized trilinear spectral capacity curve is based on the assumption that the

damping system yields prior to the yielding of the framing system (i.e., $V_d < V_y$ and $D_{yd} < D_{yf}$). Note that the strength V_d is due to the yielding damping devices in the first story, whereas the contribution of the other damping devices to the pushover and spectral capacity curves is reflected in the initial branch of the trilinear curve.

The effective period and effective damping are given by the following equations, which are valid for displacement D greater than D_{yf} (see Figure 7-5):

$$T_{eff} = 2\pi \left(\frac{D}{A_y + A_d} \right)^{1/2} \quad (7-54)$$

$$\beta_{eff} = \beta_i \left(\frac{1}{1 + A_d/A_y} \right)^{1/2} + \frac{2q_H \left(1 - \frac{1}{\mu_f} \right) + 2 \left(\frac{A_d}{A_y} \right) \left(1 - \frac{1}{\mu_d} \right)}{\pi \left(1 + A_d/A_y \right)} \quad (7-55)$$

where μ_f and μ_d are the displacement ductility ratio for the frame and the damping system, respectively, which are defined as follows::

$$\mu_f = \frac{D}{D_{yf}} \quad , \quad \mu_d = \frac{D}{D_{yd}} \quad (7-56)$$

Use of (7-54) and (7-55) requires the construction of a trilinear representation of the pushover curve of the building inclusive of the yielding damping system. For well-behaved framing systems, plastic analysis can be used to construct the pushover curve, as described in Appendix D.

It is convenient to define an elastoplastic representation of the spectral capacity curve as shown in Figure 7-5. Accordingly,

$$T_{eff} = T_1 \sqrt{\mu} \quad (7-57)$$

$$\beta_{eff} = \beta_i + \frac{2q_H}{\pi} \left(1 - \frac{1}{\mu} \right) \quad (7-58)$$

$$\mu = \frac{D}{D_y} \quad (7-59)$$

where T_I is the initial effective period calculated using the initial slope of the elastoplastic spectral capacity curve:

$$T_I = 2\pi \left(\frac{D_o}{b(A_y + A_d)} \right)^{1/2} \quad (7-60)$$

where b is a parameter so that the elastoplastic curve best represents the trilinear curve, D_o is the spectral displacement at the intersection of the trilinear and the elastoplastic representation of the pushover curve and other terms have been defined previously.

Moreover, the yield displacement is given by

$$D_y = \frac{g \cdot (A_y + A_d) \cdot T_I^2}{4\pi^2} \quad (7-61)$$

Parameter b may be taken equal to 0.6 in consistency with a similar approach followed in FEMA (1997) or it may be obtained by use of the “equal energy” approach.

7.6 Quality Factor, q_H

By definition, the quality factor q_H (called the hysteresis loop adjustment factor in NEHRP, 2000) is equal to the actual area of the hysteresis loop (consider this to be the base shear-roof displacement loop converted to spectral capacity form) divided by the area of the assumed elastoplastic representation of the loop. The actual area of the hysteresis loop is not known but can be assumed on the basis of the “quality” of the structural system. Presumably a steel special moment frame designed and constructed using of current seismic provisions would have very good hysteretic characteristics, so that q_H should be close to unity. However, an older non-ductile building would be assigned a smaller value of q_H , say 0.2 as is recommended in FEMA (1997).

Another approach to selecting values for the quality factor is by utilizing this factor to calibrate the simplified analysis procedure to predict the seismic base shear prescribed by the equivalent lateral force procedure for buildings without damping systems (NEHRP, 1997). Consider that the ground motion is described by the design response spectrum with parameters S_{DS} , S_{DI} and T_s per NEHRP (1997). Consider now a building without a damping system having a period T_I under elastic conditions, effective period T_{eff} and effective damping β_{eff} under inelastic conditions when subjected to the design ground motion. Assume that both T_I and T_{eff} are larger than T_s (period lies in the constant velocity region of the spectrum) and that the residual mode has period T_R that is less than T_s and damping ratio is equal to 0.05. Moreover, assume that the building exhibits elastoplastic behavior. The base shear can be calculated using (7-15) and using the SRSS combination rule:

$$V = \left\{ \left(\frac{\overline{W}_I S_{DI}}{T_{eff} B} \right)^2 + \left(\overline{W}_R S_{DS} \right)^2 \right\}^{1/2} \quad (7-62)$$

where \overline{W}_I and \overline{W}_R are given by (7-16) and (7-20), respectively, and B is the damping coefficient related to the damping ratio β_{eff} . The latter is given by

$$\beta_{eff} = \frac{2q_H}{\pi} \left(1 - \frac{1}{\mu} \right) \quad (7-63)$$

where μ is the displacement ductility ratio. The effective period is given by (7-35).

Equation (7-62) predicts the base shear strength of the building, V_y . The base shear strength may be predicted by multiplying the seismic base shear prescribed in NEHRP (1997) by the system overstrength factor Ω_o :

$$V_y = \frac{S_{DI} \overline{W}}{T_I R} \Omega_o \quad (7-64)$$

in which the importance factor has been ignored. Equating (7-62) and (7-64), using (7-35) and recognizing that $\mu = R_\mu = R/\Omega_o$ since T_I and $T_{eff} > T_s$, results in the following equation for B :

$$B = \left\{ \left(\frac{W}{\bar{W}_I} \right)^2 \left(\frac{\Omega_0}{R} \right) - \left(\frac{\bar{W}_R}{\bar{W}_I} \right)^2 \left(\frac{S_{DS}}{S_{DI}} \right)^2 \left(\frac{R}{\Omega_0} \right) T_I^2 \right\}^{-1/2} \quad (7-65)$$

The damping coefficient B may be related to the effective damping by empirical equations of the kind of (3-4). However, the following simple equation approximates very well the relation between B and β_{eff} in NEHRP (2000) and is used herein:

$$B = 0.73 + 3.27 \beta_{eff} \quad (7-66)$$

Substitution of (7-66) and (7-63) with $\mu = R_\mu = R/\Omega_0$ in (7-65) and recognizing that $S_{DI}/S_{DS} = T_s$, results in the following equation for q_H :

$$q_H = \frac{\left\{ \left(\frac{W}{\bar{W}_I} \right)^2 \left(\frac{\Omega_0}{R} \right) - \left(\frac{\bar{W}_R}{\bar{W}_I} \right)^2 \left(\frac{T_I}{T_s} \right)^2 \left(\frac{R}{\Omega_0} \right) \right\}^{-1/2} - 0.73}{2.08 \left(1 - \frac{\Omega_0}{R} \right)} \quad (7-67)$$

Equation (7-67) reveals a complex relation between q_H the ductility-based portion of the R -factor, $R_\mu = R/\Omega_0$, period ratio T_I/T_s and some general dynamic characteristics of the structure. As an approximation, $W/\bar{W}_I \approx 1.33$ and $\bar{W}_R/\bar{W}_I \approx 0.33$ (see Constantinou, 1998), so that q_H is primarily related to T_I/T_s and R/Ω_0 . Moreover, (7-67) sometimes predicts either complex values or values larger than unity. For such cases q_H should be set equal to unity. Accordingly,

$$q_H \approx \frac{\left\{ 1.77 \left(\frac{\Omega_0}{R} \right) - 0.11 \left(\frac{T_I}{T_s} \right)^2 \left(\frac{R}{\Omega_0} \right) \right\}^{-1/2} - 0.73}{2.08 \left(1 - \frac{\Omega_0}{R} \right)} \leq 1.0 \text{ for } T_I \geq T_s \quad (7-68)$$

Equation (7-68) predicts values of q_H which increase with increasing values of (R/Ω_0) , which is proper. However, the dependency of q_H on the period ratio T_I/T_s is complicated by the fact that large values of this ratio result in complex values of the damping coefficient B . The problem

may be traced to (7-62), in which the contribution of the residual mode $\overline{W}_R S_{DS}$ is larger than the base shear strength given by (7-64). That is, the simplified method of analysis overpredicts the base shear force.

An equation similar to (7-68) may be derived for T_1 , T_{eff} and T_R less than T_s . In this case the displacement ductility ratio is given by (7-6) so that

$$q_H \approx \frac{\left\{ 1.77 \left(\frac{\Omega_0}{R} \right) - 0.11 \right\}^{-1/2} - 0.73}{2.08 \left\{ 1 - 2 \left(1 + \frac{R^2}{\Omega_0^2} \right)^{-1/2} \right\}} \leq 1.0 \text{ for } T_1 < T_s \quad (7-69)$$

Equations (7-68) and (7-69) have been used to prepare Table 7-1, in which $(R/\Omega_0 I)$ has been used instead of (R/Ω_0) . It is apparent that a simple rule to describe the dependency of q_H on various parameters is not easy to develop. NEHRP (2000) utilizes a simple, highly approximate but conservative rule that relates q_H to T_1/T_s as follows.

$$0.5 \leq q_H = 0.67 \frac{T_s}{T_1} \leq 1.0 \quad (7-70)$$

The relation correctly predicts the trend towards $q_H = 1.0$ in the constant acceleration domain of the spectrum but is conservative for flexible structures.

7.7 Minimum Allowable Base Shear

The application of a simplified method of analysis requires that a minimum allowable base shear be specified. On the basis of the results presented in Section 6 of this report which were incorporated into NEHRP (2000), the minimum allowable base shear V_{min} for the design of the seismic-force-resisting system is

$$V_{min} = \frac{V}{B} \geq 0.75V \quad (7-71)$$

where V is the seismic base shear specified for a building without a damping system, and B is the damping coefficient for the damping ratio β_1 of the elastic building in the fundamental mode (the damping ratio β_1 includes the inherent damping and the added damping).

The limit $0.75V$ typically dictates the minimum strength for buildings with viscous or viscoelastic damping systems since $\beta_1 \geq 0.15$ and $B \geq 1.35$, and therefore $1/B \leq 0.74$. In buildings with yielding or hysteretic damping systems, the limit V/B may dictate design depending on the strength and yield displacement characteristics of the frame (exclusive of the damping system) and of the damping devices. One may then question the usefulness of a hysteretic damping system since the goal of drift reduction may be achieved by merely increasing the sections of the seismic-force-resisting system, an approach that is typically followed today. The addition of a hysteretic damping system will reduce displacements and increase building strength while limiting significant inelastic action to the damping system, which does not form part of gravity framing system. In the event of a major earthquake, only the dampers should be damaged (due to inelastic action). These dampers could be easily replaced after the earthquake with little or no impact on the gravity framing.

Equation (7-71) provides the seismic base shear, that is, the resultant of lateral forces acting on the building when the first plastic hinge forms. When the design of the seismic-force-resisting system is based on plastic analysis principles, the required base shear strength V_y is needed. On the basis of Section 7.2 (see Fig. 7-1), $V_y = V_{min}\Omega_0$. However, this equation would be valid if factors R and C_d were correctly specified to be equal (see Section 7.2). Until such inconsistency in the values of R and C_d is eliminated NEHRP (2000) presents equations which imply that

$$V_y = V_{min}\Omega_0 \frac{C_d}{R} \quad (7-72)$$

Equation (7-72) is used in the examples presented in Section 8 to arrive at the required base shear strength of the building. Plastic analysis principles are then used to size the seismic-force-resisting system to have base shear strength V_y and an acceptable collapse mechanism.

7.8 NEHRP (2000), Appendix to Chapter 13, Structures with Damping Systems

Appendix A contains the Appendix to Chapter 13 of NEHRP (2000) for the analysis and design of buildings with damping systems. This version of the Appendix was approved by the Provisions Update Committee in late 1999.

Appendix A describes two simplified analysis procedures: equivalent lateral force analysis procedure (ELF) and response spectrum-analysis-procedure (RSA). These procedures are largely based on the presentations of Sections 4 and 7 except as described below:

- (1) The calculated base shear in NEHRP (2000) is the base shear at the formation of the first plastic hinge, whereas equation (7-15) describes the base shear strength for the yielding building. Note that the design base shear is equal to the base shear strength divided by the system overstrength factor Ω_o . However, NEHRP (2000) divides by factor $\Omega_o C_d/R$ (see equations A13.4.3.4-1 and A13.4.3.4-2) to arrive at a conservative estimate of the base shear. This conservatism will be removed when C_d is specified equal to R .
- (2) NEHRP (2000) utilizes equations for the effective fundamental mode period and the effective damping which, strictly speaking, are valid for buildings with elastoplastic behavior and linear viscous damping systems. Valid equations for nonlinear viscous damping systems are presented in Section 7.5.2, viscoelastic damping systems in Section 7.5.3, and yielding damping systems in Section 7.5.4 and Appendix D.
- (3) NEHRP (2000) presents equations to calculate the roof displacement (e.g., equation A13.4.4.3-1) and accordingly defines the effective ductility as the ratio of the maximum roof displacement to the roof displacement at the effective yield of the seismic-force-resisting-system. Herein, the effective ductility demand (or displacement ductility ratio) is defined as the ratio of the maximum displacement to the effective yield displacement in the first mode spectral representation of the building. The two effective ductility demands are equal.
- (4) NEHRP (2000) replaces $(2/\pi)$ of equation (7-37) with $(0.64-\beta_i)$ in equation A13.3.2.2-1 allow for the direct addition of inherent damping ratio β_i in equation A13.3.2-2.

- (5) NEHRP (2000) utilizes pseudo-velocity to calculate the maximum velocity. Accordingly, velocities in the fundamental mode tend to be underestimated, whereas velocities in the higher modes tend to be overestimated (see Section 4.9 and Table 4-6). Examples presented in Section 8 indicate that after combination of the modal drift velocities, the error in the resultant drift velocity is significantly reduced. Analyses using the correction factors of Table 4-6 show only minor improvements in the prediction of velocity-dependent forces.
- (6) NEHRP (2000) utilizes the load combination factors CF_1 and CF_2 presented herein and described in (4-35), (4-39), (4-41) and (4-42) but defines them as force coefficients C_{mFD} and C_{mFV} , respectively, and presents them in tabular form.
- (7) NEHRP (2000) specifies maximum effective ductility demands (equations A13.3.5-1 and A13.3.5-2) that are consistent with (7-7) and (7-8) but uses $(R/\Omega_0 I)$ instead of (R/Ω_0) , where I is the occupancy importance factor. That is, the ductility-based portion of the R -factor and the maximum ductility demand are reduced for important structures.
- (8) NEHRP (2000) contains criteria for assessing the safety of the building, which include allowable story drift limits (Section A13.7.2). These limits are set equal to (R/C_d) times the allowable story drift for buildings without damping systems. The reason for this difference is that the values for R and C_d are not equal. Accordingly, the procedures described in NEHRP (2000) for buildings with damping systems predict the actual displacement response of the building, whereas the corresponding procedures for buildings without damping systems predict a smaller displacement since C_d is typically less than R . Accordingly, the specified drift limits for buildings are (C_d/R) times less than what the limits should be had the displacement prediction been correct. The NEHRP (2000) corrects for this discrepancy by increasing the drift limits by factor (R/C_d) .

7.9 Conclusions

The theoretical basis of the equivalent lateral force and the response spectrum analysis procedures of NEHRP (2000) has been presented. Moreover, procedures for calculating the effective damping and effective period, and the higher mode damping ratios for buildings with

nonlinear viscous damping systems, viscoelastic damping systems and yielding damping systems have been developed. These procedures are not presented in NEHRP (2000) but are needed for the application of the NEHRP (2000) analysis methods.

TABLE 7-1 Values of Quality Factor q_H predicted by Equations (7-68) and (7-69)

$R/\Omega_o I$ \ T_1/T_s	< 1	1	1.2	1.5	1.7	2.0	> 2.0
4/3	1.0	0.35	0.41	0.51	0.61	0.82	1.0
2	1.0	0.47	0.57	0.8	1.0	1.0	1.0
8/3	1.0	0.70	1.0	1.0	1.0	1.0	1.0
3	1.0	0.88	1.0	1.0	1.0	1.0	1.0
≥ 4	1.0	1.0	1.0	1.0	1.0	1.0	1.0

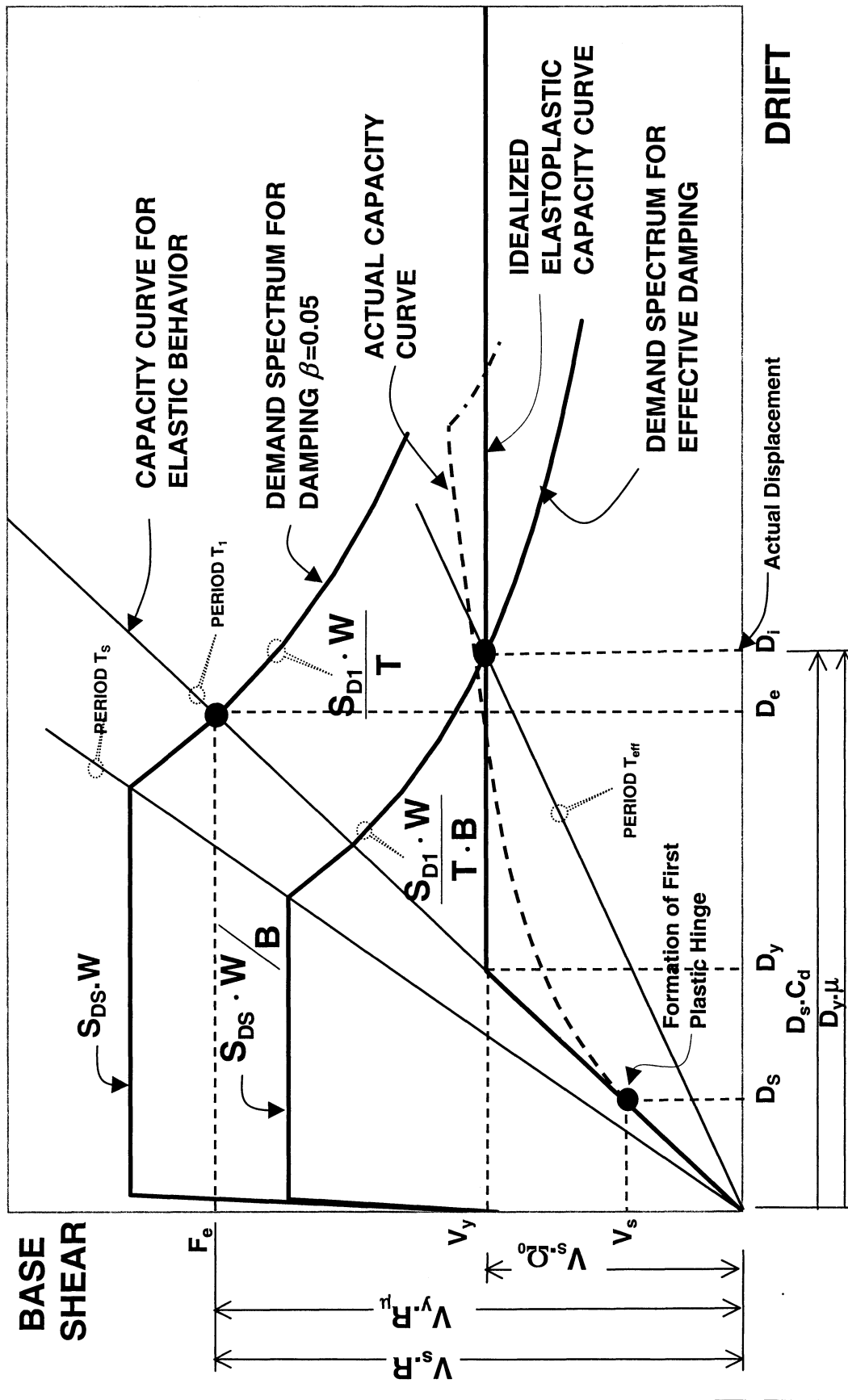


FIGURE 7-1 Structural Response and Relation Between Response Quantities

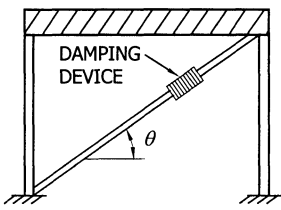
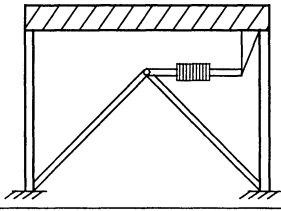
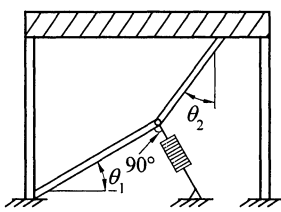
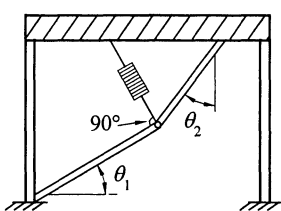
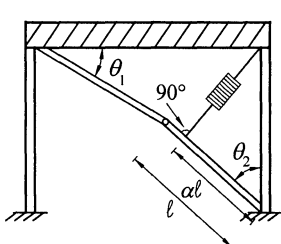
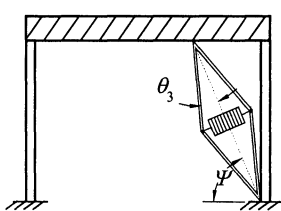
	CONFIGURATION	DISPLACEMENT AMPLIFICATION FACTOR
Diagonal		$f = \cos \theta$
Chevron		$f = 1.00$
Lower Toggle		$f = \frac{\sin \theta_2}{\cos(\theta_1 + \theta_2)}$
Upper Toggle		$f = \frac{\sin \theta_2}{\cos(\theta_1 + \theta_2)} + \sin \theta_1$
Reverse Toggle		$f = \frac{\alpha \cos \theta_1}{\cos(\theta_1 + \theta_2)} - \cos \theta_2$
Scissor-Jack		$f = \frac{\cos \psi}{\tan \theta_3}$

FIGURE 7-2 Displacement Amplification Factors for Various Damping System Configurations

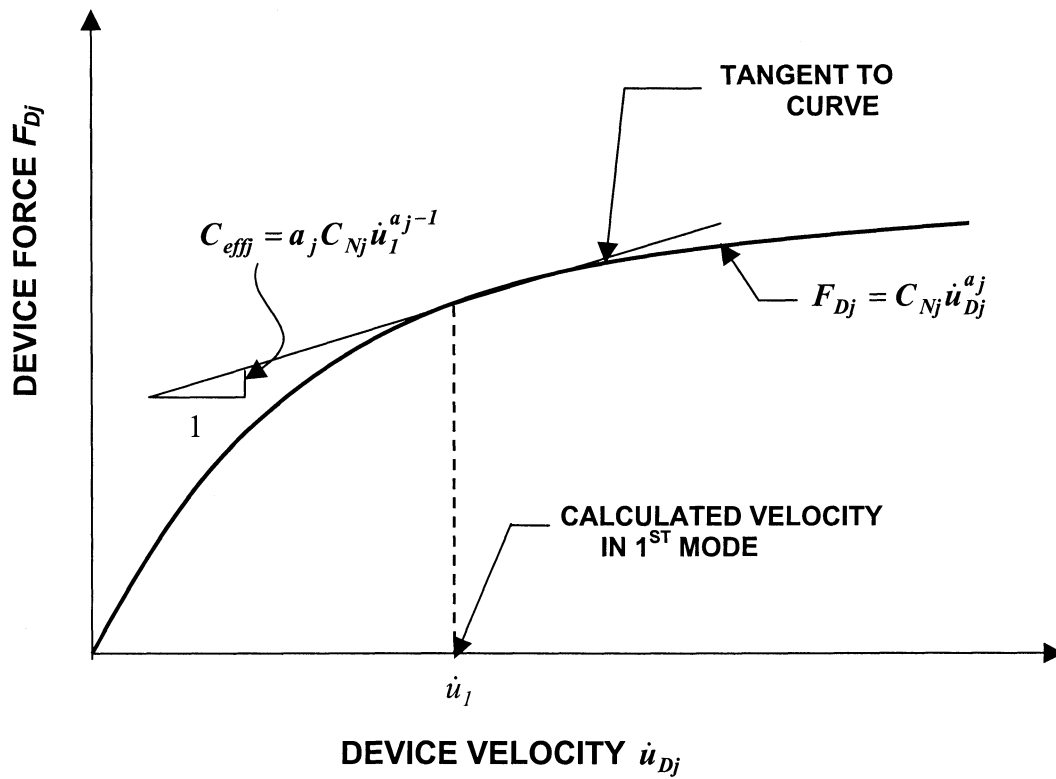


FIGURE 7-3 Effective Damping Constant of Nonlinear Viscous Damping Device for Higher Mode Response Calculation

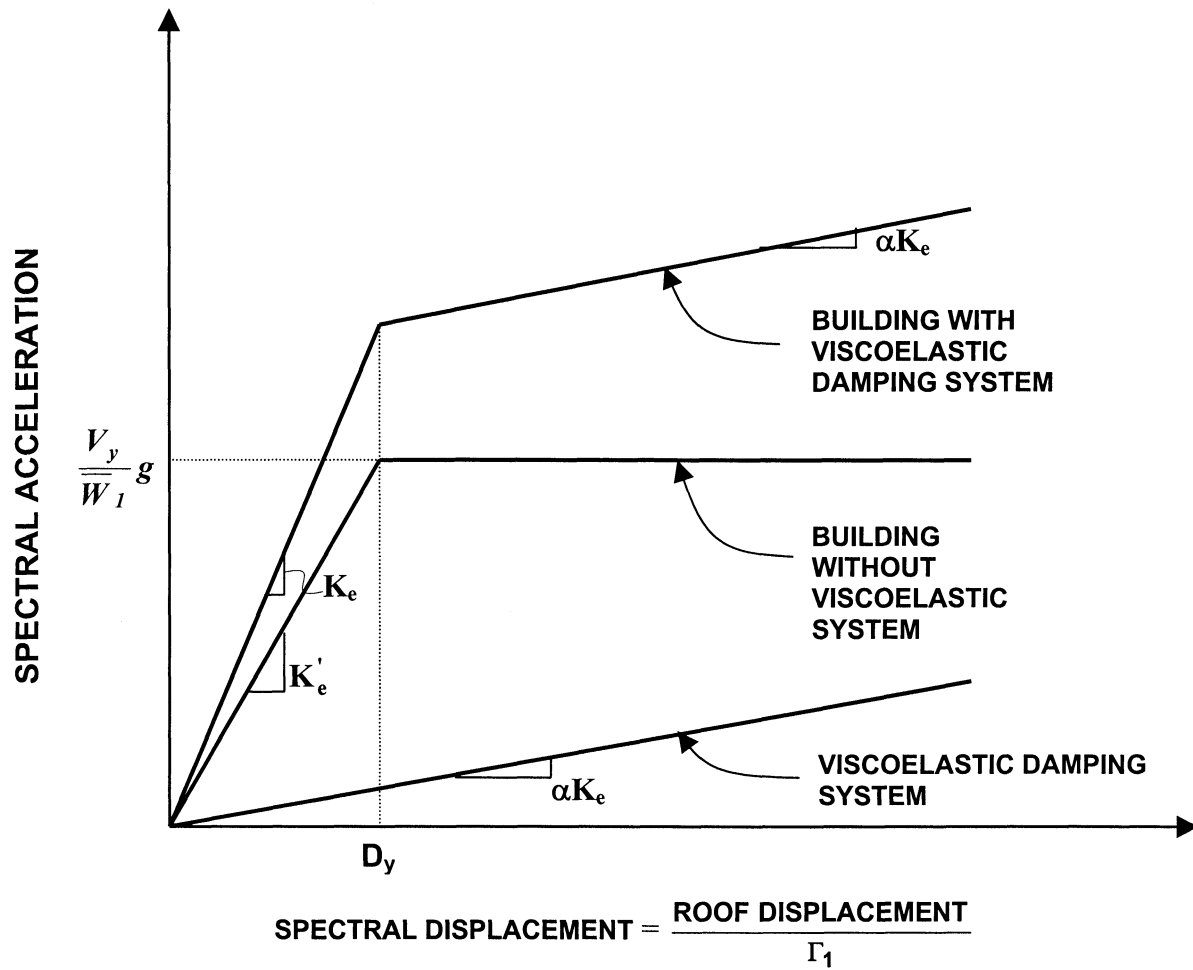


FIGURE 7-4 Idealized Spectral Capacity Curves of Building Without and With a Viscoelastic Damping System

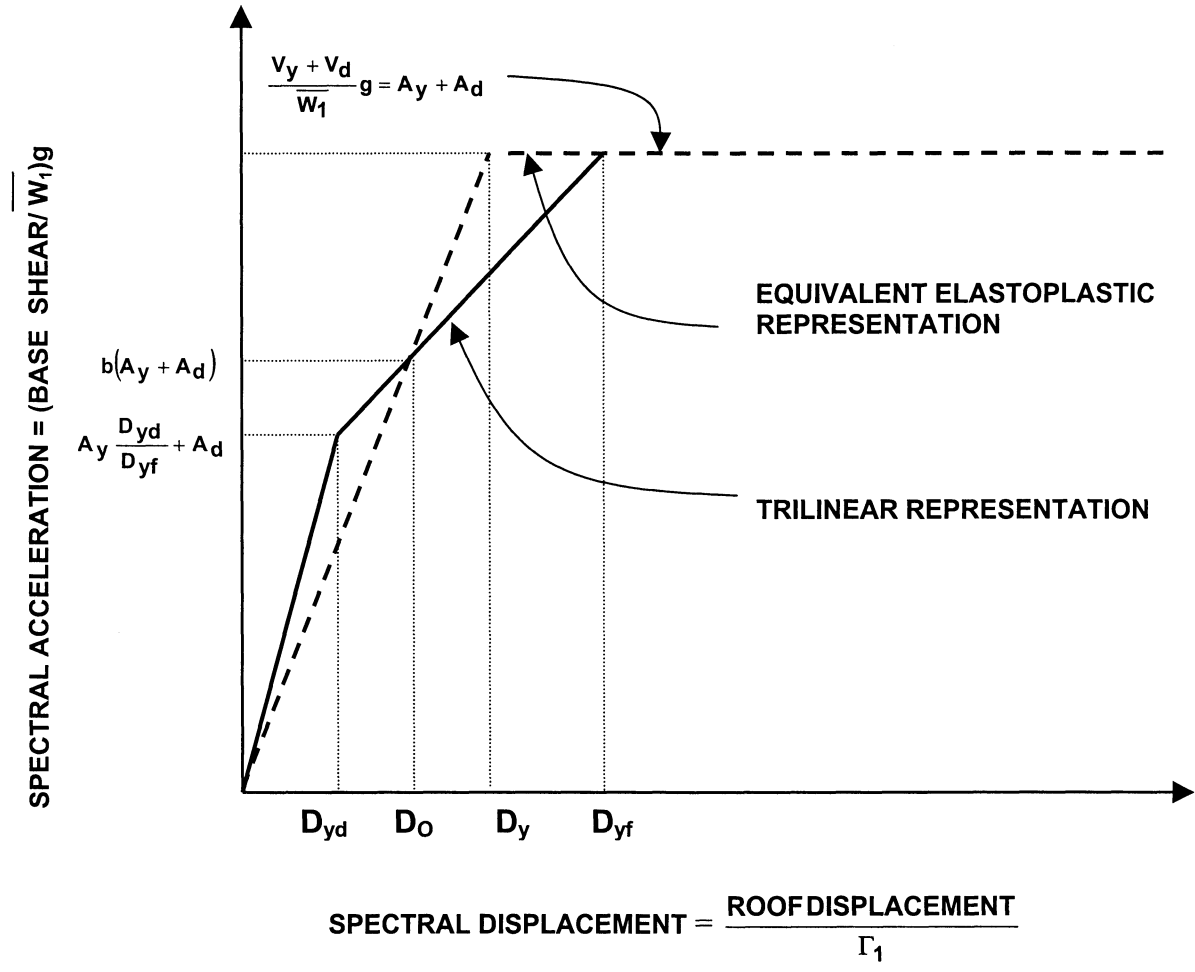


FIGURE 7-5 Idealized Trilinear and Equivalent Elastoplastic Spectral Capacity Curves of Building with a Yielding Damping

SECTION 8

EVALUATION OF METHODS OF ANALYSIS AND DESIGN OF BUILDINGS WITH DAMPING SYSTEMS

8.1 Introduction

This section presents examples of design and analysis of buildings with damping systems. The analyses were performed using the NEHRP (2000) equivalent lateral force and response-spectrum methods and the FEMA (1997) Method 2, except as modified below:

- (1) In the application of NEHRP (2000) and FEMA (1997) Method 2, the load combination factors CF_1 and CF_2 described by (4-35), (4-39), (4-41) and (4-42) were used instead either of the corresponding factors in FEMA (1997) and the force coefficients C_{mFD} and C_{mFV} listed in NEHRP (2000). This modification is of minor significance in the application of the NEHRP (2000) methods of analysis and it was done for convenience because it is easier to utilize equations rather than tables when the analysis is performed in a spreadsheet. However, the modification is of some significance for the calculation of the maximum acceleration using Method 2 of FEMA (1997).
- (2) In the application of the NEHRP (2000) methods of analysis, the procedures described in Section 7 for the calculation of the effective damping, the effective period and the added strength and stiffness were followed. The procedures described in NEHRP (2000) are valid for linear viscous damping systems and for viscoelastic and yielding damping systems provided that the strength and stiffness added by the damping system are included in the mathematical model but only approximate for nonlinear viscous damping systems.
- (3) The velocity correction factors presented in Section 4.10 were used in selected examples to demonstrate the significance of the correction procedure for multi-degree-of-freedom systems.

- (4) The pushover analysis required by Method 2 of FEMA (1997) was performed using the recommended modal and uniform distributions of lateral load, and additional distributions based on the first mode and the adaptive patterns.

The examples presented below involve three- and six-story special steel moment frame buildings with linear viscous, nonlinear viscous, viscoelastic and yielding damping systems installed in diagonal or chevron brace configurations. Each of these frames was designed based on the procedures of NEHRP (2000) to have a base shear strength of $0.6V_y$ to V_y , where V_y is defined in Table 8-1, and subsequently analyzed using the NEHRP (2000) and the FEMA (1997), Method 2 procedures. In all analyses, the seismic excitation was described by the response spectrum of NEHRP (1997) and FEMA (1997) with parameters $S_{DS} = 1.0$, $S_{D1} = 0.6$ and $T_s = 0.6$ sec. Each example building was also analyzed using nonlinear response history analysis using the twenty scaled motions presented in Section 3.2. The nonlinear response-history analysis data were used to study the usefulness and accuracy of the approximate methods of analysis.

8.2 Design of 3-Story and 6-Story Reference Frames

The reference frames were special steel moment frames in 3-story and 6-story buildings without damping systems. These frames were designed to meet the minimum base shear and drift limits of NEHRP (1997), Section 5.3. Later in this section, these frames are compared with the corresponding frames with damping systems to judge the benefits and drawbacks offered by the damping systems.

Appendix B presents a description of the geometry, the design parameters and loads for the example building. Figure B-1 shows the plan view and elevation of the building. The lateral force-resisting system is composed of two special steel moment frames in each direction. For such frames, NEHRP (1997) assigns $R = 8$, $C_d = 5.5$, and $\Omega_o = 3$. Also presented in Appendix B is the design of the 3-story and 6-story reference frames that satisfy the NEHRP drift limit $\Delta_d = 0.02 h_{sx}$, where h_{sx} is the story height. Torsional effects are not included in this study. The final designs are shown in Figures B-3 and B-4, for the 3-story and the 6-story reference frames, respectively.

The weight of the 3-story reference frame W_o is approximately 215 kN (48.4 kips), and the fundamental period of vibration T_o is 1.07 sec (determined from eigenvalue analysis using IDARC2D Version 5.0, Valles et al., 1996). The minimum required base shear strength of this frame V_y , that is, the design base shear V according to NEHRP (1997) times the factor $C_d \cdot \Omega_o / R$, is 1626 kN (366 kips). The actual base shear strength V_{yo} ranges between 2223 kN (500 kips) and 2775 kN (624 kips), depending on the distribution of lateral load (established using the plastic analysis approach of Appendix C, and confirmed by pushover analysis using program SAP-2000NL). That is, an overstrength ratio between 1.37 and 1.70 is obtained as a result of the drift limit criteria. The weight of the 6-story reference frame W_o is approximately 504 kN (113 kips) and has a fundamental period $T_o = 1.90$ sec. The minimum required strength V_y is 2108 kN (474 kips), and the actual strength V_{yo} ranges between 2748 kN (618 kips) and 3646 kN (820 kips) depending on the distribution of lateral load, which represents an overstrength ratio between 1.30 and 1.73.

8.3 Design of 3-Story and 6-Story Frames with Damping Systems

Frames with damping systems may be designed in accordance with NEHRP (2000) for a seismic base shear of not less than $0.75V$, where V is the seismic base shear for the frame without a damping system. Equivalently, frames with damping systems may be designed to have a base shear strength exclusive of the damping system not less than $0.75V_y$, where V_y is the base shear strength of the frame without a damping system designed for seismic base shear V in accordance with NEHRP (1997).

Frames were designed for the building shown in Figure 8-1, with heights of three and of six stories. These frames have base shear strength in the range of 60 to 100% of V_y . Subsequently, damping systems are added to these frames and proportioned in accordance to NEHRP (2000) to meet the drift criteria. Six frames were designed: five 3-story frames with approximate base shear strengths of 60, 75, 80, 90, and 100% of V_y , and one 6-story frame with base shear strength of 75% of V_y . These frames are classified as 3S-60, 3S-75, 3S-80, 3S-90, 3S-100 and 6S-75, respectively, in which the first number denotes the number of stories and the second number denotes the percentage ratio of the actual base shear strength of the damped frame exclusive of the damping system, V_{ya} , to the base shear strength of the frame without the damping system

designed for seismic base shear V in accordance with NEHRP (1997), V_y . In each case, the base shear strength of the frame was calculated by using the plastic analysis method described in Appendix C.

Table 8-1 presents a summary of the characteristics of the six frames. Information is presented in terms of strength ratios (V_{ya}/V_y and V_{ya}/V_{yo}), weight ratio (weight of damped frame to weight of reference frame, W/W_o), lateral drift ratio of the frame without the damping system (actual maximum drift to allowed drift, Δ_{max}/Δ_a), and the period ratio (fundamental period of the damped frame to period of the reference frame, T/T_o). The maximum story drift Δ_{max} was obtained by the procedures described in NEHRP, 1997. The data of Table 8-1 show that the base shear strengths of the frames with damping systems, V_{ya} , are substantially lower than the strengths of the reference frames that were designed to meet the NEHRP drift criteria. Ratios of V_{ya}/V_{yo} ranged between 0.44 for frame 3S-60 and 0.73 for frame 3S-100.

The frames exclusive of the damping systems do not meet the drift criteria of 1997 NEHRP (less than or equal to $0.02 h_{sx}$). Damping systems were designed for these frames to reduce drifts to acceptable levels. For example, frame 3S-75 with a linear viscous damping system that provides an added damping ratio of 0.10 in the first mode under elastic conditions meets the drift criteria of NEHRP (2000). The benefits offered by the damping system include (a) substantial reduction of the required strength of the frame, (b) lower floor and smaller foundations on average.

A total of nine examples utilizing the six frames of Table 8-1 were analyzed. The frames with the damping systems in these examples are illustrated in Figures 8-1 to 8-9 and are briefly described below:

- (1) Example No.1: frame 3S-60 with linear viscous damping system to provide 10% viscous damping ratio when assuming elastic frame behavior (Fig. 8-1). Detailed calculations are presented in Appendix E.
- (2) Example No.2: frame 3S-75 with linear viscous damping system to provide 10% viscous damping ratio when assuming elastic frame behavior (Fig. 8-2). Detailed calculations are presented in Appendices E and I.

- (3) Example No.3: frame 3S-90 with linear viscous damping system to provide 10% viscous damping ratio when assuming elastic frame behavior (Fig. 8-3). Detailed calculations are presented in Appendix E.
- (4) Example No.4: frame 3S-100 with linear viscous damping system to provide 20% viscous damping ratio when assuming elastic frame behavior (Fig. 8-4). Detailed calculations are not presented for this example.
- (5) Example No.5: frame 6S-75 with linear viscous damping system to provide 10% viscous damping ratio when assuming elastic frame behavior (Fig. 8-5). Detailed calculations are presented in Appendix E.
- (6) Example No.6: frame 3S-80 with nonlinear viscous damping system to provide 10% viscous damping ratio when assuming elastic frame behavior in the design basis earthquake (DBE) (Fig. 8-6). Detailed calculations are presented in Appendix F.
- (7) Example No.7: frame 3S-80 with nonlinear viscous damping system to provide 20% viscous damping ratio when assuming elastic frame behavior in the maximum considered earthquake (MCE) (Fig. 8-7). Detailed calculations are presented in Appendix F.
- (8) Example No.8: frame 3S-75 with viscoelastic solid damping system to provide 8.5% viscous damping ratio when assuming elastic frame behavior (Fig. 8-8). Detailed calculations are presented in Appendix G.
- (9) Example No.9: frame 3S-75 with metallic yielding damping system (Fig. 8-9). Detailed calculations are presented in Appendix H.

Appendices E through H present detailed calculations for the NEHRP (2000) simplified methods of analysis. Appendix I presents detailed calculations for the FEMA (1997) Method 2 (as modified herein) Example No.2 (3S-75 with linear viscous damping system).

8.4 Nonlinear Time History Analysis

Nonlinear time-history analysis was performed using Version 5.0 of program IDARC2D (Valles et al., 1996). Apart from the known capabilities of this program for the analysis of yielding systems, versions 4.0 and 5.0 of this program have enhanced capabilities for pushover analysis and elements for modeling the behavior of damping systems. These elements include a hysteretic element for modeling metallic yielding, friction, linear and nonlinear viscous, and Kelvin and Maxwell elements.

Viscous damping devices were directly modeled in program IDARC2D, Version 5.0 in their diagonal configurations, including the effect of the flexibility of the bracing to which these devices were attached. However, complexities arose in modeling viscoelastic and metallic yielding devices. Specifically:

- (1) The behavior of viscoelastic solid damping devices could not be directly modeled by the three-parameter model. This model is one of a spring of stiffness K_1 and of a Maxwell element with a spring of stiffness K_2 and a dashpot of constant C_2 in parallel as shown in Figure D-5. However, the program did not accept two elements connected to the same nodes. The problem was circumvented as shown in Figure 8-10. The utilized model captured correctly the behavior of the damping device in the horizontal direction but did not correctly account for the transfer of load from the devices to the frame. The latter was judged to be of significance only for the assessment of the safety of the frame. Moreover, the utilized model did not allow for the direct calculation of the peak force in the damping devices. Rather, force histories in each of the two branches of the element had to be exported to a spreadsheet and then added.
- (2) The chevron brace configuration could not be modeled in IDARC2D because the program produced erroneous results. Accordingly, the metallic yielding damping system was modeled as shown in Figure 8-11, which produced the correct lateral behavior but did not correctly account for the transfer of load from the devices to the frame. Again, this was judged to be of significance only for the safety assessment of the frame.

The frames of examples No.1 to 9 were analyzed as follows:

- (1) Examples No.1, 2, 3, 5, 6, 8 and 9 were analyzed for the design basis earthquake (DBE) and the maximum considered earthquake (MCE). The DBE consisted of the 20 scaled motions described in Section 3 and presented in Table 3-2. The MCE consisted of the DBE acceleration histories multiplied in amplitude by 1.5. Peak response quantities were obtained for each motion and values are presented for minimum, maximum, average, and average plus one standard deviation (1σ) responses.
- (2) Examples No.2 and No.4 were analyzed with selected near-fault ground motions to assess the validity of the NEHRP (2000) methods of analysis. The motions were the Sylmar 90 degree, and Newhall 360 degree motions from the 1994 Northridge earthquake, Pacoima Dam S16E motion from the 1971 San Fernando earthquake. These motions have strong near-fault characteristics with peak ground velocities of 0.77 m/s, 0.95 m/s and 1.1 m/s, respectively. The peak ground accelerations of these records were 0.6g, 0.59g and 1.17g, respectively. Examples No.2 and No.4 are used, together with the reference 3-story frame (illustrated in Fig. B-3), to study the extent of inelastic action and damage in frames with and without damping systems.
- (3) Example No.7 was analyzed only for MCE shaking since the design of the damping system was based on providing an effective damping ratio of 20% in this earthquake when elastic frame behavior is assumed.

8.5 Comparison of Results of Simplified Methods of Analysis to Results of Nonlinear Time History Analysis

Comparisons of results of the simplified methods of analysis to the results of nonlinear time-history analysis are presented in Tables 8-2 to 8-19. These tables present results obtained using the following procedures:

- (1) NEHRP(2000) Equivalent Lateral Force (ELF) and Response Spectrum Analysis (RSA) procedures. Each of these methods was applied per Section 8.1 and again with the modification of the higher mode periods calculated as $T_m\sqrt{\mu}$, where μ is the ductility demand calculated from the analysis of the first mode response.

- (2) Method 2 of FEMA (1997) as described in Section 8.1 using four different lateral force patterns. Of these patterns, two are described in FEMA (1997). The other two are one proportional to the first mode, and the second is an adaptive pattern where the lateral loads are adjusted during the pushover analysis on the basis of the calculated resistance of the various structural elements. It has been argued that the adaptive pattern of loads best captures the behavior of the yielding structure (Valles et al., 1996).

The presented results include:

- (1) Peak interstory drifts.
- (2) Peak interstory velocities.
- (3) Peak damper forces.
- (4) Story shear forces at the instance of maximum displacement (when velocities are zero).
- (5) Maximum story shears (including the viscous component).
- (6) Maximum floor accelerations.

The IDARC2D input files for the pushover and nonlinear time-history analysis are presented in Appendix K.

A study of the results in Tables 8-2 to 8-19 reveals the following:

- (1) The use of period $T_m\sqrt{\mu}$ instead of T_m for higher modes with NEHRP (2000) methods of analysis produces improved predictions of response compared with the average of the nonlinear time-history analysis. The improvement is primarily seen in the prediction of the shear force. For example, Table 8-3 presents results of the response spectrum analysis method for the story shear forces at maximum displacement as 871, 917 and 1458 kN when using period T_m . The prediction when using period $T_m\sqrt{\mu}$ is 629, 894 and 1218 kN. The average values of shear force in the nonlinear time-history analysis are 547, 985 and 1212 kN for the three stories.

- (2) The simplified procedures predict conservative estimates of story drift which consistently fall between average and the average plus 1σ results of the nonlinear time-history analysis.
- (3) The correction of pseudo-velocity by use of the factors of Table 4-6 improves the predictions of interstory velocity and damper force (see Tables 8-2 and 8-3). Although the improvement in the prediction is not significant, it appears that the correction is simple enough to implement so that its use is warranted. This is demonstrated in Tables 8-2 and 8-3 where values in bold were obtained by use of the revised velocity correction factors of Table 4-6.
- (4) The use of the adaptive load pattern in the application of Method 2 of FEMA(1997) did not produce any significant improvement in the prediction of the peak response over the use of the maximum among the responses predicted by use of the modal and uniform load patterns. Actually the use of the adaptive pattern resulted in a systematic underprediction of the maximum base shear (including the viscous component). This is best seen in Table 8-17 in which key design parameters are summarized.
- (5) The prediction of key design parameters such as the peak damper force and the maximum base shear force differs considerably among the various simplified methods of analysis. Table 8-17 presents a summary of these predictions for the MCE. However, despite these differences, the prediction is generally within 30% of the average of the nonlinear time history analysis. Such accuracy is most acceptable for simplified methods of analysis. Moreover, it is recognized that the predictions of the simplified methods deviate the most from the results of nonlinear time history analysis in the case of the 6-story structure.
- (6) The Equivalent Lateral Force method of NEHRP (2000) tends to overpredict the damper forces and frame member actions in the lower stories. This overprediction is primarily caused by the contribution of the residual mode to the total response. The residual mode shape (see eq. 7-22) has a substantial component associated with the displacements of the lower floors of the building (e.g., see values for one of the analyzed 3-story buildings in Table E-7 and for the analyzed 6-story building in Table E-10 of Appendix E). As seen in tables E-7 and E-10, the residual mode resembles second mode of vibration but has substantially larger modal displacements in the lower floors and larger modal weight. At the

same time this results in an under prediction of the response in the upper part of the building.

- (7) The simplified methods of analysis of NEHRP (2000) produce systematically conservative results on the story drift and results of acceptable accuracy on the damper forces and story shear forces (within 30%) in near-fault ground motions. As seen in Tables 8-18 and 8-19, there is no substantial improvement of the prediction of the simplified methods of analysis when the actual damped spectra of the near-fault motions are used. This provides some evidence that the damping coefficients in NEHRP (2000) apply to near-fault motions. However, the utilized near-fault motions and the analyzed structures are too few to provide definitive evidence on the validity of the simplified methods of analysis for near-fault motions.

8.6 Implications of Errors in the Calculation of Base Shear Strength

The base shear strength of the structure for a pattern of lateral loads proportional to the first mode is needed for the correct calculation of the contribution to the response by the first mode of vibration. Errors in the calculation of the base shear strength have effects which were investigated by analyzing the structures of examples No.1 and No.3 with incorrectly assumed base shear strength as follows:

- (1) Example No.1 with an assumed base shear strength of 1310 kN rather than the actual strength of 976 kN used in the analysis. The actual strength was close to the one calculated by the procedures of Appendix C and is presented in Appendix E, Section E-3.
- (2) Example No.3 with an assumed base shear strength of 991 kN rather than the actual strength of 1464 kN (see Appendix E, Section E-3).

Results for the Equivalent Lateral Force method are presented in part 3 of Table 8-20. Evidently, the displacement prediction is unaffected due to the fact that is controlled by the elastic displacement lower limit. Moreover, overprediction of strength results in underprediction of the ductility demand, but this will unlikely be of any significance since the ductility demand is typically well below the limit (NEHRP, 2000, Section A13.3.5 and Section 7.2 herein). It also results in overprediction of story shear forces, which is conservative. However, underprediction

of strength results in underprediction of story shear forces, and generally member actions, and overprediction of the ductility demand.

8.7 Effect of Viscous Damping Forces on Pushover Curve

It has been presumed in the analysis herein that the pushover curves of frames with viscous damping systems are identical to those exclusive of the damping system. This is an approximation, which likely introduces errors in the prediction of response by the simplified methods of analysis. For example, Figures 8-12 and 8-13 present calculated base shear force-first story drift loops for examples No.1 and No.2 using one of the 20 scaled motions adapted the nonlinear time-history analysis. The loops of the shear force exclusive of the damping component (dashed line in Figs. 8-12 and 8-13) do not show the expected bilinear hysteretic shape. Rather, they show a shape that closely resembles the loops for the total shear. This demonstrates that the pushover curve is affected by the viscous damping forces, likely by inducing rotations of the column ends. This phenomenon, which cannot be accounted for by the current methods of pushover analysis, affects the maximum value of member actions, which can be substantially underestimated.

8.8 Comparison of Pattern and Extend Damage in Frames without and with Damping Systems

The NEHRP (2000) procedures allow the strength of a building to be reduced below that of conventional construction if damping systems are added to the frame. For example, compare the frame of Figure B-3 (without damping devices) to the frame of Figure 8-2 (with linear viscous damping system). The two frames meet the drift and safety criteria of NEHRP (1997) and NEHRP (2000), respectively. As seen in Table 8-1, the frame with the damping system (3S-75) has a base shear strength (for a pattern of lateral loads proportional to the first mode) that is 55% of that of the frame without the damping system (referred to as the reference frame).

The pattern of plastic hinge formation and some key response quantities were investigated in (a) the reference 3-story frame (Fig. B-3), (b) the 3-story 3S-75 frame with linear viscous damping system (Example No.2, Fig. 8-2), and (c) the 3-story 3S-100 frame with linear viscous damping system (Example No.4, Fig. 8-4). It should be noted that case (b) is that of the damped frame

that just meets the NEHRP (2000) drift and safety criteria, whereas case (c) is a stronger and highly damped frame. This frame is more representative of a design for substantial improvement of performance. The frames were analyzed using the scaled Northridge Century, component 360 degrees of Table 3-2. This motion produced responses in the frames that were similar in value to the average responses calculated using the 20 scaled motions. Analysis were performed for the DBE (the scaled Northridge record) and then again for the MCE (same motion multiplied by factor 1.5). The three frames were then analyzed using the three near-fault motions: Sylmar 90 degrees, Newhall 360 degrees, and Pacoima Dam S16E.

Figures 8-14 through 8-19 present the results of these analyses. Each graph in these figures identifies the seismic excitation, presents key response quantities such as interstory drift ratios, peak roof displacements, base shear forces (including the damping component and peak plastic hinge rotations, and the location and sequence of formation of plastic hinges. Concentrating first on the performance of the frames in the DBE and the MCE, it is observed that:

- (1) Frame 3S-75 (Figure 8-15) with the damping system (that just meets the drift criteria of NEHRP) exhibits less drift, less plastic hinge rotation and substantially less base shear force than the reference frame without a damping system.
- (2) Frame 3S-100 (Figure 8-16) with the highly damped system performs better in both the DBE and the MCE than the lightly damped 3S-75 frame. However the performance in terms of drift ratios and the maximum plastic hinge rotation is only marginally better in the MCE.
- (3) The maximum DBE drift ratio of 0.028 (see Fig. 8-14) exceeds the limit of 0.02. This frame was designed using the equivalent lateral force method of NEHRP (1997), in which drift is calculated as the elastic displacement for the “reduced” lateral forces multiplied by the factor C_d . The actual drift is R/C_d times larger, that is, $0.02 \times R/C_d = 0.02 \times 8/5.5 = 0.029$.

For the near-fault earthquake motions, we observe that the lightly damped 3S-75 performs substantially better than the reference frame in the Pacoima motion, performs marginally better than the reference frame in the Newhall motion and performs worst in the Sylmar motion. The

highly damped 3S-100 frame outperforms the other two frames in terms of maximum displacements and the plastic hinge rotations.

Buildings designed with damping systems to meet the minimum criteria of NEHRP (2000) perform comparably to or better than buildings designed without damping systems to meet the minimum criteria of NEHRP (1997). Moreover, buildings with viscous damping systems offer the advantage of lower base shear force than conventional buildings without damping systems.

8.9 Conclusions

The simplified methods of analysis of NEHRP (2000) and Method 2 of FEMA (1997), as modified herein, provide systematically conservative predictions of drift, and predictions of acceptable accuracy for damper forces and member actions. These force predictions may differ by as much as $\pm 30\%$ from the average forces calculated by dynamic analysis. Interestingly, the simplified methods produced results of acceptable accuracy in near-fault seismic excitations. However, the utilized near-fault motions and analyzed structures were too few to provide conclusive evidence. Further studies with near-fault motions are warranted.

Buildings with damping systems designed to meet the minimum drift and strength criteria of NEHRP(2000) perform comparably to or better than conventional buildings without damping systems.

TABLE 8-1 Characteristics of Example Frames Exclusive of the Damping System

Frame	Number of Stories	Strength Ratio		Weight Ratio W/W_o	Drift Ratio* Δ_{max}/Δ_a	Period Ratio T/T_o
		V_{ya}/V_y	V_{yo}/V_{yo}			
3S-60	3	0.60	0.44	0.52	1.69	1.66
3S-75	3	0.75	0.55	0.57	1.50	1.48
3S-80	3	0.80	0.59	0.57	1.45	1.42
3S-90	3	0.90	0.66	0.70	1.27	1.29
3S-100	3	1.00	0.73	0.76	1.24	1.24
6S-75	6	0.75	0.58	0.60	1.35	1.37

Subscript "o" denotes property of the reference frame of Section 8.2.

Properties of reference frame of Section 8.2:

3-Story: $V_{yo}=2223 \text{ kN}$; $V_y= 1626 \text{ kN}$; $W_o=215 \text{ kN}$; $T_o=1.07 \text{ sec}$

6-Story: $V_{yo}=2748 \text{ kN}$; $V_y= 2108 \text{ kN}$; $W_o=504 \text{ kN}$; $T_o=1.90 \text{ sec}$

* Frames exclusive of the damping system do not meet the drift criteria.
Damping systems are added to meet the drift criteria.

Allowable story drift is $\Delta_a = 0.02 h_{sx}$

V_{yo} = base shear strength of reference frame (which meets the drift criteria)

V_{ya} = base shear strength of damped frame exclusive of damping system

V_y = base shear strength of frame without a damping system designed for base shear V in accordance with NEHRP (1997).

T = period of damped frame exclusive of damping system

TABLE 8-2 Comparison of Results of Simplified Methods of Analysis to Results of Nonlinear Time History Analysis. Case of Example No.1: 3-Story (0.60 V_y) with Linear Viscous Damping System. Analysis for the DBE

Response Quantity	SIMPLIFIED METHOD OF ANALYSIS											NONLINEAR TIME HISTORY ANALYSIS (IDARC 2D- Version 5.0)						
	NEHRP(2000)					METHOD 2 (FEMA 274)						Min.	Avg.	Max.				
	Higher Modes Using T_m		Higher Modes Using $T_m \sqrt{\mu}$			LATERAL FORCE PATTERN												
	ELF	RSA	ELF	RSA	mode 1	Cvx	Unif	Adpt	Avg. +1 σ	Max.								
Story Drift (mm.)	3	95	98	119	120	82	102	114	72	64	116	108	60	119	109	151	122	
Interstory Velocity (mm/sec)	3	367	364	509	441	355	362	524	461	527	489	537	498	569	542	554	529	690
	2	458	454	365	394	443	451	372	400	391	401	394	402	420	416	392	395	625
	1	405	359	290	277	383	354	298	285	263	253	257	243	274	259	261	250	520
Damper Force (kN)	3	261	259	361	313	252	257	372	327	374	347	381	353	404	384	393	375	492
	2	325	322	259	280	314	320	264	284	277	285	279	285	298	295	278	280	446
	1	287	255	206	197	272	251	211	202	187	180	182	172	195	184	185	177	371
Story Shear at Max. Disp. (kN)	3	510	642	849	1267	492	588	860	1172	516	515	579	883	1098	1357	494	901	734
	2	853	1221	1267	1267	849	860	1172	1140	895	883	1098	1357	494	901	901	901	1272
	1	1306	1221	1267	1267	1267	1267	1172	1140	1140	1136	1357	1357	1357	1357	1140	1140	1316
Max. Story Shear (kN)	3	572	566	727	706	551	548	685	664	626	611	629	614	698	688	618	607	849
	2	938	941	933	939	932	937	930	936	968	972	958	961	1174	1175	974	976	1286
	1	1338	1328	1246	1243	1291	1284	1201	1198	1164	1163	1156	1153	1385	1383	1161	1159	1795
Floor Acceleration (g)	3	0.365	0.361	0.464	0.451	0.352	0.350	0.437	0.424	0.400	0.390	0.402	0.392	0.446	0.439	0.394	0.387	0.577
	2	0.167	0.167	0.294	0.285	0.166	0.166	0.279	0.270	0.281	0.269	0.286	0.273	0.298	0.287	0.284	0.271	0.452
	1	0.402	0.387	0.301	0.293	0.370	0.357	0.275	0.266	0.286	0.277	0.302	0.292	0.297	0.287	0.291	0.281	0.551

Values in bold indicate results obtained using the revised velocity correction factors of Table 4-6.

TABLE 8-3 Comparison of Results of Simplified Methods of Analysis to Results of Nonlinear Time History Analysis. Case of Example No.1: 3-Story (0.60 V_y) with Linear Viscous Damping System. Analysis for the MCE

Response Quantity	S T O R Y	SIMPLIFIED METHOD OF ANALYSIS										NONLINEAR TIME HISTORY ANALYSIS (IDARC 2D- Version 5.0)						
		NEHRP(2000)					METHOD 2 (FEMA 274)					Min.	Avg.	Max.				
		Higher Modes Using T_m		Higher Modes Using $T_m \sqrt{\mu}$		LATERAL FORCE PATTERN			LATERAL FORCE PATTERN									
ELF	RSA	ELF	RSA	mode 1	Cvx	Unif	Adpt	mode 1	Cvx	Unif	Adpt	Avg.	+1σ					
Story Drift (mm.)	3	145	149	149	159	198	193	203	189	67	124	164	207					
	2	181	174	186	174	142	147	143	149	70	142	191	244					
	1	121	108	129	111	101	122	101	109	44	107	154	210					
Interstory Velocity (mm/sec)	3	497	494	725	619	452	484	704	636	735	737	699	690	683	695	741	919	
	2	620	616	461	514	563	604	491	533	496	495	464	472	544	540	511	728	835
	1	580	509	397	376	503	491	396	387	370	366	384	397	393	392	378	633	808
Damper Force (kN)	3	353	351	515	440	321	344	499	452	522	523	496	490	536	557	485	493	656
	2	440	437	327	365	400	429	349	379	352	351	329	335	386	383	365	363	596
	1	412	362	282	267	357	348	281	275	263	260	273	282	279	278	268	270	577
Story Shear at Max. Disp. (kN)	3	645	871	575	629	527	513	581	488	347	547	683	796					
	2	893	917	872	894	929	871	1103	899	725	985	1145	1503					
	1	1616	1458	1455	1218	1165	1105	1353	1112	912	1212	1355	1507					
Max. Story Shear (kN)	3	729	720	993	958	646	648	781	755	715	710	687	678	769	774	663	662	1004
	2	1021	1026	1011	1022	993	1006	997	1007	1029	1032	965	969	1210	1213	1003	1005	1505
	1	1652	1633	1482	1475	1455	1451	1260	1258	1205	1207	1158	1163	1404	1408	1162	1166	2176
Floor Acceleration (g)	3	0.465	0.459	0.634	0.611	0.412	0.413	0.499	0.482	0.456	0.453	0.439	0.433	0.491	0.494	0.423	0.423	0.688
	2	0.175	0.176	0.404	0.388	0.171	0.172	0.334	0.319	0.332	0.316	0.312	0.296	0.337	0.323	0.310	0.293	0.572
	1	0.599	0.577	0.446	0.433	0.484	0.472	0.339	0.325	0.340	0.324	0.306	0.291	0.326	0.308	0.315	0.296	0.763

Values in bold indicate results obtained using the revised velocity correction factors of Table 4-6.

**TABLE 8-4 Comparison of Results of Simplified Methods of Analysis to Results of Nonlinear Time History Analysis.
Case of Example No.2: 3-Story (0.75V_y) with Linear Viscous Damping System. Analysis for the DBE**

Response Quantity	S T O R Y	SIMPLIFIED METHOD OF ANALYSIS										NONLINEAR TIME HISTORY ANALYSIS (IDARC 2D- Version 5.0)			
		NEHRP(2000)					METHOD 2 (FEMA 274)					Min.	Avg.	Avg. +1σ	Max.
		Higher Modes Using T_m		Higher Modes Using $T_m \sqrt{\mu}$			LATERAL FORCE PATTERN								
		ELF	RSA	ELF	RSA	mode 1	Cvx	Unif	Adpt						
Story Drift (mm.)	3	88	89	88	91	115	98	101	100	39	82	104	114		
	2	104	99	105	100	90	104	99	103	40	92	120	137		
	1	71	62	72	63	54	59	61	57	25	63	85	103		
Interstory Velocity (mm/sec)	3	391	490	383	516	566	506	532	518	250	447	543	610		
	2	464	371	454	375	388	420	438	422	228	442	545	604		
	1	411	281	396	291	260	269	290	267	133	322	409	469		
Damper Force (kN)	3	312	391	305	411	452	404	424	413	199	357	434	487		
	2	370	296	362	299	309	335	350	336	182	353	436	483		
	1	328	224	316	232	208	215	231	213	106	257	327	375		
Story Shear at Max. Disp. (kN)	3	585	696	574	677	604	557	650	568	360	556	695	840		
	2	1046	1059	1043	1056	1093	1068	1308	1086	560	1055	1246	1458		
	1	1506	1424	1482	1408	1366	1340	1613	1362	694	1339	1568	1699		
Max. Story Shear (kN)	3	663	791	650	783	743	678	770	692	378	650	792	887		
	2	1139	1137	1136	1135	1176	1155	1394	1173	606	1182	1400	1464		
	1	1552	1458	1522	1442	1395	1370	1650	1391	800	1577	1897	2095		
Floor Acceleration (g)	3	0.423	0.505	0.415	0.500	0.474	0.433	0.491	0.442	0.254	0.437	0.529	0.588		
	2	0.203	0.320	0.202	0.315	0.312	0.311	0.335	0.316	0.170	0.324	0.406	0.504		
	1	0.414	0.303	0.392	0.292	0.291	0.293	0.284	0.302	0.181	0.355	0.479	0.609		

**TABLE 8-5 Comparison of Results of Simplified Methods of Analysis to Results of Nonlinear Time History Analysis.
Case of Example No.2: 3-Story (0.75V_y) with Linear Viscous Damping System. Analysis for the MCE**

Response Quantity	S T O R Y	SIMPLIFIED METHOD OF ANALYSIS										NONLINEAR TIME HISTORY ANALYSIS (IDARC 2D- Version 5.0)			
		NEHRP(2000)					METHOD 2 (FEMA 274)					Min.	Avg.	Avg. +1σ	Max.
		Higher Modes Using T _m		Higher Modes Using T _m √μ			LATERAL FORCE PATTERN								
		ELF	RSA	ELF	RSA	mode 1	Cvx	Unif	Adpt						
Story	3	132	133	134	143	152	150	157	155	58	118	156	179		
Drift (mm.)	2	156	149	159	150	146	151	146	148	59	131	166	187		
	1	106	94	112	96	103	103	97	95	37	96	133	176		
Interstory Velocity (mm/sec)	3	525	686	486	723	620	618	658	631	374	597	725	875		
	2	623	461	577	483	550	561	605	573	341	587	719	771		
	1	587	376	521	395	389	391	411	386	199	464	596	717		
Damper Force (kN)	3	419	547	388	577	495	493	525	503	299	477	579	699		
	2	497	368	460	385	438	448	483	457	272	469	575	616		
	1	468	300	416	315	310	312	327	308	159	370	476	573		
Story Shear at Max. Disp. (kN)	3	710	907	654	753	537	533	636	541	476	639	784	978		
	2	1074	1104	1061	1087	1088	1072	1323	1100	831	1183	1340	1592		
	1	1788	1630	1662	1482	1345	1331	1626	1364	1040	1487	1720	2254		
Max. Story Shear (kN)	3	818	1042	753	924	710	705	809	718	564	777	915	1088		
	2	1214	1210	1195	1199	1211	1199	1453	1230	907	1379	1580	1684		
	1	1846	1664	1692	1527	1408	1393	1690	1421	1198	1917	2242	2519		
Floor Acceleration (g)	3	0.522	0.665	0.480	0.590	0.453	0.450	0.516	0.458	0.380	0.525	0.618	0.740		
	2	0.211	0.426	0.207	0.382	0.339	0.341	0.369	0.347	0.255	0.417	0.514	0.613		
	1	0.615	0.446	0.519	0.373	0.346	0.350	0.368	0.375	0.272	0.506	0.664	0.811		

**TABLE 8-6 Comparison of Results of Simplified Methods of Analysis to Results of Nonlinear Time History Analysis.
Case of Example No.3: 3-Story (0.90V_y) with Linear Viscous Damping System. Analysis for the DBE**

Response Quantity	S T O R Y	SIMPLIFIED METHOD OF ANALYSIS										NONLINEAR TIME HISTORY ANALYSIS (IDARC 2D- Version 5.0)			
		NEHRP(2000)					METHOD 2 (FEMA 274)					Min.	Avg.	Avg. +1σ	Max.
		Higher Modes Using T_m		Higher Modes Using $T_m\sqrt{\mu}$			LATERAL FORCE PATTERN		LATERAL FORCE PATTERN						
		ELF	RSA	ELF	RSA	mode 1	Cvx	Unif	Adpt	mode 1	Cvx	Unif	Adpt		
Story	3	81	81	82	83	92	89	100	93	42	79	99	110		
Drift (mm.)	2	90	87	91	87	88	90	87	88	43	81	104	116		
	1	59	52	61	53	50	50	44	49	23	51	66	79		
Interstory Velocity (mm/sec)	3	410	481	417	499	511	503	561	494	276	439	531	577		
	2	456	372	464	375	418	424	465	408	263	414	500	598		
	1	396	267	409	275	260	262	265	251	143	287	352	380		
Damper Force (kN)	3	360	422	366	438	449	442	493	434	244	388	470	510		
	2	401	327	408	329	368	372	408	358	233	366	442	529		
	1	348	235	359	241	229	230	233	221	126	254	311	336		
Story Shear at Max. Disp. (kN)	3	675	775	667	761	651	645	786	593	445	687	830	983		
	2	1239	1255	1238	1253	1280	1268	1586	1174	805	1233	1441	1636		
	1	1734	1652	1714	1639	1572	1559	1911	1443	818	1604	1903	2219		
Max. Story Shear (kN)	3	767	878	762	871	783	775	927	726	474	747	889	1027		
	2	1339	1341	1339	1340	1375	1363	1688	1269	836	1396	1629	1680		
	1	1784	1688	1766	1676	1608	1596	1947	1478	883	1892	2284	2503		
Floor Acceleration (g)	3	0.489	0.560	0.486	0.556	0.500	0.494	0.591	0.463	0.320	0.493	0.583	0.666		
	2	0.238	0.350	0.237	0.346	0.336	0.337	0.371	0.316	0.172	0.381	0.477	0.582		
	1	0.434	0.314	0.423	0.305	0.296	0.295	0.328	0.297	0.200	0.387	0.520	0.691		

TABLE 8-7 Comparison of Results of Simplified Methods of Analysis to Results of Nonlinear Time History Analysis. Case of Example No.3: 3-Story (0.90V_y) with Linear Viscous Damping System. Analysis for the MCE

Response Quantity	S T O R Y	SIMPLIFIED METHOD OF ANALYSIS										NONLINEAR TIME HISTORY ANALYSIS (IDARC 2D- Version 5.0)			
		NEHRP(2000)					METHOD 2 (FEMA 274)					Min.	Avg.	Avg. +1σ	Max.
		Higher Modes Using T_m		Higher Modes Using $T_m\sqrt{\mu}$			LATERAL FORCE PATTERN								
		ELF	RSA	ELF	RSA	mode 1	Cvx	Unif	Adpt						
Story	3	121	122	125	131	147	143	155	156	63	114	146	164		
Drift (mm.)	2	135	130	139	130	129	133	125	129	66	118	152	171		
	1	88	78	96	81	74	73	72	67	35	79	107	129		
Interstory Velocity (mm/sec)	3	545	663	531	760	693	675	755	710	411	604	722	849		
	2	607	461	592	477	576	589	616	604	369	564	678	736		
	1	565	355	542	395	372	371	392	380	214	415	525	612		
Damper Force (kN)	3	479	582	467	667	609	593	663	624	364	534	638	751		
	2	533	405	520	419	506	517	541	531	326	498	600	651		
	1	496	312	476	347	327	326	345	334	189	367	464	541		
Story Shear at Max. Disp. (kN)	3	793	976	744	899	678	668	812	642	467	723	895	1156		
	2	1252	1286	1242	1273	1326	1320	1605	1242	1116	1361	1499	1605		
	1	2009	1848	1893	1768	1661	1662	1978	1590	1120	1786	2005	2268		
Max. Story Shear (kN)	3	921	1122	872	1093	889	873	1031	871	664	899	1061	1251		
	2	1399	1404	1390	1394	1468	1467	1751	1398	1211	1625	1831	2040		
	1	2074	1886	1943	1810	1710	1709	2030	1628	1321	2314	2701	3087		
Floor Acceleration (g)	3	0.588	0.716	0.556	0.698	0.567	0.557	0.658	0.556	0.441	0.600	0.700	0.826		
	2	0.245	0.456	0.240	0.438	0.403	0.403	0.439	0.401	0.299	0.551	0.730	0.936		
	1	0.643	0.460	0.565	0.417	0.433	0.448	0.442	0.468	0.299	0.551	0.730	0.936		

TABLE 8-8 Comparison of Results of Simplified Methods of Analysis to Results of Nonlinear Time History Analysis. Case of Example No.5: 6-Story (0.75V_y) with Linear Viscous Damping System. Analysis for the DBE

Response Quantity	S T O R Y	SIMPLIFIED METHOD OF ANALYSIS										NONLINEAR TIME HISTORY ANALYSIS (IDARC 2D- Version 5.0)			
		NEHRP(2000)					METHOD 2 (FEMA 274)					Min.	Avg.	Avg. +1σ	Max.
		Higher Modes Using T_m		Higher Modes Using $T_m \sqrt{\mu}$			LATERAL FORCE PATTERN								
		ELF	RSA	ELF	RSA	RSA	mode 1	Cvx	Unif	Adpt					
Story Drift (mm.)	6	53	64	53	67	67	72	60	66	26	41	50	61		
	5	79	84	79	85	88	89	79	89	38	65	84	106		
	4	85	85	85	85	96	97	92	98	41	75	101	127		
	3	86	85	86	85	91	88	95	92	39	73	100	131		
	2	71	71	71	72	67	63	78	67	31	59	80	107		
	1	68	41	70	41	34	33	39	32	18	34	44	56		
Interstory Velocity (mm/sec)	6	132	348	130	349	325	344	297	310	99	190	234	265		
	5	196	299	193	293	299	301	280	293	131	243	294	316		
	4	212	248	209	251	266	266	267	265	142	255	315	355		
	3	215	222	211	226	245	242	260	244	138	272	341	423		
	2	177	198	174	197	214	201	241	213	126	259	337	433		
	1	345	147	325	148	131	128	142	130	83	183	250	339		
Damper Force (kN)	6	205	540	201	542	504	534	461	481	153	295	364	411		
	5	304	464	299	454	464	467	434	454	204	377	456	490		
	4	403	471	396	476	505	505	506	502	270	485	598	675		
	3	407	421	400	428	465	458	494	463	262	516	649	804		
	2	454	508	446	505	548	514	617	546	323	662	863	1109		
	1	884	376	832	378	336	328	364	333	212	469	640	869		
Story Shear at Max. Disp. (kN)	6	397	558	386	516	415	413	444	383	205	278	325	369		
	5	940	956	921	910	866	834	1005	803	489	677	776	831		
	4	1240	1218	1227	1203	1182	1126	1434	1098	751	976	1107	1232		
	3	1391	1436	1391	1428	1427	1356	1752	1325	863	1211	1376	1463		
	2	1653	1647	1639	1619	1597	1517	1957	1480	960	1442	1636	1699		
	1	2294	1813	2219	1764	1683	1605	2045	1561	1032	1689	1967	2112		

TABLE 8-8 Continued

Response Quantity	S T O R Y	SIMPLIFIED METHOD OF ANALYSIS										NONLINEAR TIME HISTORY ANALYSIS (IDARC 2D- Version 5.0)			
		NEHRP(2000)					METHOD 2 (FEMA 274)					Min.	Avg.	Avg. +1σ	Max.
		Higher Modes Using T_m		Higher Modes Using $T_m \sqrt{\mu}$			LATERAL FORCE PATTERN								
		ELF	RSA	ELF	RSA	RSA	mode 1	Cvx	Unif	Adpt					
Max. Story Shear (kN)	6	427	736	414	705	613	629	610	577	222	334	390	408		
	5	967	1069	945	1025	993	965	1112	932	536	756	862	888		
	4	1321	1338	1306	1326	1321	1269	1561	1242	751	1056	1198	1352		
	3	1499	1543	1498	1538	1550	1478	1875	1450	867	1268	1429	1495		
	2	1742	1769	1725	1743	1730	1641	2105	1617	987	1579	1813	1868		
	1	2369	1861	2271	1818	1726	1643	2105	1602	1102	1948	2293	2416		
Floor Acceleration (g)	6	0.273	0.469	0.264	0.450	0.391	0.401	0.389	0.368	0.149	0.225	0.265	0.279		
	5	0.214	0.263	0.210	0.255	0.260	0.262	0.272	0.243	0.122	0.176	0.205	0.231		
	4	0.170	0.263	0.169	0.254	0.242	0.246	0.244	0.232	0.100	0.189	0.235	0.279		
	3	0.187	0.233	0.178	0.217	0.231	0.233	0.224	0.228	0.117	0.232	0.298	0.351		
	2	0.249	0.244	0.229	0.227	0.228	0.225	0.229	0.227	0.155	0.298	0.392	0.491		
	1	0.439	0.196	0.408	0.186	0.231	0.224	0.222	0.238	0.176	0.365	0.494	0.643		

**TABLE 8-9 Comparison of Results of Simplified Methods of Analysis to Results of Nonlinear Time History Analysis.
Case of Example No.5: 6-Story (0.75V_y) with Linear Viscous Damping System. Analysis for the MCE**

Response Quantity	S T O R Y	SIMPLIFIED METHOD OF ANALYSIS										NONLINEAR TIME HISTORY ANALYSIS (IDARC 2D- Version 5.0)			
		NEHRP(2000)					METHOD 2 (FEMA 274)					Min.	Avg.	Avg. +1σ	Max.
		Higher Modes Using T _m		Higher Modes Using T _m √μ			LATERAL FORCE PATTERN								
		ELF	RSA	ELF	RSA	mode 1	Cvx	Unif	Adpt						
Story Drift (mm.)	6	79	97	80	105	76	73	61	49	36	53	65	77		
	5	118	126	119	130	111	107	95	74	59	88	112	138		
	4	128	128	129	129	130	128	118	89	67	106	141	173		
	3	129	127	130	128	142	143	137	96	62	107	146	184		
	2	107	107	108	108	129	132	141	86	47	90	124	161		
	1	101	62	111	63	66	70	105	44	26	56	81	110		
Interstory Velocity (mm/sec)	6	171	513	160	485	437	438	367	288	133	249	302	325		
	5	254	424	238	393	379	386	340	261	188	319	383	410		
	4	275	336	258	332	342	336	317	248	197	346	425	480		
	3	278	291	260	299	312	301	304	232	203	380	480	584		
	2	230	266	215	257	288	291	296	212	172	374	490	617		
	1	512	207	424	202	207	212	290	144	124	278	372	497		
Damper Force (kN)	6	265	795	248	753	677	680	569	447	206	386	469	505		
	5	394	657	369	610	588	599	528	405	292	495	594	636		
	4	522	637	489	629	648	638	601	470	374	657	808	911		
	3	528	552	494	566	591	571	577	440	385	722	911	1109		
	2	589	681	551	658	739	745	759	543	441	957	1253	1580		
	1	1312	530	1086	518	529	543	743	368	319	711	953	1271		
Story Shear at Max. Disp. (kN)	6	498	771	441	562	653	669	608	462	222	318	378	467		
	5	1123	1152	1018	943	1015	1026	1080	816	636	790	895	1018		
	4	1361	1317	1289	1222	1257	1214	1425	1093	960	1102	1200	1321		
	3	1392	1490	1389	1442	1452	1372	1710	1308	1112	1349	1476	1534		
	2	1789	1778	1707	1634	1665	1595	1942	1478	1303	1645	1790	1814		
	1	2948	2060	2580	1804	1885	1831	2151	1608	1472	1932	2100	2254		

TABLE 8-9 Continued

Response Quantity	S T O R Y	SIMPLIFIED METHOD OF ANALYSIS										NONLINEAR TIME HISTORY ANALYSIS (IDARC 2D- Version 5.0)			
		NEHRP(2000)					METHOD 2 (FEMA 274)					Min.	Avg.	Avg. +1σ	Max.
		Higher Modes Using T_m		Higher Modes Using $T_m\sqrt{\mu}$			LATERAL FORCE PATTERN								
		ELF	RSA	RSA	ELF	RSA	mode 1	Cvx	Unif	Adpt					
Max. Story Shear (kN)	6	527	1042	461	871	890	902	796	614	294	399	457	492		
	5	1130	1321	1015	1124	1171	1182	1207	917	701	897	1007	1092		
	4	1459	1493	1376	1407	1442	1396	1563	1219	967	1236	1366	1481		
	3	1550	1643	1539	1604	1623	1540	1868	1426	1116	1489	1641	1733		
	2	1894	1950	1801	1817	1877	1812	2157	1623	1357	1937	2137	2281		
	1	3052	2116	2568	1888	1970	1923	2331	1670	1655	2592	3002	3455		
Floor Acceleration (g)	6	0.336	0.665	0.294	0.556	0.568	0.576	0.508	0.392	0.194	0.272	0.315	0.325		
	5	0.250	0.339	0.229	0.299	0.323	0.318	0.287	0.239	0.156	0.213	0.249	0.299		
	4	0.192	0.358	0.188	0.301	0.345	0.339	0.296	0.246	0.141	0.247	0.306	0.372		
	3	0.251	0.327	0.211	0.261	0.324	0.331	0.268	0.224	0.175	0.321	0.409	0.481		
	2	0.364	0.357	0.279	0.273	0.357	0.362	0.291	0.240	0.220	0.434	0.569	0.715		
	1	0.658	0.292	0.522	0.241	0.288	0.287	0.279	0.193	0.265	0.544	0.736	0.965		

TABLE 8-10 Comparison of Results of Simplified Methods of Analysis to Results of Nonlinear Time History Analysis. Case of Example No.6: 3-Story (0.80 V_p) with Nonlinear Viscous Damping System Designed for 10% Damping Ratio in the DBE. Analysis for the DBE

Response Quantity	S T O R Y	SIMPLIFIED METHOD OF ANALYSIS										NONLINEAR TIME HISTORY ANALYSIS (IDARC 2D- Version 5.0)				
		NEHRP(2000)					METHOD 2 (FEMA 274)					Min.	Avg.	Max.		
		Higher Modes Using T_m		Higher Modes Using $T_m \sqrt{\mu}$			LATERAL FORCE PATTERN									
		ELF	RSA	ELF	RSA	mode I	Cvx	Unif	Adpt							
Story Drift (mm.)	3	87	88	88	433	597	92	98	102	102	109	103	39	80	104	119
Interstory Velocity (mm/sec)	2	103	96	104	75	62	96	106	103	103	61	63	40	86	114	131
Damper Force (kN)	1	72	61	75	433	597	62	62	62	63	61	63	22	58	79	99
Story Shear at Max. Disp. (kN)	3	440	559	433	597	846	597	564	581	569	617	569	254	484	600	664
Max. Story Shear (kN)	2	520	382	511	388	1110	388	522	519	519	565	519	232	441	546	595
Floor Acceleration (g)	1	489	311	477	327	1547	327	342	344	345	367	345	141	311	398	449
	3	268	300	266	266	789	312	303	307	304	315	304	216	299	333	350
	2	291	261	289	262	1110	262	291	290	290	303	290	207	285	317	331
	1	286	225	281	230	1547	230	234	235	235	243	235	161	240	271	288
	3	659	803	650	650	1547	789	591	606	571	691	571	422	671	849	1032
	2	1100	1112	1098	1098	1110	1110	1097	1130	1076	1359	1076	676	1108	1311	1507
	1	1682	1560	1662	1662	1547	1547	1386	1424	1354	1682	1354	689	1420	1679	1819
	3	752	889	703	703	846	846	701	720	686	811	686	446	738	905	1042
	2	1223	1229	1166	1166	1173	1173	1219	1251	1197	1483	1197	697	1225	1446	1578
	1	1757	1633	1702	1702	1585	1585	1466	1504	1435	1766	1435	779	1617	1945	2100
	3	0.480	0.568	0.449	0.449	0.540	0.540	0.448	0.459	0.438	0.518	0.438	0.300	0.494	0.599	0.681
	2	0.213	0.349	0.211	0.211	0.343	0.343	0.307	0.310	0.297	0.337	0.297	0.162	0.353	0.446	0.543
	1	0.486	0.362	0.471	0.471	0.353	0.353	0.327	0.328	0.318	0.341	0.318	0.169	0.366	0.491	0.620

TABLE 8-11 Comparison of Results of Simplified Methods of Analysis to Results of Nonlinear Time History Analysis. Case of Example No.6: 3-Story (0.80 V_y) with Nonlinear Viscous Damping System Designed for 10% Damping Ratio in the DBE. Analysis for the MCE

Response Quantity	S T O R Y	SIMPLIFIED METHOD OF ANALYSIS										NONLINEAR TIME HISTORY ANALYSIS (IDARC 2D- Version 5.0)			
		NEHRP(2000)					METHOD 2 (FEMA 274)					Min.	Avg.	Avg. +1σ	Max.
		Higher Modes Using T_m		Higher Modes Using $T_m\sqrt{\mu}$			LATERAL FORCE PATTERN								
		ELF	RSA	ELF	RSA	mode 1	Cvx	Unif	Adpt						
Story	3	136	138	141	155	168	164	177	170	170	61	124	162	183	
Drift (mm.)	2	160	150	167	150	156	157	156	157	157	62	131	173	199	
	1	112	94	124	100	110	112	108	110	110	31	94	134	173	
Interstory Velocity (mm/sec)	3	620	813	586	918	795	770	838	779	779	406	686	856	1064	
	2	732	492	691	529	679	660	719	666	666	354	614	752	840	
	1	725	436	671	485	480	471	503	470	470	205	468	603	720	
Damper Force (kN)	3	316	367	307	397	363	359	369	360	360	273	356	397	443	
	2	343	294	334	301	330	326	340	327	327	255	336	372	394	
	1	359	265	340	279	278	275	284	275	275	194	294	334	364	
Story Shear at Max. Disp. (kN)	3	840	1095	791	938	625	602	706	590	590	440	719	930	1223	
	2	1138	1165	1125	1152	1132	1089	1350	1076	1076	943	1218	1341	1432	
	1	2098	1861	1985	1696	1430	1375	1686	1358	1358	894	1547	1771	1912	
Max. Story Shear (kN)	3	930	1178	847	1010	758	733	845	726	726	614	909	1093	1328	
	2	1279	1293	1207	1226	1267	1224	1488	1211	1211	990	1446	1629	1827	
	1	2166	1927	2025	1741	1528	1474	1787	1455	1455	1187	1937	2239	2445	
Floor Acceleration (g)	3	0.594	0.752	0.540	0.645	0.484	0.468	0.539	0.463	0.463	0.416	0.608	0.724	0.879	
	2	0.222	0.476	0.218	0.427	0.335	0.323	0.359	0.318	0.318	0.249	0.462	0.580	0.688	
	1	0.737	0.545	0.673	0.475	0.355	0.335	0.363	0.336	0.336	0.272	0.529	0.690	0.838	

TABLE 8-12 Comparison of Results of Simplified Methods of Analysis to Results of Nonlinear Time History Analysis. Case of Example No.7: 3-Story (0.80 V_y) with Nonlinear Viscous Damping System Designed for 20% Damping Ratio in the MCE. Analysis for the MCE

Response Quantity	S T O R Y	SIMPLIFIED METHOD OF ANALYSIS										NONLINEAR TIME HISTORY ANALYSIS (IDARC 2D- Version 5.0)			
		NEHRP(2000)					METHOD 2 (FEMA 274)					Min.	Avg.	Avg. +1 σ	Max.
		Higher Modes Using T_m		Higher Modes Using $T_m \sqrt{\mu}$			LATERAL FORCE PATTERN								
		ELF	RSA	ELF	RSA	mode 1	Cvx	Unif	Adpt						
Story	3	106	108	108	116	108	116	121	120	126	120	42	75	97	115
Drift (mm.)	2	125	118	127	118	127	118	129	136	122	126	53	100	132	148
	1	87	74	91	77	91	77	75	71	80	79	36	79	109	132
Interstory Velocity (mm/sec)	3	508	660	483	729	483	729	611	605	634	584	235	453	566	655
	2	599	435	569	448	569	448	604	646	589	563	298	520	635	745
	1	572	363	530	392	530	392	392	406	398	374	214	412	535	623
Damper Force (kN)	3	634	724	621	767	621	767	696	690	706	679	462	641	717	770
	2	689	614	674	619	674	619	693	714	685	668	520	686	759	822
	1	688	537	656	556	656	556	556	568	560	542	440	611	697	752
Story Shear at Max. Disp. (kN)	3	717	913	683	861	683	861	593	582	667	551	382	613	833	1298
	2	1114	1139	1105	1130	1105	1130	1141	1129	1336	1069	1014	1350	1561	1845
	1	1815	1673	1737	1619	1737	1619	1435	1446	1651	1335	1343	1732	1907	2165
Max. Story Shear (kN)	3	1003	1192	884	1099	884	1099	952	942	1029	908	510	784	934	1087
	2	1480	1476	1355	1358	1355	1358	1508	1508	1693	1428	1133	1570	1778	2007
	1	2051	1885	1905	1774	1905	1774	1686	1684	1918	1594	1466	2172	2487	2646
Floor Acceleration (g)	3	0.640	0.761	0.564	0.701	0.564	0.701	0.607	0.601	0.657	0.579	0.351	0.545	0.642	0.734
	2	0.221	0.426	0.216	0.412	0.216	0.412	0.370	0.376	0.372	0.344	0.281	0.449	0.543	0.660
	1	0.619	0.450	0.564	0.426	0.564	0.426	0.398	0.442	0.353	0.349	0.233	0.506	0.662	0.833

**TABLE 8-13 Comparison of Results of Simplified Methods of Analysis to Results of Nonlinear Time History Analysis.
Case of Example No.8: 3-Story (0.75 V_y) with Viscoelastic Damping System. Analysis for the DBE**

Response Quantity	S T O R Y	SIMPLIFIED METHOD OF ANALYSIS										NONLINEAR TIME HISTORY ANALYSIS (IDARC 2D- Version 5.0)		
		NEHRP(2000)					METHOD 2 (FEMA 274)					Min.	Avg.	Max.
		Higher Modes Using T _m		Higher Modes Using T _m √μ			LATERAL FORCE PATTERN							
		ELF	RSA	ELF	RSA	mode 1	Cvx	Unif	Adpt	Avg. +1σ				
Story Drift (mm.)	3	76	78	76	80	91	91	84	90	41	94	123	139	
	2	98	94	98	94	92	92	95	93	42	94	122	143	
	1	71	64	72	65	56	55	61	59	25	59	79	105	
Interstory Velocity (mm/sec)	3	375	485	372	507	566	553	537	551	275	493	611	725	
	2	482	401	479	407	404	375	418	382	241	440	539	574	
	1	430	315	425	324	304	289	320	301	132	308	395	495	
Damper Force (kN)	3	391	464	393	492	526	514	496	514	240	466	592	718	
	2	504	432	506	436	415	394	431	400	215	432	538	575	
	1	424	324	427	334	292	278	311	294	120	296	385	462	
Story Shear at Max. Disp. (kN)	3	653	786	646	775	810	755	808	734	156	866	1128	1316	
	2	1273	1293	1272	1292	1333	1144	1380	1155	707	1267	1522	1752	
	1	1773	1693	1758	1685	1739	1544	1787	1533	751	1407	1705	2045	
Max. Story Shear (kN)	3	716	853	710	847	903	847	896	830	532	963	1173	1367	
	2	1354	1361	1352	1360	1411	1223	1463	1236	753	1405	1672	1769	
	1	1818	1732	1804	1725	1773	1573	1828	1568	922	1642	1977	2231	
Floor Acceleration (g)	3	0.457	0.544	0.453	0.540	0.576	0.540	0.572	0.530	0.356	0.644	0.785	0.915	
	2	0.251	0.351	0.251	0.348	0.369	0.351	0.367	0.340	0.186	0.342	0.448	0.560	
	1	0.422	0.337	0.409	0.331	0.338	0.341	0.327	0.321	0.202	0.378	0.512	0.648	

**TABLE 8-14 Comparison of Results of Simplified Methods of Analysis to Results of Nonlinear Time History Analysis.
Case of Example No.8: 3-Story (0.75 V_y) with Viscoelastic Damping System. Analysis for the MCE**

Response Quantity	S T O R Y	SIMPLIFIED METHOD OF ANALYSIS										NONLINEAR TIME HISTORY ANALYSIS (IDARC 2D- Version 5.0)					
		NEHRP(2000)					METHOD 2 (FEMA 274)					Min.	Avg.	Max.			
		Higher Modes Using T _m		Higher Modes Using T _m √μ			LATERAL FORCE PATTERN										
		ELF	RSA	ELF	RSA	mode 1	Cvx	Unif	Adpt	Avg. +1σ							
Story	3	114	117	116	128	116	116	119	126	114	116	119	126	62	132	177	210
Drift (mm.)	2	147	140	150	141	150	141	146	147	149	157	146	147	63	130	169	196
	1	106	96	112	100	112	100	102	106	105	114	102	106	37	90	123	158
Interstory Velocity (mm/sec)	3	515	691	490	768	490	768	697	803	703	675	697	803	411	678	838	1048
	2	662	527	630	559	630	559	566	607	568	559	566	607	357	580	711	801
	1	615	430	570	465	570	465	437	478	450	446	437	478	198	445	576	738
Damper Force (kN)	3	558	671	560	799	560	799	665	757	658	641	665	757	285	625	724	627
	2	718	603	721	632	721	632	610	640	611	619	610	640	343	550	669	711
	1	616	460	620	508	620	508	455	492	467	477	455	492	178	430	564	675
Story Shear at Max. Disp. (kN)	3	802	1036	764	936	764	936	858	786	894	806	858	786	711	1066	1266	1392
	2	1424	1465	1415	1455	1415	1455	1504	1281	1447	1273	1504	1281	1036	1479	1680	1787
	1	2155	2005	2064	1927	2064	1927	1917	1746	1887	1670	1917	1746	1098	1548	1735	1916
Max. Story Shear (kN)	3	891	1130	851	1050	851	1050	999	956	1023	938	999	956	782	1224	1433	1645
	2	1541	1557	1527	1548	1527	1548	1634	1402	1571	1407	1634	1402	1129	1655	1888	2035
	1	2215	2053	2125	1986	2125	1986	1994	1797	1959	1750	1994	1797	1381	2007	2326	2664
Floor Acceleration (g)	3	0.569	0.721	0.543	0.670	0.543	0.670	0.638	0.610	0.653	0.599	0.638	0.610	0.535	0.812	0.880	0.945
	2	0.282	0.464	0.280	0.438	0.280	0.438	0.422	0.447	0.433	0.401	0.422	0.447	0.279	0.452	0.575	0.699
	1	0.624	0.494	0.557	0.448	0.557	0.448	0.355	0.360	0.404	0.388	0.355	0.360	0.303	0.547	0.728	0.937

**TABLE 8-15 Comparison of Results of Simplified Methods of Analysis to Results of Nonlinear Time History Analysis.
Case of Example No.9: 3-Story (0.75 V_p) with Metallic Yielding Damping System. Analysis for the DBE**

Response Quantity	S T O R Y	SIMPLIFIED METHOD OF ANALYSIS						NONLINEAR TIME HISTORY ANALYSIS (IDARC 2D- Version 5.0)				
		NEHRP(2000)			METHOD 2 (FEMA 274)			Min.	Avg.	Avg. +1 σ	Max.	
		Higher Modes Using T_m	Higher Modes Using $T_m\sqrt{\mu}$	Higher Modes Using $T_m\sqrt{\mu}$	LATERAL FORCE PATTERN	LATERAL FORCE PATTERN						
		ELF	RSA	ELF	RSA	mode 1	Cvx	Unif				
Story	3	100	107	105	119	116	116	111	111	106	129	155
Drift (mm.)	2	119	112	124	113	111	114	108	108	95	123	147
	1	82	72	93	76	83	80	85	85	68	91	121
Max. Story Shear (kN)	3	855	1041	855	1041	856	856	916	916	1111	1330	1408
	2	1351	1361	1351	1361	1409	1388	1626	1626	1638	1922	2235
	1	2165	1952	2165	1952	1816	1797	2077	2077	2030	2214	2422
Floor Acceleration (g)	3	0.546	0.664	0.546	0.664	0.546	0.546	0.585	0.585	0.705	0.841	0.886
	2	0.258	0.444	0.258	0.444	0.404	0.410	0.426	0.426	0.602	0.779	0.991
	1	0.657	0.473	0.657	0.473	0.415	0.434	0.402	0.402	0.677	0.915	1.302

TABLE 8-16 Comparison of Results of Simplified Methods of Analysis to Results of Nonlinear Time History Analysis. Case of Example No.9: 3-Story (0.75 V_y) with Metallic Yielding Damping System. Analysis for the MCE

Response Quantity	S T O R Y	SIMPLIFIED METHOD OF ANALYSIS										NONLINEAR TIME HISTORY ANALYSIS (IDARC 2D- Version 5.0)			
		NEHRP(2000)					METHOD 2 (FEMA 274)					Min.	Avg.	Avg. +1σ	Max.
		Higher Modes Using T _m		Higher Modes Using T _m √μ			LATERAL FORCE PATTERN								
		ELF	RSA	ELF	RSA	mode 1	Cvx	Unif							
Story	3	150	160	166	200	205	201	193	75	157	200	235			
Drift (mm.)	2	178	168	197	170	171	177	165	78	142	190	228			
	1	123	109	157	121	141	140	136	47	104	146	195			
Max. Story Shear (kN)	3	1102	1417	1102	1200	955	959	1015	957	1318	1546	1647			
	2	1413	1434	1413	1434	1471	1446	1680	1510	1845	2101	2434			
	1	2731	2342	2731	2122	1898	1875	2152	1939	2217	2418	2738			
Floor Acceleration (g)	3	0.703	0.905	0.703	0.766	0.610	0.612	0.648	0.607	0.836	0.982	1.052			
	2	0.272	0.606	0.272	0.543	0.472	0.477	0.490	0.469	0.742	0.932	1.164			
	1	0.980	0.702	0.980	0.619	0.526	0.541	0.515	0.530	0.849	1.109	1.556			

TABLE 8-17 Summary of Key Results Produced by Various Methods of Analysis

Quantity	3-STORY No.2, 0.75V _y , Linear Viscous, MCE			6-STORY No.5, 0.75V _y , Linear Viscous, MCE			3-STORY No.6, 0.8V _y , Nonlinear Viscous, MCE			3-STORY No.8, 0.75V _y , Viscoelastic, MCE			3-STORY No.9, 0.75V _y , Metallic Devices, MCE								
	ELF	RSA	FEMANTHA (1997)	ELF	RSA	FEMANTHA (1997)	ELF	RSA	FEMANTHA (1997)	ELF	RSA	FEMANTHA (1997)	ELF	RSA	FEMANTHA (1997)						
Drift (mm)	156	149	157	131	118	126	107	88	160	150	177	131	147	140	157	132	178	168	201	157	
Damper Force (kN)	497	547	525	477	394	795	680	495	359	367	369	356	718	671	665	625	NA	NA	NA	NA	NA
Max. Base Shear (kN)	1846	1664	1690	1917	3052	2116	2331	2592	2166	1927	1787	1937	2215	2053	1994	2007	2731	2342	2152	2217	
			1421				1670				1455				1797						

FEMA(1997): maximum response among the two calculated for the modal and uniform load patterns.

NTHA: maximum average value.

6-STORY: values represent the maximum per two floors with same dampers.

Value in bold is peak response calculated using the adaptive load pattern.

TABLE 8-18 Comparison of Results of Simplified Methods of Analysis to Results of Nonlinear Time History Analysis. Case of Example No.2: 3-Story (0.75V_y) with Linear Viscous Damping System Designed for 10% Damping Ratio. Analysis for Near-Fault Ground Motions

Response Quantity	S T O R Y	SYLMAR 90°						NEWHALL 360°						PACOIMA DAM S16E					
		Using B		Using Actual Spectra		Using B		Using Actual Spectra		Using B		Using Actual Spectra		Using B		Using Actual Spectra			
		ELF	RSA	NTHA	ELF	RSA	ELF	RSA	NTHA	ELF	RSA	ELF	RSA	ELF	RSA	NTHA	ELF	RSA	
Story Drift (mm.)	3	145	147	107	103	105	155	152	108	142	142	172	179	125	174	176	204	204	
	2	172	168	118	122	116	184	171	124	169	159	204	203	151	207	204	132	126	
	1	111	105	72	83	73	130	107	86	117	100	127	127	119	132	126			
Damper Force (kN)	3	383	504	484	349	461	566	608	567	507	605	421	672	457	439	535	521	469	
	2	454	364	380	415	311	672	443	497	602	423	500	519	517	521	469	418	329	
	1	393	285	277	381	253	661	344	332	571	337	350	389	413	418	329			
Max. Story Shear (kN)	3	715	943	802	701	900	1015	1102	926	903	1097	642	1184	681	723	930	1193	1240	
	2	1173	1152	1305	1142	1127	1301	1241	1538	1245	1193	1175	1328	1361	1193	1240	1610	1573	
	1	1617	1558	1664	1612	1521	2239	1715	1911	2008	1695	1441	1807	1879	1610	1573			

Using B: Simplified analysis procedures were applied using the actual 5%-damped spectrum of each earthquake motion, and the damping coefficient B from NEHRP (2000)

Using Actual Spectra: Simplified procedures were applied using the actual damped spectrum of each earthquake

**TABLE 8-19 Comparison of Results of Simplified Methods of Analysis to Results of Nonlinear Time History Analysis.
Case of Example No.4: 3-Story (1.0V_y) with Linear Viscous Damping System Designed for 20% Damping Ratio.
Analysis for Near-Fault Ground Motions**

Response Quantity	S T O R Y	SYLMAR 90°				NEWHALL 360°				PACOIMA DAM S16E						
		Using B		Using Actual Spectra		Using B		Using Actual Spectra		Using B		Using Actual Spectra				
		ELF	RSA	NTHA	ELF	RSA	ELF	RSA	NTHA	ELF	RSA	ELF	RSA			
Story Drift (mm.)	3	70	70	66	70	70	125	124	89	105	106	129	135	87	112	112
	2	85	82	85	84	82	150	148	111	126	123	155	153	115	134	132
	1	55	49	53	53	49	93	88	74	80	74	94	93	81	82	79
Damper Force (kN)	3	707	760	705	658	791	1036	1076	943	943	1072	960	1596	862	858	1000
	2	854	698	771	791	707	1245	1103	1221	1134	978	1152	1080	1165	1032	978
	1	707	471	538	609	485	956	703	812	894	663	840	876	880	756	640
Max. Story Shear (kN)	3	987	1053	669	937	1089	1196	1298	831	1137	1308	1145	1960	807	1070	1254
	2	1697	1648	1692	1676	1659	1934	1875	2075	1855	1802	1920	1920	1925	1829	1858
	1	2035	1890	2345	1949	1914	2259	2076	2918	2203	2061	2164	2164	2674	2070	2051

Using B: Simplified analysis procedures were applied using the actual 5%-damped spectrum of each earthquake motion, and the damping coefficient B from NEHRP (2000)

Using Actual Spectra: Simplified procedures were applied using the actual damped spectrum of each earthquake

TABLE 8-20 Results of Analysis of Example No.1 and No.3 Using Assumed and Actual Base Shear Strengths for the DBE

Quantity	Units	Example No.1		Example No.3	
		Using Assumed Strength V_y (kN) 1310	Using Actual Strength V_y (kN) 976	Using Assumed Strength V_y (kN) 991	Using Actual Strength V_y (kN) 1464
1. Elastic Response					
Damping Ratio, β_{ve}		0.100	0.100	0.100	0.100
Total Damping Ratio, β_{v+l}		0.150	0.150	0.150	0.150
Elastic Displacement, D_{el}	mm	274	274	215	215
2. Roof Displacement and Base Shear					
Assumed Ductility, μ		1.10	1.43	1.86	1.23
Effective Period, T_{ID}	sec	1.87	2.13	1.88	1.53
Hysteretic Damping, β_H		0.027	0.089	0.136	0.055
Effective Damping, β_{eff}		0.182	0.258	0.322	0.216
Displacement, D_{ID}	mm	268	264	212	208
Corrected Displacement, D_{ID}	mm	274	274	215	215
Seismic Coefficient, C_s		0.108	0.082	0.083	0.123
Seismic Base Shear, V_l	kN	635	481	480	712
Yield Displacement, D_y	mm	244	185	114	169
Computed Ductility, μ		1.12	1.48	1.88	1.27
3. Response at Stage of Maximum Displacement					
Lateral Floor Displacement, δ_i	mm	275	275	216	216
		183	183	137	137
		80	80	59	59
Story Drift, Δ_i	mm	95	95	81	81
		119	119	90	90
		80	80	59	59
Design Lateral Forces, F_i	kN	291	247	259	327
		296	227	231	331
		537	532	555	562
Actual Story Shear Forces, V_i	kN	600	510	534	675
		1109	853	851	1239
		1562	1306	1354	1734

In parts 1 and 2 of the table quantities for the 1st mode are presented.

In part 3 the total response using the ELF method is presented.

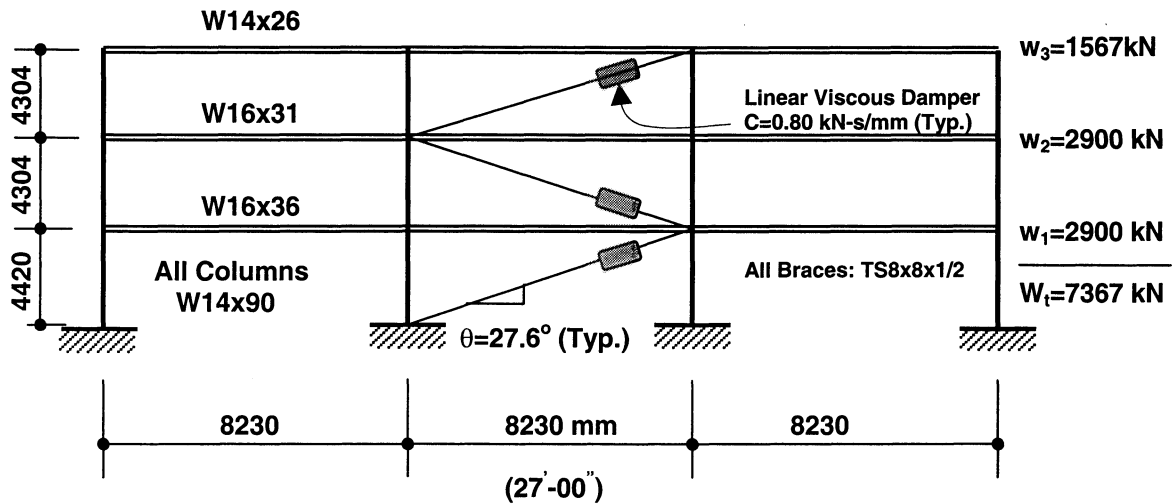


FIGURE 8-1 Example No.1: Frame 3S-60 with Linear Viscous Damping System to Provide 10% Viscous Damping Ratio when Assuming Elastic Frame Behavior

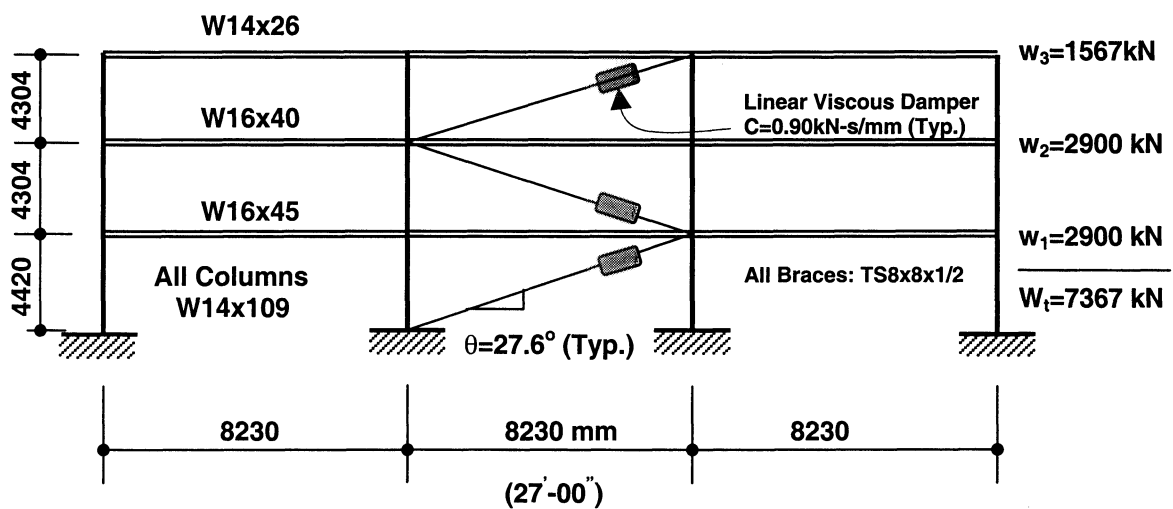


FIGURE 8-2 Example No.2: Frame 3S-75 with Linear Viscous Damping System to Provide 10% Viscous Damping Ratio when Assuming Elastic Frame Behavior

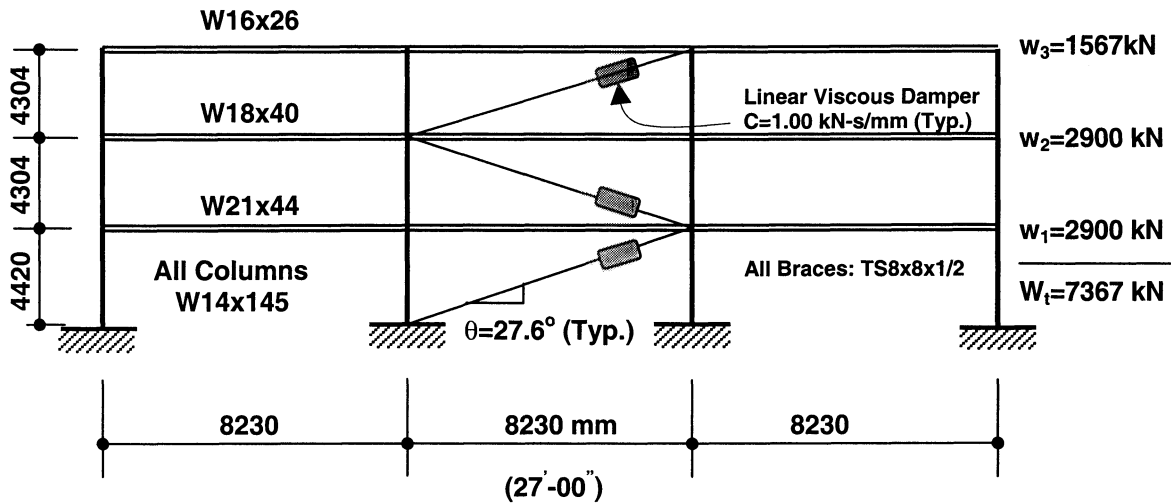


FIGURE 8-3 Example No.3: Frame 3S-90 with Linear Viscous Damping System to Provide 10% Viscous Damping when Assuming Elastic Frame Behavior

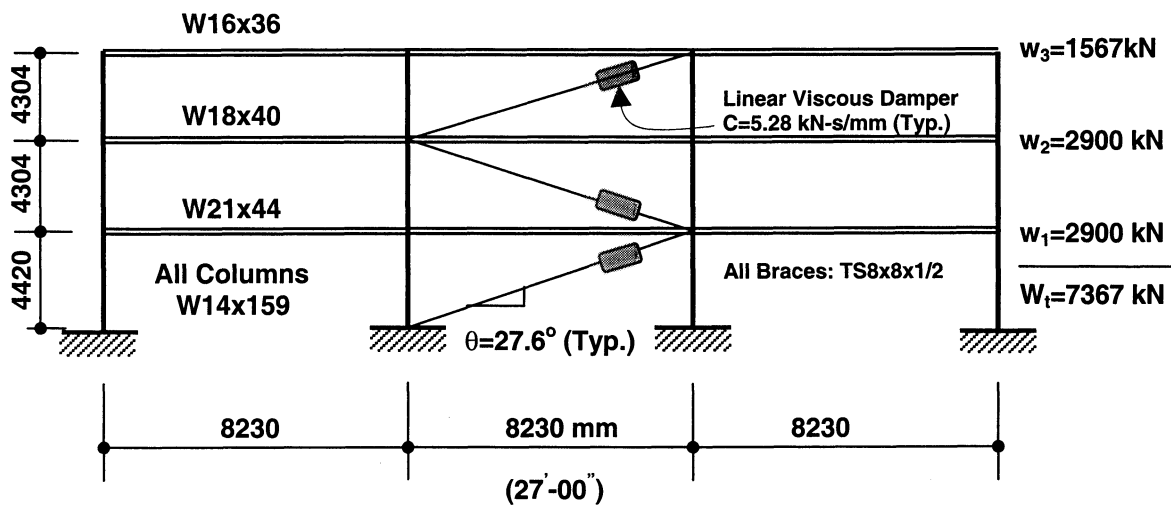


FIGURE 8-4 Example No.4: Frame 3S-100 with Linear Viscous Damping System to Provide 20% Viscous Damping Ratio when Assuming Elastic Frame Behavior

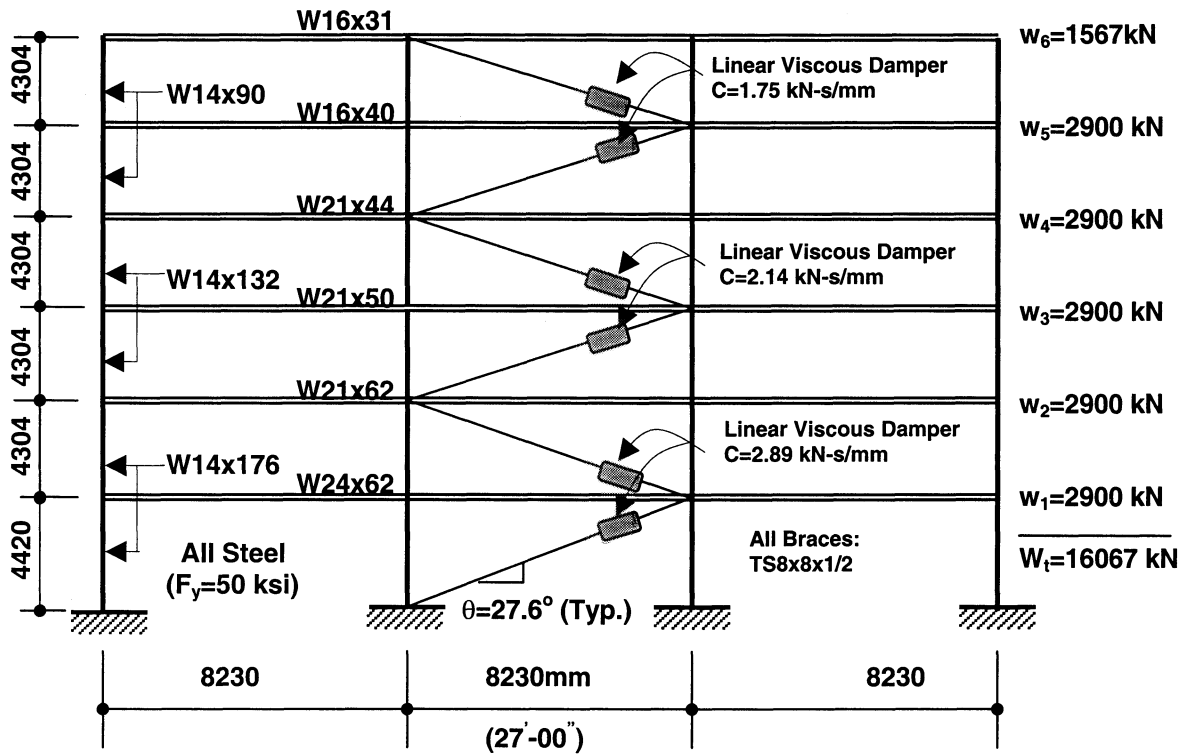


FIGURE 8-5 Example No.5: Frame 6S-75 with Linear Viscous Dampers to Provide 10% Viscous Damping Ratio when Assuming Elastic Frame Behavior

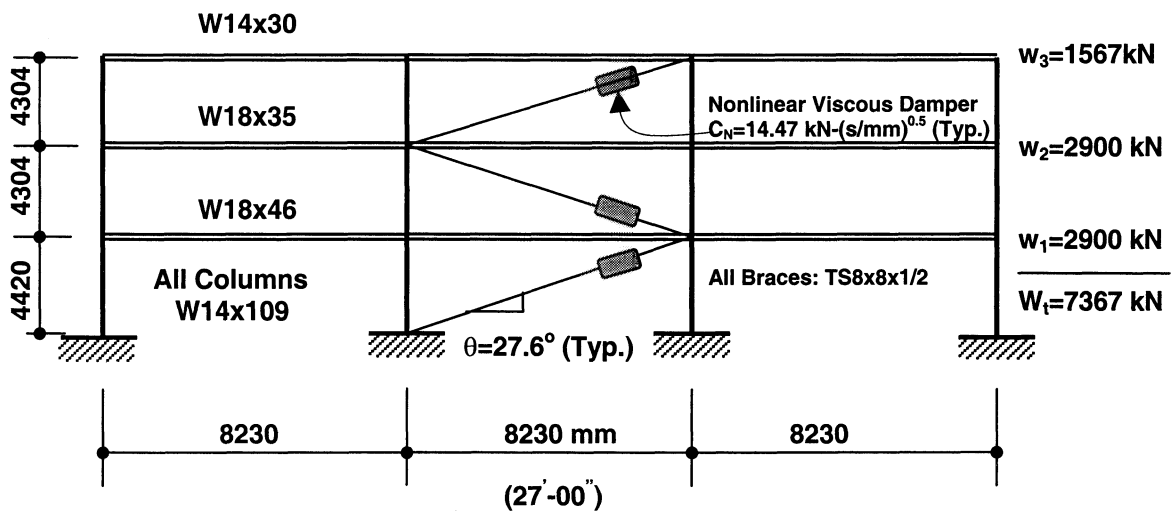


FIGURE 8-6 Example No.6: Frame 3S-80 with Nonlinear Viscous Damping System to Provide 10% Viscous Damping Ratio when Assuming Elastic Frame Behavior in the DBE

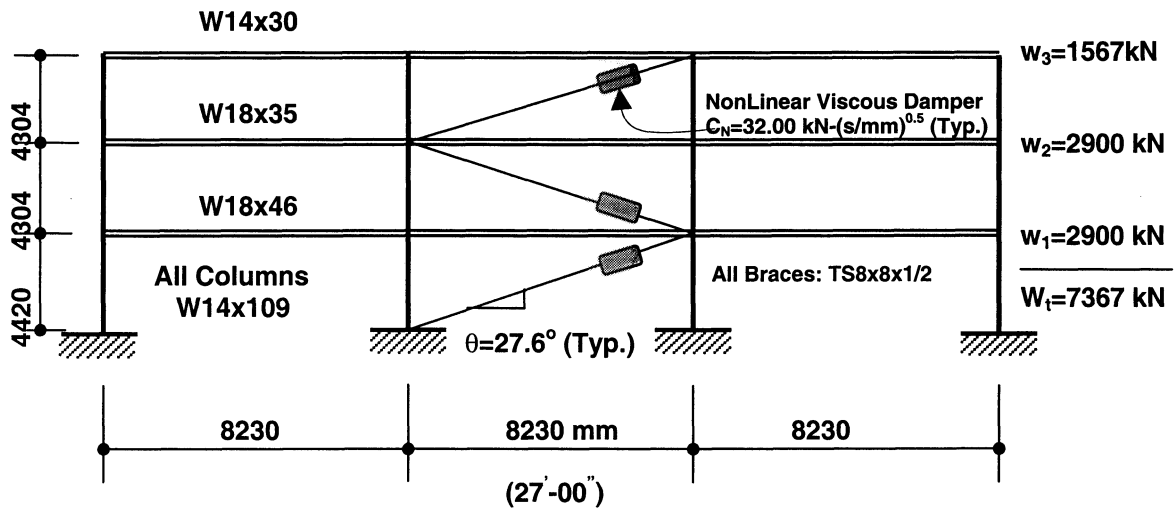


FIGURE 8-7 Example No.7: Frame 3S-80 with Nonlinear Viscous Damping System to Provide 20% Viscous Damping Ratio when Assuming Elastic Frame Behavior in the MCE

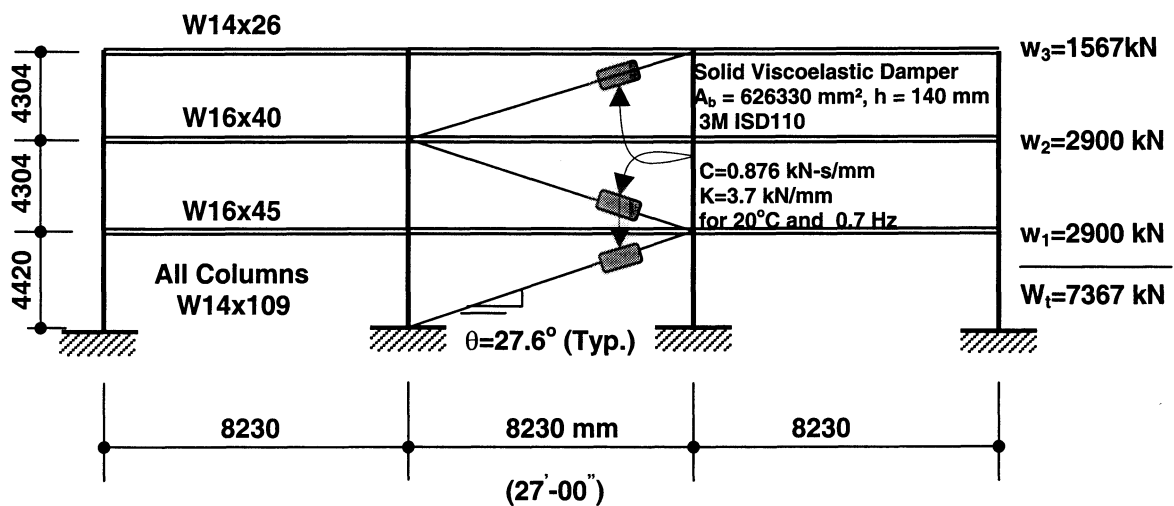


FIGURE 8-8 Example No.8: Frame 3S-75 with Viscoelastic Solid Damping System to Provide 8.5% Viscous Damping Ratio when Assuming Elastic Frame Behavior

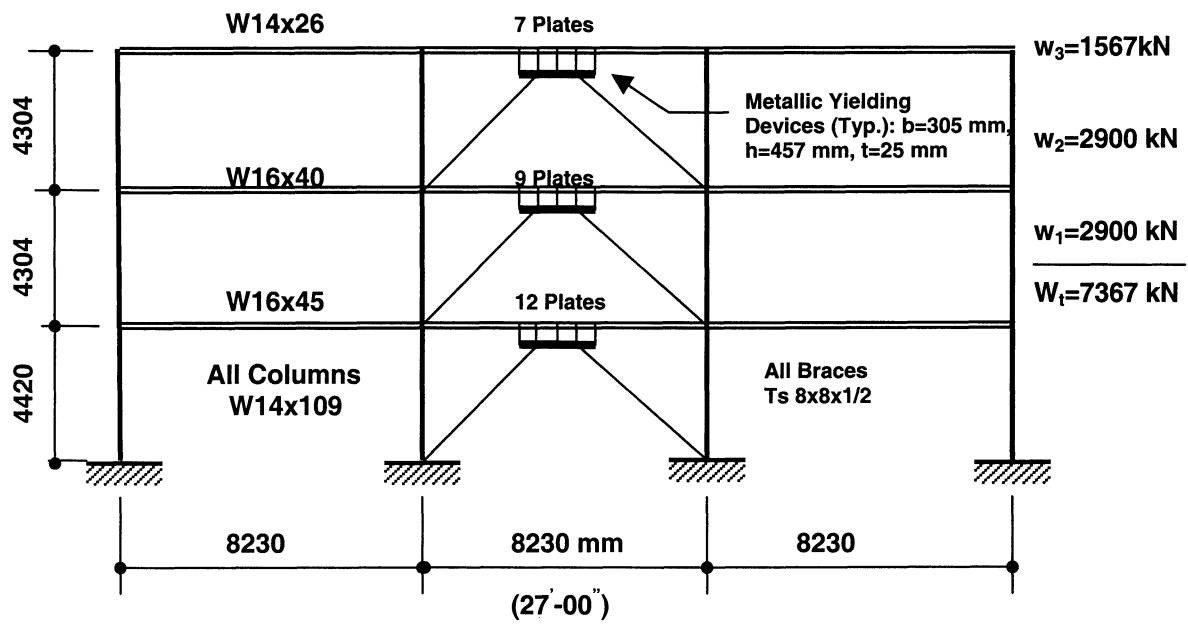
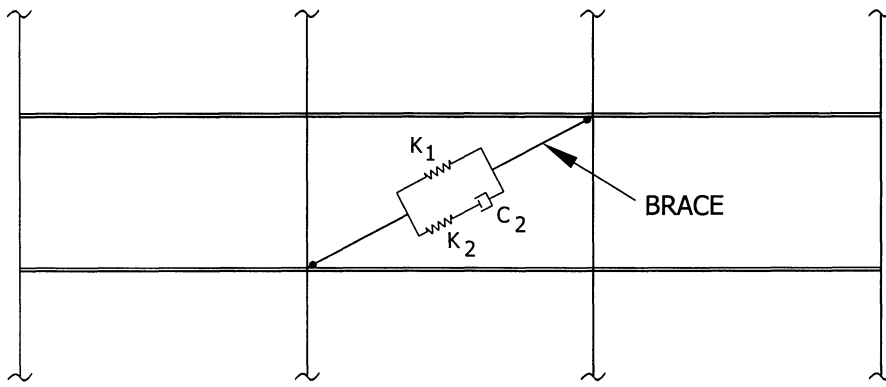
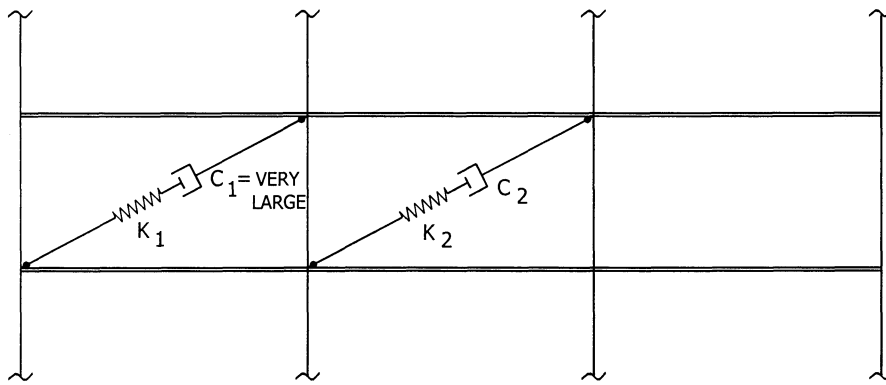


FIGURE 8-9 Example No.9: Frame 3S-75 with Metallic Yielding Damping System

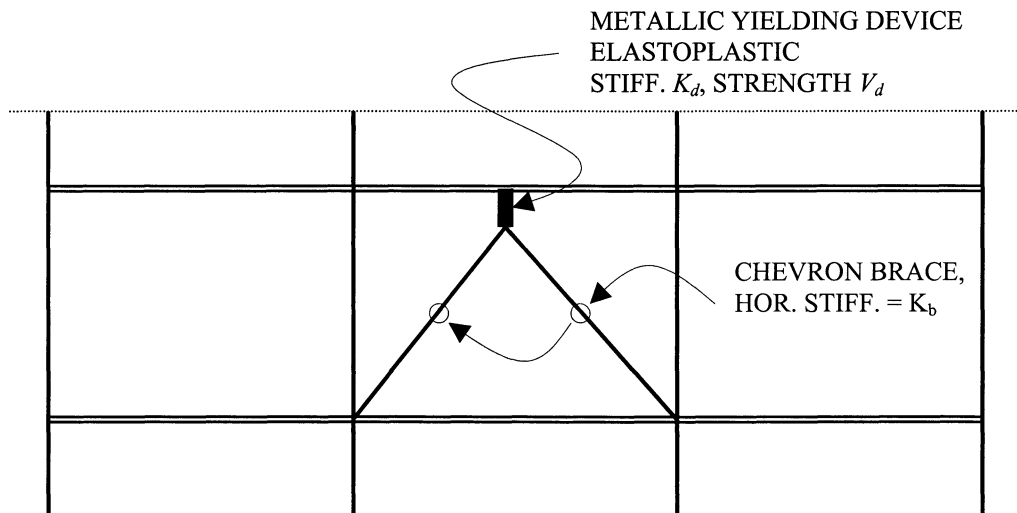


DESIRED MODEL

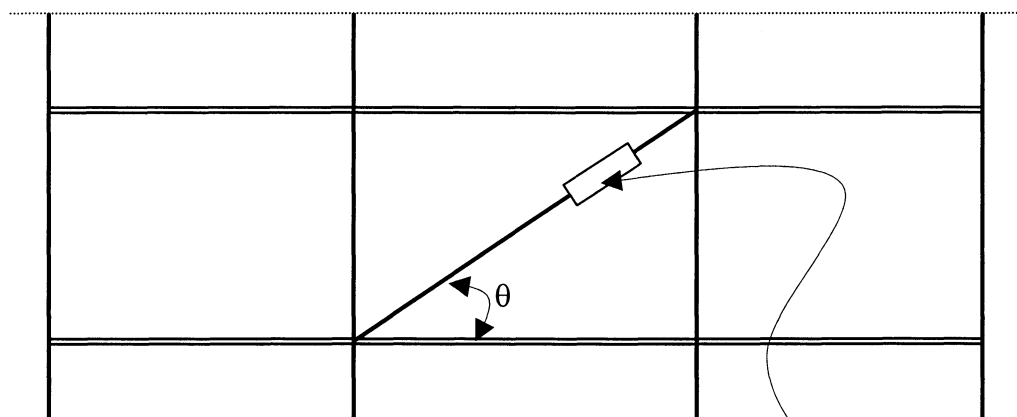


UTILIZED MODEL

FIGURE 8-10 Modeling of Viscoelastic Solid Damping Device in Program IDARC2D



DESIRED MODEL



UTILIZED MODEL

ELASTOPLASTIC ELEMENT

$$\text{STIFF.} = \frac{K_d \cdot K_b}{K_d + K_b \cos^2 \theta}$$

$$\text{STRENGTH} = V_d / \cos \theta$$

FIGURE 8-11 Modeling of Metallic Yielding Damping Device in Program IDARC2D

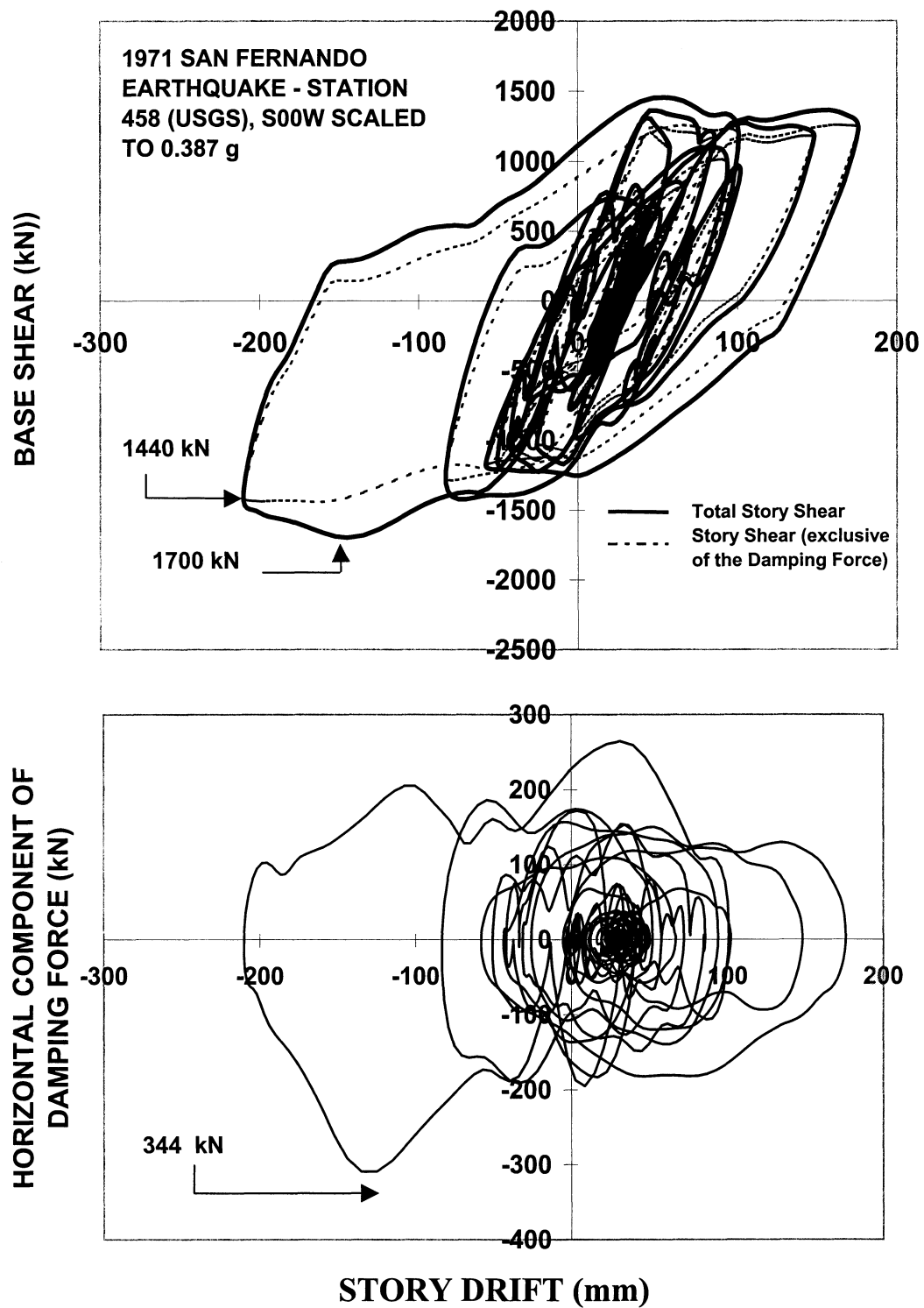


FIGURE 8-12 Base Shear-First Story Drift Loops of Frame of Example No.1: 3-Story (0.60V_y) with Linear Viscous Damping System in Scaled San Fernando, Station 458, Component S00W Earthquake (see Table 3-2)

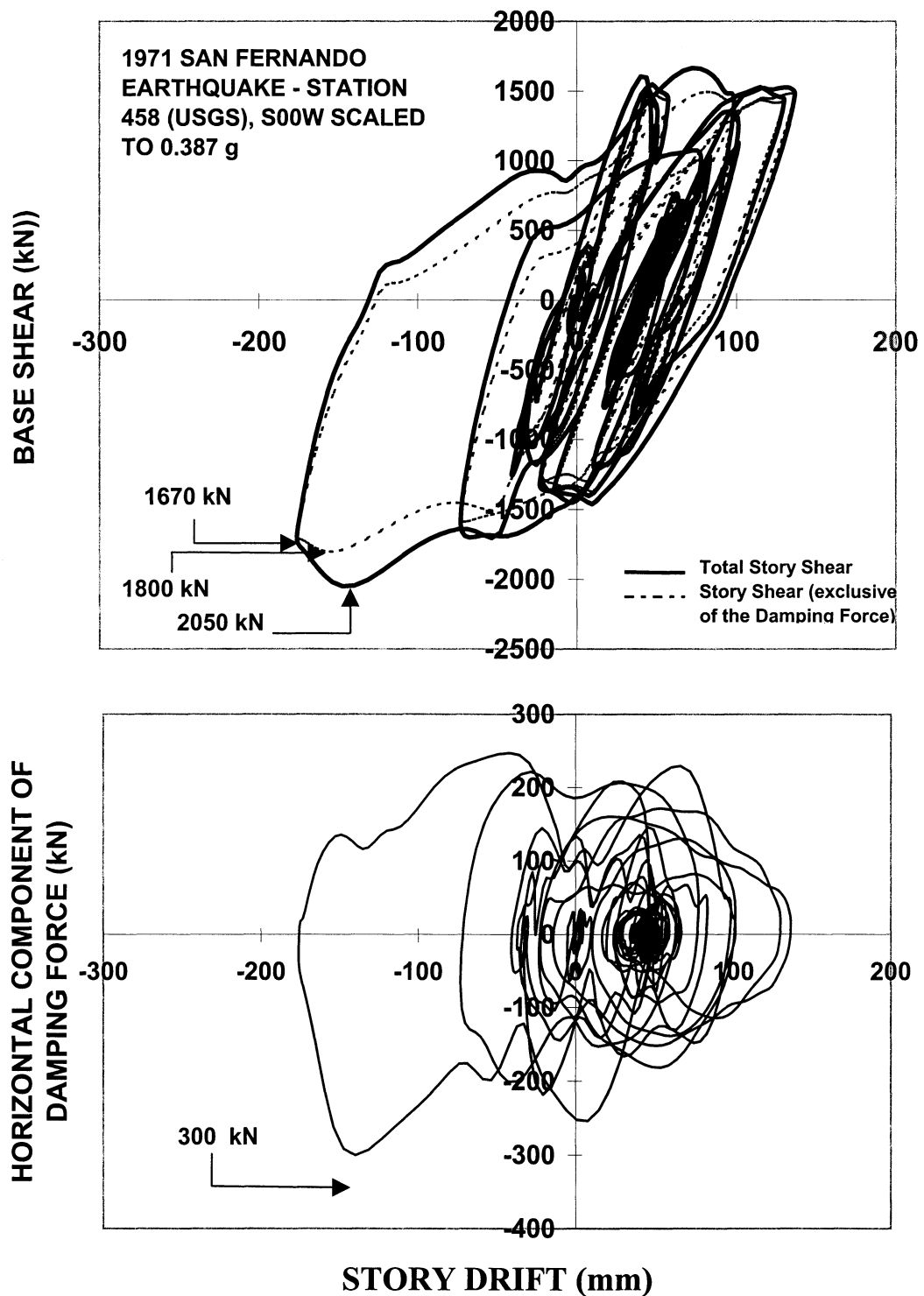
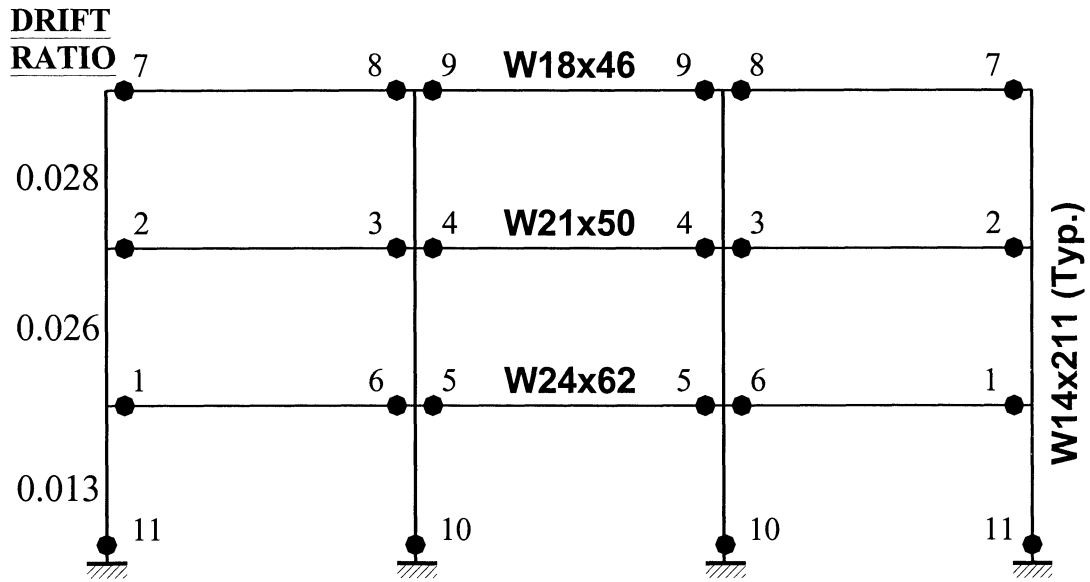


FIGURE 8-13 Base Shear-First Story Drift Loops of Frame of Example No.2: 3-Story (0.75Vy) with Linear Viscous Damping System in Scaled San Fernando, Station 458, Component S00W Earthquake (see Table 3-2)

DBE



MCE

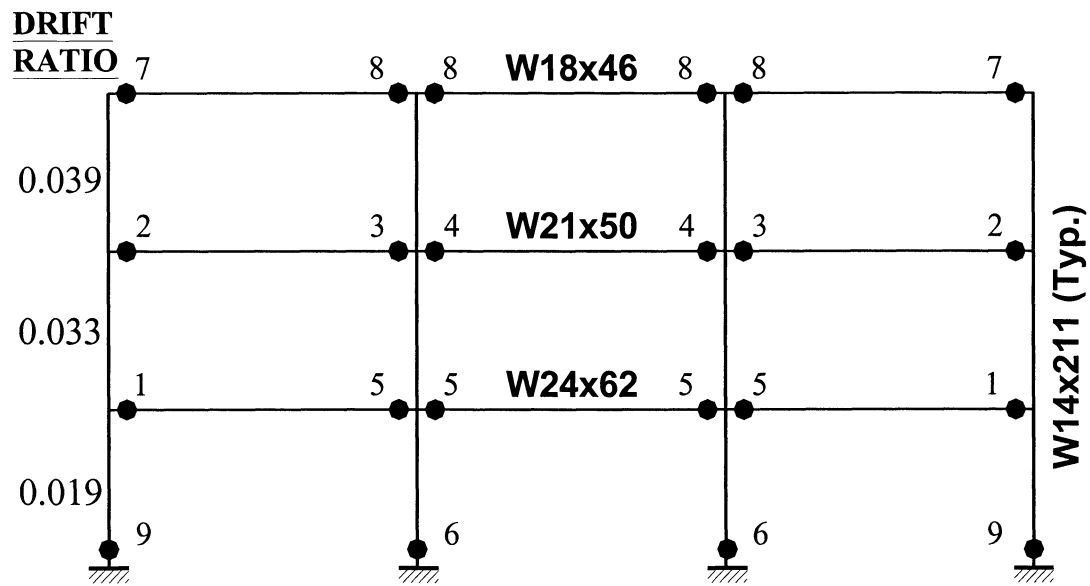
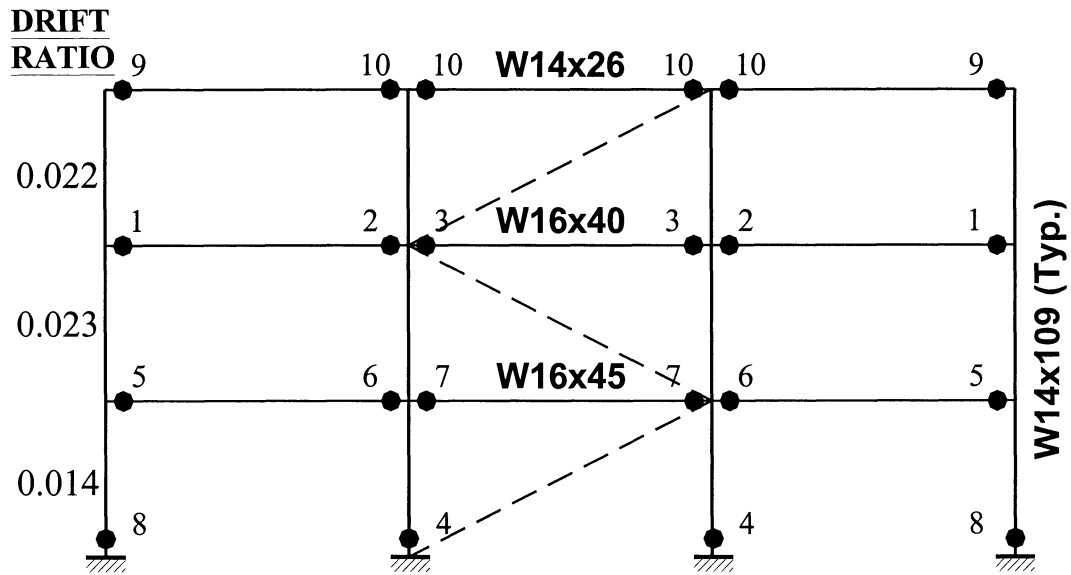


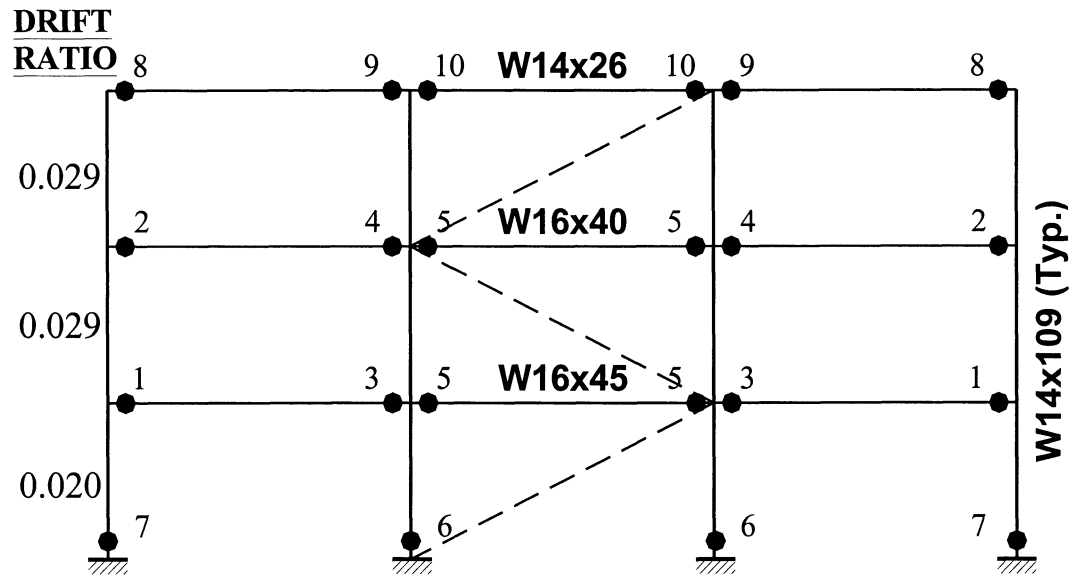
FIGURE 8-14 Plastic Hinge Formation and Key Response Quantities of Frame without Damping System in DBE and MCE

DBE



$D_{\text{roof}} = 240 \text{ mm}$, Peak $\theta_p = 0.0094 \text{ rad}$, $V_{\text{max}} = 1782 \text{ kN}$

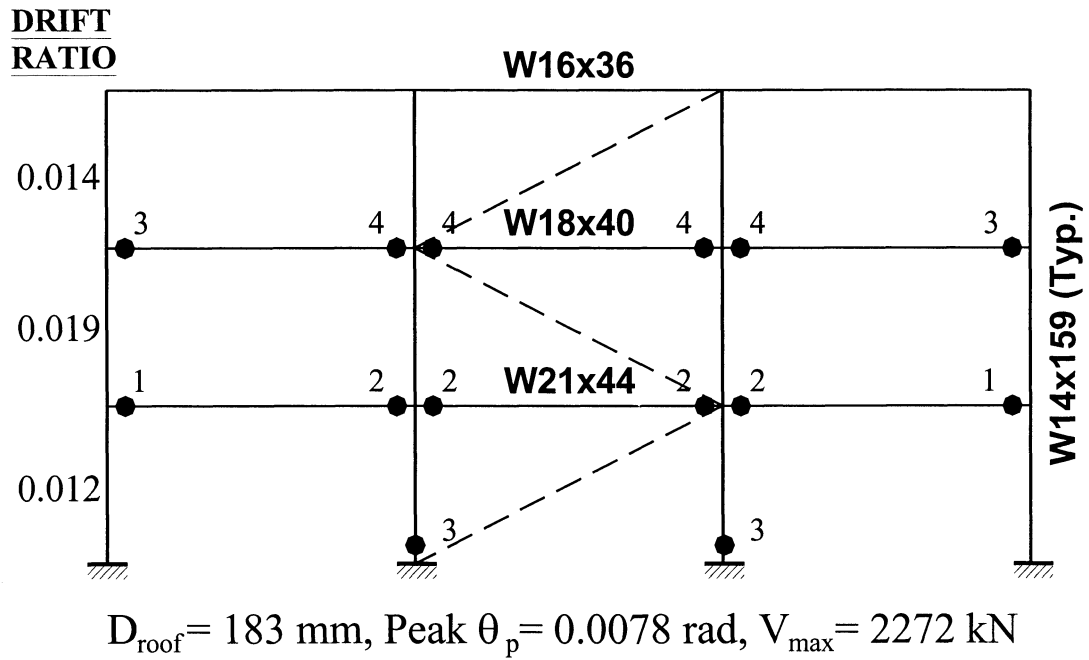
MCE



$D_{\text{roof}} = 312 \text{ mm}$, Peak $\theta_p = 0.0156 \text{ rad}$, $V_{\text{max}} = 1964 \text{ kN}$

FIGURE 8-15 Plastic Hinge Formation and Key Response Quantities of Frame 3S-75 with Linear Viscous Damping System (damping ratio of 10%) in DBE and MCE

DBE



MCE

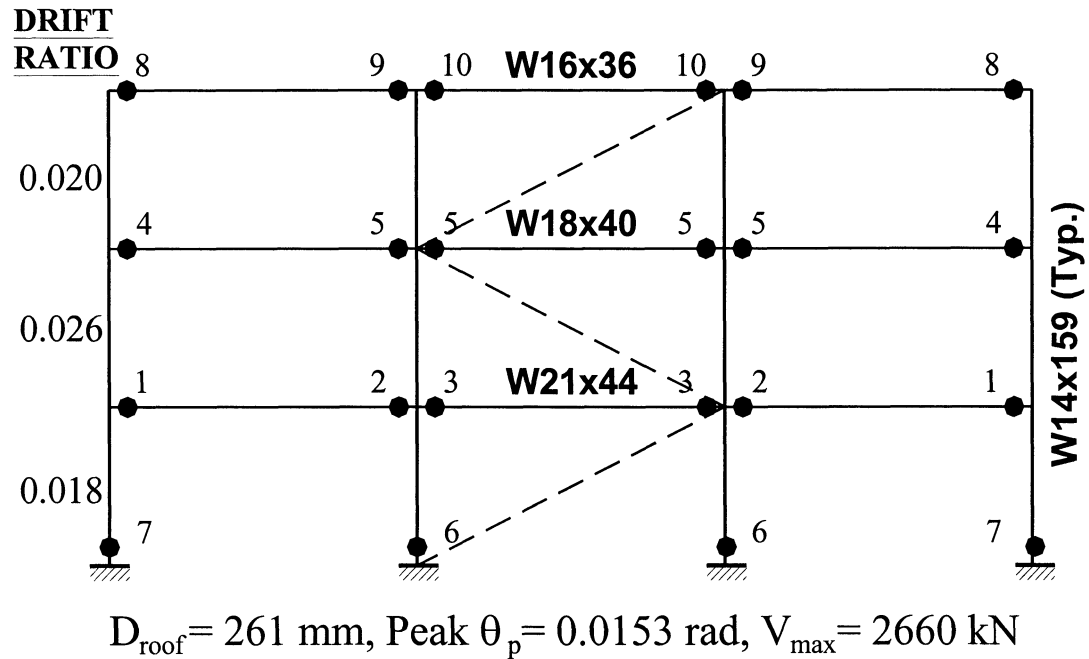


FIGURE 8-16 Plastic Hinge Formation and Key Response Quantities of Frame 3S-100 with Linear Viscous Damping System (damping ratio of 20%) in DBE and MCE

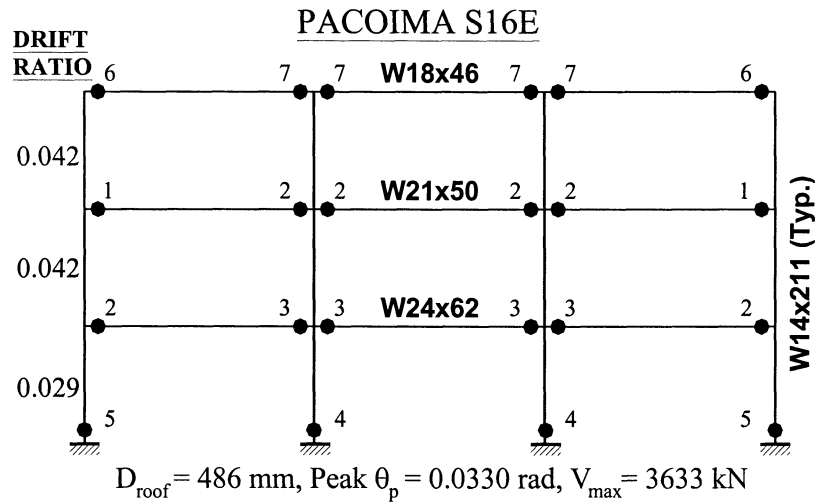
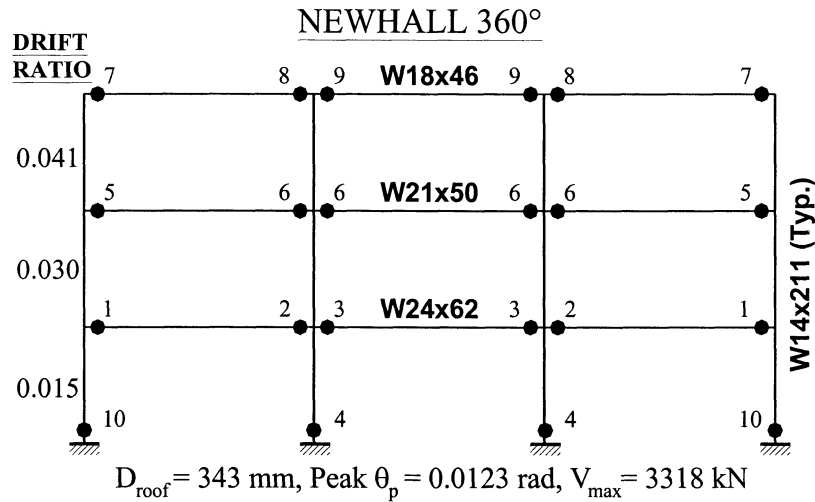
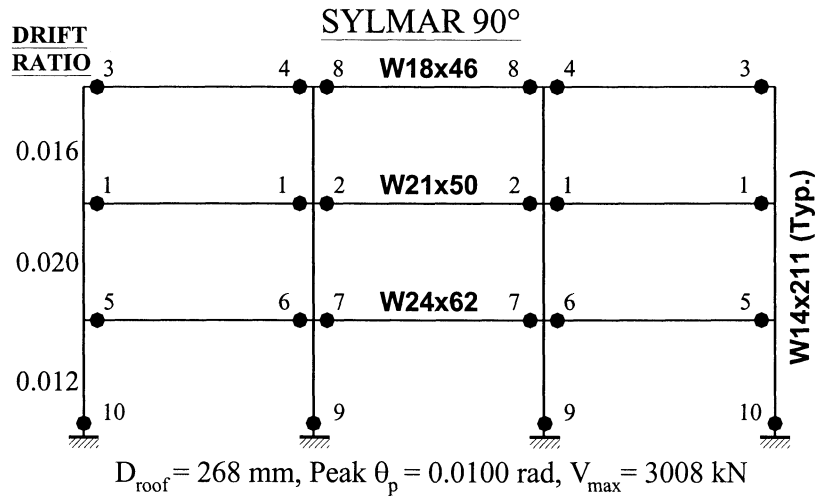


FIGURE 8-17 Plastic Hinge Formation and Key Response Quantities of Frame without Damping System in Near-Fault Seismic Excitation

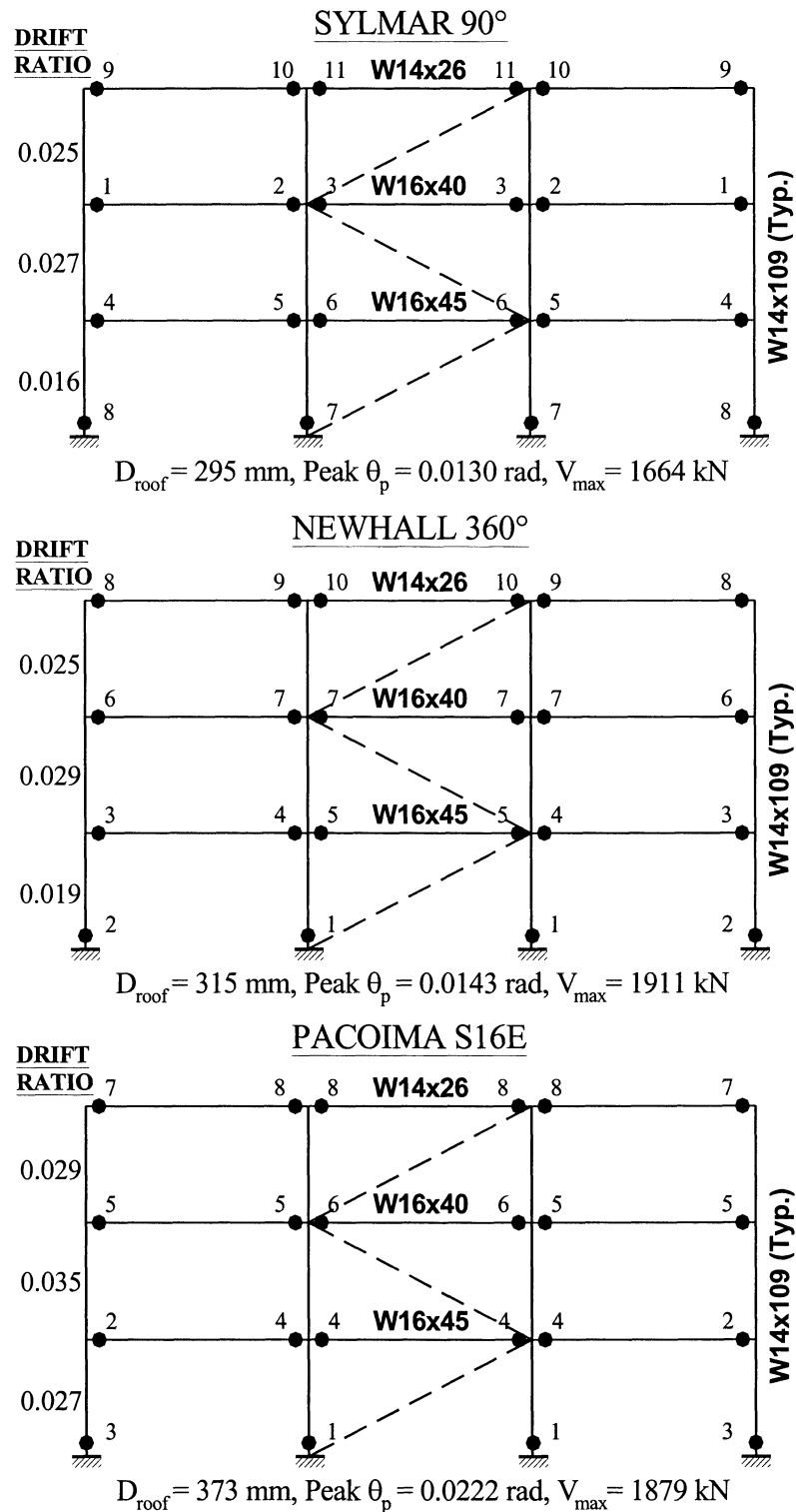


FIGURE 8-18 Plastic Hinge Formation and Key Response Quantities of Frame 3S-75 with Linear Viscous Damping System (damping ratio of 10%) in Near-Fault Seismic Excitation

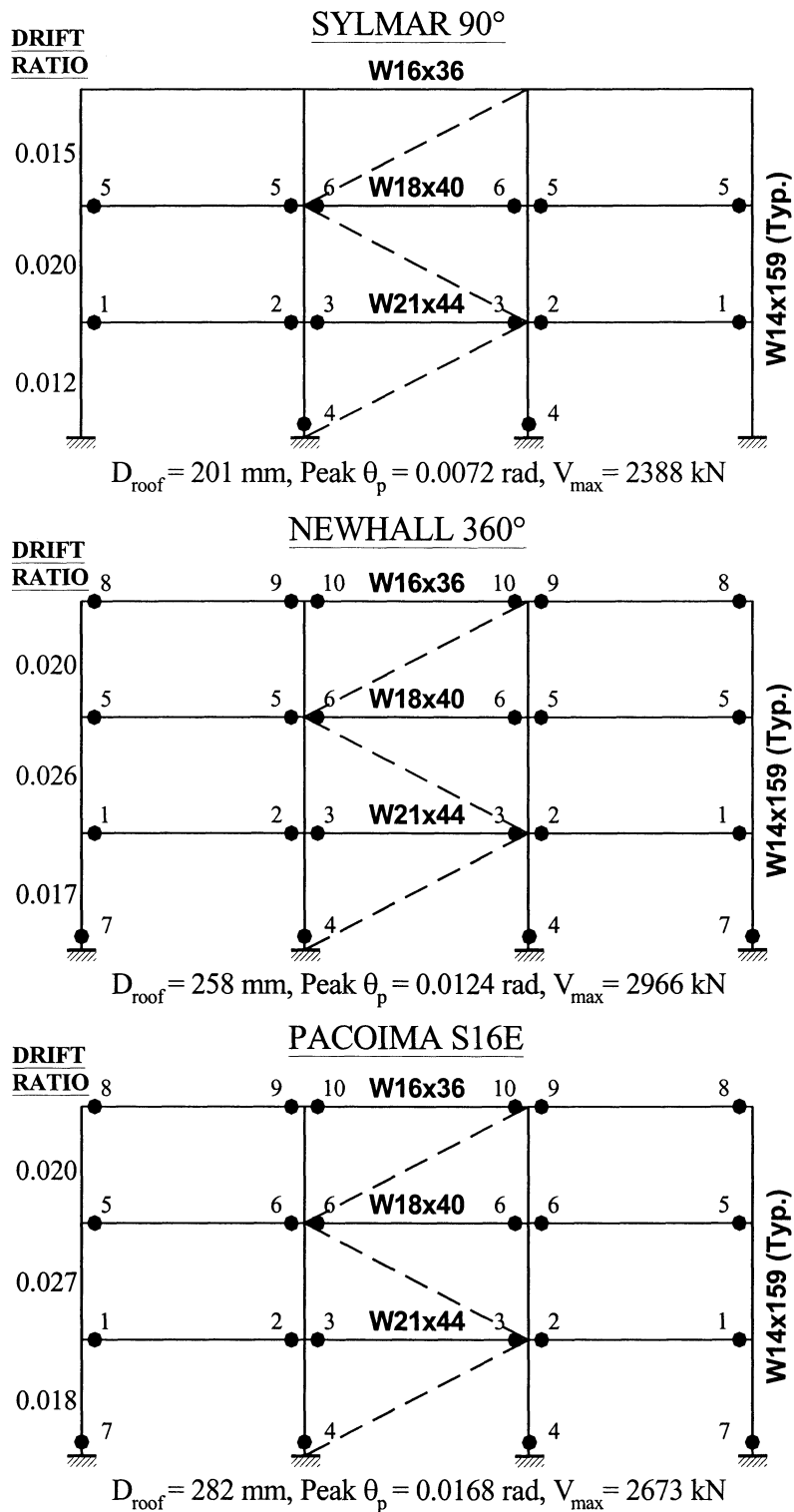


FIGURE 8-19 Plastic Hinge Formation and Key Response Quantities of Frame 3S-100 with Linear Viscous Damping System (damping ratio of 20%) in Near-Fault Seismic Excitation

SECTION 9

SUMMARY, CONCLUSIONS AND RECOMMENDATIONS

9.1 Summary

This report presented the development and evaluation of simplified procedures of analysis and design for structures with passive energy dissipation systems. This study concentrated on the evaluation of the inelastic response of buildings with passive metallic-yielding, viscoelastic, and viscous (linear and nonlinear) energy dissipation systems. This report served to validate robust linear procedures (equivalent-lateral-force and response-spectrum methods) for the analysis and design of new buildings with passive energy dissipation systems that are included in the *2000 NEHRP Recommended Provisions for Seismic Regulations for New Buildings, Appendix to Chapter 13* (NEHRP 2000).

The first task of this study concentrated on the modification of response spectra for levels of damping exceeding 5 percent of critical. Based on the analysis of response of structural systems to selected ground motions, which did not include records on soft soil sites or records with near-fault characteristics, new values of the damping coefficient B were obtained. These new values of the damping coefficient are valid for viscous damping in the range of 2 to 100 percent of critical and were utilized for the evaluation of simplified methods of analysis of yielding single-degree-of-freedom systems with energy dissipation devices. The results of this study were in good agreement with the results of nonlinear time history analysis.

A calibrated relation for the ratio of maximum inelastic displacement to maximum elastic displacement, C_I , was established. The coefficient C_I was expressed as a function of the post-elastic to elastic stiffness, α (range ≤ 0.5), the elastic period, T_e , the viscous damping ratio under elastic conditions, β_v (range of 0.05 to 0.30), the ductility portion of the R-factor, R_μ , and the period T_s , which characterizes the corner point in the design response spectrum.

A systematic study of the ductility demands on damped and undamped structures was presented to determine whether the addition of viscous damping to a building would result in comparable displacement ductility demands. Damped and undamped bilinear hysteretic single-degree-of-freedom systems structures were considered. Undamped structures were characterized by the

elastic period, T_e ; the ductility-based portion of R -factor, R_μ ; the ratio of the post-elastic to elastic stiffness, α ; and the inherent damping ratio, $\beta_i = 0.05$. Values of $T_e = 0.2$ to 2.0 sec, $\alpha = 0.05$, 0.15 , 0.25 and 0.50 , and $R_\mu = 2.0$, 3.33 and 5.0 were considered. Damped structures were characterized by the same parameters β_i , α , and R_μ , a value of elastic period T_{ed} larger than T_e , and added linear viscous damping ratio $\beta_v = 0.15$ and 0.25 under elastic conditions. The calculated average, maximum and minimum displacement ductility ratios in the damped and undamped structures were nearly the same for the same values of R_μ and α .

The core of this research project focuses on the development and evaluation of simplified procedures for the analysis of buildings with damping systems. The theoretical basis of the equivalent lateral force and the response spectrum analysis procedures of NEHRP (2000) was presented. A modification of Method 2 of FEMA (1997) was also presented. Procedures for calculating the effective damping and effective period, and the higher mode damping ratios for buildings with nonlinear viscous damping systems, viscoelastic damping systems and yielding damping systems were developed. The application of these procedures was illustrated through the analysis of 3- and 6-story steel special moment frames with passive energy dissipation devices (viscous, viscoelastic, and metallic yielding devices). Some examples were analyzed utilizing the actual damped spectra of three preselected near-fault motions. Results provided by the simplified procedures were validated by comparison to the results of nonlinear time history analysis carried out using IDARC2D.

In addition, approximate methods for the evaluation of the pushover curve of multiple-degree-of-freedom structures with viscous, viscoelastic, and metallic yielding devices were presented in this study. Important considerations in the design of metallic yielding and viscoelastic solid damping devices were identified, and sample calculations for the analysis of structures with passive damping systems were presented.

9.2 Conclusions

Key conclusions of this study are:

- (1) The proposed values of the damping coefficient B for the modification of response spectra for levels of damping greater than 5 percent of critical provided results that were in good

agreement with the results of nonlinear time history analysis of single-degree-of-freedom systems.

- (2) The proposed equation for the coefficient C_I predicts reasonably well the ratio of maximum inelastic displacement to maximum displacement under elastic conditions of systems with a wide range of values of post-elastic to elastic stiffness ratio, α , viscous damping ratio under elastic conditions, β_v ; the ductility portion of the R-factor, R_μ ; and the elastic period T_e .
- (3) The calculated average, maximum and minimum displacement ductility ratios in damped and undamped structures were nearly the same for the same values of R_μ and α . On the basis of these results, and those presented by Wu and Hanson (1989), NEHRP (2000) permits the design of structures with damping systems for a seismic base shear that is smaller than that required for undamped (conventional) structures.
- (4) Simplified methods of analysis of yielding single-degree-of-freedom systems with energy dissipation devices, including the correction for velocity prediction, produced estimates of peak displacement, peak velocity, and peak acceleration (including the viscous component), which were in good agreement with the average of results of nonlinear time history analysis. The simplified method of analysis is not error-free. However, it is simple to apply, it systematically converges, and produces results of sufficient accuracy for design purposes.
- (5) The application of the simplified methods of analysis of NEHRP (2000) and Method 2 of FEMA 274(1997), as modified in this study, to steel special moment frames with damping systems, provided systematically conservative predictions of drift, and predictions of acceptable accuracy for damper forces and member actions. These force predictions may differ by as much as $\pm 30\%$ from the average forces calculated by dynamic analysis. The greatest deviation occurred in the case of the analyzed 6-story frame.
- (6) The simplified methods produced results of acceptable accuracy for near-fault seismic excitations. However, the number of near-fault motions and analyzed structures considered were too few, and broad conclusions were not drawn. Further studies with near-fault motions are warranted.

- (7) Buildings with damping systems designed to meet the minimum drift and strength criteria of NEHRP (2000) perform comparably to, or better than, conventional buildings without damping systems. Buildings with viscous damping systems can be designed for a lower base shear force than conventional buildings without damping systems for similar performance.
- (8) The approximate methods presented for the construction of the pushover curve of buildings with or without damping systems on the basis of plastic analysis can be utilized with confidence. The developed procedure is an alternate approach to determining the base shear strength of buildings by avoiding the use of pushover analysis.
- (9) The pushover curve of buildings with viscous damping systems is affected by the viscous damping forces, likely by inducing additional rotations of the column ends. This phenomenon, which cannot be accounted for by the current methods of pushover analysis, can lead to underestimation of the maximum value of member actions.
- (10) The procedures developed and evaluated in this study validate the accuracy of simplified methods of analysis of buildings with passive energy dissipation systems. These procedures provided the basis for the implementation of robust linear procedures (equivalent lateral force and response-spectrum methods) for the development of national standards for implementing passive energy dissipation systems in buildings.

9.3 Recommendations for Future Research

It is important to emphasize that the procedures presented in this study have been developed for the analysis of buildings with passive energy dissipation devices taking into account a seismic demand compatible with the 1997 NEHRP spectra for soils type C or D. Neither near-fault characteristics nor soft soil effects have been considered. Also, the evaluation of these procedures has been limited to a few examples of 3- and 6-story steel special moment frames. While the results of these examples show that the procedures are accurate to predict global response, it is fair to say that more studies might be necessary to bound its application. In consequence, the following recommendations are made:

- (1) The number of examples presented in this study is limited. Application of the simplified procedures to a broader variety of structures with different conditions of height and

distribution of passive energy dissipation devices is encouraged to confirm results of this study.

- (2) Further studies of structures with damping systems with near-fault motions is recommended to seek for conclusive evidence of the validity, or the need for adjustments, of the simplified procedures.
- (3) It is desirable to evaluate the applicability of these procedures to the analysis of response of buildings in soft soil sites.

SECTION 10

REFERENCES

1. Bracci, J.M., Kunnath, S.K. and Reinhorn, A.M. (1997), "Seismic Performance and Retrofit Evaluation of Reinforced Concrete Structures", *Journal of Structural Engineering*, ASCE, 123(1), 3-10.
2. Chang, G.A and Mander, J.B. (1994), "Seismic Energy Based Fatigue Damage Analysis of Bridge Columns: Part II – Evaluation of Seismic Demand" Technical Report NCEER-94-0013, National Center for Earthquake Engineering Research, University at Buffalo, State University of New York, Buffalo, N.Y.
3. Chopra, A.K. and Goel, R.K. (1999), "Evaluation of NSP to Estimate Seismic Deformation: SDF Systems", *Journal of Structural Engineering*, American Society of Civil Engineers, 126(4), 482-490.
4. Chopra, A.K. (1995), "Dynamics of Structures", Prentice Hall, Englewood Cliffs, N.J.
5. Clough, R.W and Penzien, J. (1975), "Dynamics of Structures", McGraw-Hill, New York, N.Y.
6. Coffin, L. F. Jr. (1954), "A Study of Effects of Cyclic Thermal Stresses on a Ductile Metal", *Trans.*, American Society of Mechanical Engineers, New York, 76, 931-950.
7. Computers and Structures Inc. (1998), "SAP-2000NL V7.11: Integrated Finite Element Analysis and Design of Structures", Computers and Structures Inc., Berkeley, CA.
8. Constantinou, M.C. and Sigaher, N. (2000), "Energy Dissipation System Configurations for Improved Performance", *Proceedings of the 2000 Structures Congress & Exposition*, ASCE, Philadelphia, PA.
9. Constantinou, M.C. and Symans, M.D. (1992), "Experimental and Analytical Investigation of Structures with Supplemental Fluid Viscous Dampers", Technical Report NCEER-92-0032, National Center for Earthquake Engineering Research, University at Buffalo, State University of New York, Buffalo, N.Y.
10. Constantinou, M.C., Soong, T.T. and Dargush, G.F. (1998), "Passive Energy Dissipation Systems for Structural Design and Retrofit", Monograph Series No.1, Multidisciplinary Center for Earthquake Engineering Research, University at Buffalo, State University of New York at Buffalo, Buffalo, N.Y.
11. Constantinou, M.C. (1998), "An Introduction to Passive Energy Dissipation", Spring Seminar, Structural Engineers Association of Northern California (SEAONC), San Francisco, CA.

12. Eberhard, M.O. and Sozen, M.A. (1993), "Behavior-Based Method to Determine Design Shear in Earthquake-Resistant Walls", *Journal of Structural Engineering*, ASCE, 119: (2) 619-640.
13. Fajfar, P. and Fischinger, M. (1988), "N2 – A Method for Non-Linear Seismic Analysis of Regular Structures", *Proceedings of the Ninth World Conference on Earthquake Engineering*, Tokyo-Kyoto, Japan.
14. FEMA - Federal Emergency Management Agency (1997), "NEHRP Guidelines for the Seismic Rehabilitation of Buildings" and "NEHRP Commentary on the Guidelines for the Seismic Rehabilitation of Buildings", Reports No. FEMA-273 and FEMA-274, Washington, D.C.
15. Freeman, S.A., Nicoletti, J.P., and Tyrell, J.V. (1975), "Evaluation of Existing Buildings for Seismic Risk – A Case Study of Puget Sound Naval Shipyard, Bremerton, Washington", *Proceedings of the First U.S. National Conference on Earthquake Engineering*, Earthquake Engineering Research Institute, Oakland, California.
16. Freeman, S.A. (1978), "Prediction of Response of Concrete Buildings to Severe Earthquake Motion", *Douglas McHenry International Symposium on Concrete and Concrete Structures*, SP-66, American Concrete Institute, Detroit, MI, 589-605.
17. Gomez, J.D. (2000), "Evaluation of Simplified Methods of Analysis of Yielding Structures with Energy Dissipation Systems", Master of Science Thesis, Department of Civil, Structural and Environmental Engineering, University at Buffalo, State University of New York, Buffalo, N.Y.
18. Iwan, W.D. and Gates, N.C. (1979a), "The Effective Period and Damping of a Class of Hysteretic Structures", *Earthquake Engineering and Structural Dynamics*, 7(3), 199-211.
19. Iwan, W.D. and Gates, N.C. (1979b), "Estimating Earthquake Response of Simple Hysteretic Structures", *Journal of Engineering Mechanics Division*, ASCE, 105 (EM3), 391-405.
20. Kelly, J.M., Skinner, M.S. and Beucke, K.E. (1980). "Experimental Testing of an Energy Absorbing Base Isolation System", Technical Report No.UCB/EERC-80/35, Earthquake Engineering Research Center, University of California, Berkeley, CA.
21. Koh, S. K. and Stephens, R.I. (1991), "Mean Stress Effects on Low Cycle Fatigue for High Strength Steel", *Fatigue Fracture of Engineering Materials and Structures*, 14(4), 413-428.
22. Mander, J.B., Priestley, M.J.N. and Park, R. (1984), "Seismic Design of Bridge Piers", Department of Civil Engineering, University of Canterbury, Report 84-2, February.
23. Mander, J. B., Panthaki, F. D. and Kasalanati, A. (1994), "Low-Cycle Fatigue Behavior of Reinforcing Steel", *Journal of Materials in Civil Engineering*, 6 (4), 453-467.

24. Manson, S. S. (1953), "Behavior of Materials Under Conditions of Thermal Stress", Heat Transfer Symposium, Engineering Research Institute, University of Michigan, Ann Arbor, 9-75.
25. Miranda, E. and Bertero, V.V. (1994), "Evaluation of Strength Reduction Factors for Earthquake-Resistant Design", *Earthquake Spectra*, 10(2), 357-379.
26. Miranda, E. (1993), "Site-Dependent Strength Reduction Factors", *Journal of Structural Engineering*, ASCE, Vol. 119, No.12, 3503-3519.
27. Nassar, A.A. and Krawinkler, H. (1991). " Seismic demands for SDOF and MDOF Systems", Report No. 95, John Blume Earthquake Engineering Research Center, Stanford University, Stanford, California.
28. NEHRP - National Earthquake Hazard Reduction Program (1994), "NEHRP Recommended Provisions for Seismic Regulations for New Buildings and Other Structures", Federal Emergency Management Agency, Report No. FEMA 222A, Washington, D.C.
29. NEHRP - National Earthquake Hazard Reduction Program (1997), "NEHRP Recommended Provisions for Seismic Regulations for New Buildings and Other Structures", Federal Emergency Management Agency, Report No. FEMA 302, Washington, D.C.
30. NEHRP - National Earthquake Hazard Reduction Program (2000), "NEHRP Recommended Provisions for Seismic Regulations for New Buildings and Other Structures", Appendix to Chapter 13, Structures with Damping Systems, Federal Emergency Management Agency, Washington, D.C., published in March 2001 as Reports FEMA 368 and 369.
31. Newmark, N.M and Hall, W.J. (1969), "Seismic Design Criteria for Nuclear Reactor Facilities", *Proceedings Fourth World Conference on Earthquake Engineering*, Santiago, Chile, 2, B-4, 37-50.
32. Newmark, N.M. and Hall, W.J. (1973), "Seismic Design Criteria for Nuclear Reactor Facilities", Report No.46, *Building Practices for Disaster Mitigation*, National Bureau of Standards, U.S. Department of Commerce, pp. 209-236.
33. Newmark, N.M. and Hall, W.J. (1982), "Earthquake Spectra and Design", *Earthquake Engineering Research Institute*, Oakland, California.
34. Newmark, N.M and Rosenblueth, E. (1971), "Fundamentals of Earthquake Engineering", Prentice-Hall, Englewood Cliffs, N.J.
35. Novak, M. and El Hifnawy, L. (1983), "Effect of Soil-Structure Interaction on Damping of Structures". *Earthquake Engineering and Structural Dynamics*, 11(5), 595-621.

36. Pekhan, G., Mander J.B., and Chen S.S. (1999), "Design and Retrofit Methodology for Buildings Structures with Supplemental Energy Dissipating Systems", Technical Report MCEER-99-0021, Multidisciplinary Center for Earthquake Engineering Research, University at Buffalo, State University of New York, Buffalo, N.Y.
37. Reinhorn, A.M., Li, C., and Constantinou, M.C. (1995), "Experimental and Analytical Investigation of Seismic Retrofit of Structures with Supplemental Damping Part I: Fluid Viscous Damping Devices", Technical Report NCEER-95-0001, National Center for Earthquake Engineering Research, University at Buffalo, State University of New York, Buffalo, N.Y.
38. Riddell, R. and Newmark, N.M. (1979), "Statistical Analysis of the Response of Nonlinear Systems Subjected to Earthquakes", Structural Research Series No.468, Department of Civil Engineering, University of Illinois, Urbana.
39. Riddell, R., Hidalgo, P., and Cruz, E. (1989), "Response Modification Factors for Earthquake Resistant design of Short Period Structures, Earthquake Spectra, 5(3), 571-590.
40. Sadek, F., Mohraz, B. and Riley, M.A. (1999), "Linear Static and Dynamic Procedures for Structures with Velocity-Dependent Supplemental Dampers," Building and Fire Research Laboratory, National Institute of Standards and Technology, Gaithersburg, MD.
41. SEAOC- Structural Engineers Association of California (1999), "Recommended Lateral Force Requirements and Commentary", Sacramento, CA.
42. Seleemah, A.A., and Constantinou, M.C. (1997), "Investigation of Seismic Response of Buildings with Linear and Nonlinear Fluid Viscous Dampers", Technical Report NCEER-97-004, National Center for Earthquake Engineering Research, University at Buffalo, State University of New York, Buffalo, N.Y.
43. Soong, T.T. and Dargush, G.F. (1997), "Passive Energy Dissipation Systems in Structural Engineering", John Wiley & Sons Ltd., London (UK) and New York (USA).
44. Tsai, K.C., Cheng, H.W., Hong, C.P. and Su, Y.F. (1993), "Design of Steel Triangular Plate Energy Absorbers for Seismic-Resistant Construction", Earthquake Spectra, 9(3), 505-528.
45. Tsopeles, P., Constantinou, M.C., Kircher, C.A. and Whittaker, A.S. (1997), "Evaluation of Simplified Methods of Analysis for Yielding Structures". Technical Report No. NCEER 97-0012, National Center for Earthquake Engineering Research, University at Buffalo, State University of New York, Buffalo, N.Y.
46. Tyler, R.G. (1978a), "A Tenacious Base Isolation System Using Round Steel Bars", Bulletin of the New Zealand National Society for Earthquake Engineering, 11(4), 273-281.
47. Tyler, R.G. (1978b), "Tapered Steel Energy Dissipators for Earthquake Resistant Structures". Bulletin of the New Zealand National Society for Earthquake Engineering 11(4), 282-294.

48. Uang, C. and Bertero, V.V. (1990), "Evaluation of Seismic Energy in Structures", *Earthquake Engineering and Structural Dynamics*, 19(1), 77-90.
49. Valles, R.E., Reinhorn, A.M., Kunnath, S.K., Li, C. and Madan, A. (1996), "IDARC2D Version 4.0: A Computer Program for the Inelastic Damage Analysis of Buildings", Technical Report NCEER-96-0010, National Center for Earthquake Engineering Research, University at Buffalo, State University of New York, Buffalo, N.Y. Information on Version 5.0 of IDARC2D can be found at <http://civil.eng.buffalo.edu/idarc2d50/>.
50. Veletsos, A.S. and Meek, J.W. (1974), "Dynamic Behavior of Building-Foundation Systems", *Earthquake Engineering and Structural Dynamics*, 3(2), 121-138.
51. Vidic, T., Fajfar, P. and Fischinger, M. (1992), "A procedure for Determining Consistent Inelastic Design Spectra", Proc. Workshop on Nonlinear Seismic Analysis of RC Structures, Bled, Slovenia.
52. Watanabe A., Hitomi, Y., Saeki, E., Wada, A., and Fujimoto, M. (1988), "Properties of Brace Encased in Buckling-Restraining Concrete and Steel Tube", Proceedings of Ninth World Conference on Earthquake Engineering, Tokyo-Kyoto, Japan, Paper No.6-7-4, Vol. IV, pp. 719-724.
53. Whittaker, A. S., Aiken, I., Bergman, D., Clark, P., Kelly, J. and Scholl, R. (1993), "Code Requirements for the Design and Implementation of Passive Energy Dissipation Systems". *Proceedings*, ATC-17-1, Seminar on Seismic Isolation, Passive Energy Dissipation, and Active Control, Applied Technology Council, Redwood City, California.
54. Wu, J., and Hanson, R.D. (1989), "Study of Inelastic Spectra with High Damping", *Journal of Structural Engineering*, ASCE, 115(6), 1412-1431.
55. Zimmer, M. (1999) "Characterization of Viscoelastic Materials for use in Seismic Energy Dissipation Systems", Master of Science Thesis, Department of Civil, Structural and Environmental Engineering, University at Buffalo, State University of New York, Buffalo, N.Y.

APPENDIX A

**NEHRP 2000 – APPENDIX TO CHAPTER 13: STRUCTURES WITH DAMPING
SYSTEMS**

SCOPE: 1997 Provisions Appendix to Chapter 13 and Provisions and Commentary Chapter 2

PROPOSAL FOR CHANGE:

Revise the 1997 Provisions Appendix to Chapter 13 as follows:

Appendix to Chapter 13

**~~PASSIVE ENERGY DISSIPATION SYSTEMS~~
~~STRUCTURES WITH DAMPING SYSTEMS~~**

~~Passive energy dissipation systems may be used as part of the lateral-force-resisting system of a structure when special detailing is used to provide results equivalent to those obtained by use of conventional structural systems. The design criteria for structures using passive energy dissipation systems shall be consistent with the minimum requirements of an equivalent conventional structure based on these Provisions.~~

~~The design of structures using passive energy dissipation systems shall be based on rational methods of analysis, incorporating the most appropriate analysis methods, including nonlinear time-history dynamic analysis. The stiffness and damping properties of damping devices shall be accurately modeled in the analysis and shall be based on tested and independently verified data from testing of such devices. Such testing shall have subjected the devices to loads, displacements, and other imposed conditions that are consistent with design conditions.~~

~~A design review of the passive energy dissipation system and related test programs shall be performed by an independent team of registered design professionals in the appropriate disciplines and others experienced in seismic analysis methods and the theory and application of energy dissipation systems. The scope of this design review shall be consistent with that required by these Provisions for the isolation system of seismically isolated structures.~~

A13.1 GENERAL: Every structure with a damping system and every portion thereof shall be designed and constructed in accordance with the requirements of this appendix and the applicable requirements of Chapter 1.

Exception: Motion and accelerations of seismically isolated structures which contain damping devices across the plane of isolation shall be determined in accordance with the provisions of Chapter 13. Testing and strength requirements of damping devices and other elements of the damping system shall be determined in accordance with the applicable provisions of this Appendix.

A13.2 CRITERIA SELECTION:

A13.2.1 Basis for Design: The procedure and limitations for the design of *structures* with a *damping system* shall be determined considering zoning, site characteristics, vertical acceleration, cracked section properties of concrete and masonry members, *Seismic Use Group*, configuration, structural system, and height in accordance with Sec. 5.2, except as noted below.

A13.2.2 Seismic Use Group: All portions of the *structure* shall be assigned a *Seismic Use Group* in accordance with the requirements of Sec. 1.3.

A13.2.3 Seismic Design Category: Each *structure* shall be assigned to a *Seismic Design Category* based on the *Seismic Use Group* and the design spectral response acceleration in accordance with Sec. 4.2.

Exception: *Seismic Design Category A structures* with a *damping system* shall be designed using the design spectral response acceleration determined in accordance with Sec. 4.1.2.5 and the analysis methods and design provisions required for *Seismic Design Category B structures*.

A13.2.4 Configuration Requirements: *Structure* design shall consider the combination of forces that occur in the basic *seismic-force-resisting system* and the *damping system*, as defined in the following sections.

A13.2.4.1 Seismic-Force-Resisting System: *Structures* that contain a *damping system* are required to have a basic *seismic-force-resisting system* that, in each lateral direction, shall conform to one of the types indicated in Table 5.2.2.

The design of the *seismic-force-resisting system* in each direction shall comply with the requirements of Section A13.7.1 and the following:

1. The materials, detailing, construction and inspection of the *seismic-force-resisting system* shall meet all applicable requirements defined by the *Seismic Design Category*.
2. The lateral stiffness of the *seismic-force-resisting system* used to determine elastic periods and displacements shall include the modeling requirements of Sections 5.3.7 and 5.4.2.
3. The seismic base shear used for design of the *seismic-force-resisting system* shall not be less than V_{min} , where V_{min} is determined as the greater of the following values:

$$V_{min} = \frac{V}{B_{V+1}} \quad (\text{A13.2.4.1-1})$$

$$V_{min} = 0.75V \quad (\text{A13.2.4.1-2})$$

where:

-
- V = total design shear at the *base* of the *structure* in the direction of interest, as determined using the procedure of Sec. 5.3, including Sec.5.3.3 (kip or kN), and
- B_{v+l} = numerical coefficient as set forth in Table A13.3.1 for effective damping equal to the sum of viscous damping in the fundamental mode of vibration of the *structure* in the direction of interest, β_{vm} ($m = 1$), plus inherent damping, β_l , and period of *structure* equal to T_l .

Exception: Seismic base shear used for design of the *seismic-force-resisting system* shall not be taken as less than $1.0V$, if either of the following conditions apply:

1. In the direction of interest, the *damping system* has less than two *damping devices* on each floor level, configured to resist torsion.
2. The *seismic-force-resisting system* has a vertical irregularity of Type 1b (Table 5.2.3.3) or a plan irregularity of Type 1b (Table 5.2.3.2).
4. Minimum strength requirements for *elements* of the *seismic-force-resisting-system* that are also *elements* of the *damping system* or are otherwise required to resist forces from damping devices shall meet the additional requirements of Section A13.7.3.

A13.2.4.2 Damping System: Elements of the *damping system* shall be designed to remain elastic for design loads including unreduced seismic forces of *damping devices* as required in Section A13.7.3, unless it is shown by analysis or test that inelastic response of *elements* would not adversely affect *damping system* function and inelastic response is limited in accordance with the requirements of Section A13.7.3.4.

A13.2.5 Seismic Criteria:

A13.2.5.1 Design Spectra: Spectra of the *design earthquake* and the *maximum considered earthquake* developed in accordance with Sec. 13.4.4.1 shall be used for the design and analysis of all *structures* with a *damping system*. Site-specific design spectra shall be developed and used for design of *structures* with a *damping system* if any one of the following conditions apply:

1. The *structure* is located on a Class F site or
2. The *structure* is located at a site with S_1 greater than 0.60g.

A13.2.5.2 Time Histories: Ground-motion time histories of the *design earthquake* and the *maximum considered earthquake* developed in accordance with Sec. 13.4.4.2 shall be used for design and analysis of all *structures* with a *damping system* if either of the following conditions apply:

1. The *structure* is located at a site with S_1 greater than 0.60g.
2. The *damping system* is explicitly modeled and analyzed using the time history analysis method.

A13.2.6 Selection of Analysis Procedure:

A13.2.6.1 General: A structural analysis shall be made for all *structures* with a *damping system* in accordance with the requirements of this section. The structural analysis shall use linear procedures, nonlinear procedures, or a combination of linear and nonlinear procedures as described below.

The *seismic-force-resisting system* shall be designed using the procedures of either Section A13.2.6.2 or Section A13.2.6.3.

The *damping system* may be designed using the procedures of either Section A13.2.6.2 or A13.2.6.3, subject to the limitations set forth in these sections. *Damping systems* not meeting these limitations shall be designed using the nonlinear analysis methods as required in Section A13.6.

A13.2.6.2 Equivalent Lateral Force Analysis Procedure: *Structures* with a *damping system* designed using the equivalent lateral force analysis procedure of Sec. A13.4 shall be subject to the following limitations:

1. In the direction of interest, the *damping system* has at least two *damping devices* in each story, configured to resist torsion.
2. The total effective damping of the fundamental mode, $\beta_{mD}(m = 1)$, of the *structure* in the direction of interest is not greater than 35 percent of critical.
3. The *seismic-force-resisting system* does not have a vertical irregularity of Type 1a, 1b, 2, or 3 (Table 5.2.3.3) or a plan irregularity of Type 1a or 1b (Table 5.2.3.2).
4. Floor diaphragms are rigid (Section 5.2.31).
5. The height of the *structure* above the *base* does not exceed 100 feet (30 meters).
6. Peak dynamic response of the *structure* and elements of the *damping system* are confirmed by nonlinear time history analysis, when required by Sec. A13.2.6.4.3.

A13.2.6.3 Response Spectrum Analysis: *Structures* with a *damping system* meeting the limitations of Section A13.2.6.2 may be designed using the response spectrum analysis procedure of Sec. A13.5 and *structures* not meeting the limitations of Section A13.2.6.2 shall be designed using the response spectrum analysis procedure of Sec. A13.5, subject to the following limitations:

1. In the direction of interest, the *damping system* has at least two *damping devices* in each story, configured to resist torsion,
2. The total effective damping of the fundamental mode, $\beta_{mD}(m = 1)$, of the *structure* in the direction of interest is not greater than 35 percent of critical, and
3. Peak dynamic response of the *structure* and *elements* of the *damping system* are confirmed by nonlinear time history analysis, when required by Sec. A13.2.6.4.3.

A13.2.6.4 Nonlinear Analysis:

A13.2.6.4.1 General: Nonlinear analysis procedures of A13.6 are permitted for design of all *structures* with *damping systems* and shall be used for design of *structures* with *damping systems* not meeting linear analysis criteria of Sec. A13.2.6.3.

Nonlinear time history analysis shall be used to confirm peak dynamic response of the *structure* and elements of the *damping system* if the *structure* is located at a site with S_1 greater than 0.60g.

The nonlinear force-deflection characteristics of elements of the *seismic-force-resisting system* shall be modeled as required by Section 5.7.1 and 5.8.1. The nonlinear force-deflection characteristics of *damping devices* shall be modeled, as required, to explicitly account for device dependence on frequency, amplitude and duration of seismic loading.

A13.2.6.4.2 Nonlinear Static Analysis: Structures with a *damping system* designed using the nonlinear static analysis procedure of Sec. A13.6 shall be subject to the following limitations:

1. Peak dynamic response of the *structure* and elements of the *damping system* is confirmed by nonlinear time history analysis, when required by Sec. A13.2.6.4.3.

A13.2.6.4.3 Nonlinear Time History Analysis: Structures with a *damping system* may be designed using the nonlinear time history analysis procedure of Sec. A13.6 without limitation.

Nonlinear time history analysis shall be used to confirm peak dynamic response of the *structure* and *elements* of the *damping system* for structures with a *damping system* if the following conditions applies:

1. The *structure* is located at site with S_1 greater than 0.60g.

A13.3 DAMPED RESPONSE MODIFICATION:

A13.3.1 General: As required in Sections A13.4 and A13.5, response of the *structure* shall be modified for the effects of the *damping system* using coefficients prescribed in Table A13.3.1.

Table A13.3.1 Damping Coefficient, B_{V+D} , B_{ID} , B_D , B_{IM} , B_{mD} or B_{mM}

Effective Damping, β	Period of the Structure $\geq T_g/5$
$\leq 2\%$	0.8
5%	1.0
10%	1.2
20%	1.5
30%	1.8
40%	2.1
50%	2.4
60%	2.7
70%	3.0
80%	3.3
90%	3.6
$\geq 100\%$	4.0

¹The damping coefficient is equal to 1.0 at a period of the structure equal to 0 second for all values of effective damping. Interpolation may be used for intermediate values of effective damping at periods of the structure between 0 second and $T_g/5$ seconds.

A13.3.2 Effective Damping: The effective damping at the *design displacement*, β_{mD} , and at the *maximum displacement*, β_{mM} , of the m^{th} mode of vibration of the *structure* in the direction under consideration shall be calculated as follows:

$$\beta_{mD} = \beta_I + \beta_{Vm} \sqrt{\mu_D} + \beta_{HD} \tag{A13.3.2-1}$$

$$\beta_{mM} = \beta_I + \beta_{vm} \sqrt{\mu_M} + \beta_{HM} \quad (\text{A13.3.2-2})$$

where:

- β_{HD} = component of effective damping of the *structure* in the direction of interest due to post-yield hysteretic behavior of the *seismic-force-resisting system* and elements of the *damping system* at effective ductility demand, μ_D ,
- β_{HM} = component of effective damping of the *structure* in the direction of interest due to post-yield hysteretic behavior of the *seismic-force-resisting system* and elements of the *damping system* at effective ductility demand, μ_M ,
- β_I = component of effective damping of the *structure* due to the inherent dissipation of energy by elements of the *structure*, at or just below the effective yield displacement of the *seismic-force-resisting system*,
- β_{vm} = component of effective damping of the m^{th} mode of vibration of the *structure* in the direction of interest due to viscous dissipation of energy by the *damping system*, at or just below the effective yield displacement of the *seismic-force-resisting system*,
- μ_D = effective ductility demand on the *seismic-force-resisting system* in the direction of interest due to the *design earthquake*, and
- μ_M = effective ductility demand on the *seismic-force-resisting system* in the direction of interest due to the *maximum considered earthquake*.

Unless analysis or test data supports other values, the effective ductility demand of higher modes of vibration in the direction of interest shall be taken as 1.0.

A13.3.2.1 Inherent Damping: Inherent damping, β_I , shall be based on the material type, configuration and behavior of the *structure* and nonstructural components responding dynamically at or just below yield of the *seismic-force-resisting system*. Unless analysis or test data supports other values, inherent damping shall be taken as not greater than 5% of critical for all modes of vibration.

A13.3.2.2 Hysteretic Damping: Hysteretic damping of the *seismic-force-resisting system* and elements of the *damping system* shall be based either on test or analysis, or in accordance with the following equations:

$$\beta_{HD} = q_H (0.64 - \beta_I) \left(1 - \frac{1}{\mu_D} \right) \quad (\text{A13.3.2.2-1})$$

$$\beta_{HM} = q_H (0.64 - \beta_I) \left(1 - \frac{1}{\mu_M} \right) \quad (\text{A13.3.2.2-2})$$

where:

- q_H = hysteresis loop adjustment factor, as defined in Sec. A13.3.3,
- μ_D = effective ductility demand on the *seismic-force-resisting system* in the direction of interest due to the *design earthquake*, as defined in Sec. A.13.3.4, and
- μ_M = effective ductility demand on the *seismic-force-resisting system* in the direction of interest due to the *maximum considered earthquake*, as defined in Sec. A13.3.4.

Unless analysis or test data supports other values, the hysteretic damping of higher modes of vibration in the direction of interest shall be taken as zero.

A13.3.2.3 Viscous Damping: Viscous damping of the m^{th} mode of vibration of the *structure*, β_{vm} , shall be calculated as follows:

$$\beta_{vm} = \frac{\sum_j W_{mj}}{4\pi W_m} \quad (\text{A13.3.2.3-1})$$

$$W_m = \frac{1}{2} \sum_i F_{im} \delta_{im} \quad (\text{A13.3.2.3-2})$$

where:

- W_{mj} = work done by j^{th} damping device in one complete cycle of dynamic response corresponding to the m^{th} mode of vibration of the *structure* in the direction of interest at modal displacements, δ_{im} ,
- W_m = maximum strain energy in the m^{th} mode of vibration of the *structure* in the direction of interest at modal displacements, δ_{im} ,
- F_{im} = m^{th} mode inertial force at Level i (or mass point),
- δ_{im} = deflection of Level i (or mass point) in the m^{th} mode of vibration at the center of rigidity of the *structure* in the direction under consideration.

Viscous modal damping of *displacement-dependent damping devices* shall be based on a response amplitude equal to the effective yield displacement of the *structure*.

The calculation of the work done by individual *damping devices* shall consider orientation and participation of each device with respect to the mode of vibration of interest. The work done by individual *damping devices* shall be reduced as required to account for the flexibility of *elements*, including pins, bolts, gusset plates, brace extensions, and other components that connect *damping devices* to other *elements* of the *structure*.

A13.3.3 Hysteresis Loop Adjustment Factor: Hysteretic damping of the *seismic-force-resisting system* and elements of the *damping system* shall consider pinching and other effects that reduce the area of the hysteresis loop during repeated cycles of earthquake demand. Unless

analysis or test data support other values, the fraction of full hysteretic loop area of the *seismic-force-resisting system* used for design shall be taken as equal to the factor, q_H , as defined below:

$$q_H = 0.67 \frac{T_s}{T_l} \quad (\text{A13.3.3-1})$$

where:

- T_s = period, in seconds, defined by the ratio, S_{Dl}/S_{Ds}
 T_l = period, in seconds of the fundamental mode of vibration of the *structure* in the direction of the interest

The value of q_H shall not be taken as greater than 1.0, and need not be taken as less than 0.5.

A13.3.4 Effective Ductility Demand: The effective ductility demand of *seismic-force-resisting system* due to the *design earthquake*, μ_D , and due to the *maximum considered earthquake*, μ_M , shall be calculated as the ratio of the fundamental mode displacement, D_{ID} or D_{IM} , to effective yield displacement, D_Y :

$$\mu_D = \frac{D_{ID}}{D_Y} \geq 1.0 \quad (\text{A13.3.4-1})$$

$$\mu_M = \frac{D_{IM}}{D_Y} \geq 1.0 \quad (\text{A13.3.4-2})$$

$$D_Y = \left(\frac{g}{4\pi^2} \right) \left(\frac{\Omega_o C_d}{R} \right) \Gamma_l C_{sl} T_l^2 \quad (\text{A13.3.4-3})$$

where:

- D_{ID} = fundamental mode *design displacement* at the center of rigidity of the roof level of the *structure* in the direction under consideration, Sec. A13.4.4.3 (in. or mm),
 D_{IM} = fundamental mode *maximum displacement* at the center of rigidity of the roof level of *structure* in the direction under consideration, Sec. A13.4.4.6 (in. or mm),
 D_Y = displacement at the center of rigidity of the roof level of the *structure* at the effective yield point of the *seismic-force-resisting system*, Sec. A13.3.4 (in. or mm),
 R = response modification factor from Table 5.2.2,
 C_d = deflection amplification factor from Table 5.2.2,
 Ω_o = system overstrength factor from Table 5.2.2,

-
- Γ_1 = participation factor of the fundamental mode of vibration of the *structure* in the direction of interest, Sec. A13.4.3.3 or Sec. A13.5.3.3 ($m = 1$),
 - C_{S1} = *seismic response coefficient* (dimensionless) of the fundamental mode of vibration of the *structure* in the direction of interest, Sec. A13.4.3.4 or Sec. A13.5.3.4 ($m = 1$), and
 - T_1 = period, in seconds, of the fundamental mode of vibration of the *structure* in the direction of interest.

Design earthquake ductility demand, μ_D , shall not exceed the maximum value of effective ductility demand, μ_{max} , given in section A13.3.5.

A13.3.5 Maximum Effective Ductility Demand: For determination of the hysteresis loop adjustment factor, hysteretic damping and other parameters, ductility demand used for design of the *structure* shall not exceed the maximum value of effective ductility demand, μ_{max} , as defined below:

For $T_1 < T_S$:

$$\mu_{max} = \frac{1}{2} \left(\left(\frac{R}{\Omega_o I} \right)^2 + 1 \right) \quad (\text{A13.3.5-1})$$

For $T_{1D} \geq T_S$:

$$\mu_{max} = \frac{R}{\Omega_o I} \quad (\text{A13.3.5-2})$$

where:

- I = the occupancy importance factor determined in accordance with Sec. 1.4.
- T_{1D} = effective period, in seconds, of the fundamental mode of vibration of the *structure* at the *design displacement* in the direction under consideration.

For periods: $T_1 \leq T_S \leq T_{1D}$, interpolation shall be used to determine μ_{max} .

A13.4 EQUIVALENT LATERAL FORCE ANALYSIS PROCEDURE:

A13.4.1 General: This section provides required minimum standards for equivalent lateral force analysis of *structures* with a *damping system*. For purposes of analysis, the *structure* is considered to be fixed at the *base*. See Sec. A13.2.6 for limitations on the use of this procedure.

Seismic base shear and lateral forces at floors used for design of the *seismic-force-resisting system* shall be based on the procedures of Section A13.4.3. Seismic forces, displacements and velocities used for design of the *damping system* shall be based on the procedures of Section A13.4.4.

The load combinations and acceptance criteria of Section A13.7 shall be used to check design responses of *seismic-force-resisting* and *damping systems*, respectively.

A13.4.2 Modeling Requirements: *Elements* of the *seismic-force-resisting system* shall be modeled in a manner consistent with the requirements of Section 5.3.

Elements of the *damping system* shall be modeled as required to determine design forces transferred from *damping devices* to both the ground and the *seismic-force-resisting system*. The effective stiffness of *velocity-dependent damping devices* shall be modeled.

Damping devices need not be explicitly modeled provided effective damping is calculated in accordance with the procedures of Section A13.3 and used to modify response as required in Sections A13.4.3 and A13.4.4.

The stiffness and damping properties of the *damping devices* used in the models shall be based on or verified by testing of the *damping devices* as specified in Sec. A13.10.

A13.4.3 Seismic-Force-Resisting-System Design Response:

A13.4.3.1 Seismic Base Shear: The seismic *base shear*, V , of the *seismic-force-resisting system* in a given direction shall be determined as the combination of the two modal components, V_I and V_R , in accordance with the following equation:

$$V = \sqrt{V_I^2 + V_R^2} \geq V_{min} \quad (\text{A13.4.3.1-1})$$

where:

- V_I = design value of the seismic *base shear* of the fundamental mode in a given direction of response (kip or kN),
- V_R = design value of the seismic *base shear* of the residual mode in a given direction (kip or kN), and
- V_{min} = minimum allowable value of *base shear* permitted for design of the *seismic-force-resisting-system* of the *structure* in direction of the interest (kip or kN).

A13.4.3.2 Fundamental Mode Base Shear: Fundamental mode *base shear*, V_I , shall be determined in accordance with the following equation:

$$V_I = C_{s1} \overline{W}_I \quad (\text{A13.4.3.2-1})$$

where:

- \overline{W}_I = the effective fundamental mode *gravity load* including portions of the *live load* as defined by Eq. 5.4.5-2 for $m = 1$ (kip or kN).

A13.4.3.3 Fundamental Mode Properties: Fundamental mode shape, ϕ_{i1} , and participation factor, Γ_I , shall be determined by either dynamic analysis of elastic structural properties and deformational characteristics of the resisting elements or in accordance with the following equations:

$$\phi_{i1} = \frac{h_i}{h_r} \quad (\text{A13.4.3.3-1})$$

$$\Gamma_i = \frac{\overline{W}_i}{\sum_{i=1}^n w_i \phi_{i1}} \quad (\text{A13.4.3.3-2})$$

where:

- h_i = the height of the *structure* above the *base* to Level i (ft or m),
- h_r = the height of the *structure* above the *base* to the roof level (ft or m),
- w_i = the portion of the total *gravity load*, W , located or assigned to Level i .

The fundamental period, T_1 , shall be determined either by dynamic analysis of elastic structural properties and deformational characteristics of the resisting *elements*, or in accordance with the following equation:

$$T_1 = 2\pi \sqrt{\frac{\sum_{i=1}^n w_i \delta_i^2}{g \sum_{i=1}^n f_i \delta_i}} \quad (\text{A13.4.3.3-3})$$

where:

- f_i = lateral force at Level i of the *structure* distributed in accordance with Formula 5.3.4-2, and
- δ_i = elastic deflection at Level i of the *structure* due to applied lateral forces f_i .

A13.4.3.4 Fundamental Mode Seismic Response Coefficient: The fundamental mode seismic response coefficient, C_{S1} , shall be determined in accordance with the following equations:

For $T_{1D} < T_S$:

$$C_{S1} = \left(\frac{R}{C_d} \right) \frac{S_{DS}}{\Omega_o B_{1D}} \quad (\text{A13.4.3.4-1})$$

For $T_{1D} \geq T_S$:

$$C_{S1} = \left(\frac{R}{C_d} \right) \frac{S_{D1}}{T_{1D} (\Omega_o B_{1D})} \quad (\text{A13.4.3.4-2})$$

where:

-
- S_{DS} = the design spectral response acceleration in the short period range as determined from Sec. 4.1.2.5,
 S_{DI} = the design spectral response acceleration at a period of 1 second as determined from Sec. 4.1.2.5,
 B_{ID} = numerical coefficient as set forth in Table A13.3.1 for effective damping equal to β_{mD} ($m = 1$) and period of the *structure* equal to T_{ID} ,

A13.4.3.5 Effective Fundamental Mode Period Determination: The effective fundamental mode period at the *design earthquake*, T_{ID} , and at the *maximum considered earthquake*, T_{IM} , shall be based either on explicit consideration of the post-yield force deflection characteristics of the *structure* or in accordance with the following equations:

$$T_{ID} = T_I \sqrt{\mu_D} \quad (\text{A13.4.3.5-1})$$

$$T_{IM} = T_I \sqrt{\mu_M} \quad (\text{A13.4.3.5-2})$$

where:

- T_{IM} = effective period, in seconds, of the fundamental mode of vibration of the *structure* at the *maximum displacement* in the direction under consideration.

A13.4.3.6 Residual Mode Base Shear: Residual mode *base shear*, V_R , shall be determined in accordance with the following equation:

$$V_R = C_{SR} \overline{W}_R \quad (\text{A13.4.3.6-1})$$

where:

- C_{SR} = the residual mode *seismic response coefficient* as determined in Sec. A13.4.3.8, and
 \overline{W}_R = the effective residual mode *gravity load* of the *structure* determined in accordance with Eq. A13.4.3.7-3 (kip or kN).

A13.4.3.7 Residual Mode Properties: Residual mode shape, ϕ_{iR} , participation factor, Γ_R , effective gravity load of the *structure*, \overline{W}_R , and effective period, T_R , shall be determined in accordance with the following equations:

$$\phi_{iR} = \frac{1 - \Gamma_I \phi_{iI}}{1 - \Gamma_I} \quad (\text{A13.4.3.7-1})$$

$$\Gamma_R = 1 - \Gamma_I \quad (\text{A13.4.3.7-2})$$

$$\overline{W}_R = W - \overline{W}_I \quad (\text{A13.4.3.7-3})$$

$$T_R = 0.4T_I \quad (\text{A13.4.3.7-4})$$

A13.4.3.8 Residual Mode Seismic Response Coefficient: The residual mode seismic response coefficient, C_{SR} , shall be determined in accordance with the following equation:

$$C_{SR} = \left(\frac{R}{C_d} \right) \frac{S_{DS}}{\Omega_o B_R} \quad (\text{A13.4.3.8-1})$$

where:

B_R = Numerical coefficient as set forth in Table A13.3.1 for effective damping equal to β_R , and period of the *structure* equal to T_R .

A13.4.3.9 Design Lateral Force: Design lateral force in *elements* of the *seismic-force-resisting system* at Level i due to fundamental mode response, F_{iI} , and residual mode response, F_{iR} , of the *structure* in the direction of interest shall be determined in accordance with the following equations:

$$F_{iI} = w_i \phi_{iI} \frac{\Gamma_I}{W_I} V_I \quad (\text{A13.4.3.9-1})$$

$$F_{iR} = w_i \phi_{iR} \frac{\Gamma_R}{W_R} V_R \quad (\text{A13.4.3.9-2})$$

Design forces in *elements* of the *seismic-force-resisting system* shall be determined as the square-root-sum-of-squares of the forces due to fundamental and residual modes.

A13.4.4 Damping System Design Response:

A13.4.4.1 General: Design forces in *damping devices* and other elements of the *damping system* shall be determined on the basis of the floor deflection, story drift and story velocity response parameters described in the following sections.

Displacements and velocities used to determine maximum forces in *damping devices* at each story shall account for the angle of orientation from horizontal and consider the effects of increased response due to torsion required for design of the *seismic-force-resisting system*.

Floor deflections at Level i , δ_{iD} and δ_{iM} , design story drifts, Δ_D and Δ_M , and design story velocities, ∇_D and ∇_M , shall be calculated for both the *design earthquake* and the *maximum considered earthquake*, respectively, in accordance with the following sections.

A13.4.4.2 Design Earthquake Floor Deflection: Fundamental and residual mode deflections due to the *design earthquake*, δ_{iID} and δ_{iRD} (in. or mm), at the center of rigidity of Level i of the *structure* in the direction of interest shall be determined in accordance with the following equations:

$$\delta_{iID} = D_{iD} \phi_{iI} \quad (\text{A13.4.4.2-1})$$

$$\delta_{iRD} = D_{RD}\phi_{iR} \quad (\text{A13.4.4.2-2})$$

where:

D_{RD} = Residual mode *design displacement* at the center of rigidity of the roof level of the *structure* in the direction under consideration, Sec. A13.4.4.3 (in or mm).

The total *design earthquake* deflection at each floor of the *structure* in the direction of interest shall be calculated as the square-root-sum-of-squares of fundamental and residual mode floor deflections.

A13.4.4.3 Design Earthquake Roof Displacement: Fundamental and residual mode displacements due to the *design earthquake*, D_{ID} and D_{IR} (in or mm) at the center of rigidity of the roof level of the *structure* in the direction of interest shall be determined in accordance with the following equations:

$$D_{ID} = \left(\frac{g}{4\pi^2} \right) \Gamma_1 \frac{S_{DI} T_{ID}}{B_{ID}} \leq \left(\frac{g}{4\pi^2} \right) \Gamma_1 \frac{S_{DS} T_{ID}^2}{B_{ID}} \quad (\text{A13.4.4.3-1})$$

$$D_{RD} = \left(\frac{g}{4\pi^2} \right) \Gamma_R \frac{S_{DI} T_R}{B_R} \leq \left(\frac{g}{4\pi^2} \right) \Gamma_R \frac{S_{DS} T_R^2}{B_R} \quad (\text{A13.4.4.3-2})$$

A13.4.4.4 Design Earthquake Story Drift: *Design earthquake* story drift, Δ_D , of the *structure* in the direction of interest shall be calculated in accordance with the following equation:

$$\Delta_D = \sqrt{\Delta_{ID}^2 + \Delta_{RD}^2} \quad (\text{A13.4.4.4-1})$$

where:

Δ_{ID} = *design earthquake* story drift due to the fundamental mode of vibration of the *structure* in the direction of interest (in. or mm), and

Δ_{RD} = *design earthquake* story drift due to the residual mode of vibration of the *structure* in the direction of interest (in. or mm).

Modal *design earthquake* story drifts, Δ_{ID} and Δ_{IR} , shall be determined in accordance with Sec. 5.3.7.1 using the floor deflections of Sec. A13.4.4.2.

A13.4.4.5 Design Earthquake Story Velocity: *Design earthquake* story velocity, ∇_D , of the *structure* in the direction of interest shall be calculated in accordance with the following equations:

$$\nabla_D = \sqrt{\nabla_{ID}^2 + \nabla_{RD}^2} \quad (\text{A13.4.4.5-1})$$

$$\nabla_{ID} = 2\pi \frac{\Delta_{ID}}{T_{ID}} \quad (\text{A13.4.4.5-2})$$

$$\nabla_{RD} = 2\pi \frac{\Delta_{RD}}{T_R} \quad (\text{A13.4.4.5-3})$$

where:

- ∇_{ID} = design earthquake story velocity due to the fundamental mode of vibration of the *structure* in the direction of interest (in/sec or mm/sec), and
- ∇_{RD} = design earthquake story velocity due to the residual mode of vibration of the *structure* in the direction of interest (in/sec or mm/sec).

A13.4.4.6 Maximum Earthquake Response: Total and modal *maximum earthquake* floor deflections at Level *i*, design story drift values and design story velocity values shall be based on the formulas of Sections A13.4.2, A13.4.4 and A13.4.5, respectively, except *design earthquake* roof displacements shall be replaced by *maximum earthquake* roof displacements. *Maximum earthquake* roof displacements shall be calculated in accordance with the following equations:

$$D_{IM} = \left(\frac{g}{4\pi^2} \right) \Gamma_1 \frac{S_{MI} T_{IM}}{B_{IM}} \leq \left(\frac{g}{4\pi^2} \right) \Gamma_1 \frac{S_{MS} T_{IM}^2}{B_{IM}} \quad (\text{A13.4.4.6-1})$$

$$D_{RM} = \left(\frac{g}{4\pi^2} \right) \Gamma_R \frac{S_{MI} T_R}{B_R} \leq \left(\frac{g}{4\pi^2} \right) \Gamma_R \frac{S_{MS} T_R^2}{B_R} \quad (\text{A13.4.4.6-2})$$

where:

- S_{MI} = the *maximum considered earthquake*, 5 percent damped, spectral response acceleration at a period of 1 second adjusted for *site class* effects as defined in Sec.4.1.2.
- S_{MS} = the *maximum considered earthquake*, 5 percent damped, spectral response acceleration at short periods adjusted for *site class* effects as defined in Sec. 4.1.2.
- B_{IM} = Numerical coefficient as set forth in Table A13.3.1 for effective damping equal to β_{mM} ($m = 1$) and period of *structure* equal to T_{IM} .

A13.5 RESPONSE SPECTRUM ANALYSIS PROCEDURE

A13.5.1 General: This section provides required standards for response spectrum analysis of *structures* with a *damping system*. See Sec. A13.2.6 for limitations on the use of this procedure.

Seismic *base shear* and lateral forces at floors used for design of the *seismic-force-resisting system* shall be based on the procedures of Sec. A13.3.2. Seismic forces, displacements and velocities used for design of the *damping system* shall be based on the procedures of Section A13.3.

The load combinations and acceptance criteria of Sec. A13.7 shall be used to check design responses of *seismic-force-resisting system* and the *damping system*.

A13.5.2 Modeling and Analysis Requirements:

A13.5.2.1 General: A mathematical model of the *seismic-force-resisting system* and *damping system* shall be constructed that represents the spatial distribution of mass, stiffness and damping throughout the *structure*. The model and analysis shall conform to the requirements of Sec. 5.4.2, Sec. 5.4.3, and Sec.5.4.4 for the *seismic-force-resisting system* and to the requirements of Sec. A13.5.2.2 for the *damping system*. The stiffness and damping properties of the *damping devices* used in the models shall be based on or verified by testing of the *damping devices* as specified in Sec. A13.10.

A13.5.2.2 Damping System: The elastic stiffness of elements of the *damping system* other than *damping devices* shall be explicitly modeled. Stiffness of *damping devices* shall be modeled depending on *damping device* type:

1. *Displacement-Dependent Damping Devices:* *Displacement-dependent damping devices* shall be modeled with an effective stiffness that represents *damping device* force at the response displacement of interest (e.g., design story drift). Alternatively, the stiffness of hysteretic and friction *damping devices* may be excluded from response spectrum analysis provided design forces in *displacement-dependent damping devices*, Q_{DSD} , are applied to the model as external loads (Sec. A13.7.3.2).
2. *Velocity-Dependent Damping Devices:* *Velocity-dependent damping devices* that have a stiffness component (e.g., visco-elastic damping devices) shall be modeled with an effective stiffness corresponding to the amplitude and frequency of interest.

A13.5.3 Seismic-Force-Resisting-System Design Response:

A13.5.3.1 Seismic Base Shear: The seismic *base shear*, V , of the *structure* in a given direction shall be determined as the combination of modal components, V_m , subject to the limits of the following equation:

$$V \geq V_{min} \quad (\text{A13.5.3.1-1})$$

The seismic *base shear*, V , of the *structure* shall be determined by the square root sum of the squares or complete quadratic combination of modal *base shear* components, V_m .

A13.5.3.2 Modal Base Shear: Modal *base shear* of the m^{th} mode of vibration, V_m , of the *structure* in the direction of interest shall be determined in accordance with the following equation:

$$V_m = C_{Sm} \overline{W}_m \quad (\text{A13.5.3.2-1})$$

where:

C_{Sm} = seismic response coefficient (dimensionless) of the m^{th} mode of vibration of the *structure* in the direction of interest, Sec. A13.5.3.4 ($m = 1$) or Sec. A13.5.3.6 ($m > 1$), and

\overline{W}_m = the effective gravity load of the m^{th} mode of vibration of the *structure* determined in accordance with Eq. 5.4.5-2 (kip or kN).

A13.5.3.3 Modal Participation Factor: The modal participation factor of the m^{th} mode of vibration, Γ_m , of the *structure* in the direction of interest shall be determined in accordance with the following equation:

$$\Gamma_m = \frac{\overline{W}_m}{\sum_{i=1}^n w_i \phi_{im}} \quad (\text{A13.5.3.3-1})$$

where:

ϕ_{im} = displacement amplitude at the i^{th} level of the *structure* for the fixed base condition in the m^{th} mode of vibration in the direction of interest, normalized to unity at the roof level.

A13.5.3.4 Fundamental Mode Seismic Response Coefficient: The fundamental mode ($m = 1$) seismic response coefficient, C_{S1} , in the direction of interest shall be determined in accordance with the following equations:

For $T_{1D} < T_S$:

$$C_{S1} = \left(\frac{R}{C_d} \right) \frac{S_{DS}}{\Omega_o B_{1D}} \quad (\text{A13.5.3.4-1})$$

For $T_{1D} \geq T_S$:

$$C_{S1} = \left(\frac{R}{C_d} \right) \frac{S_{D1}}{T_{1D} (\Omega_o B_{1D})} \quad (\text{A13.5.3.4-2})$$

A13.5.3.5 Effective Fundamental Mode Period Determination: The effective fundamental mode ($m = 1$) period at the *design earthquake*, T_{1D} , and at the *maximum considered earthquake*, T_{1M} , shall be based either on explicit consideration of the post-yield nonlinear force deflection characteristics of the *structure* or determined in accordance with the following equations:

$$T_{1D} = T_1 \sqrt{\mu_D} \quad (\text{A13.4.3.5-1})$$

$$T_{1M} = T_1 \sqrt{\mu_M} \quad (\text{A13.4.3.5-2})$$

A13.5.3.6 Higher Mode Seismic Response Coefficient: Higher mode ($m > 1$) seismic response coefficient, C_{Sm} , of the m^{th} mode of vibration ($m > 1$) of the *structure* in the direction of interest shall be determined in accordance with the following equations:

For $T_m < T_S$:

$$C_{Sm} = \left(\frac{R}{C_d} \right) \frac{S_{DS}}{\Omega_o B_{mD}} \quad (\text{A13.5.3.6-1})$$

For $T_m \geq T_S$:

$$C_{Sm} = \left(\frac{R}{C_d} \right) \frac{S_{D1}}{T_m (\Omega_o B_{mD})} \quad (\text{A13.5.3.6-2})$$

where:

T_m = period, in seconds, of the m^{th} mode of vibration of the *structure* in the direction under consideration,

B_{mD} = numerical coefficient as set forth in Table A13.3.1 for effective damping equal to β_{mD} and period of the *structure* equal to T_m .

A13.5.3.7 Design Lateral Force: Design lateral force at Level i due to m^{th} mode of vibration, F_{im} , of the *structure* in the direction of interest shall be determined in accordance with the following equation:

$$F_{im} = w_i \phi_{im} \frac{\Gamma_m}{W_m} V_m \quad (\text{A13.5.3.7-1})$$

Design forces in elements of the *seismic-force-resisting system* shall be determined by the square root sum of squares or complete quadratic combination of modal design forces.

A13.5.4 Damping System Design Response:

A13.5.4.1 General: Design forces in *damping devices* and other elements of the *damping system* shall be determined on the basis of the floor deflection, story drift and story velocity response parameters described in the following sections.

Displacements and velocities used to determine maximum forces in *damping devices* at each story shall account for the angle of orientation from horizontal and consider the effects of increased response due to torsion required for design of the *seismic-force-resisting system*.

Floor deflections at Level i , δ_{iD} and δ_{imD} , design story drifts, Δ_D and Δ_M , and design story velocities, ∇_D and ∇_M , shall be calculated for both the *design earthquake* and the *maximum considered earthquake*, respectively, in accordance with the following sections.

A13.5.4.2 Design Earthquake Floor Deflection: The deflection of *structure* due to the *design earthquake* at Level i in the m^{th} mode of vibration, δ_{imD} (in. or mm), of the *structure* in the direction of interest shall be determined in accordance with the following equation:

$$\delta_{imD} = D_{mD} \phi_{im} \quad (\text{A13.5.4.2-1})$$

The total *design earthquake* deflection at each floor of the *structure* shall be calculated by the square root sum of squares or complete quadratic combination of modal *design earthquake* deflections.

A13.5.4.3 Design Earthquake Roof Displacement: Fundamental ($m = 1$) and higher mode ($m > 1$) roof displacements due to the *design earthquake*, D_{1D} and D_{mD} (in. or mm), of the *structure* in the direction of interest shall be determined in accordance with the following equations:

For $m = 1$:
$$D_{1D} = \left(\frac{g}{4\pi^2} \right) \Gamma_1 \frac{S_{D1} T_{1D}}{B_{1D}} \leq \left(\frac{g}{4\pi^2} \right) \Gamma_1 \frac{S_{DS} T_{1D}^2}{B_{1D}} \quad (\text{A13.5.4.3-1})$$

For $m > 1$:
$$D_{mD} = \left(\frac{g}{4\pi^2} \right) \Gamma_m \frac{S_{D1} T_m}{B_{mD}} \leq \left(\frac{g}{4\pi^2} \right) \Gamma_m \frac{S_{DS} T_m^2}{B_{mD}} \quad (\text{A13.5.4.3-2})$$

A13.5.4.4 Design Earthquake Story Drift: *Design earthquake* story drift of the fundamental mode, Δ_{1D} , and higher modes, Δ_{mD} ($m > 1$), of the *structure* in the direction of interest shall be calculated in accordance with Section 5.3.7.1 using modal roof displacements of Section A13.5.4.3.

Total *design earthquake* story drift, Δ_D (in. or mm), shall be determined by the square root of the sum of squares or complete quadratic combination of modal *design earthquake* drifts.

A13.5.4.5 Design Earthquake Story Velocity: *Design earthquake* story velocity of the fundamental mode, ∇_{1D} , and higher modes, ∇_{mD} ($m > 1$), of the *structure* in the direction of interest shall be calculated in accordance with the following equations:

For $m = 1$:
$$\nabla_{1D} = 2\pi \frac{\Delta_{1D}}{T_{1D}} \quad (\text{A13.5.4.5-1})$$

For $m > 1$:
$$\nabla_{mD} = 2\pi \frac{\Delta_{mD}}{T_m} \quad (\text{A13.5.4.5-1})$$

Total *design earthquake* story velocity, ∇_D (in/sec or mm/sec), shall be determined by the square root of the sum of squares or complete quadratic combination of modal *design earthquake* velocities.

A13.5.4.6 Maximum Earthquake Response: Total modal floor deflection at Level i , design story drift values and design story velocity values shall be based on the formulas of Sections A13.5.4.2, A13.5.4.4 and A13.5.4.5, respectively, except *design earthquake* roof displacement shall be replaced by *maximum earthquake* roof displacement. *Maximum earthquake* roof displacement of the *structure* in the direction of interest shall be calculated in accordance with the following equations:

For $m = 1$:
$$D_{1M} = \left(\frac{g}{4\pi^2} \right) \Gamma_1 \frac{S_{M1} T_{1M}}{B_{1M}} \leq \left(\frac{g}{4\pi^2} \right) \Gamma_1 \frac{S_{MS} T_{1M}^2}{B_{1M}} \quad (\text{A13.5.4.6-1})$$

For $m > 1$:
$$D_{mM} = \left(\frac{g}{4\pi^2} \right) \Gamma_m \frac{S_{M1} T_m}{B_{mM}} \leq \left(\frac{g}{4\pi^2} \right) \Gamma_m \frac{S_{MS} T_m^2}{B_{mM}} \quad (\text{A13.5.4.6-2})$$

where:

B_{mM} = numerical coefficient as set forth in Table A13.3.1 for effective damping equal to β_{mM} and period of the *structure* equal to T_m .

A13.6 NONLINEAR ANALYSIS PROCEDURES

A13.6.1 General: The nonlinear procedures provided in Section A13.6 supplement the nonlinear procedures of Sections 5.7 and 5.8 to accommodate the use of *damping systems*. The stiffness and damping properties of the *damping devices* used in the models shall be based on or verified by testing of the *damping devices* as specified in Sec. A13.10.

A13.6.2. Nonlinear Static Analysis: The nonlinear modeling described in Section 5.7.1 and the lateral loads described in Section 5.7.2 shall be applied to the *seismic-force-resisting system*. The resulting force-displacement curve shall be used in lieu of the assumed effective yield displacement, D_y , of Equation A13.3.4-3 to calculate the effective ductility demand due to the *design earthquake*, μ_D , and due to the *maximum considered earthquake*, μ_M , in Equations A13.3.4-1 and A13.3.4-2. The value of (R/C_d) shall be taken as 1.0 in Equations A13.4.3.4-1, A13.4.3.4-2 and A13.4.3.8-1 for the Equivalent Lateral Force Analysis Procedure, and in Equations A13.5.3.4-1, A13.5.3.4-2, A13.5.3.6-1, and A13.5.3.6-2 of the Response Spectrum Analysis Procedure.

A13.6.3 Nonlinear Response History Analysis: A nonlinear response history (time history) analysis shall utilize a mathematical model of the *structure* and the *damping system* as provided in Section 5.8 and this section. The model shall directly account for the nonlinear hysteretic behavior of *elements* of the *structure* and the *damping devices* to determine its response, through methods of numerical integration, to suites of ground motions compatible with the design response spectrum for the site.

The analysis shall be performed in accordance with Section 5.8 together with the requirements of this section.

A13.6.3.1 Damping Device Modeling: Mathematical models of *displacement-dependent damping devices* shall include the hysteretic behavior of the devices consistent with test data and accounting for all significant changes in strength, stiffness, and hysteretic loop shape. Mathematical models of *velocity-dependent damping devices* shall include the velocity coefficient consistent with test data. If this coefficient changes with time and/or temperature, such behavior shall be modeled explicitly. The elements of *damping devices* connecting damper units to the *structure* shall be included in the model.

Exception: If the properties of the *damping devices* are expected to change during the duration of the time history analysis, the dynamic response may be enveloped by the upper and lower limits of device properties. All these limit cases for variable device properties must satisfy the same conditions as if the time dependent behavior of the devices were explicitly modeled.

A13.6.3.2 Response Parameters: In addition to the response parameters given in Section 5.8.3, the *design earthquake* and *maximum considered earthquake* displacements, velocities, and forces of the *damping devices* shall be determined.

A13.7 SEISMIC LOAD CONDITIONS AND ACCEPTANCE CRITERIA:

A13.7.1 General: Design forces and displacements determined in accordance with the equivalent lateral force analysis procedures of Section A13.4 or the response spectrum analysis procedure of Section 13.5 shall be checked using the strength design criteria of these *Provisions* and the seismic loading conditions of the following sections.

A13.7.2 Seismic-Force-Resisting System: The *seismic-force-resisting system* shall meet the design provisions of Sec. 5.2.2 using seismic *base shear* and design forces determined in accordance with Section A13.4.3 or Sec A13.5.3.

The design earthquake story drift, Δ_D , as determined in either Sec. A13.4.4.4 or A13.5.4.4 shall not exceed (R/C_d) times the allowable story drift, as obtained from Table 5.2.8, considering the effects of torsion as required in Section 5.2.8.

A13.7.3 Damping System: The *damping system* shall meet the provisions of Section 5.2.2 for seismic design forces determined in accordance with Sec. A13.7.3.1 and the seismic loading conditions of Section A13.7.3.2 and Section A13.5.4.

A13.7.3.1 Modal Damping System Design Forces: Modal *damping system* design forces shall be calculated on the basis of the type of *damping devices*, and the modal design story displacements and modal design story velocities determined in accordance with either Section A13.4.4 or Section A13.5.4.

Exception: Modal design story displacements and velocities determined in accordance with either Section A13.4.4 or Section A13.5.4 shall be increased as required to envelop total design story displacements and velocities determined in accordance with Section A13.6, when Section A13.2.6.4.3 requires peak response to be confirmed by time history analysis.

1. *Displacement-Dependent Damping Devices:* Design seismic force in *displacement-dependent damping devices* shall be based on the maximum force in the device at displacements up to and including the *design earthquake* story drift, Δ_D .
2. *Velocity-Dependent Damping Devices:* Design seismic force in each mode of vibration of *velocity-dependent damping devices* shall be based on the maximum force in the device at velocities up to and including the *design earthquake* story velocity of the mode of interest.

Displacements and velocities used to determine design forces in *damping devices* at each story shall account for the angle of orientation from horizontal and consider the effects of increased floor response due to torsional motions.

A13.7.3.2 Seismic Load Conditions and Combination of Modal Responses: Seismic design force, Q_E , in each element of the *damping system* due to horizontal earthquake load shall be taken as the maximum force of the following three loading conditions:

1. Stage of Maximum Displacement: Seismic design force at the stage of maximum displacement shall be calculated in accordance with the following equation:

$$Q_E = \Omega_o \sqrt{\sum_m (Q_{mSFRS})^2} \pm Q_{DSD} \quad (\text{A13.7.3.2-1})$$

where:

Q_{mSFRS} = Force in an element of the *damping system* equal to the design seismic force of the m^{th} mode of vibration of the *seismic-force-resisting system* in the direction of interest.

Q_{DSD} = Force in an element of the *damping system* required to resist design seismic forces of *displacement-dependent damping devices*.

Seismic forces in elements of the *damping system*, Q_{DSD} , shall be calculated by imposing design forces of *displacement-dependent damping devices* on the *damping system* as pseudo-static forces. Design seismic forces of *displacement-dependent damping devices* shall be applied in both positive and negative directions at peak displacement of the *structure*.

2. Stage of Maximum Velocity: Seismic design force at the stage of maximum velocity shall be calculated in accordance with the following equation:

$$Q_E = \sqrt{\sum_m (Q_{mDSV})^2} \quad (\text{A13.7.3.2-2})$$

where:

Q_{mDSV} = Force in an element of the *damping system* required to resist design seismic forces of *velocity-dependent damping devices* due to the m^{th} mode of vibration of *structure* in the direction of interest.

Modal seismic design forces in elements of the *damping system*, Q_{mDSV} , shall be calculated by imposing modal design forces of *velocity-dependent devices* on the non-deformed *damping system* as pseudo-static forces. Modal seismic design forces shall be applied in directions consistent with the deformed shape of the mode of interest. Horizontal restraint forces shall be applied at each floor Level i of the non-deformed *damping system* concurrent with the design forces in *velocity-dependent damping devices* such that the horizontal displacement at each level of the *structure* is zero. At each floor Level i , restraint forces shall be proportional to and applied at the location of each mass point.

3. Stage of Maximum Acceleration: Seismic design force at the stage of maximum acceleration shall be calculated in accordance with the following equation:

$$Q_E = \sqrt{\sum_m (C_{mFD} \Omega_o Q_{mSFRS} + C_{mFV} Q_{mDSV})^2} \pm Q_{DSD} \quad (\text{A13.7.3.2-3})$$

The force coefficients, C_{mFD} and C_{mFV} , shall be determined from Tables A13.7.3.2.1 and A13.7.3.2.2, respectively, using values of effective damping determined in accordance with the following requirements:

- a. For fundamental-mode response ($m = 1$) in the direction of interest, the coefficients, C_{IFD} and C_{IFV} , shall be based on the velocity power term, α , that relates device force to *damping device* velocity. The effective fundamental-mode damping, shall be taken as equal to the total effective damping of the fundamental mode less the hysteretic component of damping (e.g., $\beta_{ID} - \beta_{HD}$) at the response level of interest (i.e., $\mu = \mu_D$ or $\mu = \mu_M$).
- b. For higher-mode ($m > 1$) or residual-mode response in the direction of interest, the coefficients, C_{mFD} and C_{mFV} , shall be based on a value of α equal to 1.0. The effective modal damping shall be taken as equal to the total effective damping of the mode of interest (e.g., β_{mD}). For determination of the coefficient C_{mFD} , the ductility demand shall be taken as equal to that of the fundamental mode (e.g., $\mu = \mu_D$).

Table A13.7.3.2.1 Force Coefficient, C_{mFD} ^{a, b}

Effective Damping	$\mu \leq 1.0$				$C_{mFD} = 1.0^c$
	$\alpha \leq 0.25$	$\alpha = 0.5$	$\alpha = 0.75$	$\alpha \geq 1.0$	
≤ 0.05	1.00	1.00	1.00	1.00	$\mu \geq 1.0$
0.1	1.00	1.00	1.00	1.00	$\mu \geq 1.0$
0.2	1.00	0.95	0.94	0.93	$\mu \geq 1.1$
0.3	1.00	0.92	0.88	0.86	$\mu \geq 1.2$
0.4	1.00	0.88	0.81	0.78	$\mu \geq 1.3$
0.5	1.00	0.84	0.73	0.71	$\mu \geq 1.4$
0.6	1.00	0.79	0.64	0.64	$\mu \geq 1.6$
0.7	1.00	0.75	0.55	0.58	$\mu \geq 1.7$
0.8	1.00	0.70	0.50	0.53	$\mu \geq 1.9$
0.9	1.00	0.66	0.50	0.50	$\mu \geq 2.1$
≥ 1.0	1.00	0.62	0.50	0.50	$\mu \geq 2.2$

^a Unless analysis or test data support other values, the force coefficient C_{mFD} for visco-elastic systems shall be taken as 1.0.

^b Interpolation shall be used for intermediate values of effective damping, α , and μ .

^c C_{mFD} shall be taken as equal to 1.0 for values of μ greater than or equal to the values shown.

Table A13.7.3.2.2 Force Coefficient, C_{mFV} ^{a, b}

Effective Damping	$\alpha \leq 0.25$	$\alpha = 0.5$	$\alpha = 0.75$	$\alpha \geq 1.0$
≤ 0.05	1.00	0.35	0.20	0.10
0.1	1.00	0.44	0.31	0.20
0.2	1.00	0.56	0.46	0.37
0.3	1.00	0.64	0.58	0.51
0.4	1.00	0.70	0.69	0.62
0.5	1.00	0.75	0.77	0.71
0.6	1.00	0.80	0.84	0.77

0.7	1.00	0.83	0.90	0.81
0.8	1.00	0.90	0.94	0.90
0.9	1.00	1.00	1.00	1.00
≥ 1.0	1.00	1.00	1.00	1.00

^a Unless analysis or test data support other values, the force coefficient C_{mFD} for visco-elastic systems shall be taken as 1.0.

^b Interpolation shall be used for intermediate values of effective damping, α , and μ .

A13.7.3.3 Combination of Load Effects: The effects on the *damping system* and its *components* due to *gravity loads* and *seismic forces* shall be combined in accordance with Section 5.2.7 using the effect of horizontal seismic forces, Q_E , determined in accordance with Section A13.7.3.2.

Exception: The reliability factor, ρ , shall be taken as equal to 1.0 in all cases and the special load combinations of Section 5.2.7.1 need not apply to the design of the *damping system*.

A13.7.3.4 Inelastic Response Limits: Elements of the *damping system* may exceed strength limits for design loads provided it is shown by analysis or test that:

1. Inelastic response does not adversely affect *damping system* function.
2. Element forces calculated in accordance with Sec. A13.7.3.2, using a value of Ω_o , taken as equal to 1.0, do not exceed the strength required to meet the load combinations of Sec. 5.2.7.

A13.8 DETAILED SYSTEM REQUIREMENTS:

A. 13.8.1 Damping Device Design: The design, construction and installation of *damping devices* shall be based on maximum earthquake response and the following load conditions:

1. Low-cycle, large displacement degradation due to seismic loads;
2. High-cycle, small-displacement degradation due to wind, thermal or other cyclic loads;
3. Forces or displacements due to *gravity loads*;
4. Adhesion of device parts due to corrosion or abrasion, biodegradation, moisture or chemical exposure; and
5. Exposure to environmental conditions, including but not limited to temperature, humidity, moisture, radiation (e.g., ultraviolet light) and reactive or corrosive substances (e.g., salt water).

Damping devices subject to failure by low-cycle fatigue shall resist wind forces without slip, movement, or inelastic cycling.

The design of *damping device* shall incorporate the range of thermal conditions, device wear, manufacturing tolerances, and other effects that cause device properties to vary during the lifetime of the device.

A13.8.2 Multi-Axis Movement: Connection points of *damping devices* shall provide sufficient articulation to accommodate simultaneous longitudinal, lateral, and vertical displacements of the *damping system*.

A13.8.3 Inspection and Periodic Testing: Means of access for inspection and removal of all *damping devices* shall be provided.

The *registered design professional* responsible for design of the *structure* shall establish an appropriate inspection and testing schedule for each type of *damping device* to ensure that the devices respond in a dependable manner throughout device design life. The degree of inspection and testing shall reflect the established in-service history of the *damping devices*, and the likelihood of change in properties over the design life of devices.

A13.8.4 Manufacturing Quality Control: The *registered design professional* responsible for design of the *structure* shall establish a quality control plan for the manufacture of *damping devices*. As a minimum, this plan shall include the testing requirements of Section A13.10.3.

A13.9 DESIGN REVIEW:

A13.9.1 General: Review of the design of the *damping system* and related test programs shall be performed by an independent engineering panel including persons licensed in the appropriate disciplines and experienced in seismic analysis including the theory and application of energy dissipation methods.

A13.9.2 Review Scope: The design review shall include the following:

1. Review of the earthquake ground motions used for design.
2. Review of design parameters of *damping devices*, including device test requirements, device manufacturing quality control and assurance, and scheduled maintenance and inspection requirements.
3. Review of nonlinear analysis methods incorporating the requirements of Sec. 5.8.4.
4. Review of the preliminary design of the *seismic-force-resisting system* and the *damping system*.
5. Review of the final design of the *seismic-force-resisting system* and the *damping system* and all supporting analyses.

A13.10 Required Tests of Damping Devices

A13.10.1 General: The force-velocity-displacement and damping properties used for the design of the *damping system* shall be based on the prototype tests of a selected number of *damping devices*, as specified in Sec. A13.10.2.1.

The fabrication and quality control procedures used for all prototype and production *damping devices* shall be identical.

A13.10.2 Prototype Tests.

A13.10.2.1 General: The following tests shall be performed separately on two full-size *damping devices* of each type and size used in the design, in the order listed below.

Representative sizes of each type of device may be used for prototype testing, provided both of the following conditions are met:

- (1) Fabrication and quality control procedures are identical for each type and size of devices used in the *structure*.
- (2) Prototype testing of representative sizes is accepted by the *registered design professional* responsible for design of the *structure*.

Test specimens shall not be used for construction, unless they are accepted by the *registered design professional* responsible for design of the *structure* and meet the requirements of Sec. A13.10.2 and Sec. A13.10.3.

A13.10.2.2 Data Recording: The force-deflection relationship for each cycle of each test shall be recorded.

A13.10.2.3 Sequence and Cycles of Testing: For the following test sequences, each *damping device* shall be subjected to gravity load effects and thermal environments representative of the installed condition. For seismic testing, the displacement in the devices calculated for the *maximum considered earthquake*, termed herein as the maximum earthquake device displacement, shall be used.

1. Each *damping device* shall be subjected to the number of cycles expected in the design windstorm, but not less than 2000 continuous fully reversed cycles of wind load. Wind load shall be at amplitudes expected in the design wind storm, and applied at a frequency equal to the inverse of the fundamental period of the building ($f_i = 1/T_i$).

Exception: *Damping devices* need not be subjected to these tests if they are not subject to wind-induced forces or displacements, or if the design wind force is less than the device yield or slip force.

2. Each *damping device* shall be loaded with 5 fully reversed, sinusoidal cycles at the maximum earthquake device displacement at a frequency equal to $1/T_{IM}$ as calculated in Section A13.4.3.5. Where the *damping device* characteristics vary with operating temperature, these tests shall be conducted at a minimum of 3 temperatures (minimum, ambient, and maximum) that bracket the range of operating temperatures.

Exception: *Damping devices* may be tested by alternative methods provided each of the following conditions is met:

- a. Alternative methods of testing are equivalent to the cyclic testing requirements of this section.
 - b. Alternative methods capture the dependence of the *damping device* response on ambient temperature, frequency of loading, and temperature rise during testing.
 - c. Alternative methods are accepted by the *registered design professional* responsible for the design of the *structure*.
3. If the force-deformation properties of the *damping device* at any displacement less than or equal the maximum earthquake device displacement change by more than 15 percent for

changes in testing frequency from $1/T_{IM}$ to $2.5/T_I$, then the preceding tests shall also be performed at frequencies equal to $1/T_I$ and $2.5/T_I$.

If reduced-scale prototypes are used to qualify the rate dependent properties of *damping devices*, the reduced-scale prototypes should be of the same type and materials, and manufactured with the same processes and quality control procedures, as full-scale prototypes, and tested at a similitude-scaled frequency that represents the full-scale loading rates.

A13.10.2.4 Testing Similar Devices: *Damping devices* need not be prototype tested provided that both of the following conditions are met:

- (1) The *damping device* manufacturer substantiates the similarity of previously tested devices.
- (2) All pertinent testing and other *damping device* data are made available to, and accepted by the *registered design professional* responsible for the design of the *structure*.

A13.10.2.5 Determination of Force-Velocity-Displacement Characteristics: The force-velocity displacement characteristics of a *damping device* shall be based on the cyclic load and displacement tests of prototype devices specified above. Effective stiffness of a *damping device* shall be calculated for each cycle of deformation using equation 13.9.3-1.

A13.10.2.6 Device Adequacy: The performance of a prototype *damping device* shall be assessed as adequate if all of the conditions listed below are satisfied. The 15-percent limits specified below may be increased by the *registered design professional* responsible for the design of the *structure* provided that the increased limit has been demonstrated by analysis to not have a deleterious effect on the response of the *structure*.

A13.10.2.6.1 Displacement-Dependent Devices:

1. For Section A13.10.2.3 Test 1, no signs of damage including leakage, yielding, or breakage.
2. For Section A13.10.2.3 Tests 2 and 3, the maximum force and minimum force at zero displacement for a *damping device* for any one cycle does not differ by more than plus or minus 15 percent from the average maximum and minimum forces at zero displacement as calculated from all cycles in that test at a specific frequency and temperature.
3. For Section A13.10.2.3 Tests 2 and 3, the maximum force and minimum force at maximum earthquake device displacement for a *damping device* for any one cycle does not differ by more than plus or minus 15 percent from the average maximum and minimum forces at the *maximum earthquake* device displacement as calculated from all cycles in that test at a specific frequency and temperature.
4. For Section A13.10.2.3 Tests 2 and 3, the area of hysteresis loop (E_{loop}) of a *damping device* for any one cycle does not differ by more than plus or minus 15 percent from the average area of the hysteresis loop as calculated from all cycles in that test at a specific frequency and temperature.

-
5. The average maximum and minimum forces at zero displacement and maximum earthquake displacement, and the average area of the hysteresis loop (E_{loop}), calculated for each test in the sequence of Section A13.10.2.3 Tests 2 and 3, shall not differ by more than plus or minus 15 percent from the target values specified by the *registered design professional* responsible for the design of the *structure*.

A13.10.2.6.2 Velocity-Dependent Devices:

1. For Section A13.10.2.3 Test 1, no signs of damage including leakage, yielding, or breakage.
2. For *velocity-dependent damping devices* with stiffness, the effective stiffness of a *damping device* in any one cycle of Tests 2 and 3 of Section A13.10.2.3 does not differ by more than plus or minus 15 percent from the average effective stiffness as calculated from all cycles in that test at a specific frequency and temperature.
3. For Section A13.10.2.3 Tests 2 and 3, the maximum force and minimum force at zero displacement for a *damping device* for any one cycle does not differ by more than plus or minus 15 percent from the average maximum and minimum forces at zero displacement as calculated from all cycles in that test at a specific frequency and temperature.
4. For Section A13.10.2.3 Tests 2 and 3, the area of hysteresis loop (E_{loop}) of a *damping device* for any one cycle does not differ by more than plus or minus 15 percent from the average area of the hysteresis loop as calculated from all cycles in that test at a specific frequency and temperature.
5. The average maximum and minimum forces at zero displacement, effective stiffness (for *damping devices* with stiffness only), and average area of the hysteresis loop (E_{loop}) calculated for each test in the sequence of Section A13.10.2.3 Tests 2 and 3, shall not differ by more than plus or minus 15 percent from the target values specified by the *registered design professional* responsible for the design of the *structure*.

A13.10.3 Production Testing:

Prior to installation in a building, *damping devices* shall be tested to ensure that their force-velocity-displacement characteristics fall within the limits set by the *registered design professional* responsible for the design of the *structure*. All devices need not be tested. The scope and frequency of the production-testing program shall be determined by the *registered design professional* responsible for the design of the *structure*.

Add the following definitions to *Provisions and Commentary Sec. 2.1*:

Damping Device: A flexible structural *element* of the *damping system* that dissipates energy due to relative motion of each end of the device. *Damping devices* include all pins, bolts gusset plates, brace extensions and other components required to connect damping devices to the other *elements* of the *structure*. *Damping devices* may be classified as either displacement-dependent or velocity-dependent, or a combination thereof, and may be configured to act in either a linear or nonlinear manner.

Damping System: The collection of structural *elements* that includes all individual *damping devices*, all structural *elements* or bracing required to transfer forces from *damping devices* to the base of the *structure* and all structural *elements* required to transfer forces from *damping devices* to the *seismic-force-resisting system*.

Displacement-Dependent Damping Device: The force response of a *displacement-dependent damping device* is primarily a function of the relative displacement, between each end of the device. The response is substantially independent of the relative velocity between each end of the device, and/or the excitation frequency.

Velocity-Dependent Damping Device: The force-displacement relation for a *velocity-dependent damping device* is primarily a function of the relative velocity between each end of the device, and may also be a function of the relative displacement between each end of the device.

Revise the following definitions in *Provisions and Commentary Sec. 2.2:*

- Q_E The effect of horizontal seismic forces~~building forces~~ (kip or kN); see Sec. 5.2.6 or Sec. A13.7.2.
- T The ~~fundamental~~ period (sec) of the fundamental mode of vibration of the structure in the direction of interest,~~building~~ as determined in Sec. 5.3.3. ~~or the modal period (sec) of the building modified as appropriate to account for the effective stiffness of the energy dissipation system (Sec. A.13.xx).~~
- T_m The ~~modal~~ period of vibration (sec) of the m^{th} mode of vibration of the structure in the direction of interest, ~~building~~ as determined in Sec. 5.4.5 or Sec. A13.5.
- V The total design shear at the base of the *structure* in the direction of interest, as determined using the procedure of Sec. 5.3, including Sec.5.3.3 (kip or kN).
- W The total gravity load of the structure ~~building~~ as defined in Sec. 5.3.2 (kip or kN). For calculation of seismically isolated building *structure* period, W , is the total seismic dead load weight of the *structure building* as defined in ~~Sec. 5.5.2 and 5.5.3~~ above the isolation system (kip or kN).
- \overline{W} The effective gravity load of the structure ~~building~~ as defined in Sec. 5.5.2 and 5.5.3 (kip or kN)
- \overline{W}_m The effective ~~modal~~ gravity load of m^{th} mode of vibration of the structure determined in accordance with Eq. 5.4.5-1 (kip or kN).
- V_i The design value of the seismic base shear of the fundamental mode in a given direction, as determined in Sec. 5.4.8 or Sec. A13.4.3.2 (kip or kN).
- ϕ_{im} The displacement amplitude at the i^{th} level of the structure building for the fixed base condition ~~when vibrating in its m^{th} mode in the m^{th} mode of vibration in the direction of interest, normalized to unity at the roof level~~, Sec. 5.4.5 and Sec. A13.5.

Add the following definitions to *Provisions and Commentary Sec. 2.2:*

- B_{ID} Numerical coefficient as set forth in Table A13.3.1 for effective damping equal to β_{mD} ($m = 1$) and period of *structure* equal to T_{ID} .
- B_{IM} Numerical coefficient as set forth in Table A13.3.1 for effective damping equal to β_{mM} ($m = 1$) and period of *structure* equal to T_{IM} .
- B_{mD} Numerical coefficient as set forth in Table A13.3.1 for effective damping equal to β_{mD} and period of *structure* equal to T_m .
- B_{mM} Numerical coefficient as set forth in Table A13.3.1 for effective damping equal to β_{mM} and period of *structure* equal to T_m .
- B_R Numerical coefficient as set forth in Table A13.3.1 for effective damping equal to β_R and period of *structure* equal to T_R .
- B_{V+I} Numerical coefficient as set forth in Table A13.3.1 for effective damping equal to the sum of viscous damping in the fundamental mode of vibration of the *structure* in the direction of interest, β_{vm} ($m = 1$), plus inherent damping, β_i , and period of *structure* equal to T_I .
- C_{mFD} Force coefficient as set forth in Table A13.7.3.2.1.
- C_{mFV} Force coefficient as set forth in Table A13.7.3.2.2.
- C_{SI} *Seismic response coefficient* (dimensionless) of the fundamental mode of vibration of the *structure* in the direction of interest, Sec. A13.4.3.4 or Sec. A13.5.3.4 ($m = 1$).
- C_{Sm} *Seismic response coefficient* (dimensionless) of the m^{th} mode of vibration of the *structure* in the direction of interest, Sec. A13.5.3.4 ($m = 1$) or Sec. A13.5.3.6 ($m > 1$).
- C_{SR} *Seismic response coefficient* (dimensionless) of the residual mode of vibration of the *structure* in the direction of interest, Sec. A13.4.3.8.
- D_{ID} Fundamental mode *design displacement* at the center of rigidity of the roof level of the *structure* in the direction under consideration, Sec. A13.4.4.3 (in. or mm).
- D_{IM} Fundamental mode *maximum displacement* at the center of rigidity of the roof level of the *structure* in the direction under consideration, Sec. A13.4.4.6 (in. or mm).
- D_{mD} *Design displacement* at the center of rigidity of the roof level of the *structure* due to the m^{th} mode of vibration in the direction under consideration, Sec. A13.5.4.3 (in. or mm).
- D_{mM} *Maximum displacement* at the center of rigidity of the roof level of the *structure* due to the m^{th} mode of vibration in the direction under consideration, Sec. A13.5.4.6 (in. or mm).
- D_{RD} Residual mode *design displacement* at the center of rigidity of the roof level of the *structure* in the direction under consideration, Sec. A13.4.4.3 (in. or mm).

-
- D_{RM} Residual mode *maximum displacement* at the center of rigidity of the roof level of the *structure* in the direction under consideration, Sec. A13.4.4.6 (in. or mm).
- D_Y Displacement at the center of rigidity of the roof level of the *structure* at the effective yield point of the *seismic-force-resisting system*, Sec. A13.3.4 (in. or mm).
- f_i Lateral force at Level i of the *structure* distributed approximately in accordance with Equation 5.3.4-2, Sec. A13.4.3.3.
- F_{iI} Inertial force at Level i (or mass point i) in the fundamental mode of vibration of the *structure* in the direction of interest, Sec. A13.4.3.9.
- F_{im} Inertial force at Level i (or mass point i) in the m^{th} mode of vibration of the *structure* in the direction of interest, Sec. A13.5.3.7.
- F_{iR} Inertial force at Level i (or mass point i) in the residual mode of vibration of the *structure* in the direction of interest, Sec. A13.4.3.9.
- h_r Height of the *structure* above the *base* to the roof level (ft or m), Sec. A13.4.3.3.
- q_H Hysteresis loop adjustment factor as determined in Sec. A13.3.3.
- Q_{DSD} Force in an element of the *damping system* required to resist design seismic forces of *displacement-dependent damping devices*, Sec. A13.7.3.2.
- Q_{mDSV} Force in an element of the *damping system* required to resist design seismic forces of *velocity-dependent damping devices* due to the m^{th} mode of vibration of *structure* in the direction of interest, Sec. A13.7.3.2.
- Q_{mSFRS} Force in an element of the *damping system* equal to the design seismic force of the m^{th} mode of vibration of the *seismic force resisting system* in the direction of interest, A13.7.3.2.
- T_I Period, in seconds, of the fundamental mode of vibration of the *structure* in the direction of interest, Sec. A13.4.3.3.
- T_{ID} Effective period, in seconds, of the fundamental mode of vibration of the *structure* at the *design displacement* in the direction under consideration, as prescribed by Sec. A13.4.3.5 or Sec. A13.5.3.5.
- T_{IM} Effective period, in seconds, of the fundamental mode of vibration of the *structure* at the *maximum displacement* in the direction under consideration, as prescribed by Sec. A13.4.3.5 or Sec. A13.5.3.5.
- T_m Period, in seconds, of the m^{th} mode of vibration of the *structure* in the direction under consideration, Sec. A13.5.3.6.
- T_R Period, in seconds, of the residual mode of vibration of the *structure* in the direction under consideration, Sec. A13.4.3.7.

V_m	Design value of the seismic <i>base shear</i> of the m^{th} mode of vibration of the <i>structure</i> in the direction of interest, Sec. 5.4.5 or Sec. A13.5.3.2 (kip or kN).
V_{min}	Minimum allowable value of <i>base shear</i> permitted for design of the <i>seismic-force-resisting system</i> of the <i>structure</i> in the direction of interest, Sec. A13.2.4.1 (kip or kN).
V_R	Design value of the seismic <i>base shear</i> of the residual mode of vibration of the <i>structure</i> in a given direction, as determined in Sec. A13.4.3.6 (kip or kN).
\overline{W}_1	Effective fundamental mode <i>gravity load</i> of the <i>structure</i> including portions of the live load determined in accordance with Eq. 5.4.5-2 for $m = 1$ (kip or kN).
\overline{W}_R	Effective residual mode <i>gravity load</i> of the <i>structure</i> determined in accordance with Eq. A13.4.3.7-3 (kip or kN).
α	Velocity power term relating <i>damping device</i> force to <i>damping device</i> velocity.
β_{mD}	Total effective damping of the m^{th} mode of vibration of the <i>structure</i> in the direction of interest at the <i>design displacement</i> , Sec. A13.3.2.
β_{mM}	Total effective damping of the m^{th} mode of vibration of the <i>structure</i> in the direction of interest at the <i>maximum displacement</i> , Sec. A13.3.2.
β_{HD}	Component of effective damping of the <i>structure</i> in the direction of interest due to post-yield hysteretic behavior of the <i>seismic-force-resisting system</i> and elements of the <i>damping system</i> at effective ductility demand, μ_D , Sec. A13.3.2.2.
β_{HM}	Component of effective damping of the <i>structure</i> in the direction of interest due to post-yield hysteretic behavior of the <i>seismic-force-resisting system</i> and elements of the <i>damping system</i> at effective ductility demand, μ_M , Sec. A13.3.2.2.
β_I	Component of effective damping of the <i>structure</i> due to the inherent dissipation of energy by elements of the <i>structure</i> , at or just below the effective yield displacement of the <i>seismic-force-resisting system</i> , Sec. A13.3.2.1.
β_R	Total effective damping in the residual mode of vibration of the <i>structure</i> in the direction of interest, calculated in accordance with Sec. A13.3.2 ($\mu_D = 1.0$ and $\mu_M = 1.0$).
β_{Vm}	Component of effective damping of the m^{th} mode of vibration of the <i>structure</i> in the direction of interest due to viscous dissipation of energy by the <i>damping system</i> , at or just below the effective yield displacement of the <i>seismic-force-resisting system</i> , Sec. A13.3.2.3.
δ_i	Elastic deflection of Level i of the <i>structure</i> due to applied lateral force, f_i , Sec. A13.4.3.3 (in. or mm).
δ_{i1D}	Fundamental mode <i>design earthquake</i> deflection of Level i at the center of rigidity of the <i>structure</i> in the direction under consideration, Sec. A13.4.4.2 (in. or mm).

δ_{iD}	Total <i>design earthquake</i> deflection of Level <i>i</i> at the center of rigidity of the <i>structure</i> in the direction under consideration, Sec. A13.4.4.2 (in. or mm).
δ_{iM}	Total <i>maximum earthquake</i> deflection of Level <i>i</i> at the center of rigidity of the <i>structure</i> in the direction under consideration, Sec. A13.4.4.2 (in. or mm).
δ_{iRD}	Residual mode <i>design earthquake</i> deflection of Level <i>i</i> at the center of rigidity of the <i>structure</i> in the direction under consideration, Sec. A13.4.4.2 (in. or mm).
δ_{im}	Deflection of Level <i>i</i> in the m^{th} mode of vibration at the center of rigidity of the <i>structure</i> in the direction under consideration, Sec. A13.5(in. or mm).
Δ_{iD}	<i>Design earthquake</i> story drift due to the fundamental mode of vibration of the <i>structure</i> in the direction of interest, Sec. A13.4.4.4 (in. or mm).
Δ_D	Total <i>design earthquake</i> story drift of the <i>structure</i> in the direction of interest, Sec. A13.4.4.4 (in. or mm).
Δ_M	Total <i>maximum earthquake</i> story drift of the <i>structure</i> in the direction of interest, Sec. A13.4.4.6 (in. or mm).
Δ_{mD}	<i>Design earthquake</i> story drift due to the m^{th} mode of vibration of the <i>structure</i> in the direction of interest, Sec. A13.4.4.4 (in. or mm).
Δ_{RD}	<i>Design earthquake</i> story drift due to the residual mode of vibration of the <i>structure</i> in the direction of interest, Sec. A13.4.4.4 (in. or mm).
μ	Effective ductility demand on the <i>seismic-force-resisting system</i> in the direction of interest.
μ_D	Effective ductility demand on the <i>seismic-force-resisting system</i> in the direction of interest due to the <i>design earthquake</i> , Sec. A.13.4.
μ_M	Effective ductility demand on the <i>seismic-force-resisting system</i> in the direction of interest due to the <i>maximum considered earthquake</i> , Sec. A13.4.
μ_{max}	Maximum allowable effective ductility demand on the <i>seismic-force-resisting system</i> due to <i>design earthquake</i> , Sec. A13.3.5.
ϕ_{iI}	Displacement amplitude at Level <i>i</i> of the fundamental mode of vibration of the <i>structure</i> in the direction of interest, normalized to unity at the roof level, Sec. A13.4.3.3.
ϕ_{iR}	Displacement amplitude at Level <i>i</i> of the residual mode of vibration of the <i>structure</i> in the direction of interest, normalized to unity at the roof level, Sec. A13.4.3.7.
Γ_1	Participation factor of the fundamental mode of vibration of the <i>structure</i> in the direction of interest, Sec. A13.4.3.3 or Sec. A13.5.3.3 ($m = 1$).
Γ_m	Participation factor of the m^{th} mode of vibration of the <i>structure</i> in the direction of interest, Sec. A13.5.3.3.

-
- Γ_R Participation factor of the residual mode of vibration of the *structure* in the direction of interest, Sec. A13.4.3.7.
- ∇_{ID} *Design earthquake* story velocity due to the fundamental mode of vibration of the *structure* in the direction of interest, Sec. A13.4.4.5 (in/sec or mm/sec).
- ∇_D Total *design earthquake* story velocity of the *structure* in the direction of interest, Sec. A13.4.4.5 (in/sec or mm/sec).
- ∇_M Total *maximum earthquake* story velocity of the *structure* in the direction of interest, Sec. A13.4.4.6 (in/sec or mm/sec).
- ∇_{mD} *Design earthquake* story velocity due to the m^{th} mode of vibration of the *structure* in the direction of interest, Sec. A13.4.4.5 (in/sec or mm/sec).
- ∇_{RD} *Design earthquake* story velocity due to the residual mode of vibration of the *structure* in the direction of interest, Sec. A13.4.4.5 (in/sec or mm/sec).

APPENDIX B

DESCRIPTION OF EXAMPLE BUILDINGS WITHOUT DAMPING SYSTEMS AND DESIGN OF LATERAL FORCE RESISTING SYSTEMS PER NEHRP (1997)

B.1 Introduction

This appendix presents a description of the 3-story and the 6-story buildings that are utilized in the development of design examples for damping systems, in the application of the NEHRP (2000) and FEMA (1997) methods of analysis and in the assessment of the accuracy of these methods. Moreover, the appendix presents the design of special steel moment frames for these buildings without damping systems to meet the strength and drift criteria of NEHRP (1997). A comparison of these frames to those of the same buildings with damping systems illustrates the benefits and drawbacks offered by the damping systems.

B.2 Description of 3-Story Building

This residential building is of regular configuration, constructed of steel, 41.15 m (135') x 41.15 m (135') in plan, and 13.028 m (42'-9") high. A typical floor plan and a typical elevation are shown in Figure B-1. Columns are spaced at 8.23 m (27'-0") o.c. Wind and earthquake resistance is provided by two three-span special moment frames in each direction, located on the perimeter of the building and are indicated by heavy lines in Figure B-1. Floors are assumed to behave as rigid diaphragms, and torsional effects are not considered. Moreover, the building is assumed to be located at a site characterized by a design response spectrum with parameters $S_{D1} = 0.6$, $S_{DS} = 1.0$, $T_s = 0.6$ sec. per NEHRP (1997).

Design Parameters

The building is designed to meet 1997 NEHRP Recommended Provisions for Seismic Regulations for New Buildings and Other Structures.

Loads

Roof Dead Load:	1.68 kN/m^2 (35 psf)
Roof Live Load:	0.96 kN/m^2 (20 psf)
Floor Dead load:	3.35 kN/m^2 (70 psf)
Floor Live Load:	1.68 kN/m^2 (35 psf)
Cladding:	1.20 kN/m^2 (25 psf)

Reduced floor live load of 35 psf is assumed for all floors for convenience. Unreduced live load is 40 psf.

Material

Steel with yield strength:	$F_y = 0.345 \text{ kN/mm}^2$ (50 ksi)
----------------------------	--

Weight of the Building

Third Floor (roof):	$w_3 = 3,134 \text{ kN}$
Second Floor:	$w_2 = 5,800 \text{ kN}$
First Floor:	$w_1 = 5,800 \text{ kN}$
	<hr/>
	$W_T = 14,734 \text{ kN}$

Design Coefficients per Table 5.2.2, 1997 NEHRP

For Special Steel Moment Frame

Response Modification Factor:	$R = 8.0$
System Overstrength Factor:	$\Omega_0 = 3.0$
Deflection Amplification Factor:	$C_d = 5.5$

Allowable Story Drift per Table 5.2.8, 1997 NEHRP

For Seismic Group I:	$\Delta_a = 0.02h_{sx}$
----------------------	-------------------------

Evaluation of Design Gravity Loads

Gravity loads on beams are summarized in Table B-1 using the loads described in Section B.3.1 and the tributary width to each beam of the special steel moment frame.

Table B-1 Uniform Gravity Loads on Beams of Typical Special Steel Moment Frame

Floor i	Tributary Width (m)	Floor Dead Load (kN/m)	Cladding (kN/m)	Total Dead Load (kN/m)	Live Load (kN/m)	1.2D+1.6L (kN/m)
3	4.725	7.9	2.6	10.5	4.5	19.8
2	4.725	15.8	5.2	21.0	8.0	38.0
1	4.725	15.8	5.2	21.0	8.0	38.0

B.3 Design of Typical 3-Story Special Steel Moment Frame

Seismic Base Shear V and Minimum Required Base Shear Strength V_y

Fundamental Period of the Structure, T (per Chapter 5.3.3, NEHRP, 1997)

Approximate fundamental period T_a (eq. 5.3.3.1-1):

$$T_a = C_t (h_n)^{\frac{3}{4}}$$

$$C_t = 0.035$$

$$T_a = 0.035(42.74)^{\frac{3}{4}} \quad \therefore T_a = 0.585 \text{ sec}$$

$$T \leq C_u \cdot T_a$$

$$C_u = 1.2 \quad (\text{For } S_{DI} > 0.4, \text{ Table 5.5.3})$$

$$T \leq 1.2 \times 0.585 = 0.702 \quad \therefore T = 0.70 \text{ sec}$$

Seismic Response Coefficient, C_s (eq. 5.3.2.1-2)

$$C_s = \frac{S_{DI}}{RT} = \frac{0.6}{8 \times 0.70} = 0.107$$

Seismic Base Shear, V (eq. 5.3.2)

$$V = C_s \cdot W_T$$

$$V = 0.107 \times 14,734 \quad \therefore V = 1,577 \text{ kN (355 kips)}$$

The design base shear of each frame is $V = 788.5 \text{ kN (177.5 kips)}$. This does not include the additional component due to torsion, which is neglected in this

example. Accordingly, the minimum required base shear strength of the frame V_y (see Section 7 herein) is

$$V_y = V \cdot \frac{C_d \cdot \Omega_o}{R} = 788.5 \times \frac{5.5 \times 3.0}{8} = 1,626 \text{ kN (366 kips)}$$

Vertical Distribution of Seismic Forces

The vertical distribution of the seismic forces is described in Section 5.3.4 (NEHRP, 1997).

$$C_{vxi} = \frac{W_i h_i^k}{\sum_{j=1}^n W_j h_j^k} \quad \text{for } T = 0.70 \text{ sec} \quad k = 1.10$$

As required by eq. (5.2.7-1), evaluation of the seismic load E requires the calculation of the redundancy reliability factor ρ . Using eq. (5.2.4.2) with a typical floor area of 1,693 m² (18,225 ft²) and a value of $r_{max} = 0.10$, the factor ρ is calculated as

$$\rho = 2 - \frac{20}{0.10 \cdot \sqrt{18225}} = 1.26$$

The lateral seismic forces are presented in Table B-2.

Table B-2 Lateral Seismic Forces for 3-Story Frame

Floor	w_i^* (kN)	h_i (m)	$w_i h_i^k$	C_{vxi}	F_{xi} (kN)	ρF_{xi} (kN)
3	1567	13.03	5.27E+04	0.363	286	360
2	2900	8.72	6.27E+04	0.432	341	430
1	2900	4.42	2.97E+04	0.204	161	203

*: Reactive weight of each frame

$$\sum_{i=1}^N w_i h_i^k = 145,100$$

Preliminary Design of Beams

Beams are proportioned for the maximum of the bending moments obtained from gravity loads, and load combination given by $U = 1.2D + 0.5L \pm E$. The corresponding bending moments are estimated as

$$M_{uG} = \frac{q_u l^2}{12} \quad q_u = 1.2D + 1.6L \quad (\text{for gravity loads})$$

$$M_{u(G+E)} = (1.2q_D + 0.5q_L) \frac{L^2}{12} + \rho M_E \quad (\text{for gravity + seismic loads})$$

Computations of the design bending moments for beams are presented in Table B-3

TABLE B-3 Calculation of Design Bending Moments of Beams

Level	1.2D + 1.6L (kN/m)	1.2D + 0.5L (kN/m)	M_{uG} (kN.m)	ρM_E (kN.m)	M_{G+E} (kN.m)
Roof	19.8	14.9	102.3	129.1	205.8
2	38.0	29.2	196.3	420.1	571.3
1	38.0	29.2	196.3	785.9	937.1

It may be noted that the governing design moments of the beams result from the combination of gravity and seismic loads in all floors. Accordingly the following sections are selected as follows:

Third Floor: $W14x26$, $\phi M_p = 205 \text{ kN.m}$

Second Floor: $W21x50$, $\phi M_p = 560 \text{ kN.m}$

First Floor: $W24x76$, $\phi M_p = 1016 \text{ kN.m}$

Preliminary Design of Columns

Columns are proportioned to satisfy strong column/weak beam conditions, that is the sum of the columns moment capacity must be greater than the sum of beam moment capacities at any joint. W14 sections are assumed. Plastic hinges in beams are assumed to form at a distance of $(d_c/2+d_b)$, where d_c and d_b are the depth of the column and beam sections, respectively, at any joint. It is further assumed that all columns have the same section along the entire height of the 3-story building.

Interior joints at the first floor represent the most critical location for the design of the column. A factor of 1.25 is applied to the sum of the beam moments to assure strong column/weak beam mechanism. With reference to Figure B-2:

Beam section: W24x76 $M_{pb} = 1129 \text{ kN} \cdot \text{m} \text{ (833}^{\text{'k}} \text{)}$

Location of plastic hinge: $L' = \frac{d_c}{2} + d_b = \frac{356}{2} + 610 = 788 \text{ mm} \text{ (2.6')}$

Beam effective length: $L_p = 8230 - 2 \cdot 788 = 6654 \text{ mm} = 6.654 \text{ m} \text{ (21.8')}$

Shear at plastic hinge: $V_p = \frac{2M_p}{L_p} = \frac{2 \times 1129}{6.654} = 340 \text{ kN} \text{ (76.5 kips)}$

Column total moment: $M_c = 2(M_{pb} + V_p L') \times 1.25$
 $= 2(1129 + 340 \times 0.788) \times 1.25$
 $= 3492 \text{ kN} \cdot \text{m} \text{ (2576}^{\text{'k}} \text{)}$

Moment in first-story column: $M_{pc} = 0.6 M_c$
(assumed) $M_{pc} = 0.6 \times 3492 = 2095 \text{ kN} \cdot \text{m} \text{ (1545}^{\text{'k}} \text{)}$

Required plastic section modulus: $Z_x = \frac{2095 \cdot 1000}{0.345} = 6,072,464 \text{ mm}^3 \text{ (371 in}^3 \text{)}$

Try W14x211: $Z_x = 6,390,955 \text{ mm}^3 \text{ (390 in}^3 \text{)}$

The fundamental period of the proposed frame obtained by eigenvalue analysis was $T_1 = 1.12$ sec. Seismic forces evaluated on the basis of this period were used to perform elastic analysis of the frame using program SAP-2000NL. The story drift obtained in the third floor exceeded the allowable limit by 10%. The design of the frame was altered by adjusting the sections to satisfy the drift criteria. Figure B-3 shows the preliminary design of the frame. Observe that the sections have changed with respect to those established using the strength criteria.

Calculation of Story Drifts

For calculation of story drifts, the actual period of the building was utilized (see Section 5.3.7.1, NEHRP, 1997) and the lateral forces were calculated.

Period of the revised frame: $T_1 = 1.07$ sec (based in eigenvalue analysis in program SAP-2000NL)

Seismic response coefficient: $C_s = \frac{0.6}{8 \times 1.07} = 0.07$

Seismic base shear: $V = 0.07 \times \frac{14734}{2} = 516$ kN (116.0 kips)

Table B-4 shows a summary of the calculations carried out to evaluate the story drifts Δ_i of the frame. Lateral floor displacements δ_{xe} are obtained from elastic analysis of the frame performed in program SAP-2000NL. Note that for $T_1 = 1.07$ sec, the exponent k is equal to 1.285.

TABLE B-4 Calculation of Story Drifts of 3-Story Frame

Level	h_i (m)	w_i (kN)	$w_i h_i^k$	C_{vx}	F_{xi} (kN)	δ_{xe} (mm)	$C_d \delta_{xe}$ (mm)	Δ_i (mm)	Δ/h_{sx}
3	13.03	1567	42440	0.3897	201	36	198	66	0.015
2	8.72	2900	46877	0.4305	222	24	132	82	0.019
1	4.42	2900	19578	0.1798	93	9	50	50	0.011

$$\sum w_i h_i^k = 108,895$$

As shown in Table B-4, the value of story drifts satisfy the NEHRP (1997) limit of $0.02h_{sx}$, therefore the preliminary design of this frame is satisfactory. The weight of the designed frame is 215 kN (48.4 kips).

B.4 Design of 6-Story Special Steel Moment Frame

Consider that the building of Figure B-1 has six stories. Assume that the number and distribution of special steel moment frames remains as shown. Furthermore, assume that the interstory height and floors weights also remain unchanged. This section presents the design of the 6-story special steel moment frame following the same approach as in the 3-story example.

Seismic Base Shear V and Minimum Required Strength V_y

Fundamental Period of Building, T (per Chapter 5.3.3, NEHRP, 1997)

Height of the structure: $h_n = 4420 + 5 \times 4304 = 25940 \text{ mm (85.1')}$

Approximate period: $T_a = 0.035(85.10)^{3/4} = 0.98 \text{ sec}$

Upper bound period: $T_1 = 1.2 \times 0.98 = 1.18 \text{ sec}$

Seismic Response Coefficient, C_s

$$C_s = \frac{0.6}{8 \times 1.18} = 0.0636$$

Seismic Base Shear

Total weight of building: $W_T = 3134 + 5 \times 5800 = 32,134 \text{ kN (7,227 kips)}$

Seismic weight per frame: $W = 16,067 \text{ kN (3,614 kips)}$

Seismic base shear: $V = 0.0636 \times 16067 = 1,022 \text{ kN (230 kips)}$

Minimum required base shear strength: $V_y = 1022 \times \frac{5.5 \times 3}{8} = 2,108 \text{ kN (474 kips)}$

Vertical Distribution of Seismic Forces

Exponent k (for $T=1.18 \text{ sec.}$): $k = 1.34$

Redundancy reliability factor: $\rho = 1.26$

Calculations of the vertical distribution of seismic forces per frame are presented in Table B-5.

TABLE B-5 Lateral Seismic Forces for 6-Story Frame

Level	w_i (kN)	h_i (m)	$w_i h_i^k$	C_{vxi}	F_{xi} (kN)	ρF_{xi} (kN)
6	1567	25.94	1.23E+05	0.2054	210	265
5	2900	21.63	1.78E+05	0.2982	305	384
4	2900	17.33	1.33E+05	0.2215	226	285
3	2900	13.03	0.94E+05	0.1511	154	194
2	2900	8.72	0.53E+05	0.0883	91	115
1	2900	4.42	0.21E+05	0.0355	36	45

$$\sum_{i=1}^N w_i h_i^k = 602,000$$

Preliminary Design of Beams

Beams are proportioned for the maximum of the bending moments obtained from gravity loads according to load combination $U_1 = 1.2D + 1.6L$, and combination of gravity and seismic loads according to load combination $U_2 = 1.2D + 0.5L \pm E$. The moments were calculated on the basis of the equations presented in B.5.3 herein and the selected beams sections are shown in Table B-6.

TABLE B-6 Summary of Design Moments and Selected Beam Sections

Level	M_{uG} (kN.m)	$M_{1.2D+0.5L}$ (kN.m)	ρM_E (kN.m)	$M_{u(G+E)}$ (kN.m)	Section	$\phi_b M_p$ (kN.m)
6	102.3	76.7	95.0	171.8	W14x26	204.6
5	196.3	151.2	327.8	479.1	W21x44	485.2
4	196.3	151.2	567.8	719.0	W21x62	731.9
3	196.3	151.2	739.6	890.8	W24x68	900.0
2	196.3	151.2	850.4	1001.2	W24x76	1016.5
1	196.3	151.2	907.8	1059.0	W24x84	1138.4

Preliminary Design of Columns

Columns are proportioned to satisfy strong column/weak beam conditions. Columns have splices at two-story intervals. The design moment of the bottom column at a splice is assumed to take 60% of the sum of the moment capacities of beams at the interior joints, including the additional moment produced by the shear at the plastic hinges.

The effect of the axial load in reducing the moment capacity of the columns is taken into account according to $M_{pc} = Z_x (F_y - P_u/A_c)$. The ultimate axial load in columns is established using the load combination $U = 1.2D \pm E + 0.5L$ (eq. A4-5, AISC LRFD, 1995) with E given by eq. 5.2.7-1, NEHRP (1997). Gravity axial loads are established from Table B-1, and $\rho = 1.26$ (eq. 5.2.4.2, NEHRP, 1997). Table B-7 presents a summary of the calculations and the selected column sections.

The natural period of the proposed frame T_1 obtained by eigenvalue analysis was $T_1 = 2.16$ sec. Seismic forces evaluated on the basis of this period were used to perform elastic analysis of the frame using program SAP-2000NL. The story drifts obtained exceeded the allowable limit by up to 40%. That is, the design of the moment frame (without damping system) is governed by drift limits rather than strength criteria.

TABLE B-7 Summary of Design Moments and Selected Column Sections

Stories	Beam Section	M_{pb} (kN.m)	L' (m)	L_p (m)	V_p (kN)	ΣM_{pb} (kN.m)	$0.6M_c$ (kN.m)	Section
1-2	W24x84	1264.4	7.88	6.65	380	3910.9	2346.6	W14x257
3-4	W24x68	999.9	7.88	6.65	301	3092.7	1855.6	W14x211
5-6	W21x44	539.1	7.11	6.81	158	1628.6	977.0	W14x109

The design of the frame was altered by adjusting the sections to satisfy the drift criteria. Figure B-4 shows the preliminary design of the frame. Observe that the sections have been increased in size from those needed to satisfy the strength requirements.

Calculation of Story Drifts

Seismic forces are evaluated using the fundamental period obtained by eigenvalue analysis of the proposed design of the frame shown in Figure B-4:

$$\begin{aligned} \text{Fundamental period:} \quad & T_1 = 1.90 \text{ sec} \\ \text{Seismic coefficient:} \quad & C_S = \frac{0.6}{8 \times 1.90} = 0.0395 \\ \text{Seismic base shear:} \quad & V = 0.0395 \times 16067 = 635 \text{ kN (142.8 kips)} \\ \text{Exponent:} \quad & k = 1.70 \end{aligned}$$

Table B-8 presents a summary of the calculations carried out for the 6-story frame shown in Figure B-4. Static analysis to obtain elastic displacements was performed using program SAP-2000NL. As shown in Table B-8, the drifts at all stories satisfy the limit of $0.02 h_{sx}$. The frame weighs approximately 504 kN (113 kips), compared with the initial design, which did not meet the drift criteria, that weighed 370 kN (83 kips).

Table B-8 Calculation of Story Drifts of 6-Story Frame

Level	w_i (kN)	h_i (m)	$w_i h_i^k$	C_{vx}	F_{xi} (kN)	δ_{xe} (mm)	$C_d \delta_{xe}$ (mm)	Δ_i (mm)	Δ_i/h_{sx}
6	1567	25.94	3.97E+05	0.2355	150	70	385	49	0.014
5	2900	21.64	5.40E+05	0.3200	203	61	336	77	0.018
4	2900	17.33	3.70E+05	0.2195	139	47	259	77	0.018
3	2900	13.03	2.28E+05	0.1251	86	33	182	77	0.018
2	2900	8.72	1.15E+05	0.0683	43	19	105	66	0.015
1	2900	4.42	0.36E+05	0.0216	14	7	39	39	0.009

$$\sum_{i=1}^N w_i h_i^k : 16.86E+05$$

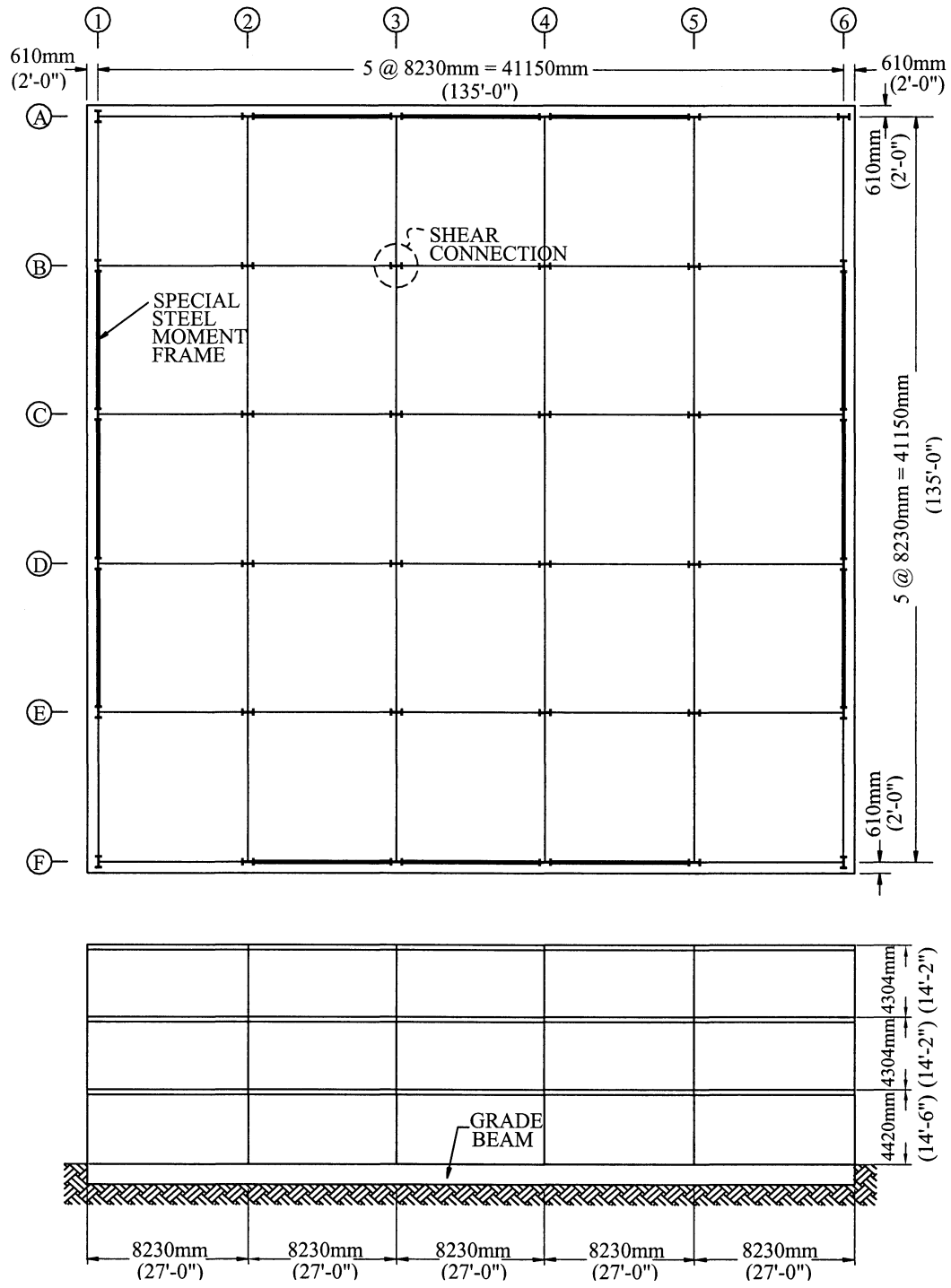
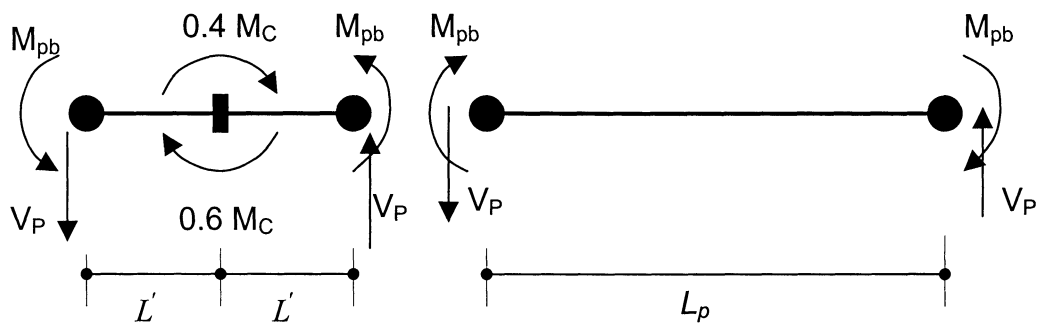
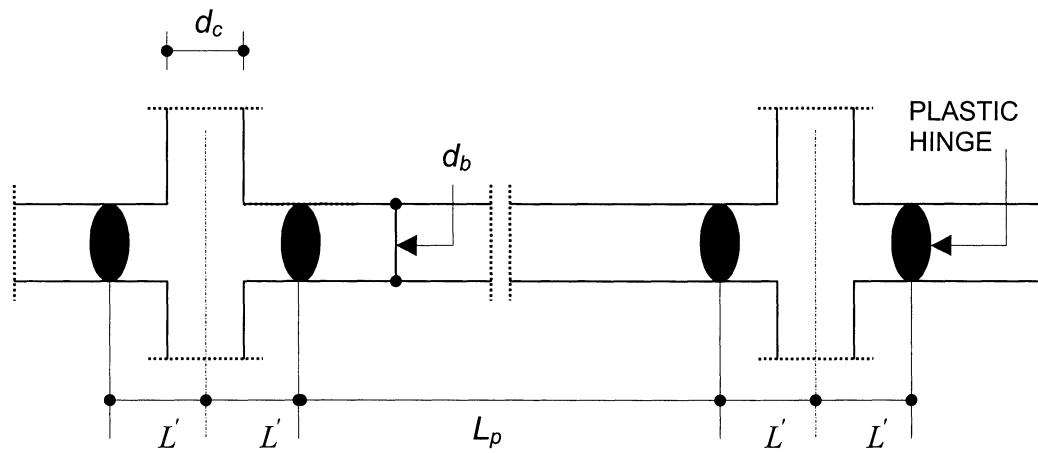


FIGURE B-1 Plan View and Elevation of Example 3-Story Building



$$M_C = 2 \left[M_{pb} + V_p L' \right]$$

(effect of shear forces due to gravity loads ignored)

FIGURE B-2 Geometry and Equilibrium at Interior Beam to Column Joint at First Floor

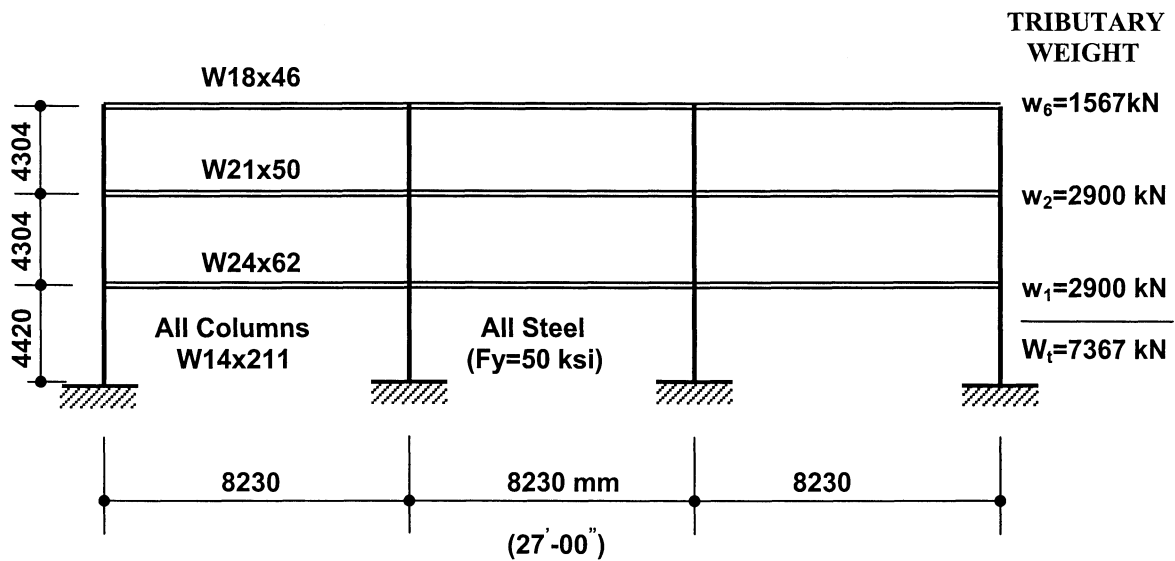


FIGURE B-3 3-Story Special Steel Moment Frame Designed to Meet NEHRP (1997) Criteria without a Damping System

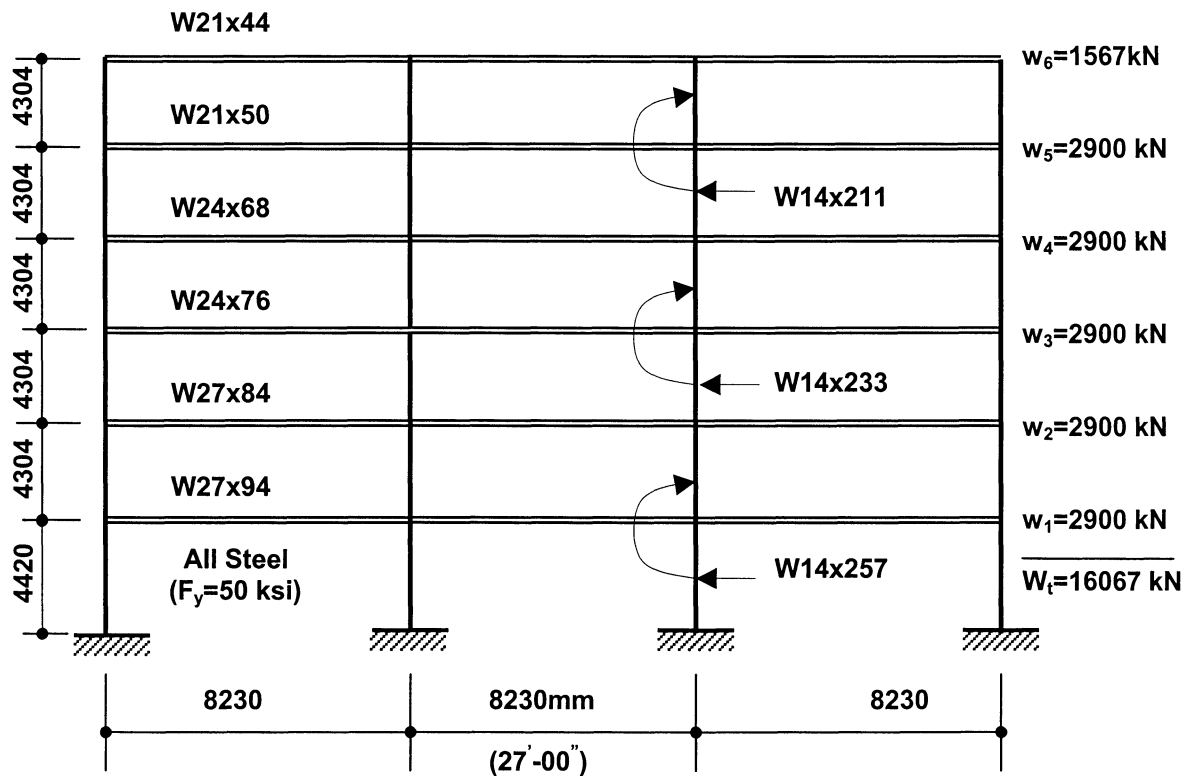


FIGURE B-4 6-Story Special Steel Moment Frame Designed to Meet NEHRP (1997) Criteria without a Damping System

APPENDIX C

APPROXIMATE CONSTRUCTION OF PUSHOVER CURVE OF BUILDINGS WITHOUT AND WITH DAMPING SYSTEMS ON THE BASIS OF PLASTIC ANALYSIS

C.1 Introduction

This appendix presents a plastic analysis-based approach to construct the pushover curve of moment-frame buildings without viscous, viscoelastic or metallic yielding damping systems. A simple method to determine the base shear strength of these systems is developed that applies under the following assumptions: (a) a proper collapse mechanism, consisting of plastic hinges at the beam ends and column bases, develops, (b) the pattern of lateral load remains constant during pushover, (c) plastic hinges develop at both ends of beams at equal distances from the centerline of columns, and (d) the frame exhibits elastoplastic behavior. The developed procedure is intended as an alternate approach to determining the base shear strength of buildings by avoiding the use of pushover analysis. It should be noted that the pushover curve may be approximately constructed when the base shear strength is known as follows: the behavior of the structural frame, exclusive of the damping system, is assumed to be elastoplastic and the ascending branch of the elastoplastic pushover curve is determined on the basis of the elastic stiffness of the frame. When the pattern of loads is proportioned to the first mode of the frame, the stiffness is directly related to the fundamental elastic period of the frame.

C.2 Base Shear Strength of Buildings without Damping Systems

The procedure described in this section applies for moment frames without damping systems. However, the procedure applies also to frames with purely viscous damping systems since such systems do not exhibit any stiffness or strength. Rather, it is assumed that the damping forces merely reduce the displacement demand due to the increased viscous damping. However, as discussed in Section 8 the situation is more complex and pure viscous damping may alter the pushover curve.

Consider the N-story, n-bay moment frame subjected to an arbitrary distribution of lateral load as shown in Figure C-1(a). Different span length, story height, and corresponding beam and column ultimate bending capacities are assumed at any level. The base shear strength of the frame, V_y , is defined as the base shear of the frame at the collapse stage (Figure C-1(b)).

Based on the assumptions stated above, the work done by the forces applied to the structure must be equal to the energy dissipated at plastic hinge locations, that is,

$$\sum_{i=1}^N F_i \cdot D_i = \sum_{k=1}^K M_{pck} \cdot \theta + 2 \sum_{i=1}^N \sum_{j=1}^n M_{pbij} \cdot \beta_{ij} \quad (\text{C-1})$$

where F_i = lateral load applied at level i , D_i = lateral displacement of level i , M_{pck} = plastic moment at base of first-story column at column line k , M_{pbij} = plastic moment of beam at level i and span j , β_{ij} = rotation of beam plastic hinge at level i and span j , and θ = rotation of plastic hinge at base of columns. From Figure C-1(c), β_{ij} can be calculated by

$$\beta_{ij} = \theta \cdot \left(\frac{1}{1 - 2\alpha_{ij}} \right) \quad (\text{C-2})$$

where α_{ij} = length factor for beam hinge location at level i and span j (see Fig. C-1(c)).

Equilibrium of forces in the horizontal direction of the whole structure at the collapse stage requires that the sum of lateral forces must equal the base shear strength, V_y , that is,

$$\sum_{i=1}^N F_i = \sum_{i=1}^N \lambda_i V_y = V_y \quad (\text{C-3})$$

where the lateral force at any level, F_i , are expressed as a fraction of the base shear strength, $F_i = \lambda_i V_y$. Parameter λ_i is a force distribution factor that depends on the lateral force pattern (first mode, modal, uniform, etc.) utilized to push over the structure (see Section 8). Substitution of (C-2) and (C-3) in (C-1) results in

$$V_y = \frac{I}{\sum_{i=1}^N (\lambda_i \cdot h_i)} \cdot \left\{ \sum_{k=1}^K M_{pck} + \left[2 \sum_{i=1}^N \sum_{j=1}^n (M_{pbij} \cdot \chi_{ij}) \right] \right\} \quad (C-4)$$

where, h_i = height of level i above the hinge at the base of the structure as shown in Figure C-1(b), and

$$\chi_{ij} = \frac{I}{1 - 2\alpha_{ij}} \quad (C-5)$$

Equation (C-4) applies to frames of any geometry provided the collapse mechanism is as shown in Figure C-1(b). However, in practical applications it is common to have same size first-story columns, so that $M_{pck} = M_{pc}$, and same size beams, so that $M_{pbij} = M_{pbi}$ in all spans of a level. Accordingly $\chi_{ij} = \chi_i = I/(1 - 2\alpha_i)$ and (C-4) takes the simpler form:

$$V_y = \frac{I}{\sum_{i=1}^N (\lambda_i \cdot h_i)} \cdot \left\{ (n+1)M_{pc} + 2n \cdot \sum_{i=1}^N (M_{pbi} \cdot \chi_i) \right\} \quad (C-6)$$

An idealized elastoplastic representation of the pushover curve of a building is characterized by the base shear strength, V_y , and the yield displacement, D_y , as shown in Figure C-2. These quantities vary depending on the pattern of lateral load applied to the system. Consider that the pattern of lateral load is proportional to the first mode of the frame under elastic conditions. The yield displacement can be obtained from the relation between the base shear strength V_y and the fundamental period of the building under elastic conditions, T_1 :

$$D_y = \left(\frac{g}{4\pi^2} \right) \cdot \Gamma_1 \cdot \left(\frac{V_y}{\overline{W}_1} \right) \cdot T_1^2 \quad (C-7)$$

where Γ_1 = first modal participation factor and \overline{W}_1 = first modal weight.

C.2.1 Example C-1

Consider the frame depicted in Figure C-3(a). Assume that plastic hinges in beams form at distance of half the depth of the column section plus one depth of the beam section ($d_c/2+d_b$), and in columns at a distance of one depth (d_c) of column section from the base of the frame. Consider also a lateral force pattern proportional to the first mode.

General Information

Number and Length of Spans:	$n = 3 ; L_b = 8230 \text{ mm}$
Number of Stories:	$N = 3$
Material Properties:	$F_y = 345 \text{ MPa (50 ksi)}$
Column Properties:	W14x109 ($d_c=356 \text{ mm}; M_{pc}=1084 \text{ kN-m}$)
Beam Properties:	
Third floor:	W14x26 ($d_b=356 \text{ mm}; M_{pb3} = 227 \text{ kN-m}$)
Second Floor:	W16x40 ($d_b=406 \text{ mm}; M_{pb2} = 412 \text{ kN-m}$)
First-Floor:	W16x45 ($d_b=406 \text{ mm}; M_{pb1} = 465 \text{ kN-m}$)
Floors Weight:	$w_3 = 1,567 \text{ kN}; w_2 = w_1 = 2,900 \text{ kN}$
Story Height:	$h_3=12,928 \text{ mm}; h_2=8,624 \text{ mm}; h_1=4,320 \text{ mm}$
Eigenvalue Analysis:	$T_1 = 1.58 \text{ sec.}; \{\phi_1\}^T = [1.000, 0.657, 0.250]; \bar{W}_1 = 5871 \text{ kN} ; \Gamma_1 = 1.399$

Evaluation of Parameters α_i , χ_i , and $M_{pbi} \chi_i$

Parameter α_i is calculated according to $\alpha_i = (d_c/2+d_b)/L_b$, and χ_i is calculated by (C-5).

Floor i	M_{pbi} (kN-m)	α_i	χ_i	$M_{pbi} \chi_i$ (kN-m)
3	227	0.065	1.149	261
2	412	0.071	1.166	480
1	465	0.071	1.166	542

$$\sum_{i=1}^N M_{pbi} \cdot \chi_i = 1283 \text{ kN.m}$$

$$\text{Evaluation of Term } \left[(n+1)M_{pc} + 2n \sum_{i=1}^N M_{pbi} \cdot \chi_i \right]$$

$$\left[(n+1)M_{pc} + 2n \sum_{i=1}^N M_{pbi} \cdot \chi_i \right] = (3+1) \cdot 1084 + 2 \cdot 3 \cdot 1283 = 12034 \text{ kN} \cdot \text{m}$$

First-Mode Pattern Base Shear Strength and Yield Displacement

Calculation of the base shear strength using (C-6) requires evaluation of the term $\sum_{i=1}^N \lambda_i \cdot h_i$,

where parameter λ_i is for the first-mode lateral force pattern. This pattern is described by

$$\lambda_i = \frac{w_i \phi_{i1}}{\sum_{m=1}^N w_m \phi_{m1}}. \text{ Calculations are summarized below:}$$

Floor i	w_i (kN)	ϕ_{i1}	h_i (mm)	$w_i \cdot \phi_{i1}$ (kN)	λ_i	$\lambda_i \cdot h_i$ (mm)
3	1567	1.000	12670	1567	0.3734	4731
2	2900	0.657	8367	1905	0.4539	3798
1	2900	0.250	4063	725	0.1727	702

$$\sum_{i=1}^N w_i \cdot \phi_{i1} = 4197 \text{ kN}$$

$$\sum_{i=1}^N \lambda_i \cdot h_i = 9231 \text{ mm}$$

Note that in the calculation of h_i it was assumed that plastic hinges form at a distance of 356 mm (14") from the base of the structure. Equation (C-6) gives the base shear strength

$$V_y = \left(\frac{1}{9229} \right) \cdot (12034 \cdot 1000) = 1304 \text{ kN}$$

Moreover, the yield displacement is calculated by use of (C-7):

$$D_y = \left(\frac{9810}{4\pi^2}\right) \times 1.4 \times \left(\frac{1304}{5871}\right) \times 1.58^2 = 192 \text{ mm}$$

Modal (C_{vx}) Pattern Base Shear Strength

Calculation of the base shear strength using (C-6) requires evaluation of the term $\sum_{i=1}^N \lambda_i \cdot h_i$,

where parameter λ_i for the modal (C_{vx}) lateral force pattern is described by $\lambda_i = \frac{w_i h_i^k}{\sum_{m=1}^N w_m h_m^k}$. In

this case of period of $T = 1.58$ sec, the exponent k (NEHRP, 1997) is equal to 1.54. Calculations are summarized below:

Floor <i>i</i>	w_i (kN)	h_i (mm)	h_i (mm)	$w_i \cdot h_i^k \times 10^6$	λ_i	$\lambda_i \cdot h_i$ (mm)
3	1567	13028	12670	3404	0.4259	5396
2	2900	8724	8367	3397	0.4250	3556
1	2900	4420	4063	1192	0.1491	606

$$\sum_{i=1}^N w_i \cdot h_i^k = 7993$$

$$\sum_{i=1}^N \lambda_i \cdot h_i = 9558$$

The base shear strength of the frame for the modal (C_{vx}) lateral force pattern is obtained from (C-6) as

$$V_y = \left(\frac{1}{9558}\right) \cdot (12034 \cdot 1000) = 1259 \text{ kN}$$

Uniform Pattern Base Shear Strength

Calculation of the base shear strength using (C-6) requires evaluation of the term $\sum_{i=1}^N \lambda_i \cdot h_i$.

Parameter λ_i for the uniform lateral force pattern is described by $\lambda_i = \frac{w_i}{\sum_{i=1}^N w_i}$. Calculations are

summarized below:

Floor	w_i (kN)	λ_i	h_i (mm)	$\lambda_i \cdot h_i$ (mm)
3	1567	0.2127	12670	2695
2	2900	0.3936	8367	3294
1	2900	0.3936	4063	1600

$$\sum_{i=1}^N \lambda_i \cdot h_i^* = 7589 \text{ mm}$$

Thus, the base shear strength of the frame for the uniform lateral force pattern is obtained from (C-6) as

$$V_y = \left(\frac{1}{7589} \right) \cdot (12034 \cdot 1000) = 1586 \text{ kN}$$

Pushover Analysis

Pushover analysis of the frame was performed by using program SAP-2000 NL (version 7.11). The results of the pushover analysis are compared to the predictions of the simple analysis. Two cases are examined for this example: a) pushover analysis without gravity loads and P- Δ effects, and b) pushover analysis with gravity load equal to 14 kN/m at the top floor, and 28 kN/m at the lower floors, and with the P- Δ effects included. Additionally, it is assumed that joints are stiffened within a length equal to half the height of the depth of the column in the horizontal

direction, and half the depth of the beam in the vertical direction. At the base, it is assumed that the length of the stiffened portion is equal to the depth of the column section. In this analysis, hinges at beams and columns are modeled to have elastoplastic behavior without considering the effect of axial load. The lateral load is proportional to the first mode. Results are summarized in Tables C-1 and C-2, and are illustrated in Figure C-4. It may be observed the results of plastic analysis compare very well to those of the pushover analysis for all patterns of lateral loads examined.

C.2.2 Examples C-2, C-3, C-4 and C-5

Figures C-3 (b), (c), (d) and (e) show the frames analyzed in examples C-2 through C-5, respectively. Following the same procedure presented in example C-1, the base shear strength V_y of each of these examples was obtained using the plastic analysis approach for the aforementioned pattern of lateral loads. Observe that while the frames of examples C-1, C-2 and C-3 are symmetrical with equal beam sizes at all levels, constant column sections, and equal span lengths, the frame of example C-4 has different (asymmetrical) span lengths and column sizes per column line. In this case the more general expression given by (C-4) was utilized for evaluation of the base shear strength. Furthermore, the 6-story, 3-span frame of example C-5 is included to verify the accuracy of the plastic analysis approach to predict the base shear strength of systems in which the effect of axial loads might be significant. Pushover analysis was performed using program SAP-2000 NL (version 7.11) following the approach of example C-1. However, in example C-5 plastic hinges at the columns were modeled considering the P-M interaction relationship.

C.2.3 Analysis and Results of Examples C-1 through C-5

Table C-1 presents a summary of the results obtained by the plastic analysis approach and by the pushover analyses performed with program SAP-2000NL. It may be observed that the base shear strength predicted by plastic analysis compares well with that predicted by program SAP-2000NL for the case when the gravity load and P- Δ effects are not included. Moreover, plastic analysis slightly overpredicts the base shear strength obtained by SAP-2000NL for the case when gravity load and P- Δ effects are included. It is also evident that consideration of gravity load and

P- Δ effects reduces the capacity of the frame. Additionally, consideration of the P-M interaction relationship in the modeling of plastic hinges in columns of example C-5 (6-story frame) results in a decrease of the capacity of the frame, but still the prediction by the plastic analysis approach is acceptable for practical purposes.

The approximate method presented herein has been derived on the basis of the assumption that plastic hinges develop in all beams along the height of the building. It is possible that a particular frame reaches its capacity without developing plastic hinges at all beams. This is likely to occur when the uniform lateral load pattern is applied in tall frames, and depending on the relative beam/column stiffness and plastic capacities. For instance, example C-5 (6-story) reaches the base shear strength under uniform pattern before hinging of the top floor beams. However, the prediction of the base shear strength by the plastic analysis approach was still acceptable for practical purposes.

On the basis of the results presented in this section, it can be stated that the plastic analysis approach can be used with confidence in the prediction of the base shear strength of moment frames with (or without) viscous damping systems provided that the frames have regular geometry, and uniform distribution of strength and stiffness.

C.3 Pushover Curves of Buildings with Yielding Damping Systems

In this section plastic analysis is utilized for the approximate construction of the pushover curve of buildings with yielding damping devices. It is assumed that all the damping devices yield prior to yielding of the framing system.

Consider the frame with damping devices in chevron type configuration subjected to a prescribed pattern of lateral load as shown in Figure C-5a. As the lateral load increases, yielding of the damping devices occurs at a specific story as shown in Figure C-5(b). In this case, yielding of the devices at the second story is shown. As the lateral load increases further, all damping devices yield while the frame is still elastic as illustrated in Figure C-5(c). Eventually a plastic collapse mechanism develops as shown in Figure C-5(d).

Figure C-6 shows a pushover curve and a trilinear representation of the pushover curve of a building with a yielding damping system. The various stages of the pushover illustrated in Figure C-5 are represented by the points a, b, c, and d on the pushover curve of Figure C-6. Segments OA, AB, and BC define the trilinear representation of the pushover curve. Segment OA represents the behavior of the combined system prior to yielding of the damping devices. The stiffness of the system in this portion of the curve, K_t , is equal to the sum of the global stiffness of the frame, K_f , and of the devices, K_d . Segment AB represents the behavior of the system after yielding of the devices. The stiffness of the system in this segment is equal to the stiffness of the frame, K_f .

Consider that a frame with metallic yielding devices is pushed laterally by loads that are proportional to the first mode resulting in the displacements D_i . The displacement of floor i , D_i , can be related to the roof displacement by $D_i = \phi_{i1} \cdot D_{roof}$. Accordingly, the interstory drift between levels j and i can be written as, $\Delta_j = D_j - D_i$, or $\Delta_j = (\phi_{j1} - \phi_{i1}) \cdot D_{roof}$, or $\Delta_j = \phi_{rj} \cdot D_{roof}$, where ϕ_{rj} is the modal drift. When yielding of the damping devices occurs at story j , the interstory drift can be written as $\Delta_{yj} = \phi_{rj} \cdot D_{roof\ yj}$, from where the displacement of the roof when yielding of the devices at level j occurs can be expressed as

$$D_{roof\ yj} = \frac{\Delta_{yj}}{\phi_{rj}} \quad (C-8)$$

The displacement of the roof when all damping devices yield (point A in Figure C-6), D_{yd} , can be defined as the maximum value of the displacement obtained by (C-8)

$$D_{yd} = \max_j \left(\frac{\Delta_{yj}}{\phi_{rj}} \right) \quad (C-9)$$

Using the modal properties of the combined system, it can be shown that base shear of the building when all damping devices yield, $V_d + K_f \cdot D_{yd}$ (see Fig. C-6) is given by

$$V_d + K_f D_{yd} = \left(\frac{4\pi^2}{gT_{lc}^2} \right) \cdot \left(\frac{D_{yd}}{\Gamma_1} \right) \cdot \bar{W}_1 \quad (\text{C-10})$$

where, T_{lc} = fundamental period of the combined system, Γ_1 = first modal participation factor of the combined system, and \bar{W}_1 = first modal weight of the combined system.

The base shear strength of the system, V , is equal to the sum of the yield strength of the frame, V_y , and the strength of the devices in the first story, V_{d1} , when yielding of both the frame and the devices occurs, that is

$$V = V_y + V_d = V_y + V_{d1} \quad (\text{C-11})$$

Of interest is to note that strength V_d is contributed by the yielding damping devices at the first story, whereas the contribution of the other damping devices to the pushover curve is reflected in the initial branch of the trilinear pushover curve. However, the above assumptions are true if the yielding of the damping devices does not change the plastic collapse mechanism of the frame, which may often occur.

Equations (C-9), (C-10) and (C-11) are sufficient to characterize the trilinear representation of the behavior of the combined system. Note that the yield displacement of the frame (exclusive of the devices) D_{yf} is presumed known. Moreover, definition of an equivalent elastoplastic representation of the pushover curve as shown in Figure C-7 is desirable for application of simplified analysis procedures. The effective initial stiffness, K_1 , of the equivalent elastoplastic representation can be defined as the slope of the straight line that intersects the trilinear curve at a base shear equal to bV , where b is a parameter selected so that the elastoplastic curve best represent the trilinear curve. Herein a value of b equal to 0.6 is used in consistency with a similar approach followed in FEMA (1997). The value of the roof displacement at the intersection point, D_o , can be easily established on the basis of Figure C-7 and the modal properties of the frame (without damping devices) as

$$D_o = \left(\frac{g}{4\pi^2} \right) \cdot \Gamma_{1f} \cdot \left(\frac{0.6V - V_d}{\bar{W}_{1f}} \right) \cdot T_{1f}^2 \quad (\text{C-12})$$

where, Γ_{1f} = first modal participation factor of the frame (without damping devices), T_{1f} = fundamental period of the frame (without damping devices), and \overline{W}_{1f} = first modal weight (without damping devices).

The effective initial (secant) period, T_1 , of the structure inclusive of the damping system in its equivalent elastoplastic representation can be expressed as

$$T_1 = 2\pi \cdot \sqrt{\frac{D_0/\Gamma_1}{\left(\frac{0.6V}{\overline{W}_1}\right) \cdot g}} \quad (\text{C-13})$$

Accordingly, the yield displacement of the equivalent elastoplastic representation is given by

$$D_y = \left(\frac{g}{4\pi^2}\right) \cdot \Gamma_1 \cdot T_1^2 \cdot \left(\frac{V}{\overline{W}_1}\right) \quad (\text{C-14})$$

Equations (C-11),(C-13) and (C-14), along with the modal properties of the combined system (under elastic conditions) can be directly used in the application of the simplified analysis procedures.

It should be noted that parameters D_y , and D_o are defined herein as the values of the roof displacement at which, respectively, yielding occurs and the base shear equals 0.6V. However, in Section 7.5.4 the same symbols are used to denote the corresponding quantities in the spectral representation of the pushover curve. That is, the two quantities differ by factor Γ_1 as illustrated in Figure 7-4.

C.3.1 Example C-6

Consider the 3-story special steel moment frame with triangular metallic yielding devices (Tsai et al., 1993) as shown in Figure C-8(a). The devices are made of steel with yield strength $F_y = 248$ MPa (36 ksi) and the dimensions shown in Figure C-8(b). They are supported on steel square tube TS8x8x1/2 braces in a chevron configuration. The base shear strength of the frame

exclusive of the damping devices and for a lateral load pattern proportional to the first mode is $V_y = 1220$ kN (275 kips) and the corresponding yield displacement is $D_{yf} = 182$ mm. The base shear strength and the yield displacement of the frame exclusive of the yielding damping devices were determined by the procedures described in Section C.2. Eigenvalue analysis of the frame exclusive of the damping devices gave: $T_{1f} = 1.58$ sec, $\bar{W}_{1f} = 5871$ kN, and $\Gamma_{1f} = 1.399$. Eigenvalue analysis of the frame inclusive of the damping devices gave: $T_{1c} = 1.133$ sec, $\{\phi_{1c}\}^T = [1.000 \quad 0.708 \quad 0.296]$, $\{\phi_{1j}\}^T = [0.292 \quad 0.412 \quad 0.296]$, $\bar{W}_1 = 6125$ kN and $\Gamma_1 = 1.3676$. Calculations for the construction of the pushover curve of the building follow.

General Information

Number of yielding steel devices per story

First story:	$N_1 = 12$
Second Story:	$N_2 = 9$
Third Story:	$N_3 = 7$

Dimensions of yielding steel devices: $b = 305$ mm; $h = 457$ mm; $t = 25.4$ mm
(see Fig. C-8)

Yield strength of the yielding steel devices: $F_y = 248$ MPa (36 ksi)

Young's Modulus: $E = 200$ kN/mm²

Yield Strength and Stiffness of Damping Devices

The yield strength V_d of yielding steel devices is given by (D-5) in Appendix D.

$$V_{di} = N_i \frac{F_y b t^2}{4h} = N_i \frac{0.248 \times 305 \times 25.4^2}{4 \times 457} = 26.70 N_i$$

$$V_{d1} = 26.7 \times 12 = 320 \text{ kN}$$

$$V_{d2} = 26.7 \times 9 = 240 \text{ kN}$$

$$V_{d3} = 26.7 \times 7 = 187 \text{ kN}$$

$$K_{di} = N_i \frac{Ebt^3}{6h_i^3} = N_i \frac{200 \times 305 \times 25.4^3}{6 \times 457^3} = 1.746 N_i$$

$$K_{d1} = 1.746 \times 12 = 21.0 \text{ kN/mm}$$

$$\therefore K_{d2} = 1.746 \times 9 = 15.7 \text{ kN/mm}$$

$$K_{d3} = 1.746 \times 7 = 12.2 \text{ kN/mm}$$

Yield Displacement of Damping Devices

The yield displacement of the devices is given by (D-3) as $\Delta_{yi} = \frac{3}{2} \cdot \left(\frac{F_y}{E} \cdot \frac{h^2}{t} \right)_i$. Accordingly,

$$\Delta_{yi} = \frac{3}{2} \times \left(\frac{0.248}{200} \times \frac{457^2}{25.4} \right)_i = 15.3 \text{ mm}$$

It may be noted that since the devices in all stories have the same dimensions h and t and are made of the same material, the yield displacement is the same in all stories.

Evaluation of D_{yd}

According to (C-9), D_{yd} is equal to the maximum value of the ratio Δ_{yi}/ϕ_{rj} , for $j=1$ to the number of stories. Since the yield displacement in this case is constant, it is obvious that the maximum ratio occurs at the story for which ϕ_{rj} is minimum, that is,

$$D_{yd} = \frac{15.3}{0.292} = 52.4 \text{ mm}$$

Evaluation of $V_d + K_f D_{yd}$

$V_d + K_f D_{yd}$ is given by (C-10)

$$V_d + K_f D_{yd} = \left(\frac{4\pi^2}{9810 \times 1.133^2} \right) \times \left(\frac{52.4}{1.3676} \right) \times 6125 = 735.7 \text{ kN}$$

Base Shear Strength of Frame Inclusive of Damping System, V

According to (C-11), the base shear strength V is equal to the sum of the base shear strength of the frame V_y (exclusive of the damping devices) and the yield strength of the devices in the first story V_{dl} . Accordingly,

$$V = V_y + V_{dl} = 1220 + 320 = 1540 \text{ kN}$$

The values of D_{yd} , $V_d + K_f D_{yd}$ and V , along with the yield displacement of the frame D_{yf} are sufficient to define the trilinear representation of the pushover curve of the system.

Evaluation of Displacement D_0

Using (C-12)

$$D_0 = \left(\frac{9810}{4\pi^2} \right) \times 1.399 \times \left(\frac{0.6 \times 1540 - 320}{5871} \right) \times 1.58^2 = 89.3 \text{ mm}$$

Effective Initial (secant) Period T_1

Using (C-13)

$$T_1 = 2\pi \sqrt{\frac{89.3 / 1.3676}{\left(\frac{0.6 \times 1540}{6125} \right) \times 9810}} = 1.320 \text{ sec}$$

Yield Displacement D_y

Using (C-14)

$$D_y = \left(\frac{9810}{4\pi^2} \right) \times 1.3676 \times \left(\frac{1540}{6125} \right) \times 1.320^2 = 148.9 \text{ mm}$$

The base shear strength V and the corresponding yield displacement D_y are sufficient to characterize the elastoplastic representation of the trilinear curve of the frame.

Pushover Curve

Pushover analysis of the structure inclusive of the damping devices was performed using program SAP-2000NL. The structure was pushed with loads proportional to the first mode. Hinges in beams and columns were modeled using elastoplastic models of behavior. Hinges in beams were assumed to form at the faces of the columns, while hinges were assumed to form in the columns at a height of 356 mm (14 in.) from the base. Joints were assumed to be stiff within a distance equal to half the depth of the beam (or column) section. A similar model was utilized to perform the pushover analysis of the frame without the damping devices.

Figure C-9 presents the pushover curves obtained by program SAP-2000NL for the frame with and without the damping devices. Also shown are the trilinear and the elastoplastic representations of the pushover curve as constructed using the approximate procedures presented in this section. Evidently, the presented simplified analysis procedure predicts very well the pushover curve of the frame with a yielding damping system.

C.4 Pushover Curve of Buildings with Viscoelastic Damping systems

Viscoelastic damping systems increase both the stiffness and the strength of a building as shown in Figure C-10. The bilinear representation of the pushover curve in this case is characterized by the yield displacement D_y , the base shear strength V_y , and the post-elastic to elastic stiffness ratio α . These parameters are related to the properties and geometry of the damping system and the base shear strength, V_{yf} , and yield displacement, D_{yf} , of the frame exclusive of the damping system. The latter may be determined by the procedures described in Section C.2.

Consider a frame with solid viscoelastic devices subjected to a prescribed pattern of lateral loads as shown in Figure C-11 (a). Each viscoelastic device is characterized by the effective stiffness, K_j , and effective damping constant, C_j . However, for the pushover analysis only the stiffness part is considered as illustrated in Figure C-11 (b). These stiffnesses represent the

storage stiffness of each device evaluated at the fundamental frequency of the system (Constantinou et al., 1998).

The global initial stiffness K_t of the combined system is equal to the sum of the stiffnesses of the frame (exclusive of the devices) and the stiffness provided by the devices. It can be shown that K_t can be expressed as function of the fundamental period of the frame inclusive of the damping devices, T_1 , the first modal participation factor Γ_1 and the first modal weight \bar{W}_1 of the combined system

$$K_t = \left(\frac{2\pi}{T_1} \right)^2 \cdot \frac{\bar{W}_1}{\Gamma_1 \cdot g} \quad (\text{C-15})$$

Period T_1 and the modal properties of the frame inclusive of the damping devices can be determined by eigenvalue analysis. However, when a complete vertical distribution of the damping devices is used, the fundamental mode shapes of the frame with and without the damping system have small differences so that the mode shape of the frame without the damping system may be used. Accordingly, (7-49) and (7-53) may be used to estimate period T_1 and parameter α .

Construction of the pushover curve requires knowledge of the yield displacement D_y . This displacement is assumed to be the one of the frame exclusive of the damping systems, which can be calculated by the procedures of section C.2. It follows that the base shear strength of the combined system is given by

$$V_y = \left(\frac{4\pi^2}{g \cdot T_1^2} \right) \cdot \left(\frac{\bar{W}_1}{\Gamma_1} \right) \cdot D_y \quad (\text{C-16})$$

C.4.1 Example C-7

Consider the 3-story special steel moment frame with the uniform vertical distribution of viscoelastic devices shown in Figure C-12(a). Each of these viscoelastic devices has bonded area equal to $A_b = 626,330 \text{ mm}^2$ (four 15.5 by 15.5 in. areas) and thickness $h = 140 \text{ mm}$ (5.5 in.) made of material 3M ISD110 (Zimmer, 1999) with approximate storage and loss shear moduli

$G' \approx G'' = 0.83 \text{ MPa}$ at temperature of 20° C and frequency of about 0.7 Hz . Note that stiffness K is the storage stiffness and damping constant C is the loss stiffness divided by frequency as described by equation (7-43). Note that the frequency is the frequency of the mode of interest. In this case the frequency is that of the first mode of the frame inclusive of the damping system estimated by (7-49) with $\eta = 1.0$. It should be noted that the dimensions of the viscoelastic devices appear large. The large dimensions resulted from the restriction of a shear strain amplitude in the viscoelastic material of 100% in the maximum considered earthquake (1.5 times the design basis earthquake). Such limit appears reasonable at this time but improvements in the materials and bonding processes may justify higher limits. These devices provide additional viscous damping ratio of 0.086 under elastic conditions. The damping ratio β_{V1} was calculated on the basis of (7-29) with $f_j = \cos \theta_j$ and using the mode shape and period T_1 of the frame inclusive of the damping devices (including the storage stiffness of the devices). However, the same result was obtained when use was made of the mode shape of the frame exclusive of the damping system and the period based on (7-49).

The base shear strength of the frame (exclusive of the damping devices) is 1220 kN (275 kips) and the corresponding yield displacement is 182 mm. Eigenvalue analysis of the frame (exclusive of the devices) gave: $T_{1f} = 1.58 \text{ sec}$, $\{\phi_{i1}\}^T = [1.000 \ 0.657 \ 0.250]$, $\bar{W}_{1f} = 5871 \text{ kN}$, and $\Gamma_{1f} = 1.399$. Eigenvalue analysis of the frame inclusive of the damping devices gave: $T_{1c} = 1.473 \text{ sec}$, $\{\phi_{i1}\}^T = [1.000 \ 0.684 \ 0.275]$, $\bar{W}_1 = 6013 \text{ kN}$ and $\Gamma_1 = 1.38$. The results of the eigenvalue analysis of the frame with the damping devices are presented for the purpose of demonstrating (a) the usefulness of (7-49) in predicting the period, and (b) that the modal properties of the frame with the damping devices are basically the same as those of the frame exclusive of the damping system.

General Information

Base shear strength of the frame (w/o devices):	$V_{yf} = 1220 \text{ kN}$
Yield displacement of the frame (w/o devices):	$D_{yf} = 182 \text{ mm}$
Damping constant of the devices	$C_j = 0.876 \text{ kN-s/mm}$

Storage stiffness of the devices :

$$K_j = 3.70 \text{ kN-s/mm}$$

Calculation of Initial Stiffness, K_t

Stiffness K_t was evaluated by (C-15) using the approximate period given by (7-49) with $\eta = 1.0$ and the modal properties of the frame without damping devices:

$$T_1 \approx 1.58x \sqrt{1 - \frac{2x0.086}{1.0}} = 1.44 \text{ sec}$$

$$K_t = \left(\frac{2\pi}{1.44} \right)^2 x \frac{5871}{1.399x9810} = 8.1 \text{ kN / mm}$$

Also use of (C-15) with the modal properties of the frame inclusive of the damping system gives

$$K_t = \left(\frac{2\pi}{1.473} \right)^2 x \frac{6013}{1.38 \cdot 9810} = 8.1 \text{ kN / mm}$$

Base Shear Strength of the Combined System, V_y

Using (C-16)

$$V_y = \left(\frac{4\pi^2}{9810x1.44^2} \right) x \left(\frac{5871}{1.399} \right) x 182 = 1482 \text{ kN}$$

Post-Elastic to Elastic Stiffness Ratio, α

Using (7-53)

$$\alpha = \frac{2x0.086}{1.0} = 0.172$$

Pushover Analysis

Pushover analysis of the frame with the damping devices as shown in Figure C-11(b) was performed in program SAP-2000NL. The structure was pushed over by forces proportional to the first mode using the modal properties of the combined system under elastic conditions. Hinges in

beams and columns were modeled as elastoplastic elements. Hinges in beams were assumed to form at the faces of the columns while hinges at the base of the structure are assumed to develop at a height of 356 mm (14 in.) above the base. Joints were assumed to be stiff within a distance equal to half the depth of the beam (or column) section.

Figure C-13(a) present the pushover curves of the frame with and without the damping system as obtained by program SAP-2000NL and compares them to the results of approximate analysis. Evidently, the approximate analysis predicts well the pushover curve. It is of interest to observe that the addition of the viscoelastic devices caused an increase of about 20% in both the strength and the stiffness of the frame.

Examples C-8 and C-9

Example C-8 is also a 3-story frame as shown in Figure C-12 (b) but much stiffer and stronger than the frame of example C-7. The damping devices provide an additional viscous damping β_{V1} equal to 0.06 under elastic conditions. The base shear strength of the frame (exclusive of the devices) is 3210 kN (722 kips) and the corresponding yield displacement is 173 mm. Eigenvalue analysis of the combined system (frame with damping devices) gave: $T_{1c} = 1.365$ sec, $\{\phi_{i1}\}^T = [1.000 \ 0.792 \ 0.413]$, $\bar{W}_1 = 11955$ kN and $\Gamma_1 = 1.31$. Using these modal properties:

$$(C-15): \quad K_t = \left(\frac{2\pi}{1.365} \right)^2 \times \frac{11955}{1.31 \times 9810} = 19.7 \text{ kN/mm}$$

$$(C-16): \quad V_y = \left(\frac{4\pi^2}{9810 \times 1.365^2} \right) \times \left(\frac{11955}{1.31} \right) \times 173 = 3410 \text{ kN}$$

$$(7-53): \quad \alpha = \frac{2 \times 0.06}{1.0} = 0.12$$

Figure C-13(b) compares the approximate pushover curve to that obtained by analysis using program SAP-2000NL. The comparison is very good.

Example C-9 is a 6-story frame as shown in Figure C-12(c). The viscoelastic devices provide an

additional viscous damping β_{VI} equal to 0.12 under elastic conditions. The base shear strength of the frame (exclusive of the damping devices) is 1730 kN (389 kips) and the corresponding yield displacement is 360 mm. Eigenvalue analysis of the combined system (frame with damping devices) gave: $T_{1c} = 2.367$ sec, $\{\phi_{i1}\}^T = [1.000 \ 0.893 \ 0.717 \ 0.568 \ 0.302 \ 0.113]$, $\bar{W}_1 = 12392$ kN and $\Gamma_1 = 1.39$. Using these modal properties:

$$(C-15): \quad K_t = \left(\frac{2\pi}{2.363} \right)^2 \times \frac{12392}{1.39 \times 9810} = 6.4 \text{ kN/mm}$$

$$(C-16): \quad V_y = \left(\frac{4\pi^2}{9810 \times 2.363^2} \right) \times \left(\frac{12392}{1.39} \right) \times 360 = 2313 \text{ kN}$$

$$(7-53): \quad \alpha = \frac{2 \times 0.12}{1.0} = 0.24$$

The pushover curve in this case is also constructed using program SAP-2000NL and utilizing the first mode lateral load distribution and the modal properties of the combined system under elastic conditions. Plastic hinges in beams were modeled using an elastoplastic model, whereas plastic hinges in the columns were modeled using the M-P interaction relationship. Gravity loads and P- Δ effects were also included in the analysis. As shown in Figure C-13(c) the approximate pushover curve compares well with the one obtained by program SAP-2000NL although it may be seen that the predicted strength is about 7% larger than the actual one.

TABLE C-1 Comparison of Base Shear Strength Calculated by Plastic Analysis and Analysis Using Program SAP-2000NL

Example	Lateral Load Pattern	Plastic Analysis	SAP-2000NL Pushover	
			V_y (kN)	
		V_y (kN)	A	B
C-1	First Mode	1304	1312	1272
	Modal (C_{vx})	1259	1263	1227
	Uniform	1585	1592	1530
C-2	First Mode	1744	1765	1734
	Modal (C_{vx})	1718	1734	1707
	Uniform	2133	2161	2112
C-3	First Mode	2435	2450	2419
	Modal (C_{vx})	2421	2454	2423
	Uniform	2990	3015	2970
C-4	First Mode	3314	3295	3210
	Modal (C_{vx})	3130	3068	2992
	Uniform	3698	3695	3584
C-5	First Mode	1848	1881	1730
	Modal (C_{vx})	1666	1690	1574
	Uniform	2375	2410	2188

A = pushover analysis without gravity load and P- Δ effects

B = pushover analysis with gravity load and P- Δ effects

TABLE C-2 Comparison of Yield Displacement Calculated by Plastic Analysis and Analysis Using Program SAP-2000NL

Example	First Mode Properties				Plastic Analysis		SAP-2000 Pushover	
							Analysis with P- Δ and Gravity Loads Effects	
	T_1 (sec)	\overline{W}_1 (kN)	Γ_1	Weight (kN)	V_y (kN)	D_y (mm)	V_y (kN)	D_y (mm)
C-1	1.580	5871	1.40	7368	1304	192	1272	188
C-2	1.331	5803	1.41	7367	1744	186	1734	185
C-3	1.119	5749	1.41	7367	2435	186	2419	185
C-4	1.403	11934	1.32	13339	3314	179	3210	173
C-5	2.678	12081	1.41	16067	1848	385	1730	360

Pattern of Lateral Loads Proportional to First Mode

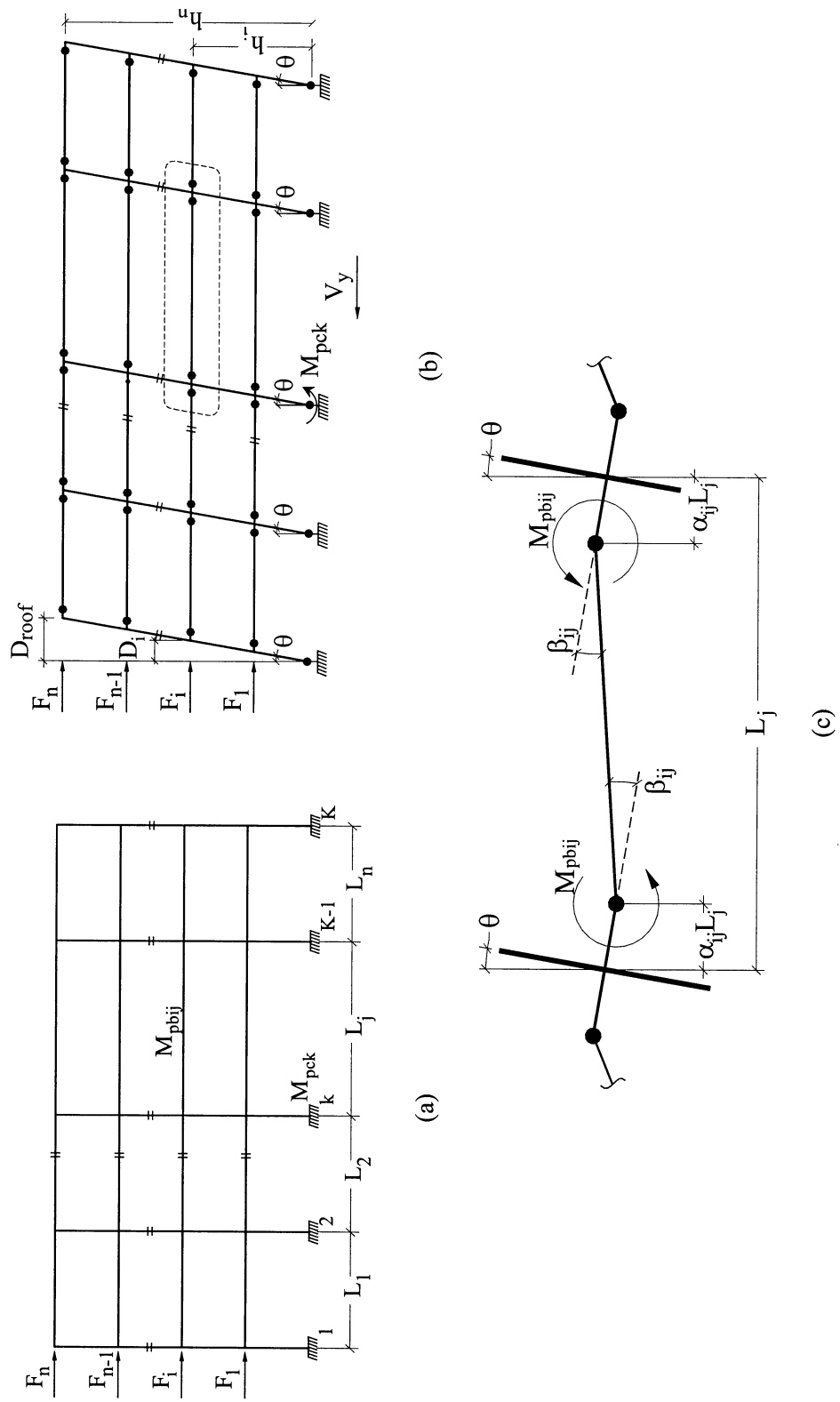


FIGURE C-1 N-Story, n-Bay Moment Frame and Assumed Collapse Mechanism

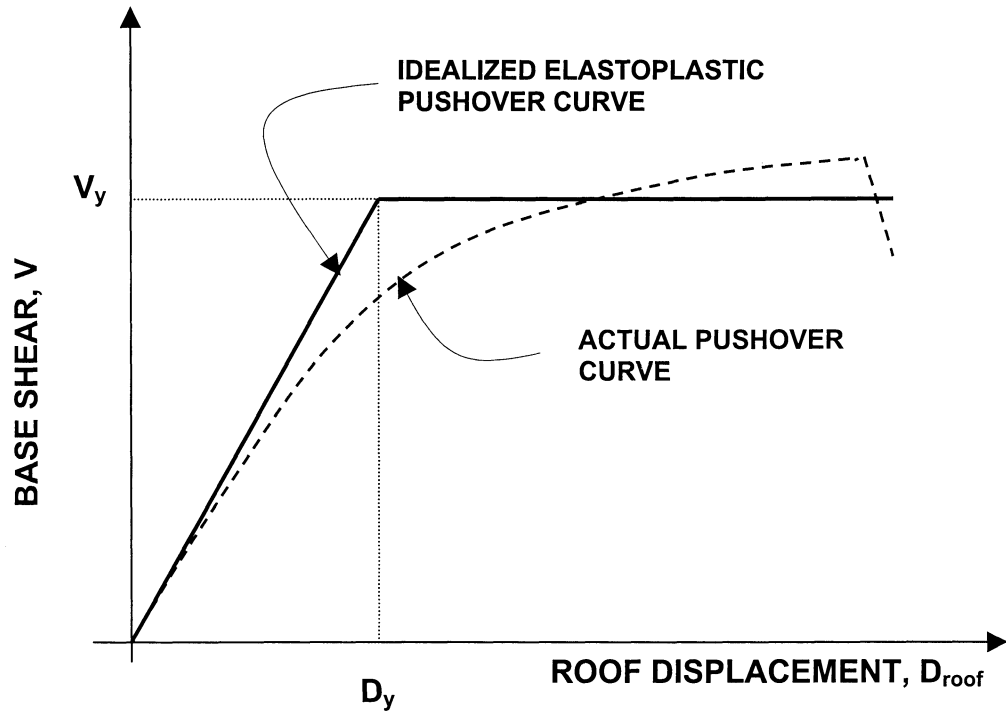
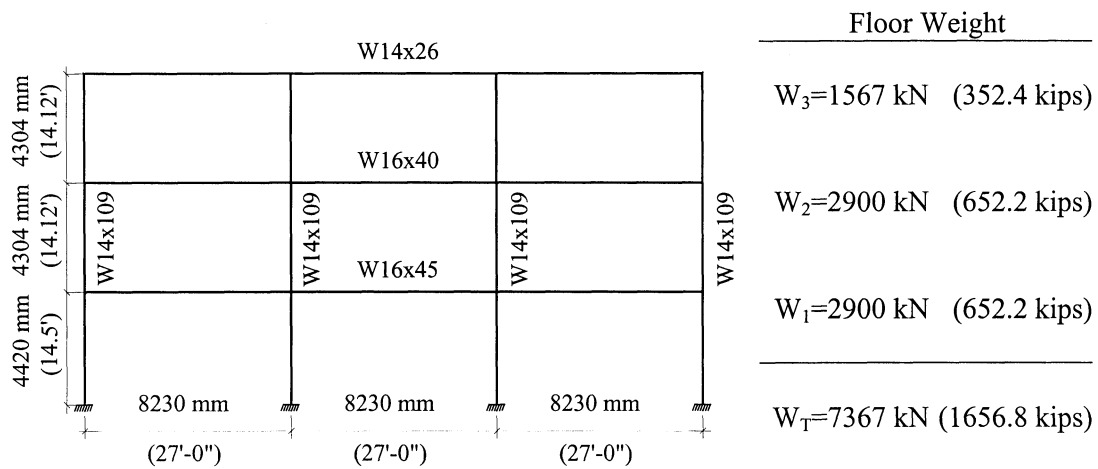
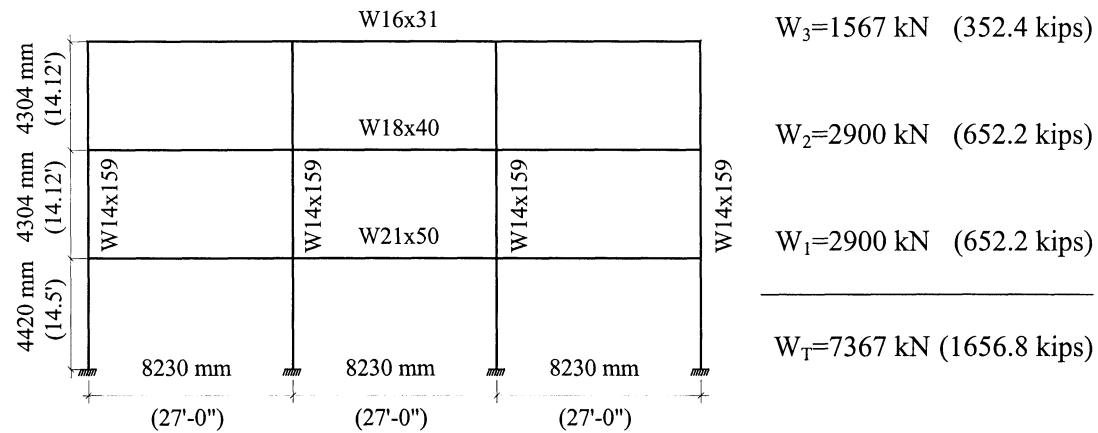


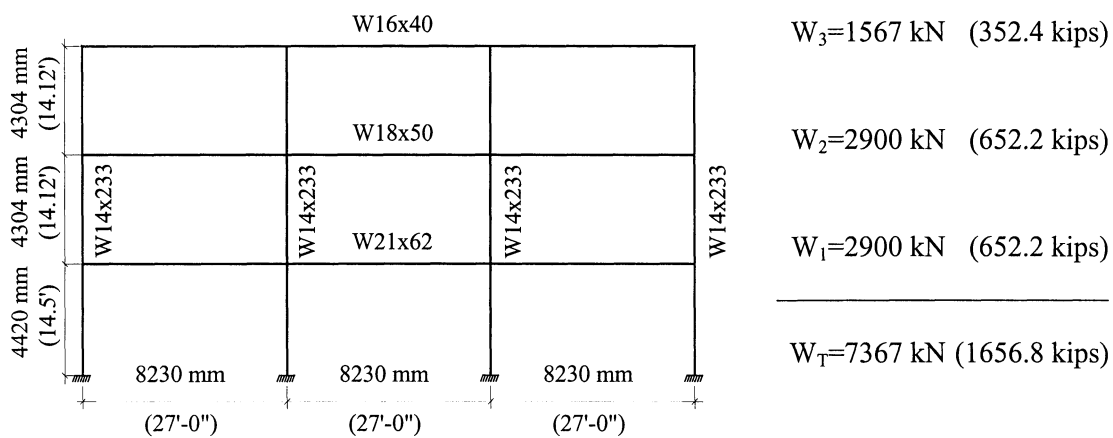
FIGURE C-2 Bilinear Representation of Pushover Curve of Building without a Damping System (or with a Viscous Damping System)



(a) Example C-1

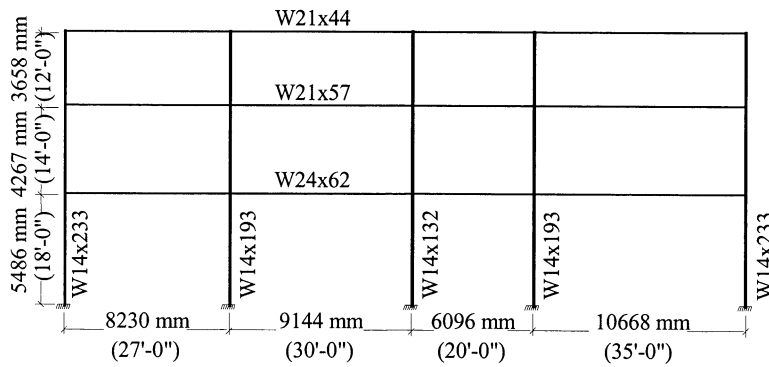


(b) Example C-2



(c) Example C-3

FIGURE C-3 Analyzed Steel Moment Frames



Floor Weight

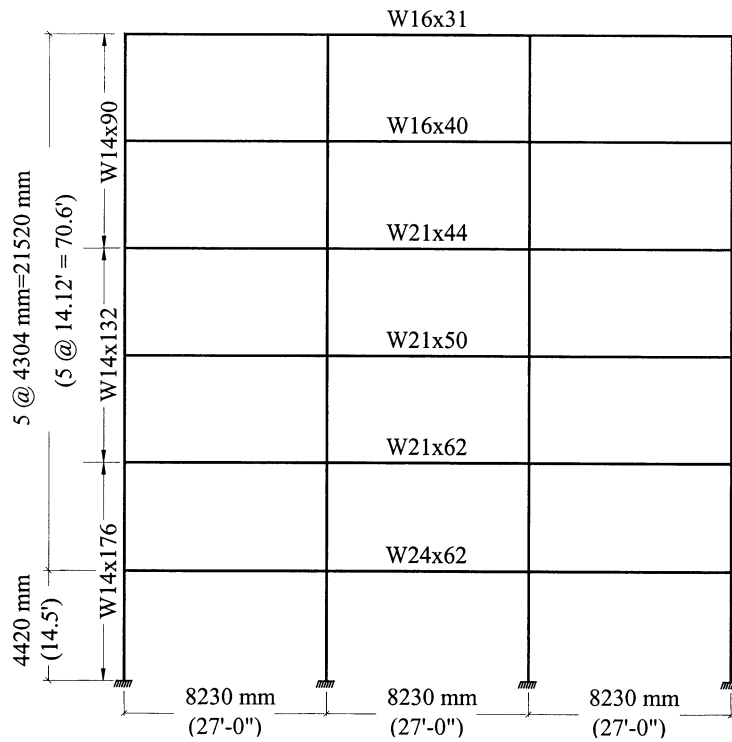
$$W_3 = 2668 \text{ kN} \quad (600 \text{ kips})$$

$$W_2 = 5336 \text{ kN} \quad (1200 \text{ kips})$$

$$W_1 = 5336 \text{ kN} \quad (1200 \text{ kips})$$

$$W_T = 13340 \text{ kN} \quad (3000 \text{ kips})$$

(d) Example C-4



$$W_6 = 1567 \text{ kN} \quad (352.4 \text{ kips})$$

$$W_5 = 2900 \text{ kN} \quad (652.2 \text{ kips})$$

$$W_4 = 2900 \text{ kN} \quad (652.2 \text{ kips})$$

$$W_3 = 2900 \text{ kN} \quad (652.2 \text{ kips})$$

$$W_2 = 2900 \text{ kN} \quad (652.2 \text{ kips})$$

$$W_1 = 2900 \text{ kN} \quad (652.2 \text{ kips})$$

$$W_T = 16067 \text{ kN} \quad (3613.4 \text{ kips})$$

(e) Example C-5

FIGURE C-3 continued

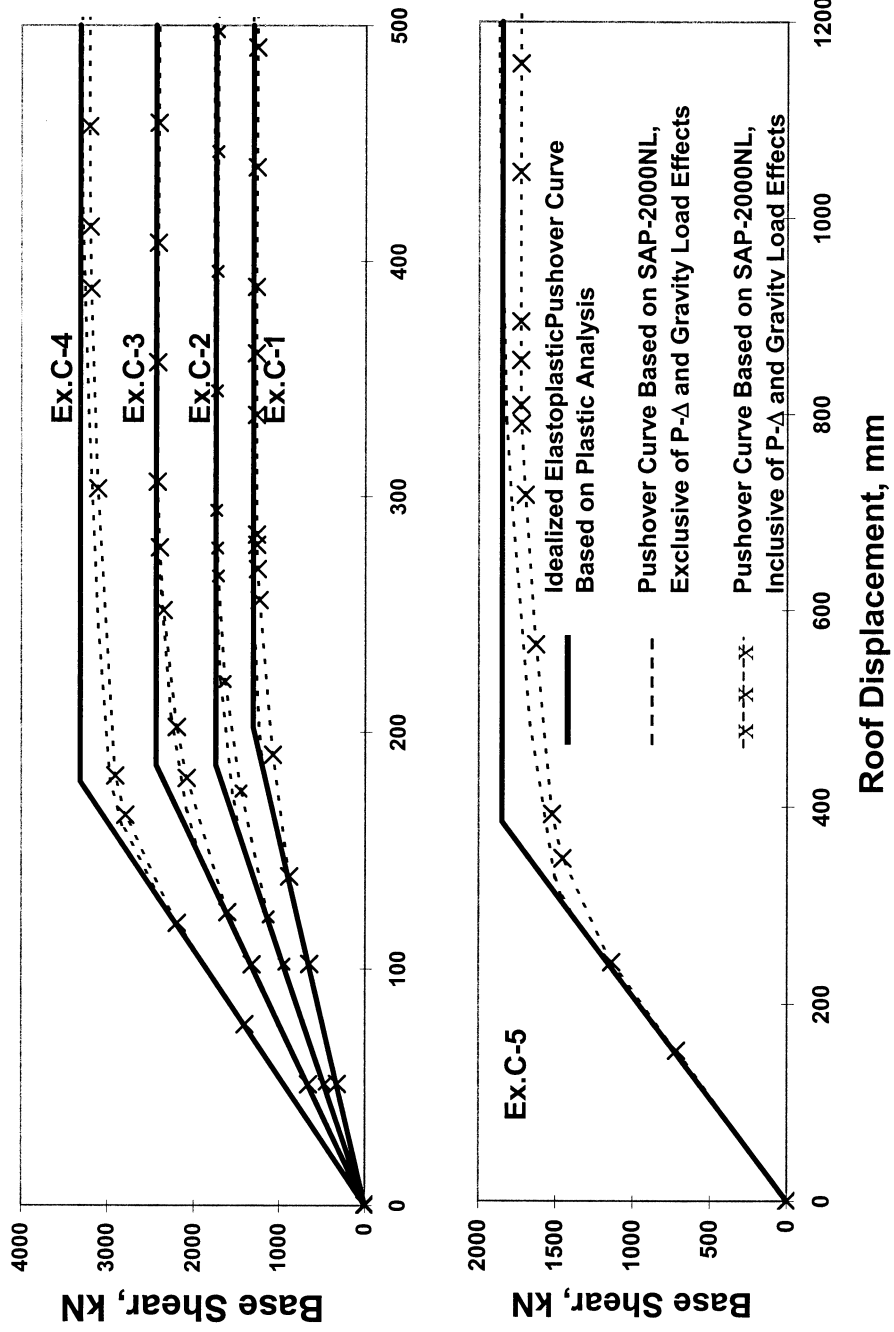
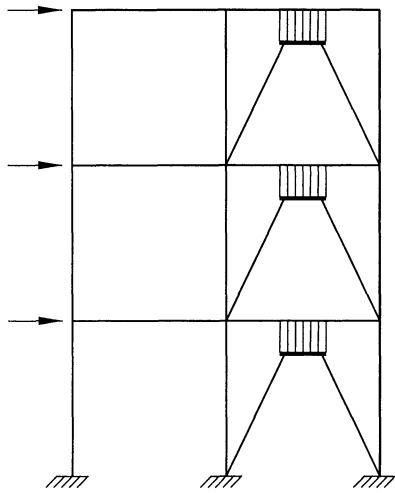


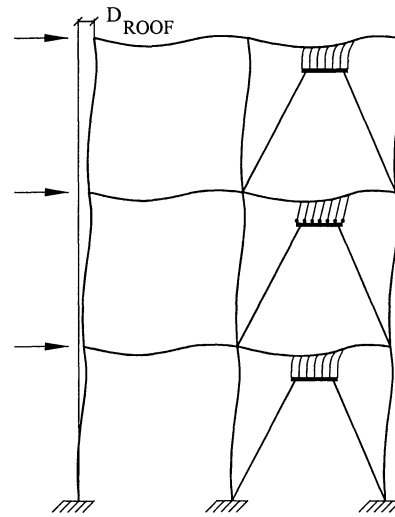
FIGURE C-4 Comparison of Idealized Elastoplastic Pushover Curves Based on Plastic Analysis and Pushover Curves Calculated Using Program SAP-2000NL

ELASTIC BEHAVIOR



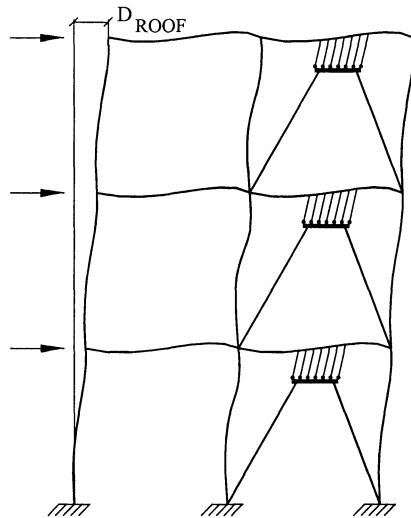
(a)

FIRST YIELDING IN DAMPING DEVICES



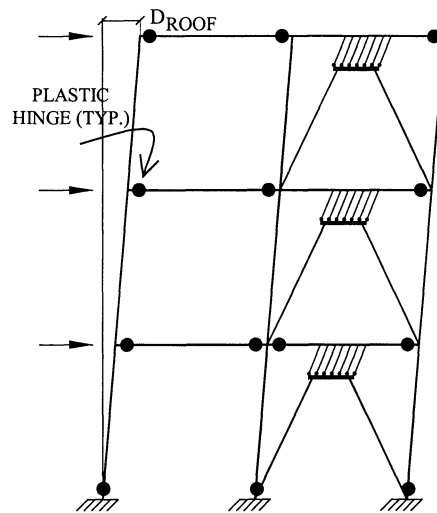
(b)

YIELDING IN ALL DAMPING DEVICES, FRAME STILL ELASTIC



(c)

COLLAPSE MECHANISM



(d)

FIGURE C-5 Frame with Metallic Damping Devices

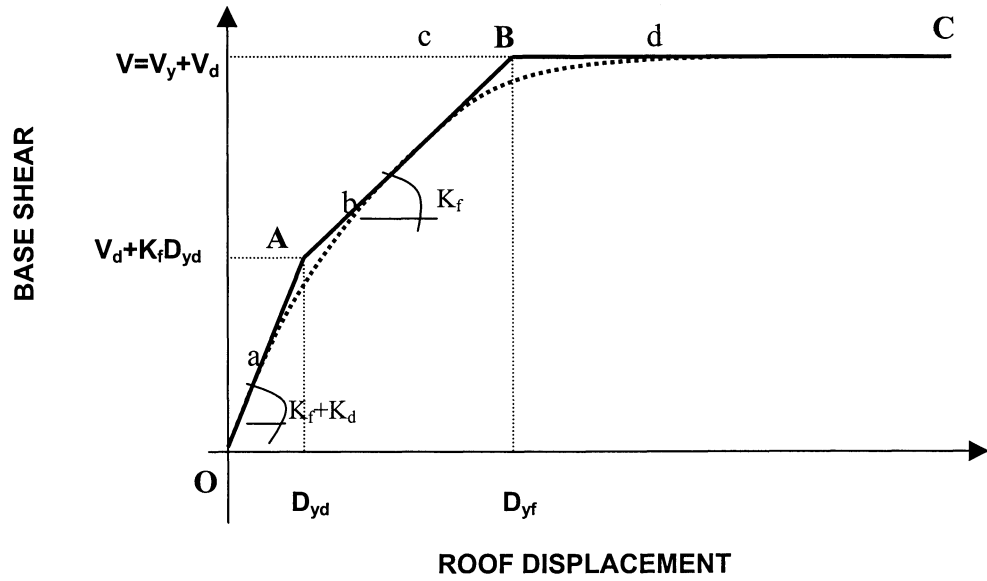


FIGURE C-6 Trilinear Representation of Pushover Curve of Building with Yielding Damping System

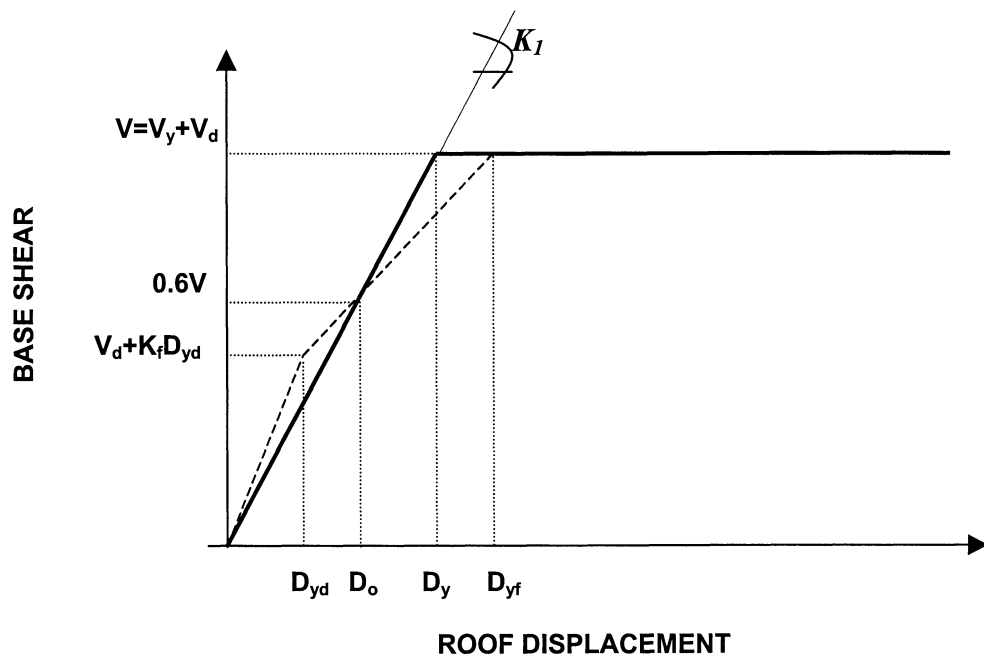
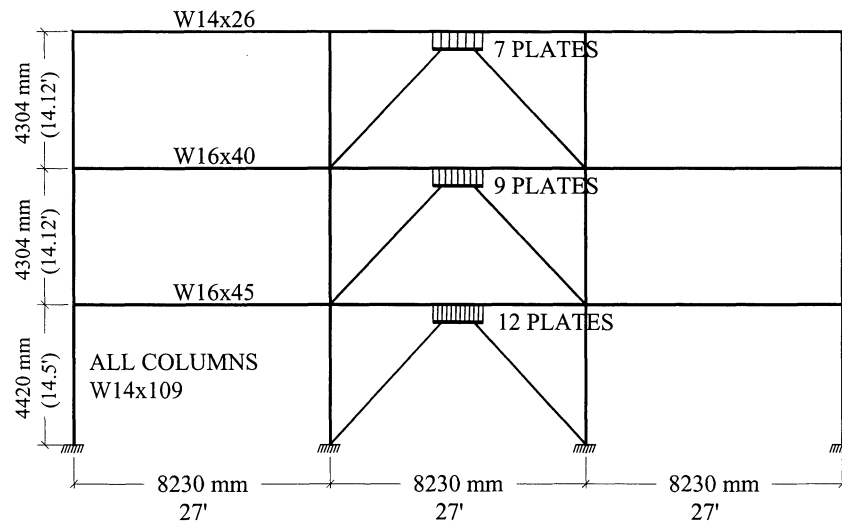
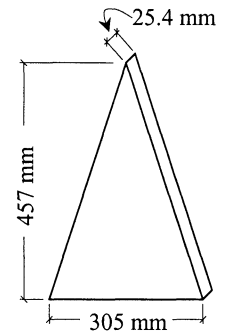


FIGURE C-7 Trilinear and Equivalent Elastoplastic Representation of Pushover Curve of Building with Yielding Damping System



(a)



$F_y = 248 \text{ MPa}$
(= 36 ksi)

(b)

FIGURE C-8 Frame of Example C-6 with Metallic Yielding Devices

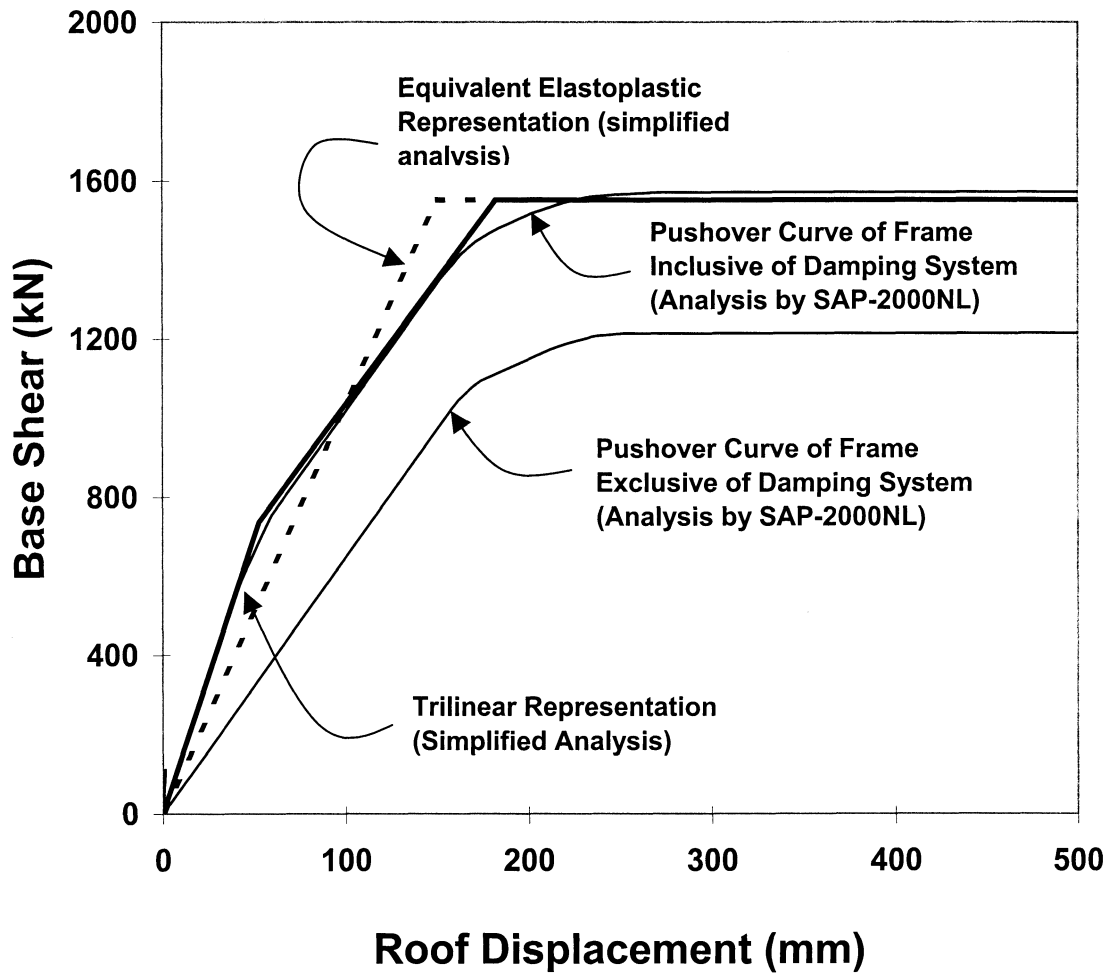


FIGURE C-9 Comparison of Pushover Curves of Frame with and without Yielding Damping System Obtained by Simplified Analysis and by Computer Analysis

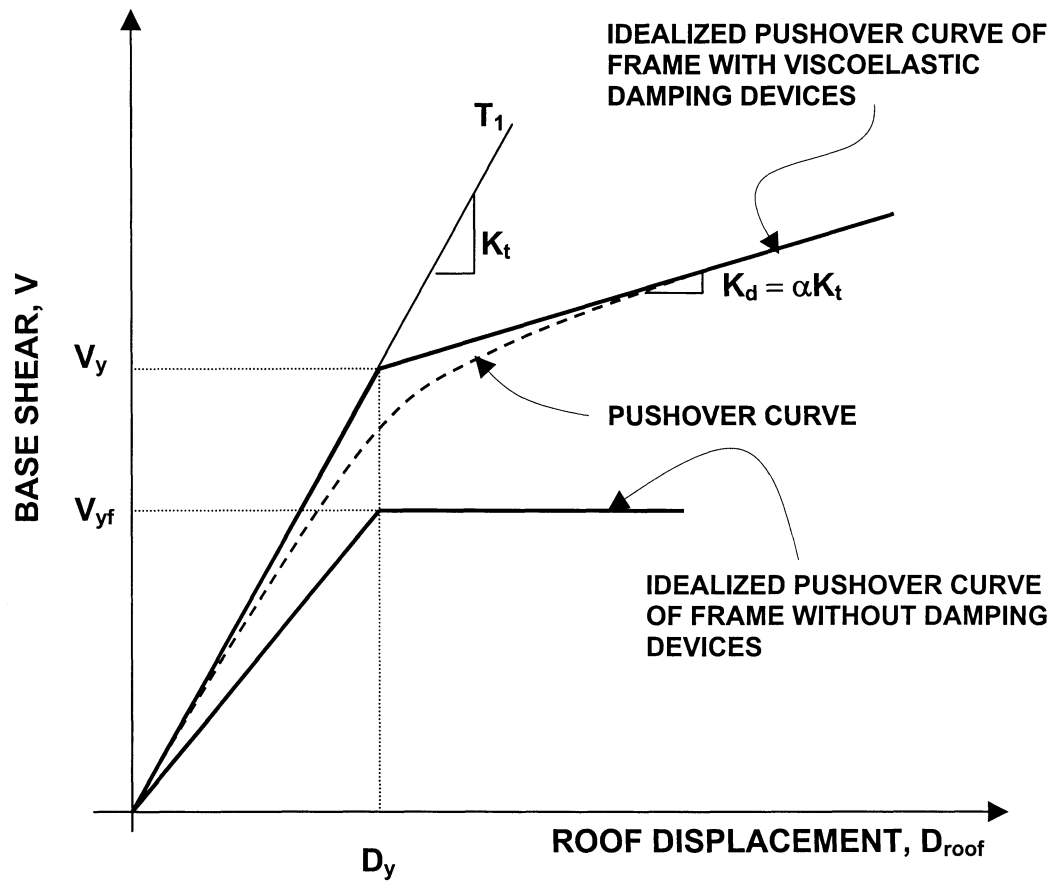


FIGURE C-10 Pushover Curves of Frame with Viscoelastic Damping Devices

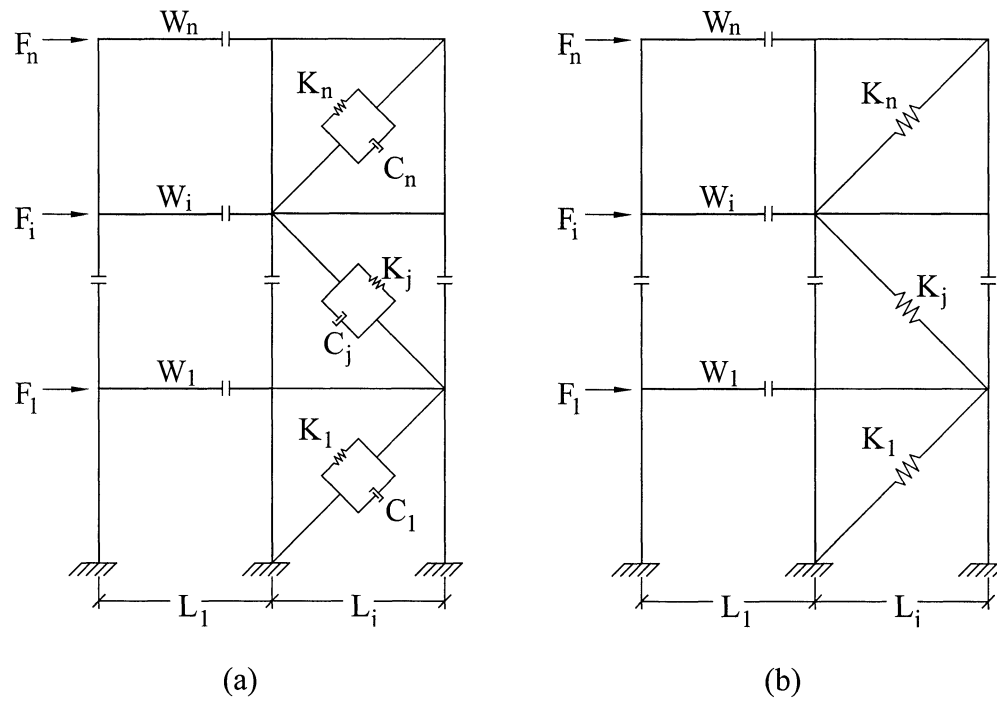
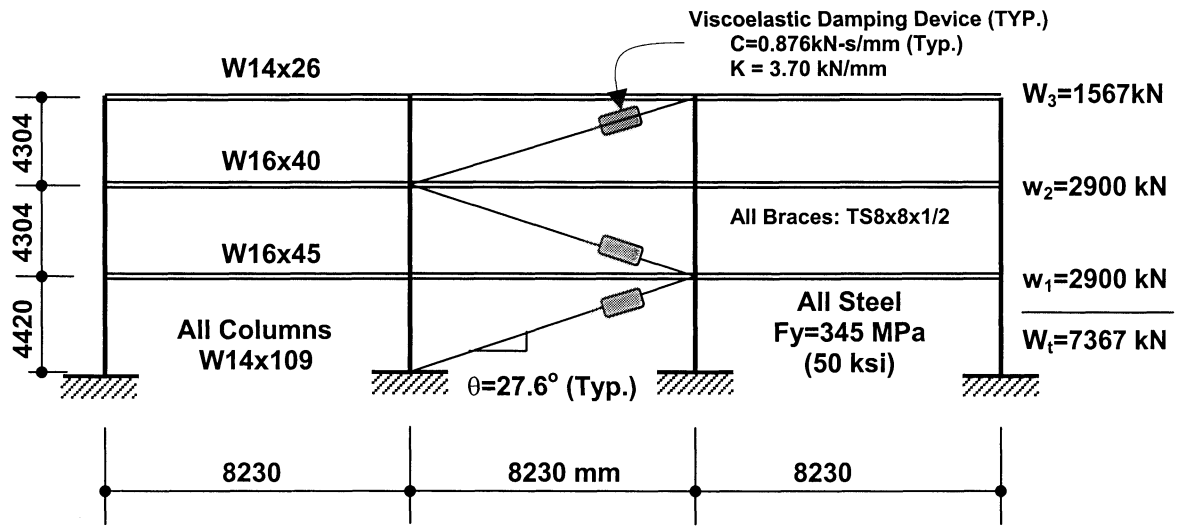
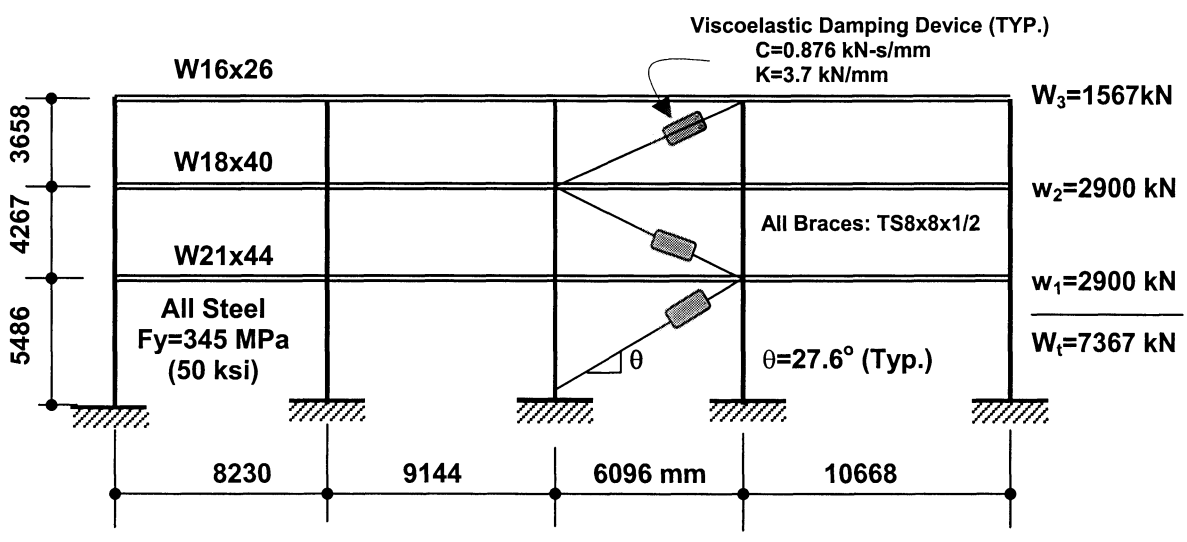


FIGURE C-11 Frame with Viscoelastic Damping System

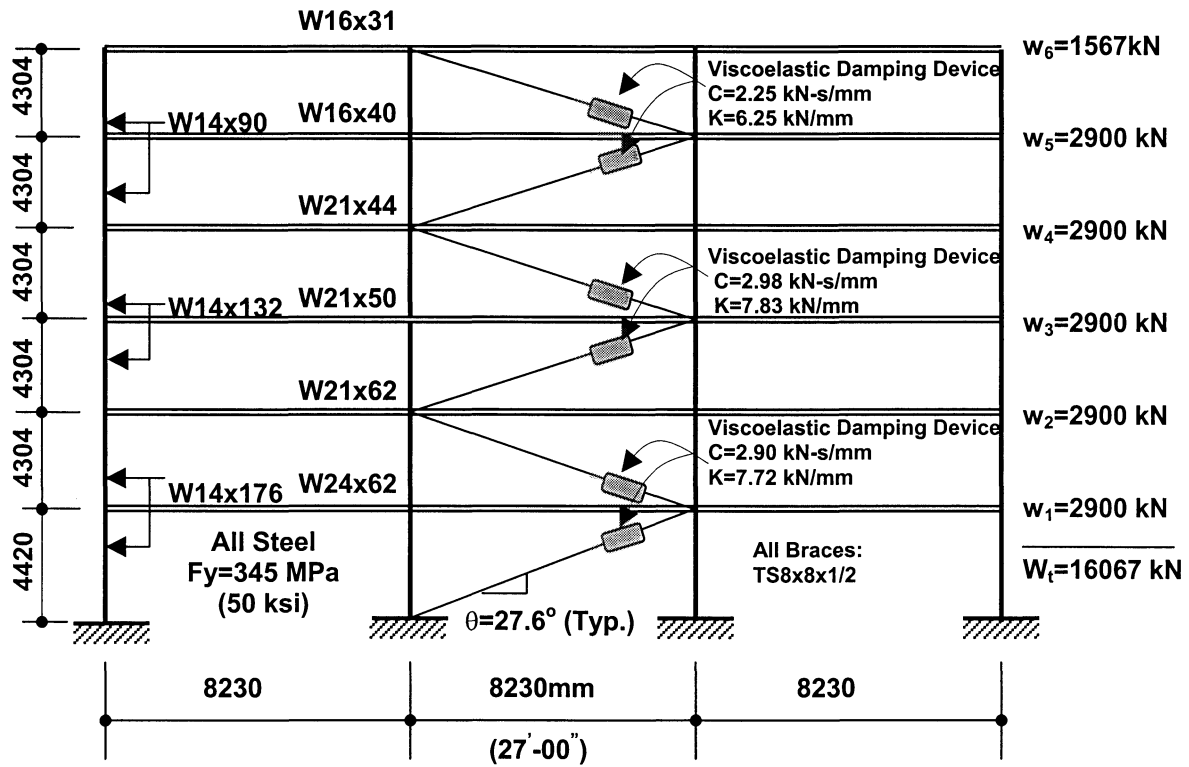


(a)



(b)

FIGURE C-12 Examples of Steel Moment Frames with Viscoelastic Solid Devices



(c)

FIGURE C-12 Examples of Steel Moment Frames with Viscoelastic Solid Devices
(continued)

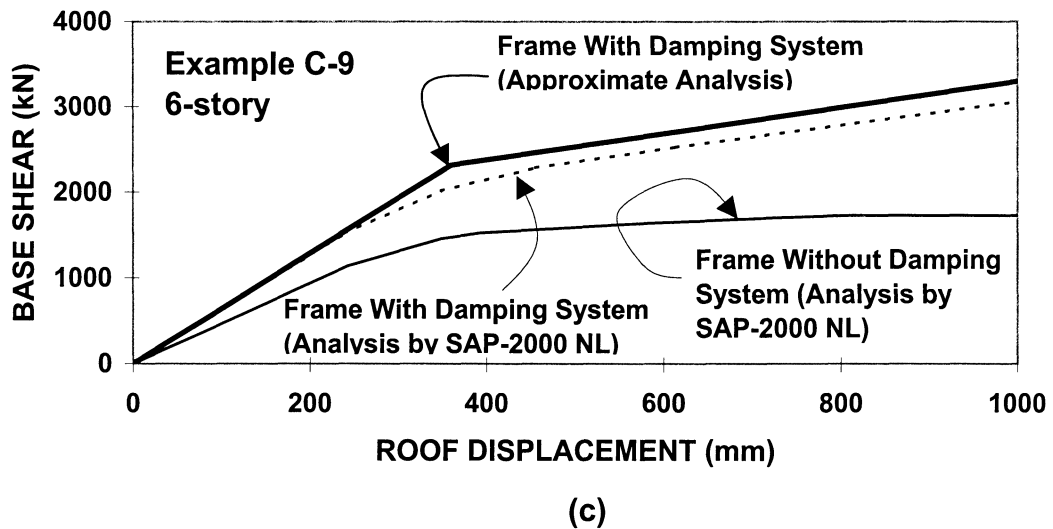
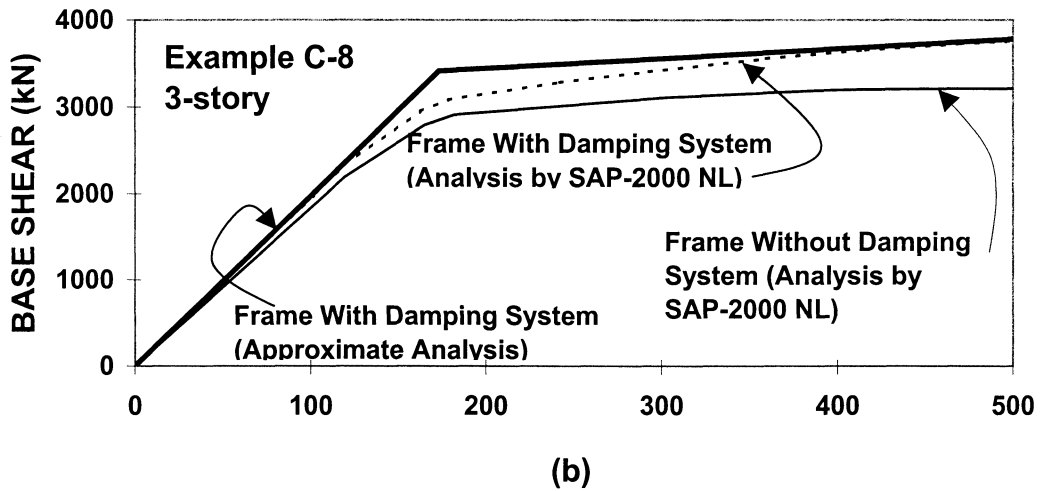
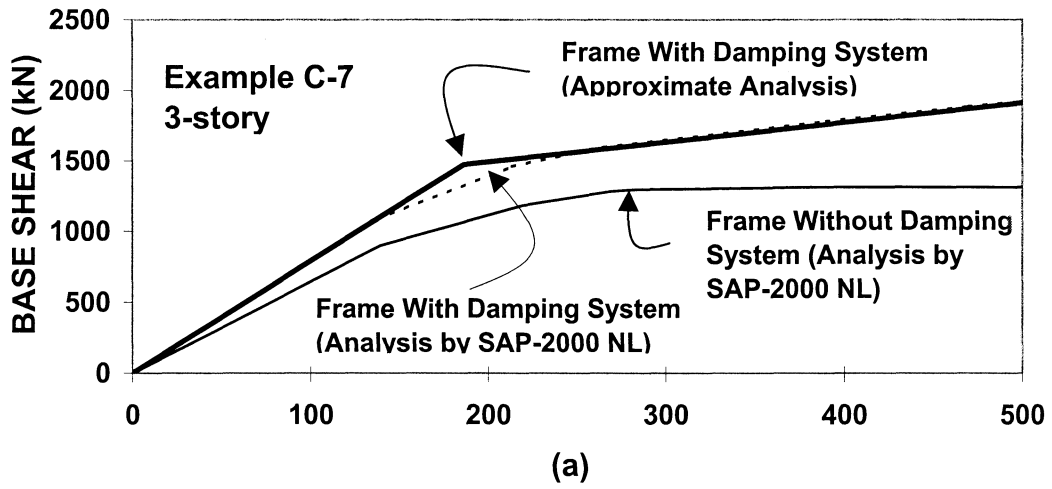


FIGURE C-13 Comparison of Pushover Curves of Buildings with Viscoelastic Damping Systems

APPENDIX D

CONSIDERATIONS IN THE DESIGN OF

METALLIC YIELDING AND VISCOELASTIC SOLID DAMPING DEVICES

D.1 Introduction

This appendix presents some information on metallic yielding and on viscoelastic solid damping devices, which is of significance in their design. In the case of metallic yielding devices, the presentation concentrates on triangular plate devices (Tsai et al., 1993) since this type of device is utilized in the examples presented in this work. The information presented in this appendix can also be applied to other types of metallic yielding devices such as the unbonded steel braces (Watanabe et al., 1988). In the case of viscoelastic devices, information is presented on the mechanical properties of one commonly available and used material, 3M ISD110 (Soong and Dargush, 1997). Data from Zimmer (1999), who conducted an extensive experimental study to evaluate the properties of this material for a wide range of frequency, temperature, and strain are presented.

D.2 Metallic Yielding Devices

Triangular plate damping devices or T-ADAS devices (Tsai et al., 1993; Soong and Dargush, 1997; Constantinou et al., 1998) are shaped and loaded as shown in Figure D-1. The triangular shape ensures yielding over the entire height of the device.

Triangular plate elements were originally conceived as damping devices in seismic isolation systems (Tyler, 1978a; Tyler, 1978b). The original work of Tyler consisted of experiments and design procedures for a variety of yielding steel devices, including triangular and round devices. An important consideration in the design of these devices is low-cycle fatigue. The approach followed herein in the design of these devices is to specify the number of cycles that the device should be capable of sustaining in either the design-basis earthquake or maximum-considered earthquake. Various studies on low-cycle fatigue relate the maximum strain or plastic strain to the number of cycles, N_f , at failure (Manson, 1953; Coffin, 1954; Koh and Stephens, 1991;

Mander et al., 1994). In general, a relation between the amplitude of strain (half the strain range) and the number of cycles at failure, N_f , may be written in the form:

$$\varepsilon_{max} = AN_f^{-b} \quad (D-1)$$

Values $A = 0.08$ and $b = 0.3$ result in an equation which reasonably represents the low-cycle fatigue behavior of low strength steel devices. Note that this behavior is typically different from that of specimens of the steel used in these devices (e.g., see Tyler, 1978a).

Utilizing this relation and requiring that $N_f = 100$ in the design-basis earthquake, the allowable maximum strain in the plate is calculated to be $\varepsilon_{max} = 0.02$. Moreover, the maximum displacement ductility in the device, μ_d , calculated as the ratio of the maximum and yield displacements at the point of application of the load, D_{max} and D_y , respectively, may be shown to be for the triangular plate device

$$\mu_d = \frac{D_{max}}{D_y} = \frac{2}{3} \left(\frac{\varepsilon_{max}}{\varepsilon_y} \right) \quad (D-2)$$

where ε_y is the yield strain of the material. Note that for an unbonded brace (brace in uniaxial tension and compression without instability problems), $\mu_d = \varepsilon_{max} / \varepsilon_y$. Accordingly, use of A36 steel (minimum yield stress $250 \text{ MPa} = 36 \text{ ksi}$) with $\varepsilon_y = 0.00125$ results in maximum allowable strain $\varepsilon_{max} = 0.02$ and allowable ductility demand $\mu_d = 10.7$ for triangular plate devices.

To understand the implications of these limits on strain and ductility for triangular plate devices, one has to relate the yield displacement D_y and the maximum displacement D_{max} of the device to the yield strain ε_y , the maximum strain ε_{max} and the geometry of the device. It is easily derived that

$$D_y = \frac{3}{2} \left(\frac{\varepsilon_y h^2}{t} \right) \quad (D-3)$$

$$D_{max} = \left(\frac{\varepsilon_{max} h^2}{t} \right) \quad (D-4)$$

Based on NEHRP (2000), the drift limit in the design-basis earthquake is R/C_d times the allowable story drift. For a special steel moment frame, seismic group I, the drift limit is $(R/C_d)(0.02h_{sx})$ or about $(8/5.5)(0.02 \times 4000 \text{ mm}) = 116 \text{ mm}$. Consider a design in which triangular plate devices are designed in a chevron configuration to have a displacement of not much less than 116 mm in the design-basis earthquake. For A36 steel with $\varepsilon_{max} = 0.02$ and using (D-4) results in the requirement that $h^2/t = 5,800 \text{ mm}$. Selecting $t = 25.4 \text{ mm}$ (1 in.), $h = 384 \text{ mm}$ (15 in.). The width, b (typically less than h) and the number of triangular plates are selected in order to achieve the desired yield strength. For this calculation, the yield strength V_d of a single triangular plate may be calculated by

$$V_d = \left(\frac{F_y b t^2}{4h} \right) \quad (\text{D-5})$$

where F_y = yield stress of steel.

As an example, consider a singular triangular plate device with dimensions $b = 305 \text{ mm}$, $h = 457 \text{ mm}$, $t = 25.4 \text{ mm}$ with $F_y = 250 \text{ MPa}$ (A36 steel). It has yield strength $V_d = 26.9 \text{ kN}$ and allowed maximum displacement $D_{max} = 165 \text{ mm}$ in the design-basis earthquake (for $N_f = 100$). For this displacement, the maximum strain in the device is $\varepsilon_{max} = 0.02$. By comparison, consider that unbonded steel braces are used rather than triangular plate devices. The braces are installed in the diagonal configuration at an angle $\theta = 28^\circ$ with an effective length of $9,300 \text{ mm}$. For a drift of 165 mm in the design-basis earthquake, the brace axial deformation is 146 mm and therefore the maximum strain is $146/9,300 = 0.016$. At this strain the predicted number of cycles to failure is 213, which is very good.

For the maximum-considered earthquake, the displacement is approximately 1.75 times larger, so that for the triangular plate devices $D_{max} = 289 \text{ mm}$, $\varepsilon_{max} = 0.035$ and $N_f = 16$, which is arguably sufficient. For the unbonded steel brace device, $D_{max} = 256 \text{ mm}$, $\varepsilon_{max} = 0.027$ and $N_f = 37$, which is very good

D.3 Viscoelastic Solid Devices

Information on viscoelastic solid devices may be found in Soong and Dargush (1997), Constantinou et al. (1998) and FEMA (1997). Herein, we present a brief description of the

behavior of these devices, mechanical data for viscoelastic material 3M ISD110 and a simple procedure for the mathematical modeling of these devices for dynamic response-history analysis.

Figure D-2 presents typical force-displacement loops of a full size device with bonded area $A_b = 92,903 \text{ mm}^2$ and thickness $h = 88.9 \text{ mm}$ (Zimmer, 1999). It was subjected to 10 cycles of displacement of amplitudes equal to the thickness (i.e., shear strain $\gamma = u_o / h = 1.0$). The substantial reduction of effective stiffness and energy dissipated per cycle is a result of the increase in temperature of the device from 20° C to 26.9° C during testing. The effect of temperature, whether ambient or due to heating, is an important consideration in the design of buildings with these devices.

Figure D-3 illustrates an idealized loop of a viscoelastic device, in which the physical significance of the storage stiffness K' and the loss stiffness K'' is presented. These properties are extracted from experimental data and transformed to values of the storage-shear modulus $G' = K' h / A_b$ and the loss shear modulus $G'' = K'' h / A_b$.

Zimmer (1999) conducted an extensive experimental study on viscoelastic material 3M ISD110 and concluded that shear strain in the range of 25 to 100% does not have significant effect on the mechanical properties of the material. Rather, temperature and frequency have important effects on the properties, which were quantified in the range of 10 to 50° C and 0.1 to 3 Hz, respectively. Figure D-4 presents data on the storage- and loss-shear moduli of this material as a function of temperature and frequency. The trends seen in this figure are identical to those identified in Soong and Dargush (1997) but the values of the moduli in Figure D-4 are lower than those reported in Soong and Dargush (1997), which were obtained from tests at low strains, with the majority of the tests conducted at a strain level of 5%.

Various models for the modeling the dynamic behavior of viscoelastic solid devices have been proposed and described in Soong and Dargush (1997) and Constantinou et al. (1998). Of these, the simplest is Kelvin model, which consists of a spring of stiffness K and a dashpot (linear viscous device) of constant C in parallel (see Figure C-11(a)). These parameters are defined as

$$K = \left(\frac{G' A_b}{h} \right) \tag{D-6}$$

$$C = \left(\frac{G'' A_b}{h\omega} \right) \quad (\text{D-7})$$

where ω is the frequency of vibration, which is typically selected to be the fundamental frequency of the structure. The Kelvin model is appropriate for simplified analysis for which the frequency is assumed and subsequently confirmed. This approach was followed for the application of the simplified methods of analysis using the data of Figure D-4 and similar data in non-logarithmic scale in Zimmer (1999).

The simplest models that are capable of capturing the frequency dependence of these devices are either the Standard Linear Solid described in FEMA (1997) or the Three-Parameter Model depicted in Figure D-5, for which the predictions are identical to those of the Standard Linear Solid. The Three-Parameter Model has been utilized herein for performing dynamic response-history analysis. The parameters of this model are obtained from

$$K_1 = \left(\frac{A_b}{h} \right) G_0 \quad (\text{D-8})$$

$$K_2 = \left(\frac{A_b}{h} \right) (G_\infty - G_0) \quad (\text{D-9})$$

$$C_1 = \left(\frac{G_\infty - G_0}{\omega_m} \right) \left(\frac{A_b}{h} \right) \quad (\text{D-10})$$

in which G_0 is the storage-shear modulus at zero frequency, G_∞ is the storage-shear modulus at very large frequencies and ω_m is the frequency at which the loss-shear modulus is maximum. Values of parameters G_0 , G_∞ and ω_m have been presented in Zimmer (1999) as a function of temperature. Table D-1 presents the calibrated values of these parameters used in the analyses of Appendix G. It should be noted that the effect of temperature rise due to viscous heating cannot be captured with this model. Rather, bounding analysis after analytically calculating the temperature rise needs to be performed.

TABLE D-1 Values of Parameters in Three-Parameter Model (Zimmer, 1999)

Temperature (°C)	G_0 (MPa)	G_∞ (MPa)	ω_m (rad/sec)
10	1.66	12.02	16.08
15	0.98	8.83	18.66
20	0.56	5.99	24.94
22	0.50	4.43	26.08
24	0.43	3.98	27.02
26	0.35	3.16	26.70
28	0.28	2.46	26.14
30	0.25	1.94	25.76
35	0.16	1.05	24.00
40	0.14	0.78	28.65
45	0.10	0.43	24.88
50	0.10	0.35	24.13

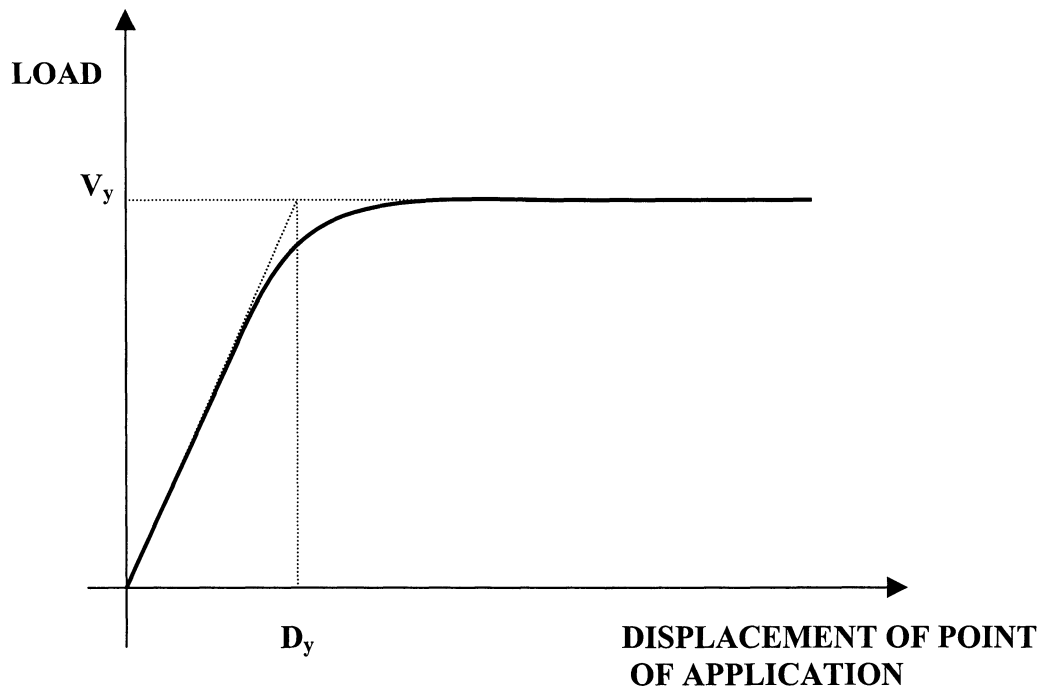
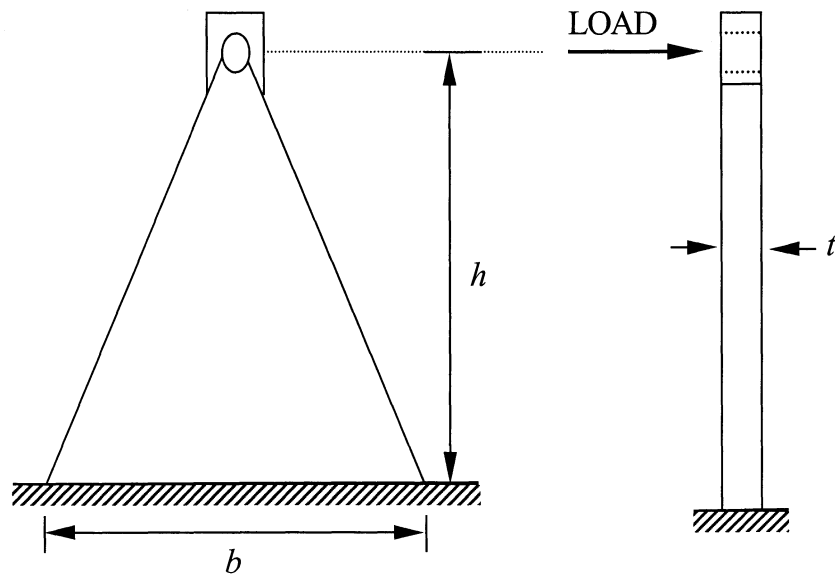


FIGURE D-1 Illustration of Triangular Plate Damping Device And Assumed Behavior

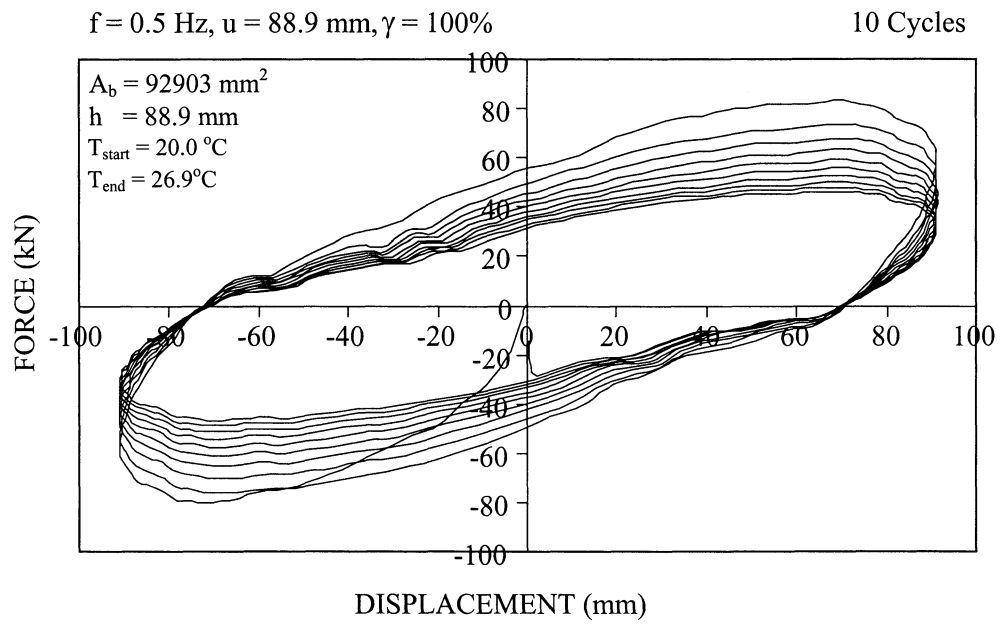


FIGURE D-2 Typical Force-Displacement Loops of Viscoelastic Solid Device (Zimmer, 1999)

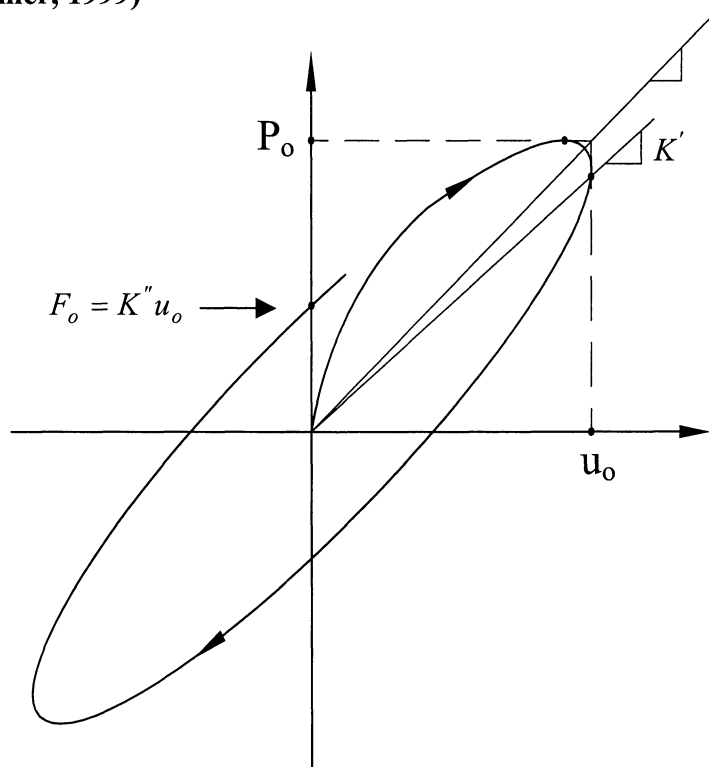
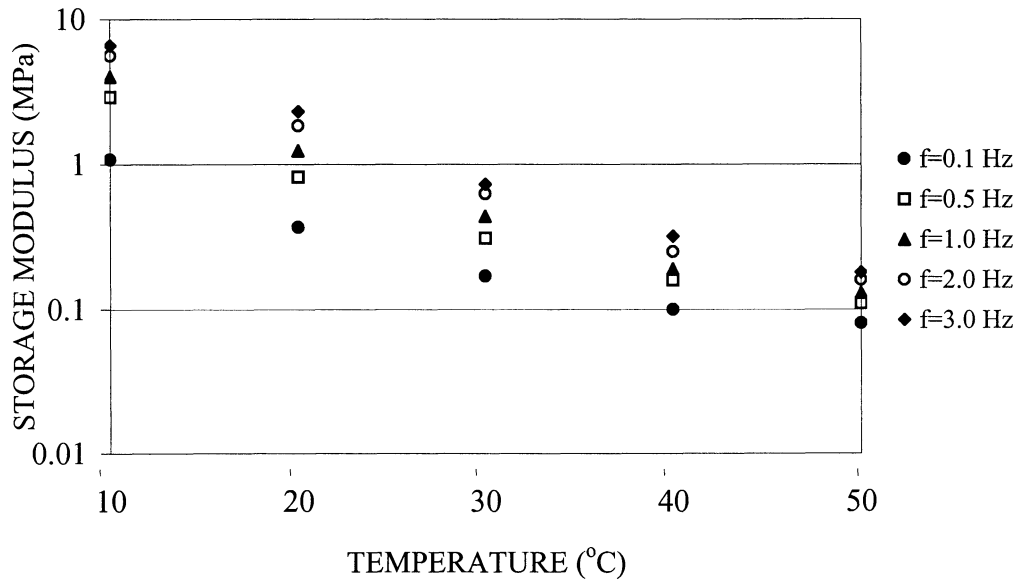


FIGURE D-3 Idealized Force-Displacement Loop of Viscoelastic Material and Illustration of Mechanical Properties

STORAGE MODULUS G'



LOSS MODULUS G''

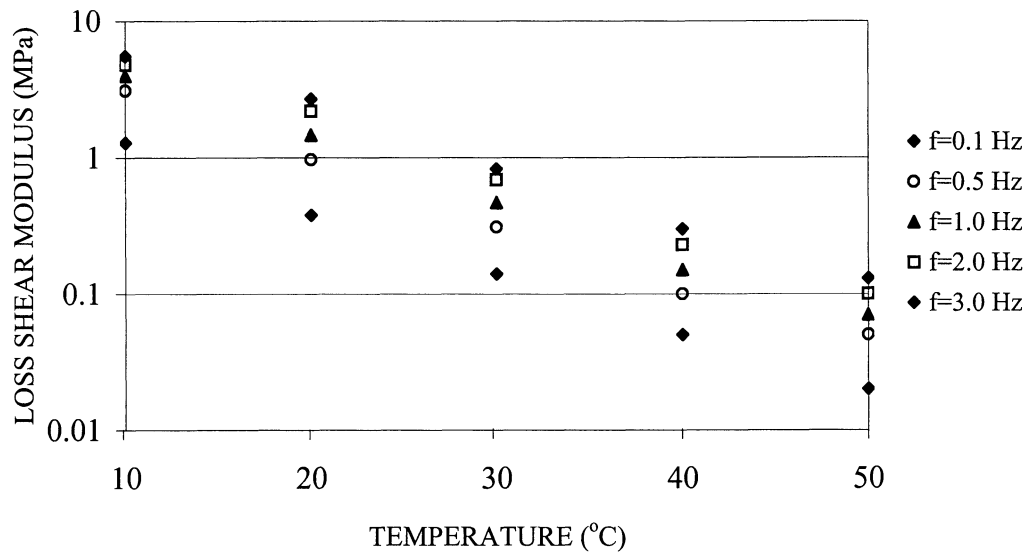


FIGURE D-4 Dependence of Storage and Loss Shear Moduli on Frequency and Temperature

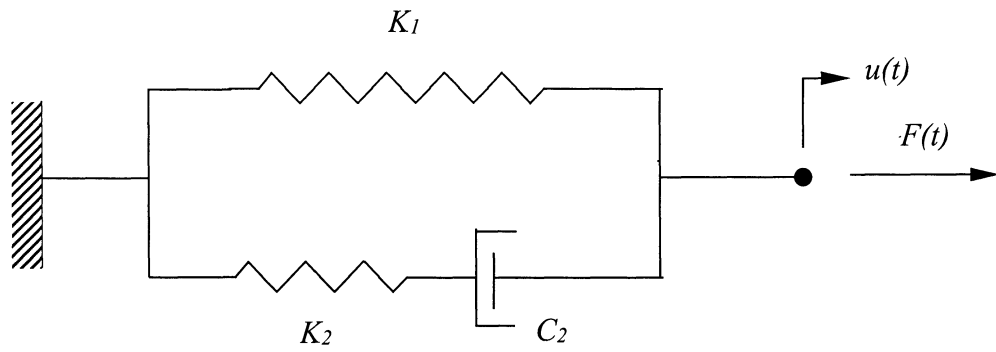


FIGURE D-5 The Three-Parameter Model

APPENDIX E
DETAILED CALCULATIONS FOR THE SIMPLIFIED ANALYSIS OF
3-STORY AND 6-STORY FRAMES WITH LINEAR VISCOUS DAMPING
SYSTEM

E.1 Introduction

This appendix presents detailed calculations in the application of the equivalent lateral force (ELF) and of the response spectrum analysis (RSA) procedures of NEHRP (2000) for the analysis of buildings with linear viscous damping systems. These procedures are applied as described in Appendix A subject to the modifications described in Section 8.1.

The presentation in this appendix consists of:

- (a) Detailed calculations for the 3-story special steel moment frame 3S-75 shown in Figure 8-2 and denoted as example No.2 in Section 8.
- (b) Summary calculations for the 3-story special steel moment frames 3S-60 and 3S-90 shown in Figures 8-1 and 8-3 and denoted as examples No.1 and No.3 in Section 8, respectively.
- (c) Summary calculations for the 6-story special steel moment frame 6S-75 shown in Figure 8-5 and denoted as example No.5 in Section 8.

E.2 Detailed Calculations for 3-Story Frame 3S-75 with Linear Viscous Damping System

Parameters

Tributary Weight

Third Floor (roof): $w_3 = 1567 \text{ kN}$

Second Floor: $w_2 = 2900 \text{ kN}$

First Floor: $w_1 = 2900 \text{ kN}$

Design Coefficients per Table 5.2.2, 1997 NEHRP

For Special Steel Moment Frame

Response Modification Factor: $R = 8.0$

System Overstrength Factor: $\Omega_0 = 3.0$

Deflection Amplification Factor: $C_d = 5.5$

Importance Factor: $I = 1.0$

Description of the System

The analyzed frame is a special steel moment frame with a linear viscous damping system as shown in Figure 8-2. This frame is one of two such frames in each principal direction of a building with the plan and elevation shown in Figure B-1 in Appendix B. In the analysis of the building, torsional effects were disregarded for simplicity. The building is located at a site characterized by a design response spectrum with parameters $S_{D1} = 0.6$, $S_{DS} = 1.0$ and $T_s = 0.6$ sec per NEHRP (1997). This characterization is that of the design-basis earthquake (DBE). The maximum-considered earthquake (MCE) is characterized by a response spectrum with ordinates 1.5 larger than those of the DBE.

The damping system of the frame (as well as of each of the other four identical frames of the building in Figure B-1) consists of linear viscous damping devices installed in the diagonal configuration as shown in Figure 8-2. The damping ratio in the fundamental mode of vibration of the frame under elastic conditions is $\beta_{VI} = 0.10$ (damping provided by damping system) plus an assumed inherent damping ratio $\beta_I = 0.05$ for a total damping ratio $\beta_{VI} + \beta_I = 0.15$. The corresponding damping coefficient $B_{V+I} = 1.35$ (Table A13.3.1 and Table 3-3, column for B_I , conservative values). On the basis of NEHRP (2000) Section A13.2.4.1, the seismic base shear for the design of this frame is $V_{min} = 0.75V$, where V is determined by the procedures of NEHRP (1997), Section 5.3. The seismic base shear V was determined in Section B.3 to be 788.5 kN, so that $V_{min} = 0.75V = 0.75 \times 788.5 = 591.4$ kN.

The approach followed herein to design the frame started with the calculation of the required base shear strength of the frame V_y per (7-72), so that

$$V_y = V_{min} \cdot \frac{\Omega_o \cdot C_d}{R} = 591.4x \frac{3x5.5}{8} = 1220 \text{ kN}$$

The frame was then designed to have a proper collapse mechanism (weak beam/strong columns) and to have a base shear strength equal to approximately 1220 kN when pushed over by lateral loads proportional to the first mode of the frame under elastic conditions. Subsequently, the frame was analyzed by the plastic analysis procedure of Appendix C.2 was calculated to be $V_y = 1220$ kN. The model utilized for the plastic analysis was as shown in Figure C-1 with distance $a_{ij}L_j$ equal to $d_c/2$, where $d_c =$ column depth. That is, hinges were assumed to form at the beam to column interface. Note that the analyses in the examples of Appendix C were based on a different location of the plastic hinge. The selection of the location of the hinges at distance $d_c/2$ was based on the corresponding limitation for the location of the beam plastic hinges in Program IDARC2D-version 5.0. This program was later utilized in the dynamic response history analysis of the frame and it was desirable to have consistency between the simplified model and the model in this computer program.

Eigenvalue analysis of the frame performed in program IDARC 2D-version 5.0 gave: $T_1 = 1.58$ sec, $\{\phi_{i1}\}^T = [1.000 \ 0.657 \ 0.250]$, $T_2 = 0.49$ sec, $\{\phi_{i2}\}^T = [1.000 \ -0.560 \ -0.690]$ and $T_3 = 0.24$ sec, $\{\phi_{i3}\}^T = [1.000 \ -1.618 \ 2.096]$.

Modal Properties of Frame

The modal weights (or effective modal gravity loads), \bar{W}_m , are given by (7-16), while the corresponding modal participation factors, Γ_m , are given by (7-12) or (A13.4.3.3.-2).

First Mode

$$\bar{W}_1 = \frac{(1567 \times 1.000 + 2900 \times 0.657 + 2900 \times 0.250)^2}{(1567 \times 1.000^2 + 2900 \times 0.657^2 + 2900 \times 0.250^2)} = \frac{4197.3^2}{3000.0} = 5872.4 \text{ kN}$$

$$\Gamma_1 = \frac{4197.3}{3000.0} = 1.3991$$

Second Mode

$$\bar{W}_2 = \frac{[1567 \times 1.000 + 2900 \times (-0.560) + 2900 \times (-0.690)]^2}{(1567 \times 1.000^2 + 2900 \times -0.560^2 + 2900 \times -0.690^2)} = \frac{(-2058)^2}{3857.13} = 1098.1 \text{ kN}$$

$$\Gamma_2 = \frac{-2058}{3857.13} = -0.5336$$

Third Mode

$$\bar{W}_3 = \frac{[1567 \times 1.000 + 2900 \times (-1.618) + 2900 \times (2.096)]^2}{[1567 \times 1.000^2 + 2900 \times (-1.618)^2 + 2900 \times 2.096^2]} = \frac{2953.2^2}{21899.31} = 398.3 \text{ kN}$$

$$\Gamma_3 = \frac{2953.2}{21899.31} = 0.1349$$

The effective weights and participation factors were adjusted to add up to the total weight and unity, respectively. The adjusted values are: $\bar{W}_1 = 5871 \text{ kN}$, $\bar{W}_2 = 1098 \text{ kN}$, $\bar{W}_3 = 398 \text{ kN}$ and $\Gamma_1 = 1.3985$, $\Gamma_2 = -0.5334$, $\Gamma_3 = 0.1349$.

Residual Mode

Using (A13.4.3.7-3)

$$\bar{W}_R = 7367 - 5871 = 1496 \text{ kN}$$

Using (A13.4.3.7-2)

$$\Gamma_R = 1 - 1.3985 = -0.3985$$

The residual mode shape was calculated by using (A13.4.3.7-1) as

$$\phi_R = \frac{\begin{Bmatrix} 1.0 \\ 1.0 \\ 1.0 \end{Bmatrix} - 1.3985 \begin{Bmatrix} 1.000 \\ 0.657 \\ 0.250 \end{Bmatrix}}{1 - 1.3985} = \begin{Bmatrix} 1.0000 \\ -0.2037 \\ -1.6321 \end{Bmatrix}$$

Viscous Damping Ratios under Elastic Conditions

Equation (7-29) was used to calculate the damping ratio in each mode using

$C_j = 0.9 \text{ kN} \cdot \text{s} / \text{mm}$ and $f_j = \cos \theta_j$, where $\theta_j = 27.6^\circ$ (see Figure 8-2).

$$\beta_{vm} = \left(\frac{T_m}{4\pi} \right) \frac{\sum_j C_j \cos^2 \theta_j \phi_{rj}^2}{\sum_i \left(\frac{w_i}{g} \right) \phi_{im}^2}$$

First Mode (T₁= 1.58 sec)

Modal Drift

$$\{\phi_r\}_1 = \begin{Bmatrix} 1 - 0.657 \\ 0.657 - 0.25 \\ 0.25 \end{Bmatrix} = \begin{Bmatrix} 0.343 \\ 0.407 \\ 0.250 \end{Bmatrix}, \quad \sum_i w_i \phi_{i1}^2 = 3000.0$$

$$\beta_{V1} = \left(\frac{1.58}{4\pi} \right) \frac{0.9 \times \cos^2 27.6^\circ \times 9810 \times (0.343^2 + 0.407^2 + 0.25^2)}{3000} = 0.10$$

Second Mode (T₂= 0.49 sec)

Modal Drift

$$\{\phi_r\}_2 = \begin{Bmatrix} 1 - (-0.5600) \\ -0.5600 - (-0.6900) \\ -0.6900 \end{Bmatrix} = \begin{Bmatrix} 1.560 \\ 0.130 \\ -0.690 \end{Bmatrix}, \quad \sum_i w_i \phi_{i2}^2 = 3857.1 \text{ kN}$$

$$\beta_{V2} = \left(\frac{0.49}{4\pi} \right) \times 0.90 \times \cos^2 27.6^\circ \times 9810 \times \frac{(1.560^2 + 0.130^2 + 0.690^2)}{3857.10} = 0.205$$

Third Mode (T₃=0.24 sec)

Modal Drift

$$\{\phi_r\}_3 = \begin{Bmatrix} 1 - (-1.6180) \\ -1.6180 - 2.0960 \\ 2.0960 \end{Bmatrix} = \begin{Bmatrix} 2.6180 \\ -3.7140 \\ 2.0960 \end{Bmatrix}, \quad \sum_i w_i \phi_{i3}^2 = 21899.31 \text{ kN}$$

$$\beta_{V3} = \left(\frac{0.24}{4\pi} \right) \times 0.90 \times \cos^2 27.6^\circ \times 9810 \times \frac{(2.618^2 + 3.714^2 + 2.096^2)}{21899.31} = 0.151$$

Residual Mode ($T_R = 0.4T_1 = 0.632$ sec, A13.4.3.7-4)

Modal Drift

$$\{\phi_r\}_R = \begin{Bmatrix} 1 - (-0.2037) \\ -0.2037 - (-1.6321) \\ -1.6321 \end{Bmatrix} = \begin{Bmatrix} 1.2037 \\ 1.4284 \\ -1.6321 \end{Bmatrix}$$

$$w_i \phi_{rj}^2 = 1567 \times 1.000^2 + 2900 \times (-0.2037)^2 + 2900 \times (-1.6321)^2 = 9412.21$$

$$\beta_{VR} = \left(\frac{0.632}{4\pi} \right) \times 0.90 \times \cos^2 27.6^\circ \times 9810 \times \frac{(1.2037^2 + 1.4284^2 + (-1.6321)^2)}{9412.21} = 0.228$$

CALCULATION OF RESPONSE IN DESIGN BASIS EARTHQUAKE**FIRST MODE RESPONSE ($T_1 = 1.58$ sec $> T_s$)****Inelastic Roof Displacement**Assumed Effective Ductility: $\mu_D = 1.29$ Effective Period: $T_{1D} = T_1 \sqrt{\mu_D} = 1.58 \sqrt{1.29} = 1.795$ sec (A13.4.3.5-1)**Effective Damping Ratio**

$$\text{Quality Factor: } q_H = 0.67 \frac{T_s}{T_1} = 0.67 \times \frac{0.60}{1.58} = 0.254 < 0.50 \quad (\text{A13.3.3-1})$$

Use $q_H = 0.5$

$$\text{Hysteretic Damping: } \beta_{HD} = 0.50 \times (0.64 - 0.05) \left(1 - \frac{1}{1.29} \right) = 0.066 \quad (\text{A13.3.2.2-1})$$

$$\text{Effective Damping: } \beta_{1D} = 0.05 + 0.10 \sqrt{1.29} + 0.066 = 0.23 \quad (\text{A13.3.2-1})$$

$$\text{Damping Coefficient: } B_{1D} = 1.59 \quad (\text{Table A13.3.1})$$

Roof Displacement, D_{1D} For $T_{1D} > T_s$

$$D_{1D} = \left(\frac{9810}{4\pi^2} \right) \times |1.3985| \times 0.6 \times \frac{1.795}{1.59} = 235 \text{ mm} \quad (\text{A13.4.4.3-1})$$

Total viscous damping ratio under elastic conditions: $\beta_{V+I} = 0.10 + 0.05 = 0.15$

Damping coefficient: $B = 1.35$ (Table A13.3.1)

The roof displacement for elastic behavior of the frame is:

$$D = \left(\frac{9810}{4\pi^2} \right) \times |1.3985| \times 0.6 \times \frac{1.58}{1.35} = 244 \text{ mm}$$

Since $D_{1D} < D$, use $D_{1D} = 244 \text{ mm}$

Base Shear, V_I

$$\text{Seismic Coefficient:} \quad C_{s1} = \left(\frac{8}{5.5} \right) \times \frac{0.6}{1.795 \times (3 \times 1.59)} = 0.102 \quad (\text{A13.4.3.4-2})$$

$$\text{Base Shear} \quad V_I = 0.102 \times 5871 = 598.84 \text{ kN} \quad (\text{A13.4.3.2-1})$$

The contribution of the first mode to the base shear strength of the frame is given by (7-72)

$$V_y = V_I \frac{\Omega_o C_d}{R} = 598.84 \times \frac{3 \times 5.5}{8} = 1235 \text{ kN}$$

The calculated contribution to the base shear strength of 1235 kN is nearly identical to the actual base shear strength of 1220 kN. Had the two were different, the assumed ductility demand would have been incorrect and the process should be repeated with a new assumed ductility demand.

Displacement at Effective Yield (Yield Displacement), D_y

$$D_y = \left(\frac{g}{4\pi^2} \right) \left(\frac{\Omega_o \cdot C_d}{R} \right) \Gamma_I \cdot C_S \cdot T_I^2 \quad (\text{A13.3.4-3})$$

$$D_y = \left(\frac{9810}{4\pi^2} \right) \left(\frac{3 \times 5.5}{8} \right) \times |1.3985| \times 0.102 \times 1.58^2 = 183 \text{ mm}$$

Effective Ductility Demand μ_D

$$\mu_D = \frac{D_{ID}}{D_y} \quad (\text{A13.3.4-1})$$

$$\mu_D = \frac{244}{183} = 1.33 \approx 1.29 \text{ (assumed)}, \text{ no further iteration is necessary.}$$

$$\mu_{max} = \frac{R}{\Omega_o I} \quad (\text{A13.3.5-2})$$

$$\mu_{max} = \frac{8}{3 \times 1.0} = 2.667 \quad \mu_D < \mu_{max}$$

The difference between the estimated and the assumed ductility demand is due to adjustment of the inelastic displacement to meet the condition that it is not less than the elastic displacement.

Response at Stage of Maximum Displacement

Lateral Floor Displacements, $\delta_{i_{ID}}$, and Story Drifts, $\Delta_{i_{ID}}$

$$\delta_{i_{ID}} = D_{ID} \cdot \phi_{i_1} \quad (\text{A13.4.4.2-1})$$

$$\delta_{i_{ID}} = 244 \times \begin{Bmatrix} 1.0000 \\ 0.6570 \\ 0.2500 \end{Bmatrix} = \begin{Bmatrix} 244.00 \\ 160.31 \\ 61.00 \end{Bmatrix} \text{ mm}$$

$$\Delta_{i_{ID}} = \begin{Bmatrix} 83.69 \\ 99.31 \\ 61.00 \end{Bmatrix} \text{ mm}$$

Design Lateral Forces, F_{i_1} , Design Story Shears, V_{i_1} , and Accelerations, A_{i_1}

$$F_{i_1} = w_i \cdot \phi_{i_1} \cdot \frac{\Gamma_i}{\bar{W}_1} \cdot V_1 \quad (\text{A13.4.3.9-1})$$

$$F_{i1} = \begin{Bmatrix} 1567 \times 1.0 \times \frac{1.3985}{5871} \times 598.84 \\ 2900 \times 0.657 \times \frac{1.3985}{5871} \times 598.84 \\ 2900 \times 0.250 \times \frac{1.3985}{5871} \times 598.84 \end{Bmatrix} = \begin{Bmatrix} 224 \\ 272 \\ 103 \end{Bmatrix} \text{ kN}$$

$$A_{i1} = \left(\frac{F_{i1}}{w_i} \right) \times \left(\frac{C_d \cdot \Omega_o}{R} \right)$$

$$A_{i1} = \begin{Bmatrix} 224/1567 \\ 272/2900 \\ 103/2900 \end{Bmatrix} \times \left(\frac{5.5 \times 3}{8} \right) = \begin{Bmatrix} 0.295 \\ 0.193 \\ 0.073 \end{Bmatrix} \text{ g}$$

$$V_{i1} = \begin{Bmatrix} 224 \\ 496 \\ 599 \end{Bmatrix} \text{ kN}$$

Note that the actual story shear forces (=strength) are equal to $V_{i1} \frac{\Omega_o C_d}{R}$

Response at Stage of Maximum Velocity

Story Velocity, ∇_{i1D}

$$\nabla_{i1D} = \frac{2\pi}{T_{1D}} \cdot \Delta_{i1D}, \quad \nabla_{i1D} = \frac{2\pi}{1.795} \cdot \begin{Bmatrix} 84 \\ 99 \\ 61 \end{Bmatrix} = \begin{Bmatrix} 294 \\ 347 \\ 214 \end{Bmatrix} \text{ mm / sec} \quad (\text{A13.4.4.5-2})$$

Force in Damping Devices, Fd_{i1D}

$$Fd_{i1D} = C_i \cdot \nabla_{i1D} \cdot \cos \theta_i, \quad Fd_{i1D} = 0.90 \times \begin{Bmatrix} 294 \\ 347 \\ 214 \end{Bmatrix} \times \cos 27.6 = \begin{Bmatrix} 235 \\ 277 \\ 171 \end{Bmatrix} \text{ kN} \quad (7-23)$$

Horizontal Component of Damping Forces, Vd_{iD}

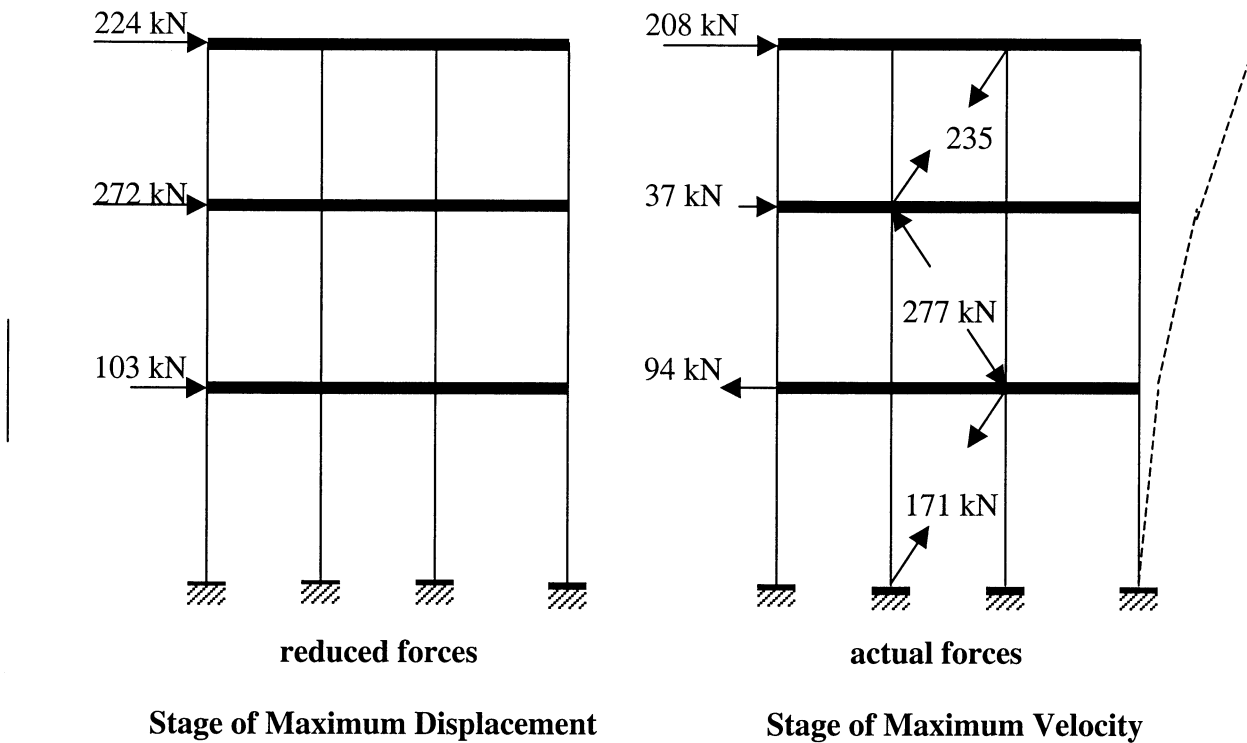
$$Vd_{iD} = Fd_{iD} \times \cos 27.6 = \begin{Bmatrix} 235 \\ 277 \\ 171 \end{Bmatrix} \times \cos 27.6 = \begin{Bmatrix} 208 \\ 245 \\ 151 \end{Bmatrix} \text{ kN}$$

Horizontal Inertia Forces, F_{iDI}

$$F_{iDI} = \begin{Bmatrix} 208 \\ 245 - 208 \\ 151 - 245 \end{Bmatrix} = \begin{Bmatrix} 208 \\ 37 \\ -94 \end{Bmatrix} \text{ kN}$$

Seismic Design Forces

Illustrated below are the seismic design forces



Response at Stage of Maximum Acceleration

Force Coefficients

$$\text{Effective viscous damping: } \beta_{eff} = \beta_i + \beta_{v_i} \sqrt{\mu_D} = 0.05 + 0.10 \sqrt{1.33} = 0.165$$

$$CF_1 = \cos \left[\tan^{-1} (2\beta_{eff}) \right] \quad (4-41)$$

$$CF_1 = \cos \left[\tan^{-1} (2 \times 0.165) \right] = 0.950$$

$$CF_1 \mu = 0.95 \times 1.33 = 1.264 > 1.0 \quad \therefore \text{use } CF_1 = 1.0$$

$$CF_2 = \sin \left[\tan^{-1} (2\beta_{eff}) \right] \quad (4-39)$$

$$CF_2 = \sin \left[\tan^{-1} (2 \times 0.165) \right] = 0.313$$

Note that coefficients CF_1 and CF_2 are identical to coefficients C_{IFD} and C_{IFV} in Tables A13.7.3.2.1 and A13.7.3.2.2 of NEHRP (2000). Using effective damping of 0.165 in these tables, $C_{IFD} = 1.0$ and $C_{IFV} = 0.311$, that is, almost exactly the values derived by use of (4-39) and (4-41).

Maximum Lateral Inertia Forces

Maximum actual lateral inertia forces per floor are calculated according to

$$F_{i_j, max} = CF_1 \cdot |F_{i_j}|_{Max Disp} \cdot \frac{C_d \Omega_o}{R} + CF_2 \cdot |F_{i_{D1}}|_{Max Velocity}$$

$$F_{i_j, max} = 1.0 \times \begin{Bmatrix} |224| \\ |272| \\ |103| \end{Bmatrix} \times \left(\frac{3 \times 5.5}{8} \right) + 0.313 \times \begin{Bmatrix} |208| \\ |37| \\ |-94| \end{Bmatrix} = \begin{Bmatrix} 527 \\ 573 \\ 242 \end{Bmatrix} \text{ kN}$$

Maximum Acceleration

The maximum floor accelerations are calculated by

$$A_{i_j, max} = \frac{F_{i_j, max}}{w_i}$$

$$A_{i_j, max} = \begin{Bmatrix} 527/1567 \\ 573/2900 \\ 242/2900 \end{Bmatrix} = \begin{Bmatrix} 0.336 \\ 0.198 \\ 0.083 \end{Bmatrix}$$

Maximum Story Shear, $V_{i1,max}$

$$V_{i1,max} = CF_1 \cdot |V_{i1}|_{Max\ Disp} \cdot \frac{C_d \Omega_o}{R} + CF_2 \cdot |Vd_{i1D}|_{Max\ Velocity}$$

$$V_{i1,max} = 1.000 \times \begin{Bmatrix} 224 \\ 496 \\ 599 \end{Bmatrix} \times \left(\frac{3 \times 5.5}{8} \right) + 0.313 \times \begin{Bmatrix} 208 \\ 245 \\ 151 \end{Bmatrix} = \begin{Bmatrix} 527 \\ 1100 \\ 1283 \end{Bmatrix} \text{ kN}$$

SECOND MODE RESPONSE ($T_2=0.49$ sec < T_s)

Effective Damping Ratio: $\beta_{2D} = 0.205 + 0.05 = 0.255 \quad \therefore B_{2D} = 1.665$ (Table A13.3.1)

Roof Displacement, D_{2D}

$$D_{2D} = \left(\frac{g}{4\pi^2} \right) \times \Gamma_2 \times \frac{S_{DS} T_2^2}{B_{2D}} \quad (\text{A13.5.4.3-2})$$

$$D_{2D} = \left(\frac{9810}{4\pi^2} \right) \times |-0.5334| \times \frac{1.0 \times 0.49^2}{1.665} = 19.11 \text{ mm}$$

Seismic Base Shear, V_2

$$V_2 = C_{S2} \cdot \bar{W}_2 \quad (\text{A13.5.3.2-1})$$

$$C_{S2} = \left(\frac{R}{C_d} \right) \frac{S_{DS}}{\Omega_o B_{2D}} \quad (\text{A13.5.3.6-1})$$

$$C_{S2} = \left(\frac{8}{5.5} \right) \frac{1.0}{3 \times 1.665} = 0.291$$

$$V_2 = 0.291 \times 1098 = 319.5 \text{ kN}$$

Response at Stage of Maximum Displacement

Lateral Floor Displacement, δ_{i2D} , and Story Drifts, A_{i2D}

$$\delta_{i2D} = D_{2D} \cdot \phi_{i2} \quad (\text{A13.5.4.2-1})$$

$$\delta_{i2D} = 19.11 \times \begin{Bmatrix} 1.000 \\ -0.560 \\ -0.690 \end{Bmatrix} = \begin{Bmatrix} 19.11 \\ -10.70 \\ -13.19 \end{Bmatrix} \text{ mm}$$

$$A_{i2D} = \begin{Bmatrix} 29.81 \\ 2.49 \\ -13.19 \end{Bmatrix} \text{ mm}$$

Design Lateral Forces, F_{i2} , Design Story Shears, V_{i2} , and Accelerations, A_{i2}

$$F_{i2} = w_i \cdot \phi_{i2} \cdot \frac{\Gamma_2}{W_2} \cdot V_2 \quad (\text{A13.5.3.7-1})$$

$$F_{i2} = \begin{Bmatrix} 1567 \times 1.000 \times \frac{|-0.5334|}{1098} \times 319.5 \\ 2900 \times (-0.560) \times \frac{|-0.5334|}{1098} \times 319.5 \\ 2900 \times (-0.690) \times \frac{|-0.5334|}{1098} \times 319.5 \end{Bmatrix} = \begin{Bmatrix} 243 \\ -252 \\ -311 \end{Bmatrix} \text{ kN}$$

$$A_{i2} = \left(\frac{F_{i2}}{W_i} \right) \times \left(\frac{C_d \cdot \Omega_o}{R} \right)$$

$$A_{i2} = \begin{Bmatrix} 243/1567 \\ -252/2900 \\ -311/2900 \end{Bmatrix} \times \left(\frac{5.5 \times 3}{8} \right) = \begin{Bmatrix} 0.320 \\ -0.179 \\ -0.221 \end{Bmatrix} g$$

$$V_{i2} = \begin{Bmatrix} 243 \\ -9 \\ -320 \end{Bmatrix} \text{ kN}$$

Response at Stage of Maximum Velocity

Story Velocity, $\nabla_{i_{2D}}$

$$\nabla_{i_{2D}} = \frac{2\pi}{T_{2D}} \cdot \Delta_{i_{2D}}, \quad \nabla_{i_{2D}} = \frac{2\pi}{0.49} \times \begin{Bmatrix} 29.81 \\ 2.49 \\ -13.19 \end{Bmatrix} = \begin{Bmatrix} 382.2 \\ 31.9 \\ -169.1 \end{Bmatrix} \text{ mm/sec} \quad (\text{A13.5.4.5-2})$$

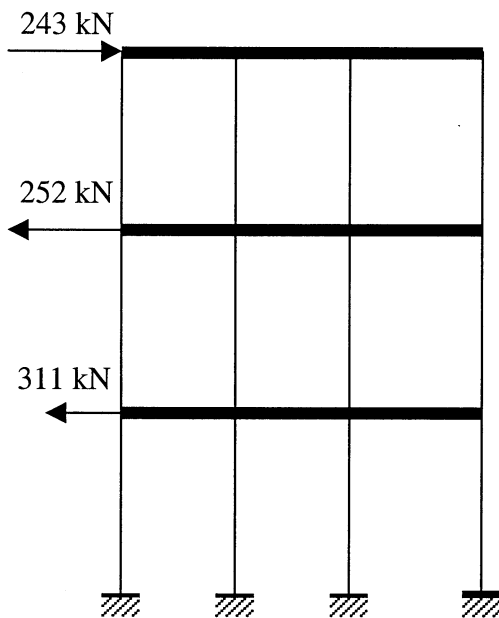
Forces in Damping Devices, $F_{d_{i_{2D}}}$

$$F_{d_{i_{2D}}} = C_i \cdot \nabla_{i_2} \cdot \cos \theta_i, \quad F_{d_{i_{2D}}} = 0.90 \times \begin{Bmatrix} 382.2 \\ 31.9 \\ -169.1 \end{Bmatrix} \times \cos 27.6^\circ = \begin{Bmatrix} 305 \\ 25 \\ -135 \end{Bmatrix} \text{ kN} \quad (7-23)$$

Horizontal component of Damping Forces, $V_{d_{i_{2D}}}$, and Horiz. Inertia Forces, $F_{i_{D2}}$

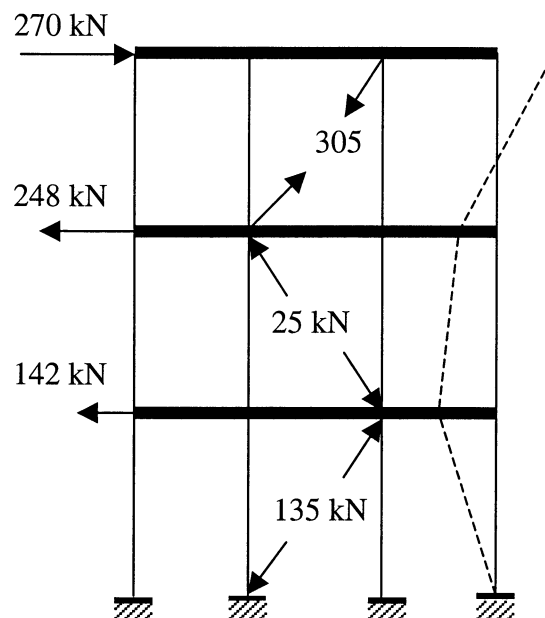
$$V_{d_{i_{2D}}} = \begin{Bmatrix} 305 \\ 25 \\ -135 \end{Bmatrix} \times \cos 27.6 = \begin{Bmatrix} 270 \\ 22 \\ -120 \end{Bmatrix} \text{ kN}, \quad F_{i_{D2}} = \begin{Bmatrix} 270 \\ 22 - 270 \\ -120 - 22 \end{Bmatrix} = \begin{Bmatrix} 270 \\ -248 \\ -142 \end{Bmatrix} \text{ kN}$$

Seismic Design Forces



reduced forces

Stage of Maximum Displacement



actual forces

Stage of Maximum Velocity

Response at Stage of Maximum Acceleration

Force Coefficients

$$\beta_{eff_2} = 0.205 \times \sqrt{1.0} + 0.05 = 0.255$$

$$CF_1 = \cos \left[\tan^{-1} \left(2\beta_{eff_2} \right) \right], \quad CF_1 = \cos \left[\tan^{-1} (2 \times 0.255) \right] = 0.891 \quad (4-41)$$

$$CF_2 = \sin \left[\tan^{-1} \left(2\beta_{eff_2} \right) \right], \quad CF_2 = \sin \left[\tan^{-1} (2 \times 0.255) \right] = 0.454 \quad (4-39)$$

Maximum Lateral Inertia Forces

$$F_{i_2,max} = CF_1 \cdot |F_{i_2}|_{Max\ Disp} \cdot \frac{C_d \Omega_o}{R} + CF_2 \cdot |F_{i_{2D}}|_{Max\ Velocity}$$

$$F_{i_2,max} = 0.891 \times \begin{Bmatrix} |243| \\ |-252| \\ |-311| \end{Bmatrix} \times \left(\frac{3 \times 5.5}{8} \right) + 0.454 \times \begin{Bmatrix} |270| \\ |-248| \\ |-142| \end{Bmatrix} = \begin{Bmatrix} 571.6 \\ 577.2 \\ 637.9 \end{Bmatrix} \text{ kN}$$

Maximum Acceleration

$$A_{i_2,max} = \frac{F_{i_2,max}}{w_i}, \quad A_{i_2} = \begin{Bmatrix} 571.6/1567 \\ -577.2/2900 \\ -637.9/2900 \end{Bmatrix} = \begin{Bmatrix} 0.364 \\ 0.199 \\ 0.220 \end{Bmatrix}$$

Maximum Story Shear, $V_{i_2,max}$

$$V_{i_2,max} = CF_1 \cdot |V_{i_2}|_{Max\ Disp} \cdot \frac{C_d \Omega_o}{R} + CF_2 \cdot |Vd_{i_2D}|_{Max\ Velocity}$$

$$V_{i_2,max} = 0.891 \times \begin{Bmatrix} |243| \\ |-9| \\ |-320| \end{Bmatrix} \times \left(\frac{3 \times 5.5}{8} \right) + 0.454 \times \begin{Bmatrix} |270| \\ |22| \\ |-120| \end{Bmatrix} = \begin{Bmatrix} 569 \\ 27 \\ 643 \end{Bmatrix} \text{ kN}$$

THIRD MODE RESPONSE ($T_3=0.24 \text{ sec} < T_s$)

$$\text{Effective Damping Ratio: } \beta_{3D} = 0.151 + 0.05 = 0.201 \quad \therefore B_{3D} = 1.503 \quad (\text{Table A13.3.1})$$

Roof Displacement, D_{3D}

$$D_{3D} = \left(\frac{g}{4\pi^2} \right) \times \Gamma_3 \times \frac{S_{DS} T_3^2}{B_{3D}} \quad (\text{A13.5.4.3-2})$$

$$D_{3D} = \left(\frac{9810}{4\pi^2} \right) \times |0.1349| \times \frac{1.0 \times 0.24^2}{1.503} = 1.28 \text{ mm}$$

Seismic Base Shear, V_3

$$V_3 = C_{S3} \cdot \bar{W}_3 \quad (\text{A13.5.3.2-1})$$

$$C_{S3} = \left(\frac{R}{C_d} \right) \frac{S_{DS}}{\Omega_o B_{3D}} \quad (\text{A13.5.3.6-1})$$

$$C_{S3} = \left(\frac{8}{5.5} \right) \frac{1.0}{3 \times 1.503} = 0.323$$

$$V_3 = 0.323 \times 398 = 128.6 \text{ kN}$$

Response at Stage of Maximum Displacement

Lateral Floor Displacement, $\delta_{i_{3D}}$, and Story Drifts, $\Delta_{i_{3D}}$

$$\delta_{i_{3D}} = D_{3D} \cdot \phi_{i_3} \quad (\text{A13.5.4.2-1})$$

$$\delta_{i_{3D}} = 1.28 \times \begin{Bmatrix} 1.000 \\ -1.618 \\ 2.096 \end{Bmatrix} = \begin{Bmatrix} 1.28 \\ -2.07 \\ 2.68 \end{Bmatrix} \text{ mm}$$

$$\Delta_{i_{3D}} = \begin{Bmatrix} 3.35 \\ -4.75 \\ 2.68 \end{Bmatrix} \text{ mm}$$

Design Lateral Forces, F_{i_3} , Design Story Shears, V_{i_3} , and Floor Accelerations, A_{i_3}

$$F_{i_3} = w_i \cdot \phi_{i_3} \cdot \frac{\Gamma_3}{\bar{W}_3} \cdot V_3 \quad (\text{A13.5.3.7-1})$$

$$F_{i3} = \begin{Bmatrix} 1567 \times 1.000 \times \frac{|0.1348|}{398} \times 128.6 \\ 2900 \times (-1.618) \times \frac{|0.1348|}{398} \times 128.6 \\ 2900 \times 2.096 \times \frac{|0.1348|}{398} \times 128.6 \end{Bmatrix} = \begin{Bmatrix} 68 \\ -204 \\ 265 \end{Bmatrix} \text{ kN}$$

$$A_{i3} = \left(\frac{F_{i3}}{W_i} \right) \times \left(\frac{C_d \cdot \Omega_o}{R} \right)$$

$$A_{i3} = \begin{Bmatrix} 68/1567 \\ -204/2900 \\ 265/2900 \end{Bmatrix} \times \left(\frac{5.5 \times 3}{8} \right) = \begin{Bmatrix} 0.090 \\ -0.146 \\ 0.188 \end{Bmatrix} \text{ g}$$

$$V_{i3} = \begin{Bmatrix} 68 \\ -136 \\ 129 \end{Bmatrix} \text{ kN}$$

Response at Stage of Maximum Velocity

Story Velocity, ∇_{i3D}

$$\nabla_{i3D} = \frac{2\pi}{T_3} \cdot \Delta_{i3}, \quad \nabla_{i3D} = \frac{2\pi}{0.24} \times \begin{Bmatrix} 3.35 \\ -4.75 \\ 2.68 \end{Bmatrix} = \begin{Bmatrix} 87.7 \\ -124.4 \\ 70.2 \end{Bmatrix} \text{ mm/sec} \quad (\text{A13.5.4.5-2})$$

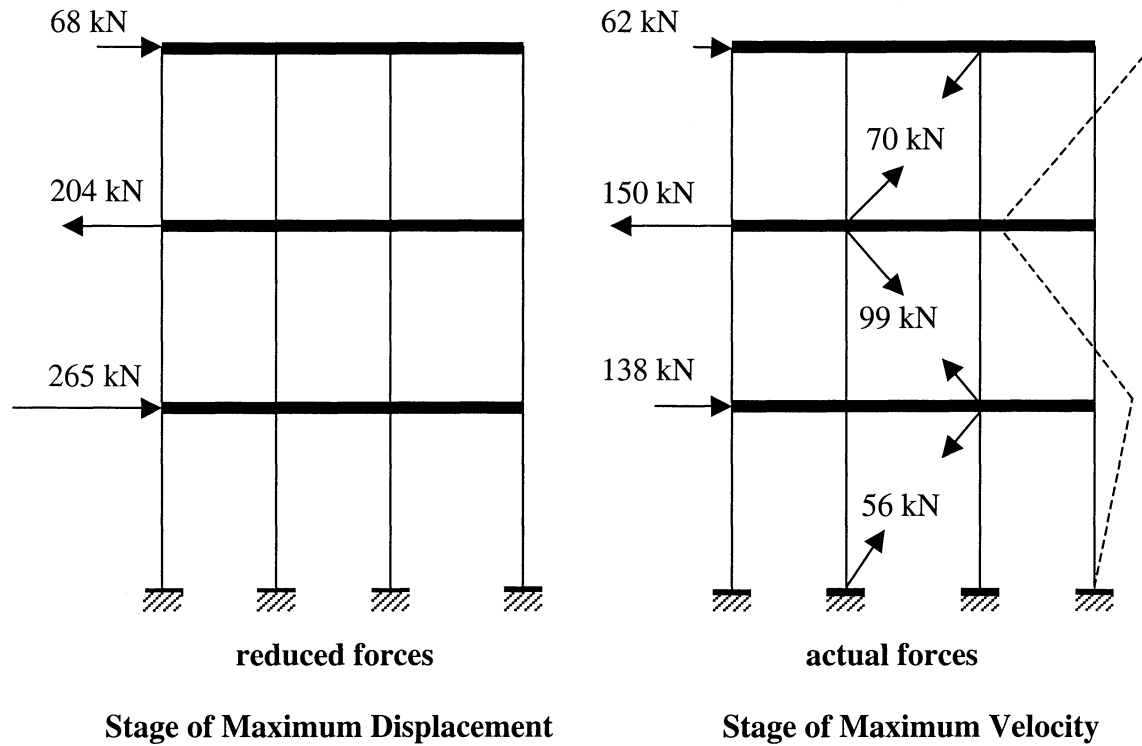
Forces in Damping Devices, Fd_{i3D}

$$Fd_{i3D} = C_i \cdot \nabla_{i3D} \cdot \cos \theta_i, \quad Fd_{i3D} = 0.90 \times \begin{Bmatrix} 87.7 \\ -124.4 \\ 70.2 \end{Bmatrix} \times \cos 27.6^\circ = \begin{Bmatrix} 70 \\ -99 \\ 56 \end{Bmatrix} \text{ kN} \quad (7-23)$$

Horizontal component of Damping Forces, Vd_{i3D} , and Horiz. Inertia Forces, F_{iD3}

$$Vd_{i3D} = \begin{Bmatrix} 70 \\ -99 \\ 56 \end{Bmatrix} \times \cos 27.6 = \begin{Bmatrix} 62 \\ -88 \\ 50 \end{Bmatrix} \text{ kN}, \quad F_{iD3} = \begin{Bmatrix} 62 \\ -88 - 62 \\ 50 - (-88) \end{Bmatrix} = \begin{Bmatrix} 62 \\ -150 \\ 138 \end{Bmatrix} \text{ kN}$$

Seismic Design Forces



Response at Stage of Maximum Acceleration

Force Coefficients

$$\beta_{eff_3} = 0.151 \times \sqrt{1.0} + 0.05 = 0.201$$

$$CF_1 = \cos \left[\tan^{-1} \left(2\beta_{eff_3} \right) \right], \quad CF_1 = \cos \left[\tan^{-1} (2 \times 0.201) \right] = 0.928 \quad (4-41)$$

$$CF_2 = \sin \left[\tan^{-1} \left(2\beta_{eff_3} \right) \right], \quad CF_2 = \sin \left[\tan^{-1} (2 \times 0.201) \right] = 0.373 \quad (4-39)$$

Maximum Lateral Inertia Forces

$$F_{i_3, max} = CF_1 \cdot |F_{i_3}|_{Max Disp} \cdot \frac{C_d \Omega_o}{R} + CF_2 \cdot |F_{i_{D3}}|_{Max Velocity}$$

$$F_{i_3, max} = 0.928 \times \begin{Bmatrix} |68| \\ |-204| \\ |265| \end{Bmatrix} \times \left(\frac{3 \times 5.5}{8} \right) + 0.373 \times \begin{Bmatrix} |62| \\ |-150| \\ |138| \end{Bmatrix} = \begin{Bmatrix} 153.3 \\ 446.4 \\ 558.7 \end{Bmatrix} \text{ kN}$$

Maximum Acceleration

$$A_{i_3,max} = \frac{F_{i_3,max}}{w_i}, \quad A_{i_3} = \left\{ \begin{array}{l} 153.3/1567 \\ 446.4/2900 \\ 558.7/2900 \end{array} \right\} = \left\{ \begin{array}{l} 0.098 \\ 0.154 \\ 0.193 \end{array} \right\}$$

Maximum Story Shear, $V_{i_3,max}$

$$V_{i_3,max} = CF_1 \cdot |V_{i_3}|_{Max\ Disp} \cdot \frac{C_d \cdot \Omega_o}{R} + CF_2 \cdot |V_{di_3D}|_{Max\ Velocity}$$

$$V_{i_3,max} = 0.928 \times \left\{ \begin{array}{l} |68| \\ |-136| \\ |129| \end{array} \right\} \times \left(\frac{3 \times 5.5}{8} \right) + 0.373 \times \left\{ \begin{array}{l} |62| \\ |-88| \\ |50| \end{array} \right\} = \left\{ \begin{array}{l} 153 \\ 293 \\ 266 \end{array} \right\} \text{ kN}$$

RESIDUAL MODE RESPONSE ($T_R=0.632 \text{ sec} > T_s$)

Effective Damping Ratio: $\beta_{RD} = 0.228 + 0.05 = 0.278 \quad \therefore B_{RD} = 1.734$ (Table A13.3.1)

Roof Displacement, D_{RD}

$$D_{RD} = \left(\frac{g}{4\pi^2} \right) \times \Gamma_R \times \frac{S_{DI} T_R}{B_{RD}} \quad (\text{A13.4.4.3-2})$$

For $T_R > T_o$

$$D_{RD} = \left(\frac{9810}{4\pi^2} \right) \times |-0.3985| \times \frac{0.6 \times 0.632}{1.734} = 21.66 \text{ mm}$$

Seismic Base Shear, V_R

$$V_R = C_{SR} \cdot \bar{W}_R \quad (\text{A13.4.3.6-1})$$

$$C_{SR} = \left(\frac{R}{C_d} \right) \frac{S_{Ds}}{\Omega_o B_{RD}}, \quad C_{SR} = \left(\frac{8}{5.5} \right) \frac{1.0}{3 \times 1.734} = 0.28 \quad (\text{A13.4.3.8-1})$$

$$V_R = 0.28 \times 1496 = 418.9 \text{ kN}$$

Response at Stage of Maximum Displacement

Lateral Floor Displacement, δ_{i_R} , and Story Drifts, Δ_{i_R}

$$\delta_{i_R} = D_{RD} \cdot \phi_{i_R} \quad (\text{A13.4.4.2-2})$$

$$\delta_{i_R} = 21.66 \times \begin{Bmatrix} 1.000 \\ -0.2037 \\ -1.6321 \end{Bmatrix} = \begin{Bmatrix} 21.66 \\ -4.41 \\ -35.35 \end{Bmatrix} \text{ mm}$$

$$\Delta_{i_R} = \begin{Bmatrix} 26.07 \\ 30.94 \\ -35.35 \end{Bmatrix} \text{ mm}$$

Design Lateral Forces, F_{i_R} , Design Story Shears, V_{i_R} , and Floor Accelerations, A_{i_R}

$$F_{i_R} = w_i \cdot \phi_{i_R} \cdot \frac{\Gamma_R}{\bar{W}_R} \cdot V_R \quad (\text{A13.4.3.9-2})$$

$$F_{i_R} = \begin{Bmatrix} 1567 \times 1.000 \times \frac{|-0.3985|}{1496} \times 418.9 \\ 2900 \times (-0.2037) \times \frac{|-0.3985|}{1496} \times 418.9 \\ 2900 \times (-1.6321) \times \frac{|-0.3985|}{1496} \times 418.9 \end{Bmatrix} = \begin{Bmatrix} 175 \\ -66 \\ -528 \end{Bmatrix} \text{ kN}$$

$$A_{i_R} = \left(\frac{F_{i_R}}{w_i} \right) \times \left(\frac{C_d \cdot \Omega_o}{R} \right)$$

$$A_{i_R} = \begin{Bmatrix} 175/1567 \\ -66/2900 \\ -528/2900 \end{Bmatrix} \times \left(\frac{5.5 \times 3}{8} \right) = \begin{Bmatrix} 0.230 \\ -0.047 \\ -0.376 \end{Bmatrix} \text{ g}$$

$$V_{i_R} = \begin{Bmatrix} 175 \\ 109 \\ -419 \end{Bmatrix} \text{ kN}$$

Response at Stage of Maximum Velocity

Story Velocity, ∇_{iRD}

$$\nabla_{iRD} = \frac{2\pi}{T_R} \cdot \Delta_{iRD}, \quad \nabla_{iRD} = \frac{2\pi}{0.632} \times \begin{Bmatrix} 26.07 \\ 30.94 \\ -35.35 \end{Bmatrix} = \begin{Bmatrix} 259.2 \\ 307.6 \\ -351.4 \end{Bmatrix} \text{ mm/sec} \quad (\text{A13.4.4.5-3})$$

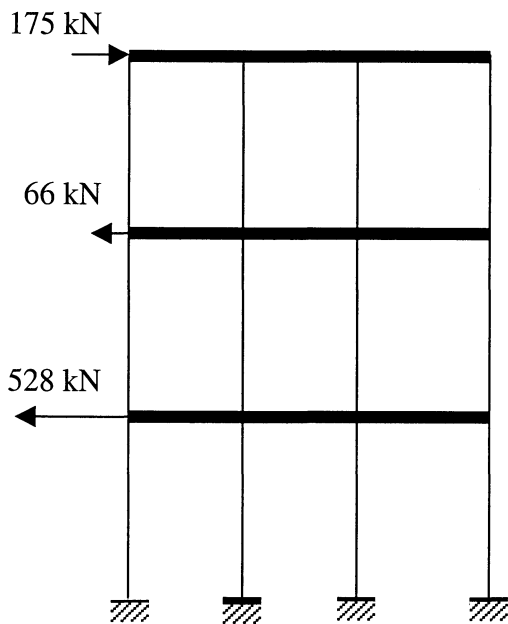
Forces in Damping Devices, Fd_{iRD}

$$Fd_{iRD} = C_i \cdot \nabla_{iRD} \cdot \cos \theta_i, \quad Fd_{iRD} = 0.90 \cdot \begin{Bmatrix} 259.2 \\ 307.6 \\ -351.4 \end{Bmatrix} \times \cos 27.6^\circ = \begin{Bmatrix} 207 \\ 245 \\ -280 \end{Bmatrix} \text{ kN} \quad (7-23)$$

Horizontal component of Damping Forces, Vd_{iRD} , and Horiz. Inertia Forces, F_{iDR}

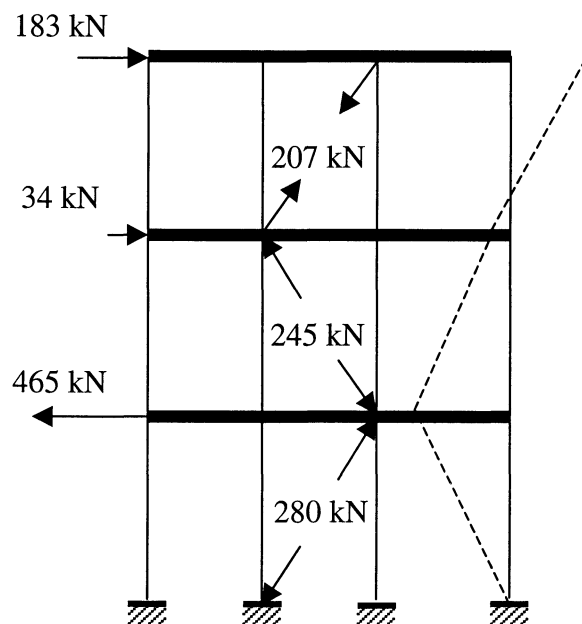
$$Vd_{iRD} = \begin{Bmatrix} 207 \\ 245 \\ -280 \end{Bmatrix} \times \cos 27.6^\circ = \begin{Bmatrix} 183 \\ 217 \\ -248 \end{Bmatrix} \text{ kN}, \quad F_{iDR} = \begin{Bmatrix} 183 \\ 217 - 183 \\ -248 - 217 \end{Bmatrix} = \begin{Bmatrix} 183 \\ 34 \\ -465 \end{Bmatrix} \text{ kN}$$

Seismic Design Forces



reduced forces

Stage of Maximum Displacement



actual forces

Stage of Maximum Velocity

Response at Stage of Maximum Acceleration

Force Coefficients

$$\beta_{eff_R} = 0.228 \times \sqrt{1.0} + 0.05 = 0.278$$

$$CF_1 = \cos \left[\tan^{-1} (2\beta_{eff_R}) \right], \quad CF_1 = \cos \left[\tan^{-1} (2 \times 0.278) \right] = 0.874 \quad (4-41)$$

$$CF_2 = \sin \left[\tan^{-1} (2 \times 0.278) \right] = 0.486$$

Maximum Lateral Inertia Forces

$$F_{i_R,max} = CF_1 \cdot \left| F_{i_R} \right|_{Max Disp} \cdot \frac{C_d \Omega_o}{R} + CF_2 \cdot \left| F_{i_{DR}} \right|_{Max Velocity}$$

$$F_{i_R,max} = 0.874 \times \begin{Bmatrix} |175| \\ |-66| \\ |-528| \end{Bmatrix} \times \left(\frac{3 \times 5.5}{8} \right) + 0.486 \times \begin{Bmatrix} |183| \\ |34| \\ |-465| \end{Bmatrix} = \begin{Bmatrix} 404.4 \\ 135.5 \\ 1177.8 \end{Bmatrix} \text{ kN}$$

Maximum Acceleration

$$A_{i_R,max} = \frac{F_{i_R,max}}{w_i}, \quad A_{i_R,max} = \begin{Bmatrix} 404.4/1567 \\ 135.5/2900 \\ 1177.8/2900 \end{Bmatrix} = \begin{Bmatrix} 0.258 \\ 0.047 \\ 0.406 \end{Bmatrix}$$

Maximum Story Shear, $V_{i_R,max}$

$$V_{i_R,max} = CF_1 \cdot \left| V_{i_R} \right|_{Max Disp} \cdot \frac{C_d \Omega_o}{R} + CF_2 \cdot \left| V_{i_{RD}} \right|_{Max Velocity}$$

$$V_{i_R,max} = 0.874 \times \begin{Bmatrix} |175| \\ |109| \\ |-419| \end{Bmatrix} \times \left(\frac{3 \times 5.5}{8} \right) + 0.486 \times \begin{Bmatrix} |183| \\ |217| \\ |-248| \end{Bmatrix} = \begin{Bmatrix} 404 \\ 302 \\ 876 \end{Bmatrix} \text{ kN}$$

Total responses resulting from modal combinations were calculated by use of the SRSS combination rule. Table E-1 presents a summary of the modal properties of the frame and Tables E-2 and E-3 present summaries of the results of the analysis for each mode and the total response calculated by both the ELF and the RSA procedures for the DBE and MCE, respectively.

E.3 Summary Calculations for 3-Story Frames 3S-60 and 3S-90 with Linear Viscous Damping Systems

Frame 3S-60 is shown in Figure 8-1 and is described as example No.1 in Section 8. This special moment frame does not meet the minimum seismic base shear requirement of NEHRP(2000) since it has been designed for $V_{min} = 0.6V = 0.6 \times 788.5 = 473 \text{ kN}$, or equivalently, it has been designed to have a base shear strength equal to $V_y = V_{min} \cdot \Omega_o \cdot C_d / R = 473 \times 3.0 \times 5.5 / 8 = 976 \text{ kN}$ for a pattern of lateral loads proportional to the first mode. Its actual base shear strength for this pattern of loads was calculated by the procedures of Appendix C.2 (beam hinges at the beam to column interface) to be $V_y = 971 \text{ kN}$. Summary calculations for this frame are presented in Tables E-4, E-5 and E-6.

Frame 3S-90 is shown in Figure 8-3 and is described as example No.3 in Section 8. The frame has been designed for seismic base shear equal to $V_{min} = 0.90V = 0.9 \times 788.5 = 709.7 \text{ kN}$, or equivalently it has been designed to have a base shear strength $V_y = V_{min} \cdot \Omega_o \cdot C_d / R = 709.7 \times 3.0 \times 5.5 / 8 = 1464 \text{ kN}$ for a pattern of lateral loads proportional to the first mode. The base shear strength of the frame for this pattern of loads was calculated by the procedures of Appendix C.2 to be $V_y = 1468 \text{ kN}$. Summary calculations for this frame are presented in Tables E-7, E-8, and E-9.

E.4 Summary Calculations for 6-Story Frame 6S-75 with Linear Viscous Damping System

Frame 6S-75 is the 6-story frame shown in Figure 8-5 and described as Example No.5 in Section 8. It has been designed for seismic base shear equal to $V_{min} = 0.75V$, where V was calculated in accordance with Section 5.3 of NEHRP (1997). That is, period $T = 1.2 \times 0.035 \times (85.1)^{0.75} = 1.18 \text{ sec}$, $C_s = \frac{S_{D1}}{T(R/I)} = \frac{0.6}{1.18(8/1)} = 0.0636$, $V = C_s W = 0.0636 \times 16,067 = 1022 \text{ kN}$, and $V_{min} = 0.75 \times 1022 = 767 \text{ kN}$. Actually, the frame was designed to have a base shear strength for a pattern of lateral loads proportional to the first mode $V_y = V_{min} \cdot \Omega_o \cdot C_d / R = 767 \times 3.0 \times 5.5 / 8 = 1582 \text{ kN}$. The frame was analyzed using the procedures of Appendix C.2 and its actual base shear strength was found to be $V_y = 1597 \text{ kN}$. Summary calculations for this frame are presented in Tables E-10, E-11, and E-12.

TABLE E-1 Modal Properties of Frame 3S-75

Quantity	Mode 1	Mode 2	Mode 3	Residual Mode
T_m , sec	1.58	0.49	0.24	0.632
$\{\phi_m\}$	1.000 0.657 0.250	1.000 -0.560 -0.690	1.000 -1.618 2.096	1.0000 -0.2037 -1.6321
\bar{W}_m , kN	5871	1098	398	1496
Γ_m	1.3985	-0.5334	0.1349	-0.3985

TABLE E-2 Modal Response Calculations for Example No.2: 3-Story Frame ($V_{min}=0.75V$) with Linear Viscous Damping System. Analysis for the DBE

Quantity	Units	Mode 1 (m=1)	Mode 2 (m=2)	Mode 3 (m=3)	Mode R (m=R)	SRSS	
						ELF	RSA
1. Elastic Response							
Damping Ratio, β_{ve}		0.100	0.205	0.151	0.228		
Total Damping Ratio, β_{v+l}		0.150	0.255	0.201	0.278		
Damping Coefficient, B_m		1.350	1.665	1.503	1.734		
Elastic Displacement, D_{em}	mm	244	19	1	22		
2. Roof Displacement and Base Shear							
Assumed Ductility, μ		1.29	1	1	1		
Effective Period, T_{ID}	sec	1.795	0.490	0.240	0.632		
Eff. Visc. Damp. Ratio, $\beta_v\sqrt{\mu}$		0.114	0.205	0.151	0.228		
Hysteretic Damping, β_H		0.066	0	0	0		
Effective Damping, β_m		0.230	0.255	0.201	0.278		
Damping Coefficient, B_m		1.590	1.665	1.503	1.734		
Displacement, D_{mD}	mm	235					
Corrected Displacement, D_{mD}	mm	244	19	1	22		
Seismic Coefficient, C_s		0.102	0.291	0.323	0.280		
Seismic Base Shear, V_m	kN	599	320	128	418	730	691
Yield Displacement, D_y	mm	182	-----	-----	-----		
Computed Ductility, μ		1.34	-----	-----	-----		
3. Response at Stage of Maximum Displacement							
Lateral Floor Displacement, δ_{ij}	mm	244	19	1	22		
		160	-11	-2	-4		
		61	-13	3	-35		
Story Drift, Δ_{jm}	mm	84	30	3	26	88	89
		99	2	-5	31	104	99
		61	-13	3	-35	71	62
Design Lateral Forces, F_{im}	kN	223	243	68	175		
		272	-252	-204	-66		
		103	-311	264	-527		
Floor Acceleration, A_{im}	g	0.294	0.320	0.090	0.230	0.373	0.444
		0.193	-0.179	-0.145	-0.047	0.199	0.301
		0.074	-0.221	0.188	-0.375	0.382	0.299
Actual Story Shear Forces, V_{jm}	kN	461	502	141	360	585	696
		1021	-18	-280	224	1046	1059
		1234	-659	265	-863	1506	1424

TABLE E-2 continued

4. Response at Stage of Maximum Velocity							
Drift Velocity, ∇_{im}	mm/sec	293	382	88	259	391	490
		348	32	-125	308	464	371
		214	-169	70	-351	411	281
Force in Damping Devices, $F_{d_{jm}}$	kN	234	305	70	207	312	391
		277	25	-100	245	370	296
		170	-135	56	-280	328	224
Horizontal Damper Force, $V_{d_{jm}}$	kN	207	270	62	183		
		246	23	-88	217		
		151	-120	50	-248		
5. Response at Stage of Maximum Acceleration							
Ductility, μ		1.34	1.00	1.00	1.00		
Ef. Visc. Damp. Rat., $\beta_1 + \beta_v \sqrt{\mu}$		0.166	0.255	0.201	0.278		
Parameter δ		0.320	0.472	0.382	0.507		
Coefficient CF_1		0.949	0.891	0.928	0.874		
Product $CF_1 \cdot \mu$		1.270	0.891	0.928	0.874		
Force Coefficient, CF_1 or C_{mFD}		1.000	0.891	0.928	0.874		
Force Coefficient, CF_2 or C_{mFV}		0.315	0.454	0.373	0.486		
Max.Floor Acc., $A_{im,max}$	g	0.336	0.364	0.098	0.258	0.423	0.505
		0.197	0.199	0.154	0.047	0.203	0.320
		0.084	0.219	0.192	0.406	0.414	0.303
Maximum Story Shear, $V_{j_{m,max}}$ (actual)	kN	526	570	154	404	663	791
		1098	26	293	302	1139	1137
		1282	642	264	875	1552	1458

TABLE E-3 Modal Response Calculations for Example No.2: 3-Story Frame ($V_{\min}=0.75V$) with Linear Viscous Damping System. Analysis for the MCE

Quantity	Units	Mode 1 (m=1)	Mode 2 (m=2)	Mode 3 (m=3)	Mode R (m=R)	SRSS	
						ELF	RSA
1. Elastic Response							
Damping Ratio, β_{ve}		0.100	0.205	0.151	0.228		
Total Damping Ratio, β_{v+I}		0.150	0.255	0.201	0.278		
Damping Coefficient, B_m		1.350	1.665	1.503	1.734		
Elastic Displacement, D_{em}	mm	366	29	2	32		
2. Roof Displacement and Base Shear							
Assumed Ductility, μ		2	1	1	1		
Effective Period, T_{ID}	sec	2.23	0.49	0.24	0.63		
Eff. Visc. Damp. Ratio, $\beta_v\sqrt{\mu}$		0.141	0.205	0.151	0.228		
Hysteretic Damping, β_H		0.148	0	0	0		
Effective Damping, β_m		0.339	0.255	0.201	0.278		
Damping Coefficient, B_m		1.917	1.665	1.503	1.734		
Displacement, D_{mD}	mm	365					
Corrected Displacement, D_{mD}	mm	366	29	2	32		
Seismic Coefficient, C_s		0.102	0.437	0.484	0.419		
Seismic Base Shear, V_m	kN	598	480	193	627	867	790
Yield Displacement, D_y	mm	182	-----	-----	-----		
Computed Ductility, μ		2	-----	-----	-----		
3. Response at Stage of Maximum Displacement							
Lateral Floor Displacement, δ_{ij}	mm	366	29	2	32		
		241	-16	-3	-7		
		92	-20	4	-53		
Story Drift, Δ_{jm}	mm	126	45	5	39	132	133
		149	4	-7	46	156	149
		92	-20	4	-53	106	94
Design Lateral Forces, F_{im}	kN	223	365	102	262		
		271	-378	-306	-99		
		103	-466	396	-791		
Floor Acceleration, A_{im}	g	0.294	0.480	0.135	0.345	0.453	0.579
		0.193	-0.269	-0.218	-0.070	0.205	0.396
		0.073	-0.332	0.282	-0.563	0.567	0.441
Actual Story Shear Forces, V_{jm}	kN	460	753	211	540	710	907
		1020	-27	-420	337	1074	1104
		1233	-989	397	-1295	1788	1630

TABLE E-3 continued

4. Response at Stage of Maximum Velocity							
Drift Velocity, ∇_{im}	mm/sec	353	573	132	389	525	686
		419	48	-187	461	623	461
		257	-254	106	-527	587	376
Force in Damping Devices, $F_{d_{jm}}$	kN	282	457	105	310	419	547
		334	38	-149	368	497	368
		205	-202	84	-420	468	300
Horizontal Damper Force, $V_{d_{jm}}$	kN	250	405	93	275		
		296	34	-132	326		
		182	-179	75	-373		
5. Response at Stage of Maximum Acceleration							
Ductility, μ		2	1	1	1		
Ef. Visc. Damp. Rat., $\beta_1 + \beta_v \sqrt{\mu}$		0.192	0.255	0.201	0.278		
Parameter δ		0.366	0.472	0.382	0.507		
Coefficient CF_1		0.934	0.891	0.928	0.874		
Product $CF_1 \cdot \mu$		1.875	0.891	0.928	0.874		
Force Coefficient, CF_1 or C_{mFD}		1.000	0.891	0.928	0.874		
Force Coefficient, CF_2 or C_{mFV}		0.358	0.454	0.373	0.486		
Max.Floor Acc., $A_{im,max}$	g	0.351	0.546	0.147	0.387	0.522	0.665
		0.199	0.298	0.231	0.070	0.211	0.426
		0.088	0.329	0.288	0.609	0.615	0.446
Maximum Story Shear, $V_{j_{m,max}}$ (actual)	kN	550	855	230	606	818	1042
		1126	40	439	453	1214	1210
		1298	962	396	1313	1846	1664

TABLE E-4 Modal Properties of Frame 3S-60

Quantity	Mode 1	Mode 2	Mode 3	Residual Mode
T_m , sec	1.78	0.54	0.27	0.712
$\{\phi_{im}\}$	1.000 0.667 0.252	1.000 -0.543 -0.707	1.000 -1.550 1.957	1.000 -0.184 -1.658
\bar{W}_m , kN	5889	1094	384	1478
Γ_m	1.3917	-0.5316	0.1399	-0.3917

TABLE E-5 Modal Response Calculations for Example No.1: 3-Story Frame ($V_{\min}=0.60V$) with Linear Viscous Damping System. Analysis for the DBE

Quantity	Units	Mode 1 (m=1)	Mode 2 (m=2)	Mode 3 (m=3)	Mode R (m=R)	SRSS	
						ELF	RSA
1. Elastic Response							
Damping Ratio, β_{Ve}		0.100	0.199	0.153	0.229		
Total Damping Ratio, β_{V+I}		0.150	0.249	0.203	0.279		
Damping Coefficient, B_m		1.350	1.647	1.509	1.737		
Elastic Displacement, D_{em}	mm	274	23	2	24		
2. Roof Displacement and Base Shear							
Assumed Ductility, μ		1.43	1	1	1		
Effective Period, T_{ID}	sec	2.129	0.540	0.270	0.712		
Eff. Visc. Damp. Ratio, $\beta_{V\sqrt{\mu}}$		0.120	0.199	0.153	0.229		
Hysteretic Damping, β_H		0.089	0	0	0		
Effective Damping, β_m		0.258	0.249	0.203	0.279		
Damping Coefficient, B_m		1.674	1.647	1.509	1.737		
Displacement, D_{mD}	mm	264					
Corrected Displacement, D_{mD}	mm	274	23	2	24		
Seismic Coefficient, C_s		0.082	0.294	0.321	0.279		
Seismic Base Shear, V_m	kN	481	322	123	413	634	592
Yield Displacement, D_y	mm	185	-----	-----	-----		
Computed Ductility, μ		1.48	-----	-----	-----		
3. Response at Stage of Maximum Displacement							
Lateral Floor Displacement, δ_{ij}	mm	274	23	2	24		
		182	-13	-3	-4		
		69	-17	3	-40		
Story Drift, Δ_{jm}	mm	91	36	4	28	95	98
		114	4	-6	35	119	114
		69	-17	3	-40	80	71
Design Lateral Forces, F_{im}	kN	178	245	70	171		
		220	-246	-202	-58		
		83	-321	255	-526		
Floor Acceleration, A_{im}	g	0.234	0.323	0.093	0.226	0.325	0.410
		0.156	-0.175	-0.144	-0.041	0.162	0.275
		0.059	-0.228	0.181	-0.374	0.378	0.297
Actual Story Shear Forces, V_{jm}	kN	367	506	145	353	510	642
		821	-2	-271	234	853	864
		992	-664	255	-850	1306	1221

TABLE E-5 continued

4. Response at Stage of Maximum Velocity							
Drift Velocity, ∇_{im}	mm/sec	269	420	100	250	367	509
		335	45	-137	311	458	365
		204	-192	76	-350	405	290
Force in Damping Devices, $F_{d_{jm}}$	kN	191	298	71	177	261	361
		238	32	-97	221	325	259
		144	-137	54	-249	287	206
Horizontal Damper Force, $V_{d_{jm}}$	kN	169	264	63	157		
		211	28	-86	196		
		128	-121	48	-220		
5. Response at Stage of Maximum Acceleration							
Ductility, μ		1.48	1.00	1.00	1.00		
Ef. Visc. Damp. Rat., $\beta_1 + \beta_2 \sqrt{\mu}$		0.172	0.249	0.203	0.279		
Parameter δ		0.331	0.462	0.386	0.509		
Coefficient CF_1		0.946	0.895	0.927	0.873		
Product $CF_1 \cdot \mu$		1.402	0.895	0.927	0.873		
Force Coefficient, CF_1 or C_{mFD}		1.000	0.895	0.927	0.873		
Force Coefficient, CF_2 or C_{mFV}		0.325	0.446	0.376	0.487		
Max.Floor Acc., $A_{im,max}$	g	0.269	0.364	0.101	0.246	0.365	0.464
		0.161	0.193	0.152	0.043	0.167	0.294
		0.068	0.227	0.186	0.396	0.402	0.301
Maximum Story Shear, $V_{jm,max}$ (actual)	kN	422	571	158	385	572	727
		889	15	284	300	938	933
		1033	649	254	850	1338	1246

TABLE E-6 Modal Response Calculations for Example No.1: 3-Story Frame ($V_{\min}=0.60V$) with Linear Viscous Damping System. Analysis for the MCE

Quantity	Units	Mode 1 (m=1)	Mode 2 (m=2)	Mode 3 (m=3)	Mode R (m=R)	SRSS	
						ELF	RSA
1. Elastic Response							
Damping Ratio, β_{Ve}		0.100	0.199	0.153	0.229		
Total Damping Ratio, β_{v+l}		0.150	0.249	0.203	0.279		
Damping Coefficient, B_m		1.350	1.647	1.509	1.737		
Elastic Displacement, D_{em}	mm	410	35	3	36		
2. Roof Displacement and Base Shear							
Assumed Ductility, μ		2.26	1	1	1		
Effective Period, T_{ID}	sec	2.68	0.54	0.27	0.71		
Eff. Visc. Damp. Ratio, $\beta_v\sqrt{\mu}$		0.150	0.199	0.153	0.229		
Hysteretic Damping, β_H		0.164	0	0	0		
Effective Damping, β_m		0.365	0.249	0.203	0.279		
Damping Coefficient, B_m		1.995	1.647	1.509	1.737		
Displacement, D_{mD}	mm	417					
Corrected Displacement, D_{mD}	mm	417	35	3	36		
Seismic Coefficient, C_s		0.082	0.442	0.482	0.419		
Seismic Base Shear, V_m	kN	481	483	185	619	784	707
Yield Displacement, D_y	mm	185	-----	-----	-----		
Computed Ductility, μ		2.26	-----	-----	-----		
3. Response at Stage of Maximum Displacement							
Lateral Floor Displacement, δ_{ij}	mm	417	35	3	36		
		278	-19	-4	-7		
		105	-25	5	-60		
Story Drift, Δ_{jm}	mm	139	54	6	42	145	149
		173	6	-9	53	181	174
		105	-25	5	-60	121	108
Design Lateral Forces, F_{im}	kN	178	368	106	257		
		220	-370	-303	-87		
		83	-481	383	-788		
Floor Acceleration, A_{im}	g	0.235	0.484	0.139	0.338	0.412	0.556
		0.156	-0.263	-0.216	-0.062	0.168	0.374
		0.059	-0.342	0.272	-0.561	0.564	0.441
Actual Story Shear Forces, V_{jm}	kN	368	759	218	530	645	871
		822	-4	-407	351	893	917
		993	-996	382	-1275	1616	1458

TABLE E-6 continued

4. Response at Stage of Maximum Velocity							
Drift Velocity, ∇_{im}	mm/sec	326	630	149	375	497	725
		407	67	-206	467	620	461
		247	-289	115	-525	580	397
Force in Damping Devices, $F_{d_{jm}}$	kN	232	447	106	266	353	515
		289	48	-146	332	440	327
		175	-205	81	-373	412	282
Horizontal Damper Force, $V_{d_{jm}}$	kN	205	396	94	236		
		256	42	-129	294		
		155	-182	72	-330		
5. Response at Stage of Maximum Acceleration							
Ductility, μ		2	1	1	1		
Ef. Visc. Damp. Rat., $\beta_I + \beta_v \sqrt{\mu}$		0.200	0.249	0.203	0.279		
Parameter δ		0.381	0.462	0.386	0.509		
Coefficient CF_1		0.928	0.895	0.927	0.873		
Product $CF_1 \cdot \mu$		2.098	0.895	0.927	0.873		
Force Coefficient, CF_1 or C_{mFD}		1.000	0.895	0.927	0.873		
Force Coefficient, CF_2 or C_{mFV}		0.372	0.446	0.376	0.487		
Max.Floor Acc., $A_{im,max}$	g	0.283	0.546	0.151	0.369	0.465	0.634
		0.163	0.290	0.229	0.064	0.175	0.404
		0.072	0.341	0.278	0.595	0.599	0.446
Maximum Story Shear, $V_{jm,max}$ (actual)	kN	444	856	237	578	729	993
		917	22	426	449	1021	1011
		1051	973	381	1275	1652	1482

TABLE E-7 Modal Properties of Frame 3S-90

Quantity	Mode 1	Mode 2	Mode 3	Residual Mode
T_m , sec	1.38	0.43	0.21	0.552
$\{\phi_m\}$	1.000	1.000	1.000	1.000
	0.639	-0.586	-1.648	-0.241
	0.237	-0.697	2.146	-1.622
\bar{W}_m , kN	5799	1170	398	1568
Γ_m	1.4105	-0.5426	0.1322	-0.4105

TABLE E-8 Modal Response Calculations for Example No.3: 3-Story Frame ($V_{\min}=0.90V$) with Linear Viscous Damping System. Analysis for the DBE

Quantity	Units	Mode 1 (m=1)	Mode 2 (m=2)	Mode 3 (m=3)	Mode R (m=R)	SRSS	
						ELF	RSA
1. Elastic Response							
Damping Ratio, β_{Ve}		0.100	0.198	0.146	0.218		
Total Damping Ratio, β_{V+I}		0.150	0.248	0.196	0.268		
Damping Coefficient, B_m		1.350	1.644	1.488	1.704		
Elastic Displacement, D_{em}	mm	215	15	1	18		
2. Roof Displacement and Base Shear							
Assumed Ductility, μ		1.23	1	1	1		
Effective Period, T_{ID}	sec	1.530	0.430	0.210	0.552		
Eff. Visc. Damp. Ratio, $\beta_{V\sqrt{\mu}}$		0.111	0.198	0.146	0.218		
Hysteretic Damping, β_H		0.055	0	0	0		
Effective Damping, β_m		0.216	0.248	0.196	0.268		
Damping Coefficient, B_m		1.548	1.644	1.488	1.704		
Displacement, D_{mD}	mm	208					
Corrected Displacement, D_{mD}	mm	215	15	1	18		
Seismic Coefficient, C_s		0.123	0.295	0.326	0.285		
Seismic Base Shear, V_m	kN	712	345	130	446	840	802
Yield Displacement, D_y	mm	169	-----	-----	-----		
Computed Ductility, μ		1.27	-----	-----	-----		
3. Response at Stage of Maximum Displacement							
Lateral Floor Displacement, δ_{ij}	mm	215	15	1	18		
		137	-9	-2	-4		
		51	-11	2	-30		
Story Drift, Δ_{jm}	mm	78	24	3	23	81	81
		86	2	-4	25	90	87
		51	-11	2	-30	59	52
Design Lateral Forces, F_{im}	kN	271	251	67	183		
		321	-272	-206	-81		
		119	-323	268	-549		
Floor Acceleration, A_{im}	g	0.357	0.330	0.089	0.241	0.431	0.494
		0.228	-0.193	-0.146	-0.058	0.235	0.333
		0.085	-0.230	0.191	-0.391	0.400	0.311
Actual Story Shear Forces, V_{jm}	kN	560	517	139	377	675	775
		1222	-44	-285	209	1239	1255
		1467	-711	267	-924	1734	1652

TABLE E-8 continued

4. Response at Stage of Maximum Velocity							
Drift Velocity, ∇_{im}	mm/sec	319	351	77	258	410	481
		355	25	-110	287	456	372
		209	-154	62	-337	396	267
Force in Damping Devices, $F_{d_{jm}}$	kN	280	309	68	226	360	422
		312	22	-97	252	401	327
		184	-136	55	-296	348	235
Horizontal Damper Force, $V_{d_{jm}}$	kN	248	274	60	200		
		276	19	-86	223		
		163	-120	49	-262		
5. Response at Stage of Maximum Acceleration							
Ductility, μ		1.27	1.00	1.00	1.00		
Ef. Visc. Damp. Rat., $\beta_1 + \beta_2 \sqrt{\mu}$		0.163	0.248	0.196	0.268		
Parameter δ		0.315	0.460	0.374	0.492		
Coefficient CF_1		0.951	0.896	0.931	0.881		
Product $CF_1 \cdot \mu$		1.209	0.896	0.931	0.881		
Force Coefficient, CF_1 or C_{mFD}		1.000	0.896	0.931	0.881		
Force Coefficient, CF_2 or C_{mFV}		0.310	0.444	0.365	0.472		
Max. Floor Acc., $A_{im,max}$	g	0.406	0.373	0.097	0.273	0.489	0.560
		0.231	0.212	0.155	0.055	0.238	0.350
		0.097	0.227	0.194	0.423	0.434	0.314
Maximum Story Shear, $V_{j_{m,max}}$ (actual)	kN	637	585	151	427	767	878
		1307	48	297	290	1339	1341
		1518	690	267	938	1784	1688

TABLE E-9 Modal Response Calculations for Example No.3: 3-Story Frame ($V_{min}=0.90V$) with Linear Viscous Damping System. Analysis for the MCE

Quantity	Units	Mode 1 (m=1)	Mode 2 (m=2)	Mode 3 (m=3)	Mode R (m=R)	SRSS	
						ELF	RSA
1. Elastic Response							
Damping Ratio, β_{Ve}		0.100	0.198	0.146	0.218		
Total Damping Ratio, β_{V+I}		0.150	0.248	0.196	0.268		
Damping Coefficient, B_m		1.350	1.644	1.488	1.704		
Elastic Displacement, D_{em}	mm	322	23	1	27		
2. Roof Displacement and Base Shear							
Assumed Ductility, μ		1.90	1	1	1		
Effective Period, T_{ID}	sec	1.90	0.43	0.21	0.55		
Eff. Visc. Damp. Ratio, $\beta_v\sqrt{\mu}$		0.138	0.198	0.146	0.218		
Hysteretic Damping, β_H		0.140	0	0	0		
Effective Damping, β_m		0.328	0.248	0.196	0.268		
Damping Coefficient, B_m		1.884	1.644	1.488	1.704		
Displacement, D_{mD}	mm	318					
Corrected Displacement, D_{mD}	mm	322	23	1	27		
Seismic Coefficient, C_s		0.122	0.442	0.489	0.427		
Seismic Base Shear, V_m	kN	706	517	195	669	973	897
Yield Displacement, D_y	mm	168	-----	-----	-----		
Computed Ductility, μ		1.92	-----	-----	-----		
3. Response at Stage of Maximum Displacement							
Lateral Floor Displacement, δ_{ij}	mm	322	23	1	27		
		206	-13	-2	-7		
		76	-16	3	-44		
Story Drift, Δ_{jm}	mm	116	36	4	34	121	122
		130	3	-6	38	135	130
		76	-16	3	-44	88	78
Design Lateral Forces, F_{im}	kN	269	376	101	275		
		318	-408	-309	-122		
		118	-485	402	-824		
Floor Acceleration, A_{im}	g	0.354	0.495	0.133	0.361	0.506	0.623
		0.226	-0.290	-0.220	-0.087	0.242	0.428
		0.084	-0.345	0.286	-0.586	0.592	0.456
Actual Story Shear Forces, V_{jm}	kN	555	776	209	566	793	976
		1211	-66	-428	314	1252	1286
		1455	-1066	401	-1385	2009	1848

TABLE E-9 continued

4. Response at Stage of Maximum Velocity							
Drift Velocity, ∇_{im}	mm/sec	384	527	116	386	545	663
		428	37	-166	430	607	461
		252	-232	94	-505	565	355
Force in Damping Devices, $F_{d_{jm}}$	kN	338	463	102	339	479	582
		376	32	-146	378	533	405
		222	-204	82	-444	496	312
Horizontal Damper Force, $V_{d_{jm}}$	kN	299	410	90	301		
		333	29	-129	335		
		197	-180	73	-393		
5. Response at Stage of Maximum Acceleration							
Ductility, μ		2	1	1	1		
Ef. Visc. Damp. Rat., $\beta_I + \beta_v \sqrt{\mu}$		0.189	0.248	0.196	0.268		
Parameter δ		0.361	0.460	0.374	0.492		
Coefficient CF_1		0.936	0.896	0.931	0.881		
Product $CF_1 \cdot \mu$		1.800	0.896	0.931	0.881		
Force Coefficient, CF_1 or C_{mFD}		1.000	0.896	0.931	0.881		
Force Coefficient, CF_2 or C_{mFV}		0.353	0.444	0.365	0.472		
Max.Floor Acc., $A_{im,max}$	g	0.422	0.560	0.145	0.409	0.588	0.716
		0.230	0.318	0.232	0.082	0.245	0.456
		0.101	0.341	0.292	0.635	0.643	0.460
Maximum Story Shear, $V_{jm,max}$ (actual)	kN	661	877	227	641	921	1122
		1329	71	446	435	1399	1404
		1524	1035	400	1407	2074	1886

TABLE E-10 Modal Properties of Frame 6S-75

Quantity	Mode 1	Mode 2	Mode 3	Mode 4	Mode 5	Mode 6	Resid. Mode
T_m, sec	2.60	0.93	0.51	0.33	0.23	0.17	1.04
$\{\phi_m\}$	1.000	1.000	1.000	1.000	1.000	1.000	1.000
	0.872	0.289	-0.456	-1.148	-1.721	-2.200	0.565
	0.682	-0.411	-0.709	0.435	2.660	5.569	-0.082
	0.476	-0.698	0.175	0.872	-2.112	-10.369	-0.783
	0.268	-0.582	0.784	-0.634	-0.293	14.923	-1.491
	0.096	-0.249	0.487	-0.845	2.383	-15.385	-2.076
W_m, kN	12045	2129	917	449	296	230	4022
Γ_m	1.4163	-0.6613	0.3853	-0.1988	-0.0701	-0.0115	-0.4163

**TABLE E-11 Modal Response Calculations for Example No.5: 6-Story Frame
($V_{min}=0.75V$) with Linear Viscous Damping System. Analysis for the DBE**

Quantity	Units	Mode 1	Mode 2	Mode 3	Mode 4	Mode 5	Mode 6	Mode R	SRSS		
		(m=1)	(m=2)	(m=3)	(m=4)	(m=5)	(m=6)	(m=R)	ELF	RSA	
1. Elastic Response											
Damping Ratio, β_{ve}		0.103	0.286	0.365	0.354	0.326	0.320	0.456			
Total Damping Ratio, β_{v+l}		0.153	0.336	0.415	0.404	0.376	0.370	0.506			
Damping Coefficient, B_m		1.359	1.908	2.145	2.112	2.028	2.010	2.418			
Elastic Displacement, D_{em}	mm	404.0	48.1	11.6	2.5	0.5	0.0	26.7			
2. Roof Displacement and Base Shear											
Assumed Ductility, μ		1.25	1.00	1.00	1.00	1.00	1.00	1.00			
Effective Period, T_{ID}	sec	2.91	0.93	0.51	0.33	0.23	0.17	1.04			
Eff. Visc. Damp. Ratio, $\beta_{v\sqrt{\mu}}$		0.115	0.286	0.365	0.354	0.326	0.320	0.456			
Hysteretic Damping, β_H		0.059	0.000	0.000	0.000	0.000	0.000	0.000			
Effective Damping, β_m		0.224	0.336	0.415	0.404	0.376	0.370	0.506			
Damping Coefficient, B_m		1.572	1.908	2.145	2.112	2.028	2.010	2.418			
Displacement, D_{mb}	mm	390	-----	-----	-----	-----	-----	-----			
Corrected Displacement, D_{md}	mm	404	48.1	11.6	2.5	0.5	0.0	26.7			
Seismic Coefficient, C_s		0.064	0.164	0.226	0.230	0.239	0.241	0.201			
Seismic Base Shear, V_m	kN	767	349	207	103	71	56	806	1113		878
Yield Displacement, D_y	mm	312	-----	-----	-----	-----	-----	-----			
Computed Ductility, μ		1.29	-----	-----	-----	-----	-----	-----			

TABLE E-11 continued

Quantity	Units	Mode 1 (m=1)	Mode 2 (m=2)	Mode 3 (m=3)	Mode 4 (m=4)	Mode 5 (m=5)	Mode 6 (m=6)	Mode R (m=R)	SRSS	
									ELF	RSA
3. Response at Stage of Maximum Displacement										
Lateral Floor Displacement, δ_{ij}	mm	404	48	12	3	0	0	27		
		352	14	-5	-3	-1	0	15		
		276	-20	-8	1	1	0	-2		
		192	-34	2	2	-1	0	-21		
		108	-28	9	-2	0	1	-40		
		39	-12	6	-2	1	-1	-55		
Story Drift, Δ_{jm}	mm	52	34	17	5	1	0	12	53	64
		77	34	3	-4	-2	0	17	79	84
		83	14	-10	-1	2	1	19	85	85
		84	-6	-7	4	-1	-1	19	86	85
		69	-16	3	1	1	1	16	71	71
		39	-12	6	-2	1	-1	-55	68	41
Design Lateral Forces, F_{im}	kN	141	170	136	72	26	4	131		
		228	91	-115	-152	-84	-18	137		
		178	-129	-179	58	129	45	-20		
		124	-219	44	115	-103	-83	-189		
		70	-183	198	-84	-14	120	-361		
		25	-78	123	-112	116	-124	-502		
Floor Acceleration, A_{im}	g	0.186	0.224	0.180	0.094	0.035	0.006	0.172	0.253	0.356
		0.162	0.065	-0.082	-0.108	-0.059	-0.013	0.097	0.189	0.229
		0.127	-0.092	-0.127	0.041	0.092	0.032	-0.014	0.128	0.228
		0.089	-0.156	0.031	0.082	-0.073	-0.059	-0.135	0.161	0.221
		0.050	-0.130	0.141	-0.060	-0.010	0.085	-0.257	0.261	0.224
		0.018	-0.056	0.087	-0.080	0.082	-0.088	-0.357	0.358	0.179
Actual Story Shear Forces, V_{jm}	kN	291	350	281	148	54	9	270	397	558
		762	538	44	-166	-118	-27	552	940	956
		1129	271	-325	-47	148	65	511	1240	1218
		1386	-181	-234	191	-63	-107	120	1391	1436
		1531	-559	174	18	-93	140	-624	1653	1647
		1582	-720	428	-213	146	-115	-1661	2294	1813

TABLE E-11 continued

Quantity	Units	Mode 1	Mode 2	Mode 3	Mode 4	Mode 5	Mode 6	Mode R	SRSS		
		(m=1)	(m=2)	(m=3)	(m=4)	(m=5)	(m=6)	(m=R)	ELF	RSA	
4. Response at Stage of Maximum Velocity											
Drift Velocity, $\dot{V}_{i,m}$	mm/sec	112	231	208	104	34	5	70	132	348	
		166	227	36	-77	-54	-12	104	196	299	
Force in Damping Devices, $F d_{j,m}$	kN	180	93	-126	-21	59	24	113	212	248	
		182	-38	-87	73	-23	-38	114	215	222	
Horizontal Damper Force, $V d_{j,m}$	kN	150	-108	42	10	-33	46	94	177	198	
		84	-81	70	-41	30	-23	-335	345	147	
		173	358	323	162	52	8	109	205	540	
		257	352	56	-119	-84	-18	162	304	464	
		341	177	-240	-40	112	46	214	403	471	
		344	-71	-165	139	-43	-73	216	407	421	
		385	-277	109	26	-85	118	242	454	508	
		215	-207	178	-105	76	-60	-857	884	376	
		154	317	286	143	46	7	97	181	478	
		228	312	50	-106	-75	-16	143	269	411	
		302	157	-212	-36	100	41	190	357	417	
		305	-63	-146	123	-38	-64	192	361	373	
		341	-245	96	23	-75	104	214	403	450	
		190	-184	158	-93	67	-53	-760	783	333	

TABLE E-11 continued

Quantity	Units	Mode 1	Mode 2	Mode 3	Mode 4	Mode 5	Mode 6	Mode R	SRSS		
		(m=1)	(m=2)	(m=3)	(m=4)	(m=5)	(m=6)	(m=R)	ELF	RSA	
5. Response at Stage of Maximum Acceleration											
Ductility, μ		1.29	1.00	1.00	1.00	1.00	1.00	1.00	1.00		
Ef. Visc. Damp. Rat., $\beta_T + \beta \sqrt{\mu}$		0.17	0.34	0.42	0.40	0.38	0.37	0.51			
Parameter δ		0.32	0.59	0.69	0.68	0.64	0.64	0.79			
Coefficient CF_1		0.95	0.83	0.77	0.78	0.80	0.80	0.70			
Product $CF_1 \cdot \mu$		1.23	0.83	0.77	0.78	0.80	0.80	0.70			
Force Coefficient, CF_1 or C_{mFD}		1.00	0.83	0.77	0.78	0.80	0.80	0.70			
Force Coefficient, CF_2 or C_{mFY}		0.32	0.56	0.64	0.63	0.60	0.59	0.71			
		0.217	0.299	0.255	0.131	0.045	0.007	0.165	0.273		0.469
		0.187	0.114	0.074	0.107	0.063	0.013	0.103	0.214		0.263
		0.160	0.106	0.145	0.040	0.094	0.034	0.057	0.170		0.263
		0.122	0.142	0.056	0.090	0.066	0.061	0.142	0.187		0.233
		0.087	0.155	0.130	0.051	0.024	0.090	0.233	0.249		0.244
		0.039	0.082	0.102	0.082	0.080	0.082	0.438	0.439		0.196
Max.Floor Acc., $A_{m,max}$	g	340	468	399	205	71	11	258	427		736
		834	621	66	195	140	32	490	967		1069
		1225	313	386	59	178	76	494	1321		1338
		1483	186	274	226	74	124	221	1499		1543
		1639	601	196	28	119	175	591	1742		1769
		1643	700	430	224	157	124	1708	2369		1861
Maximum Story Shear, $V_{jm,max}$ (actual)	kN										

**TABLE E-12 Modal Response Calculations for Example No.5: 6-Story Frame
($V_{min}=0.75V$) with Linear Viscous Damping System. Analysis for the MCE**

Quantity	Units	Mode 1	Mode 2	Mode 3	Mode 4	Mode 5	Mode 6	Mode R	SRSS	
		(m=1)	(m=2)	(m=3)	(m=4)	(m=5)	(m=6)	(m=R)	ELF	RSA
1. Elastic Response										
Damping Ratio, β_{ve}		0.103	0.286	0.365	0.354	0.326	0.320	0.456		
Total Damping Ratio, β_{v+l}		0.153	0.336	0.415	0.404	0.376	0.370	0.506		
Damping Coefficient, B_m		1.359	1.908	2.145	2.112	2.028	2.010	2.418		
Elastic Displacement, D_{em}	mm	606	72.1	17.4	3.8	0.7	0.1	40.0		
2. Roof Displacement and Base Shear										
Assumed Ductility, μ		1.93	1.00	1.00	1.00	1.00	1.00	1.00		
Effective Period, T_{ID}	sec	3.61	0.93	0.51	0.33	0.23	0.17	1.04		
Eff. Visc. Damp. Ratio, $\beta_{v\sqrt{\mu}}$		0.143	0.286	0.365	0.354	0.326	0.320	0.456		
Hysteretic Damping, β_H		0.142	0.000	0.000	0.000	0.000	0.000	0.000		
Effective Damping, β_m		0.335	0.336	0.415	0.404	0.376	0.370	0.506		
Damping Coefficient, B_m		1.905	1.908	2.145	2.112	2.028	2.010	2.418		
Displacement, D_{md}	mm	601	---	---	---	---	---	---		
Corrected Displacement, D_{md}	mm	606	72.1	17.4	3.8	0.7	0.1	40.0		
Seismic Coefficient, C_s		0.063	0.246	0.339	0.344	0.359	0.362	0.301		
Seismic Base Shear, V_m	kN	764	524	311	155	106	83	1210	1431	998
Yield Displacement, D_y	mm	311	---	---	---	---	---	---		
Computed Ductility, μ		1.95	---	---	---	---	---	---		

TABLE E-12 continued

Quantity	Units	Mode 1	Mode 2	Mode 3	Mode 4	Mode 5	Mode 6	Mode R	SRSS		
		(m=1)	(m=2)	(m=3)	(m=4)	(m=5)	(m=6)	(m=R)	ELF	RSA	
3. Response at Stage of Maximum Displacement											
Lateral Floor Displacement, δ_{ij}	mm	606	72	17	4	1	0	40			
		528	21	-8	-4	-1	0	23			
		413	-30	-12	2	2	0	-3			
		288	-50	3	3	-1	-1	-31			
		162	-42	14	-2	0	1	-60			
		58	-18	8	-3	2	-1	-83			
Story Drift, Δ_{jm}	mm	78	51	25	8	2	0	17	79	97	
		115	50	4	-6	-3	0	26	118	126	
		125	21	-15	-2	3	1	28	128	128	
		126	-8	-11	6	-1	-2	28	129	127	
		104	-24	5	1	-2	2	23	107	107	
		58	-18	8	-3	2	-1	-83	101	62	
Design Lateral Forces, F_{jm}	kN	141	255	205	107	39	7	196			
		227	136	-173	-228	-125	-27	205			
		178	-194	-269	86	194	67	-30			
		124	-329	66	173	-154	-125	-284			
		70	-274	297	-126	-21	180	-541			
		25	-117	184	-168	174	-185	-754			
Floor Acceleration, A_{jm}	g	0.185	0.335	0.269	0.141	0.052	0.009	0.258	0.318	0.492	
		0.162	0.097	-0.123	-0.162	-0.089	-0.019	0.146	0.218	0.292	
		0.126	-0.138	-0.191	0.061	0.138	0.048	-0.021	0.128	0.311	
		0.088	-0.234	0.047	0.123	-0.110	-0.089	-0.202	0.221	0.316	
		0.050	-0.195	0.211	-0.090	-0.015	0.128	-0.385	0.388	0.331	
		0.018	-0.084	0.131	-0.119	0.124	-0.132	-0.536	0.536	0.267	
Actual Story Shear Forces, V_{jm}	kN	290	526	422	221	81	13	405	498	771	
		759	807	66	-249	-178	-41	827	1123	1152	
		1125	407	-488	-71	222	97	766	1361	1317	
		1381	-272	-351	286	-95	-161	180	1392	1490	
		1525	-838	261	27	-139	210	-936	1789	1778	
		1576	-1080	642	-319	219	-172	-2491	2948	2060	

TABLE E-12 continued

Quantity	Units	Mode 1	Mode 2	Mode 3	Mode 4	Mode 5	Mode 6	Mode R	SRSS	
		(m=1)	(m=2)	(m=3)	(m=4)	(m=5)	(m=6)	(m=R)	ELF	RSA
4. Response at Stage of Maximum Velocity										
Drift Velocity, $\nabla_{i,m}$	mm/sec	135	346	312	156	51	7	105	171	513
		200	341	54	-115	-82	-18	156	254	424
Force in Damping Devices, $F_{d,jm}$	kN	217	140	-190	-32	89	36	170	275	336
		219	-56	-131	110	-34	-58	171	278	291
		181	-162	64	15	-50	69	142	230	266
		101	-121	104	-61	44	-35	-502	512	207
		209	537	484	242	79	11	163	265	795
		311	529	84	-179	-127	-27	243	394	657
Horizontal Damper Force, $V_{d,jm}$	kN	412	265	-360	-60	169	69	322	522	637
		416	-107	-248	208	-64	-109	325	528	552
		464	-415	163	39	-128	177	363	589	681
		259	-311	268	-157	114	-90	-1286	1312	530
		185	476	429	215	70	10	145	235	704
		275	469	75	-158	-112	-24	215	349	582
		365	235	-319	-53	149	61	285	463	565
		368	-95	-220	184	-57	-97	288	468	489
		412	-368	145	35	-113	156	321	522	604
		230	-275	237	-140	101	-79	-1140	1163	470

TABLE E-12 continued

Quantity	Units	Mode 1	Mode 2	Mode 3	Mode 4	Mode 5	Mode 6	Mode R	SRSS		
		(m=1)	(m=2)	(m=3)	(m=4)	(m=5)	(m=6)	(m=R)	ELF	RSA	
5. Response at Stage of Maximum Acceleration											
Ductility, μ		1.95	1.00	1.00	1.00	1.00	1.00	1.00	1.00		
Ef. Visc. Damp. Rat., $\beta_1 + \beta_2 \sqrt{\mu}$		0.19	0.34	0.42	0.40	0.38	0.37	0.51			
Parameter δ		0.37	0.59	0.69	0.68	0.64	0.64	0.79			
Coefficient CF_1		0.93	0.83	0.77	0.78	0.80	0.80	0.70			
Product $CF_1 \cdot \mu$		1.82	0.83	0.77	0.78	0.80	0.80	0.70			
Force Coefficient, CF_1 or C_{mFD}		1.00	0.83	0.77	0.78	0.80	0.80	0.70			
Force Coefficient, CF_2 or C_{mFV}		0.36	0.56	0.64	0.63	0.60	0.59	0.71			
		0.228	0.448	0.382	0.196	0.068	0.011	0.247	0.336	0.665	
		0.196	0.171	0.111	0.160	0.095	0.020	0.155	0.250	0.339	
		0.172	0.160	0.217	0.059	0.141	0.051	0.085	0.192	0.358	
		0.134	0.213	0.085	0.136	0.099	0.091	0.213	0.251	0.327	
		0.101	0.233	0.194	0.077	0.036	0.135	0.349	0.364	0.357	
		0.046	0.122	0.153	0.123	0.120	0.122	0.656	0.658	0.292	
		357	702	599	307	107	17	387	527	1042	
		858	931	98	293	209	48	734	1130	1321	
		1257	469	579	89	268	114	741	1459	1493	
		1514	279	411	339	110	187	331	1550	1643	
		1673	901	293	43	179	262	887	1894	1950	
		1659	1050	645	336	236	185	2561	3052	2116	
Maximum Story Shear, $V_{j,m,max}$ (actual)	kN										

APPENDIX F
DETAILED CALCULATIONS FOR THE SIMPLIFIED ANALYSIS OF A 3-STORY
FRAME WITH NONLINEAR VISCOUS DAMPING SYSTEM

F.1 Introduction

This appendix presents detailed calculations in the application of the equivalent lateral force (ELF) and response-spectrum analysis (RSA) procedures of NEHRP(2000) for the analysis of buildings with nonlinear viscous damping systems. These procedures are applied as described in Appendix A subject to the modifications described in Section 8.1 and Section 7.5.2. The presentation in the appendix consists of:

- (1) Detailed calculations for the 3-story special steel moment frame 3S-80 shown in Figure 8-6 and denoted as example No.6 in Section 8.
- (2) Summary calculations for the 3-story special steel moment frame 3S-80 shown in Figure 8-7 and denoted as example No.7 in Section 8.

F.2 Detailed Calculations for 3-Story Frame 3S-80 with Nonlinear Damping System
(Example No.6)

Parameters

The seismic tributary weights are: for the third floor 1567 kN, and 2900 kN for the second and first floors. The design coefficients per Table 5.2.2 of the 1997 NEHRP Recommended Provisions for special steel moment frames are: $R = 8.0$, $\Omega_o = 3.0$, $C_d = 5.5$, and $I = 1.0$.

Description of the System

The analyzed frame is a special steel moment frame with a nonlinear viscous damping system as shown in Figure 8-6. This frame is one of two such frames in each principal direction of the building with the plan and elevation shown in Figure B-1 of Appendix B. Torsional effects were disregarded in the analysis. The building is located at a site characterized by a design response spectrum with parameters $S_{DI} = 0.6$, $S_{DS} = 1.0$ and $T_s = 0.6$ sec per NEHRP (1997). This characterization is that of the design basis-earthquake (DBE). The maximum considered

earthquake (MCE) is characterized by a response spectrum with ordinates 1.5 larger than those of the DBE.

The damping system in the frame (as well as each of the other four identical frames of the building in Figure B-1) consists of nonlinear viscous damping devices with velocity exponent $a = 0.5$, installed in the diagonal configuration shown in Figure 8-6. The damping ratio in the fundamental mode of vibration of the frame under elastic conditions for the design basis earthquake is $\beta_{VI} = 0.10$ (damping provided by the damping system) plus an assumed inherent damping ratio $\beta_I = 0.05$ for a total damping ratio $\beta_{VI} + \beta_I = 0.15$. The corresponding damping coefficient is $B_{V+I} = 1.35$ (Table A13.3.1 and Table 3-3, column for B_1 , conservative values). The seismic base shear strength for the design of this frame was selected to be $0.80V$, which is larger than the minimum required on the basis of NEHRP (2000) Section A13.2.4.1, $V_{min} = 0.75V$, where V is determined by the procedures of NEHRP (1997), Section 5.3. The seismic base shear V has been determined in Section B.3 to be 788.5 kN , so that $0.80V = 0.80 \times 788.5 = 630.8 \text{ kN}$.

The approach followed to design the frame started with the calculation of the required base shear strength of the frame V_y , per (7-72) with $0.80V$ in place of V_{min} , such that

$$V_y = (0.80V) \cdot \frac{\Omega_o \cdot C_d}{R} = 630.8 \times \frac{3 \times 5.5}{8} = 1301 \text{ kN}$$

The frame was then designed to have a base shear strength equal to approximately 1301 kN when pushed over by lateral loads proportional to the first mode of the frame under elastic conditions. Subsequently, the frame was analyzed by the plastic analysis procedure of Appendix C.2 and $V_y = 1260 \text{ kN}$ ($\approx 0.78V$). Note that pushover analysis of the frame performed with program IDARC2D-Version 5.0 gave $V_y = 1262 \text{ kN}$. The model utilized for the plastic analysis is shown in Figure C-1 with distance $a_{ij}L_j$ equal to $d_c/2$, where d_c is the column depth. Thus, hinges were assumed to form at the beam-to-column interface.

Eigenvalue analysis of the frame performed in program IDARC2D-Version 5.0 gave: $T_1 = 1.52$ sec, $\{\phi_{i1}\}^T = [1.000 \quad 0.655 \quad 0.248]$, $T_2 = 0.48$ sec, $\{\phi_{i2}\}^T = [1.000 \quad -0.555 \quad -0.711]$ and $T_3 = 0.24$ sec, $\{\phi_{i3}\}^T = [1.000 \quad -1.578 \quad 1.992]$. The modal properties of the frame are summarized in Table F-1.

CALCULATION OF RESPONSE IN DESIGN BASIS EARTHQUAKE

FIRST MODE RESPONSE ($T_1 = 1.52$ sec)

Viscous Damping Ratio under Elastic Conditions

Equation (7-32) gives the damping ratio. For $\alpha = 0.5$ and $\lambda = 3.496$, (7-32) becomes

$$\beta_{V1} = 0.556 \cdot \left(\frac{T}{2\pi} \right)^{3/2} \frac{\sum_j C_{N1} \cdot (\cos \theta_j \cdot \phi_{rj})^{3/2}}{(D_{roof})^{1/2} \cdot \sum_i \left(\frac{w_i}{g} \right) \phi_{i1}^2}$$

Observe that application of (7-32) requires estimation of the roof displacement for elastic behavior. Assume that a damping constant of $C_{N1} = 14.47 \text{ kN} \cdot (\text{s/mm})^{0.5}$ provides a viscous damping ratio of $\beta_{V1} = 0.10$. The procedure to evaluate β_{V1} is as follows:

Effective viscous damping ratio (under elastic conditions): $\beta_{V+I} = 0.05 + 0.10 = 0.15$

Damping Coefficient: $B_{V+I} = 1.35$ (Table A13.3.1)

The roof displacement for elastic behavior of the frame is:

$$D = \left(\frac{9810}{4\pi^2} \right) \times |1.3994| \times \frac{0.6}{1.35} \times 1.52 = 234.92 \text{ mm}$$

Viscous damping ratio (under elastic conditions)

Modal Drift

$$\{\phi_r\}_I = \begin{Bmatrix} 1 - 0.655 \\ 0.655 - 0.248 \\ 0.248 \end{Bmatrix} = \begin{Bmatrix} 0.345 \\ 0.407 \\ 0.248 \end{Bmatrix}, \quad \sum_i w_i \phi_{i1}^2 = 2989.5$$

$$\beta_{V1} = 0.556 \times \left(\frac{1.52}{2\pi} \right)^{3/2} \times 9810 \times 14.47 \times (\cos^{1.5} 27.6^\circ) \times \frac{(0.345^{1.5} + 0.407^{1.5} + 0.248^{1.5})}{\sqrt{235 \times 2989.5}}$$

$$\beta_{V1} = 0.10$$

Had the viscous damping ratio been different, the computations would have to be repeated for a new value of C_{N1} .

Roof Displacement

Assumed Effective Ductility: $\mu_D = 1.27$

Effective Period: $T_{ID} = 1.52(1.27)^{1/2} = 1.713 \text{ sec}$ (A13.4.3.5-1)

Effective Damping Ratio

Quality factor: $q_H = 0.67 \times \frac{0.6}{1.52} = 0.26 < 0.50$ (A13.3.3.-1)

Hysteretic Damping: $\beta_{HD} = 0.50 \times (0.64 - 0.05) \times \left(1 - \frac{1}{1.27}\right) = 0.0627$ (A13.3.2.2-1)

Effective Damping: $\beta_{ID} = 0.05 + 0.10 \times (1.27)^{3/4} + 0.0627 = 0.232$ (7-40)

Damping Coefficient: $B_{ID} = 1.596$ (Table A13.3.1)

Roof Displacement: $D_{ID} = \left(\frac{9810}{4\pi^2}\right) \times |1.3994| \times \frac{0.6 \times 1.713}{1.596} = 223.94 \text{ mm}$ (A13.4.4.3-1)

Corrected Displacement: Since $D_{ID} < D$, use $D_{ID} = 234.92 \text{ mm}$

Base Shear

Seismic coefficient: $C_{s1} = \left(\frac{8}{5.5}\right) \times \frac{0.6}{1.713 \times (3 \times 1.596)} = 0.1064$ (A13.4.3.4-2)

Base shear: $V_1 = 0.1064 \times 5861 = 623.6 \text{ kN}$ (A13.4.3.2-1)

The contribution of the first mode to the base shear strength of the frame is given by (7-72)

$$V_y = V_1 \frac{\Omega_o \cdot C_d}{R} = 623.6 \times \frac{3 \times 5.5}{8} = 1286 \text{ kN}$$

The calculated contribution to the base shear strength of 1286 is close to the actual base shear strength of 1260 kN.

Displacement at Effective Yield (Yield Displacement) D_y

$$D_y = \left(\frac{9810}{4\pi^2} \right) \times \left(\frac{3 \times 5.5}{8} \right) \times |1.3994| \times 0.1064 \times 1.52^2 = 176.3 \text{ mm} \quad (\text{A13.3.4-3})$$

Effective Ductility Demand: $\mu_D = \frac{235}{176} = 1.33 \approx 1.27$ (A13.3.4-1)

$$\mu_{max} = \frac{8}{3 \times 1} = 2.667 \quad (\text{A13.5-2})$$

$$\mu_D < \mu_{max}$$

The difference between the estimated and the assumed ductility demand is due to the correction of the roof displacement to meet the condition that it is not less than the elastic displacement.

Response at Stage of Maximum Displacement

Lateral Floor Displacements, δ_{iID} , and Story Drifts, Δ_{iID}

$$\delta_{iID} = 234.92 \times \begin{Bmatrix} 1.000 \\ 0.655 \\ 0.248 \end{Bmatrix} = \begin{Bmatrix} 234.92 \\ 153.87 \\ 58.26 \end{Bmatrix} \text{ mm} \quad (\text{A13.4.4.2-1})$$

$$\Delta_{iID} = \begin{Bmatrix} 81.05 \\ 95.61 \\ 58.26 \end{Bmatrix} \text{ mm}$$

Design Lateral Forces, F_{iI} , Design Story Shears, V_{iI} , and Accelerations, A_{iI}

$$F_{i_l} = \begin{Bmatrix} 1567 \times 1.0 \times \frac{1.3994}{5860} \times 623.6 \\ 2900 \times 0.655 \times \frac{1.3994}{5860} \times 623.6 \\ 2900 \times 0.248 \times \frac{1.3994}{5860} \times 623.6 \end{Bmatrix} = \begin{Bmatrix} 233 \\ 283 \\ 107 \end{Bmatrix} \text{ kN} \quad (\text{A13.4.3.9-1})$$

$$A_{i_l} = \frac{F_{i_l}}{w_i} \cdot \left(\frac{C_d \Omega_o}{R} \right) = \begin{Bmatrix} \frac{233}{1567} \\ \frac{283}{2900} \\ \frac{107}{2900} \end{Bmatrix} \times \left(\frac{5.5 \times 3}{8} \right) = \begin{Bmatrix} 0.307 \\ 0.201 \\ 0.076 \end{Bmatrix} \text{ g}$$

Observe that for calculation of A_{i_l} , lateral inertia forces are multiplied by factor $C_d \cdot \Omega_o / R$ to convert them into real (unreduced) forces.

$$V_{i_l} = \begin{Bmatrix} 233 \\ 516 \\ 623 \end{Bmatrix} \text{ kN}$$

Response at Stage of Maximum Velocity

$$\text{Story Velocity:} \quad \nabla_{i_{1D}} = \frac{2\pi}{1.713} \times \begin{Bmatrix} 81.05 \\ 95.61 \\ 58.26 \end{Bmatrix} = \begin{Bmatrix} 297.3 \\ 350.7 \\ 213.7 \end{Bmatrix} \frac{\text{mm}}{\text{sec}} \quad (\text{A13.4.4.5-2})$$

$$\text{Force in Damping Devices:} \quad F_{d_{i_{1D}}} = 14.47 \times \begin{Bmatrix} \frac{1}{297.3^2} \\ \frac{1}{350.7^2} \\ \frac{1}{213.7^2} \end{Bmatrix} \times (\cos 27.6^\circ)^{0.5} = \begin{Bmatrix} 235 \\ 255 \\ 199 \end{Bmatrix} \text{ kN} \quad (7-30)$$

Response at Stage of Maximum Acceleration

Force Coefficients

Effective viscous damping: $\beta_{V+I} = 0.05 + 0.10 \times (1.33)^{0.75} = 0.174$

Parameter δ :
$$\delta = \left(\frac{2\pi \times 0.5}{3.496} \times 0.174 \right)^{\frac{2}{3}} = 0.290 \text{ rads} \quad (4-35)$$

Force Coefficient CF_1 :
$$CF_1 = \cos \delta = \cos(0.290) = 0.958 \quad (4-41)$$

$$CF_1 \cdot \mu = 0.958 \times 1.33 = 1.274 > 1.0 \quad \therefore \text{ use } CF_1 = 1.000$$

Force Coefficient CF_2 :
$$CF_2 = [\sin(0.290)]^{\frac{1}{2}} = 0.535 \quad (4-39)$$

Maximum Lateral Inertia Forces

$$F_{i_l, max} = CF_1 \cdot \left| F_{i_l} |_{Max \text{ Disp}} \right| \cdot \frac{C_d \Omega_o}{R} + CF_2 \cdot \left| F_{i_{D1}} |_{Max \text{ Velocity}} \right|$$

$$F_{i_l, max} = 1.0 \times \begin{Bmatrix} 233 \\ 283 \\ 107 \end{Bmatrix} \times \left(\frac{3 \times 5.5}{8} \right) + 0.535 \times \begin{Bmatrix} 208 \\ 18 \\ -50 \end{Bmatrix} = \begin{Bmatrix} 592 \\ 593 \\ 247 \end{Bmatrix} \text{ kN}$$

Maximum Floor Accelerations

$$A_{i_l, max} = \frac{F_{i_l, max}}{w_i} = \begin{Bmatrix} 592 / 1567 \\ 593 / 2900 \\ 247 / 2900 \end{Bmatrix} = \begin{Bmatrix} 0.378 \\ 0.204 \\ 0.085 \end{Bmatrix} \text{ g}$$

Maximum Story Shear

$$V_{i_l, max} = 1.0 \times \begin{Bmatrix} 481 \\ 1064 \\ 1285 \end{Bmatrix} + 0.531 \times \begin{Bmatrix} 208 \\ 226 \\ 176 \end{Bmatrix} = \begin{Bmatrix} 592 \\ 1185 \\ 1379 \end{Bmatrix} \text{ (kN)}$$

SECOND MODE RESPONSE ($T_2=0.48 \text{ sec} < T_s$)

Effective Damping Ratio

Damping Constant in Higher Modes

$$C_i = \frac{1}{2} C_{Ni} \nabla_{i1}^{-\frac{1}{2}} = \frac{1}{2} \times 14.47 \times \begin{Bmatrix} (297 \times \cos 27.6)^{-\frac{1}{2}} \\ (352 \times \cos 27.6)^{-\frac{1}{2}} \\ (213 \times \cos 27.6)^{-\frac{1}{2}} \end{Bmatrix} = \begin{Bmatrix} 0.446 \\ 0.410 \\ 0.527 \end{Bmatrix} \text{ kN} \cdot \text{s/mm} \quad (7-41)$$

Viscous Damping Ratio under Elastic Conditions

$$\beta_{V2} = \left(\frac{0.48}{4\pi} \right) \times \left(\frac{\cos^2 27.6^\circ}{1/9810} \right) \times \left[\frac{0.446 \times 1.555^2 + 0.410 \times 0.156^2 + 0.527 \times (-0.711)^2}{1567 \times 1.0^2 + 2900 \times (-0.555)^2 + 2900 \times (-0.711)^2} \right] \quad (7-29)$$

$$\beta_{V2} = 0.101$$

Effective Damping Ratio: $\beta_{2D} = 0.101 + 0.05 = 0.151$

Damping Coefficient: $B_{2D} = 1.353$ (Table A13.3.1)

Roof Displacement: $D_{2D} = \left(\frac{9810}{4\pi^2} \right) \times |-0.5360| \times \frac{1.0}{1.353} \times 0.48^2 = 22.67 \text{ mm}$ (A13.5.4.3-2)

Seismic Base Shear

Seismic coefficient: $C_{S2} = \left(\frac{8}{5.5} \right) \times \frac{1.0}{3 \times 1.353} = 0.3584$ (A13.5.3.6-1)

Base shear: $V_2 = 0.3584 \times 1128 = 404.27 \text{ kN}$ (A13.5.3.2-1)

Response at Stage of Maximum Displacement

Lateral Floor Displacement, δ_{i2D} , and Story Drifts, Δ_{i2D}

$$\delta_{i2D} = 22.67 \times \begin{Bmatrix} 1.000 \\ -0.555 \\ -0.711 \end{Bmatrix} = \begin{Bmatrix} 22.67 \\ -12.58 \\ -16.12 \end{Bmatrix} \text{ mm} \quad (A13.5.4.2-1)$$

$$\Delta_{i2D} = \begin{Bmatrix} 35.25 \\ 3.54 \\ -16.12 \end{Bmatrix} \text{ mm}$$

Design Lateral Forces, F_{i2} , Design Story Shears, V_{i2} , and Accelerations, A_{i2}

$$F_{i2} = \begin{Bmatrix} 1567 \times 1.0 \times \frac{|-0.536|}{1128} \times 404.27 \\ 2900 \times (-0.555) \times \frac{|-0.536|}{1128} \times 404.27 \\ 2900 \times (-0.711) \times \frac{|-0.536|}{1128} \times 404.27 \end{Bmatrix} = \begin{Bmatrix} 301.0 \\ -309.2 \\ -396.1 \end{Bmatrix} \text{ kN} \quad (\text{A13.5.3.7-1})$$

$$A_{i2} = \frac{F_{i2}}{w_i} \cdot \left(\frac{C_d \cdot \Omega_o}{R} \right) = \begin{Bmatrix} \frac{301.0}{1567} \\ \frac{-309.2}{2900} \\ \frac{-396.1}{2900} \end{Bmatrix} \times \frac{3 \times 5.5}{8} = \begin{Bmatrix} 0.396 \\ -0.220 \\ -0.282 \end{Bmatrix} \text{ g}$$

$$V_{i2} = \begin{Bmatrix} 301.0 \\ -8.2 \\ -404.3 \end{Bmatrix} \text{ kN}$$

Response at Stage of Maximum Velocity

$$\text{Story Velocity} \quad \nabla_{i2D} = \left(\frac{2\pi}{0.48} \right) \times \begin{Bmatrix} 35.25 \\ 3.54 \\ -16.12 \end{Bmatrix} = \begin{Bmatrix} 461.4 \\ 46.3 \\ -211.0 \end{Bmatrix} \frac{\text{mm}}{\text{sec}} \quad (\text{A13.5.4.5-2})$$

$$\text{Forces in Damping Devices:} \quad Fd_{i2D} = \begin{Bmatrix} 0.446 \times 461.4 \\ 0.410 \times 46.3 \\ 0.527 \times (-211) \end{Bmatrix} \times \cos 27.6 = \begin{Bmatrix} 182.4 \\ 16.8 \\ -98.5 \end{Bmatrix} \text{ kN} \quad (7-23)$$

Response at Stage of Maximum Acceleration

Force Coefficients

$$\beta_{v2} = 0.05 + 0.101 = 0.151$$

$$CF_1 = \cos[\tan^{-1}(2 \times 0.151)] = 0.957 \quad (4-41)$$

$$CF_2 = \sin[\tan^{-1}(2 \times 0.151)] = 0.289 \quad (4-39)$$

Maximum Inertia Forces and Floor Accelerations

$$F_{i2,max} = 0.957 \times \begin{Bmatrix} |301.0| \\ |-309.2| \\ |-396.1| \end{Bmatrix} \times \left(\frac{3 \times 5.5}{8} \right) + 0.289 \times \begin{Bmatrix} |162| \\ |-147| \\ |-102| \end{Bmatrix} = \begin{Bmatrix} 640.9 \\ 652.8 \\ 811.3 \end{Bmatrix} \text{ kN}$$

$$A_{i2,max} = \frac{F_{i2,max}}{w_i} = \begin{Bmatrix} 640.9 / 1567 \\ 652.8 / 2900 \\ 811.3 / 2900 \end{Bmatrix} = \begin{Bmatrix} 0.409 \\ 0.225 \\ 0.280 \end{Bmatrix} \text{ g}$$

Maximum Story Shear

$$V_{i2,max} = 0.957 \times \begin{Bmatrix} |301.0| \\ |-8.2| \\ |-404.3| \end{Bmatrix} \times \left(\frac{3 \times 5.5}{8} \right) + 0.289 \times \begin{Bmatrix} |162| \\ |15| \\ |-87| \end{Bmatrix} = \begin{Bmatrix} 641 \\ 20 \\ 823 \end{Bmatrix} \text{ kN}$$

THIRD MODE RESPONSE ($T_3 = 0.24 \text{ sec} < T_s$)

Effective Damping Ratio

Viscous Damping Ratio under Elastic Conditions

$$\beta_{v3} = \left(\frac{0.24}{4\pi} \right) \times \frac{\cos^2 27.6 \times [0.446 \times 2.578^2 + 0.410 \times 3.57^2 + 0.526 \times 1.992^2]}{(1/9810) \times [1567 \times 1.0^2 + 2900 \times 1.578^2 + 2900 \times 1.992^2]} \quad (7-29)$$

$$\beta_{v3} = 0.075$$

Effective Damping Ratio: $\beta_{3D} = 0.075 + 0.05 = 0.125$

Damping Coefficient: $B_3 = 1.275$ (Table A13.3.1)

Roof Displacement: $D_{3D} = \left(\frac{9810}{4\pi^2} \right) \times |0.1363| \times \frac{1.0}{1.275} \times 0.24^2 = 1.53 \text{ mm}$ (A13.5.4.3-2)

Seismic Base Shear

$$\text{Seismic Coefficient: } C_{S3} = \frac{8}{5.5} \times \frac{1.0}{3 \times 1.275} = 0.380 \quad (\text{A13.5.3.6-1})$$

$$\text{Base Shear: } V_3 = 0.380 \times 378 = 143.74 \text{ kN} \quad (\text{A13.5.3.2-1})$$

Response at Stage of Maximum Displacement

Lateral Floor Displacement, δ_{i3D} , and Story Drifts, Δ_{i3D}

$$\delta_{i3D} = 1.53 \times \begin{Bmatrix} 1.0 \\ -1.578 \\ 1.992 \end{Bmatrix} = \begin{Bmatrix} 1.53 \\ -2.41 \\ 3.05 \end{Bmatrix} \text{ mm} \quad (\text{A13.5.4.2-1})$$

$$\Delta_{i3D} = \begin{Bmatrix} 3.94 \\ -5.45 \\ 3.05 \end{Bmatrix} \text{ mm}$$

Design Lateral Forces, F_{i3} , Design Story Shears, V_{i3} , and Floor Accelerations, A_{i3}

$$F_{i3} = \begin{Bmatrix} 1567 \times 1.0 \times \frac{|0.1363|}{378} \times 143.74 \\ 2900 \times (-1.578) \times \frac{|0.1363|}{378} \times 143.74 \\ 2900 \times 1.992 \times \frac{|0.1363|}{378} \times 143.74 \end{Bmatrix} = \begin{Bmatrix} 81.2 \\ -237.2 \\ 299.4 \end{Bmatrix} \text{ kN} \quad (\text{A13.5.3.7-1})$$

$$A_{i3} = \frac{F_{i3}}{w_i} \cdot \left(\frac{C_d \Omega_o}{R} \right) = \begin{Bmatrix} \frac{81.2}{1567} \\ -\frac{237.2}{2900} \\ \frac{299.4}{2900} \end{Bmatrix} \times \left(\frac{3 \times 5.5}{3} \right) = \begin{Bmatrix} 0.107 \\ -0.169 \\ 0.213 \end{Bmatrix} \text{ g}$$

$$V_{i3} = \begin{Bmatrix} 81.2 \\ -156.0 \\ 143.4 \end{Bmatrix} \text{ kN}$$

Response at Stage of Maximum Velocity

$$\text{Story Velocity:} \quad \nabla_{i_{3D}} = \left(\frac{2\pi}{0.24} \right) \times \begin{Bmatrix} 3.94 \\ -5.45 \\ 3.05 \end{Bmatrix} = \begin{Bmatrix} 103.1 \\ -142.7 \\ 79.8 \end{Bmatrix} \frac{\text{mm}}{\text{sec}} \quad (\text{A13.5.4.5-2})$$

$$\text{Forces in Damping Devices:} \quad Fd_{i_{3D}} = \begin{Bmatrix} 0.446 \times 103.1 \\ 0.410 \times (-142.7) \\ 0.527 \times 79.8 \end{Bmatrix} \times \cos 27.6 = \begin{Bmatrix} 40.8 \\ -51.9 \\ 37.3 \end{Bmatrix} \text{ kN} \quad (7-23)$$

Response at Stage of Maximum Acceleration

Force Coefficients

$$\beta_{v3} = 0.075 + 0.05 = 0.125$$

$$CF_1 = \cos[\tan^{-1}(2 \times 0.125)] = 0.970 \quad (4-41)$$

$$CF_2 = \sin[\tan^{-1}(2 \times 0.125)] = 0.243$$

Maximum Inertia Forces and Floor Acceleration

$$F_{i_{3,max}} = 0.970 \times \begin{Bmatrix} |81.2| \\ |-237.2| \\ |299.4| \end{Bmatrix} \times \left(\frac{3 \times 5.5}{8} \right) + 0.243 \times \begin{Bmatrix} |36.16| \\ |82.15| \\ |79.05| \end{Bmatrix} = \begin{Bmatrix} 171.2 \\ 494.5 \\ 618.2 \end{Bmatrix} \text{ kN}$$

$$A_{i_{3,max}} = \frac{F_{i_{3,max}}}{w_i} = \begin{Bmatrix} 171.2 / 1567 \\ 494.5 / 2900 \\ 618.2 / 2900 \end{Bmatrix} = \begin{Bmatrix} 0.109 \\ 0.171 \\ 0.213 \end{Bmatrix} \text{ g}$$

Maximum Story Shear

$$V_{i_{3,max}} = 0.970 \times \begin{Bmatrix} |81.2| \\ |-156| \\ |143| \end{Bmatrix} \times \left(\frac{3 \times 5.5}{8} \right) + 0.243 \times \begin{Bmatrix} |36.16| \\ |-45.99| \\ |35.06| \end{Bmatrix} = \begin{Bmatrix} 171 \\ 323 \\ 295 \end{Bmatrix} \text{ kN}$$

RESIDUAL MODE RESPONSE ($T_R = 0.4 \times 1.52 = 0.608 \text{ sec} > T_s$)

Effective Damping Ratio

Viscous damping ratio under elastic conditions:

$$\beta_{VR} = \left(\frac{0.608}{4\pi} \right) \times \frac{\cos^2 27.6 \times [0.446 \times 1.209^2 + 0.410 \times 1.426^2 + 0.527 \times 1.635^2]}{(1/9810) \times [1567 \times 1.0^2 + 2900 \times (-0.2088)^2 + 2900 \times (-1.6348)^2]} \quad (7-29)$$

$$\beta_{VR} = 0.114$$

Effective Damping Ratio: $\beta_{RD} = 0.114 + 0.05 = 0.164$

Damping Coefficient: $B_{RD} = 1.392$ (Table A13.3.1)

Roof Displacement: $D_{RD} = \left(\frac{9810}{4\pi^2} \right) \times |-0.3994| \times \frac{0.6}{1.392} \times 0.608 = 26.01 \text{ mm}$

Seismic coefficient: $C_{SR} = \left(\frac{8}{5.5} \right) \times \frac{1.0}{3 \times 1.392} = 0.3483$ (A13.4.3.8-1)

Base shear: $V_R = 0.3483 \times 1506 = 524.54 \text{ kN}$ (A13.4.3.6-1)

Response at Stage of Maximum Displacement

Lateral Floor Displacement, δ_{iR} , and Story Drifts, Δ_{iR}

$$\delta_{iR} = 26.01 \times \begin{Bmatrix} 1.000 \\ -0.2088 \\ -1.6348 \end{Bmatrix} = \begin{Bmatrix} 26.01 \\ -5.43 \\ -42.52 \end{Bmatrix} \text{ mm} \quad (A13.4.4.2-2)$$

$$\Delta_{iR} = \begin{Bmatrix} 31.44 \\ 37.09 \\ -42.52 \end{Bmatrix} \text{ mm}$$

Design Lateral Forces, F_{iR} , Design Story Shears, V_{iR} , and Floor Accelerations, A_{iR}

$$F_{iR} = \begin{Bmatrix} 1567 \times 1.0 \times \frac{|-0.3994|}{1506} \times 524.54 \\ 2900 \times (-0.2088) \times \frac{|-0.3994|}{1506} \times 524.54 \\ 2900 \times (-1.6348) \times \frac{|-0.3994|}{1506} \times 524.54 \end{Bmatrix} = \begin{Bmatrix} 218.0 \\ -84.2 \\ -659.5 \end{Bmatrix} \text{ kN} \quad (A13.4.3.9-2)$$

$$A_{iR} = \frac{F_{iR}}{w_i} \left(\frac{C_d \Omega_o}{R} \right) = \begin{Bmatrix} \frac{218.0}{1567} \\ -84.2 \\ \frac{2900}{2900} \\ \frac{-659.5}{2900} \end{Bmatrix} \times \left(\frac{3 \times 5.5}{8} \right) = \begin{Bmatrix} 0.287 \\ -0.060 \\ -0.469 \end{Bmatrix} g$$

$$V_{iR} = \begin{Bmatrix} 218.0 \\ 133.8 \\ -525.7 \end{Bmatrix} kN$$

Response at Stage of Maximum Velocity

Story Velocity:
$$\nabla_{iRD} = \left(\frac{2\pi}{0.608} \right) \times \begin{Bmatrix} 31.44 \\ 37.09 \\ -42.52 \end{Bmatrix} = \begin{Bmatrix} 324.9 \\ 383.3 \\ -439.4 \end{Bmatrix} \frac{mm}{sec} \quad (A13.4.4.5-3)$$

Forces in Damping Devices:
$$Fd_{iRD} = \begin{Bmatrix} 0.446 \times 324.9 \\ 0.410 \times 383.3 \\ 0.527 \times (-439.4) \end{Bmatrix} \cos 27.6^\circ = \begin{Bmatrix} 128.4 \\ 139.3 \\ -205.2 \end{Bmatrix} kN$$

Response at Stage of Maximum Acceleration

Force Coefficients

$$\beta_{VR} = 0.114 + 0.05 = 0.164$$

$$CF_1 = \cos[\tan^{-1}(2 \times 0.164)] = 0.950 \quad (4-41)$$

$$CF_2 = \sin[\tan^{-1}(2 \times 0.164)] = 0.312 \quad (4-39)$$

Maximum Inertia Forces and Floor Acceleration

$$F_{iR,max} = 0.950 \times \begin{Bmatrix} |218.0| \\ |-84.2| \\ |-659.5| \end{Bmatrix} \times \left(\frac{3 \times 5.5}{8} \right) + 0.312 \times \begin{Bmatrix} |113.8| \\ |9.6| \\ |-305.3| \end{Bmatrix} = \begin{Bmatrix} 462.64 \\ 167.97 \\ 1387.46 \end{Bmatrix} kN$$

$$A_{iR,max} = \frac{F_{iR,max}}{w_i} = \begin{Bmatrix} 462.64 / 1567 \\ 167.97 / 2900 \\ 1387.46 / 2900 \end{Bmatrix} = \begin{Bmatrix} 0.295 \\ 0.058 \\ 0.478 \end{Bmatrix} g$$

Maximum Story Shear:

$$V_{iR,max} = 0.950 \times \begin{Bmatrix} |218.0| \\ |133.8| \\ |-525.7| \end{Bmatrix} \times \left(\frac{3 \times 5.5}{8} \right) + 0.312 \times \begin{Bmatrix} |113.8| \\ |123.5| \\ |-181.8| \end{Bmatrix} = \begin{Bmatrix} 463 \\ 301 \\ 1087 \end{Bmatrix} \text{ kN}$$

Total responses resulting from modal combinations were calculated by use of the SRSS combination rule. Table F-1 presents a summary of the modal properties of the frame and Tables F-2 and F-3 present summaries of the results of the analysis for each mode and the total response calculated by both the ELF and RSA procedures for the DBE and the MCE, respectively.

F.3 Summary Calculations for 3-Story Frame 3S-80 with Nonlinear Viscous Damping (Example No.7)

Frame 3S-80 with nonlinear viscous damping system to provide a viscous damping ratio under elastic conditions of $\beta_{VI} = 0.20$ in the MCE is described as example No.7 in Section 8 and is shown in Figure 8-7. It may be noted that this frame is the same frame of example No.6, with higher damping. Summary calculations for this frame are presented in Table F-4 for the maximum considered earthquake.

TABLE F-1 Modal Properties of Frame 3S-80

Quantity	Mode 1	Mode 2	Mode 3	Residual Mode
T_m , sec	1.52	0.48	0.24	0.608
$\{\phi_{im}\}$	1.000	1.000	1.000	1.0000
	0.655	-0.555	-1.578	-0.2088
	0.248	-0.711	1.992	-1.6348
\bar{W}_m , kN	5861	1128	378	1506
Γ_m	1.3994	-0.5357	0.1363	-0.3994

TABLE F-2 Modal Response Calculations for Example No.6: 3-Story Frame ($V_{\min}=0.80V$) with 10% NonLinear Viscous Damping in the DBE.

Analysis for the DBE

Quantity	Units	Mode 1 (m=1)	Mode 2 (m=2)	Mode 3 (m=3)	Mode R (m=R)	SRSS	
						ELF	RSA
1. Elastic Response							
Damping Ratio, β_{Ve}		0.100	0.101	0.075	0.114		
Total Damping Ratio, β_{V+I}		0.150	0.151	0.125	0.164		
Damping Coefficient, B_m		1.350	1.353	1.275	1.392		
Elastic Displacement, D_{em}	mm	235	23	2	26		
2. Roof Displacement and Base Shear							
Assumed Ductility, μ		1.27	1	1	1		
Effective Period, T_{ID}	sec	1.713	0.480	0.240	0.608		
Eff. Visc. Damp. Ratio, $\beta_v \mu^{1-\frac{\alpha}{2}}$		0.120	0.101	0.075	0.114		
Hysteretic Damping, β_H		0.063	0	0	0		
Effective Damping, β_m		0.232	0.151	0.125	0.164		
Damping Coefficient, B_m		1.596	1.353	1.275	1.392		
Displacement, D_{mD}	mm	224					
Corrected Displacement, D_{mD}	mm	235	23	2	26		
Seismic Coefficient, C_s		0.106	0.358	0.380	0.348		
Seismic Base Shear, V_m	kN	624	404	144	524	815	757
Yield Displacement, D_y	mm	176	-----	-----	-----		
Computed Ductility, μ		1.33	-----	-----	-----		
3. Response at Stage of Maximum Displacement							
Lateral Floor Displacement, δ_{ij}	mm	235	23	2	26		
		154	-13	-2	-5		
		58	-16	3	-43		
Story Drift, Δ_{jm}	mm	81	35	4	31	87	88
		96	4	-5	37	103	96
		58	-16	3	-43	72	61
Design Lateral Forces, F_{im}	kN	233	301	81	218		
		283	-309	-237	-84		
		107	-396	299	-660		
Floor Acceleration, A_{im}	g	0.307	0.396	0.107	0.287	0.420	0.512
		0.201	-0.220	-0.169	-0.060	0.210	0.342
		0.076	-0.282	0.213	-0.469	0.475	0.361
Actual Story Shear Forces, V_{jm}	kN	481	620	168	450	659	803
		1065	-17	-322	276	1100	1112
		1286	-833	296	-1084	1682	1560

TABLE F-2 continued

4. Response at Stage of Maximum Velocity							
Drift Velocity, ∇_{im}	mm/sec	297	461	103	325	440	559
		351	46	-143	383	520	382
		214	-211	80	-439	489	311
Force in Damping Devices, $F_{d_{jm}}$	kN	235	182	41	128	268	300
		255	17	-52	139	291	261
		199	-98	37	-205	286	225
Horizontal Damper Force, $V_{d_{jm}}$	kN	208	162	36	114		
		226	15	-46	124		
		176	-87	33	-181		
5. Response at Stage of Maximum Acceleration							
Ductility, μ		1.33	1.00	1.00	1.00		
Ef. Visc. Damp. Rat. $\beta_1 + \beta_V \mu^{1-\frac{a}{2}}$		0.174	0.151	0.125	0.164		
Parameter δ		0.290	0.293	0.245	0.317		
Coefficient CF_1		0.958	0.957	0.970	0.950		
Product $CF_1 \cdot \mu$		1.277	0.957	0.970	0.950		
Force Coefficient, CF_1 or C_{mFD}		1.000	0.957	0.970	0.950		
Force Coefficient, CF_2 or C_{mFV}		0.535	0.289	0.243	0.312		
Max.Floor Acc., $A_{im,max}$	g	0.378	0.409	0.109	0.295	0.480	0.568
		0.204	0.225	0.171	0.058	0.213	0.349
		0.085	0.280	0.213	0.478	0.486	0.362
Maximum Story Shear, $V_{jm,max}$ (actual)	kN	593	641	171	463	752	889
		1186	20	323	301	1223	1229
		1380	823	295	1087	1757	1633

TABLE F-3 Modal Response Calculations for Example No.6: 3-Story Frame ($V_{\min}=0.80V$) with 10% NonLinear Viscous Damping in the DBE.

Analysis for the MCE

Quantity	Units	Mode 1 (m=1)	Mode 2 (m=2)	Mode 3 (m=3)	Mode R (m=R)	SRSS	
						ELF	RSA
1. Elastic Response							
Damping Ratio, β_{ve}		0.082	0.091	0.067	0.103		
Total Damping Ratio, β_{v+l}		0.132	0.141	0.117	0.153		
Damping Coefficient, B_m		1.296	1.323	1.251	1.359		
Elastic Displacement, D_{em}	mm	367	35	2	40		
2. Roof Displacement and Base Shear							
Assumed Ductility, μ		2.02	1	1	1		
Effective Period, T_{ID}	sec	2.160	0.480	0.240	0.608		
Eff. Visc. Damp. Ratio, $\beta_v \mu^{1-\frac{\alpha}{2}}$		0.139	0.091	0.067	0.103		
Hysteretic Damping, β_H		0.149	0	0	0		
Effective Damping, β_m		0.338	0.141	0.117	0.153		
Damping Coefficient, B_m		1.914	1.323	1.251	1.359		
Displacement, D_{mD}	mm	353					
Corrected Displacement, D_{mD}	mm	367	35	2	40		
Seismic Coefficient, C_s		0.106	0.550	0.581	0.535		
Seismic Base Shear, V_m	kN	619	620	219	806	1016	903
Yield Displacement, D_y	mm	175	-----	-----	-----		
Computed Ductility, μ		2.10	-----	-----	-----		
3. Response at Stage of Maximum Displacement							
Lateral Floor Displacement, δ_{ij}	mm	367	35	2	40		
		240	-19	-4	-8		
		91	-25	5	-65		
Story Drift, Δ_{jm}	mm	127	54	6	48	136	138
		149	5	-8	57	160	150
		91	-25	5	-65	112	94
Design Lateral Forces, F_{im}	kN	231	461	124	335		
		281	-474	-363	-129		
		106	-607	458	-1013		
Floor Acceleration, A_{im}	g	0.305	0.607	0.163	0.441	0.536	0.699
		0.200	-0.337	-0.258	-0.092	0.220	0.469
		0.076	-0.432	0.326	-0.721	0.725	0.546
Actual Story Shear Forces, V_{jm}	kN	477	952	256	691	840	1095
		1056	-26	-492	424	1138	1165
		1275	-1278	452	-1666	2098	1861

TABLE F-3 continued

4. Response at Stage of Maximum Velocity							
Drift Velocity, ∇_{im}	mm/sec	368	708	158	499	620	813
		435	71	-219	589	732	492
		265	-324	122	-675	725	436
Force in Damping Devices, $F_{d_{jm}}$	kN	261	251	56	177	316	367
		284	23	-71	192	343	294
		222	-135	51	-283	359	265
Horizontal Damper Force, $V_{d_{jm}}$	kN	232	223	50	157		
		252	21	-63	171		
		196	-120	45	-250		
5. Response at Stage of Maximum Acceleration							
Ductility, μ		2.10	1.00	1.00	1.00		
Ef. Visc. Damp. Rat $\beta_1 + \beta_V \mu^{1-\frac{\alpha}{2}}$		0.193	0.141	0.117	0.153		
Parameter δ		0.311	0.275	0.230	0.297		
Coefficient CF_1		0.952	0.962	0.974	0.956		
Product $CF_1 \cdot \mu$		1.998	0.962	0.974	0.956		
Force Coefficient, CF_1 or C_{mFD}		1.000	0.962	0.974	0.956		
Force Coefficient, CF_2 or C_{mFV}		0.553	0.271	0.228	0.293		
Max. Floor Acc., $A_{im,max}$	g	0.386	0.623	0.166	0.451	0.594	0.752
		0.203	0.343	0.260	0.089	0.222	0.476
		0.086	0.429	0.326	0.732	0.737	0.545
Maximum Story Shear, $V_{j_{m,max}}$ (actual)	kN	605	976	261	707	930	1178
		1195	30	493	455	1279	1293
		1384	1263	451	1666	2166	1927

TABLE F-4 Modal Response Calculations for Example No.7: 3-Story Frame ($V_{\min}=0.80V$) with 20% NonLinear Viscous Damping in the MCE.

Analysis for the MCE

Quantity	Units	Mode 1 (m=1)	Mode 2 (m=2)	Mode 3 (m=3)	Mode R (m=R)	SRSS	
						ELF	RSA
1. Elastic Response							
Damping Ratio, β_{ve}		0.200	0.212	0.156	0.239		
Total Damping Ratio, β_{v+l}		0.250	0.262	0.206	0.289		
Damping Coefficient, B_m		1.650	1.686	1.518	1.767		
Elastic Displacement, D_{em}	mm	288	27	2	31		
2. Roof Displacement and Base Shear							
Assumed Ductility, μ		1.53	1	1	1		
Effective Period, T_{ID}	sec	1.880	0.480	0.240	0.608		
Eff. Visc. Damp. Ratio, $\beta_v \mu^{1-\frac{\alpha}{2}}$		0.275	0.212	0.156	0.239		
Hysteretic Damping, β_H		0.102	0	0	0		
Effective Damping, β_m		0.427	0.262	0.206	0.289		
Damping Coefficient, B_m		2.181	1.686	1.518	1.767		
Displacement, D_{mD}	mm	270					
Corrected Displacement, D_{mD}	mm	288	27	2	31		
Seismic Coefficient, C_s		0.106	0.431	0.479	0.412		
Seismic Base Shear, V_m	kN	624	487	181	620	879	812
Yield Displacement, D_y	mm	176	-----	-----	-----		
Computed Ductility, μ		1.63	-----	-----	-----		
3. Response at Stage of Maximum Displacement							
Lateral Floor Displacement, δ_{ij}	mm	288	27	2	31		
		189	-15	-3	-6		
		72	-19	4	-50		
Story Drift, Δ_{jm}	mm	99	42	5	37	106	108
		117	4	-7	44	125	118
		72	-19	4	-50	87	74
Design Lateral Forces, F_{im}	kN	233	362	102	258		
		283	-372	-299	-100		
		107	-476	377	-779		
Floor Acceleration, A_{im}	g	0.307	0.477	0.135	0.339	0.457	0.583
		0.201	-0.265	-0.213	-0.071	0.213	0.394
		0.076	-0.339	0.268	-0.554	0.559	0.439
Actual Story Shear Forces, V_{jm}	kN	481	747	211	531	717	913
		1065	-20	-405	326	1114	1139
		1286	-1003	373	-1281	1815	1673

TABLE F-4 continued

4. Response at Stage of Maximum Velocity							
Drift Velocity, ∇_{im}	mm/sec	332	555	130	384	508	660
		392	56	-180	453	599	435
		239	-254	101	-519	572	363
Force in Damping Devices, $F_{d_{jm}}$	kN	549	459	108	317	634	724
		597	42	-137	345	689	614
		466	-248	98	-506	688	537
Horizontal Damper Force, $V_{d_{jm}}$	kN	487	407	95	281		
		529	38	-121	305		
		413	-219	87	-449		
5. Response at Stage of Maximum Acceleration							
Ductility, μ		1.63	1.00	1.00	1.00		
Ef. Visc. Damp. Rat. $\beta_l + \beta_v \mu^{1-\frac{\alpha}{2}}$		0.339	0.262	0.206	0.289		
Parameter δ		0.453	0.483	0.391	0.524		
Coefficient CF_1		0.899	0.886	0.925	0.866		
Product $CF_1 \cdot \mu$		1.470	0.886	0.925	0.866		
Force Coefficient, CF_1 or C_{mFD}		1.000	0.886	0.925	0.866		
Force Coefficient, CF_2 or C_{mFV}		0.661	0.464	0.381	0.500		
Max. Floor Acc., $A_{im,max}$	g	0.513	0.543	0.148	0.383	0.640	0.761
		0.211	0.293	0.225	0.065	0.221	0.426
		0.103	0.341	0.275	0.610	0.619	0.450
Maximum Story Shear, $V_{j_{m,max}}$ (actual)	kN	803	850	231	601	1003	1192
		1415	35	421	435	1480	1476
		1559	990	378	1334	2051	1885

APPENDIX G

DETAILED CALCULATIONS FOR THE SIMPLIFIED ANALYSIS OF A 3-STORY FRAME WITH VISCOELASTIC DAMPING SYSTEM

G.1 Introduction

This appendix presents detailed calculations in the application of the equivalent lateral force (ELF) and response-spectrum analysis (RSA) procedures of NEHRP (2000) for the analysis of buildings with viscoelastic damping systems. These procedures are applied as described in Appendix A subject to the modifications described in Sections 7.5.3 and 8.1 herein. The presentation in the appendix consists of detailed calculations for the 3-story special steel moment frame 3S-75 shown in Figure 8-8 and denoted as example No.8 in Section 8.

G.2 Detailed Calculations for 3-Story Frame 3S-75 with Viscoelastic Damping System

Parameters

The seismic tributary weights are: for the third floor 1567 kN, and 2900 kN for the second and first floors. The design coefficients per Table 5.2.2 of the 1997 NEHRP Recommended Provisions for special steel moment frames are: $R = 8.0$, $\Omega_o = 3.0$, $C_d = 5.5$, and $I = 1.0$.

Description of the System

The analyzed frame is the 3-story special steel moment frame with a viscoelastic damping system shown in Figure 8-8. The damping system in the frame consists of solid viscoelastic damping devices installed in the diagonal configuration, made of material 3M ISD110 (Zimmer, 1999), and designed to sustain 100% strain in the MCE. Each of these devices has a bonded area of $A_b = 626,330 \text{ mm}^2$ and thickness $h = 140 \text{ mm}$ with approximate storage- and loss-shear moduli $G' \approx G'' = 0.83 \text{ MPa}$ at a temperature of 20°C and frequency of about 0.7Hz in the first mode. The corresponding stiffness and damping constant are, respectively, $K = 3.71 \text{ kN/mm}$ and $C = 0.871 \text{ kN.s/mm}$. The damping ratio in the fundamental mode of vibration of the frame is $\beta_{vl} = 0.086$ (damping provided by the damping system) plus an assumed inherent damping ratio $\beta_l =$

0.05 for a total damping ratio of $\beta_{VI} + \beta_I = 0.136$. The corresponding damping coefficient is $B_{V+I} = 1.308$ (Table A13.3.1). Using Section A13.2.4.1 of NEHRP (2000), the seismic base shear for the design of this frame is controlled by $V_{min} = V/B_{V+I}$ (per eq. A13.2.4.1-1), where the seismic base shear V has been determined in Section B.3 to be 788.5 kN, so that $V_{min} = 788.5/1.308 = 602.8$ kN. The required base shear strength of the frame V_y per (7-72) is $V_y = 602.8 \times 3 \times 5.5/8 = 1243.3$ kN. The base shear strength of the frame (inclusive of the damping devices) is $V_y = 1482$ kN (see example C-7) which is larger than the required base shear strength. Example C-7 also gives the yield displacement of the system $D_y = 182$ mm, the initial stiffness, $K_e = 8.10$ kN/mm, and the post-elastic stiffness, $\alpha K_e = 1.39$ kN/mm.

Eigenvalue analysis of the frame using program SAP-2000NL (using springs of stiffness K corresponding to a frequency of 0.70 Hz to model the contribution of stiffness of the devices in each story) gave: $T_1 = 1.473$ sec, $\{\phi_{i1}\}^T = [1.000 \ 0.683 \ 0.275]$, $T_2 = 0.475$ sec, $\{\phi_{i2}\}^T = [1.000 \ -0.498 \ -0.698]$ and $T_3 = 0.253$ sec, $\{\phi_{i3}\}^T = [1.000 \ -1.504 \ 1.911]$. These properties, the modal weights and participations factors are presented in Table G-1. Note that the higher mode periods and shapes could be calculated using the stiffness of the viscoelastic devices at the respective modal frequencies (not 0.7 Hz). However, such an approach produces mode shapes that do not satisfy the orthogonality conditions.

Viscous Damping Ratio under Elastic Conditions

Equation (7-29) was used to calculate the damping ratio in each mode with $f_j = \cos \theta_j$, where $\theta_j = 27.6^\circ$ (see Figure 8-2). To start-off the analysis for the first mode, its period was estimated as 0.70 Hz using (7-49) as shown in example C7 of Appendix C. The damping ratio under elastic conditions using $C = 0.871$ kN.s/mm was $\beta_{VI} = 0.086$. Because of the frequency dependence of these properties, properties were re-evaluated for higher modes. The procedure for each higher mode started by assuming that its frequency was equal to the frequency calculated by eigenvalue analysis using properties calculated for a frequency equal to the first mode frequency. Using the calculated higher mode frequency, the storage and loss shear moduli, G' and G'' , respectively, were obtained from Figure G-1. The storage stiffness K_j was then calculated using (7-43). The higher mode frequency and corresponding eigenvectors were then calculated by eigenvalue

analysis of the frame with spring constant K_j in each story. This process was repeated until the calculated and assumed frequencies converged. The damping constant C_j and damping ratio β_v were then calculated using the modal frequency corresponding to the actual period in Table G-2 and the mode shape shown in the same table. Within the context of approximate analysis, the calculation of the damping ratios could have been instead based on the modal properties in Table G-1. The result would have been slightly different values of damping ratios for the second and third modes. For the residual mode, the damping constant of the device and damping ratio were directly evaluated by using the frequency corresponding to $T_R = 0.4T_1$ and the eigenvectors obtained from the eigenvalue analysis for the first mode. Table G-2 summarizes the calculations of the elastic period T_m , damping constant C_j and viscous damping β_{vm} ratio under elastic conditions for each mode.

FIRST-MODE RESPONSE ($T_1=1.473$ sec)

Roof Displacement

Assumed Effective Ductility: $\mu_D = 1.21$

Parameter α : $\alpha = 2\beta_{v1}/\eta = 2 \times 0.086 / 1 = 0.172$ (7-53)

Effective Period: $T_{ID} = 1.473 \sqrt{\frac{1.21}{1 + 0.172 \times 1.21 - 0.172}} = 1.592 \text{ sec}$ (7-50)

Effective Damping Ratio:

Quality Factor: $q_H = 0.67 \times \frac{0.6}{1.592} = 0.253 < 0.50$ (A13.3.3-1)

use $q_H = 0.50$

Hysteretic Damping: $\beta_{HD} = (0.64 - 0.05) \times 0.5 \times \left(\frac{1}{1 + 0.172 \times 1.21 - 0.172} - \frac{1}{1.21} \right) = 0.041$ (7-51)

Effective Damping: $\beta_{ID} = 0.05 + 0.086 \sqrt{\frac{1.21}{1 + 0.172 \times 1.21 - 0.172}} + 0.041 = 0.184$ (7-51)

Damping Coefficient: $B_{ID} = 1.452$ (Table A13.3.1)

Roof Displacement: $D_{ID} = \left(\frac{9810}{4\pi^2} \right) \times |1.361| \times \frac{0.6}{1.452} \times 1.592 = 222.48 \text{ mm}$ (A13.3.2-1)

Corrected Roof Displacement:

The effective viscous damping ratio is $\beta_{v+I} = 0.086 + 0.05 = 0.135$, and the corresponding damping coefficient from Table (A13.3.1) is $B_{v+I} = 1.308$. Accordingly, the displacement of the roof for elastic behavior is

$$D = \left(\frac{9810}{4\pi^2} \right) \times |1.361| \times \frac{0.6}{1.308} \times 1.473 = 228.51 \text{ mm}$$

Since $D_{ID} < D$, use $D_{ID} = 228.51 \text{ mm}$

Base Shear

$$\text{Seismic Coefficient: } C_{SI} = \left(\frac{8}{5.5} \right) \times \frac{0.6}{1.592 \times 3 \times 1.452} = 0.1259 \quad (\text{A13.4.3.4-2})$$

$$\text{Base Shear: } V_I = 0.1259 \times 5991.7 = 754 \text{ kN} \quad (\text{A13.4.3.2-1})$$

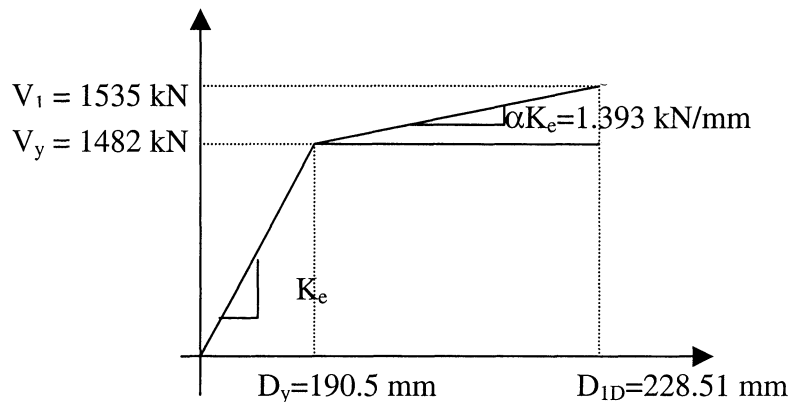
Displacement at Effective Yield (Yield Displacement)

$$D_y = \left(\frac{9810}{4\pi^2} \right) \times \left(\frac{3 \times 5.5}{8} \right) \times |1.361| \times 0.1259 \times 1.473^2 = 190.5 \text{ mm} \quad (\text{A13.3.4-3})$$

$$\text{Effective Ductility Demand: } \mu_D = \frac{228.51}{190.5} = 1.20 \quad (\text{A13.3.4-1})$$

$$\mu_D < \mu_{max} = \frac{8}{3 \times 1.0} = 2.67$$

The contribution of the restoring force from the devices must be added to the yield strength of the frame to obtain its base shear strength at displacement D_{ID} and compare it with the calculated one.



The contribution of the restoring force to the base shear is

$$V_{IR} = 1.393 \times (228.51 - 190.50) = 53 \text{ kN}$$

The base shear strength at displacement D_{ID} is

$$V_I = 1482 + 53 = 1535 \text{ kN}$$

The contribution of the first mode to the base shear strength of the frame is given by (7-72)

$$V_I = 754 \times \left(\frac{3 \times 5.5}{8} \right) = 1555 \text{ kN}$$

This compares well with the base shear strength at displacement D_{ID} , taking into account that the base shear force of 754 kN includes the contribution of the damper restoring force, which is an actual force, and should not be multiplied by the factor in parenthesis. Since this contribution is small, it is acceptable for simplified analysis.

Response at Stage of Maximum Displacement

Lateral Floor Displacements, δ_{iID} , and Story Drifts, Δ_{iID}

$$\delta_{iID} = 228.51 \times \begin{Bmatrix} 1.000 \\ 0.683 \\ 0.275 \end{Bmatrix} = \begin{Bmatrix} 228.51 \\ 156.07 \\ 62.84 \end{Bmatrix} \text{ mm} \quad (\text{A13.4.4.2-1})$$

$$\Delta_{iID} = \begin{Bmatrix} 72.44 \\ 93.23 \\ 62.84 \end{Bmatrix} \text{ mm}$$

Design Lateral Forces, F_{iI} , Design Story Shears, V_{iI} , and Accelerations, A_{iI}

$$F_{iI} = \begin{Bmatrix} 1567 \times 1.000 \times \frac{1.361}{5991.7} \times 754 \\ 2900 \times 0.683 \times \frac{1.361}{5991.7} \times 754 \\ 2900 \times 0.275 \times \frac{1.361}{5991.7} \times 754 \end{Bmatrix} = \begin{Bmatrix} 268.34 \\ 339.23 \\ 136.59 \end{Bmatrix} \text{ kN} \quad (\text{A13.4.3.9-1})$$

$$A_{iI} = \frac{F_{iI}}{w_i} \cdot \left(\frac{C_d \Omega_o}{R} \right) = \begin{Bmatrix} \frac{268.34}{1567} \\ \frac{339.23}{2900} \\ \frac{136.59}{2900} \end{Bmatrix} \times \left(\frac{3 \times 5.5}{8} \right) = \begin{Bmatrix} 0.353 \\ 0.241 \\ 0.097 \end{Bmatrix} g$$

$$V_{i1} = \begin{Bmatrix} 268.34 \\ 607.57 \\ 744.16 \end{Bmatrix} \text{ kN}$$

Damper Axial Restoring Force F_{ir1}

$$F_{ir1} = Kd_{i1D} \cdot \Delta_{i1D} \cdot \cos \theta_i, \quad F_{ir1} = 3.71 \times \begin{Bmatrix} 72.44 \\ 93.23 \\ 62.84 \end{Bmatrix} \times \cos 27.6^\circ = \begin{Bmatrix} 238.17 \\ 306.52 \\ 206.61 \end{Bmatrix} \text{ kN}$$

Response at Stage of Maximum Velocity

Story Velocity, ∇_{i1D}

$$\nabla_{i1D} = \frac{2\pi}{1.592} \begin{Bmatrix} 72.44 \\ 93.23 \\ 62.84 \end{Bmatrix} = \begin{Bmatrix} 285.90 \\ 367.95 \\ 248.01 \end{Bmatrix} \text{ mm/sec} \quad (\text{A13.5.4.5-1})$$

Force in Damping Devices, Fd_{i1D}

$$Fd_{i1D} = 0.871 \times \begin{Bmatrix} 285.90 \\ 367.95 \\ 248.01 \end{Bmatrix} \cos 27.6^\circ = \begin{Bmatrix} 220.68 \\ 284.01 \\ 191.44 \end{Bmatrix} \text{ kN} \quad (7-23)$$

Horizontal Component of Damping Forces, Vd_{i1D}

$$Vd_{i1D} = \begin{Bmatrix} 220.68 \\ 284.01 \\ 191.44 \end{Bmatrix} \cos 27.6^\circ = \begin{Bmatrix} 195.57 \\ 251.69 \\ 169.66 \end{Bmatrix} \text{ kN}$$

Horizontal Inertia Forces, F_{iD1}

$$F_{iD1} = \begin{Bmatrix} 195.57 \\ 251.69 - 195.57 \\ 169.66 - 251.69 \end{Bmatrix} = \begin{Bmatrix} 195.57 \\ 56.12 \\ -82.03 \end{Bmatrix} \text{ kN}$$

Maximum Axial Damping Force, F_{D11}

The response at maximum velocity is obtained as the combination of the viscous and the restoring force components of the dampers as follows:

Storage and Loss Shear Moduli: $G'(\omega) = G''(\omega) = 0.83 \text{ MPa}$ (Table G-2)

Loss Factor: $\eta = \frac{G''(\omega)}{G'(\omega)} = 1.0$ (7-44)

$$\begin{aligned} \tan^{-1} \eta &= \tan^{-1} (1.0) = 0.785 \\ \cos (\tan^{-1} \eta) &= \cos (0.785) = 0.707 \\ \sin (\tan^{-1} \eta) &= \sin (0.785) = 0.707 \end{aligned}$$

$$F_{D_{i1}} = 0.707 \times \begin{Bmatrix} |238.17| \\ |306.52| \\ |206.61| \end{Bmatrix} + 0.707 \times \begin{Bmatrix} |220.68| \\ |284.01| \\ |191.44| \end{Bmatrix} = \begin{Bmatrix} 324 \\ 418 \\ 281 \end{Bmatrix} \text{ kN}$$

Response at Stage of Maximum Acceleration

Force Coefficients

Ductility demand: $\mu_D = 1.20$

Effective viscous damping: $\beta_{eff} = 0.05 + 0.086 \sqrt{\frac{1.20}{1 + 0.172 \times 1.20 - 0.172}} = 0.143$ (7-51)

Parameter δ : $\delta = \tan^{-1} (2 \times 0.143) = 0.279$ (4-36)

Force Coefficient CF_1 :

$$CF_1 = \cos (0.279) = 0.961$$

$$CF_1 \mu = 0.961 \times 1.20 = 1.15 > 1.000 \quad \text{use } CF_1 = 1.0 \quad (4-41)$$

Force Coefficient CF_2 : $CF_2 = \sin (0.279) = 0.275$ (4-39)

Maximum Lateral Inertia Forces

$$F_{i1,max} = CF_1 \cdot |F_{i1}|_{Max Disp} \cdot \frac{C_d \Omega_o}{R} + CF_2 \cdot |F_{i_{D1}}|_{Max Velocity}$$

$$F_{i1,max} = 1.0 \times \begin{Bmatrix} |268.34| \\ |339.23| \\ |136.59| \end{Bmatrix} \times \left(\frac{3 \times 5.5}{8} \right) + 0.275 \times \begin{Bmatrix} |195.57| \\ |56.12| \\ |-82.03| \end{Bmatrix} = \begin{Bmatrix} 607 \\ 715 \\ 304 \end{Bmatrix} \text{ kN}$$

Maximum Acceleration, $A_{i1,max}$

$$A_{i1,max} = \frac{F_{i1,max}}{w_i} = \left\{ \begin{array}{l} \frac{607}{1567} \\ \frac{715}{2900} \\ \frac{304}{2900} \end{array} \right\} = \left\{ \begin{array}{l} 0.387 \\ 0.247 \\ 0.105 \end{array} \right\} g$$

Maximum Story Shear, $V_{i1,max}$

$$V_{i1,max} = 1.0 \times \left\{ \begin{array}{l} 268.34 \\ 607.57 \\ 744.16 \end{array} \right\} \times \frac{5.5 \times 3}{8} + 0.275 \times \left\{ \begin{array}{l} 195.57 \\ 251.69 \\ 169.96 \end{array} \right\} = \left\{ \begin{array}{l} 607 \\ 1322 \\ 1582 \end{array} \right\} kN$$

SECOND MODE RESPONSE ($T_2 = 0.475$ sec)

Elastic Response

Viscous Damping Ratio: $\beta_{v2} = 0.149$

Effective Damping Ratio: $\beta_{2D} = 0.05 + 0.149 = 0.199$ (A13.3.2-1)

Damping Coefficient: $B_{1D} = 1.497$ (Table A13.3.1)

Roof Displacement: $D_{2D} = \left(\frac{9810}{4\pi^2} \right) \times |-0.505| \times \frac{1.0 \times 0.475^2}{1.497} = 18.91 \text{ mm}$ (A13.5.4.3-2)

Base Shear

Seismic Coefficient: $C_{S2} = \left(\frac{8}{5.5} \right) \times \frac{1.0}{3 \times 1.497} = 0.3239$ (A13.5.3.6-2)

Base Shear: $V_2 = 0.3239 \times 973.6 = 315.35 \text{ kN}$ (A13.5.3.2-1)

Required base shear strength: $V_2 = 315.35 \times \left(\frac{3 \times 5.5}{8} \right) = 650 \text{ kN}$

Response at Stage of Maximum Displacement

Lateral Floor Displacement, δ_{i_2D} , and Story Drifts, Δ_{i_2D}

$$\delta_{i_2D} = 18.91 \times \begin{Bmatrix} 1.000 \\ -0.498 \\ -0.698 \end{Bmatrix} = \begin{Bmatrix} 18.91 \\ -9.42 \\ -13.20 \end{Bmatrix} \text{ mm} \quad (\text{A13.5.4.2-1})$$

$$\Delta_{i_2D} = \begin{Bmatrix} 28.33 \\ 3.78 \\ -13.20 \end{Bmatrix} \text{ mm}$$

Design Lateral Forces, F_{i_2}

$$F_{i_2} = \begin{Bmatrix} 1567 \times 1.000 \times \frac{|-0.505|}{973.6} \times 315.35 \\ 2900 \times (-0.498) \times \frac{|-0.505|}{973.6} \times 315.35 \\ 2900 \times (-0.698) \times \frac{|-0.505|}{973.6} \times 315.35 \end{Bmatrix} = \begin{Bmatrix} 256.31 \\ -236.22 \\ -331.11 \end{Bmatrix} \text{ kN} \quad (\text{A13.5.3.7-1})$$

Floor Acceleration, A_{i_2}

$$A_{i_2} = \frac{F_{i_2} \cdot \left(\frac{\Omega_o C_d}{R} \right)}{w_i} = \begin{Bmatrix} \frac{256.31}{1567} \\ -236.22 \\ \frac{2900}{-331.10} \\ \frac{2900}{2900} \end{Bmatrix} \times \left(\frac{3 \times 5.5}{8} \right) = \begin{Bmatrix} 0.337 \\ -0.168 \\ -0.236 \end{Bmatrix} \text{ g}$$

Story Shears, V_{i_2}

$$V_{i_2} = \begin{Bmatrix} 256.31 \\ 20.09 \\ -311.01 \end{Bmatrix} \text{ kN}$$

Damper Axial Restoring Force F_{ir_2}

$$F_{ir_2} = K d_{i_2D} \cdot \Delta_{i_2D} \cdot \cos \theta_i$$

$$K_{j_2} = \frac{G'(\omega) A_b}{h} = \frac{1.90 \times 10^{-3} \times 626330}{140} = 8.5 \text{ kN/mm}$$

$$F_{ir_2} = 8.5 \times \begin{Bmatrix} 28.33 \\ 3.78 \\ -13.20 \end{Bmatrix} \cos 27.6^\circ = \begin{Bmatrix} 213.40 \\ 28.47 \\ -99.43 \end{Bmatrix} \text{ kN}$$

Response at Stage of Maximum Velocity

Story Velocity, ∇_{i_2D}

$$\nabla_{i_2D} = \frac{2\pi}{0.475} \begin{Bmatrix} 28.33 \\ 3.78 \\ -13.20 \end{Bmatrix} = \begin{Bmatrix} 374.74 \\ 50.00 \\ -174.61 \end{Bmatrix} \text{ mm/sec} \quad (\text{A13.5.4.5-2})$$

Forces in Damping Devices, Fd_{i_2D}

$$Fd_{i_2D} = 0.730 \times \begin{Bmatrix} 374.74 \\ 50.00 \\ -174.61 \end{Bmatrix} \times \cos 27.6^\circ = \begin{Bmatrix} 242.43 \\ 32.35 \\ -112.96 \end{Bmatrix} \text{ kN} \quad (7-23)$$

Horizontal component of Damping Forces, Vd_{i_2D}

$$Vd_{i_2D} = \begin{Bmatrix} 242.43 \\ 32.35 \\ -112.96 \end{Bmatrix} \times \cos 27.6^\circ = \begin{Bmatrix} 214.84 \\ 28.67 \\ -100.11 \end{Bmatrix} \text{ kN}$$

Maximum Axial Damping Force, $F_{D_{i_2}}$

Storage and Loss Shear Moduli: $G'(\omega) = 1.90 \text{ MPa}$; $G''(\omega) = 2.30 \text{ MPa}$ (Table G-2)

Loss Factor:
$$\eta = \frac{G''(\omega)}{G'(\omega)} = \frac{2.30}{1.90} = 1.211 \quad (7-44)$$

Maximum Axial Damping Force

$$\begin{aligned} \tan^{-1} \eta &= \tan^{-1} (1.211) = 0.8803 \\ \cos (\tan^{-1} \eta) &= \cos (0.8803) = 0.6369 \\ \sin (\tan^{-1} \eta) &= \sin (0.8803) = 0.7709 \end{aligned}$$

$$F_{D_{i2}} = 0.6369 \times \begin{Bmatrix} |213.40| \\ |28.47| \\ |-99.43| \end{Bmatrix} + 0.7709 \times \begin{Bmatrix} |242.43| \\ |32.35| \\ |-112.96| \end{Bmatrix} = \begin{Bmatrix} 323 \\ 43 \\ 150 \end{Bmatrix} \text{ kN}$$

Response at Stage of Maximum Acceleration

Force Coefficients

Effective viscous damping ratio: $\beta_{\text{eff}} = 0.05 + 0.149 = 0.199$

Parameter δ
$$\delta = \tan^{-1} (2 \times 0.199) = 0.379 \quad (4-36)$$

Force coefficient CF_1 :
$$CF_1 = \cos (0.379) = 0.929 \quad (4-41)$$

Force Coefficient CF_2 :
$$CF_2 = \sin (0.379) = 0.370 \quad (4-39)$$

Maximum Lateral Inertia Forces

$$F_{i2,max} = 0.929 \times \begin{Bmatrix} |256.31| \\ |-236.22| \\ |-331.10| \end{Bmatrix} \times \left(\frac{3 \times 5.5}{8} \right) + 0.370 \times \begin{Bmatrix} |214.84| \\ |-186.17| \\ |-128.78| \end{Bmatrix} = \begin{Bmatrix} 570.06 \\ 521.50 \\ 682.06 \end{Bmatrix} \text{ kN}$$

Maximum Acceleration

$$A_{i2,max} = F_{i2,max} / w_i \quad , \quad A_{i2,max} = \begin{Bmatrix} 570.60/1567 \\ 521.50/2900 \\ 682.06/2900 \end{Bmatrix} = \begin{Bmatrix} 0.364 \\ 0.180 \\ 0.235 \end{Bmatrix}$$

Maximum Story Shear, $V_{i_2,max}$

$$V_{i_2,max} = CF_1 \cdot |V_{i_2}|_{Max\ Disp} \cdot \frac{C_d \Omega_o}{R} + CF_2 \cdot |Vd_{i_2D}|_{Max\ Velocity}$$
$$V_{i_2,max} = 0.929 \times \begin{Bmatrix} |256.31| \\ |20.09| \\ |-311.01| \end{Bmatrix} \times \left(\frac{3 \times 5.5}{8} \right) + 0.370 \times \begin{Bmatrix} |214.84| \\ |28.67| \\ |-100.11| \end{Bmatrix} = \begin{Bmatrix} 571 \\ 49 \\ 633 \end{Bmatrix} \text{ kN}$$

THIRD MODE RESPONSE ($T_3 = 0.253$ sec)

Elastic Response

Viscous Damping Ratio: $\beta_v = 0.076$ (TABLE G-2)

Effective damping ratio: $\beta_{3D} = 0.05 + 0.076 = 0.126$ (A13.3.3-1)

Damping Coefficient: $B_{3D} = 1.278$ (Table A13.3.1)

Roof Displacement, D_{3D} :

$$D_{3D} = \left(\frac{9810}{4\pi^2} \right) \times |0.144| \times \frac{1.0 \times 0.253^2}{1.503} = 1.79 \text{ mm} \quad (\text{A13.5.4.3-2})$$

Base Shear

Seismic Coefficient: $C_{s3} = \left(\frac{8}{5.5} \right) \times \frac{1.0}{3 \times 1.278} = 0.3794$ (A13.5.3.6-2)

Base Shear: $V_3 = 0.3794 \times 401.7 = 152.41 \text{ kN}$ (A13.5.3.2-1)

Required Base Shear Strength: $V_3 = \left(\frac{3 \times 5.5}{8} \right) \times 152.41 = 314 \text{ kN}$

Response at Stage of Maximum Displacement

Lateral Floor Displacement, $\delta_{i_{3D}}$, and Story Drifts, $\Delta_{i_{3D}}$

$$\delta_{i_{3D}} = 1.79 \times \begin{Bmatrix} 1.000 \\ -1.504 \\ 1.911 \end{Bmatrix} = \begin{Bmatrix} 1.79 \\ -2.69 \\ 3.42 \end{Bmatrix} \text{ mm}, \quad \Delta_{i_3} = \begin{Bmatrix} 4.48 \\ -6.11 \\ 3.42 \end{Bmatrix} \text{ mm} \quad (\text{A13.5.4.2-1})$$

Design Lateral Forces, F_{i3}

$$F_{i3} = \begin{Bmatrix} 1567 \times 1.000 \times \frac{|0.144|}{398} \times 152.41 \\ 2900 \times (-1.504) \times \frac{|0.144|}{398} \times 152.41 \\ 2900 \times 1.911 \times \frac{|0.144|}{398} \times 152.41 \end{Bmatrix} = \begin{Bmatrix} 85.61 \\ -238.30 \\ 302.78 \end{Bmatrix} \text{ kN} \quad (\text{A13.5.3.7-1})$$

Floor Accelerations, A_{i3}

$$A_{i3} = \begin{Bmatrix} \frac{85.61}{1567} \\ \frac{-238.30}{2900} \\ \frac{302.78}{2900} \end{Bmatrix} \times \left(\frac{3 \times 5.5}{8} \right) = \begin{Bmatrix} 0.113 \\ -0.170 \\ 0.215 \end{Bmatrix} \text{ g}$$

Design Story Shears, V_{i3}

$$V_{i3} = \begin{Bmatrix} 85.61 \\ -152.69 \\ 150.09 \end{Bmatrix} \text{ kN}$$

Damper Axial Restoring Force F_{ir3}

$$K_{j3} = \frac{G'(\omega)A_b}{h} = \frac{3.20 \times 10^{-3} \times 626330}{140} = 14.32 \text{ kN/mm} \quad (7.43)$$

$$F_{ir3} = K d_{i3D} \cdot \Delta_{i3D} \cdot \cos \theta_i = 14.32 \times \begin{Bmatrix} 4.48 \\ -6.11 \\ 3.42 \end{Bmatrix} \times \cos 27.6^\circ = \begin{Bmatrix} 56.85 \\ -77.54 \\ 43.40 \end{Bmatrix} \text{ kN}$$

Response at Stage of Maximum Velocity

Story Velocity, ∇_{i3D}

$$\nabla_{i3D} = \frac{2\pi}{0.253} \begin{Bmatrix} 4.48 \\ -6.11 \\ 3.42 \end{Bmatrix} = \begin{Bmatrix} 111.26 \\ -151.74 \\ 84.93 \end{Bmatrix} \text{ mm/sec} \quad (\text{A13.5.4.5-1})$$

Forces in Damping Devices, $F_{d_{i3D}}$

$$F_{d_{i3D}} = 0.456 \times \begin{Bmatrix} 111.26 \\ -151.74 \\ 84.93 \end{Bmatrix} \times \cos 27.6^\circ = \begin{Bmatrix} 44.96 \\ -61.32 \\ 34.32 \end{Bmatrix} \text{ kN} \quad (7-23)$$

Horizontal Component of the Viscous Damping Force

$$V_{d_{i3D}} = \begin{Bmatrix} 44.96 \\ -61.32 \\ 34.32 \end{Bmatrix} \cos 27.6^\circ = \begin{Bmatrix} 39.84 \\ -54.34 \\ 30.41 \end{Bmatrix} \text{ kN}$$

Maximum Axial Damping Force, $F_{D_{i3}}$

Storage and Shear Moduli: $G'(\omega) = 3.20 \text{ MPa}$; $G''(\omega) = 2.70 \text{ MPa}$ (Table G-2)

Loss Factor:
$$\eta = \frac{G''(\omega)}{G'(\omega)} = \frac{2.70}{3.20} = 0.844 \quad (7-44)$$

Maximum Axial Damping Force

$$\begin{aligned} \tan^{-1} \eta &= \tan^{-1} (0.844) = 0.701 \\ \cos (\tan^{-1} \eta) &= \cos (0.701) = 0.764 \\ \sin (\tan^{-1} \eta) &= \sin (0.701) = 0.645 \end{aligned}$$

$$F_{D_{i3}} = 0.764 \times \begin{Bmatrix} |56.85| \\ |-77.54| \\ |43.40| \end{Bmatrix} + 0.645 \times \begin{Bmatrix} |44.96| \\ |-61.32| \\ |34.32| \end{Bmatrix} = \begin{Bmatrix} 72 \\ 99 \\ 55 \end{Bmatrix} \text{ kN}$$

Response at Stage of Maximum Acceleration

Force Coefficients

Effective viscous damping ratio: $\beta_{\text{eff}} = 0.05 + 0.076 = 0.126$

Parameter δ :
$$\delta = \tan^{-1} (2 \times 0.126) = 0.247 \quad (4-36)$$

$$\text{Force coefficient } CF_1: \quad CF_1 = \cos(0.247) = 0.970 \quad (4-41)$$

$$\text{Force Coefficient } CF_2: \quad CF_2 = \sin(0.252) = 0.245 \quad (4-39)$$

Maximum Lateral Inertia Forces

$$F_{i_3,max} = 0.970 \times \begin{Bmatrix} |85.61| \\ |-238.30| \\ |302.78| \end{Bmatrix} \times \left(\frac{3 \times 5.5}{8} \right) + 0.245 \times \begin{Bmatrix} |39.84| \\ |-94.18| \\ |84.75| \end{Bmatrix} = \begin{Bmatrix} 181.03 \\ 499.82 \\ 626.51 \end{Bmatrix} \text{ kN}$$

Maximum Acceleration

$$A_{i_3,max} = F_{i_3,max} / w_i, \quad A_{i_3,max} = \begin{Bmatrix} 181.03/1567 \\ 499.82/2900 \\ 626.51/2900 \end{Bmatrix} = \begin{Bmatrix} 0.116 \\ 0.172 \\ 0.216 \end{Bmatrix}$$

Maximum Story Shear, $V_{i_2,max}$

$$V_{i_3,max} = CF_1 \cdot |V_{i_3}|_{Max\ Disp} \cdot \frac{C_d \Omega_o}{R} + CF_2 \cdot |V_{d_{i_3D}}|_{Max\ Velocity}$$

$$V_{i_3,max} = 0.970 \times \begin{Bmatrix} |85.61| \\ |-152.69| \\ |150.09| \end{Bmatrix} \times \left(\frac{3 \times 5.5}{8} \right) + 0.245 \times \begin{Bmatrix} |39.84| \\ |-54.34| \\ |30.41| \end{Bmatrix} = \begin{Bmatrix} 181 \\ 319 \\ 308 \end{Bmatrix} \text{ kN}$$

RESIDUAL MODE RESPONSE ($T_R = 0.589 \text{ sec} < T_s$)

Elastic Response

$$\text{Viscous Damping Ratio: } \beta_{RD} = 0.196 \quad (\text{Table G-2})$$

$$\text{Effective Damping Ratio: } B_{RD} = 0.05 + 0.196 = 0.246 \quad (\text{A13.3.3-1})$$

$$\text{Damping Coefficient: } B_R = 1.638 \quad (\text{Table A13.3.1})$$

$$\text{Roof Displacement: } D_{RD} = \left(\frac{9810}{4\pi^2} \right) \times |-0.361| \times \frac{0.6 \times 0.589^2}{1.638} = 19.00 \text{ mm} \quad (\text{A13.4.4.3-2})$$

Base Shear

$$\text{Seismic Coefficient: } C_{SR} = \left(\frac{8}{5.5} \right) \times \frac{1.0}{3 \times 1.638} = 0.296 \quad (\text{A13.4.3.8-1})$$

$$\text{Base Shear: } V_R = 0.265 \times 1375.3 = 407.09 \text{ kN} \quad (\text{A13.4.3.6-1})$$

$$\text{Required Base Shear Strength: } V_R = \left(\frac{3 \times 5.5}{8} \right) \times 407.09 = 840 \text{ kN}$$

Response at Stage of Maximum Displacement

Lateral Floor Displacement, δ_{iR} , and Story Drifts, Δ_{iR}

$$\delta_{iR} = 19 \times \begin{Bmatrix} 1.000 \\ -0.195 \\ -1.733 \end{Bmatrix} = \begin{Bmatrix} 19.00 \\ -3.71 \\ -32.93 \end{Bmatrix} \text{ mm} \quad (\text{A13.4.4.2-2})$$

$$\Delta_{iR} = \begin{Bmatrix} 22.71 \\ 29.22 \\ -32.93 \end{Bmatrix} \text{ mm}$$

Design Lateral Forces, F_{iR}

$$F_{iR} = \begin{Bmatrix} 1567 \times 1.000 \times \frac{|-0.361|}{1375.3} \times 407.09 \\ 2900 \times (-0.195) \times \frac{|-0.361|}{1375.3} \times 407.09 \\ 2900 \times (-1.733) \times \frac{|-0.361|}{1375.3} \times 407.09 \end{Bmatrix} = \begin{Bmatrix} 167.44 \\ -60.43 \\ -537.03 \end{Bmatrix} \text{ kN} \quad (\text{A13.4.3.9-2})$$

Floor Acceleration, A_{iR}

$$A_{iR} = \begin{Bmatrix} \frac{167.44}{1567} \\ \frac{-60.43}{2900} \\ \frac{-537.03}{2900} \end{Bmatrix} \times \left(\frac{3 \times 5.5}{8} \right) = \begin{Bmatrix} 0.220 \\ -0.043 \\ -0.382 \end{Bmatrix} \text{ g}$$

Story Shears, V_{iR}

$$V_{iR} = \begin{Bmatrix} 167.44 \\ 107.01 \\ -430.02 \end{Bmatrix} \text{ kN}$$

Damper Axial Restoring Force F_{iR}

$$K_{jR} = \frac{G'(\omega)A_b}{h} = \frac{1.40 \times 10^{-3} \times 626330}{140} = 6.26 \text{ kN/mm} \quad (7.43)$$

$$F_{iR} = K d_{iR} \cdot \Delta_{iR} \cdot \cos \theta_i = 6.26 \times \begin{Bmatrix} 22.71 \\ 29.22 \\ -32.93 \end{Bmatrix} \times \cos 27.6^\circ = \begin{Bmatrix} 126.00 \\ 162.10 \\ -182.68 \end{Bmatrix} \text{ kN}$$

Response at Stage of Maximum Velocity

Story Velocity, ∇_{iRD}

$$\nabla_{iRD} = \frac{2\pi}{0.589} \times \begin{Bmatrix} 22.71 \\ 29.22 \\ -32.93 \end{Bmatrix} = \begin{Bmatrix} 242.26 \\ 311.71 \\ -351.28 \end{Bmatrix} \text{ mm/sec} \quad (\text{A13.4.4.5.-3})$$

Forces in Damping Devices, Fd_{iRD}

$$Fd_{iRD} = 0.831 \times \begin{Bmatrix} 242.26 \\ 311.71 \\ -351.28 \end{Bmatrix} \cos 27.6^\circ = \begin{Bmatrix} 178.41 \\ 229.55 \\ -258.69 \end{Bmatrix} \text{ kN} \quad (7-23)$$

Horizontal Component of the Viscous Damping Force

$$Vd_{iRD} = \begin{Bmatrix} 178.41 \\ 229.55 \\ -258.69 \end{Bmatrix} \cos 27.6^\circ = \begin{Bmatrix} 158.11 \\ 203.43 \\ -229.25 \end{Bmatrix} \text{ kN}$$

Maximum Axial Damping Force, $F_{D_{iR}}$

Storage and Shear Moduli: $G'(\omega) = 1.4 \text{ MPa}$; $G''(\omega) = 1.98 \text{ MPa}$ (Table G-2)

Loss Factor: $\eta = \frac{1.98}{1.40} = 1.414$ (7-44)

$$\begin{aligned} \tan^{-1} \eta &= \tan^{-1}(1.414) &&= 0.955 \\ \cos(\tan^{-1} \eta) &= \cos(0.955) &&= 0.578 \\ \sin(\tan^{-1} \eta) &= \sin(0.955) &&= 0.816 \end{aligned}$$

$$F_{D_{iR}} = 0.578 \times \begin{Bmatrix} |126.00| \\ |162.10| \\ |-182.68| \end{Bmatrix} + 0.816 \times \begin{Bmatrix} |178.41| \\ |229.55| \\ |-258.69| \end{Bmatrix} = \begin{Bmatrix} 218 \\ 281 \\ 317 \end{Bmatrix} \text{ kN}$$

Response at Stage of Maximum Acceleration

Force Coefficients

$$\text{Effective viscous damping ratio: } \beta_{\text{eff}} = 0.05 + 0.196 = 0.246$$

$$\text{Parameter } \delta: \quad \delta = \tan^{-1} (2 \times 0.246) = 0.457 \quad (4-36)$$

$$\text{Force coefficient } CF_1: \quad CF_1 = \cos (0.457) = 0.897 \quad (4-41)$$

$$\text{Force Coefficient } CF_2: \quad CF_2 = \sin (0.457) = 0.441 \quad (4-39)$$

Maximum Lateral Inertia Forces

$$F_{iR,max} = 0.897 \times \begin{Bmatrix} |167.44| \\ |-60.43| \\ |-537.03| \end{Bmatrix} \times \left(\frac{3 \times 5.5}{8} \right) + 0.441 \times \begin{Bmatrix} |158.11| \\ |45.32| \\ |-432.68| \end{Bmatrix} = \begin{Bmatrix} 379.50 \\ 131.79 \\ 1184.35 \end{Bmatrix} \text{ kN}$$

Maximum Acceleration

$$A_{iR,max} = F_{iR,max} / w_i, \quad A_{iR,max} = \begin{Bmatrix} 379.50/1567 \\ 131.79/2900 \\ 1184.35/2900 \end{Bmatrix} = \begin{Bmatrix} 0.242 \\ 0.045 \\ 0.408 \end{Bmatrix}$$

Maximum Story Shear, $V_{iR,max}$

$$V_{iR,max} = 0.897 \times \begin{Bmatrix} |167.44| \\ |107.01| \\ |-430.02| \end{Bmatrix} \times \left(\frac{3 \times 5.5}{8} \right) + 0.441 \times \begin{Bmatrix} |158.11| \\ |203.43| \\ |-229.25| \end{Bmatrix} = \begin{Bmatrix} 380 \\ 288 \\ 897 \end{Bmatrix} \text{ kN}$$

Total responses resulting from modal combinations were calculated by use of the SRSS combination rule. Table G-1 presents a summary of the modal properties of the frame (inclusive of the damping devices) and Table G-2 presents a summary of the calculations of the storage stiffness and loss stiffness and viscous damping ratio under elastic conditions of the system at each mode. Tables G-3 and G-4 present summaries of the results of the analysis for each mode and the total response obtained by both the ELF and RSA procedures for the DBE and MCE, respectively.

TABLE G-1 Modal Properties of Frame 3S-75 with Viscoelastic Devices

Quantity	Mode 1	Mode 2	Mode 3	Residual Mode
T_m , sec	1.473	0.475	0.253	0.589
$\{\phi_{im}\}$	1.000 0.683 0.275	1.000 -0.498 -0.698	1.000 -1.504 1.911	1.000 -0.195 -1.733
\bar{W}_m , kN	5991.7	973.6	401.7	1375.3
Γ_m	1.361	-0.505	0.144	-0.361

TABLE G-2 Calculation of Storage Stiffness, Loss Stiffness of Viscoelastic Damping Devices and Viscous Damping Ratio under Elastic Conditions

Mode	Period (assumed) sec	Frequency f Hz	G' MPa	G'' MPa	K_j kN/mm (7-43)	Period (actual) sec	Mode Shape	C_j kN.s/mm (7-43)	β_v (7-29)
1	1.44	0.70	0.83	0.83	3.71	1.473	1.000 0.683 0.275	0.871	0.086
2	0.475	2.11	1.90	2.30	8.50	0.446	1.000 -0.457 -0.692	0.730	0.149
3	0.253	3.95	3.20	2.70	14.30	0.237	1.000 -1.285 1.723	0.456	0.076
Residual	0.589	1.70	1.40	1.98	6.26	0.589	1.000 -0.195 -1.733	0.831	0.196

- Values of G' and G'' at given frequencies are obtained from Figure G-1.
- Mode shape calculated in analysis using the stiffness of viscoelastic devices at frequency equal to frequency of mode (0.7 Hz for 1st, 2.24 Hz for 2nd and 4.22 Hz for 3rd).

**TABLE G-3 Modal Response Calculations for Example No.8: 3-Story Frame
($V_{min}=0.75 V_y$) with Viscoelastic Damping System. Analysis for the DBE**

Quantity	Units	Mode 1 (m=1)	Mode 2 (m=2)	Mode 3 (m=3)	Mode R (m=R)	SRSS	
						ELF	RSA
1. Elastic Response							
Damping Ratio, β_{ve}		0.086	0.149	0.076	0.196		
Total Damping Ratio, β_{v+I}		0.136	0.199	0.126	0.246		
Damping Coefficient, B_m		1.308	1.497	1.278	1.638		
Elastic Displacement, D_{em}	mm	229	19	2	19		
2. Roof Displacement and Base Shear							
Assumed Ductility, μ		1.21	1.0	1.0	1.0		
Effective Period, T_{ID}	sec	1.592	0.475	0.253	0.589		
Eff. Viscous Damping Ratio, β_v		0.093	0.149	0.076	0.196		
Hysteretic Damping, β_H		0.041	0.000	0.000	0.000		
Effective Damping, β_m		0.184	0.199	0.126	0.246		
Damping Coefficient, B_m		1.452	1.497	1.278	1.638		
Displacement, D_{mD}	mm	222	19	2	19		
Corrected Displacement, D_{mD}	mm	229	0.324	0.379	0.296		
Seismic Coefficient, C_s	kN	0.126	315	152	407	857	831
Seismic Base Shear, V_m	mm	754	-----	-----	-----		
Yield Displacement, D_y		191	-----	-----	-----		
Computed Ductility, μ		1.20	-----	-----	-----		

TABLE G-3 continued

3. Response at Stage of Maximum Displacement									
Lateral Floor Displacement, δ_{ij}	mm	229	19	2	19	2	19		
		156	-9	-3	-4				
		63	-13	3	-33				
Story Drift, Δ_{jm}	mm	72	28	4	23		76	78	
		93	4	-6	29		98	94	
		63	-13	3	-33		71	64	
Design Lateral Forces, F_{im} (including restoring force)	kN	268	257	86	167				
		339	-236	-239	-60				
		137	-331	303	-537				
Floor Acceleration, A_{im}	g	0.353	0.338	0.113	0.220				
		0.241	-0.168	-0.170	-0.043				
		0.097	-0.236	0.216	-0.382				
Actual Story Shear Forces, V_{jm} (including restoring force)	kN	554	529	177	345		653	786	
		1254	41	-316	221		1273	1293	
		1535	-642	310	-887		1773	1693	

TABLE G-3 continued

4. Response at Stage of Maximum Velocity									
Drift Velocity, V_{im}	mm/sec	286	375	112	242	375	485		
		368	50	-152	312	482	401		
		248	-175	85	-351	430	315		
Force in Damping Devices, $F_{d_{jm}}$ (viscous component)	kN	221	243	45	178	284	331		
		284	32	-62	230	365	292		
		191	-113	34	-259	322	225		
Horizontal Damper Force, $V_{d_{jm}}$ (viscous force)	kN	196	215	40	158				
		252	29	-55	203				
		170	-100	31	-229				
Lateral Force (viscous component)	kN	196	215	40	158				
		56	-186	-95	45				
		-82	-129	85	-433				
G'	MPa	0.830	1.900	3.200	1.400				
G''	MPa	0.830	2.300	2.700	1.980				
η		1.000	1.211	0.844	1.414				
$\tan^{-1}\eta$		0.785	0.880	0.701	0.955				
$\cos(\tan^{-1}\eta)$		0.707	0.637	0.764	0.577				
$\sin(\tan^{-1}\eta)$		0.707	0.771	0.645	0.817				
Force in Damping Devices, $F_{d_{jm}}$ (combination of viscous and restoring forces)	kN	325	323	73	218	391	464		
		418	43	99	281	504	432		
		282	151	56	317	424	324		

TABLE G-3 continued

5. Response at Stage of Maximum Acceleration									
Ductility, μ	1.20	1.00	1.00	1.00	1.00	1.00	1.00	1.00	
Eff. Damp. Excluding Hysteretic	0.143	0.199	0.126	0.246					
Parameter δ	0.278	0.379	0.247	0.457					
Coefficient CF_1	0.962	0.929	0.970	0.897					
Product $CF_1 \cdot \mu$	1.154	0.929	0.970	0.897					
Force Coefficient, CF_1 or C_{nFD}	1.000	0.929	0.970	0.897					
Force Coefficient, CF_2 or C_{nFV}	0.274	0.370	0.244	0.441					
Lateral Force F_{in}	607	571	181	380					
(combination of restoring and viscous forces)	715	522	501	132					
	304	683	628	1185					
Max.Floor Acc., $A_{in,max}$	0.388	0.364	0.116	0.242	0.457	0.544			
	0.247	0.180	0.173	0.045	0.251	0.351			
	0.105	0.235	0.216	0.409	0.422	0.337			
Maximum Story Shear, $V_{jm,max}$	607	571	181	380	716	853			
(actual)	1323	49	319	288	1354	1361			
	1582	634	308	897	1818	1732			

**TABLE G-4 Modal Response Calculations for Example No.8: 3-Story Frame
($V_{min}=0.75 V_y$) with Viscoelastic Damping System. Analysis for the MCE**

Quantity	Units	Mode 1 (m=1)	Mode 2 (m=2)	Mode 3 (m=3)	Mode R (m=R)	SRSS	
						ELF	RSA
1. Elastic Response							
Damping Ratio, β_{ve}		0.086	0.149	0.076	0.196		
Total Damping Ratio, β_{v+I}		0.136	0.199	0.126	0.246		
Damping Coefficient, B_m		1.308	1.497	1.278	1.638		
Elastic Displacement, D_{em}	mm	343	28	3	29		
2. Roof Displacement and Base Shear							
Assumed Ductility, μ		1.86	1.0	1.0	1.0		
Effective Period, T_{ID}	sec	1.875	0.475	0.253	0.589		
Eff. Viscous Damping Ratio, β_v		0.109	0.149	0.076	0.196		
Hysteretic Damping, β_H		0.098	0.000	0.000	0.000		
Effective Damping, β_m		0.258	0.199	0.126	0.246		
Damping Coefficient, B_m		1.674	1.497	1.278	1.638		
Displacement, D_{mD}	mm	341					
Corrected Displacement, D_{mD}	mm	343	28	3	29		
Seismic Coefficient, C_s		0.139	0.486	0.569	0.444		
Seismic Base Shear, V_m	kN	833	473	229	611	1033	985
Yield Displacement, D_y	mm	210	-----	-----	-----		
Computed Ductility, μ		1.63	-----	-----	-----		

TABLE G-4 continued

3. Response at Stage of Maximum Displacement									
Lateral Floor Displacement, δ_{ij}	mm	343	28	3	29				
		234	-14	-4	-6				
		94	-20	5	-49				
Story Drift, Δ_{jm}	mm	109	43	7	34	114	117		
		140	6	-9	44	147	140		
		94	-20	5	-49	106	96		
Design Lateral Forces, F_{im} (including restoring force)	kN	297	385	129	251				
		375	-355	-358	-91				
		151	-497	455	-806				
Floor Acceleration, A_{im}	g	0.390	0.506	0.169	0.331				
		0.267	-0.252	-0.255	-0.064				
		0.107	-0.354	0.324	-0.573				
Actual Story Shear Forces, V_{jm} (including restoring force)	kN	612	794	265	518	802	1036		
		1385	62	-473	331	1424	1465		
		1696	-963	465	-1330	2155	2005		

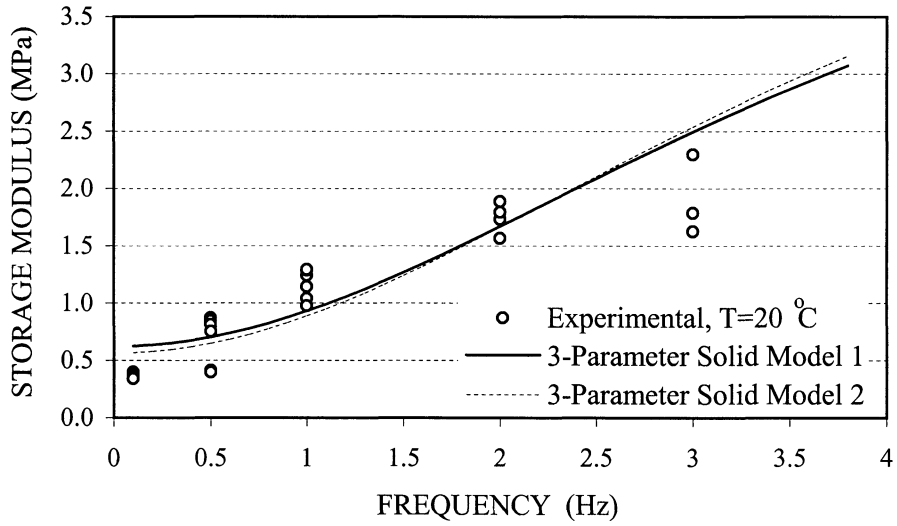
TABLE G-4 continued

4. Response at Stage of Maximum Velocity									
Drift Velocity, V_{im}	mm/sec	364	563	168	363	515	691		
		469	75	-229	468	662	527		
		316	-262	128	-527	615	430		
Force in Damping Devices, F_{djm} (viscous component)	kN	281	364	68	268	388	465		
		362	49	-92	344	499	377		
		244	-170	52	-388	458	301		
Horizontal Damper Force, V_{djm} (viscous force)	kN	249	323	60	237				
		321	43	-82	305				
		216	-150	46	-344				
Lateral Force (viscous component)	kN	249	323	60	237				
		72	-280	-142	68				
		-105	-193	128	-649				
G'	MPa	0.830	1.900	3.200	1.400				
G''	MPa	0.830	2.300	2.700	1.980				
η		1.000	1.211	0.844	1.414				
$\tan^{-1}\eta$		0.785	0.880	0.701	0.955				
$\cos(\tan^{-1}\eta)$		0.707	0.637	0.764	0.577				
$\sin(\tan^{-1}\eta)$		0.707	0.771	0.645	0.817				
Force in Damping Devices, F_{djm} (combination of viscous and restoring forces)	kN	452	485	109	328	558	671		
		581	65	149	422	718	603		
		392	226	83	475	616	460		

TABLE G-4 continued

5. Response at Stage of Maximum Acceleration									
	1.63	1.00	1.00	1.00	1.00	1.00	1.00	1.00	
Ductility, μ									
Eff. Damp. Excluding Hysteretic	0.154	0.199	0.126	0.246					
Parameter δ	0.299	0.379	0.247	0.457					
Coefficient CF_1	0.956	0.929	0.970	0.897					
Product $CF_1 \cdot \mu$	1.557	0.929	0.970	0.897					
Force Coefficient, CF_1 or C_{mFD}	1.000	0.929	0.970	0.897					
Force Coefficient, CF_2 or C_{mFV}	0.295	0.370	0.244	0.441					
Lateral Force F_{im}	685	857	272	570					
(combination of restoring and viscous forces)	794	783	751	198					
	342	1024	942	1777					
Max.Floor Acc., $A_{im,max}$	0.437	0.547	0.174	0.364					0.721
	0.274	0.270	0.259	0.068					0.464
	0.118	0.353	0.325	0.613					0.494
Maximum Story Shear, $V_{jm,max}$	685	857	272	570					1130
(actual)	1479	74	479	432					1557
	1760	950	462	1345					2053

STORAGE MODULUS G'



LOSS MODULUS G''

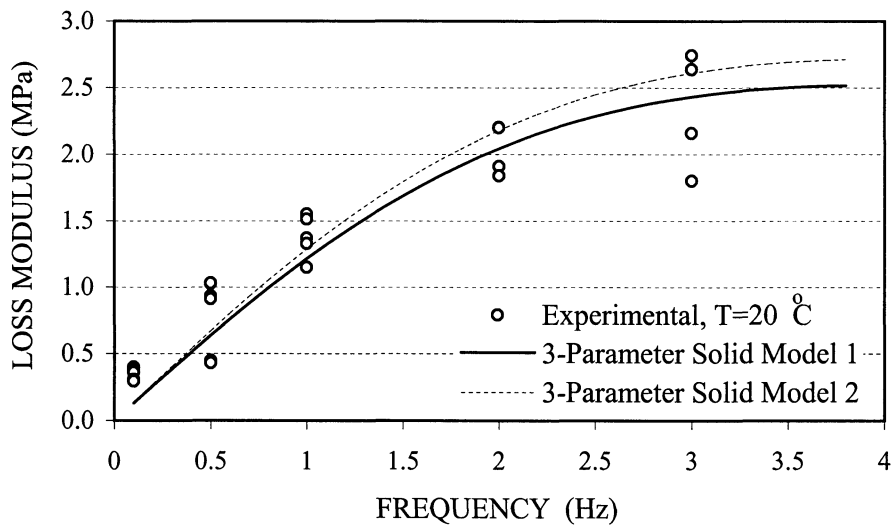


FIGURE G-1 Storage and Loss Modulus of Viscoelastic Damping Device at Temperature $T = 20\text{ }^{\circ}\text{C}$ (Zimmer, 2000)

APPENDIX H

DETAILED CALCULATIONS FOR THE SIMPLIFIED ANALYSIS OF A 3-STORY FRAME WITH YIELDING DAMPING SYSTEM

H.1 Introduction

This appendix presents detailed calculations in the application of the equivalent lateral force procedure (ELF) and response-spectrum analysis (RSA) procedures of NEHRP (2000) for the analysis of buildings with yielding damping systems. These procedures are applied as described in Appendix A subject to the modifications described in Sections 7.5.4 and in Section 8.1. The presentation in the appendix consists of detailed calculations for the 3-story steel moment frame 3S-75 shown in Figure 8-9 and described as example No.9 in Section 8.

H.2 Detailed Calculations for 3-Story Frame 3S-75 with Metallic Yielding Damping Devices

Parameters

The seismic tributary weights of the third, second and first floors are 1567 kN, 2900 kN, and 2900 kN, respectively. The design coefficients per Table 5.2.2 1997 NEHRP Recommended Provisions for special steel moment frames are $R = 8.0$, $\Omega_o = 3.0$, $C_d = 5.5$, and $I = 1.0$. The devices are made of steel ($F_y = 248$ MPa) with dimensions base x height x thickness of 305 mm x 457 mm x 25.4 mm (12"x18"x1").

Description of the System

The analyzed frame is the 3-story special steel moment frame with the yielding damping system shown in Figure 8-9. The damping system of the frame consists of triangular metallic yielding devices (Tsai et al., 1993) shown in Figure C-8(a). Section C.3.1 presents calculations for yield strength and yield displacement of these devices at the first story of this frame, $V_d = 320$ kN and $D_{yd} = 52.4$ mm, respectively. The base shear strength and yield displacement of the frame exclusive of the damping system, are $V_{yf} = 1220$ kN, and $D_{yf} = 182$ mm. The base shear strength of the frame inclusive of the damping system is $V = 1220 + 320 = 1540$ kN. Moreover, Section C.3.1 provides the yield displacement and effective initial (secant) period of the equivalent bilinear representation of the combined system (frame plus yielding devices) as $D_y =$

148.9 mm, and $T_1 = 1.320$ sec, respectively (see Fig. C-7). The required base shear strength was calculated by use of (7-72) to be $V_{min} \cdot \Omega_0 \cdot C_d / R$ in which V_{min} is the greater of V/B_{V+I} (equation A13.2.4-1) and $0.75V$ (equation A13.2.4.1-2). The seismic base shear V was calculated in Section B.3 to be 788.5 kN. Coefficient B_{V+I} was interpreted as the damping coefficient corresponding to the effective damping of the frame inclusive of the yielding damping system at displacement just below the effective yield displacement of the frame exclusive of the damping system. That is, at this level of displacements there is inelastic action in the yielding system. Therefore, the effective damping was calculated by use of (7-55) with $\mu_f = 1.0$, $A_d/A_y = 320/1220 = 0.26$, and $\mu_d = 182/52.4 = 3.47$. The result is

$$\beta_1 = 0.05 \left(\frac{1}{1+0.26} \right)^{1/2} + \frac{2 \times 0.26 \times \left(1 - \frac{1}{3.47} \right)}{\pi(1+0.26)} = 0.138$$

The corresponding damping coefficient is $B_{V+I} = 1.314$ (Table A13.3.1). Thus, $V_{min} = V/B_{V+I} = 788.5/1.314 = 600$ kN (which is greater than $0.75V=591$ kN). The required base shear strength of the frame (7-72) is $V_y = 600 \times 3 \times 5.5/8 = 1237.5$ kN. The base shear strength of the frame (exclusive of the damping system) is $V_{yf} = 1220$ kN which is close to the required base shear strength.

The application of the ELF method of analysis of NEHRP (2000) requires that the period and mode shape of the first mode of vibration of the frame inclusive of the damping system is determined. Modal analysis of the frame inclusive of the metallic devices resulted in $T_1 = 1.133$ sec $\{\phi_{i1}\}^T = [1.0 \ 0.708 \ 0.296]$. However, direct use of the NEHRP (2000) analysis procedure requires that the effective initial (secant) period for the elastoplastic representation of the frame inclusive of the damping system is utilized. This period was calculated in Section C.3.1 using (C-13) to be $T_1 = 1.320$ sec. Since this period was calculated by simple procedures without the use of a computer model of the frame, the first mode shape was assumed to be that of the frame exclusive of the damping system: $\{\phi_{i1}\}^T = [1.0 \ 0.657 \ 0.250]$. Note that this mode shape is very close to the one of the frame inclusive of the damping system and that both mode shapes represent approximations to a more approximate mode shape that should have been calculated using effective member stiffnesses.

A similar complexity arises in the application of the RSA method of NEHRP (2000). Calculation of the modal properties of the frame inclusive of the damping system would require the use of effective stiffnesses for the yielding damping devices. To avoid such analysis and within the context of approximate analysis, the modal properties were calculated as follows:

- (a) The effective initial (secant) period $T_1 = 1.320$ sec was used for the first mode.
- (b) The periods $T_2 = 0.49$ sec and $T_3 = 0.24$ sec of the frame exclusive of the damping devices were used for the second and third modes, respectively. Note that the second- and third-mode periods of the frame inclusive of the damping devices (for elastic conditions of the metallic damping devices) are 0.40 sec and 0.23 sec, respectively. Use of effective stiffnesses for the metallic devices in the computer analysis would have resulted in values of periods T_2 and T_3 between 0.49 and 0.40 sec and between 0.24 and 0.23 sec, respectively. Such accuracy is, apparently, of little significance in an approximate analysis.
- (c) The mode shapes of the frame exclusive of the damping system were used. That is, $\{\phi_{i1}\}^T = [1.0 \ 0.657 \ 0.250]$, $\{\phi_{i2}\}^T = [1.0 \ -0.560 \ -0.690]$, and $\{\phi_{i3}\}^T = [1.0 \ -1.618 \ 2.096]$. By comparison, the mode shapes of the frame inclusive of the metallic yielding devices (for elastic conditions of these devices) are $[1.0 \ 0.708 \ 0.296]$, $[1.0 \ -0.472 \ -0.675]$ and $[1.0 \ -1.548 \ 1.840]$, respectively. Again, values of the modal displacements between these two bounding cases could have been used but it is apparent that this would have been of little significance in an approximate analysis.

The utilized modal properties of the frame are summarized in Table H-1. The yield displacement of the equivalent bilinear representation ($D_y = 148.9$ mm) was utilized for calculations of effective ductility demand.

CALCULATION OF RESPONSE IN DESIGN BASIS EARTHQUAKE

FIRST MODE RESPONSE ($T_1=1.320$ sec)

Equations (7-54) and (7-55) were used to calculate effective period and effective damping ratio in the first mode. The following two equations, defined in Figure 7-5, were needed:

$$A_d = \frac{V_d}{W_1} g = \frac{320}{5871} g = 0.055 g$$

$$A_y = \frac{V_{yf}}{W_1} g = \frac{1220}{5871} g = 0.208 g$$

Inelastic Roof Displacement

Assumed Effective Ductility: $\mu_D = 1.46$

Assumed Roof Displacement: $D_{1D} = \mu_D \cdot D_y = 1.46 \times 148.9 = 217.39 \text{ mm}$ (A13.3.4-1)

$$\text{Spectral Roof Displacement: } D = \frac{D_{1D}}{\Gamma_1} = \frac{217.39}{|1.3986|} = 155.43 \text{ mm}$$

Effective Period: $T_{1D} = 2 \times \pi \times \left(\frac{155.43}{(0.055 + 0.208) \times 9810} \right)^{1/2} = 1.544 \text{ sec}$ (7-54)

Effective Damping Ratio:

Ductility Ratio for the Frame: $\mu_f = \frac{217.39}{182} = 1.195$ (7-56)

Ductility Ratio for the Damping System: $\mu_d = \frac{217.39}{52.4} = 4.149$ (7-56)

Quality Factor: $q_H = 0.67 \times \frac{0.6}{1.320} = 0.30 < 0.50$ (A13.3.3-1)

use $q_H = 0.50$

Hysteretic Damping (hysteretic component in (7-55)):

$$\beta_{HD} = \frac{2 \times 0.5 \times \left(1 - \frac{1}{1.195} \right) + 2 \times 0.26 \times \left(1 - \frac{1}{4.149} \right)}{\pi \times (1 + 0.26)} = 0.141$$

Effective Damping: $\beta_{1D} = 0.05 \times \left(\frac{1}{1 + 0.26} \right)^{1/2} + 0.141 = 0.186$ (7-55)

Damping Coefficient: $B_{1D} = 1.458$ (Table A13.3.1)

Roof Displacement: $D_{1D} = \left(\frac{9810}{4\pi^2}\right) \times |1.3986| \times \frac{0.6}{1.458} \times 1.544 = 221 \text{ mm}$ (A13.4.4.3-1)

Corrected Roof Displacement

The roof displacement for elastic behavior of the frame is:

$$D = \left(\frac{9810}{4\pi^2}\right) \times |1.3986| \times \frac{0.6}{1.0} \times 1.320 = 275 \text{ mm}$$

Since $D_{1D} < D$, use $D_{1D} = 275 \text{ mm}$

Base Shear

Seismic Coefficient: $C_{s1} = \left(\frac{8}{5.5}\right) \times \frac{0.6}{1.544 \times (3 \times 1.458)} = 0.1292$ (A13.4.3.4-1)

Base Shear: $V_1 = 0.1292 \times 5871 = 758.5 \text{ kN}$ (A13.4.3.1-1)

The contribution of the first mode to the base shear strength of the frame is given by (7-72)

$$V_1 = 758.5 \times \frac{3 \times 5.5}{8} = 1565 \text{ kN}$$

The calculated contribution to the base shear strength of 1565 kN is very close to the actual base shear strength of 1540 kN.

Displacement at Effective Yield (Yield Displacement) D_y

$$D_y = \left(\frac{9810}{4\pi^2}\right) \times \left(\frac{3 \times 5.5}{8}\right) \times |1.3986| \times 0.1292 \times 1.320^2 = 161 \text{ mm}$$
 (A13.3.4-3)

Effective Ductility Demand: $\mu_D = \frac{275}{161} = 1.71$ (A13.3.4-1)

$$\mu_D < \mu_{MAX} = 2.67$$

The difference between the calculated and the assumed ductility demand is due to adjustment of the inelastic displacement to meet the condition that it is not less than the elastic displacement.

Response at stage of maximum displacement

Lateral Floor Displacements, δ_{iID} , and Story Drifts, Δ_{iID}

$$\delta_{iID} = 275 \times \begin{Bmatrix} 1.000 \\ 0.657 \\ 0.250 \end{Bmatrix} = \begin{Bmatrix} 275 \\ 181 \\ 69 \end{Bmatrix} \text{ mm} \quad (\text{A13.4.4.2-1})$$

$$\Delta_{iID} = \begin{Bmatrix} 94 \\ 112 \\ 69 \end{Bmatrix} (\text{mm})$$

Design Lateral Forces, F_{iI} , Design Story Shears, V_{iI} , and Accelerations, A_{iI}

$$F_{iI} = \begin{Bmatrix} 1567 \times 1.000 \times \frac{1.3986}{5871} \times 758.5 \\ 2900 \times 0.659 \times \frac{1.3986}{5871} \times 758.5 \\ 2900 \times 0.250 \times \frac{1.3986}{5871} \times 758.5 \end{Bmatrix} = \begin{Bmatrix} 283 \\ 345 \\ 131 \end{Bmatrix} \text{ kN} \quad (\text{A13.4.3.9-1})$$

$$A_{iI} = \frac{F_{iI}}{w_i} \cdot \left(\frac{C_d \cdot \Omega_o}{R} \right) \begin{Bmatrix} \frac{283}{1567} \\ \frac{345}{2900} \\ \frac{131}{2900} \end{Bmatrix} \times \left(\frac{3 \times 5.5}{8} \right) = \begin{Bmatrix} 0.373 \\ 0.245 \\ 0.093 \end{Bmatrix} \text{ g}$$

$$V_{iI} = \begin{Bmatrix} 283 \\ 628 \\ 759 \end{Bmatrix} \text{ kN}$$

SECOND MODE RESPONSE ($T_2 = 0.49 < T_s$)

Effective Damping Ratio: $\beta_{2D} = 0.05$ $B_{2D} = 1.0$

Roof Displacement: $D_{2D} = \left(\frac{9810}{4\pi^2} \right) \times |-0.533| \times \frac{1.0}{1.0} \times 0.49^2 = 32 \text{ mm}$ (A13.5.4.3-2)

Seismic Base Shear:

Seismic Coefficient: $C_{S2} = \left(\frac{8}{5.5} \right) \times \frac{1.0}{3 \times 1.0} = 0.485$ (A13.5.3.6-1)

Base Shear: $V_2 = 0.485 \times 1098 = 533 \text{ kN}$ (A13.5.3.2-1)

Response at Stage of Maximum Displacement

Lateral Floor Displacement, $\delta_{i_{2D}}$, and Story Drifts, $\Delta_{i_{2D}}$

$$\delta_{i_{2D}} = 32 \times \begin{Bmatrix} 1.000 \\ -0.560 \\ -0.690 \end{Bmatrix} = \begin{Bmatrix} 32 \\ -18 \\ -22 \end{Bmatrix} \text{ mm} \quad (\text{A13.5.4.2-1})$$

$$\Delta_{i_{2D}} = \begin{Bmatrix} 50 \\ 4 \\ -22 \end{Bmatrix} \text{ mm}$$

Design Lateral Forces, F_{i_2} , Design Story Shears, V_{i_2} , and Accelerations, A_{i_2}

$$F_{i_2} = \begin{Bmatrix} 1567 \times 1.0 \times \frac{|-0.533|}{1098} \times 533 \\ 2900 \times (-0.560) \times \frac{|-0.533|}{1098} \times 533 \\ 2900 \times (-0.690) \times \frac{|-0.533|}{1098} \times 533 \end{Bmatrix} = \begin{Bmatrix} 405 \\ -420 \\ -518 \end{Bmatrix} \text{ kN} \quad (\text{A13.5.3.7-1})$$

$$A_{i_2} = \frac{F_{i_2}}{w_i} \cdot \left(\frac{C_d \Omega_o}{R} \right) = \left\{ \begin{array}{c} 405 \\ 1567 \\ -420 \\ 2900 \\ -518 \\ 2900 \end{array} \right\} \times \left(\frac{3 \times 5.5}{8} \right) = \left\{ \begin{array}{c} 0.533 \\ -0.299 \\ -0.368 \end{array} \right\} g$$

$$V_{i_2} = \left\{ \begin{array}{c} 405 \\ -15 \\ -533 \end{array} \right\} kN$$

THIRD MODE RESPONSE ($T_3 = 0.24 \text{ sec} < T_s$)

Effective Damping Ratio: $\beta_{3D} = 0.05$ $B_{3D} = 1.0$

Roof Displacement: $D_{3D} = \left(\frac{9810}{4\pi^2} \right) \times |0.135| \times \frac{1.0}{1.0} \times 0.24^2 = 2 \text{ mm}$ (A13.5.4.3-2)

Seismic Base Shear:

Seismic Coefficient: $C_{s3} = \left(\frac{8}{5.5} \right) \times \frac{1.0}{3 \times 1.0} = 0.485$

(A13.5.3.6-1)

Base Shear: $V_3 = 0.485 \times 398 = 193 \text{ kN}$ (A13.5.3.2-1)

Response at Stage of Maximum Displacement

Lateral Floor Displacement, $\delta_{i_{3D}}$, and Story Drifts, $\Delta_{i_{3D}}$

$$\delta_{i_{3D}} = 2 \times \left\{ \begin{array}{c} 1.000 \\ -1.618 \\ 2.096 \end{array} \right\} = \left\{ \begin{array}{c} 2 \\ -3 \\ 4 \end{array} \right\} \text{ mm} \quad (\text{A13.5.4.2-1})$$

$$\Delta_{i_{3D}} = \left\{ \begin{array}{c} 5 \\ -7 \\ 4 \end{array} \right\} \text{ mm}$$

Design Lateral Forces, F_{i3} , Design Story Shears, V_{i3} , and Floor Accelerations, A_{i3}

$$F_{i3} = \begin{Bmatrix} 1567 \times 1.0 \times \frac{|0.135|}{398} \times 193 \\ 2900 \times (-1.618) \times \frac{|0.135|}{398} \times 193 \\ 2900 \times (2.096) \times \frac{|0.135|}{398} \times 193 \end{Bmatrix} = \begin{Bmatrix} 103 \\ -307 \\ 398 \end{Bmatrix} \text{ kN} \quad (\text{A13.5.3.7-1})$$

$$A_{i3} = \frac{F_{i2}}{w_i} \cdot \left(\frac{C_d \Omega_o}{R} \right) = \begin{Bmatrix} \frac{103}{1567} \\ \frac{-307}{2900} \\ \frac{398}{2900} \end{Bmatrix} \times \left(\frac{3 \times 5.5}{8} \right) = \begin{Bmatrix} 0.136 \\ -0.218 \\ 0.283 \end{Bmatrix} \text{ g}$$

$$V_{i3} = \begin{Bmatrix} 103 \\ -204 \\ 194 \end{Bmatrix} \text{ kN}$$

RESIDUAL MODE RESPONSE ($T_R = 0.4 \times 1.320 = 0.528 \text{sec} < T_s$)

Effective Damping Ratio: $\beta_{RD} = 0.05$ $B_{RD} = 1.0$

Roof Displacement: $D_{RD} = \left(\frac{9810}{4\pi^2} \right) \times |-0.399| \times \frac{1.0}{1.0} \times 0.528^2 = 28 \text{ mm}$ (A13.4.4.3-2)

Seismic Base Shear:

Seismic Coefficient: $C_{SR} = \left(\frac{8}{5.5} \right) \times \frac{1.0}{3 \times 1.0} = 0.485$ (A13.4.3.8-1)

Base Shear: $V_R = 0.485 \times 1496 = 725 \text{ kN}$ (A13.4.3.6-1)

Response at Stage of Maximum Displacement

Lateral Floor Displacement, δ_{iR} , and Story Drifts, Δ_{iR}

$$\delta_{iRD} = 28 \times \begin{Bmatrix} 1.000 \\ -0.2036 \\ -1.6318 \end{Bmatrix} = \begin{Bmatrix} 28 \\ -6 \\ -46 \end{Bmatrix} \text{ mm} \quad (\text{A13.4.4.2-2})$$

$$\Delta_{iRD} = \begin{Bmatrix} 34 \\ 40 \\ -46 \end{Bmatrix} \text{ mm}$$

Design Lateral Forces, F_{iR} , Design Story Shears, V_{iR} , and Floor Accelerations, A_{iR}

$$F_{iR} = \begin{Bmatrix} 1567 \times 1.0 \times \frac{|-0.399|}{1496} \times 725 \\ 2900 \times (-0.2024) \times \frac{|-0.399|}{1496} \times 725 \\ 2900 \times (-1.6292) \times \frac{|-0.399|}{1496} \times 725 \end{Bmatrix} = \begin{Bmatrix} 303 \\ -114 \\ -915 \end{Bmatrix} \text{ kN} \quad (\text{A13.5.3.7-1})$$

$$A_{iR} = \frac{F_{iR}}{w_i} \cdot \left(\frac{C_d \Omega_o}{R} \right) = \begin{Bmatrix} \frac{303}{1567} \\ \frac{-114}{2900} \\ \frac{-915}{2900} \end{Bmatrix} \times \left(\frac{3 \times 5.5}{8} \right) = \begin{Bmatrix} 0.399 \\ -0.081 \\ 0.651 \end{Bmatrix} \text{ g}$$

$$V_{iR} = \begin{Bmatrix} 303 \\ 189 \\ -726 \end{Bmatrix} \text{ kN}$$

Total responses resulting from modal combinations were calculated by use of the SRSS combination rule. Tables H-2 and H-3 present summaries of the results of the analysis for each mode and the total response calculated by both the ELF and RSA procedures for the DBE and MCE, respectively.

TABLE H-1 Modal Properties of Frame 3S-75

<i>Dynamic Properties</i>				
Quantity	Mode 1 (m=1)	Mode 2 (m=2)	Mode 3 (m=3)	Residual Mode (m=R)
T_m sec	1.320	0.49	0.24	0.528
$\{\phi_m\}$	1.000 0.657 0.250	1.000 -0.560 -0.690	1.000 -1.618 2.096	1.0000 -0.2036 -1.6318
\bar{W}_m , kN (7-12)	5871	1098	398	1496
Γ_m (7-16)	1.3986	-0.5334	0.1348	-0.3986

Note that period T_l is the effective initial (secant) period of the equivalent bilinear representation of the pushover curve of the frame (see Section C.3.1).

TABLE H-2 Modal Response Calculations for Example No.9: 3-Story Frame with Triangular Metallic Yielding Devices. Analysis for the DBE

Quantity	Units	Mode 1 (m=1)	Mode 2 (m=2)	Mode 3 (m=3)	Mode R (m=R)	SRSS	
						ELF	RSA
1. Elastic Response							
Damping Ratio, β_{Ve}		0.050	0.050	0.050	0.050		
Damping Coefficient, B_m		1.000	1.000	1.000	1.000		
Elastic Displacement, D_{em}	mm	275	32	2	28		
2. Roof Displacement and Base Shear							
Assumed Ductility, μ		1.46	1.00	1.00	1.00		
Effective Period, T_{ID}	sec	1.544	0.490	0.240	0.528		
Hysteretic Damping, β_H		0.141	0	0	0		
Effective Damping, β_m		0.186	0.050	0.050	0.050		
Damping Coefficient, B_m		1.458	1.000	1.000	1.000		
Displacement, D_{mD}	mm	221					
Corrected Displacement, D_{mD}	mm	275	32	2	28		
Seismic Coefficient, C_S		0.129	0.485	0.485	0.485		
Seismic Base Shear, V_m	kN	759	532	193	725	1050	947
Yield Displacement, D_y	mm	161	-----	-----	-----		
Computed Ductility, μ		1.71	-----	-----	-----		
3. Response at Stage of Maximum Displacement							
Lateral Floor Displacement, δ_{ij}	mm	275	32	2	28		
		181	-18	-3	-6		
		69	-22	4	-45		
Story Drift, Δ_{jm}	mm	94	50	5	33	100	107
		112	4	-7	39	119	112
		69	-22	4	-45	82	72
Design Lateral Forces, F_{im}	kN	283	405	102	303		
		344	-420	-307	-114		
		131	-517	397	-914		
Floor Acceleration, A_{im}	g	0.373	0.533	0.135	0.399	0.546	0.664
		0.245	-0.299	-0.218	-0.081	0.258	0.444
		0.093	-0.368	0.283	-0.650	0.657	0.473
Actual Story Shear Forces, V_{jm}	kN	584	836	211	625	855	1041
		1294	-30	-421	389	1351	1361
		1564	-1098	398	-1497	2165	1952

TABLE H-3 Modal Response Calculations for Example No.9: 3-Story Frame with Triangular Metallic Yielding Devices. Analysis for the MCE

Quantity	Units	Mode 1 (m=1)	Mode 2 (m=2)	Mode 3 (m=3)	Mode R (m=R)	SRSS	
						ELF	RSA
1. Elastic Response							
Damping Ratio, β_{Ve}		0.050	0.050	0.050	0.050		
Damping Coefficient, B_m		1.000	1.000	1.000	1.000		
Elastic Displacement, D_{em}	mm	413	48	3	41		
2. Roof Displacement and Base Shear							
Assumed Ductility, μ		2.35	1.00	1.00	1.00		
Effective Period, T_{ID}	sec	1.959	0.490	0.240	0.528		
Hysteretic Damping, β_H		0.233	0	0	0		
Effective Damping, β_m		0.278	0.050	0.050	0.050		
Damping Coefficient, B_m		1.734	1.000	1.000	1.000		
Displacement, D_{mD}	mm	353					
Corrected Displacement, D_{mD}	mm	413	48	3	41		
Seismic Coefficient, C_s		0.128	0.727	0.727	0.727		
Seismic Base Shear, V_m	kN	754	798	290	1088	1324	1136
Yield Displacement, D_y	mm	160	-----	-----	-----		
Computed Ductility, μ		2.57	-----	-----	-----		
3. Response at Stage of Maximum Displacement							
Lateral Floor Displacement, δ_{ij}	mm	413	48	3	41		
		271	-27	-5	-8		
		103	-33	6	-68		
Story Drift, Δ_{jm}	mm	142	74	8	50	150	160
		168	6	-11	59	178	168
		103	-33	6	-68	123	109
Design Lateral Forces, F_{im}	kN	281	608	154	454		
		342	-630	-460	-171		
		130	-776	596	-1372		
Floor Acceleration, A_{im}	g	0.370	0.800	0.202	0.598	0.703	0.905
		0.243	-0.448	-0.327	-0.122	0.272	0.606
		0.093	-0.552	0.424	-0.976	0.980	0.702
Actual Story Shear Forces, V_{jm}	kN	581	1254	317	937	1102	1417
		1286	-46	-632	584	1413	1434
		1555	-1646	597	-2245	2731	2342

APPENDIX I

DETAILED CALCULATIONS FOR THE ANALYSIS OF A 3-STORY FRAME WITH LINEAR VISCOUS DAMPING SYSTEM USING THE FEMA 274 METHOD 2 NONLINEAR STATIC PROCEDURE

I.1 Introduction

This appendix presents detailed calculations of the application of Method 2 of FEMA, 1997 for the analysis of a building with a linear viscous damping system. This method is applied as described in Section 2 subject to the modifications described in Section 8.1. The application of this method is illustrated in Figure 2-1.

In this appendix detailed calculations are presented, for the 3-story special steel moment frame 3S-75 shown in Figure 8-2 and denoted as example No.2 in Section 8, using a distribution of lateral load based on the first mode pattern.

I.2 Detailed Calculations for 3-Story Frame 3S-75 with Linear Viscous Damping System

Design Parameters and Modal Properties

The design parameters for, and a description of the 3-story special steel moment frame 3S-75, example No.2 are presented in Section E.2. The modal properties of the frame are presented in Table I.1.

Pushover Analysis

Pushover analysis is performed in IDARC2D-Version 4.0 (Valles et al., 1996) using a distribution of lateral load consistent with the first mode pattern. Table I.1 presents the lateral load distribution patterns utilized in the analysis. Elastoplastic behavior is assumed in the modeling of the plastic hinges. Parameters utilized for modeling of the plastic hinges are summarized in Table I-1. In addition it has been assumed that joints are stiffened within a length of half the depth of the beam ($d_b/2$) section in the vertical direction, and of half the depth of the column section ($d_c/2$) in the horizontal direction. In the first-story columns, the rigid offset above the base of the column is assumed to be equal to the column depth (d_c). Gravity load and P- Δ effects are disregarded in this analysis.

Table I-2 shows the values of base shear, V_I at increments of roof displacement, D_{roof} , of 0.50 mm. It also shows the corresponding values of shear and drifts per story. Figure I-1(a) shows the pushover curve of the building and the sequence of yielding at several steps of the analysis. It also shows the approximate bilinear representation of the pushover curve, giving an approximate base shear strength, V_y , equal to 1232 kN and a displacement at yielding, D_y , of 182 mm. Figure I-1(b) shows the force displacement relationship of each story and its bilinear representation.

Modal Properties of the Frame at Various Stages of the Pushover Analysis

This section is included to illustrate the variation of the modal properties of the frame under inelastic action. Modal properties of the frame were obtained by eigenvalue analysis performed in program IDARC2D using the effective stiffness of each story at three different values of assumed roof displacement. At each assumed roof displacement, the story drift, Δ_j , and the story shear V_j were obtained from Table I-2. The effective stiffness at each story was obtained as $K_{eff} = V_j/\Delta_j$.

Eigenvalue analysis of the frame at the assumed displacement was performed using a shear building type of representation. Models were utilized in which the beams and columns sections were modified to approximately represent the reduction of stiffness due to yielding. Figure I-2 shows the shear type and the modified frame model of the structure that was used for eigenvalue analysis at different values of assumed roof displacement. In both models, the lateral stiffness at

each story was nearly equal with the corresponding effective stiffness at the assumed roof displacement as calculated in the pushover analysis. Table I-3 presents a summary of the modal properties of the frame at each value of assumed roof displacement. Substantial differences in the values of modal properties and effective viscous damping obtained by using both the shear building and the modified model representations of the frame are observed. It is evident that the modal properties of the frame at the various stages of pushover analysis examined depend strongly on the mathematical model, especially for the higher modes. This is an important issue when dealing with systems with rate-dependent damping devices. Magnitude and distribution of damping forces are significantly influenced by the modal properties of the building. Consequently, the model of the frame must represent the actual behavior of the building as close as possible. The “modified model” seems to be a more reasonable approach. Herein the results obtained by eigenvalue analysis of the modified frame are utilized for application of Method 2.

CALCULATION OF RESPONSE IN THE DESIGN BASIS EARTHQUAKE

FIRST MODE RESPONSE ($T_1=1.58$ sec)

Roof Displacement for Elastic Behavior

Viscous Damping Ratio (under elastic conditions): $\beta_{vI} = 0.10$

Effective Viscous Damping Ratio: $\beta_{v+I} = 0.10 + 0.05 = 0.15$

Damping Coefficient: $B_{v+I} = 1.35$ (Table A13.3.1)

Roof Displacement: $D = \left(\frac{9810}{4\pi^2} \right) \times |1.399| \times \frac{0.6}{1.35} \times 1.58 = 244 \text{ mm}$

Assumed Roof Displacement: $D_{ID} = 244 \text{ mm}$

For convenience the roof displacement is assumed to be equal to the elastic displacement.

Modal Properties at Assumed Roof Displacement

Table I-3 presents the results of the eigenvalue analysis for the assumed roof displacement.

Displacement Ductility Ratio: $\mu_D = \frac{244}{182} = 1.34$ (7-36)

Effective Period: from eigenvalue analysis, $T_{eff} = 1.808 \text{ sec}$ (Table I-3)

To facilitate the displacement calculation by iteration, the effective period is calculated using (4-18) with spectral displacement, $S_d = 244 / (1.0 \times 1.449) = 168.4 \text{ mm}$ and spectral acceleration, $S_a = 1232 / 5565 = 0.22 \text{ g}$, and it is found to be $T_{eff} = 1.750 \text{ sec}$.

Note that (7-35) gives: $T_{eff} = T_1 \sqrt{\mu} = 1.58 \sqrt{1.34} = 1.829 \text{ sec}$

Effective Damping Ratio:

Effective Viscous Damping: $\beta_{V1} = 0.130$ (Table I-3)

(use of equation 7-29 with effective period and mode shape per Table I-3)

Quality Factor: $q_H = 0.67 \times \frac{0.6}{1.750} = 0.230 < 0.5$

use $q_H = 0.5$

(use q_H in NEHRP (2000) for consistency)

Hysteretic Damping Ratio: $\beta_{HD} = (0.64 - 0.05) \times 0.5 \times \left(1 - \frac{1}{1.34}\right) = 0.075$

(note use of term $2/\pi - \beta_i$ rather than $2/\pi$ for consistency with NEHRP, 2000)

Effective Damping Ratio: $\beta_{eff} = 0.05 + 0.130 + 0.075 = 0.255$ (7-37)

Damping Coefficient: $B = 1.666$

(use of damping coefficient in NEHRP, 2000 for consistency)

Spectral Capacity Curve

To convert the bilinear representation of the pushover curve to a spectral capacity curve, it is necessary to determine the spectral coordinates at yielding of the frame, and at several other stages of pushover. Herein we utilize three points to define the spectral capacity curve by means of (2-2) and (2-4) and the properties presented in Tables I-1 and I-3, and figure I-1 at different assumed roof displacements, as follows:

$$\text{At yielding } (D_y=182 \text{ mm}): S_{ay} = \frac{1232 \text{ g}}{5871} = 0.21 \text{ g}, \quad S_{dy} = \frac{\delta_r}{\phi_{r1}\Gamma_1} = \frac{182}{1.0 \times 1.399} = 130 \text{ mm}$$

$$\text{At assumed } D_{roof} = 244 \text{ mm}: S_a = \frac{1232 \text{ g}}{5565} = 0.22 \text{ g}, \quad S_d = \frac{\delta_r}{\phi_{r1}\Gamma_1} = \frac{244}{1.0 \times 1.449} = 168 \text{ mm}$$

$$\text{At assumed } D_{roof} = 419 \text{ mm}: S_a = \frac{1232 \text{ g}}{5820} = 0.21 \text{ g}, \quad S_d = \frac{\delta_r}{\phi_{r1}\Gamma_1} = \frac{419}{1.0 \times 1.437} = 292 \text{ mm}$$

Note that the spectral acceleration is not constant as it should have been in an elastoplastic model. The difference is a result of the approximate nature of the analysis. However, the difference is small and we proceed using $S_a = 0.22 \text{ g}$.

Design Demand Curve

The design demand curve is established by using (2-5) and (3-1) and the damping coefficients from Table A13.3.1. Figure 2-2 shows the design demand curves for damping ratios from 5% to 100% for the design-basis earthquake.

Calculated Roof Displacement

Figure I-3 (a) shows the spectral capacity curve of the frame and the design demand curves for damping ratios of 0.15 and 0.26. The spectral displacement S_d is established at the intersection of the spectral capacity curve and the design demand curve for $\beta_{eff} = 0.255$. Note that the same point is also defined at the intersection of the straight line corresponding to the effective period at the assumed displacement, $T_{eff} = 1.750 \text{ sec}$, and the design demand curve for $\beta_{eff} = 0.255$. The spectral displacement at the intersection is $S_d = 156.6 \text{ mm}$. Accordingly, the calculated roof displacement is obtained from (2-4) as

$$D_{1D} = 156.6 \times |1.449| = 227 \text{ mm}$$

Since the calculated roof displacement, $D_{1D} = 227 \text{ mm}$, is less than the assumed displacement 244 mm , iteration was performed using the modal properties corresponding to displacement 244 mm , but changing the period of the structure based on the new assumed displacement. This resulted to a spectral displacement of $S_d = 157 \text{ mm}$ corresponding to a spectral acceleration $S_a = 0.2214 \text{ g}$, $T_{eff} = 1.689 \text{ sec}$ and a displacement $D_{1D} = 227 \text{ mm}$.

Corrected Roof Displacement

Since the calculated roof displacement $D_{1D} = 227 \text{ mm}$ is less than the elastic displacement $D = 244 \text{ mm}$, then take $D_{1D} = 244 \text{ mm}$. The spectral displacement for elastic behavior of the frame is shown in Figure I-3 (a) at the intersection of the straight line corresponding to the fundamental period of the frame ($T_1 = 1.58 \text{ sec}$) and the design demand curve for $\beta_{V+I} = 0.15$.

Base Shear

The base shear can be obtained from (2-2) as

$$V_1 = S_a \cdot \bar{W}_1 = 0.2214 \times 5565 = 1232 \text{ kN}$$

Response at Stage of Maximum Displacement

Lateral Floor Displacements, δ_{i1D} , and Story Drifts, Δ_{i1D}

$$\delta_{i1D} = 244 \times \begin{Bmatrix} 1.000 \\ 0.574 \\ 0.210 \end{Bmatrix} = \begin{Bmatrix} 244 \\ 140 \\ 51 \end{Bmatrix} \text{ mm}$$

Note that here use was made of the mode shape of the modified frame at a roof displacement equal to 244 mm (elastic displacement) and not the elastic mode shape (see Table I-1). One could have used the elastic mode shape.

$$\Delta_{i1D} = \begin{Bmatrix} 104 \\ 89 \\ 51 \end{Bmatrix} \text{ mm}$$

Design Lateral Forces, F_{i_l} , Design Story Shears, V_{i_l} , and Accelerations, A_{i_l}

$$F_{i_l} = \begin{Bmatrix} 1567 \times 1.0 \times \frac{1.449}{5565} \times 1232 \\ 2900 \times 0.574 \times \frac{1.449}{5565} \times 1232 \\ 2900 \times 0.210 \times \frac{1.449}{5565} \times 1232 \end{Bmatrix} = \begin{Bmatrix} 503 \\ 534 \\ 195 \end{Bmatrix} \text{ kN}$$

$$A_{i_l} = \frac{F_{i_l}}{w_i} = \begin{Bmatrix} \frac{503}{1567} \\ \frac{534}{2900} \\ \frac{195}{2900} \end{Bmatrix} = \begin{Bmatrix} 0.321 \\ 0.184 \\ 0.067 \end{Bmatrix} \text{ g}$$

$$V_{i_l} = \begin{Bmatrix} 503 \\ 1037 \\ 1232 \end{Bmatrix} \text{ kN}$$

Response at Stage of Maximum Velocity

Story Velocity, $\nabla_{i_{1D}}$

Calculated as pseudovelocity

$$\nabla_{i_l} = \left(\frac{2\pi}{1.750} \right) \times \begin{Bmatrix} 104 \\ 89 \\ 51 \end{Bmatrix} = \begin{Bmatrix} 373 \\ 320 \\ 183 \end{Bmatrix} \text{ mm/sec}$$

Force in Damping Devices, $Fd_{i_{1D}}$

$$Fd_{i_{1D}} = 0.90 \times \begin{Bmatrix} 373 \\ 320 \\ 183 \end{Bmatrix} \cos 27.6^\circ = \begin{Bmatrix} 298 \\ 255 \\ 146 \end{Bmatrix} \text{ kN} \quad (7-23)$$

Horizontal Component of Damping Forces, Vd_{i1D}

$$Vd_{i1D} = \begin{Bmatrix} 298 \\ 255 \\ 146 \end{Bmatrix} \cos 27.6^\circ = \begin{Bmatrix} 264 \\ 226 \\ 129 \end{Bmatrix} \text{ kN}$$

Response at Stage of Maximum Acceleration

Force Coefficients

Effective Viscous Damping: $\beta_{v1} = 0.05 + 0.130 = 0.180$

Parameter δ : $\delta = \tan^{-1}(2 \times 0.180) = 0.346$

Coefficient CF_1 :

$$CF_1 = \cos(0.346) = 0.941 \quad (4-41)$$

$$CF_1 \mu = 0.941 \times 1.34 = 1.26 > 1.00 \quad \text{use } CF_1 = 1.0$$

Coefficient CF_2 : $CF_2 = \sin(0.346) = 0.339 \quad (4-39)$

(note that we used the revised coefficients CF_1 and CF_2 in 2000 NEHRP)

Maximum Lateral Inertia Forces

$$F_{i1,max} = 1.0 \times \begin{Bmatrix} |503| \\ |534| \\ |195| \end{Bmatrix} + 0.339 \times \begin{Bmatrix} |264| \\ |-38| \\ |-95| \end{Bmatrix} = \begin{Bmatrix} 592 \\ 547 \\ 227 \end{Bmatrix} \text{ kN}$$

Maximum floor acceleration, $A_{i1,max}$

$$A_{i1,max} = \begin{Bmatrix} 592/1567 \\ 547/2900 \\ 227/2900 \end{Bmatrix} = \begin{Bmatrix} 0.378 \\ 0.189 \\ 0.078 \end{Bmatrix}$$

Maximum Story Shear, $V_{i1,max}$

$$V_{i1,max} = CF_1 \cdot |V_{i1}|_{Max \text{ Disp}} + CF_2 \cdot |Vd_{i1D}|_{Max \text{ Velocity}}$$

$$V_{i1,max} = 1.0 \times \begin{Bmatrix} |503| \\ |1037| \\ |1232| \end{Bmatrix} + 0.339 \times \begin{Bmatrix} |264| \\ |226| \\ |129| \end{Bmatrix} = \begin{Bmatrix} 592 \\ 1114 \\ 1276 \end{Bmatrix} \text{ kN}$$

SECOND MODE RESPONSE ($T_2=0.732 \text{ sec} > T_s$)

The higher mode responses are calculated without constructing the spectral-capacity and design-demand curves due to the assumption of elastic behavior. The graphical solution is also presented.

Roof Displacement

Viscous Damping Ratio: $\beta_{v2} = 0.344$ (Table I-3)

Effective Damping Ratio: $\beta_{2D} = 0.344 + 0.05 = 0.394$

Damping Coefficient: $B_{2D} = 2.082$ (Table A13.3.1)

Roof Displacement: $D_{2D} = \left(\frac{9810}{4\pi^2} \right) \times |-0.528| \times \frac{0.6}{2.082} \times 0.732 = 27.7 \text{ mm}$

Seismic Base Shear

Figure I-3(b) shows the design demand curve for $\beta_{2D} = 0.394$ and the spectral capacity curve of the second mode denoted by the straight line corresponding to period $T_2 = 0.732 \text{ sec}$. The corresponding spectral acceleration is obtained at the intersection point as $S_a = 0.394 \text{ g}$. Accordingly, the base shear is obtained from (2-2) as

$$V_2 = 0.394 \times 1091 = 430 \text{ kN}$$

Response at Stage of Maximum Displacement

Lateral Floor Displacement, $\delta_{i_{2D}}$, and Story Drifts, $\Delta_{i_{2D}}$

$$\delta_{i_{2D}} = 27.7 \times \begin{Bmatrix} 1.000 \\ -0.737 \\ -0.516 \end{Bmatrix} = \begin{Bmatrix} 27.7 \\ -20.4 \\ -14.3 \end{Bmatrix} \text{ mm}$$

$$\Delta_{i2D} = \begin{Bmatrix} 48.1 \\ -6.1 \\ -14.3 \end{Bmatrix} \text{ mm}$$

Design Lateral Forces, F_{i2} , Design Story Shears, V_{i2} , and Accelerations, A_{i2}

$$F_{i2} = \begin{Bmatrix} 1567 \times 1.0 \times \frac{|-0.528|}{1091} \times 430 \\ 2900 \times (-0.737) \times \frac{|-0.528|}{1091} \times 430 \\ 2900 \times (-0.516) \times \frac{|-0.528|}{1091} \times 430 \end{Bmatrix} = \begin{Bmatrix} 326 \\ -445 \\ -311 \end{Bmatrix} \text{ kN}$$

$$A_{i2} = \frac{F_{i2}}{w_i} = \begin{Bmatrix} \frac{326}{1567} \\ \frac{-445}{2900} \\ \frac{-311}{2900} \end{Bmatrix} = \begin{Bmatrix} 0.208 \\ -0.153 \\ -0.107 \end{Bmatrix} \text{ g}$$

$$V_{i2} = \begin{Bmatrix} 326 \\ -119 \\ -430 \end{Bmatrix} \text{ kN}$$

Response at Stage of Maximum Velocity

$$\text{Story Velocity, } \nabla_{i2D} \quad \nabla_{i2D} = \left(\frac{2\pi}{0.732} \right) \times \begin{Bmatrix} 48.1 \\ -6.1 \\ -14.3 \end{Bmatrix} = \begin{Bmatrix} 413 \\ -52 \\ -123 \end{Bmatrix} \frac{\text{mm}}{\text{sec}}$$

$$\text{Forces in Damping Devices: } Fd_{i2D} = 0.90 \times \begin{Bmatrix} 413 \\ -52 \\ -123 \end{Bmatrix} \times \cos 27.6 = \begin{Bmatrix} 329 \\ -41 \\ -98 \end{Bmatrix} \text{ kN} \quad (7-23)$$

Response at Stage of Maximum Acceleration

Force Coefficients

$$\beta_{v2} = 0.05 + 0.344 = 0.394$$

$$CF_1 = \cos[\tan^{-1}(2 \times 0.394)] = 0.785 \quad (4-41)$$

$$CF_2 = \sin[\tan^{-1}(2 \times 0.394)] = 0.619 \quad (4-39)$$

Maximum Lateral Inertia Forces

$$F_{i2,max} = 0.785 \times \begin{Bmatrix} |326| \\ |-445| \\ |-311| \end{Bmatrix} + 0.619 \times \begin{Bmatrix} |292| \\ |-329| \\ |-50| \end{Bmatrix} = \begin{Bmatrix} 435 \\ 551 \\ 275 \end{Bmatrix} \text{ kN}$$

Maximum floor acceleration, $A_{i2,max}$

$$A_{i2,max} = \begin{Bmatrix} 435/1567 \\ 551/2900 \\ 275/2900 \end{Bmatrix} = \begin{Bmatrix} 0.277 \\ 0.190 \\ 0.095 \end{Bmatrix}$$

Maximum Story Shear, $V_{i2,max}$

$$V_{i2,max} = CF_1 \cdot |V_{i2}|_{Max Disp} + CF_2 \cdot |Vd_{i2D}|_{Max Velocity}$$

$$V_{i2,max} = 0.785 \times \begin{Bmatrix} |326| \\ |-119| \\ |-430| \end{Bmatrix} + 0.619 \times \begin{Bmatrix} |292| \\ |-36| \\ |-87| \end{Bmatrix} = \begin{Bmatrix} 437 \\ 116 \\ 391 \end{Bmatrix} \text{ kN}$$

THIRD MODE RESPONSE ($T_3 = 0.349 \text{ sec} < T_s$)

Roof Displacement

Viscous Damping Ratio: $\beta_{v3} = 0.199$ (Table I-3)

Effective Damping Ratio: $\beta_{3D} = 0.199 + 0.05 = 0.249$

Damping Coefficient: $B_{3D} = 1.647$ (Table A13.3.1)

Roof Displacement: $D_{3D} = \left(\frac{9810}{4\pi^2}\right) \times |0.0846| \times \frac{1.0}{1.647} \times 0.349^2 = 1.55 \text{ mm}$

Seismic Base Shear

Figure I-3(b) shows the design demand curve for $\beta_{3D} = 0.249$ and the spectral capacity curve of the second mode denoted by the straight line corresponding to period $T_3 = 0.349$ sec. The corresponding spectral acceleration is obtained at the intersection point as $S_a = 0.607$ g. Accordingly, the base shear is obtained from (2-2) as

$$V_3 = 0.607 \times 666 = 404 \text{ kN}$$

Response at Stage of Maximum Displacement

Lateral Floor Displacement, δ_{i3D} , and Story Drifts, Δ_{i3D}

$$\delta_{i3D} = 1.55 \times \begin{Bmatrix} 1.000 \\ -2.733 \\ 4.909 \end{Bmatrix} = \begin{Bmatrix} 1.55 \\ -4.2 \\ 7.6 \end{Bmatrix} \text{ mm}$$

$$\Delta_{i3D} = \begin{Bmatrix} 5.8 \\ -11.8 \\ 7.6 \end{Bmatrix} \text{ mm}$$

Design Lateral Forces, F_{i3} , Design Story Shears, V_{i3} , and Floor Accelerations, A_{i3}

$$F_{i3} = \begin{Bmatrix} 1567 \times 1.0 \times \frac{0.085}{666} \times 404 \\ 2900 \times (-2.733) \times \frac{0.085}{666} \times 404 \\ 2900 \times (4.909) \times \frac{0.085}{666} \times 404 \end{Bmatrix} = \begin{Bmatrix} 81 \\ -409 \\ 734 \end{Bmatrix} \text{ kN}$$

$$A_{i3} = \frac{F_{i2}}{w_i} = \begin{Bmatrix} \frac{81}{1567} \\ \frac{-409}{2900} \\ \frac{734}{2900} \end{Bmatrix} = \begin{Bmatrix} 0.052 \\ -0.141 \\ 0.250 \end{Bmatrix} \text{ g}$$

$$V_{i_3} = \begin{Bmatrix} 81 \\ -328 \\ 406 \end{Bmatrix} \text{ kN}$$

Response at Stage of Maximum Velocity

$$\text{Story Velocity: } \nabla_{i_{3D}} = \left(\frac{2\pi}{0.349} \right) \times \begin{Bmatrix} 5.8 \\ -11.8 \\ 7.6 \end{Bmatrix} = \begin{Bmatrix} 104 \\ -212 \\ 137 \end{Bmatrix} \frac{\text{mm}}{\text{sec}}$$

$$\text{Forces in Damping Devices: } Fd_{i_{3D}} = 0.90 \times \begin{Bmatrix} 104 \\ -212 \\ 137 \end{Bmatrix} \times \cos 27.6 = \begin{Bmatrix} 83 \\ -169 \\ 109 \end{Bmatrix} \text{ kN} \quad (7-23)$$

Response at Stage of Maximum Acceleration

Force Coefficients

$$\beta_{V3} = 0.05 + 0.199 = 0.249$$

$$CF_1 = \cos[\tan^{-1}(2 \times 0.249)] = 0.895 \quad (4-41)$$

$$CF_2 = \sin[\tan^{-1}(2 \times 0.249)] = 0.446 \quad (4-39)$$

Maximum Lateral Inertia Forces

$$F_{i_3,max} = 0.895 \times \begin{Bmatrix} |81| \\ |-409| \\ |734| \end{Bmatrix} + 0.446 \times \begin{Bmatrix} |74| \\ |-224| \\ |247| \end{Bmatrix} = \begin{Bmatrix} 105 \\ 466 \\ 767 \end{Bmatrix} \text{ kN}$$

Maximum floor acceleration, $A_{i_3,max}$

$$A_{i_3,max} = \begin{Bmatrix} 105/1567 \\ 466/2900 \\ 767/2900 \end{Bmatrix} = \begin{Bmatrix} 0.067 \\ 0.161 \\ 0.264 \end{Bmatrix}$$

Maximum Story Shear

$$V_{i_3,max} = CF_1 \cdot |V_{i_3}|_{\text{Max Disp}} + CF_2 \cdot |Vd_{i_{3D}}|_{\text{Max Velocity}}$$

$$V_{i_3,max} = 0.895 \times \begin{Bmatrix} |81| \\ |-328| \\ |406| \end{Bmatrix} + 0.446 \times \begin{Bmatrix} |74| \\ |-150| \\ |97| \end{Bmatrix} = \begin{Bmatrix} 105 \\ 360 \\ 407 \end{Bmatrix} \text{ kN}$$

TABLE I-1 Modal Properties and Modeling Information of Frame 3S-75 for Pushover Analysis in IDARC2D

<i>Modal Properties (under elastic conditions)</i>				
Quantity	Mode 1	Mode 2	Mode 3	
T_m , sec	1.58	0.49	0.24	
$\{\phi_{im}\}$	1.000	1.000	1.000	
	0.657	-0.560	-1.618	
	0.250	-0.690	2.096	
\overline{W}_m , kN	5871	1098	398	
Γ_m	1.399	-0.533	0.135	
<i>Lateral Force Distribution for Pushover</i>				
Lateral Force Factor per Level	First Mode	Modal (C_{vx})	Uniform	Adaptive
λ_3	0.3733	0.4259	0.2127	Vary. Calculated by IDARC
λ_2	0.4540	0.4250	0.3937	
λ_1	0.1727	0.1492	0.3937	
<i>Modeling Parameters for Time History Analysis</i>				
Element	Section	M_p (kN-m)	ϕ_y	ϕ_u
Beam-3 rd floor	W14x26	227	0.000310	0.015500
Beam-2 ^d floor	W16x45	411	0.000267	0.013400
Beam-1 st floor	W16x50	465	0.000267	0.013400
Column	W14x109	1084	0.000294	0.014700

**Table I-2 Base Shear-Roof Displacement and Story Shear-Story Drift Relationships
of Frame of Example No.2 for First Mode Lateral Force Pattern**

Pushover		Third Story		Second Story		First Story	
D _{roof} (mm)	Base Shear, V (kN)	Drift, Δ ₃ (mm)	Shear, V ₃ (kN)	Drift, Δ ₂ (mm)	Shear, V ₂ (kN)	Drift, Δ ₁ (mm)	Shear, V ₁ (kN)
0.0	0.0	0.0	0.0	0.0	0.0	0.0	0.0
0.7	4.4	0.2	1.7	0.3	3.7	0.2	4.4
1.3	8.8	0.5	3.3	0.5	7.4	0.3	8.8
2.0	13.3	0.7	5.0	0.8	11.0	0.5	13.3
2.6	17.7	0.9	6.6	1.1	14.7	0.7	17.7
3.3	22.1	1.1	8.3	1.3	18.4	0.8	22.1
3.9	26.5	1.4	10.0	1.6	22.1	1.0	26.5
4.6	30.9	1.6	11.6	1.9	25.7	1.1	30.9
5.3	35.4	1.8	13.3	2.1	29.4	1.3	35.4
5.9	39.8	2.0	14.9	2.4	33.1	1.5	39.8
6.6	44.2	2.3	16.6	2.7	36.8	1.6	44.2
7.2	48.6	2.5	18.3	2.9	40.5	1.8	48.6
7.9	53.0	2.7	19.9	3.2	44.1	2.0	53.0
8.5	57.5	2.9	21.6	3.5	47.8	2.1	57.5
9.2	62.6	3.2	23.2	3.7	51.5	2.3	62.6
9.9	67.0	3.4	24.9	4.0	55.2	2.5	67.0
10.5	71.5	3.6	26.6	4.3	58.9	2.6	71.5
11.2	75.9	3.8	28.2	4.5	62.5	2.8	75.9
11.8	80.3	4.1	29.9	4.8	66.2	3.0	80.3
12.5	84.7	4.3	31.5	5.1	69.9	3.1	84.7
13.1	89.1	4.5	33.2	5.3	73.6	3.3	89.1
13.8	93.6	4.7	34.9	5.6	77.2	3.4	93.6
14.5	98.0	5.0	36.5	5.9	80.9	3.6	98.0
15.1	102.4	5.2	38.2	6.1	84.6	3.8	102.4
.....	
.....	
200	1156	69	432	82	956	48	1156
.....	
.....	
244	1223	84	455	99	1008	57	1223
.....	
.....	
419	1241	146	463	160	1026	113	1241
.....	
.....	
474	1245	165	465	179	1030	130	1245
532	1249	185	466	199	1034	148	1249
593	1254	206	468	220	1037	168	1254
656	1258	227	470	241	1041	187	1258

TABLE I-3 Modal Properties of Example Frame at Various Stages of Pushover Analysis for First Mode Lateral Force Pattern.

Assumed Roof Disp. mm	Effective Modal Quantities	Shear Building Model			Modified Model of Frame		
		Mode 1 m=1	Mode 2 m=2	Mode 3 m=3	Mode 1 m=1	Mode 2 m=2	Mode 3 m=3
200	T_m, sec	1.656	0.764	0.500	1.657	0.600	0.289
	$\{\phi_{im}\}$	1.000	1.000	1.000	1.000	1.000	1.000
		0.630	-0.738	-3.063	0.612	-0.677	-2.269
		0.195	-0.393	7.230	0.222	-0.538	3.827
	\bar{W}_m, kN	5524	813	1030	5681	1025	628
	Γ_m	1.400	-0.477	0.076	1.425	-0.524	0.103
β_v	0.118	0.386	0.267	0.115	0.276	0.169	
244	$T_m (sec)$	1.807	0.833	0.553	1.808	0.732	0.349
	$\{\phi_{im}\}$	1.000	1.000	1.000	1.000	1.000	1.000
		0.638	-0.704	-2.875	0.574	-0.737	-2.733
		0.216	-0.429	6.051	0.210	-0.516	4.909
	\bar{W}_m, kN	5655	832	879	5565	1091	666
	Γ_m	1.403	-0.486	0.082	1.449	-0.528	0.085
β_v	0.123	0.411	0.304	0.135	0.343	0.199	
419	T_m, sec	2.395	1.106	0.742	2.397	1.021	0.523
	$\{\phi_{im}\}$	1.000	1.000	1.000	1.000	1.000	1.000
		0.656	-0.612	-2.578	0.608	-0.668	-2.850
		0.274	-0.505	4.185	0.248	-0.503	4.829
	\bar{W}_m, kN	6000	825	542	5820	930	576
	Γ_m	1.406	-0.493	0.087	1.437	-0.509	0.079
β_v	0.148	0.515	0.434	0.162	0.479	0.302	

Note that the modal weights and participation factors for the modified model of frame, do not add up to the total weight of the structure and unity, respectively. This is due to the fact that the mode shapes are not exactly orthogonal. This was the result of the methodology used to obtain the mode shape, which was based on averaging the modal displacements for each floor.

Adjustment of the modal weights to add up to the total weight and participation factors to add up to unity results in errors in the calculation of the story and base shears, while if they are not adjusted this discrepancy vanishes. Possible solutions are: a) enforce orthogonality by adjusting the mode shapes, or b) use the shear building model (stick model).

**TABLE I-4 Modal Properties of Example Frame at Various Stages of Pushover Analysis
for Cv, Uniform and Adaptive Patterns**

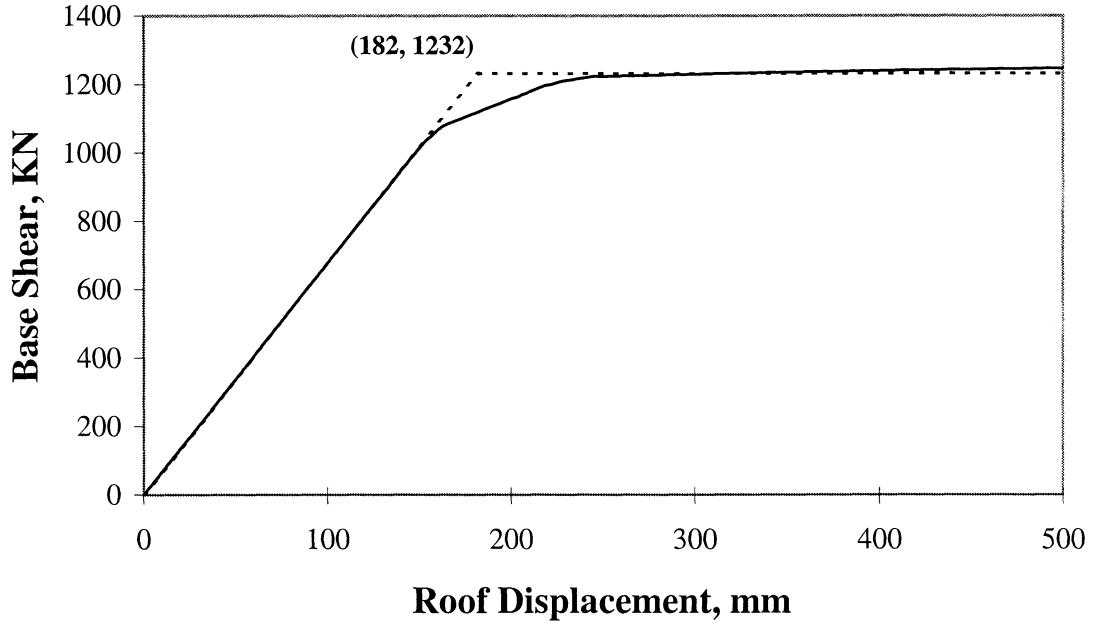
Assumed Roof Disp. mm	Effective Modal Quantities	Cv			Uniform			Adaptive		
		Mode 1 m=1	Mode 2 m=2	Mode 3 m=3	Mode 1 m=1	Mode 2 m=2	Mode 3 m=3	Mode 1 m=1	Mode 2 m=2	Mode 3 m=3
244	T_m (sec)	1.798	0.760	0.360	1.906	0.800	0.370	1.875	0.750	0.352
		1.000	1.000	1.000	1.000	1.000	1.000	1.000	1.000	1.000
	$\{\phi_{im}\}$	0.654	-0.731	-2.662	0.641	-0.736	-2.802	0.642	-0.753	-2.810
		0.233	-0.510	4.854	0.239	-0.523	4.946	0.226	-0.501	5.274
	\bar{W}_m , kN	5778	1067	694	5804	1105	636	5731	1086	722
	Γ_m	1.396	-0.525	0.088	1.409	-0.530	0.082	1.403	-0.525	0.083
	β_v	0.118	0.358	0.205	0.125	0.374	0.212	0.125	0.356	0.199
419	T_m , sec	2.282	1.044	0.530	2.330	1.091	0.540	2.282	1.063	0.510
		1.000	1.000	1.000	1.000	1.000	1.000	1.000	1.000	1.000
	$\{\phi_{im}\}$	0.661	-0.661	-2.725	0.636	-0.704	-3.046	0.639	-0.704	-2.999
		0.264	-0.510	4.645	0.250	-0.487	5.466	0.247	-0.482	5.452
	\bar{W}_m , kN	5947	932	594	5854	964	640	5841	953	662
	Γ_m	1.400	-0.510	0.083	1.416	-0.511	0.075	1.412	-0.509	0.076
	β_v	0.142	0.488	0.306	0.152	0.520	0.307	0.148	0.508	0.290

TABLE I-5 Modal Response Calculations for Example No.2: 3-Story Frame ($V_{\min}=0.75V$) with Linear Viscous Damping System Using Method 2 (FEMA, 1997) for First Mode Lateral Force Pattern. Analysis for the DBE

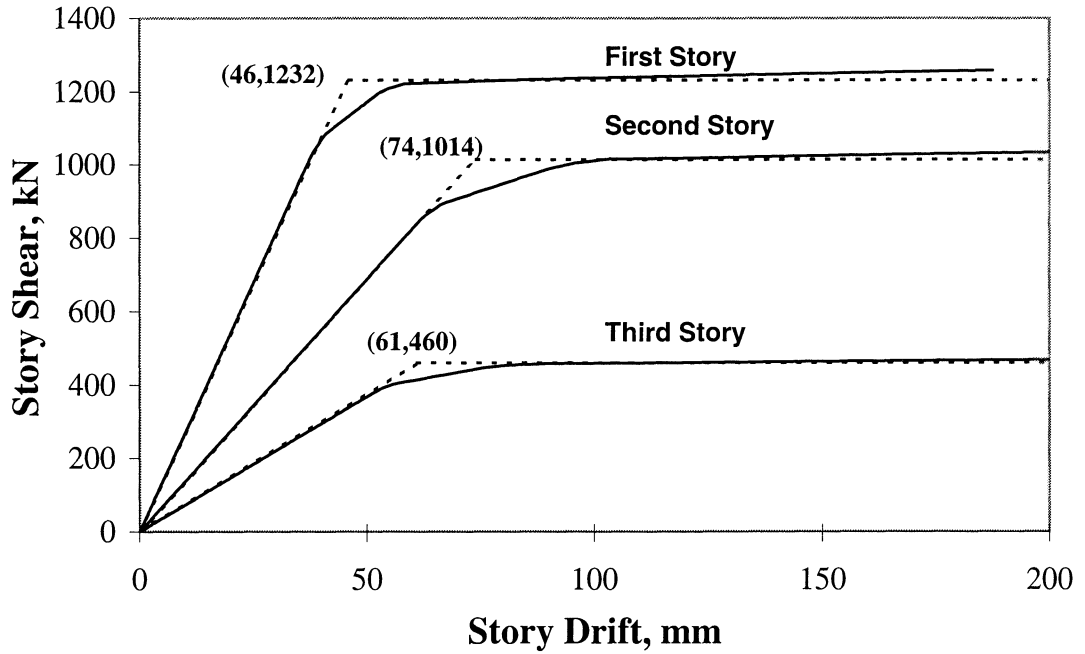
Quantity	Units	Mode 1 (m=1)	Mode 2 (m=2)	Mode 3 (m=3)	SRSS
1. Elastic Response					
Damping Ratio, β_{ve}		0.100	0.344	0.199	
Total Damping Ratio, β_{v+l}		0.150	0.000	0.000	
Damping Coefficient, B_m		1.350	0.394	0.249	
Elastic Displacement, D_{em}	mm	244	28	2	
2. Roof Displacement and Base Shear					
Assumed Displacement D_{ID}		244	28	2	
Effective Period, T_{eff}	sec	1.750	0.732	0.349	
Eff. Visc. Damp. Ratio, β_v		0.130	0.344	0.199	
Hysteretic Damping, β_H		0.075	0	0	
Effective Damping, β_m		0.255	0.394	0.249	
Damping Coefficient, B_m		1.666	2.082	1.647	
Displacement, D_{mD}	mm	227			
Corrected Displacement, D_{mD}	mm	244	28	2	
Spectral Acceleration	g	0.221	0.394	0.607	
Base Shear, V_m	kN	1232	430	405	1366
3. Response at Stage of Maximum Displacement					
Lateral Floor Displacement, δ_{ij}	mm	244	28	2	
		140	-20	-4	
		51	-14	8	
Story Drift, Δ_{jm}	mm	104	48	6	115
		89	-6	-12	90
		51	-14	8	54
Design Lateral Forces, F_{im}	kN	503	326	80	
		534	-444	-407	
		195	-311	731	
Floor Acceleration, A_{im}	g	0.321	0.208	0.051	0.386
		0.184	-0.153	-0.140	0.278
		0.067	-0.107	0.252	0.282
Story Shear Forces, V_{jm}	kN	503	326	80	604
		1037	-119	-327	1093
		1232	-430	405	1366

TABLE I-5 continued

4. Response at Stage of Maximum Velocity					
Drift Velocity, ∇_{im}	mm/sec	373	413	104	566
		319	-53	-214	388
		184	-123	137	260
Force in Damping Devices, $F_{d_{jm}}$	kN	298	329	83	452
		254	-42	-171	309
		147	-98	110	208
Horizontal Damper Force, $V_{d_{jm}}$	kN	264	292	74	
		225	-37	-151	
		130	-87	97	
5. Response at Stage of Maximum Acceleration					
Ductility, μ		1.34	1.00	1.00	
Eff. Viscous Damping Ratio		0.180	0.394	0.249	
Parameter δ		0.346	0.667	0.462	
Coefficient CF_1		0.941	0.785	0.895	
Product $CF_1 \cdot \mu$		1.261	0.785	0.895	
Force Coefficient, CF_1 or C_{mFD}		1.000	0.785	0.895	
Force Coefficient, CF_2 or C_{mFV}		0.339	0.619	0.446	
Max.Floor Acc., $A_{im,max}$	g	0.378	0.278	0.067	0.474
		0.189	0.190	0.160	0.312
		0.079	0.095	0.264	0.291
Maximum Story Shear, $V_{jm,max}$	kN	592	436	105	743
		1113	116	360	1176
		1276	391	405	1395



(a)



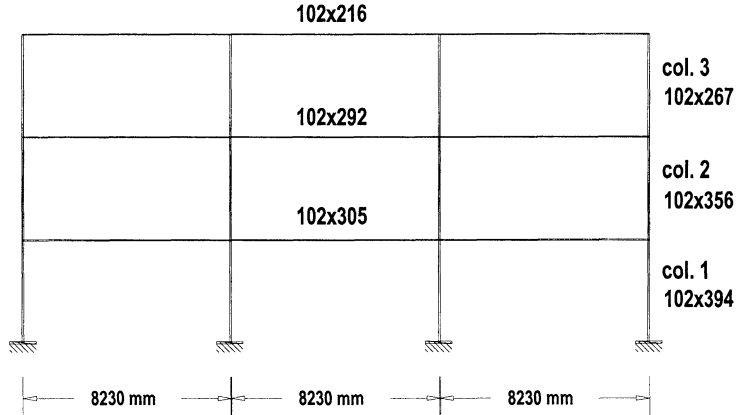
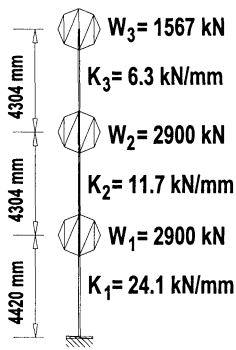
(b)

FIGURE I-1 Pushover Curve and Story Shear-Story Drift Relationships of Frame 3S-75 for First Mode Lateral Force Pattern

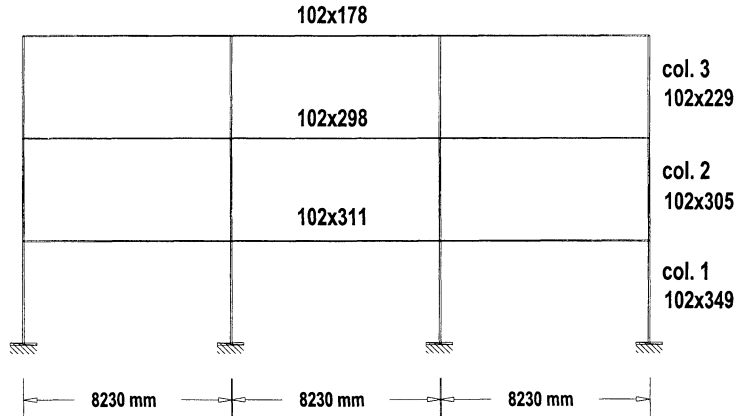
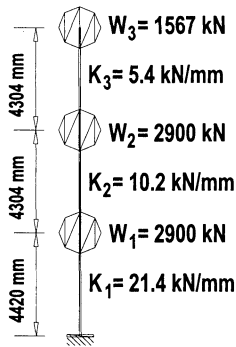
Shear Building Representation

Modified Model of the Frame

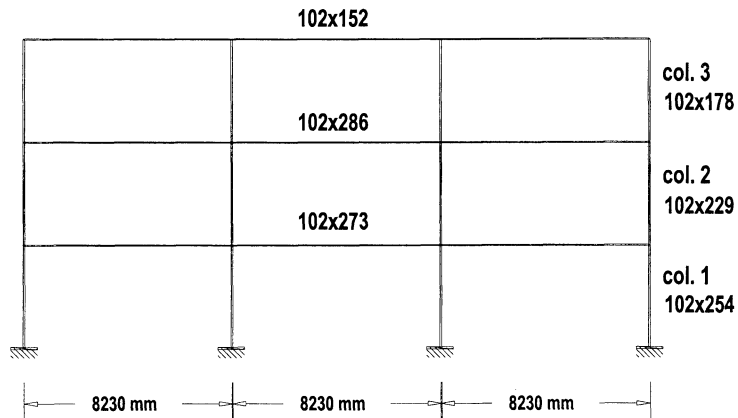
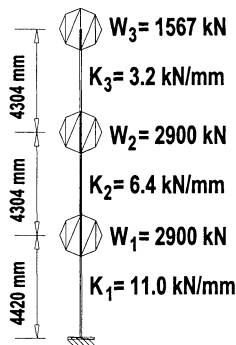
[All Elements are Rectangular Steel Sections]



(a) at assumed roof displacement $D_{roof} = 200$ mm



(b) at assumed roof displacement $D_{roof} = 244$ mm



(c) at assumed roof displacement $D_{roof} = 419$ mm

FIGURE I-2 Shear Building and Modified Model Representations of Frame 3S-75 for Eigenvalue Analysis at Different Values of Assumed Roof Displacement

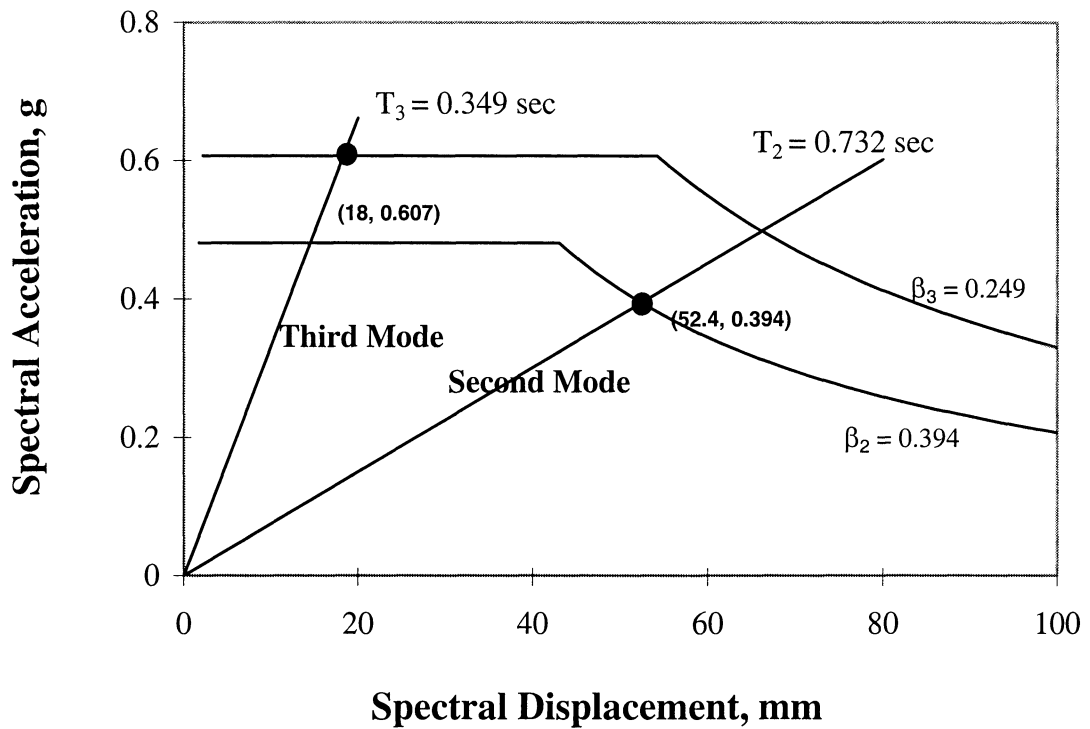
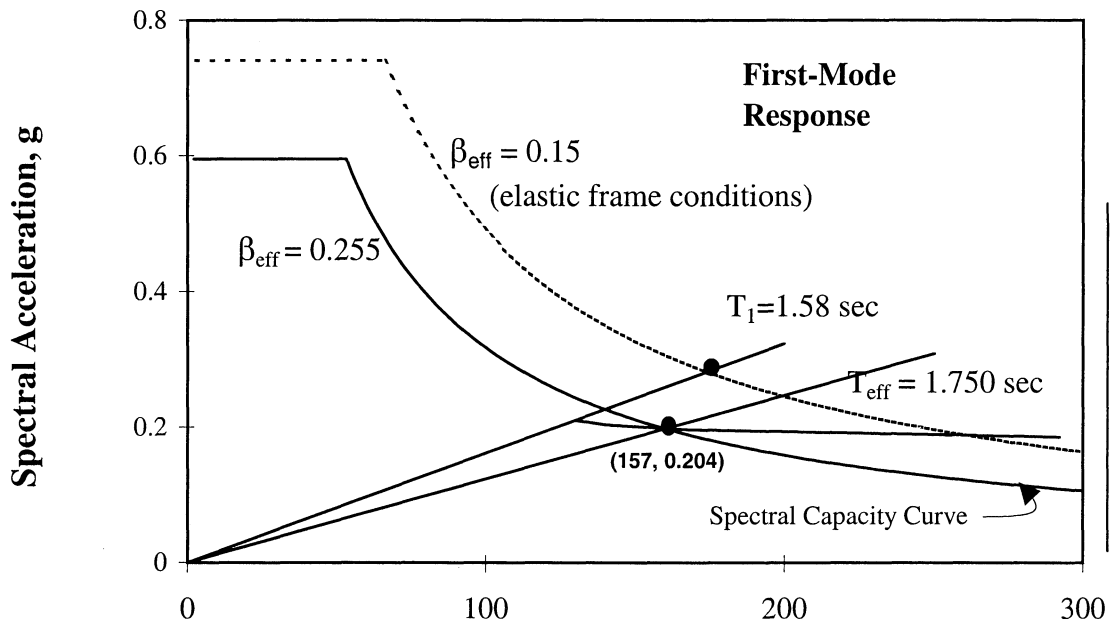


FIGURE I-3 Determination of Modal Spectral Response of Frame 3S-75 Using Method 2 (FEMA,1997)

APPENDIX J

INPUT FILES FOR EIGENVALUE AND PUSHOVER ANALYSIS OF FRAMES WITH DAMPING SYSTEMS IN PROGRAM SAP2000-NL

J.1 Introduction

This appendix contains information on the input files for the eigenvalue and pushover analysis of selected examples of frames with damping systems in program SAP2000-NL Version 7.11. The input files of the following examples are presented:

- (a) 3-story special steel moment frame designed to meet NEHRP (1997) criteria without a damping system.
- (b) Example No.2: frame 3S-75 with linear viscous damping system to provide 10% viscous damping ratio when assuming elastic frame behavior (Fig. 8-2).
- (c) Example No.5: frame 6S-75 with linear viscous damping system to provide 10% viscous damping ratio when assuming elastic frame behavior (Fig. 8-5).
- (d) Example No.8: frame 3S-75 with viscoelastic solid damping system to provide 8.5% viscous damping ratio when assuming elastic frame behavior (Fig. 8-8).
- (e) Example No.9: frame 3S-75 with metallic yielding damping system (Fig. 8-9).

Input files for the pushover analysis of the frames for three lateral force patterns are presented: (a) proportional to the first mode, (b) modal (Cvx) pattern, and (c) uniform pattern.

**SAP2000-NL VERSION 7.11 INPUT FILE FOR EIGENVALUE AND PUSHOVER
ANALYSIS OF 3-STORY SPECIAL STEEL MOMENT FRAME DESIGNED TO
MEET NEHRP (1997) CRITERIA WITHOUT A DAMPING SYSTEM**

SYSTEM

DOF=UX,UZ,RY LENGTH=IN FORCE=Kip PAGE=SECTIONS

JOINT

17 X=-486 Y=0 Z=0
18 X=-486 Y=0 Z=174
19 X=-486 Y=0 Z=343.44
20 X=-486 Y=0 Z=512.88
21 X=-162 Y=0 Z=512.88
22 X=162 Y=0 Z=512.88
23 X=486 Y=0 Z=512.88
24 X=486 Y=0 Z=343.44
25 X=486 Y=0 Z=174
26 X=486 Y=0 Z=0
27 X=-162 Y=0 Z=343.44
28 X=162 Y=0 Z=343.44
29 X=-162 Y=0 Z=174
30 X=162 Y=0 Z=174
33 X=162 Y=0 Z=0
34 X=-162 Y=0 Z=0

RESTRAINT

ADD=17 DOF=U1,U2,U3,R1,R2,R3
ADD=26 DOF=U1,U2,U3,R1,R2,R3
ADD=33 DOF=U1,U2,U3,R1,R2,R3
ADD=34 DOF=U1,U2,U3,R1,R2,R3

PATTERN

NAME=DEFAULT

MASS

ADD=20 U1=.222
ADD=21 U1=.222
ADD=22 U1=.222
ADD=23 U1=.222
ADD=18 U1=.41133
ADD=19 U1=.4121
ADD=24 U1=.4121
ADD=25 U1=.41133
ADD=27 U1=.4121
ADD=28 U1=.4121
ADD=29 U1=.41133
ADD=30 U1=.41133

MATERIAL

NAME=STEEL IDES=S M=7.324E-07 W=.000283
T=0 E=29000 U=.3 A=.0000065 FY=50
NAME=CONC IDES=C M=2.246377E-07 W=.0000868
T=0 E=3600 U=.2 A=.0000055
NAME=OTHER IDES=N M=2.246377E-07 W=.0000868
T=0 E=3600 U=.2 A=.0000055

FRAME SECTION

NAME=W14X211 MAT=STEEL A=62 J=44.6 I=2660,1030 AS=15.406,41.08 S=338.4224,130.3797
Z=390,198 R=6.550056,4.075893 T=15.72,15.8,1.56,.98,15.8,1.56 SHN=W14X211 DSG=W

NAME=W18X46 MAT=STEEL A=13.5 J=1.22 I=712,22.5 AS=6.5016,6.1105 S=78.84829,7.425743
Z=90.7,11.7 R=7.262282,1.290994 T=18.06,6.06,.605,.36,6.06,.605 SHN=W18X46 DSG=W

NAME=W21X50 MAT=STEEL A=14.7 J=1.14 I=984,24.9 AS=7.9154,5.8226 S=94.47912,7.626339
Z=110,12.2 R=8.181612,1.301491 T=20.83,6.53,.535,.38,6.53,.535 SHN=W21X50 DSG=W

NAME=W24X62 MAT=STEEL A=18.2 J=1.71 I=1550,34.5 AS=10.208,6.9227 S=130.5813,9.801136
Z=153,15.7 R=9.228479,1.376809 T=23.74,7.04,.59,.43,7.04,.59 SHN=W24X62 DSG=W

FRAME

22 J=17,18 SEC=W14X211 NSEG=2 ANG=0 IOFF=14 JOFF=12 RIGID=1
23 J=18,19 SEC=W14X211 NSEG=2 ANG=0 IOFF=12 JOFF=10.5 RIGID=1
24 J=19,20 SEC=W14X211 NSEG=2 ANG=0 IOFF=10.5 JOFF=9 RIGID=1
25 J=20,21 SEC=W18X46 NSEG=4 ANG=0 IOFF=7 JOFF=7 RIGID=1
26 J=21,22 SEC=W18X46 NSEG=4 ANG=0 IOFF=7 JOFF=7 RIGID=1
27 J=22,23 SEC=W18X46 NSEG=4 ANG=0 IOFF=7 JOFF=7 RIGID=1
28 J=23,24 SEC=W14X211 NSEG=2 ANG=0 IOFF=10.5 JOFF=9 RIGID=1
29 J=24,25 SEC=W14X211 NSEG=2 ANG=0 IOFF=12 JOFF=10.5 RIGID=1
30 J=25,26 SEC=W14X211 NSEG=2 ANG=0 IOFF=14 JOFF=12 RIGID=1
31 J=19,27 SEC=W21X50 NSEG=4 ANG=0 IOFF=7 JOFF=7 RIGID=1
32 J=27,28 SEC=W21X50 NSEG=4 ANG=0 IOFF=7 JOFF=7 RIGID=1
33 J=28,24 SEC=W21X50 NSEG=4 ANG=0 IOFF=7 JOFF=7 RIGID=1
34 J=18,29 SEC=W24X62 NSEG=4 ANG=0 IOFF=7 JOFF=7 RIGID=1
35 J=29,30 SEC=W24X62 NSEG=4 ANG=0 IOFF=7 JOFF=7 RIGID=1
36 J=30,25 SEC=W24X62 NSEG=4 ANG=0 IOFF=7 JOFF=7 RIGID=1
38 J=33,30 SEC=W14X211 NSEG=2 ANG=0 IOFF=14 JOFF=12 RIGID=1
39 J=30,28 SEC=W14X211 NSEG=2 ANG=0 IOFF=12 JOFF=10.5 RIGID=1
40 J=28,22 SEC=W14X211 NSEG=2 ANG=0 IOFF=10.5 JOFF=9 RIGID=1
41 J=34,29 SEC=W14X211 NSEG=2 ANG=0 IOFF=14 JOFF=12 RIGID=1
42 J=29,27 SEC=W14X211 NSEG=2 ANG=0 IOFF=12 JOFF=10.5 RIGID=1
43 J=27,21 SEC=W14X211 NSEG=2 ANG=0 IOFF=10.5 JOFF=9 RIGID=1

LOAD

NAME=CVX
TYPE=FORCE
ADD=20 UX=.3942
ADD=19 UX=.4301
ADD=18 UX=.1757
NAME=UNIFORM
TYPE=FORCE
ADD=20 UX=.2128
ADD=19 UX=.3936
ADD=18 UX=.3936
NAME=NEHRPSTR
TYPE=FORCE
ADD=20 UX=49.4
ADD=19 UX=55.8
ADD=18 UX=24.2

```

NAME=GAVITY
TYPE=DISTRIBUTED SPAN
  ADD=25 RD=0,1 UZ=-1,-1
  ADD=26 RD=0,1 UZ=-1,-1
  ADD=27 RD=0,1 UZ=-1,-1
  ADD=31 RD=0,1 UZ=-1,-1
  ADD=32 RD=0,1 UZ=-1,-1
  ADD=33 RD=0,1 UZ=-1,-1
  ADD=34 RD=0,1 UZ=-1,-1
  ADD=35 RD=0,1 UZ=-1,-1
  ADD=36 RD=0,1 UZ=-1,-1
NAME=NEHRPDRF
TYPE=FORCE
  ADD=20 UX=45.2
  ADD=19 UX=50
  ADD=18 UX=20.9

```

```

MODE
TYPE=EIGEN N=3 TOL=.00001

```

```

OUTPUT
; No Output Requested

```

```

END

```

```

; The following data is used for graphics, design and pushover analysis.
; If changes are made to the analysis data above, then the following data
; should be checked for consistency.

```

SAP2000 V7.11 SUPPLEMENTAL DATA

```

GRID GLOBAL X "1" -486
GRID GLOBAL X "2" -162
GRID GLOBAL X "3" 162
GRID GLOBAL X "4" 486
GRID GLOBAL Y "5" 0
GRID GLOBAL Z "6" 0
GRID GLOBAL Z "7" 174
GRID GLOBAL Z "8" 343.44
GRID GLOBAL Z "9" 512.88
MATERIAL STEEL FY 50
MATERIAL CONC FYREBAR 60 FYSHEAR 40 FC 4 FCSHEAR 4
FRAMESECTION FS1 NAME W21X62-A
STATICLOAD CVX TYPE DEAD
STATICLOAD UNIFORM TYPE DEAD
STATICLOAD NEHRPSTR TYPE DEAD
STATICLOAD GAVITY TYPE DEAD
STATICLOAD NEHRPDRF TYPE DEAD
PUSHCASE "PUSHM1" CONTROL DISP TARGET 20 JOINT 20 DOF U1
PUSHCASE "PUSHM1" PDELTA NO
PUSHCASE "PUSHM1" MINSTEPS 20 MAXNULLSTEPS 10 MAXTOTALSTEPS 220 MAXITER
10
PUSHCASE "PUSHM1" ITERTOL .0001 EVENTTOL .01
PUSHCASE "PUSHM1" LOADTYPE MODE NUMBER 1 SCALEFACTOR 1
HINGE "USER" TYPE M3 SYMMETRIC
HINGE "USER" TYPE M3 B 1 1 C 50 1 D 50 .2 E 80 .2
HINGE "USER" TYPE M3 IO 2 LS 4 CP 6
FRAMEHINGE 22 HINGE "USER" RDISTANCE .0805

```

FRAMEHINGE 22 HINGE "USER" RDISTANCE .9224
FRAMEHINGE 23 HINGE "USER" RDISTANCE .0797
FRAMEHINGE 23 HINGE "USER" RDISTANCE .9292
FRAMEHINGE 24 HINGE "USER" RDISTANCE .0708
FRAMEHINGE 24 HINGE "USER" RDISTANCE .938
FRAMEHINGE 25 HINGE "USER" RDISTANCE .03086
FRAMEHINGE 25 HINGE "USER" RDISTANCE .969
FRAMEHINGE 26 HINGE "USER" RDISTANCE .03086
FRAMEHINGE 26 HINGE "USER" RDISTANCE .969
FRAMEHINGE 27 HINGE "USER" RDISTANCE .03086
FRAMEHINGE 27 HINGE "USER" RDISTANCE .969
FRAMEHINGE 28 HINGE "USER" RDISTANCE .0708
FRAMEHINGE 28 HINGE "USER" RDISTANCE .938
FRAMEHINGE 29 HINGE "USER" RDISTANCE .0797
FRAMEHINGE 29 HINGE "USER" RDISTANCE .9292
FRAMEHINGE 30 HINGE "USER" RDISTANCE .0805
FRAMEHINGE 30 HINGE "USER" RDISTANCE .9224
FRAMEHINGE 31 HINGE "USER" RDISTANCE .03086
FRAMEHINGE 31 HINGE "USER" RDISTANCE .969
FRAMEHINGE 32 HINGE "USER" RDISTANCE .03086
FRAMEHINGE 32 HINGE "USER" RDISTANCE .969
FRAMEHINGE 33 HINGE "USER" RDISTANCE .03086
FRAMEHINGE 33 HINGE "USER" RDISTANCE .969
FRAMEHINGE 34 HINGE "USER" RDISTANCE .03086
FRAMEHINGE 34 HINGE "USER" RDISTANCE .969
FRAMEHINGE 35 HINGE "USER" RDISTANCE .03086
FRAMEHINGE 35 HINGE "USER" RDISTANCE .969
FRAMEHINGE 36 HINGE "USER" RDISTANCE .03086
FRAMEHINGE 36 HINGE "USER" RDISTANCE .969
FRAMEHINGE 38 HINGE "USER" RDISTANCE .0805
FRAMEHINGE 38 HINGE "USER" RDISTANCE .9224
FRAMEHINGE 39 HINGE "USER" RDISTANCE .0797
FRAMEHINGE 39 HINGE "USER" RDISTANCE .9292
FRAMEHINGE 40 HINGE "USER" RDISTANCE .0708
FRAMEHINGE 40 HINGE "USER" RDISTANCE .938
FRAMEHINGE 41 HINGE "USER" RDISTANCE .0805
FRAMEHINGE 41 HINGE "USER" RDISTANCE .9224
FRAMEHINGE 42 HINGE "USER" RDISTANCE .0797
FRAMEHINGE 42 HINGE "USER" RDISTANCE .9292
FRAMEHINGE 43 HINGE "USER" RDISTANCE .0708
FRAMEHINGE 43 HINGE "USER" RDISTANCE .938
END SUPPLEMENTAL DATA

**SAP2000-NL VERSION 7.11 INPUT FILE FOR EIGENVALUE AND
PUSHOVER ANALYSIS OF EXAMPLE No.2: FRAME 3S-75 WITH LINEAR
VISCOUS DAMPING SYSTEM TO PROVIDE 10% VISCOUS DAMPING
RATIO WHEN ASSUMING ELASTIC FRAME BEHAVIOR**

SYSTEM

DOF=UX,UZ,RY LENGTH=IN FORCE=Kip PAGE=SECTIONS

JOINT

17 X=-486 Y=0 Z=0
18 X=-486 Y=0 Z=174
19 X=-486 Y=0 Z=343.44
20 X=-486 Y=0 Z=512.88
21 X=-162 Y=0 Z=512.88
22 X=162 Y=0 Z=512.88
23 X=486 Y=0 Z=512.88
24 X=486 Y=0 Z=343.44
25 X=486 Y=0 Z=174
26 X=486 Y=0 Z=0
27 X=-162 Y=0 Z=343.44
28 X=162 Y=0 Z=343.44
29 X=-162 Y=0 Z=174
30 X=162 Y=0 Z=174
33 X=162 Y=0 Z=0
34 X=-162 Y=0 Z=0

RESTRAINT

ADD=17 DOF=U1,U2,U3,R1,R2,R3
ADD=26 DOF=U1,U2,U3,R1,R2,R3
ADD=33 DOF=U1,U2,U3,R1,R2,R3
ADD=34 DOF=U1,U2,U3,R1,R2,R3

PATTERN

NAME=DEFAULT

MASS

ADD=20 U1=.228238
ADD=21 U1=.228238
ADD=22 U1=.228238
ADD=23 U1=.228238
ADD=18 U1=.4224093
ADD=19 U1=.4224093
ADD=24 U1=.4224093
ADD=25 U1=.4224093
ADD=27 U1=.4224093
ADD=28 U1=.4224093
ADD=29 U1=.4224093
ADD=30 U1=.4224093

MATERIAL

NAME=STEEL IDES=S M=7.324E-07 W=.000283
T=0 E=29000 U=.3 A=.0000065 FY=50
NAME=CONC IDES=C M=2.246377E-07 W=.0000868
T=0 E=3600 U=.2 A=.0000055

NAME=OTHER IDES=N M=2.246377E-07 W=.0000868
T=0 E=3600 U=.2 A=.0000055

FRAME SECTION

NAME=W14X109 MAT=STEEL A=32 J=7.12 I=1240,447 AS=7.518,20.934 S=173.1844,61.21191
Z=192,92.7 R=6.22495,3.737479 T=14.32,14.605,.86,.525,14.605,.86 SHN=W14X109 DSG=W
NAME=W16X40 MAT=STEEL A=11.8 J=.79 I=518,28.9 AS=4.8831,5.8875 S=64.70956,8.263045
Z=72.9,12.7 R=6.625579,1.564977 T=16.01,6.995,.505,.305,6.995,.505 SHN=W16X40 DSG=W
NAME=W16X45 MAT=STEEL A=13.3 J=1.11 I=586,32.8 AS=5.5649,6.6246 S=72.65965,9.324804
Z=82.3,14.5 R=6.637782,1.570403 T=16.13,7.035,.565,.345,7.035,.565 SHN=W16X45 DSG=W
NAME=W14X26 MAT=STEEL A=7.69 J=.36 I=245,8.91 AS=3.5471,3.5175 S=35.22646,3.546268
Z=40.2,5.54 R=5.644427,1.076405 T=13.91,5.025,.42,.255,5.025,.42 SHN=W14X26 DSG=W

FRAME

1 J=18,29 SEC=W16X45 NSEG=4 ANG=0 IOFF=10 JOFF=10 RIGID=1
2 J=29,30 SEC=W16X45 NSEG=4 ANG=0 IOFF=10 JOFF=10 RIGID=1
3 J=30,25 SEC=W16X45 NSEG=4 ANG=0 IOFF=10 JOFF=10 RIGID=1
4 J=19,27 SEC=W16X40 NSEG=4 ANG=0 IOFF=10 JOFF=10 RIGID=1
5 J=27,28 SEC=W16X40 NSEG=4 ANG=0 IOFF=10 JOFF=10 RIGID=1
6 J=28,24 SEC=W16X40 NSEG=4 ANG=0 IOFF=10 JOFF=10 RIGID=1
7 J=20,21 SEC=W14X26 NSEG=4 ANG=0 IOFF=10 JOFF=10 RIGID=1
8 J=21,22 SEC=W14X26 NSEG=4 ANG=0 IOFF=10 JOFF=10 RIGID=1
9 J=22,23 SEC=W14X26 NSEG=4 ANG=0 IOFF=10 JOFF=10 RIGID=1
22 J=17,18 SEC=W14X109 NSEG=2 ANG=0 IOFF=18 JOFF=10 RIGID=1
23 J=18,19 SEC=W14X109 NSEG=2 ANG=0 IOFF=10 JOFF=10 RIGID=1
24 J=19,20 SEC=W14X109 NSEG=2 ANG=0 IOFF=10 JOFF=9 RIGID=1
28 J=23,24 SEC=W14X109 NSEG=2 ANG=0 IOFF=10 JOFF=9 RIGID=1
29 J=24,25 SEC=W14X109 NSEG=2 ANG=0 IOFF=10 JOFF=10 RIGID=1
30 J=25,26 SEC=W14X109 NSEG=2 ANG=0 IOFF=18 JOFF=10 RIGID=1
38 J=33,30 SEC=W14X109 NSEG=2 ANG=0 IOFF=18 JOFF=10 RIGID=1
39 J=30,28 SEC=W14X109 NSEG=2 ANG=0 IOFF=10 JOFF=10 RIGID=1
40 J=28,22 SEC=W14X109 NSEG=2 ANG=0 IOFF=10 JOFF=9 RIGID=1
41 J=34,29 SEC=W14X109 NSEG=2 ANG=0 IOFF=18 JOFF=10 RIGID=1
42 J=29,27 SEC=W14X109 NSEG=2 ANG=0 IOFF=10 JOFF=10 RIGID=1
43 J=27,21 SEC=W14X109 NSEG=2 ANG=0 IOFF=10 JOFF=9 RIGID=1

LOAD

NAME=CVX
TYPE=FORCE
ADD=20 UX=.4576
ADD=19 UX=.417
ADD=18 UX=.1255
NAME=NEHRP
TYPE=FORCE
ADD=20 UX=37.79
ADD=19 UX=32.46
ADD=18 UX=8.84
NAME=GRAVITY
TYPE=DISTRIBUTED SPAN
ADD=7 RD=0,1 UZ=-.06,-.06
ADD=8 RD=0,1 UZ=-.06,-.06
ADD=9 RD=0,1 UZ=-.06,-.06
ADD=1 RD=0,1 UZ=-.13,-.13
ADD=2 RD=0,1 UZ=-.13,-.13
ADD=3 RD=0,1 UZ=-.13,-.13
ADD=4 RD=0,1 UZ=-.13,-.13

```

    ADD=5 RD=0,1 UZ=-.13,-.13
    ADD=6 RD=0,1 UZ=-.13,-.13
NAME=1STMODE
TYPE=FORCE
    ADD=20 UX=125.1
    ADD=19 UX=156.6
    ADD=18 UX=63.6
NAME=RMODE
TYPE=FORCE
    ADD=20 UX=93.9
    ADD=19 UX=-27
    ADD=18 UX=-275.7
NAME=DEAD
NAME=LIVE
NAME=1MODDBE
TYPE=FORCE
    ADD=20 UX=41.7
    ADD=19 UX=52.2
    ADD=18 UX=21.2
NAME=RMODBE
TYPE=FORCE
    ADD=20 UX=31.3
    ADD=19 UX=-9
    ADD=18 UX=-91.9
NAME=DDLL
NAME=UNIFORM
TYPE=FORCE
    ADD=20 UX=.2127
    ADD=19 UX=.39365
    ADD=18 UX=.39365

```

```

MODE
TYPE=EIGEN N=3 TOL=.00001

```

```

COMBO
NAME=DSTL1
LOAD=CVX SF=1
LOAD=NEHRP SF=1
LOAD=GRAVITY SF=1
LOAD=1STMODE SF=1
LOAD=RMODE SF=1
LOAD=DEAD SF=1
LOAD=1MODDBE SF=1
LOAD=RMODBE SF=1
LOAD=DDLL SF=1
LOAD=UNIFORM SF=1
NAME=DSTL2
LOAD=CVX SF=1
LOAD=NEHRP SF=1
LOAD=GRAVITY SF=1
LOAD=1STMODE SF=1
LOAD=RMODE SF=1
LOAD=DEAD SF=1
LOAD=LIVE SF=1
LOAD=1MODDBE SF=1
LOAD=RMODBE SF=1

```

LOAD=DDLL SF=1
LOAD=UNIFORM SF=1

OUTPUT
; No Output Requested

END

; The following data is used for graphics, design and pushover analysis.
; If changes are made to the analysis data above, then the following data
; should be checked for consistency.

SAP2000 V7.11 SUPPLEMENTAL DATA

GRID GLOBAL X "1" -486

GRID GLOBAL X "2" -162

GRID GLOBAL X "3" 162

GRID GLOBAL X "4" 486

GRID GLOBAL Y "5" 0

GRID GLOBAL Z "6" 0

GRID GLOBAL Z "7" 174

GRID GLOBAL Z "8" 343.44

GRID GLOBAL Z "9" 512.88

MATERIAL STEEL FY 50

MATERIAL CONC FYREBAR 60 FYSHEAR 40 FC 4 FCSHEAR 4

STATICLOAD CVX TYPE DEAD

STATICLOAD NEHRP TYPE DEAD

STATICLOAD GRAVITY TYPE DEAD

STATICLOAD 1STMODE TYPE DEAD

STATICLOAD RMODE TYPE DEAD

STATICLOAD DEAD TYPE DEAD

STATICLOAD LIVE TYPE LIVE

STATICLOAD 1MODDBE TYPE DEAD

STATICLOAD RMODBE TYPE DEAD

STATICLOAD DDLL TYPE DEAD

STATICLOAD UNIFORM TYPE DEAD

COMBO DSTL1 DESIGN STEEL

COMBO DSTL2 DESIGN STEEL

STEELDESIGN "AISC-ASD89"

PUSHCASE "PUSHUNO" CONTROL DISP TARGET 20 JOINT 20 DOF U1

PUSHCASE "PUSHUNO" PDELTA NO

PUSHCASE "PUSHUNO" MINSTEPS 50 MAXNULLSTEPS 50 MAXTOTALSTEPS 200

MAXITER 10

PUSHCASE "PUSHUNO" ITERTOL .0001 EVENTTOL .01

PUSHCASE "PUSHUNO" LOADTYPE MODE NUMBER 1 SCALEFACTOR -1

PUSHCASE "PUSHCVX" CONTROL DISP TARGET 20 JOINT 20 DOF U1

PUSHCASE "PUSHCVX" MINSTEPS 50 MAXNULLSTEPS 50 MAXTOTALSTEPS 200

MAXITER 10

PUSHCASE "PUSHCVX" ITERTOL .0001 EVENTTOL .01

PUSHCASE "PUSHCVX" LOADTYPE STATIC LOAD CVX SCALEFACTOR 1

PUSHCASE "PUSHUNIF" CONTROL DISP TARGET 20 JOINT 20 DOF U1

PUSHCASE "PUSHUNIF" PDELTA NO

PUSHCASE "PUSHUNIF" MINSTEPS 50 MAXNULLSTEPS 50 MAXTOTALSTEPS 200

MAXITER 10

PUSHCASE "PUSHUNIF" ITERTOL .0001 EVENTTOL .01

PUSHCASE "PUSHUNIF" LOADTYPE STATIC LOAD UNIFORM SCALEFACTOR 1

HINGE "USER" TYPE M3 SYMMETRIC

HINGE "USER" TYPE M3 B 1 1 C 6 1 D 8 1 E 10 1

HINGE "USER" TYPE M3 IO 2 LS 4 CP 6
FRAMEHINGE 22 HINGE "USER" RDISTANCE 0
FRAMEHINGE 22 HINGE "USER" RDISTANCE 1
FRAMEHINGE 23 HINGE "USER" RDISTANCE 0
FRAMEHINGE 23 HINGE "USER" RDISTANCE 1
FRAMEHINGE 24 HINGE "USER" RDISTANCE 0
FRAMEHINGE 24 HINGE "USER" RDISTANCE 1
FRAMEHINGE 28 HINGE "USER" RDISTANCE 0
FRAMEHINGE 28 HINGE "USER" RDISTANCE 1
FRAMEHINGE 29 HINGE "USER" RDISTANCE 0
FRAMEHINGE 29 HINGE "USER" RDISTANCE 1
FRAMEHINGE 30 HINGE "USER" RDISTANCE 0
FRAMEHINGE 30 HINGE "USER" RDISTANCE 1
FRAMEHINGE 38 HINGE "USER" RDISTANCE 0
FRAMEHINGE 38 HINGE "USER" RDISTANCE 1
FRAMEHINGE 39 HINGE "USER" RDISTANCE 0
FRAMEHINGE 39 HINGE "USER" RDISTANCE 1
FRAMEHINGE 40 HINGE "USER" RDISTANCE 0
FRAMEHINGE 40 HINGE "USER" RDISTANCE 1
FRAMEHINGE 41 HINGE "USER" RDISTANCE 0
FRAMEHINGE 41 HINGE "USER" RDISTANCE 1
FRAMEHINGE 42 HINGE "USER" RDISTANCE 0
FRAMEHINGE 42 HINGE "USER" RDISTANCE 1
FRAMEHINGE 43 HINGE "USER" RDISTANCE 0
FRAMEHINGE 43 HINGE "USER" RDISTANCE 1
FRAMEHINGE 1 HINGE "USER" RDISTANCE 0
FRAMEHINGE 1 HINGE "USER" RDISTANCE 1
FRAMEHINGE 2 HINGE "USER" RDISTANCE 0
FRAMEHINGE 2 HINGE "USER" RDISTANCE 1
FRAMEHINGE 3 HINGE "USER" RDISTANCE 0
FRAMEHINGE 3 HINGE "USER" RDISTANCE 1
FRAMEHINGE 4 HINGE "USER" RDISTANCE 0
FRAMEHINGE 4 HINGE "USER" RDISTANCE 1
FRAMEHINGE 5 HINGE "USER" RDISTANCE 0
FRAMEHINGE 5 HINGE "USER" RDISTANCE 1
FRAMEHINGE 6 HINGE "USER" RDISTANCE 0
FRAMEHINGE 6 HINGE "USER" RDISTANCE 1
FRAMEHINGE 7 HINGE "USER" RDISTANCE 0
FRAMEHINGE 7 HINGE "USER" RDISTANCE 1
FRAMEHINGE 8 HINGE "USER" RDISTANCE 0
FRAMEHINGE 8 HINGE "USER" RDISTANCE 1
FRAMEHINGE 9 HINGE "USER" RDISTANCE 0
FRAMEHINGE 9 HINGE "USER" RDISTANCE 1
END SUPPLEMENTAL DATA

**SAP 2000-NL VERSION 7.11 INPUT FILE FOR THE EIGNEVALUE AND
PUSHOVER ANALYSIS OF EXAMPLE No.5: FRAME 6S-75 WITH LINEAR
VISCOUS DAMPING TO PROVIDE 10% VISCOUS DAMPING RATIO WHEN
ASSUMING ELASTIC FRAME BEHAVIOR**

SYSTEM

DOF=UX,UZ,RY LENGTH=IN FORCE=Kip PAGE=SECTIONS

JOINT

1 X=-486 Y=0 Z=0
2 X=-486 Y=0 Z=174
3 X=-486 Y=0 Z=343.44
4 X=-486 Y=0 Z=512.88
5 X=-486 Y=0 Z=682.32
6 X=-486 Y=0 Z=851.76
7 X=-486 Y=0 Z=1021.2
8 X=-162 Y=0 Z=0
9 X=-162 Y=0 Z=174
10 X=-162 Y=0 Z=343.44
11 X=-162 Y=0 Z=512.88
12 X=-162 Y=0 Z=682.32
13 X=-162 Y=0 Z=851.76
14 X=-162 Y=0 Z=1021.2
15 X=162 Y=0 Z=0
16 X=162 Y=0 Z=174
17 X=162 Y=0 Z=343.44
18 X=162 Y=0 Z=512.88
19 X=162 Y=0 Z=682.32
20 X=162 Y=0 Z=851.76
21 X=162 Y=0 Z=1021.2
22 X=486 Y=0 Z=0
23 X=486 Y=0 Z=174
24 X=486 Y=0 Z=343.44
25 X=486 Y=0 Z=512.88
26 X=486 Y=0 Z=682.32
27 X=486 Y=0 Z=851.76
28 X=486 Y=0 Z=1021.2

RESTRAINT

ADD=1 DOF=U1,U2,U3,R1,R2,R3
ADD=8 DOF=U1,U2,U3,R1,R2,R3
ADD=15 DOF=U1,U2,U3,R1,R2,R3
ADD=22 DOF=U1,U2,U3,R1,R2,R3

PATTERN

NAME=DEFAULT

MASS

ADD=7 U1=.22496
ADD=14 U1=.22496
ADD=21 U1=.22496
ADD=28 U1=.22496
ADD=2 U1=.412632
ADD=3 U1=.41352
ADD=4 U1=.414958

ADD=5 U1=.416
ADD=6 U1=.4278
ADD=9 U1=.412632
ADD=10 U1=.41352
ADD=11 U1=.414958
ADD=12 U1=.416
ADD=13 U1=.4278
ADD=16 U1=.412632
ADD=17 U1=.41352
ADD=18 U1=.414958
ADD=19 U1=.416
ADD=20 U1=.4278
ADD=23 U1=.412632
ADD=24 U1=.41352
ADD=25 U1=.414958
ADD=26 U1=.416
ADD=27 U1=.4278

MATERIAL

NAME=STEEL IDES=S M=7.324E-07 W=.000283
T=0 E=29000 U=.3 A=.0000065 FY=50
NAME=CONC IDES=C M=2.246377E-07 W=.0000868
T=0 E=3600 U=.2 A=.0000055
NAME=OTHER IDES=N M=2.246377E-07 W=.0000868
T=0 E=3600 U=.2 A=.0000055

FRAME SECTION

NAME=W14X132 MAT=STEEL A=38.8 J=12.3 I=1530,548 AS=9.4557,25.278 S=208.7312,74.43124
Z=234,113 R=6.279569,3.758153 T=14.66,14.725,1.03,.645,14.725,1.03 SHN=W14X132 DSG=W
NAME=W14X176 MAT=STEEL A=51.8 J=26.5 I=2140,838 AS=12.633,34.169 S=281.2089,107.0927
Z=320,163 R=6.427499,4.02214 T=15.22,15.65,1.31,.83,15.65,1.31 SHN=W14X176 DSG=W
NAME=W16X31 MAT=STEEL A=9.12 J=.46 I=375,12.4 AS=4.367,4.0517 S=47.22922,4.488688
Z=54,7.03 R=6.412365,1.16604 T=15.88,5.525,.44,.275,5.525,.44 SHN=W16X31 DSG=W
NAME=W16X40 MAT=STEEL A=11.8 J=.79 I=518,28.9 AS=4.8831,5.8875 S=64.70956,8.263045
Z=72.9,12.7 R=6.625579,1.564977 T=16.01,6.995,.505,.305,6.995,.505 SHN=W16X40 DSG=W
NAME=W21X44 MAT=STEEL A=13 J=.77 I=843,20.7 AS=7.231,4.875 S=81.60697,6.369231
Z=95.4,10.2 R=8.052711,1.261867 T=20.66,6.5,.45,.35,6.5,.45 SHN=W21X44 DSG=W
NAME=W21X50 MAT=STEEL A=14.7 J=1.14 I=984,24.9 AS=7.9154,5.8226 S=94.47912,7.626339
Z=110,12.2 R=8.181612,1.301491 T=20.83,6.53,.535,.38,6.53,.535 SHN=W21X50 DSG=W
NAME=W21X62 MAT=STEEL A=18.3 J=1.83 I=1330,57.5 AS=8.396,8.446 S=126.727,13.95631
Z=144,21.7 R=8.525116,1.77259 T=20.99,8.24,.615,.48,8.24,.615 SHN=W21X62 DSG=W
NAME=W24X62 MAT=STEEL A=18.2 J=1.71 I=1550,34.5 AS=10.208,6.9227 S=130.5813,9.801136
Z=153,15.7 R=9.228479,1.376809 T=23.74,7.04,.59,.43,7.04,.59 SHN=W24X62 DSG=W
NAME=W14X90 MAT=STEEL A=26.5 J=4.06 I=999,362 AS=6.1688,17.182 S=142.5107,49.86226
Z=157,75.6 R=6.139879,3.695995 T=14.02,14.52,.71,.44,14.52,.71 SHN=W14X90 DSG=W
NAME=W14X26 MAT=STEEL A=7.69 J=.36 I=245,8.91 AS=3.5471,3.5175 S=35.22646,3.546268
Z=40.2,5.54 R=5.644427,1.076405 T=13.91,5.025,.42,.255,5.025,.42 SHN=W14X26 DSG=W

FRAME

1 J=1,2 SEC=W14X176 NSEG=2 ANG=0 IOFF=16 JOFF=13 RIGID=1
2 J=2,3 SEC=W14X176 NSEG=2 ANG=0 IOFF=13 JOFF=11.5 RIGID=1
3 J=3,4 SEC=W14X132 NSEG=2 ANG=0 IOFF=11.5 JOFF=11.5 RIGID=1
4 J=4,5 SEC=W14X132 NSEG=2 ANG=0 IOFF=11.5 JOFF=11.5 RIGID=1
5 J=5,6 SEC=W14X90 NSEG=2 ANG=0 IOFF=11.5 JOFF=9 RIGID=1
6 J=6,7 SEC=W14X90 NSEG=2 ANG=0 IOFF=9 JOFF=9 RIGID=1

7 J=8,9 SEC=W14X176 NSEG=2 ANG=0 IOFF=16 JOFF=13 RIGID=1
 8 J=9,10 SEC=W14X176 NSEG=2 ANG=0 IOFF=13 JOFF=11.5 RIGID=1
 9 J=10,11 SEC=W14X132 NSEG=2 ANG=0 IOFF=11.5 JOFF=11.5 RIGID=1
 10 J=11,12 SEC=W14X132 NSEG=2 ANG=0 IOFF=11.5 JOFF=11.5 RIGID=1
 11 J=12,13 SEC=W14X90 NSEG=2 ANG=0 IOFF=11.5 JOFF=9 RIGID=1
 12 J=13,14 SEC=W14X90 NSEG=2 ANG=0 IOFF=9 JOFF=9 RIGID=1
 13 J=15,16 SEC=W14X176 NSEG=2 ANG=0 IOFF=16 JOFF=13 RIGID=1
 14 J=16,17 SEC=W14X176 NSEG=2 ANG=0 IOFF=13 JOFF=11.5 RIGID=1
 15 J=17,18 SEC=W14X132 NSEG=2 ANG=0 IOFF=11.5 JOFF=11.5 RIGID=1
 16 J=18,19 SEC=W14X132 NSEG=2 ANG=0 IOFF=11.5 JOFF=11.5 RIGID=1
 17 J=19,20 SEC=W14X90 NSEG=2 ANG=0 IOFF=11.5 JOFF=9 RIGID=1
 18 J=20,21 SEC=W14X90 NSEG=2 ANG=0 IOFF=9 JOFF=9 RIGID=1
 19 J=22,23 SEC=W14X176 NSEG=2 ANG=0 IOFF=16 JOFF=13 RIGID=1
 20 J=23,24 SEC=W14X176 NSEG=2 ANG=0 IOFF=13 JOFF=11.5 RIGID=1
 21 J=24,25 SEC=W14X132 NSEG=2 ANG=0 IOFF=11.5 JOFF=11.5 RIGID=1
 22 J=25,26 SEC=W14X132 NSEG=2 ANG=0 IOFF=11.5 JOFF=11.5 RIGID=1
 23 J=26,27 SEC=W14X90 NSEG=2 ANG=0 IOFF=11.5 JOFF=9 RIGID=1
 24 J=27,28 SEC=W14X90 NSEG=2 ANG=0 IOFF=9 JOFF=9 RIGID=1
 25 J=2,9 SEC=W24X62 NSEG=4 ANG=0 IOFF=11 JOFF=11 RIGID=1
 26 J=3,10 SEC=W21X62 NSEG=4 ANG=0 IOFF=11 JOFF=11 RIGID=1
 27 J=4,11 SEC=W21X50 NSEG=4 ANG=0 IOFF=11 JOFF=11 RIGID=1
 28 J=5,12 SEC=W21X44 NSEG=4 ANG=0 IOFF=11 JOFF=11 RIGID=1
 29 J=6,13 SEC=W16X40 NSEG=4 ANG=0 IOFF=11 JOFF=11 RIGID=1
 30 J=7,14 SEC=W16X31 NSEG=4 ANG=0 IOFF=11 JOFF=11 RIGID=1
 31 J=9,16 SEC=W24X62 NSEG=4 ANG=0 IOFF=11 JOFF=11 RIGID=1
 32 J=10,17 SEC=W21X62 NSEG=4 ANG=0 IOFF=11 JOFF=11 RIGID=1
 33 J=11,18 SEC=W21X50 NSEG=4 ANG=0 IOFF=11 JOFF=11 RIGID=1
 34 J=12,19 SEC=W21X44 NSEG=4 ANG=0 IOFF=11 JOFF=11 RIGID=1
 35 J=13,20 SEC=W16X40 NSEG=4 ANG=0 IOFF=11 JOFF=11 RIGID=1
 36 J=14,21 SEC=W16X31 NSEG=4 ANG=0 IOFF=11 JOFF=11 RIGID=1
 37 J=16,23 SEC=W24X62 NSEG=4 ANG=0 IOFF=11 JOFF=11 RIGID=1
 38 J=17,24 SEC=W21X62 NSEG=4 ANG=0 IOFF=11 JOFF=11 RIGID=1
 39 J=18,25 SEC=W21X50 NSEG=4 ANG=0 IOFF=11 JOFF=11 RIGID=1
 40 J=19,26 SEC=W21X44 NSEG=4 ANG=0 IOFF=11 JOFF=11 RIGID=1
 41 J=20,27 SEC=W16X40 NSEG=4 ANG=0 IOFF=11 JOFF=11 RIGID=1
 42 J=21,28 SEC=W16X31 NSEG=4 ANG=0 IOFF=11 JOFF=11 RIGID=1

LOAD

NAME=NEHRP
 TYPE=FORCE
 ADD=7 UX=27.2
 ADD=6 UX=34.6
 ADD=5 UX=21.8
 ADD=4 UX=12
 ADD=3 UX=5.2
 ADD=2 UX=1.3
 NAME=PITO
 TYPE=FORCE
 ADD=7 UX=.1815
 ADD=6 UX=.2939
 ADD=5 UX=.2317
 ADD=4 UX=.1639
 ADD=3 UX=.0937
 ADD=2 UX=.0353
 NAME=FIRSTM
 TYPE=FORCE

```
ADD=7 UX=25.2
ADD=6 UX=40.8
ADD=5 UX=32.2
ADD=4 UX=22.7
ADD=3 UX=13
ADD=2 UX=4.9
NAME=RMODE
TYPE=FORCE
ADD=7 UX=9.84
ADD=6 UX=10.4
ADD=5 UX=-1.16
ADD=4 UX=-13.76
ADD=3 UX=-26.8
ADD=2 UX=-37.6
NAME=GRAVITY
TYPE=DISTRIBUTED SPAN
ADD=30 RD=0,1 UZ=-.085,-.085
ADD=36 RD=0,1 UZ=-.085,-.085
ADD=42 RD=0,1 UZ=-.085,-.085
ADD=25 RD=0,1 UZ=-.167,-.167
ADD=26 RD=0,1 UZ=-.167,-.167
ADD=27 RD=0,1 UZ=-.167,-.167
ADD=28 RD=0,1 UZ=-.167,-.167
ADD=29 RD=0,1 UZ=-.167,-.167
ADD=31 RD=0,1 UZ=-.167,-.167
ADD=32 RD=0,1 UZ=-.167,-.167
ADD=33 RD=0,1 UZ=-.167,-.167
ADD=34 RD=0,1 UZ=-.167,-.167
ADD=35 RD=0,1 UZ=-.167,-.167
ADD=37 RD=0,1 UZ=-.167,-.167
ADD=38 RD=0,1 UZ=-.167,-.167
ADD=39 RD=0,1 UZ=-.167,-.167
ADD=40 RD=0,1 UZ=-.167,-.167
ADD=41 RD=0,1 UZ=-.167,-.167
NAME=PUSHUNIF
TYPE=FORCE
ADD=7 UX=.0975
ADD=6 UX=.1805
ADD=2 UX=.1805
ADD=3 UX=.1805
ADD=4 UX=.1805
ADD=5 UX=.1805
NAME=UNIFORM
TYPE=FORCE
ADD=7 UX=9.752587E-02
ADD=2 UX=.1804948
ADD=3 UX=.1804948
ADD=4 UX=.1804948
ADD=5 UX=.1804948
ADD=6 UX=.1804948
```

```
MODE
TYPE=EIGEN N=6 TOL=.00001
```

```
OUTPUT
; No Output Requested
```

END

; The following data is used for graphics, design and pushover analysis.
; If changes are made to the analysis data above, then the following data
; should be checked for consistency.

SAP2000 V7.11 SUPPLEMENTAL DATA

GRID GLOBAL X "1" -486
GRID GLOBAL X "2" -162
GRID GLOBAL X "3" 162
GRID GLOBAL X "4" 486
GRID GLOBAL Y "5" 0
GRID GLOBAL Z "6" 0
GRID GLOBAL Z "7" 174
GRID GLOBAL Z "8" 343.44
GRID GLOBAL Z "9" 512.88
GRID GLOBAL Z "10" 682.32
GRID GLOBAL Z "11" 851.76
GRID GLOBAL Z "12" 1021.2
MATERIAL STEEL FY 50
MATERIAL CONC FYREBAR 60 FYSHEAR 40 FC 4 FCSHEAR 4
STATICLOAD NEHRP TYPE QUAKE
STATICLOAD PITO TYPE QUAKE
STATICLOAD FIRSTM TYPE QUAKE
STATICLOAD RMODE TYPE QUAKE
STATICLOAD GRAVITY TYPE DEAD
STATICLOAD PUSHUNIF TYPE QUAKE
STATICLOAD UNIFORM TYPE QUAKE
PUSHCASE "GRAVITY" CONTROL FORCE JOINT 7 DOF U3
PUSHCASE "GRAVITY" MINSTEPS 1 MAXNULLSTEPS 50 MAXTOTALSTEPS 200 MAXITER
10
PUSHCASE "GRAVITY" ITERTOL .0001 EVENTTOL .01
PUSHCASE "GRAVITY" LOADTYPE STATIC LOAD GRAVITY SCALEFACTOR 1
PUSHCASE "PUSHM1" CONTROL DISP TARGET 45 JOINT 7 DOF U1
PUSHCASE "PUSHM1" STARTCASE "GRAVITY"
PUSHCASE "PUSHM1" MINSTEPS 200 MAXNULLSTEPS 50 MAXTOTALSTEPS 200 MAXITER
10
PUSHCASE "PUSHM1" ITERTOL .0001 EVENTTOL .01
PUSHCASE "PUSHM1" LOADTYPE MODE NUMBER 1 SCALEFACTOR 1
PUSHCASE "UNIFORM" CONTROL DISP TARGET 36 JOINT 7 DOF U1
PUSHCASE "UNIFORM" MINSTEPS 50 MAXNULLSTEPS 50 MAXTOTALSTEPS 200
MAXITER 10
PUSHCASE "UNIFORM" ITERTOL .0001 EVENTTOL .01
PUSHCASE "UNIFORM" LOADTYPE STATIC LOAD UNIFORM SCALEFACTOR 1
HINGE "USER" TYPE M3 SYMMETRIC
HINGE "USER" TYPE M3 B 1 1 C 8 1 D 8 .2 E 10 .2
HINGE "USER" TYPE M3 IO 2 LS 4 CP 6
FRAMEHINGE 1 HINGE "Default-PMM" RDISTANCE 0
FRAMEHINGE 1 HINGE "Default-PMM" RDISTANCE 1
FRAMEHINGE 2 HINGE "Default-PMM" RDISTANCE 0
FRAMEHINGE 2 HINGE "Default-PMM" RDISTANCE 1
FRAMEHINGE 3 HINGE "Default-PMM" RDISTANCE 0
FRAMEHINGE 3 HINGE "Default-PMM" RDISTANCE 1
FRAMEHINGE 4 HINGE "Default-PMM" RDISTANCE 0
FRAMEHINGE 4 HINGE "Default-PMM" RDISTANCE 1
FRAMEHINGE 5 HINGE "Default-PMM" RDISTANCE 0

FRAMEHINGE 5 HINGE "Default-PMM" RDISTANCE 1
FRAMEHINGE 6 HINGE "Default-PMM" RDISTANCE 0
FRAMEHINGE 6 HINGE "Default-PMM" RDISTANCE 1
FRAMEHINGE 7 HINGE "Default-PMM" RDISTANCE 0
FRAMEHINGE 7 HINGE "Default-PMM" RDISTANCE 1
FRAMEHINGE 8 HINGE "Default-PMM" RDISTANCE 0
FRAMEHINGE 8 HINGE "Default-PMM" RDISTANCE 1
FRAMEHINGE 9 HINGE "Default-PMM" RDISTANCE 0
FRAMEHINGE 9 HINGE "Default-PMM" RDISTANCE 1
FRAMEHINGE 10 HINGE "Default-PMM" RDISTANCE 0
FRAMEHINGE 10 HINGE "Default-PMM" RDISTANCE 1
FRAMEHINGE 11 HINGE "Default-PMM" RDISTANCE 0
FRAMEHINGE 11 HINGE "Default-PMM" RDISTANCE 1
FRAMEHINGE 12 HINGE "Default-PMM" RDISTANCE 0
FRAMEHINGE 12 HINGE "Default-PMM" RDISTANCE 1
FRAMEHINGE 13 HINGE "Default-PMM" RDISTANCE 0
FRAMEHINGE 13 HINGE "Default-PMM" RDISTANCE 1
FRAMEHINGE 14 HINGE "Default-PMM" RDISTANCE 0
FRAMEHINGE 14 HINGE "Default-PMM" RDISTANCE 1
FRAMEHINGE 15 HINGE "Default-PMM" RDISTANCE 0
FRAMEHINGE 15 HINGE "Default-PMM" RDISTANCE 1
FRAMEHINGE 16 HINGE "Default-PMM" RDISTANCE 0
FRAMEHINGE 16 HINGE "Default-PMM" RDISTANCE 1
FRAMEHINGE 17 HINGE "Default-PMM" RDISTANCE 0
FRAMEHINGE 17 HINGE "Default-PMM" RDISTANCE 1
FRAMEHINGE 18 HINGE "Default-PMM" RDISTANCE 0
FRAMEHINGE 18 HINGE "Default-PMM" RDISTANCE 1
FRAMEHINGE 19 HINGE "Default-PMM" RDISTANCE 0
FRAMEHINGE 19 HINGE "Default-PMM" RDISTANCE 1
FRAMEHINGE 20 HINGE "Default-PMM" RDISTANCE 0
FRAMEHINGE 20 HINGE "Default-PMM" RDISTANCE 1
FRAMEHINGE 21 HINGE "Default-PMM" RDISTANCE 0
FRAMEHINGE 21 HINGE "Default-PMM" RDISTANCE 1
FRAMEHINGE 22 HINGE "Default-PMM" RDISTANCE 0
FRAMEHINGE 22 HINGE "Default-PMM" RDISTANCE 1
FRAMEHINGE 23 HINGE "Default-PMM" RDISTANCE 0
FRAMEHINGE 23 HINGE "Default-PMM" RDISTANCE 1
FRAMEHINGE 24 HINGE "Default-PMM" RDISTANCE 0
FRAMEHINGE 24 HINGE "Default-PMM" RDISTANCE 1
FRAMEHINGE 25 HINGE "USER" RDISTANCE 0
FRAMEHINGE 25 HINGE "USER" RDISTANCE 1
FRAMEHINGE 26 HINGE "USER" RDISTANCE 0
FRAMEHINGE 26 HINGE "USER" RDISTANCE 1
FRAMEHINGE 27 HINGE "USER" RDISTANCE 0
FRAMEHINGE 27 HINGE "USER" RDISTANCE 1
FRAMEHINGE 28 HINGE "USER" RDISTANCE 0
FRAMEHINGE 28 HINGE "USER" RDISTANCE 1
FRAMEHINGE 29 HINGE "USER" RDISTANCE 0
FRAMEHINGE 29 HINGE "USER" RDISTANCE 1
FRAMEHINGE 30 HINGE "USER" RDISTANCE 0
FRAMEHINGE 30 HINGE "USER" RDISTANCE 1
FRAMEHINGE 31 HINGE "USER" RDISTANCE 0
FRAMEHINGE 31 HINGE "USER" RDISTANCE 1
FRAMEHINGE 32 HINGE "USER" RDISTANCE 0
FRAMEHINGE 32 HINGE "USER" RDISTANCE 1
FRAMEHINGE 33 HINGE "USER" RDISTANCE 0

FRAMEHINGE 33 HINGE "USER" RDISTANCE 1
FRAMEHINGE 34 HINGE "USER" RDISTANCE 0
FRAMEHINGE 34 HINGE "USER" RDISTANCE 1
FRAMEHINGE 35 HINGE "USER" RDISTANCE 0
FRAMEHINGE 35 HINGE "USER" RDISTANCE 1
FRAMEHINGE 36 HINGE "USER" RDISTANCE 0
FRAMEHINGE 36 HINGE "USER" RDISTANCE 1
FRAMEHINGE 37 HINGE "USER" RDISTANCE 0
FRAMEHINGE 37 HINGE "USER" RDISTANCE 1
FRAMEHINGE 38 HINGE "USER" RDISTANCE 0
FRAMEHINGE 38 HINGE "USER" RDISTANCE 1
FRAMEHINGE 39 HINGE "USER" RDISTANCE 0
FRAMEHINGE 39 HINGE "USER" RDISTANCE 1
FRAMEHINGE 40 HINGE "USER" RDISTANCE 0
FRAMEHINGE 40 HINGE "USER" RDISTANCE 1
FRAMEHINGE 41 HINGE "USER" RDISTANCE 0
FRAMEHINGE 41 HINGE "USER" RDISTANCE 1
FRAMEHINGE 42 HINGE "USER" RDISTANCE 0
FRAMEHINGE 42 HINGE "USER" RDISTANCE 1
END SUPPLEMENTAL DATA

**SAP2000-NL VERSION 7.11 INPUT FILE FOR EIGENVALUE AND PUSHOVER
ANALYSIS OF EXAMPLE No.8: FRAME 3S-75 WITH VISCOLEASTIC SOLID
DAMPING SYSTEM TO PROVIDE 8.5% VISCOUS DAMPING RATIO WHEN
ASSUMING ELASTIC FRAME BEHAVIOR**

SYSTEM

DOF=UX,UZ,RY LENGTH=IN FORCE=Kip PAGE=SECTIONS

JOINT

17 X=-486 Y=0 Z=0
18 X=-486 Y=0 Z=174
19 X=-486 Y=0 Z=343.44
20 X=-486 Y=0 Z=512.88
21 X=-162 Y=0 Z=512.88
22 X=162 Y=0 Z=512.88
23 X=486 Y=0 Z=512.88
24 X=486 Y=0 Z=343.44
25 X=486 Y=0 Z=174
26 X=486 Y=0 Z=0
27 X=-162 Y=0 Z=343.44
28 X=162 Y=0 Z=343.44
29 X=-162 Y=0 Z=174
30 X=162 Y=0 Z=174
33 X=162 Y=0 Z=0
34 X=-162 Y=0 Z=0

RESTRAINT

ADD=17 DOF=U1,U2,U3,R1,R2,R3
ADD=26 DOF=U1,U2,U3,R1,R2,R3
ADD=33 DOF=U1,U2,U3,R1,R2,R3
ADD=34 DOF=U1,U2,U3,R1,R2,R3

PATTERN

NAME=DEFAULT

MASS

ADD=20 U1=.22488
ADD=21 U1=.22488
ADD=22 U1=.22488
ADD=23 U1=.22488
ADD=18 U1=.41606
ADD=19 U1=.41606
ADD=24 U1=.41606
ADD=25 U1=.41606
ADD=27 U1=.41606
ADD=28 U1=.41606
ADD=29 U1=.41606
ADD=30 U1=.41606

MATERIAL

NAME=STEEL IDES=S M=7.324E-07 W=.000283
T=0 E=29000 U=.3 A=.0000065 FY=50
NAME=CONC IDES=C M=2.246377E-07 W=.0000868
T=0 E=3600 U=.2 A=.0000055
NAME=OTHER IDES=N M=2.246377E-07 W=.0000868

T=0 E=3600 U=.2 A=.0000055

FRAME SECTION

NAME=W14X109 MAT=STEEL A=32 J=7.12 I=1240,447 AS=7.518,20.934 S=173.1844,61.21191
Z=192,92.7 R=6.22495,3.737479 T=14.32,14.605,.86,.525,14.605,.86 SHN=W14X109 DSG=W
NAME=W16X40 MAT=STEEL A=11.8 J=.79 I=518,28.9 AS=4.8831,5.8875 S=64.70956,8.263045
Z=72.9,12.7 R=6.625579,1.564977 T=16.01,6.995,.505,.305,6.995,.505 SHN=W16X40 DSG=W
NAME=W16X45 MAT=STEEL A=13.3 J=1.11 I=586,32.8 AS=5.5649,6.6246 S=72.65965,9.324804
Z=82.3,14.5 R=6.637782,1.570403 T=16.13,7.035,.565,.345,7.035,.565 SHN=W16X45 DSG=W
NAME=W14X26 MAT=STEEL A=7.69 J=.36 I=245,8.91 AS=3.5471,3.5175 S=35.22646,3.546268
Z=40.2,5.54 R=5.644427,1.076405 T=13.91,5.025,.42,.255,5.025,.42 SHN=W14X26 DSG=W
NAME=BRACE MAT=STEEL SH=R T=.426,.426 A=.181476 J=4.63814E-03 I=2.744462E-
03,2.744462E-03 AS=.15123,.15123

FRAME

1 J=18,29 SEC=W16X45 NSEG=4 ANG=0 IOFF=7 JOFF=7 RIGID=1
2 J=29,30 SEC=W16X45 NSEG=4 ANG=0 IOFF=7 JOFF=7 RIGID=1
3 J=30,25 SEC=W16X45 NSEG=4 ANG=0 IOFF=7 JOFF=7 RIGID=1
4 J=19,27 SEC=W16X40 NSEG=4 ANG=0 IOFF=7 JOFF=7 RIGID=1
5 J=27,28 SEC=W16X40 NSEG=4 ANG=0 IOFF=7 JOFF=7 RIGID=1
6 J=28,24 SEC=W16X40 NSEG=4 ANG=0 IOFF=7 JOFF=7 RIGID=1
7 J=20,21 SEC=W14X26 NSEG=4 ANG=0 IOFF=7 JOFF=7 RIGID=1
8 J=21,22 SEC=W14X26 NSEG=4 ANG=0 IOFF=7 JOFF=7 RIGID=1
9 J=22,23 SEC=W14X26 NSEG=4 ANG=0 IOFF=7 JOFF=7 RIGID=1
10 J=34,30 SEC=BRACE NSEG=2 ANG=0 IREL=R3 JREL=R3
12 J=27,22 SEC=BRACE NSEG=2 ANG=0 IREL=R3 JREL=R3
14 J=30,27 SEC=BRACE NSEG=2 ANG=0 IREL=R3 JREL=R3
22 J=17,18 SEC=W14X109 NSEG=2 ANG=0 IOFF=14 JOFF=8 RIGID=1
23 J=18,19 SEC=W14X109 NSEG=2 ANG=0 IOFF=8 JOFF=8 RIGID=1
24 J=19,20 SEC=W14X109 NSEG=2 ANG=0 IOFF=8 JOFF=7 RIGID=1
28 J=23,24 SEC=W14X109 NSEG=2 ANG=0 IOFF=8 JOFF=7 RIGID=1
29 J=24,25 SEC=W14X109 NSEG=2 ANG=0 IOFF=8 JOFF=8 RIGID=1
30 J=25,26 SEC=W14X109 NSEG=2 ANG=0 IOFF=14 JOFF=8 RIGID=1
38 J=33,30 SEC=W14X109 NSEG=2 ANG=0 IOFF=14 JOFF=8 RIGID=1
39 J=30,28 SEC=W14X109 NSEG=2 ANG=0 IOFF=8 JOFF=8 RIGID=1
40 J=28,22 SEC=W14X109 NSEG=2 ANG=0 IOFF=8 JOFF=7 RIGID=1
41 J=34,29 SEC=W14X109 NSEG=2 ANG=0 IOFF=14 JOFF=8 RIGID=1
42 J=29,27 SEC=W14X109 NSEG=2 ANG=0 IOFF=8 JOFF=8 RIGID=1
43 J=27,21 SEC=W14X109 NSEG=2 ANG=0 IOFF=8 JOFF=7 RIGID=1

LOAD

NAME=CVX
TYPE=FORCE
ADD=20 UX=.4162
ADD=19 UX=.4269
ADD=18 UX=.1569
NAME=NEHRP
TYPE=FORCE
ADD=20 UX=37.79
ADD=19 UX=32.46
ADD=18 UX=8.84
NAME=GRAVITY
NAME=1STMODE
TYPE=FORCE
ADD=20 UX=144
ADD=19 UX=181.3

ADD=18 UX=74.65
NAME=RMODE
TYPE=FORCE
ADD=20 UX=93.9
ADD=19 UX=-27
ADD=18 UX=-275.7
NAME=DEAD
NAME=LIVE
NAME=1MODDBE
TYPE=FORCE
ADD=20 UX=41.7
ADD=19 UX=52.2
ADD=18 UX=21.2
NAME=RMODBE
TYPE=FORCE
ADD=20 UX=31.3
ADD=19 UX=-9
ADD=18 UX=-91.9
NAME=DDLL
NAME=UNIFORM
TYPE=FORCE
ADD=20 UX=.2127
ADD=19 UX=.39365
ADD=18 UX=.39365

MODE
TYPE=EIGEN N=3 TOL=.00001

COMBO
NAME=DSTL1
LOAD=CVX SF=1
LOAD=NEHRP SF=1
LOAD=GRAVITY SF=1
LOAD=1STMODE SF=1
LOAD=RMODE SF=1
LOAD=DEAD SF=1
LOAD=1MODDBE SF=1
LOAD=RMODBE SF=1
LOAD=DDLL SF=1
LOAD=UNIFORM SF=1
NAME=DSTL2
LOAD=CVX SF=1
LOAD=NEHRP SF=1
LOAD=GRAVITY SF=1
LOAD=1STMODE SF=1
LOAD=RMODE SF=1
LOAD=DEAD SF=1
LOAD=LIVE SF=1
LOAD=1MODDBE SF=1
LOAD=RMODBE SF=1
LOAD=DDLL SF=1
LOAD=UNIFORM SF=1

OUTPUT
; No Output Requested

END

; The following data is used for graphics, design and pushover analysis.
; If changes are made to the analysis data above, then the following data
; should be checked for consistency.

SAP2000 V7.11 SUPPLEMENTAL DATA

GRID GLOBAL X "1" -486

GRID GLOBAL X "2" -162

GRID GLOBAL X "3" 162

GRID GLOBAL X "4" 486

GRID GLOBAL Y "5" 0

GRID GLOBAL Z "6" 0

GRID GLOBAL Z "7" 174

GRID GLOBAL Z "8" 343.44

GRID GLOBAL Z "9" 512.88

MATERIAL STEEL FY 50

MATERIAL CONC FYREBAR 60 FYSHEAR 40 FC 4 FCSHEAR 4

STATICLOAD CVX TYPE DEAD

STATICLOAD NEHRP TYPE DEAD

STATICLOAD GRAVITY TYPE DEAD

STATICLOAD 1STMODE TYPE DEAD

STATICLOAD RMODE TYPE DEAD

STATICLOAD DEAD TYPE DEAD

STATICLOAD LIVE TYPE LIVE

STATICLOAD 1MODDBE TYPE DEAD

STATICLOAD RMODBE TYPE DEAD

STATICLOAD DDL TYPE DEAD

STATICLOAD UNIFORM TYPE DEAD

COMBO DSTL1 DESIGN STEEL

COMBO DSTL2 DESIGN STEEL

STEELDESIGN "AISC-ASD89"

PUSHCASE "PUSHUNO" CONTROL DISP TARGET 20 JOINT 20 DOF U1

PUSHCASE "PUSHUNO" MINSTEPS 200 MAXNULLSTEPS 50 MAXTOTALSTEPS 200

MAXITER 10

PUSHCASE "PUSHUNO" ITERTOL .0001 EVENTTOL .01

PUSHCASE "PUSHUNO" LOADTYPE MODE NUMBER 1 SCALEFACTOR -1

PUSHCASE "PUSHCVX" CONTROL DISP TARGET 20 JOINT 20 DOF U1

PUSHCASE "PUSHCVX" MINSTEPS 10 MAXNULLSTEPS 50 MAXTOTALSTEPS 200

MAXITER 10

PUSHCASE "PUSHCVX" ITERTOL .0001 EVENTTOL .01

PUSHCASE "PUSHCVX" LOADTYPE STATIC LOAD CVX SCALEFACTOR 1

PUSHCASE "PUSHUNIF" CONTROL DISP TARGET 20 JOINT 20 DOF U1

PUSHCASE "PUSHUNIF" MINSTEPS 10 MAXNULLSTEPS 50 MAXTOTALSTEPS 200

MAXITER 10

PUSHCASE "PUSHUNIF" ITERTOL .0001 EVENTTOL .01

PUSHCASE "PUSHUNIF" LOADTYPE STATIC LOAD UNIFORM SCALEFACTOR 1

HINGE "USER" TYPE M3 SYMMETRIC

HINGE "USER" TYPE M3 B 1 1 C 6 1 D 8 1 E 10 1

HINGE "USER" TYPE M3 IO 2 LS 4 CP 6

FRAMEHINGE 22 HINGE "USER" RDISTANCE 0

FRAMEHINGE 22 HINGE "USER" RDISTANCE 1

FRAMEHINGE 23 HINGE "USER" RDISTANCE 0

FRAMEHINGE 23 HINGE "USER" RDISTANCE 1

FRAMEHINGE 24 HINGE "USER" RDISTANCE 0

FRAMEHINGE 24 HINGE "USER" RDISTANCE 1

FRAMEHINGE 28 HINGE "USER" RDISTANCE 0

FRAMEHINGE 28 HINGE "USER" RDISTANCE 1
FRAMEHINGE 29 HINGE "USER" RDISTANCE 0
FRAMEHINGE 29 HINGE "USER" RDISTANCE 1
FRAMEHINGE 30 HINGE "USER" RDISTANCE 0
FRAMEHINGE 30 HINGE "USER" RDISTANCE 1
FRAMEHINGE 38 HINGE "USER" RDISTANCE 0
FRAMEHINGE 38 HINGE "USER" RDISTANCE 1
FRAMEHINGE 39 HINGE "USER" RDISTANCE 0
FRAMEHINGE 39 HINGE "USER" RDISTANCE 1
FRAMEHINGE 40 HINGE "USER" RDISTANCE 0
FRAMEHINGE 40 HINGE "USER" RDISTANCE 1
FRAMEHINGE 41 HINGE "USER" RDISTANCE 0
FRAMEHINGE 41 HINGE "USER" RDISTANCE 1
FRAMEHINGE 42 HINGE "USER" RDISTANCE 0
FRAMEHINGE 42 HINGE "USER" RDISTANCE 1
FRAMEHINGE 43 HINGE "USER" RDISTANCE 0
FRAMEHINGE 43 HINGE "USER" RDISTANCE 1
FRAMEHINGE 1 HINGE "USER" RDISTANCE 0
FRAMEHINGE 1 HINGE "USER" RDISTANCE 1
FRAMEHINGE 2 HINGE "USER" RDISTANCE 0
FRAMEHINGE 2 HINGE "USER" RDISTANCE 1
FRAMEHINGE 3 HINGE "USER" RDISTANCE 0
FRAMEHINGE 3 HINGE "USER" RDISTANCE 1
FRAMEHINGE 4 HINGE "USER" RDISTANCE 0
FRAMEHINGE 4 HINGE "USER" RDISTANCE 1
FRAMEHINGE 5 HINGE "USER" RDISTANCE 0
FRAMEHINGE 5 HINGE "USER" RDISTANCE 1
FRAMEHINGE 6 HINGE "USER" RDISTANCE 0
FRAMEHINGE 6 HINGE "USER" RDISTANCE 1
FRAMEHINGE 7 HINGE "USER" RDISTANCE 0
FRAMEHINGE 7 HINGE "USER" RDISTANCE 1
FRAMEHINGE 8 HINGE "USER" RDISTANCE 0
FRAMEHINGE 8 HINGE "USER" RDISTANCE 1
FRAMEHINGE 9 HINGE "USER" RDISTANCE 0
FRAMEHINGE 9 HINGE "USER" RDISTANCE 1
END SUPPLEMENTAL DATA

**SAP2000-NL VERSION 7.11 INPUT FILE FOR EIGENVALUE AND PUSHOVER
ANALYSIS OF EXAMPLE No.9: FRAME 3S-75 WITH METALLIC YIELDING
DEVICES**

SYSTEM

DOF=UX,UZ,RY LENGTH=IN FORCE=Kip PAGE=SECTIONS

JOINT

1 X=-5.333333 Y=0 Z=156
2 X=-6 Y=0 Z=494.88
3 X=6 Y=0 Z=494.88
4 X=-6 Y=0 Z=325.44
5 X=6 Y=0 Z=325.44
6 X=-6 Y=0 Z=156
7 X=6 Y=0 Z=156
8 X=-6 Y=0 Z=512.88
9 X=6 Y=0 Z=512.88
10 X=-6 Y=0 Z=343.44
11 X=6 Y=0 Z=343.44
12 X=-6 Y=0 Z=174
13 X=6 Y=0 Z=174
14 X=-4.666667 Y=0 Z=494.88
15 X=-3.333333 Y=0 Z=494.88
16 X=-2 Y=0 Z=494.88
17 X=-486 Y=0 Z=0
18 X=-486 Y=0 Z=174
19 X=-486 Y=0 Z=343.44
20 X=-486 Y=0 Z=512.88
21 X=-162 Y=0 Z=512.88
22 X=162 Y=0 Z=512.88
23 X=486 Y=0 Z=512.88
24 X=486 Y=0 Z=343.44
25 X=486 Y=0 Z=174
26 X=-.6666667 Y=0 Z=494.88
27 X=-162 Y=0 Z=343.44
28 X=162 Y=0 Z=343.44
29 X=-162 Y=0 Z=174
30 X=162 Y=0 Z=174
31 X=.6666667 Y=0 Z=494.88
32 X=486 Y=0 Z=0
33 X=162 Y=0 Z=0
34 X=-162 Y=0 Z=0
35 X=2 Y=0 Z=494.88
36 X=3.333333 Y=0 Z=494.88
37 X=4.666667 Y=0 Z=494.88
38 X=-4.666667 Y=0 Z=325.44
39 X=-3.333333 Y=0 Z=325.44
40 X=-2 Y=0 Z=325.44
41 X=-.6666667 Y=0 Z=325.44
42 X=.6666667 Y=0 Z=325.44
43 X=2 Y=0 Z=325.44
44 X=3.333333 Y=0 Z=325.44
45 X=4.666667 Y=0 Z=325.44
46 X=-4.666667 Y=0 Z=156
47 X=-3.333333 Y=0 Z=156

48 X=-2 Y=0 Z=156
49 X=-.6666667 Y=0 Z=156
50 X=.6666667 Y=0 Z=156
51 X=2 Y=0 Z=156
52 X=3.333333 Y=0 Z=156
53 X=4.666667 Y=0 Z=156
54 X=-4.666667 Y=0 Z=512.88
55 X=-3.333333 Y=0 Z=512.88
56 X=-2 Y=0 Z=512.88
57 X=-.6666667 Y=0 Z=512.88
58 X=.6666667 Y=0 Z=512.88
59 X=2 Y=0 Z=512.88
60 X=3.333333 Y=0 Z=512.88
61 X=4.666667 Y=0 Z=512.88
62 X=-4.666667 Y=0 Z=343.44
63 X=-3.333333 Y=0 Z=343.44
64 X=-2 Y=0 Z=343.44
65 X=-.6666667 Y=0 Z=343.44
66 X=.6666667 Y=0 Z=343.44
67 X=2 Y=0 Z=343.44
68 X=3.333333 Y=0 Z=343.44
69 X=4.666667 Y=0 Z=343.44
70 X=-4.666667 Y=0 Z=174
71 X=-3.333333 Y=0 Z=174
72 X=-2 Y=0 Z=174
73 X=-.6666667 Y=0 Z=174
74 X=.6666667 Y=0 Z=174
75 X=2 Y=0 Z=174
76 X=3.333333 Y=0 Z=174
77 X=4.666667 Y=0 Z=174
78 X=5.333333 Y=0 Z=156
79 X=-5.333333 Y=0 Z=174
80 X=5.333333 Y=0 Z=174

RESTRAINT

ADD=17 DOF=U1,U2,U3,R1,R2,R3
ADD=33 DOF=U1,U2,U3,R1,R2,R3
ADD=34 DOF=U1,U2,U3,R1,R2,R3
ADD=32 DOF=U1,U2,U3,R1,R2,R3

PATTERN

NAME=DEFAULT

MASS

ADD=20 U1=.228238
ADD=21 U1=.228238
ADD=22 U1=.228238
ADD=23 U1=.228238
ADD=18 U1=.4224093
ADD=19 U1=.4224093
ADD=24 U1=.4224093
ADD=25 U1=.4224093
ADD=27 U1=.4224093
ADD=28 U1=.4224093
ADD=29 U1=.4224093
ADD=30 U1=.4224093

MATERIAL

NAME=STEEL IDES=S M=7.324E-07 W=.000283
T=0 E=29000 U=.3 A=.0000065 FY=50
NAME=CONC IDES=C M=2.246377E-07 W=.0000868
T=0 E=3600 U=.2 A=.0000055
NAME=OTHER IDES=N M=2.246377E-07 W=.0000868
T=0 E=3600 U=.2 A=.0000055
NAME=A36 IDES=S M=7.324E-07 W=.000283
T=0 E=29000 U=.3 A=.0000065 FY=36

FRAME SECTION

NAME=W14X109 MAT=STEEL A=32 J=7.12 I=1240,447 AS=7.518,20.934 S=173.1844,61.21191
Z=192,92.7 R=6.22495,3.737479 T=14.32,14.605,.86,.525,14.605,.86 SHN=W14X109 DSG=W
NAME=W16X40 MAT=STEEL A=11.8 J=.79 I=518,28.9 AS=4.8831,5.8875 S=64.70956,8.263045
Z=72.9,12.7 R=6.625579,1.564977 T=16.01,6.995,.505,.305,6.995,.505 SHN=W16X40 DSG=W
NAME=W16X45 MAT=STEEL A=13.3 J=1.11 I=586,32.8 AS=5.5649,6.6246 S=72.65965,9.324804
Z=82.3,14.5 R=6.637782,1.570403 T=16.13,7.035,.565,.345,7.035,.565 SHN=W16X45 DSG=W
NAME=W14X26 MAT=STEEL A=7.69 J=.36 I=245,8.91 AS=3.5471,3.5175 S=35.22646,3.546268
Z=40.2,5.54 R=5.644427,1.076405 T=13.91,5.025,.42,.255,5.025,.42 SHN=W14X26 DSG=W
NAME=COREB MAT=A36 SH=R T=.3333,54 A=18 J=.6640741 I=.1666667,4374 AS=15,15
NAME=FS6 MAT=STEEL A=14.4 J=217 I=131,131 AS=8,8 S=32.75,32.75 Z=39.7,39.7
R=3.01616,3.01616 T=8,8,.5,.5,0,0 SHN=TS8X8X1/2 DSG=B

NLPROP

NAME=NLPR1 TYPE=Plastic1
DOF=U1 KE=0 CE=0 K=320.32 YIELD=58.77 RATIO=0 EXP=1
NAME=NLPR3 TYPE=Plastic1
DOF=U1 KE=0 CE=0 K=223.73 YIELD=36.73 RATIO=0 EXP=1
NAME=NLPR2 TYPE=Plastic1
DOF=U1 KE=0 CE=0 K=258.36 YIELD=44 RATIO=0 EXP=1

FRAME

1 J=18,29 SEC=W16X45 NSEG=4 ANG=0 IOFF=7 JOFF=7 RIGID=1
2 J=26,57 SEC=COREB NSEG=2 ANG=0
3 J=30,25 SEC=W16X45 NSEG=4 ANG=0 IOFF=7 JOFF=7 RIGID=1
4 J=19,27 SEC=W16X40 NSEG=4 ANG=0 IOFF=7 JOFF=7 RIGID=1
5 J=41,65 SEC=COREB NSEG=2 ANG=0
6 J=28,24 SEC=W16X40 NSEG=4 ANG=0 IOFF=7 JOFF=7 RIGID=1
7 J=20,21 SEC=W14X26 NSEG=4 ANG=0 IOFF=7 JOFF=7 RIGID=1
9 J=22,23 SEC=W14X26 NSEG=4 ANG=0 IOFF=7 JOFF=7 RIGID=1
10 J=49,73 SEC=COREB NSEG=2 ANG=0
11 J=50,74 SEC=COREB NSEG=2 ANG=0
12 J=6,1 SEC=FS1 NSEG=4 ANG=0
13 J=1,46 SEC=FS1 NSEG=4 ANG=0
14 J=53,78 SEC=FS1 NSEG=4 ANG=0
15 J=78,7 SEC=FS1 NSEG=4 ANG=0
16 J=12,79 SEC=W16X45 NSEG=4 ANG=0
17 J=27,2 SEC=FS6 NSEG=2 ANG=0 IREL=R3 JREL=R3
18 J=3,28 SEC=FS6 NSEG=2 ANG=0 IREL=R3 JREL=R3
19 J=29,4 SEC=FS6 NSEG=2 ANG=0 IREL=R3 JREL=R3
20 J=5,30 SEC=FS6 NSEG=2 ANG=0 IREL=R3 JREL=R3
21 J=34,6 SEC=FS6 NSEG=2 ANG=0 IREL=R3 JREL=R3
22 J=17,18 SEC=W14X109 NSEG=2 ANG=0 IOFF=14 JOFF=8 RIGID=1
23 J=18,19 SEC=W14X109 NSEG=2 ANG=0 IOFF=8 JOFF=8 RIGID=1
24 J=19,20 SEC=W14X109 NSEG=2 ANG=0 IOFF=8 JOFF=7 RIGID=1
25 J=7,33 SEC=FS6 NSEG=2 ANG=0 IREL=R3 JREL=R3

26 J=21,8 SEC=W14X26 NSEG=4 ANG=0 IOFF=7 RIGID=1
27 J=79,70 SEC=W16X45 NSEG=4 ANG=0
28 J=23,24 SEC=W14X109 NSEG=2 ANG=0 IOFF=8 JOFF=7 RIGID=1
29 J=24,25 SEC=W14X109 NSEG=2 ANG=0 IOFF=8 JOFF=8 RIGID=1
30 J=9,22 SEC=W14X26 NSEG=4 ANG=0 JOFF=7 RIGID=1
31 J=27,10 SEC=W16X40 NSEG=4 ANG=0 IOFF=7 RIGID=1
32 J=77,80 SEC=W16X45 NSEG=4 ANG=0
33 J=11,28 SEC=W16X40 NSEG=4 ANG=0 JOFF=7 RIGID=1
34 J=29,12 SEC=W16X45 NSEG=4 ANG=0 IOFF=7 RIGID=1
35 J=80,13 SEC=W16X45 NSEG=4 ANG=0
36 J=13,30 SEC=W16X45 NSEG=4 ANG=0 JOFF=7 RIGID=1
37 J=2,14 SEC=FS1 NSEG=4 ANG=0
38 J=14,15 SEC=FS1 NSEG=4 ANG=0
39 J=30,28 SEC=W14X109 NSEG=2 ANG=0 IOFF=8 JOFF=8 RIGID=1
40 J=28,22 SEC=W14X109 NSEG=2 ANG=0 IOFF=8 JOFF=7 RIGID=1
41 J=15,16 SEC=FS1 NSEG=4 ANG=0
42 J=29,27 SEC=W14X109 NSEG=2 ANG=0 IOFF=8 JOFF=8 RIGID=1
43 J=27,21 SEC=W14X109 NSEG=2 ANG=0 IOFF=8 JOFF=7 RIGID=1
44 J=25,32 SEC=W14X109 NSEG=2 ANG=0 IOFF=14 JOFF=8 RIGID=1
45 J=16,26 SEC=FS1 NSEG=4 ANG=0
46 J=26,31 SEC=FS1 NSEG=4 ANG=0
47 J=31,35 SEC=FS1 NSEG=4 ANG=0
48 J=35,36 SEC=FS1 NSEG=4 ANG=0
49 J=36,37 SEC=FS1 NSEG=4 ANG=0
50 J=37,3 SEC=FS1 NSEG=4 ANG=0
51 J=4,38 SEC=FS1 NSEG=4 ANG=0
52 J=38,39 SEC=FS1 NSEG=4 ANG=0
53 J=39,40 SEC=FS1 NSEG=4 ANG=0
54 J=40,41 SEC=FS1 NSEG=4 ANG=0
55 J=41,42 SEC=FS1 NSEG=4 ANG=0
56 J=42,43 SEC=FS1 NSEG=4 ANG=0
57 J=43,44 SEC=FS1 NSEG=4 ANG=0
58 J=44,45 SEC=FS1 NSEG=4 ANG=0
59 J=45,5 SEC=FS1 NSEG=4 ANG=0
60 J=1,79 SEC=COREB NSEG=2 ANG=0
61 J=46,47 SEC=FS1 NSEG=4 ANG=0
62 J=47,48 SEC=FS1 NSEG=4 ANG=0
63 J=48,49 SEC=FS1 NSEG=4 ANG=0
64 J=49,50 SEC=FS1 NSEG=4 ANG=0
65 J=50,51 SEC=FS1 NSEG=4 ANG=0
66 J=51,52 SEC=FS1 NSEG=4 ANG=0
67 J=52,53 SEC=FS1 NSEG=4 ANG=0
68 J=78,80 SEC=COREB NSEG=2 ANG=0
69 J=8,54 SEC=W14X26 NSEG=4 ANG=0
70 J=54,55 SEC=W14X26 NSEG=4 ANG=0
71 J=55,56 SEC=W14X26 NSEG=4 ANG=0
72 J=56,57 SEC=W14X26 NSEG=4 ANG=0
73 J=57,58 SEC=W14X26 NSEG=4 ANG=0
74 J=58,59 SEC=W14X26 NSEG=4 ANG=0
75 J=59,60 SEC=W14X26 NSEG=4 ANG=0
76 J=60,61 SEC=W14X26 NSEG=4 ANG=0
77 J=61,9 SEC=W14X26 NSEG=4 ANG=0
78 J=10,62 SEC=W16X40 NSEG=4 ANG=0
79 J=62,63 SEC=W16X40 NSEG=4 ANG=0
80 J=63,64 SEC=W16X40 NSEG=4 ANG=0
81 J=64,65 SEC=W16X40 NSEG=4 ANG=0

82 J=65,66 SEC=W16X40 NSEG=4 ANG=0
 83 J=66,67 SEC=W16X40 NSEG=4 ANG=0
 84 J=67,68 SEC=W16X40 NSEG=4 ANG=0
 85 J=68,69 SEC=W16X40 NSEG=4 ANG=0
 86 J=69,11 SEC=W16X40 NSEG=4 ANG=0
 87 J=39,63 SEC=COREB NSEG=2 ANG=0
 88 J=70,71 SEC=W16X45 NSEG=4 ANG=0
 89 J=71,72 SEC=W16X45 NSEG=4 ANG=0
 90 J=72,73 SEC=W16X45 NSEG=4 ANG=0
 91 J=73,74 SEC=W16X45 NSEG=4 ANG=0
 92 J=74,75 SEC=W16X45 NSEG=4 ANG=0
 93 J=75,76 SEC=W16X45 NSEG=4 ANG=0
 94 J=76,77 SEC=W16X45 NSEG=4 ANG=0
 95 J=44,68 SEC=COREB NSEG=2 ANG=0
 96 J=2,8 SEC=COREB NSEG=2 ANG=0
 97 J=3,9 SEC=COREB NSEG=2 ANG=0
 98 J=60,36 SEC=COREB NSEG=2 ANG=0
 99 J=15,55 SEC=COREB NSEG=2 ANG=0
 100 J=31,58 SEC=COREB NSEG=2 ANG=0
 101 J=4,10 SEC=COREB NSEG=2 ANG=0
 102 J=5,11 SEC=COREB NSEG=2 ANG=0
 103 J=38,62 SEC=COREB NSEG=2 ANG=0
 104 J=45,69 SEC=COREB NSEG=2 ANG=0
 105 J=40,64 SEC=COREB NSEG=2 ANG=0
 106 J=43,67 SEC=COREB NSEG=2 ANG=0
 107 J=12,6 SEC=COREB NSEG=2 ANG=0
 108 J=13,7 SEC=COREB NSEG=2 ANG=0
 109 J=70,46 SEC=COREB NSEG=2 ANG=0
 110 J=77,53 SEC=COREB NSEG=2 ANG=0
 111 J=71,47 SEC=COREB NSEG=2 ANG=0
 112 J=76,52 SEC=COREB NSEG=2 ANG=0
 113 J=72,48 SEC=COREB NSEG=2 ANG=0
 114 J=75,51 SEC=COREB NSEG=2 ANG=0
 115 J=35,59 SEC=COREB NSEG=2 ANG=0
 127 J=34,29 SEC=W14X109 NSEG=2 ANG=0 IOFF=14 JOFF=8 RIGID=1
 130 J=33,30 SEC=W14X109 NSEG=2 ANG=0 IOFF=14 JOFF=8 RIGID=1

LOAD

NAME=CVX
 TYPE=FORCE
 ADD=20 UX=.3929
 ADD=19 UX=.4303
 ADD=18 UX=.1768
 NAME=NEHRP
 TYPE=FORCE
 ADD=20 UX=43.7
 ADD=19 UX=47.9
 ADD=18 UX=19.7
 NAME=GRAVITY
 TYPE=DISTRIBUTED SPAN
 ADD=7 RD=0,1 UZ=-.06,-.06
 ADD=9 RD=0,1 UZ=-.06,-.06
 ADD=26 RD=0,1 UZ=-.06,-.06
 ADD=30 RD=0,1 UZ=-.06,-.06
 ADD=1 RD=0,1 UZ=-.13,-.13
 ADD=3 RD=0,1 UZ=-.13,-.13

```

ADD=4 RD=0,1 UZ=-.13,-.13
ADD=6 RD=0,1 UZ=-.13,-.13
ADD=31 RD=0,1 UZ=-.13,-.13
ADD=33 RD=0,1 UZ=-.13,-.13
ADD=34 RD=0,1 UZ=-.13,-.13
ADD=36 RD=0,1 UZ=-.13,-.13
NAME=1STMODE
TYPE=FORCE
ADD=20 UX=125.1
ADD=19 UX=156.6
ADD=18 UX=63.6
NAME=RMODE
TYPE=FORCE
ADD=20 UX=93.9
ADD=19 UX=-27
ADD=18 UX=-275.7
NAME=DEAD
NAME=LIVE
NAME=1MODDBE
TYPE=FORCE
ADD=20 UX=41.7
ADD=19 UX=52.2
ADD=18 UX=21.2
NAME=RMODBE
TYPE=FORCE
ADD=20 UX=31.3
ADD=19 UX=-9
ADD=18 UX=-91.9
NAME=DDLL
NAME=UNIFORM
TYPE=FORCE
ADD=20 UX=.2127
ADD=19 UX=.39365
ADD=18 UX=.39365

```

```

MODE
TYPE=EIGEN N=3 TOL=.00001

```

```

COMBO
NAME=DSTL1
LOAD=CVX SF=1
LOAD=NEHRP SF=1
LOAD=GRAVITY SF=1
LOAD=1STMODE SF=1
LOAD=RMODE SF=1
LOAD=DEAD SF=1
LOAD=1MODDBE SF=1
LOAD=RMODBE SF=1
LOAD=DDLL SF=1
LOAD=UNIFORM SF=1
NAME=DSTL2
LOAD=CVX SF=1
LOAD=NEHRP SF=1
LOAD=GRAVITY SF=1
LOAD=1STMODE SF=1
LOAD=RMODE SF=1

```

LOAD=DEAD SF=1
LOAD=LIVE SF=1
LOAD=1MODDBE SF=1
LOAD=RMODBE SF=1
LOAD=DDLL SF=1
LOAD=UNIFORM SF=1

OUTPUT

; No Output Requested

END

; The following data is used for graphics, design and pushover analysis.
; If changes are made to the analysis data above, then the following data
; should be checked for consistency.

SAP2000 V7.12 SUPPLEMENTAL DATA

GRID GLOBAL X "1" -486
GRID GLOBAL X "2" -162
GRID GLOBAL X "3" -6
GRID GLOBAL X "4" 6
GRID GLOBAL X "5" 162
GRID GLOBAL X "6" 486
GRID GLOBAL Y "7" 0
GRID GLOBAL Z "8" 0
GRID GLOBAL Z "9" 156
GRID GLOBAL Z "10" 174
GRID GLOBAL Z "11" 325.44
GRID GLOBAL Z "12" 343.44
GRID GLOBAL Z "13" 494.88
GRID GLOBAL Z "14" 512.88
MATERIAL STEEL FY 50
MATERIAL A36 FY 36
MATERIAL CONC FYREBAR 60 FYSHEAR 40 FC 4 FCSHEAR 4
FRAMESECTION FS1 NAME BASEPLAT
FRAMESECTION FS2 NAME TS10X10X5/8
FRAMESECTION FS3 NAME TS8X8X1/4
FRAMESECTION FS4 NAME TS6X6X1/4
FRAMESECTION FS5 NAME TS6X6X3/8
FRAMESECTION FS6 NAME TS8X8X1/2
STATICLOAD CVX TYPE DEAD
STATICLOAD NEHRP TYPE DEAD
STATICLOAD GRAVITY TYPE DEAD
STATICLOAD 1STMODE TYPE DEAD
STATICLOAD RMODE TYPE DEAD
STATICLOAD DEAD TYPE DEAD
STATICLOAD LIVE TYPE LIVE
STATICLOAD 1MODDBE TYPE DEAD
STATICLOAD RMODBE TYPE DEAD
STATICLOAD DDLL TYPE DEAD
STATICLOAD UNIFORM TYPE DEAD
COMBO DSTL1 DESIGN STEEL
COMBO DSTL2 DESIGN STEEL
STEELDESIGN "AISC-ASD89"
PUSHCASE "GRAVITY" CONTROL FORCE JOINT 20 DOF U3
PUSHCASE "GRAVITY" PDELTA NO

PUSHCASE "GRAVITY" MINSTEPS 1 MAXNULLSTEPS 50 MAXTOTALSTEPS 200 MAXITER
 10
 PUSHCASE "GRAVITY" ITERTOL .0001 EVENTTOL .01
 PUSHCASE "GRAVITY" LOADTYPE STATIC LOAD GRAVITY SCALEFACTOR 1
 PUSHCASE "PUSHM1" CONTROL DISP TARGET 20.5152 JOINT 20 DOF U1
 PUSHCASE "PUSHM1" STARTCASE "GRAVITY"
 PUSHCASE "PUSHM1" MINSTEPS 10 MAXNULLSTEPS 50 MAXTOTALSTEPS 200 MAXITER
 10
 PUSHCASE "PUSHM1" ITERTOL .0001 EVENTTOL .01
 PUSHCASE "PUSHM1" LOADTYPE MODE NUMBER 1 SCALEFACTOR 1
 PUSHCASE "PUSHUNIF" CONTROL DISP TARGET 20.5152 JOINT 20 DOF U1
 PUSHCASE "PUSHUNIF" STARTCASE "GRAVITY"
 PUSHCASE "PUSHUNIF" MINSTEPS 10 MAXNULLSTEPS 50 MAXTOTALSTEPS 200
 MAXITER 10
 PUSHCASE "PUSHUNIF" ITERTOL .0001 EVENTTOL .01
 PUSHCASE "PUSHUNIF" LOADTYPE STATIC LOAD UNIFORM SCALEFACTOR 1
 PUSHCASE "PUSHCVX" CONTROL DISP TARGET 20.5152 JOINT 20 DOF U1
 PUSHCASE "PUSHCVX" STARTCASE "GRAVITY"
 PUSHCASE "PUSHCVX" MINSTEPS 10 MAXNULLSTEPS 50 MAXTOTALSTEPS 200
 MAXITER 10
 PUSHCASE "PUSHCVX" ITERTOL .0001 EVENTTOL .01
 PUSHCASE "PUSHCVX" LOADTYPE STATIC LOAD CVX SCALEFACTOR 1
 HINGE "USER" TYPE M3 SYMMETRIC
 HINGE "USER" TYPE M3 B 1 1 C 6 1 D 8 1 E 10 1
 HINGE "USER" TYPE M3 IO 2 LS 4 CP 6
 HINGE "USERP" TYPE M3 SYMMETRIC
 HINGE "USERP" TYPE M3 B 1 1 C 16 1 D 20 1 E 40 1
 HINGE "USERP" TYPE M3 IO 2 LS 4 CP 6
 FRAMEHINGE 22 HINGE "USER" RDISTANCE .08046
 FRAMEHINGE 22 HINGE "USER" RDISTANCE .87356
 FRAMEHINGE 23 HINGE "USER" RDISTANCE .12984
 FRAMEHINGE 23 HINGE "USER" RDISTANCE .87016
 FRAMEHINGE 24 HINGE "USER" RDISTANCE .12984
 FRAMEHINGE 24 HINGE "USER" RDISTANCE .8760623
 FRAMEHINGE 28 HINGE "USER" RDISTANCE .12984
 FRAMEHINGE 28 HINGE "USER" RDISTANCE .8760623
 FRAMEHINGE 29 HINGE "USER" RDISTANCE .12984
 FRAMEHINGE 29 HINGE "USER" RDISTANCE .87016
 FRAMEHINGE 39 HINGE "USER" RDISTANCE .12984
 FRAMEHINGE 39 HINGE "USER" RDISTANCE .87016
 FRAMEHINGE 40 HINGE "USER" RDISTANCE .12984
 FRAMEHINGE 40 HINGE "USER" RDISTANCE .8760623
 FRAMEHINGE 42 HINGE "USER" RDISTANCE .12984
 FRAMEHINGE 42 HINGE "USER" RDISTANCE .87016
 FRAMEHINGE 43 HINGE "USER" RDISTANCE .12984
 FRAMEHINGE 43 HINGE "USER" RDISTANCE .8760623
 FRAMEHINGE 1 HINGE "USER" RDISTANCE .0648
 FRAMEHINGE 1 HINGE "USER" RDISTANCE .935185
 FRAMEHINGE 3 HINGE "USER" RDISTANCE .070988
 FRAMEHINGE 3 HINGE "USER" RDISTANCE .9290125
 FRAMEHINGE 4 HINGE "USER" RDISTANCE .0648
 FRAMEHINGE 4 HINGE "USER" RDISTANCE .935185
 FRAMEHINGE 6 HINGE "USER" RDISTANCE .070988
 FRAMEHINGE 6 HINGE "USER" RDISTANCE .9290125
 FRAMEHINGE 7 HINGE "USER" RDISTANCE .0648
 FRAMEHINGE 7 HINGE "USER" RDISTANCE .935185

FRAMEHINGE 9 HINGE "USER" RDISTANCE .0648
FRAMEHINGE 9 HINGE "USER" RDISTANCE .9352
FRAMEHINGE 44 HINGE "USER" RDISTANCE .08046
FRAMEHINGE 44 HINGE "USER" RDISTANCE .87356
FRAMEHINGE 127 HINGE "USER" RDISTANCE .08046
FRAMEHINGE 127 HINGE "USER" RDISTANCE .87356
FRAMEHINGE 130 HINGE "USER" RDISTANCE .08046
FRAMEHINGE 130 HINGE "USER" RDISTANCE .87356
FRAMEHINGE 26 HINGE "USER" RDISTANCE .12963
FRAMEHINGE 26 HINGE "USER" RDISTANCE 1
FRAMEHINGE 30 HINGE "USER" RDISTANCE 0
FRAMEHINGE 30 HINGE "USER" RDISTANCE .87037
FRAMEHINGE 31 HINGE "USER" RDISTANCE .149753
FRAMEHINGE 31 HINGE "USER" RDISTANCE 1
FRAMEHINGE 33 HINGE "USER" RDISTANCE 0
FRAMEHINGE 33 HINGE "USER" RDISTANCE .858025
FRAMEHINGE 34 HINGE "USER" RDISTANCE .149753
FRAMEHINGE 34 HINGE "USER" RDISTANCE 1
FRAMEHINGE 36 HINGE "USER" RDISTANCE 0
FRAMEHINGE 36 HINGE "USER" RDISTANCE .858025
FRAMEHINGE 96 HINGE "USERP" RDISTANCE 0
FRAMEHINGE 96 HINGE "USERP" RDISTANCE 1
FRAMEHINGE 97 HINGE "USERP" RDISTANCE 0
FRAMEHINGE 97 HINGE "USERP" RDISTANCE 1
FRAMEHINGE 98 HINGE "USERP" RDISTANCE 0
FRAMEHINGE 98 HINGE "USERP" RDISTANCE 1
FRAMEHINGE 99 HINGE "USERP" RDISTANCE 0
FRAMEHINGE 99 HINGE "USERP" RDISTANCE 1
FRAMEHINGE 100 HINGE "USERP" RDISTANCE 0
FRAMEHINGE 100 HINGE "USERP" RDISTANCE 1
FRAMEHINGE 101 HINGE "USERP" RDISTANCE 0
FRAMEHINGE 101 HINGE "USERP" RDISTANCE 1
FRAMEHINGE 102 HINGE "USERP" RDISTANCE 0
FRAMEHINGE 102 HINGE "USERP" RDISTANCE 1
FRAMEHINGE 103 HINGE "USERP" RDISTANCE 0
FRAMEHINGE 103 HINGE "USERP" RDISTANCE 1
FRAMEHINGE 104 HINGE "USERP" RDISTANCE 0
FRAMEHINGE 104 HINGE "USERP" RDISTANCE 1
FRAMEHINGE 105 HINGE "USERP" RDISTANCE 0
FRAMEHINGE 105 HINGE "USERP" RDISTANCE 1
FRAMEHINGE 106 HINGE "USERP" RDISTANCE 0
FRAMEHINGE 106 HINGE "USERP" RDISTANCE 1
FRAMEHINGE 107 HINGE "USERP" RDISTANCE 0
FRAMEHINGE 107 HINGE "USERP" RDISTANCE 1
FRAMEHINGE 108 HINGE "USERP" RDISTANCE 0
FRAMEHINGE 108 HINGE "USERP" RDISTANCE 1
FRAMEHINGE 109 HINGE "USERP" RDISTANCE 0
FRAMEHINGE 109 HINGE "USERP" RDISTANCE 1
FRAMEHINGE 110 HINGE "USERP" RDISTANCE 0
FRAMEHINGE 110 HINGE "USERP" RDISTANCE 1
FRAMEHINGE 111 HINGE "USERP" RDISTANCE 0
FRAMEHINGE 111 HINGE "USERP" RDISTANCE 1
FRAMEHINGE 112 HINGE "USERP" RDISTANCE 0
FRAMEHINGE 112 HINGE "USERP" RDISTANCE 1
FRAMEHINGE 113 HINGE "USERP" RDISTANCE 0
FRAMEHINGE 113 HINGE "USERP" RDISTANCE 1

FRAMEHINGE 114 HINGE "USERP" RDISTANCE 0
FRAMEHINGE 114 HINGE "USERP" RDISTANCE 1
FRAMEHINGE 2 HINGE "USERP" RDISTANCE 0
FRAMEHINGE 2 HINGE "USERP" RDISTANCE 1
FRAMEHINGE 5 HINGE "USERP" RDISTANCE 0
FRAMEHINGE 5 HINGE "USERP" RDISTANCE 1
FRAMEHINGE 10 HINGE "USERP" RDISTANCE 0
FRAMEHINGE 10 HINGE "USERP" RDISTANCE 1
FRAMEHINGE 11 HINGE "USERP" RDISTANCE 0
FRAMEHINGE 11 HINGE "USERP" RDISTANCE 1
FRAMEHINGE 60 HINGE "USERP" RDISTANCE 0
FRAMEHINGE 60 HINGE "USERP" RDISTANCE 1
FRAMEHINGE 68 HINGE "USERP" RDISTANCE 0
FRAMEHINGE 68 HINGE "USERP" RDISTANCE 1
FRAMEHINGE 87 HINGE "USERP" RDISTANCE 0
FRAMEHINGE 87 HINGE "USERP" RDISTANCE 1
FRAMEHINGE 95 HINGE "USERP" RDISTANCE 0
FRAMEHINGE 95 HINGE "USERP" RDISTANCE 1
FRAMEHINGE 115 HINGE "USERP" RDISTANCE 0
FRAMEHINGE 115 HINGE "USERP" RDISTANCE 1
END SUPPLEMENTAL DATA

APPENDIX K

INPUT FILES FOR NONLINEAR TIME-HISTORY AND PUSHOVER ANALYSIS OF FRAMES WITH DAMPING SYSTEMS IN PROGRAM IDARCD2D

K.1 Introduction

This appendix contains information on the input files for the nonlinear time-history and pushover analysis of selected examples of frames with damping systems in program IDARC2D-Version 5.0. Figure K-1 shows the connectivity and the numbers of beams, columns and energy dissipating braces as required in this program. The input files for nonlinear time history analysis of the following examples are presented:

- (a) Example No.2: frame 3S-75 with linear viscous damping system to provide 10% viscous damping ratio when assuming elastic frame behavior (Fig. 8-2).
- (b) Example No.5: frame 6S-75 with linear viscous damping system to provide 10% viscous damping ratio when assuming elastic frame behavior (Fig. 8-5).
- (c) Example No.6: frame 3S-80 with nonlinear viscous damping system to provide 10% viscous damping ratio when assuming elastic frame behavior in the design basis earthquake (DBE) (Fig. 8-6).
- (d) Example No.8: frame 3S-75 with viscoelastic solid damping system to provide 8.5% viscous damping ratio when assuming elastic frame behavior (Fig. 8-8).
- (e) Example No.9: frame 3S-75 with metallic yielding damping system (Fig. 8-9).

Moreover, input files for the pushover analysis of example No.1: frame 3S-60 with linear viscous damping system to provide 10% viscous damping ratio when assuming elastic frame behavior (Fig. 8-1) are presented. Files for four lateral force patterns are presented: (a) proportional to the first mode, (b) modal (Cvx) pattern, (c) uniform pattern, and (d) modal adaptive pattern.

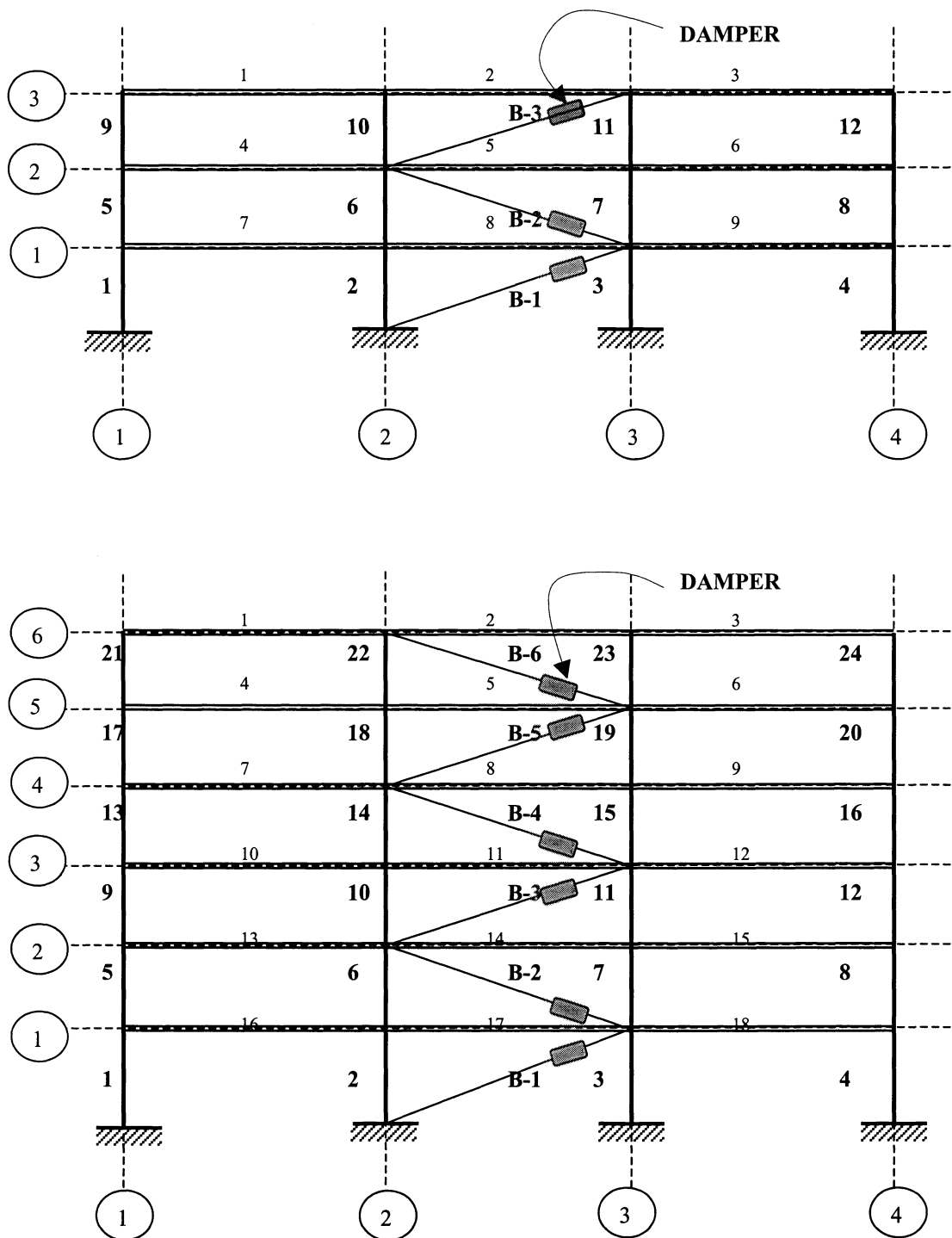


FIGURE K-1 Frame Connectivity and Member Numbers of 3- and 6-story Frame Models in Program IDARC2D

**IDARC-2D INPUT FILE FOR NONLINEAR TIME HISTORY ANALYSIS OF
EXAMPLE No.2: FRAME 3S-75 WITH LINEAR VISCOUS DAMPING SYSTEM
TO PROVIDE 10% VISCOUS DAMPING RATIO WHEN ASSUMING ELASTIC
FRAME BEHAVIOR**

EXAMPLE No.2: FRAME 3S-75 + 10% LVD. ANALYSIS FOR THE DBE.

SET A - CONTROL DATA SET

3, 1, 0, 0, 0, 0, 1, 1

SET A1 - ELEMENTS TYPE

3, 3, 0, 0, 0, 0, 1, 0, 0, 0

SET A2 - ELEMENT DATA

12, 9, 0, 0, 0, 0, 0, 3, 0

SET A3 - SYSTEM OF UNITS

1

SET A4 - FLOOR ELEVATIONS

174.0, 343.44, 512.88

SET A5 - DESCRIPTION OF IDENTICAL FRAMES

1

SET A6 - PLAN CONFIGURATION

4

SET A7 - NODAL WEIGHTS

1, 1, 0, 652.2, 0, 0

2, 1, 0, 652.2, 0, 0

3, 1, 0, 352.4, 0, 0

SET B - MATERIAL PROPERTIES SET

1

SET C - HYSTERETIC MODELING RULES

1

1, 1, 200, 0.001, 0.001, 1.0, 0

SET D - COLUMN PROPERTIES

1

SET D3 COLUMN DATA

1, 174.00, 14.0, 8.0, 0

-1 36.0E6 5.33E3 8.72E4 9.12E3 9.60E3 2.94E-4 1.47E-2 1

9.12E3 9.60E3 2.94E-4 1.47E-2 1

2, 169.44, 8.0, 8.0, 0

-1 36.0E6 5.48E3 8.72E4 9.12E3 9.60E3 2.94E-4 1.47E-2 1

9.12E3 9.60E3 2.94E-4 1.47E-2 1

3, 169.44, 8.0, 7.0, 0

-1 36.0E6 5.48E3 8.72E4 9.12E3 9.60E3 2.94E-4 1.47E-2 1

9.12E3 9.60E3 2.94E-4 1.47E-2 1

SET E - BEAM PROPERTIES

1

SET E2 - BEAM DATA

1 324.0 7.0 7.0 0

-1 7.10E6 4.11E4 1.91E3 2.01E3 3.10E-4 1.55E-2 1

1.91E3 2.01E3 3.10E-4 1.55E-2 1
 2 324.0 7.0 7.0 0
 -1 15.02E6 5.66E4 3.46E3 3.64E3 2.67E-4 1.34E-2 1
 3.46E3 3.64E3 2.67E-4 1.34E-2 1
 3 324.0 7.0 7.0 0
 -1 16.99E6 6.45E4 3.91E3 4.12E3 2.67E-4 1.34E-2 1
 3.91E3 4.12E3 2.67E-4 1.34E-2 1

BRACE PROPERTIES - J1

0 0
1 5.15 875.28 1.0

COLUMN CONNECTIVITY - L1

1,1,1,1,0,1
2,1,1,2,0,1
3,1,1,3,0,1
4,1,1,4,0,1
5,2,1,1,1,2
6,2,1,2,1,2
7,2,1,3,1,2
8,2,1,4,1,2
9,3,1,1,2,3
10,3,1,2,2,3
11,3,1,3,2,3
12,3,1,4,2,3

BEAMS CONNECTIVITY - L2

1,1,3,1,1,2
2,1,3,1,2,3
3,1,3,1,3,4
4,2,2,1,1,2
5,2,2,1,2,3
6,2,2,1,3,4
7,3,1,1,1,2
8,3,1,1,2,3
9,3,1,1,3,4

BRACES CONNECTIVITY - L8

1,1,1,1,1,0,3,2,367.77
2,1,1,1,2,1,2,3,365.63
3,1,1,1,3,2,3,2,365.63

SET M - ANALYSIS OPTION

3
SET M1 - LONG-TERM STATIC LOADING
0, 0, 0, 0

SET M3 - DYNAMIC ANALYSIS

0.5021, 0.0, 0.005, 60.0, 5, 1

HORIZONTAL ACC

0, 3000, 0.02

GROUND MOTION

EQ10.DAT
SET N1.2
0
0, 0, 0, 0, 0
SET N2 - STORY OUTPUT CONTROL
3, 0.02, 1, 2, 3
LEV1E10.OUT
LEV2E10.OUT
LEV3E10.OUT
SET N3 - ELEMENT HYSTERESIS OUTPUT
0, 1, 0, 0, 3, 0
BEAM OUTPUT
4
BRACES OUTPUT
1,2,3

**IDARC-2D INPUT FILE FOR NONLINEAR TIME HISTORY ANALYSIS OF
EXAMPLE No.5: FRAME 6S-75 WITH LINEAR VISCOUS DAMPING SYSTEM
TO PROVIDE 10% VISCOUS DAMPING RATIO WHEN ASSUMING ELASTIC
FRAME BEHAVIOR**

EXAMPLE No.5: FRAME 6S-75 + 10% LINEAR VISCOUS DAMPING. ANALYSIS
FOR THE DBE

SET A - CONTROL DATA SET

6, 1, 0, 0, 0, 1, 1, 1

SET A1 - ELEMENTS TYPE

6, 6, 0, 0, 0, 0, 3, 0, 0, 0

SET A2 - ELEMENT DATA

24, 18, 0, 0, 0, 0, 0, 6, 0

SET A3 - SYSTEM OF UNITS

1

SET A4 - FLOOR ELEVATIONS

174.0 343.44 512.88 682.32 851.76 1021.2

SET A5 - DESCRIPTION OF IDENTICAL FRAMES

1

SET A6 - PLAN CONFIGURATION

4

SET A7 - NODAL WEIGHTS

1, 1, 0, 652.2, 0, 0

2, 1, 0, 652.2, 0, 0

3, 1, 0, 652.2, 0, 0

4, 1, 0, 652.2, 0, 0

5, 1, 0, 652.2, 0, 0

6, 1, 0, 352.4, 0, 0

SET B - MATERIAL PROPERTIES SET

1

SET C - HYSTERETIC MODELING RULES

1

1, 1, 200, 0.001, 0.001, 1.0, 0

SET D - COLUMN PROPERTIES

1

SET D3 - COLUMN DATA

1, 174.00, 14.0, 12.0, 0

-1	62.1E6	8.63E3	14.7E4	1.30E4	1.37E4	2.42E-4	1.21E-2	1
				1.30E4	1.37E4	2.42E-4	1.21E-2	1

2, 169.44, 12.0, 10.5, 0

-1	62.1E6	8.87E3	14.7E4	1.34E4	1.41E4	2.49E-4	1.25E-2	1
				1.34E4	1.41E4	2.49E-4	1.25E-2	1

3, 169.44, 10.5, 10.5, 0

-1	44.4E6	6.64E3	11.0E4	9.72E3	10.2E3	2.54E-4	1.27E-2	1
				9.72E3	10.2E3	2.54E-4	1.27E-2	1

4, 169.44, 10.5, 10.5, 0

-1 44.4E6 6.64E3 11.0E4 10.1E3 10.7E3 2.64E-4 1.32E-2 1
10.1E3 10.7E3 2.64E-4 1.32E-2 1
5, 169.44, 10.5, 8.0, 0
-1 29.0E6 4.54E3 7.15E4 6.87E3 7.23E3 2.75E-4 1.37E-2 1
6.87E3 7.23E3 2.75E-4 1.37E-2 1
6, 169.44, 8.0, 8.0, 0
-1 29.0E6 4.54E3 7.15E4 7.26E3 7.64E3 2.90E-4 1.45E-2 1
7.26E3 7.64E3 2.90E-4 1.45E-2 1

SET E - BEAM PROPERTIES

1

SET E2 - BEAM DATA

1 324.0 7.0 7.0 0

-1 10.9E6 5.07E4 2.57E3 2.70E3 2.73E-4 1.37E-2 1
2.57E3 2.70E3 2.73E-4 1.37E-2 1

2 324.0 7.0 7.0 0

-1 15.0E6 5.66E4 3.46E3 3.65E3 2.67E-4 1.33E-2 1
3.46E3 3.65E3 2.67E-4 1.33E-2 1

3 324.0 7.0 7.0 0

-1 24.4E6 8.39E4 4.53E3 4.77E3 2.15E-4 1.07E-2 1
4.53E3 4.77E3 2.15E-4 1.07E-2 1

4 324.0 7.0 7.0 0

-1 28.5E6 9.19E4 5.23E3 5.50E3 2.12E-4 1.06E-2 1
5.23E3 5.50E3 2.12E-4 1.06E-2 1

5 324.0 7.0 7.0 0

-1 38.6E6 9.74E4 6.84E3 7.20E3 2.05E-4 1.03E-2 1
6.84E3 7.20E3 2.05E-4 1.03E-2 1

6 324.0 7.0 7.0 0

-1 45.0E6 11.8E4 7.27E3 7.65E3 1.87E-4 9.36E-3 1
7.27E3 7.65E3 1.87E-4 9.36E-3 1

BRACE PROPERTIES - J1

1 0

1 12.96 1142.0 1.0

2 9.620 1142.0 1.0

3 7.854 1142.0 1.0

COLUMN CONNECTIVITY - L1

1,1,1,1,0,1

2,1,1,2,0,1

3,1,1,3,0,1

4,1,1,4,0,1

5,2,1,1,1,2

6,2,1,2,1,2

7,2,1,3,1,2

8,2,1,4,1,2

9,3,1,1,2,3

10,3,1,2,2,3

11,3,1,3,2,3

12,3,1,4,2,3
13,4,1,1,3,4
14,4,1,2,3,4
15,4,1,3,3,4
16,4,1,4,3,4
17,5,1,1,4,5
18,5,1,2,4,5
19,5,1,3,4,5
20,5,1,4,4,5
21,6,1,1,5,6
22,6,1,2,5,6
23,6,1,3,5,6
24,6,1,4,5,6

BEAMS CONNECTIVITY - L2

1,1,6,1,1,2
2,1,6,1,2,3
3,1,6,1,3,4
4,2,5,1,1,2
5,2,5,1,2,3
6,2,5,1,3,4
7,3,4,1,1,2
8,3,4,1,2,3
9,3,4,1,3,4
10,4,3,1,1,2
11,4,3,1,2,3
12,4,3,1,3,4
13,5,2,1,1,2
14,5,2,1,2,3
15,5,2,1,3,4
16,6,1,1,1,2
17,6,1,1,2,3
18,6,1,1,3,4

BRACES CONNECTIVITY - L8

1,1,1,1,1,0,3,2,367.77
2,1,1,1,2,1,2,3,365.63
3,1,1,2,3,2,3,2,365.63
4,1,1,2,4,3,2,3,355.63
5,1,1,3,5,4,3,2,365.63
6,1,1,3,6,5,2,3,365.63

SET M - ANALYSIS OPTION

3

SET M1 - LONG-TERM STATIC LOADING

18, 0, 0, 0

1 0

UNIFORMLY LOADED BEAMS

1 1 0.08

1 2 0.08
1 3 0.08
2 4 0.16
2 5 0.16
2 6 0.16
2 7 0.16
2 8 0.16
2 9 0.16
2 10 0.16
2 11 0.16
2 12 0.16
2 13 0.16
2 14 0.16
2 15 0.16
2 16 0.16
2 17 0.16
2 18 0.16
SET M3 - DYNAMIC ANALYSIS
0.2331, 0.0, 0.005, 98.0, 5, 1
HORIZONTAL ACC
0, 4932, 0.02
GROUND MOTION
EQ20.DAT
SET N1.2
0
0, 0, 0, 0, 0
SET N2 - STORY OUTPUT CONTROL
6, 0.02, 1, 2, 3, 4, 5, 6
LEV1E20.OUT
LEV2E20.OUT
LEV3E20.OUT
LEV4E20.OUT
LEV5E20.OUT
LEV6E20.OUT
SET N3 - ELEMENT HYSTERESIS OUTPUT
0, 0, 0, 0, 0, 0

**IDARC-2D INPUT FILE FOR NONLINEAR TIME HISTORY ANALYSIS OF
EXAMPLE No.6: FRAME 3S-80 WITH NONLINEAR VISCOUS DAMPING
SYSTEM TO PROVIDE 10% VISCOUS DAMPING RATIO WHEN ASSUMING
ELASTIC FRAME BEHAVIOR IN THE DESIGN BASIS EARTHQUAKE**

FRAME 3S80 + 10% NONLINEAR DAMPING IN DBE - ANALYSIS FOR THE DBE

SET A - CONTROL DATA SET

3, 1, 0, 0, 0, 0, 1, 1

SET A1 - ELEMENTS TYPE

3, 3, 0, 0, 0, 0, 1, 0, 0, 0

SET A2 - ELEMENT DATA

12, 9, 0, 0, 0, 0, 0, 3, 0

SET A3 - SYSTEM OF UNITS

1

SET A4 - FLOOR ELEVATIONS

174.0, 343.44, 512.88

SET A5 - DESCRIPTION OF IDENTICAL FRAMES

1

SET A6 - PLAN CONFIGURATION

4

SET A7 - NODAL WEIGHTS

1, 1, 0, 652.2, 0, 0

2, 1, 0, 652.2, 0, 0

3, 1, 0, 352.4, 0, 0

SET B - MATERIAL PROPERTIES SET

1

SET C - HYSTERETIC MODELING RULES

1

1, 1, 200, 0.001, 0.001, 1.0, 0

SET D - COLUMN PROPERTIES

1

SET D3 - COLUMN DATA

1, 174.00, 14.0, 9.0, 0

-1	36.0E6	5.33E3	8.72E4	9.12E3	9.60E3	2.94E-4	1.47E-2	1
				9.12E3	9.60E3	2.94E-4	1.47E-2	1

2, 169.44, 9.0, 9.0, 0

-1	36.0E6	5.48E3	8.72E4	9.12E3	9.60E3	2.94E-4	1.47E-2	1
				9.12E3	9.60E3	2.94E-4	1.47E-2	1

3, 169.44, 9.0, 7.0, 0

-1	36.0E6	5.48E3	8.72E4	9.12E3	9.60E3	2.94E-4	1.47E-2	1
				9.12E3	9.60E3	2.94E-4	1.47E-2	1

SET E - BEAM PROPERTIES

1

SET E2 - BEAM DATA

1 324.0 7.0 7.0 0
 -1 8.44E6 4.33E4 2.13E3 2.37E3 3.08E-4 9.25E-3 1
 2.13E3 2.37E3 3.08E-4 9.25E-3 1
 2 324.0 7.0 7.0 0
 -1 14.8E6 6.16E4 3.16E3 3.33E3 2.47E-4 7.41E-3 1
 3.16E3 3.33E3 2.47E-4 7.41E-3 1
 3 324.0 7.0 7.0 0
 -1 20.65E6 7.52E4 4.31E3 4.54E3 2.42E-4 7.25E-3 1
 4.31E3 4.54E3 2.42E-4 7.25E-3 1

BRACE PROPERTIES - J1

0 0
 1 16.35 875.28 0.5

COLUMN CONNECTIVITY - L1

1,1,1,1,0,1
 2,1,1,2,0,1
 3,1,1,3,0,1
 4,1,1,4,0,1
 5,2,1,1,1,2
 6,2,1,2,1,2
 7,2,1,3,1,2
 8,2,1,4,1,2
 9,3,1,1,2,3
 10,3,1,2,2,3
 11,3,1,3,2,3
 12,3,1,4,2,3

BEAMS CONNECTIVITY - L2

1,1,3,1,1,2
 2,1,3,1,2,3
 3,1,3,1,3,4
 4,2,2,1,1,2
 5,2,2,1,2,3
 6,2,2,1,3,4
 7,3,1,1,1,2
 8,3,1,1,2,3
 9,3,1,1,3,4

BRACES CONNECTIVITY - L8

1,1,1,1,1,0,3,2,365.63
 2,1,1,1,2,1,2,3,365.63
 3,1,1,1,3,2,3,2,365.63

SET M - ANALYSIS OPTION

3
 SET M1 - LONG-TERM STATIC LOADING

0, 0, 0, 0

SET M3 - DYNAMIC ANALYSIS

0.258, 0.0, 0.005, 98, 5, 1

HORIZONTAL ACC

0, 4932, 0.02
GROUNDMOTION
EQ19.DAT
SET N1.2
0
0, 0, 0, 0, 0
SET N2 - STORY OUTPUT CONTROL
3, 0.02, 1, 2, 3
LEV1E19.OUT
LEV2E19.OUT
LEV3E19.OUT
SET N3 - ELEMENT HYSTERESIS OUTPUT
0, 0, 0, 0, 3, 0
braces output
1,2,3

**IDARC-2D INPUT FILE FOR NONLINEAR TIME HISTORY ANALYSIS OF
EXAMPLE No.8: FRAME 3S-75 WITH VISCOELASTIC SOLID DAMPING
SYSTEM TO PROVIDE 8.5% VISCOUS DAMPING RATIO WHEN ASSUMING
ELASTIC FRAME BEHAVIOR**

FRAME 3S-75 WITH SOLID VE DEVICES + 8.5% LINEAR VISCOUS DAMPING.

SET A - CONTROL DATA SET

3, 1, 0, 0, 0, 0, 1, 1

SET A1 - ELEMENTS TYPE

3, 3, 0, 0, 0, 0, 2, 0, 0, 0

SET A2 - ELEMENT DATA

12, 9, 0, 0, 0, 0, 0, 6, 0

SET A3 - SYSTEM OF UNITS

1

SET A4 - FLOOR ELEVATIONS

174.0, 343.44, 512.88

SET A5 - DESCRIPTION OF IDENTICAL FRAMES

1

SET A6 - PLAN CONFIGURATION

4

SET A7 - NODAL WEIGHTS

1, 1, 0, 652.2, 0, 0

2, 1, 0, 652.2, 0, 0

3, 1, 0, 352.4, 0, 0

SET B - MATERIAL PROPERTIES SET

1

SET C - HYSTERETIC MODELING RULES

1

1, 1, 200, 0.001, 0.001, 1.0, 0

SET D - COLUMN PROPERTIES

1

SET D3 - COLUMN DATA

1, 174.00, 14.0, 8.0, 0

-1 36.0E6 5.33E3 8.72E4 9.12E3 9.60E3 2.94E-4 1.47E-2 1

9.12E3 9.60E3 2.94E-4 1.47E-2 1

2, 169.44, 8.0, 8.0, 0

-1 36.0E6 5.48E3 8.72E4 9.12E3 9.60E3 2.94E-4 1.47E-2 1

9.12E3 9.60E3 2.94E-4 1.47E-2 1

3, 169.44, 8.0, 7.0, 0

-1 36.0E6 5.48E3 8.72E4 9.12E3 9.60E3 2.94E-4 1.47E-2 1

9.12E3 9.60E3 2.94E-4 1.47E-2 1

SET E - BEAM PROPERTIES

1

SET E2 - BEAM DATA

1 324.0 7.0 7.0 0

-1 7.10E6 4.11E4 1.91E3 2.01E3 3.10E-4 1.55E-2 1

1.91E3 2.01E3 3.10E-4 1.55E-2 1
 2 324.0 7.0 7.0 0
 -1 15.02E6 5.66E4 3.46E3 3.64E3 2.67E-4 1.34E-2 1
 3.46E3 3.64E3 2.67E-4 1.34E-2 1
 3 324.0 7.0 7.0 0
 -1 16.99E6 6.45E4 3.91E3 4.12E3 2.67E-4 1.34E-2 1
 3.91E3 4.12E3 2.67E-4 1.34E-2 1

VISCOELASTIC BRACE PROPERTIES - J3

0 0
 1 5.6 139.8 1.00
 2 500.0 14.4 1.00

COLUMN CONNECTIVITY - L1

1,1,1,1,0,1
 2,1,1,2,0,1
 3,1,1,3,0,1
 4,1,1,4,0,1
 5,2,1,1,1,2
 6,2,1,2,1,2
 7,2,1,3,1,2
 8,2,1,4,1,2
 9,3,1,1,2,3
 10,3,1,2,2,3
 11,3,1,3,2,3
 12,3,1,4,2,3

BEAMS CONNECTIVITY - L2

1,1,3,1,1,2
 2,1,3,1,2,3
 3,1,3,1,3,4
 4,2,2,1,1,2
 5,2,2,1,2,3
 6,2,2,1,3,4
 7,3,1,1,1,2
 8,3,1,1,2,3
 9,3,1,1,3,4

BRACES CONNECTIVITY - L8

1,1,1,1,1,0,3,2,367.77
 2,1,1,1,2,1,2,3,365.63
 3,1,1,1,3,2,3,2,365.63
 4,1,1,2,1,0,2,1,367.77
 5,1,1,2,2,1,1,2,365.63
 6,1,1,2,3,2,2,1,365.63

SET M - ANALYSIS OPTION

3
 SET M1 - LONG-TERM STATIC LOADING
 0, 0, 0, 0
 SET M3 - DYNAMIC ANALYSIS

0.2331, 0.0, 0.005, 98.0, 5, 1
HORIZONTAL ACC
0, 4932, 0.02
GROUNDMOTION
EQ20.DAT
SET N1.2
0
0, 0, 0, 0, 0
SET N2 - STORY OUTPUT CONTROL
3, 0.02, 1, 2, 3
LEV1E20.OUT
LEV2E20.OUT
LEV3E20.OUT
SET N3 - ELEMENT HYSTERESIS OUTPUT
12, 0, 0, 0, 6, 0
COLUMNS OUTPUT
1,2,3,4,5,6,7,8,9,10,11,12
BRACES OUTPUT
1,2,3,4,5,6

**IDARC-2D INPUT FILE FOR NONLINEAR TIME HISTORY ANALYSIS OF
EXAMPLE No.9: FRAME 3S-75 WITH METALLIC YIELDING DAMPING
SYSTEM**

FRAME 3S-75V METALLIC YIELDING DEVICES. ANALYSIS FOR DBE.

SET A - CONTROL DATA SET

3, 1, 0, 0, 0, 0, 1, 1

SET A1 - ELEMENTS TYPE

3, 3, 0, 0, 0, 0, 0, 3, 0, 0

SET A2 - ELEMENT DATA

12, 9, 0, 0, 0, 0, 0, 3, 0

SET A3 - SYSTEM OF UNITS

1

SET A4 - FLOOR ELEVATIONS

174.0, 343.44, 512.88

SET A5 - DESCRIPTION OF IDENTICAL FRAMES

1

SET A6 - PLAN CONFIGURATION

4

SET A7 - NODAL WEIGHTS

1, 1, 0, 652.2, 0, 0

2, 1, 0, 652.2, 0, 0

3, 1, 0, 352.4, 0, 0

SET B - MATERIAL PROPERTIES SET

1

SET C - HYSTERETIC MODELING RULES

1

1, 1, 200, 0.001, 0.001, 1.0, 0

SET D - COLUMN PROPERTIES

1

SET D3 - COLUMN DATA

1, 174.00, 14.0, 8.0, 0

-1 36.0E6 5.33E3 8.72E4 9.12E3 9.60E3 2.94E-4 1.47E-2 1
9.12E3 9.60E3 2.94E-4 1.47E-2 1

2, 169.44, 8.0, 8.0, 0

-1 36.0E6 5.48E3 8.72E4 9.12E3 9.60E3 2.94E-4 1.47E-2 1
9.12E3 9.60E3 2.94E-4 1.47E-2 1

3, 169.44, 8.0, 7.0, 0

-1 36.0E6 5.48E3 8.72E4 9.12E3 9.60E3 2.94E-4 1.47E-2 1
9.12E3 9.60E3 2.94E-4 1.47E-2 1

SET E - BEAM PROPERTIES

1

SET E2 - BEAM DATA

1 324.0 7.0 7.0 0

-1 7.10E6 4.11E4 1.91E3 2.01E3 3.10E-4 1.55E-2 1
1.91E3 2.01E3 3.10E-4 1.55E-2 1

2 324.0 7.0 7.0 0
 -1 15.02E6 5.66E4 3.46E3 3.64E3 2.67E-4 1.34E-2 1
 3.46E3 3.64E3 2.67E-4 1.34E-2 1
 3 324.0 7.0 7.0 0
 -1 16.99E6 6.45E4 3.91E3 4.12E3 2.67E-4 1.34E-2 1
 3.91E3 4.12E3 2.67E-4 1.34E-2 1

BRACE PROPERTIES - J3

0
 1 152 81.25 0.0005
 2 114 60.93 0.0005
 3 88.6 47.39 0.0005

COLUMN CONNECTIVITY - L1

1,1,1,1,0,1
 2,1,1,2,0,1
 3,1,1,3,0,1
 4,1,1,4,0,1
 5,2,1,1,1,2
 6,2,1,2,1,2
 7,2,1,3,1,2
 8,2,1,4,1,2
 9,3,1,1,2,3
 10,3,1,2,2,3
 11,3,1,3,2,3
 12,3,1,4,2,3

BEAMS CONNECTIVITY - L2

1,1,3,1,1,2
 2,1,3,1,2,3
 3,1,3,1,3,4
 4,2,2,1,1,2
 5,2,2,1,2,3
 6,2,2,1,3,4
 7,3,1,1,1,2
 8,3,1,1,2,3
 9,3,1,1,3,4

BRACES CONNECTIVITY - L8

1,1,2,1,1,0,3,2,367.77
 2,1,2,2,2,1,2,3,365.63
 3,1,2,3,3,2,3,2,365.63

SET M - ANALYSIS OPTION

3
 SET M1 - LONG-TERM STATIC LOADING
 0, 0, 0, 0
 SET M3 - DYNAMIC ANALYSIS
 0.2331, 0.0, 0.005, 98, 5, 1
 HORIZONTAL ACC
 0, 4932, 0.02

GROUNDMOTION
EQ20.DAT
SET N1.2
0
0, 0, 0, 0, 0
SET N2 - STORY OUTPUT CONTROL
3, 0.02, 1, 2, 3
LEV1E20.OUT
LEV2E20.OUT
LEV3E20.OUT
SET N3 - ELEMENT HYSTERESIS OUTPUT
0, 0, 0, 0, 3, 0
BRACES OUTPUT
1,2,3

**IDARC-2D INPUT FILE FOR PUSHOVER ANALYSIS OF EXAMPLE No.1:
 FRAME 3S-60 WITH LINEAR VISCOUS DAMPING SYSTEM TO PROVIDE
 10% VISCOUS DAMPING RATIO WHEN ASSUMING ELASTIC FRAME
 BEHAVIOR. FIRST MODE LATERAL FORCE PATTERN.**

FRAME 3S-60 - PUSHOVER ANALYSIS- FIRST MODE PATTERN

SET A - CONTROL DATA SET

3, 1, 0, 0, 0, 0, 1, 1

SET A1 - ELEMENTS TYPE

3, 3, 0, 0, 0, 0, 0, 0, 0, 0

SET A2 - ELEMENT DATA

12, 9, 0, 0, 0, 0, 0, 0, 0

SET A3 - SYSTEM OF UNITS

1

SET A4 - FLOOR ELEVATIONS

174., 343.44, 512.88

SET A5 - DESCRIPTION OF IDENTICAL FRAMES

1

SET A6 - PLAN CONFIGURATION

4

SET A7 - NODAL WEIGHTS

1, 1, 0, 652.2, 0, 0

2, 1, 0, 652.2, 0, 0

3, 1, 0, 352.4, 0, 0

SET B - MATERIAL PROPERTIES SET

1

SET C - HYSTERETIC MODELING RULES

1

1, 1, 200, 0.001, 0.001, 1.0, 0

SET D - COLUMN PROPERTIES

1

SET D3 - COLUMN DATA

1, 174.00, 14.0, 8.0, 0

-1 29.0E6 4.42E3 7.16E4 7.46E3 7.85E3 2.98E-4 1.49E-2 0.10

7.46E3 7.85E3 2.98E-4 1.49E-2 0.10

2, 169.44, 8.0, 8.0, 0

-1 29.0E6 4.54E3 7.16E4 7.46E3 7.85E3 2.98E-4 1.49E-2 0.10

7.46E3 7.85E3 2.98E-4 1.49E-2 0.10

3, 169.44, 8.0, 7.0, 0

-1 29.0E6 4.54E3 7.16E4 7.46E3 7.85E3 2.98E-4 1.49E-2 0.10

7.46E3 7.85E3 2.98E-4 1.49E-2 0.10

SET E - BEAM PROPERTIES

1

SET E2 - BEAM DATA

1 324.0 7.0 7.0 0

-1 7.10E6 4.11E4 1.91E3 2.01E3 3.10E-4 1.55E-2 0.10

			1.91E3	2.01E3	3.10E-4	1.55E-2	0.10	
2	324.0	7.0	7.0	0				
-1	10.88E6	4.60E4	2.57E3	2.70E3	2.93E-4	1.47E-2	0.10	
			2.57E3	2.70E3	2.93E-4	1.47E-2	0.10	
3	324.0	7.0	7.0	0				
-1	12.99E6	5.43E4	3.04E3	3.20E3	2.70E-4	1.35E-2	0.10	
			3.04E3	3.20E3	2.70E-4	1.35E-2	0.10	

COLUMN CONNECTIVITY - L1

1,1,1,1,0,1
 2,1,1,2,0,1
 3,1,1,3,0,1
 4,1,1,4,0,1
 5,2,1,1,1,2
 6,2,1,2,1,2
 7,2,1,3,1,2
 8,2,1,4,1,2
 9,3,1,1,2,3
 10,3,1,2,2,3
 11,3,1,3,2,3
 12,3,1,4,2,3

BEAMS CONNECTIVITY - L2

1,1,3,1,1,2
 2,1,3,1,2,3
 3,1,3,1,3,4
 4,2,2,1,1,2
 5,2,2,1,2,3
 6,2,2,1,3,4
 7,3,1,1,1,2
 8,3,1,1,2,3
 9,3,1,1,3,4

SET M - ANALYSIS OPTION

2

SET M1 - LONG-TERM STATIC LOADING

0, 0, 0, 0

SET M2 - TYPE OF PUSHOVER

1

SET M2.1 - FORCE CONTROLLED INPUT

4

SET M2.2 - USER INPUT

3

1,2,3

86.9 229.95 185.15

500 5.0

SET N1.1 - PUSHOVER SNAPSHOT CONTROL DATA

0

0 0 0 0 0

SET N2 - STORY OUTPUT CONTROL
3 1 1 2 3
PUSHM1LEV1.OUT
PUSHM1LEV2.OUT
PUSHM1LEV3.OUT
SET N3 - ELEMENT OUTPUT CONTROL
0 0 0 0 0

**IDARC-2D INPUT FILE FOR PUSHOVER ANALYSIS OF EXAMPLE No.1:
 FRAME 3S-60 WITH LINEAR VISCOUS DAMPING SYSTEM TO PROVIDE
 10% VISCOUS DAMPING RATIO WHEN ASSUMING ELASTIC FRAME
 BEHAVIOR. MODAL (Cvx) LATERAL FORCE PATTERN**

FRAME 3S-60 - PUSHOVER ANALYSIS- MODAL (Cvx) PATTERN

SET A - CONTROL DATA SET

3, 1, 0, 0, 0, 0, 1, 1

SET A1 - ELEMENTS TYPE

3, 3, 0, 0, 0, 0, 0, 0, 0, 0

SET A2 - ELEMENT DATA

12, 9, 0, 0, 0, 0, 0, 0, 0

SET A3 - SYSTEM OF UNITS

1

SET A4 - FLOOR ELEVATIONS

174., 343.44, 512.88

SET A5 - DESCRIPTION OF IDENTICAL FRAMES

1

SET A6 - PLAN CONFIGURATION

4

SET A7 - NODAL WEIGHTS

1, 1, 0, 652.2, 0, 0

2, 1, 0, 652.2, 0, 0

3, 1, 0, 352.4, 0, 0

SET B - MATERIAL PROPERTIES SET

1

SET C - HYSTERETIC MODELING RULES

1

1, 1, 200, 0.001, 0.001, 1.0, 0

SET D - COLUMN PROPERTIES

1

SET D3 - COLUMN DATA

1, 174.00, 14.0, 8.0, 0

-1	29.0E6	4.42E3	7.16E4	7.46E3	7.85E3	2.98E-4	1.49E-2	0.10
				7.46E3	7.85E3	2.98E-4	1.49E-2	0.10

2, 169.44, 8.0, 8.0, 0

-1	29.0E6	4.54E3	7.16E4	7.46E3	7.85E3	2.98E-4	1.49E-2	0.10
				7.46E3	7.85E3	2.98E-4	1.49E-2	0.10

3, 169.44, 8.0, 7.0, 0

-1	29.0E6	4.54E3	7.16E4	7.46E3	7.85E3	2.98E-4	1.49E-2	0.10
				7.46E3	7.85E3	2.98E-4	1.49E-2	0.10

SET E - BEAM PROPERTIES

1

SET E2 - BEAM DATA

1 324.0 7.0 7.0 0

-1	7.10E6	4.11E4	1.91E3	2.01E3	3.10E-4	1.55E-2	0.10
			1.91E3	2.01E3	3.10E-4	1.55E-2	0.10
2	324.0	7.0	7.0	0			
-1	10.88E6	4.60E4	2.57E3	2.70E3	2.93E-4	1.47E-2	0.10
			2.57E3	2.70E3	2.93E-4	1.47E-2	0.10
3	324.0	7.0	7.0	0			
-1	12.99E6	5.43E4	3.04E3	3.20E3	2.70E-4	1.35E-2	0.10
			3.04E3	3.20E3	2.70E-4	1.35E-2	0.10

COLUMN CONNECTIVITY - L1

1,1,1,1,0,1
2,1,1,2,0,1
3,1,1,3,0,1
4,1,1,4,0,1
5,2,1,1,1,2
6,2,1,2,1,2
7,2,1,3,1,2
8,2,1,4,1,2
9,3,1,1,2,3
10,3,1,2,2,3
11,3,1,3,2,3
12,3,1,4,2,3

BEAMS CONNECTIVITY - L2

1,1,3,1,1,2
2,1,3,1,2,3
3,1,3,1,3,4
4,2,2,1,1,2
5,2,2,1,2,3
6,2,2,1,3,4
7,3,1,1,1,2
8,3,1,1,2,3
9,3,1,1,3,4

SET M - ANALYSIS OPTION

2

SET M1 - LONG-TERM STATIC LOADING

0, 0, 0, 0

SET M2 - TYPE OF PUSHOVER

1

SET M2.1 - FORCE CONTROLLED INPUT

4

SET M2.2 - USER INPUT

3

1,2,3

70.0 210.0 220.0

500 5.0

SET N1.1 - PUSHOVER SNAPSHOT CONTROL DATA

0

0 0 0 0 0
SET N2 - STORY OUTPUT CONTROL
3 1 1 2 3
CVXLEV1.OUT
CVXLEV2.OUT
CVXLEV3.OUT
SET N3 - ELEMENT OUTPUT CONTROL
0 0 0 0 0

-1	7.10E6	4.11E4	1.91E3	2.01E3	3.10E-4	1.55E-2	0.10
			1.91E3	2.01E3	3.10E-4	1.55E-2	0.10
2	324.0	7.0	7.0	0			
-1	10.88E6	4.60E4	2.57E3	2.70E3	2.93E-4	1.47E-2	0.10
			2.57E3	2.70E3	2.93E-4	1.47E-2	0.10
3	324.0	7.0	7.0	0			
-1	12.99E6	5.43E4	3.04E3	3.20E3	2.70E-4	1.35E-2	0.10
			3.04E3	3.20E3	2.70E-4	1.35E-2	0.10

COLUMN CONNECTIVITY - L1

1,1,1,1,0,1
 2,1,1,2,0,1
 3,1,1,3,0,1
 4,1,1,4,0,1
 5,2,1,1,1,2
 6,2,1,2,1,2
 7,2,1,3,1,2
 8,2,1,4,1,2
 9,3,1,1,2,3
 10,3,1,2,2,3
 11,3,1,3,2,3
 12,3,1,4,2,3

BEAMS CONNECTIVITY - L2

1,1,3,1,1,2
 2,1,3,1,2,3
 3,1,3,1,3,4
 4,2,2,1,1,2
 5,2,2,1,2,3
 6,2,2,1,3,4
 7,3,1,1,1,2
 8,3,1,1,2,3
 9,3,1,1,3,4

SET M - ANALYSIS OPTION

2

SET M1 - LONG-TERM STATIC LOADING

0, 0, 0, 0

SET M2 - TYPE OF PUSHOVER

1

SET M2.1 - FORCE CONTROLLED INPUT

4

SET M2.2 - USER INPUT

3

1,2,3

196.8 196.8 106.4

500 5.0

SET N1.1 - PUSHOVER SNAPSHOT CONTROL DATA

0

0 0 0 0 0
SET N2 - STORY OUTPUT CONTROL
3 1 1 2 3
UNIFLEV1.OUT
UNIFLEV2.OUT
UNIFLEV3.OUT
SET N3 - ELEMENT OUTPUT CONTROL
0 0 0 0 0

**IDARC-2D INPUT FILE FOR PUSHOVER ANALYSIS OF EXAMPLE No.1:
 FRAME 3S-60 WITH LINEAR VISCOUS DAMPING SYSTEM TO PROVIDE
 10% VISCOUS DAMPING RATIO WHEN ASSUMING ELASTIC FRAME
 BEHAVIOR. MODAL ADAPTIVE FORCE PATTERN**

FRAME 3S-60 – PUSHOVER ANALYSIS. MODAL ADAPTIVE PATTERN

SET A - CONTROL DATA SET

3, 1, 0, 0, 0, 0, 1, 1

SET A1 - ELEMENTS TYPE

3, 3, 0, 0, 0, 0, 0, 0, 0

SET A2 - ELEMENT DATA

12, 9, 0, 0, 0, 0, 0, 0, 0

SET A3 - SYSTEM OF UNITS

1

SET A4 - FLOOR ELEVATIONS

174.0, 343.44, 512.88

SET A5 - DESCRIPTION OF IDENTICAL FRAMES

1

SET A6 - PLAN CONFIGURATION

4

SET A7 - NODAL WEIGHTS

1, 1, 0, 652.2, 0, 0

2, 1, 0, 652.2, 0, 0

3, 1, 0, 352.4, 0, 0

SET B - MATERIAL PROPERTIES SET

1

SET C - HYSTERETIC MODELING RULES

1

1, 1, 200, 0.001, 0.001, 1.0, 0

SET D - COLUMN PROPERTIES

1

SET D3 - COLUMN DATA

1, 174.00, 14.0, 8.0, 0

-1	29.0E6	4.42E3	7.16E4	7.46E3	7.85E3	2.98E-4	1.49E-2	0.10
				7.46E3	7.85E3	2.98E-4	1.49E-2	0.10

2, 169.44, 8.0, 8.0, 0

-1	29.0E6	4.54E3	7.16E4	7.46E3	7.85E3	2.98E-4	1.49E-2	0.10
				7.46E3	7.85E3	2.98E-4	1.49E-2	0.10

3, 169.44, 8.0, 7.0, 0

-1	29.0E6	4.54E3	7.16E4	7.46E3	7.85E3	2.98E-4	1.49E-2	0.10
				7.46E3	7.85E3	2.98E-4	1.49E-2	0.10

SET E - BEAM PROPERTIES

1

SET E2 - BEAM DATA

1 324.0 7.0 7.0 0

-1	7.10E6	4.11E4	1.91E3	2.01E3	3.10E-4	1.55E-2	0.10
			1.91E3	2.01E3	3.10E-4	1.55E-2	0.10
2	324.0	7.0	7.0	0			
-1	10.88E6	4.60E4	2.57E3	2.70E3	2.93E-4	1.47E-2	0.10
			2.57E3	2.70E3	2.93E-4	1.47E-2	0.10
3	324.0	7.0	7.0	0			
-1	12.99E6	5.43E4	3.04E3	3.20E3	2.70E-4	1.35E-2	0.10
			3.04E3	3.20E3	2.70E-4	1.35E-2	0.10

COLUMN CONNECTIVITY - L1

1,1,1,1,0,1
 2,1,1,2,0,1
 3,1,1,3,0,1
 4,1,1,4,0,1
 5,2,1,1,1,2
 6,2,1,2,1,2
 7,2,1,3,1,2
 8,2,1,4,1,2
 9,3,1,1,2,3
 10,3,1,2,2,3
 11,3,1,3,2,3
 12,3,1,4,2,3

BEAMS CONNECTIVITY - L2

1,1,3,1,1,2
 2,1,3,1,2,3
 3,1,3,1,3,4
 4,2,2,1,1,2
 5,2,2,1,2,3
 6,2,2,1,3,4
 7,3,1,1,1,2
 8,3,1,1,2,3
 9,3,1,1,3,4

SET M - ANALYSIS OPTION

2

SET M1 - LONG-TERM STATIC LOADING

0, 0, 0, 0

SET M2 - TYPE OF PUSHOVER

1

SET M2.1 - FORCE CONTROLLED INPUT

3

0.40 500 5.0

3 2 1

SET N1.1 - PUSHOVER SNAPSHOT CONTROL DATA

0

0 0 0 0 0

SET N2 - STORY OUTPUT CONTROL

3 1 1 2 3

ADAPTLEV1.OUT
ADAPTLEV2.OUT
ADAPTLEV3.OUT
SET N3 - ELEMENT OUTPUT CONTROL
0 0 0 0 0

MCEER Technical Reports

MCEER publishes technical reports on a variety of subjects written by authors funded through MCEER. These reports are available from both MCEER Publications and the National Technical Information Service (NTIS). Requests for reports should be directed to MCEER Publications, MCEER, University at Buffalo, State University of New York, Red Jacket Quadrangle, Buffalo, New York 14261. Reports can also be requested through NTIS, 5285 Port Royal Road, Springfield, Virginia 22161. NTIS accession numbers are shown in parenthesis, if available.

- NCEER-87-0001 "First-Year Program in Research, Education and Technology Transfer," 3/5/87, (PB88-134275, A04, MF-A01).
- NCEER-87-0002 "Experimental Evaluation of Instantaneous Optimal Algorithms for Structural Control," by R.C. Lin, T.T. Soong and A.M. Reinhorn, 4/20/87, (PB88-134341, A04, MF-A01).
- NCEER-87-0003 "Experimentation Using the Earthquake Simulation Facilities at University at Buffalo," by A.M. Reinhorn and R.L. Ketter, to be published.
- NCEER-87-0004 "The System Characteristics and Performance of a Shaking Table," by J.S. Hwang, K.C. Chang and G.C. Lee, 6/1/87, (PB88-134259, A03, MF-A01). This report is available only through NTIS (see address given above).
- NCEER-87-0005 "A Finite Element Formulation for Nonlinear Viscoplastic Material Using a Q Model," by O. Gyebe and G. Dasgupta, 11/2/87, (PB88-213764, A08, MF-A01).
- NCEER-87-0006 "Symbolic Manipulation Program (SMP) - Algebraic Codes for Two and Three Dimensional Finite Element Formulations," by X. Lee and G. Dasgupta, 11/9/87, (PB88-218522, A05, MF-A01).
- NCEER-87-0007 "Instantaneous Optimal Control Laws for Tall Buildings Under Seismic Excitations," by J.N. Yang, A. Akbarpour and P. Ghaemmaghami, 6/10/87, (PB88-134333, A06, MF-A01). This report is only available through NTIS (see address given above).
- NCEER-87-0008 "IDARC: Inelastic Damage Analysis of Reinforced Concrete Frame - Shear-Wall Structures," by Y.J. Park, A.M. Reinhorn and S.K. Kunnath, 7/20/87, (PB88-134325, A09, MF-A01). This report is only available through NTIS (see address given above).
- NCEER-87-0009 "Liquefaction Potential for New York State: A Preliminary Report on Sites in Manhattan and Buffalo," by M. Budhu, V. Vijayakumar, R.F. Giese and L. Baumgras, 8/31/87, (PB88-163704, A03, MF-A01). This report is available only through NTIS (see address given above).
- NCEER-87-0010 "Vertical and Torsional Vibration of Foundations in Inhomogeneous Media," by A.S. Veletsos and K.W. Dotson, 6/1/87, (PB88-134291, A03, MF-A01). This report is only available through NTIS (see address given above).
- NCEER-87-0011 "Seismic Probabilistic Risk Assessment and Seismic Margins Studies for Nuclear Power Plants," by Howard H.M. Hwang, 6/15/87, (PB88-134267, A03, MF-A01). This report is only available through NTIS (see address given above).
- NCEER-87-0012 "Parametric Studies of Frequency Response of Secondary Systems Under Ground-Acceleration Excitations," by Y. Yong and Y.K. Lin, 6/10/87, (PB88-134309, A03, MF-A01). This report is only available through NTIS (see address given above).
- NCEER-87-0013 "Frequency Response of Secondary Systems Under Seismic Excitation," by J.A. HoLung, J. Cai and Y.K. Lin, 7/31/87, (PB88-134317, A05, MF-A01). This report is only available through NTIS (see address given above).
- NCEER-87-0014 "Modelling Earthquake Ground Motions in Seismically Active Regions Using Parametric Time Series Methods," by G.W. Ellis and A.S. Cakmak, 8/25/87, (PB88-134283, A08, MF-A01). This report is only available through NTIS (see address given above).
- NCEER-87-0015 "Detection and Assessment of Seismic Structural Damage," by E. DiPasquale and A.S. Cakmak, 8/25/87, (PB88-163712, A05, MF-A01). This report is only available through NTIS (see address given above).

- NCEER-87-0016 "Pipeline Experiment at Parkfield, California," by J. Isenberg and E. Richardson, 9/15/87, (PB88-163720, A03, MF-A01). This report is available only through NTIS (see address given above).
- NCEER-87-0017 "Digital Simulation of Seismic Ground Motion," by M. Shinozuka, G. Deodatis and T. Harada, 8/31/87, (PB88-155197, A04, MF-A01). This report is available only through NTIS (see address given above).
- NCEER-87-0018 "Practical Considerations for Structural Control: System Uncertainty, System Time Delay and Truncation of Small Control Forces," J.N. Yang and A. Akbarpour, 8/10/87, (PB88-163738, A08, MF-A01). This report is only available through NTIS (see address given above).
- NCEER-87-0019 "Modal Analysis of Nonclassically Damped Structural Systems Using Canonical Transformation," by J.N. Yang, S. Sarkani and F.X. Long, 9/27/87, (PB88-187851, A04, MF-A01).
- NCEER-87-0020 "A Nonstationary Solution in Random Vibration Theory," by J.R. Red-Horse and P.D. Spanos, 11/3/87, (PB88-163746, A03, MF-A01).
- NCEER-87-0021 "Horizontal Impedances for Radially Inhomogeneous Viscoelastic Soil Layers," by A.S. Veletsos and K.W. Dotson, 10/15/87, (PB88-150859, A04, MF-A01).
- NCEER-87-0022 "Seismic Damage Assessment of Reinforced Concrete Members," by Y.S. Chung, C. Meyer and M. Shinozuka, 10/9/87, (PB88-150867, A05, MF-A01). This report is available only through NTIS (see address given above).
- NCEER-87-0023 "Active Structural Control in Civil Engineering," by T.T. Soong, 11/11/87, (PB88-187778, A03, MF-A01).
- NCEER-87-0024 "Vertical and Torsional Impedances for Radially Inhomogeneous Viscoelastic Soil Layers," by K.W. Dotson and A.S. Veletsos, 12/87, (PB88-187786, A03, MF-A01).
- NCEER-87-0025 "Proceedings from the Symposium on Seismic Hazards, Ground Motions, Soil-Liquefaction and Engineering Practice in Eastern North America," October 20-22, 1987, edited by K.H. Jacob, 12/87, (PB88-188115, A23, MF-A01). This report is available only through NTIS (see address given above).
- NCEER-87-0026 "Report on the Whittier-Narrows, California, Earthquake of October 1, 1987," by J. Pantelic and A. Reinhorn, 11/87, (PB88-187752, A03, MF-A01). This report is available only through NTIS (see address given above).
- NCEER-87-0027 "Design of a Modular Program for Transient Nonlinear Analysis of Large 3-D Building Structures," by S. Srivastav and J.F. Abel, 12/30/87, (PB88-187950, A05, MF-A01). This report is only available through NTIS (see address given above).
- NCEER-87-0028 "Second-Year Program in Research, Education and Technology Transfer," 3/8/88, (PB88-219480, A04, MF-A01).
- NCEER-88-0001 "Workshop on Seismic Computer Analysis and Design of Buildings With Interactive Graphics," by W. McGuire, J.F. Abel and C.H. Conley, 1/18/88, (PB88-187760, A03, MF-A01). This report is only available through NTIS (see address given above).
- NCEER-88-0002 "Optimal Control of Nonlinear Flexible Structures," by J.N. Yang, F.X. Long and D. Wong, 1/22/88, (PB88-213772, A06, MF-A01).
- NCEER-88-0003 "Substructuring Techniques in the Time Domain for Primary-Secondary Structural Systems," by G.D. Manolis and G. Juhn, 2/10/88, (PB88-213780, A04, MF-A01).
- NCEER-88-0004 "Iterative Seismic Analysis of Primary-Secondary Systems," by A. Singhal, L.D. Lutes and P.D. Spanos, 2/23/88, (PB88-213798, A04, MF-A01).
- NCEER-88-0005 "Stochastic Finite Element Expansion for Random Media," by P.D. Spanos and R. Ghanem, 3/14/88, (PB88-213806, A03, MF-A01).

- NCEER-88-0006 "Combining Structural Optimization and Structural Control," by F.Y. Cheng and C.P. Pantelides, 1/10/88, (PB88-213814, A05, MF-A01).
- NCEER-88-0007 "Seismic Performance Assessment of Code-Designed Structures," by H.H-M. Hwang, J-W. Jaw and H-J. Shau, 3/20/88, (PB88-219423, A04, MF-A01). This report is only available through NTIS (see address given above).
- NCEER-88-0008 "Reliability Analysis of Code-Designed Structures Under Natural Hazards," by H.H-M. Hwang, H. Ushiba and M. Shinozuka, 2/29/88, (PB88-229471, A07, MF-A01). This report is only available through NTIS (see address given above).
- NCEER-88-0009 "Seismic Fragility Analysis of Shear Wall Structures," by J-W Jaw and H.H-M. Hwang, 4/30/88, (PB89-102867, A04, MF-A01).
- NCEER-88-0010 "Base Isolation of a Multi-Story Building Under a Harmonic Ground Motion - A Comparison of Performances of Various Systems," by F-G Fan, G. Ahmadi and I.G. Tadjbakhsh, 5/18/88, (PB89-122238, A06, MF-A01). This report is only available through NTIS (see address given above).
- NCEER-88-0011 "Seismic Floor Response Spectra for a Combined System by Green's Functions," by F.M. Lavelle, L.A. Bergman and P.D. Spanos, 5/1/88, (PB89-102875, A03, MF-A01).
- NCEER-88-0012 "A New Solution Technique for Randomly Excited Hysteretic Structures," by G.Q. Cai and Y.K. Lin, 5/16/88, (PB89-102883, A03, MF-A01).
- NCEER-88-0013 "A Study of Radiation Damping and Soil-Structure Interaction Effects in the Centrifuge," by K. Weissman, supervised by J.H. Prevost, 5/24/88, (PB89-144703, A06, MF-A01).
- NCEER-88-0014 "Parameter Identification and Implementation of a Kinematic Plasticity Model for Frictional Soils," by J.H. Prevost and D.V. Griffiths, to be published.
- NCEER-88-0015 "Two- and Three- Dimensional Dynamic Finite Element Analyses of the Long Valley Dam," by D.V. Griffiths and J.H. Prevost, 6/17/88, (PB89-144711, A04, MF-A01).
- NCEER-88-0016 "Damage Assessment of Reinforced Concrete Structures in Eastern United States," by A.M. Reinhorn, M.J. Seidel, S.K. Kunnath and Y.J. Park, 6/15/88, (PB89-122220, A04, MF-A01). This report is only available through NTIS (see address given above).
- NCEER-88-0017 "Dynamic Compliance of Vertically Loaded Strip Foundations in Multilayered Viscoelastic Soils," by S. Ahmad and A.S.M. Israil, 6/17/88, (PB89-102891, A04, MF-A01).
- NCEER-88-0018 "An Experimental Study of Seismic Structural Response With Added Viscoelastic Dampers," by R.C. Lin, Z. Liang, T.T. Soong and R.H. Zhang, 6/30/88, (PB89-122212, A05, MF-A01). This report is available only through NTIS (see address given above).
- NCEER-88-0019 "Experimental Investigation of Primary - Secondary System Interaction," by G.D. Manolis, G. Juhn and A.M. Reinhorn, 5/27/88, (PB89-122204, A04, MF-A01).
- NCEER-88-0020 "A Response Spectrum Approach For Analysis of Nonclassically Damped Structures," by J.N. Yang, S. Sarkani and F.X. Long, 4/22/88, (PB89-102909, A04, MF-A01).
- NCEER-88-0021 "Seismic Interaction of Structures and Soils: Stochastic Approach," by A.S. Veletsos and A.M. Prasad, 7/21/88, (PB89-122196, A04, MF-A01). This report is only available through NTIS (see address given above).
- NCEER-88-0022 "Identification of the Serviceability Limit State and Detection of Seismic Structural Damage," by E. DiPasquale and A.S. Cakmak, 6/15/88, (PB89-122188, A05, MF-A01). This report is available only through NTIS (see address given above).
- NCEER-88-0023 "Multi-Hazard Risk Analysis: Case of a Simple Offshore Structure," by B.K. Bhartia and E.H. Vanmarcke, 7/21/88, (PB89-145213, A05, MF-A01).

- NCEER-88-0024 "Automated Seismic Design of Reinforced Concrete Buildings," by Y.S. Chung, C. Meyer and M. Shinozuka, 7/5/88, (PB89-122170, A06, MF-A01). This report is available only through NTIS (see address given above).
- NCEER-88-0025 "Experimental Study of Active Control of MDOF Structures Under Seismic Excitations," by L.L. Chung, R.C. Lin, T.T. Soong and A.M. Reinhorn, 7/10/88, (PB89-122600, A04, MF-A01).
- NCEER-88-0026 "Earthquake Simulation Tests of a Low-Rise Metal Structure," by J.S. Hwang, K.C. Chang, G.C. Lee and R.L. Ketter, 8/1/88, (PB89-102917, A04, MF-A01).
- NCEER-88-0027 "Systems Study of Urban Response and Reconstruction Due to Catastrophic Earthquakes," by F. Kozin and H.K. Zhou, 9/22/88, (PB90-162348, A04, MF-A01).
- NCEER-88-0028 "Seismic Fragility Analysis of Plane Frame Structures," by H.H-M. Hwang and Y.K. Low, 7/31/88, (PB89-131445, A06, MF-A01).
- NCEER-88-0029 "Response Analysis of Stochastic Structures," by A. Kardara, C. Bucher and M. Shinozuka, 9/22/88, (PB89-174429, A04, MF-A01).
- NCEER-88-0030 "Nonnormal Accelerations Due to Yielding in a Primary Structure," by D.C.K. Chen and L.D. Lutes, 9/19/88, (PB89-131437, A04, MF-A01).
- NCEER-88-0031 "Design Approaches for Soil-Structure Interaction," by A.S. Veletsos, A.M. Prasad and Y. Tang, 12/30/88, (PB89-174437, A03, MF-A01). This report is available only through NTIS (see address given above).
- NCEER-88-0032 "A Re-evaluation of Design Spectra for Seismic Damage Control," by C.J. Turkstra and A.G. Tallin, 11/7/88, (PB89-145221, A05, MF-A01).
- NCEER-88-0033 "The Behavior and Design of Noncontact Lap Splices Subjected to Repeated Inelastic Tensile Loading," by V.E. Sagan, P. Gergely and R.N. White, 12/8/88, (PB89-163737, A08, MF-A01).
- NCEER-88-0034 "Seismic Response of Pile Foundations," by S.M. Mamoon, P.K. Banerjee and S. Ahmad, 11/1/88, (PB89-145239, A04, MF-A01).
- NCEER-88-0035 "Modeling of R/C Building Structures With Flexible Floor Diaphragms (IDARC2)," by A.M. Reinhorn, S.K. Kunnath and N. Panahshahi, 9/7/88, (PB89-207153, A07, MF-A01).
- NCEER-88-0036 "Solution of the Dam-Reservoir Interaction Problem Using a Combination of FEM, BEM with Particular Integrals, Modal Analysis, and Substructuring," by C-S. Tsai, G.C. Lee and R.L. Ketter, 12/31/88, (PB89-207146, A04, MF-A01).
- NCEER-88-0037 "Optimal Placement of Actuators for Structural Control," by F.Y. Cheng and C.P. Pantelides, 8/15/88, (PB89-162846, A05, MF-A01).
- NCEER-88-0038 "Teflon Bearings in Aseismic Base Isolation: Experimental Studies and Mathematical Modeling," by A. Mokha, M.C. Constantinou and A.M. Reinhorn, 12/5/88, (PB89-218457, A10, MF-A01). This report is available only through NTIS (see address given above).
- NCEER-88-0039 "Seismic Behavior of Flat Slab High-Rise Buildings in the New York City Area," by P. Weidlinger and M. Ettouney, 10/15/88, (PB90-145681, A04, MF-A01).
- NCEER-88-0040 "Evaluation of the Earthquake Resistance of Existing Buildings in New York City," by P. Weidlinger and M. Ettouney, 10/15/88, to be published.
- NCEER-88-0041 "Small-Scale Modeling Techniques for Reinforced Concrete Structures Subjected to Seismic Loads," by W. Kim, A. El-Attar and R.N. White, 11/22/88, (PB89-189625, A05, MF-A01).
- NCEER-88-0042 "Modeling Strong Ground Motion from Multiple Event Earthquakes," by G.W. Ellis and A.S. Cakmak, 10/15/88, (PB89-174445, A03, MF-A01).

- NCEER-88-0043 "Nonstationary Models of Seismic Ground Acceleration," by M. Grigoriu, S.E. Ruiz and E. Rosenblueth, 7/15/88, (PB89-189617, A04, MF-A01).
- NCEER-88-0044 "SARCF User's Guide: Seismic Analysis of Reinforced Concrete Frames," by Y.S. Chung, C. Meyer and M. Shinozuka, 11/9/88, (PB89-174452, A08, MF-A01).
- NCEER-88-0045 "First Expert Panel Meeting on Disaster Research and Planning," edited by J. Pantelic and J. Stoyke, 9/15/88, (PB89-174460, A05, MF-A01).
- NCEER-88-0046 "Preliminary Studies of the Effect of Degrading Infill Walls on the Nonlinear Seismic Response of Steel Frames," by C.Z. Chrysostomou, P. Gergely and J.F. Abel, 12/19/88, (PB89-208383, A05, MF-A01).
- NCEER-88-0047 "Reinforced Concrete Frame Component Testing Facility - Design, Construction, Instrumentation and Operation," by S.P. Pessiki, C. Conley, T. Bond, P. Gergely and R.N. White, 12/16/88, (PB89-174478, A04, MF-A01).
- NCEER-89-0001 "Effects of Protective Cushion and Soil Compliancy on the Response of Equipment Within a Seismically Excited Building," by J.A. HoLung, 2/16/89, (PB89-207179, A04, MF-A01).
- NCEER-89-0002 "Statistical Evaluation of Response Modification Factors for Reinforced Concrete Structures," by H.H-M. Hwang and J-W. Jaw, 2/17/89, (PB89-207187, A05, MF-A01).
- NCEER-89-0003 "Hysteretic Columns Under Random Excitation," by G-Q. Cai and Y.K. Lin, 1/9/89, (PB89-196513, A03, MF-A01).
- NCEER-89-0004 "Experimental Study of 'Elephant Foot Bulge' Instability of Thin-Walled Metal Tanks," by Z-H. Jia and R.L. Ketter, 2/22/89, (PB89-207195, A03, MF-A01).
- NCEER-89-0005 "Experiment on Performance of Buried Pipelines Across San Andreas Fault," by J. Isenberg, E. Richardson and T.D. O'Rourke, 3/10/89, (PB89-218440, A04, MF-A01). This report is available only through NTIS (see address given above).
- NCEER-89-0006 "A Knowledge-Based Approach to Structural Design of Earthquake-Resistant Buildings," by M. Subramani, P. Gergely, C.H. Conley, J.F. Abel and A.H. Zaghaw, 1/15/89, (PB89-218465, A06, MF-A01).
- NCEER-89-0007 "Liquefaction Hazards and Their Effects on Buried Pipelines," by T.D. O'Rourke and P.A. Lane, 2/1/89, (PB89-218481, A09, MF-A01).
- NCEER-89-0008 "Fundamentals of System Identification in Structural Dynamics," by H. Imai, C-B. Yun, O. Maruyama and M. Shinozuka, 1/26/89, (PB89-207211, A04, MF-A01).
- NCEER-89-0009 "Effects of the 1985 Michoacan Earthquake on Water Systems and Other Buried Lifelines in Mexico," by A.G. Ayala and M.J. O'Rourke, 3/8/89, (PB89-207229, A06, MF-A01).
- NCEER-89-R010 "NCEER Bibliography of Earthquake Education Materials," by K.E.K. Ross, Second Revision, 9/1/89, (PB90-125352, A05, MF-A01). This report is replaced by NCEER-92-0018.
- NCEER-89-0011 "Inelastic Three-Dimensional Response Analysis of Reinforced Concrete Building Structures (IDARC-3D), Part I - Modeling," by S.K. Kunnath and A.M. Reinhorn, 4/17/89, (PB90-114612, A07, MF-A01). This report is available only through NTIS (see address given above).
- NCEER-89-0012 "Recommended Modifications to ATC-14," by C.D. Poland and J.O. Malley, 4/12/89, (PB90-108648, A15, MF-A01).
- NCEER-89-0013 "Repair and Strengthening of Beam-to-Column Connections Subjected to Earthquake Loading," by M. Corazao and A.J. Durrani, 2/28/89, (PB90-109885, A06, MF-A01).
- NCEER-89-0014 "Program EXKAL2 for Identification of Structural Dynamic Systems," by O. Maruyama, C-B. Yun, M. Hoshiya and M. Shinozuka, 5/19/89, (PB90-109877, A09, MF-A01).

- NCEER-89-0015 "Response of Frames With Bolted Semi-Rigid Connections, Part I - Experimental Study and Analytical Predictions," by P.J. DiCorso, A.M. Reinhorn, J.R. Dickerson, J.B. Radzinski and W.L. Harper, 6/1/89, to be published.
- NCEER-89-0016 "ARMA Monte Carlo Simulation in Probabilistic Structural Analysis," by P.D. Spanos and M.P. Mignolet, 7/10/89, (PB90-109893, A03, MF-A01).
- NCEER-89-P017 "Preliminary Proceedings from the Conference on Disaster Preparedness - The Place of Earthquake Education in Our Schools," Edited by K.E.K. Ross, 6/23/89, (PB90-108606, A03, MF-A01).
- NCEER-89-0017 "Proceedings from the Conference on Disaster Preparedness - The Place of Earthquake Education in Our Schools," Edited by K.E.K. Ross, 12/31/89, (PB90-207895, A012, MF-A02). This report is available only through NTIS (see address given above).
- NCEER-89-0018 "Multidimensional Models of Hysteretic Material Behavior for Vibration Analysis of Shape Memory Energy Absorbing Devices, by E.J. Graesser and F.A. Cozzarelli, 6/7/89, (PB90-164146, A04, MF-A01).
- NCEER-89-0019 "Nonlinear Dynamic Analysis of Three-Dimensional Base Isolated Structures (3D-BASIS)," by S. Nagarajaiah, A.M. Reinhorn and M.C. Constantinou, 8/3/89, (PB90-161936, A06, MF-A01). This report has been replaced by NCEER-93-0011.
- NCEER-89-0020 "Structural Control Considering Time-Rate of Control Forces and Control Rate Constraints," by F.Y. Cheng and C.P. Pantelides, 8/3/89, (PB90-120445, A04, MF-A01).
- NCEER-89-0021 "Subsurface Conditions of Memphis and Shelby County," by K.W. Ng, T-S. Chang and H-H.M. Hwang, 7/26/89, (PB90-120437, A03, MF-A01).
- NCEER-89-0022 "Seismic Wave Propagation Effects on Straight Jointed Buried Pipelines," by K. Elhadi and M.J. O'Rourke, 8/24/89, (PB90-162322, A10, MF-A02).
- NCEER-89-0023 "Workshop on Serviceability Analysis of Water Delivery Systems," edited by M. Grigoriu, 3/6/89, (PB90-127424, A03, MF-A01).
- NCEER-89-0024 "Shaking Table Study of a 1/5 Scale Steel Frame Composed of Tapered Members," by K.C. Chang, J.S. Hwang and G.C. Lee, 9/18/89, (PB90-160169, A04, MF-A01).
- NCEER-89-0025 "DYNA1D: A Computer Program for Nonlinear Seismic Site Response Analysis - Technical Documentation," by Jean H. Prevost, 9/14/89, (PB90-161944, A07, MF-A01). This report is available only through NTIS (see address given above).
- NCEER-89-0026 "1:4 Scale Model Studies of Active Tendon Systems and Active Mass Dampers for Aseismic Protection," by A.M. Reinhorn, T.T. Soong, R.C. Lin, Y.P. Yang, Y. Fukao, H. Abe and M. Nakai, 9/15/89, (PB90-173246, A10, MF-A02). This report is available only through NTIS (see address given above).
- NCEER-89-0027 "Scattering of Waves by Inclusions in a Nonhomogeneous Elastic Half Space Solved by Boundary Element Methods," by P.K. Hadley, A. Askar and A.S. Cakmak, 6/15/89, (PB90-145699, A07, MF-A01).
- NCEER-89-0028 "Statistical Evaluation of Deflection Amplification Factors for Reinforced Concrete Structures," by H.H.M. Hwang, J-W. Jaw and A.L. Ch'ng, 8/31/89, (PB90-164633, A05, MF-A01).
- NCEER-89-0029 "Bedrock Accelerations in Memphis Area Due to Large New Madrid Earthquakes," by H.H.M. Hwang, C.H.S. Chen and G. Yu, 11/7/89, (PB90-162330, A04, MF-A01).
- NCEER-89-0030 "Seismic Behavior and Response Sensitivity of Secondary Structural Systems," by Y.Q. Chen and T.T. Soong, 10/23/89, (PB90-164658, A08, MF-A01).
- NCEER-89-0031 "Random Vibration and Reliability Analysis of Primary-Secondary Structural Systems," by Y. Ibrahim, M. Grigoriu and T.T. Soong, 11/10/89, (PB90-161951, A04, MF-A01).

- NCEER-89-0032 "Proceedings from the Second U.S. - Japan Workshop on Liquefaction, Large Ground Deformation and Their Effects on Lifelines, September 26-29, 1989," Edited by T.D. O'Rourke and M. Hamada, 12/1/89, (PB90-209388, A22, MF-A03).
- NCEER-89-0033 "Deterministic Model for Seismic Damage Evaluation of Reinforced Concrete Structures," by J.M. Bracci, A.M. Reinhorn, J.B. Mander and S.K. Kunnath, 9/27/89, (PB91-108803, A06, MF-A01).
- NCEER-89-0034 "On the Relation Between Local and Global Damage Indices," by E. DiPasquale and A.S. Cakmak, 8/15/89, (PB90-173865, A05, MF-A01).
- NCEER-89-0035 "Cyclic Undrained Behavior of Nonplastic and Low Plasticity Silts," by A.J. Walker and H.E. Stewart, 7/26/89, (PB90-183518, A10, MF-A01).
- NCEER-89-0036 "Liquefaction Potential of Surficial Deposits in the City of Buffalo, New York," by M. Budhu, R. Giese and L. Baumgrass, 1/17/89, (PB90-208455, A04, MF-A01).
- NCEER-89-0037 "A Deterministic Assessment of Effects of Ground Motion Incoherence," by A.S. Veletsos and Y. Tang, 7/15/89, (PB90-164294, A03, MF-A01).
- NCEER-89-0038 "Workshop on Ground Motion Parameters for Seismic Hazard Mapping," July 17-18, 1989, edited by R.V. Whitman, 12/1/89, (PB90-173923, A04, MF-A01).
- NCEER-89-0039 "Seismic Effects on Elevated Transit Lines of the New York City Transit Authority," by C.J. Costantino, C.A. Miller and E. Heymsfield, 12/26/89, (PB90-207887, A06, MF-A01).
- NCEER-89-0040 "Centrifugal Modeling of Dynamic Soil-Structure Interaction," by K. Weissman, Supervised by J.H. Prevost, 5/10/89, (PB90-207879, A07, MF-A01).
- NCEER-89-0041 "Linearized Identification of Buildings With Cores for Seismic Vulnerability Assessment," by I-K. Ho and A.E. Aktan, 11/1/89, (PB90-251943, A07, MF-A01).
- NCEER-90-0001 "Geotechnical and Lifeline Aspects of the October 17, 1989 Loma Prieta Earthquake in San Francisco," by T.D. O'Rourke, H.E. Stewart, F.T. Blackburn and T.S. Dickerman, 1/90, (PB90-208596, A05, MF-A01).
- NCEER-90-0002 "Nonnormal Secondary Response Due to Yielding in a Primary Structure," by D.C.K. Chen and L.D. Lutes, 2/28/90, (PB90-251976, A07, MF-A01).
- NCEER-90-0003 "Earthquake Education Materials for Grades K-12," by K.E.K. Ross, 4/16/90, (PB91-251984, A05, MF-A05). This report has been replaced by NCEER-92-0018.
- NCEER-90-0004 "Catalog of Strong Motion Stations in Eastern North America," by R.W. Busby, 4/3/90, (PB90-251984, A05, MF-A01).
- NCEER-90-0005 "NCEER Strong-Motion Data Base: A User Manual for the GeoBase Release (Version 1.0 for the Sun3)," by P. Friberg and K. Jacob, 3/31/90 (PB90-258062, A04, MF-A01).
- NCEER-90-0006 "Seismic Hazard Along a Crude Oil Pipeline in the Event of an 1811-1812 Type New Madrid Earthquake," by H.H.M. Hwang and C-H.S. Chen, 4/16/90, (PB90-258054, A04, MF-A01).
- NCEER-90-0007 "Site-Specific Response Spectra for Memphis Sheahan Pumping Station," by H.H.M. Hwang and C.S. Lee, 5/15/90, (PB91-108811, A05, MF-A01).
- NCEER-90-0008 "Pilot Study on Seismic Vulnerability of Crude Oil Transmission Systems," by T. Ariman, R. Dobry, M. Grigoriu, F. Kozin, M. O'Rourke, T. O'Rourke and M. Shinozuka, 5/25/90, (PB91-108837, A06, MF-A01).
- NCEER-90-0009 "A Program to Generate Site Dependent Time Histories: EQGEN," by G.W. Ellis, M. Srinivasan and A.S. Cakmak, 1/30/90, (PB91-108829, A04, MF-A01).
- NCEER-90-0010 "Active Isolation for Seismic Protection of Operating Rooms," by M.E. Talbott, Supervised by M. Shinozuka, 6/8/9, (PB91-110205, A05, MF-A01).

- NCEER-90-0011 "Program LINEARID for Identification of Linear Structural Dynamic Systems," by C-B. Yun and M. Shinozuka, 6/25/90, (PB91-110312, A08, MF-A01).
- NCEER-90-0012 "Two-Dimensional Two-Phase Elasto-Plastic Seismic Response of Earth Dams," by A.N. Yiagos, Supervised by J.H. Prevost, 6/20/90, (PB91-110197, A13, MF-A02).
- NCEER-90-0013 "Secondary Systems in Base-Isolated Structures: Experimental Investigation, Stochastic Response and Stochastic Sensitivity," by G.D. Manolis, G. Juhn, M.C. Constantinou and A.M. Reinhorn, 7/1/90, (PB91-110320, A08, MF-A01).
- NCEER-90-0014 "Seismic Behavior of Lightly-Reinforced Concrete Column and Beam-Column Joint Details," by S.P. Pessiki, C.H. Conley, P. Gergely and R.N. White, 8/22/90, (PB91-108795, A11, MF-A02).
- NCEER-90-0015 "Two Hybrid Control Systems for Building Structures Under Strong Earthquakes," by J.N. Yang and A. Daniellians, 6/29/90, (PB91-125393, A04, MF-A01).
- NCEER-90-0016 "Instantaneous Optimal Control with Acceleration and Velocity Feedback," by J.N. Yang and Z. Li, 6/29/90, (PB91-125401, A03, MF-A01).
- NCEER-90-0017 "Reconnaissance Report on the Northern Iran Earthquake of June 21, 1990," by M. Mehrain, 10/4/90, (PB91-125377, A03, MF-A01).
- NCEER-90-0018 "Evaluation of Liquefaction Potential in Memphis and Shelby County," by T.S. Chang, P.S. Tang, C.S. Lee and H. Hwang, 8/10/90, (PB91-125427, A09, MF-A01).
- NCEER-90-0019 "Experimental and Analytical Study of a Combined Sliding Disc Bearing and Helical Steel Spring Isolation System," by M.C. Constantinou, A.S. Mokha and A.M. Reinhorn, 10/4/90, (PB91-125385, A06, MF-A01). This report is available only through NTIS (see address given above).
- NCEER-90-0020 "Experimental Study and Analytical Prediction of Earthquake Response of a Sliding Isolation System with a Spherical Surface," by A.S. Mokha, M.C. Constantinou and A.M. Reinhorn, 10/11/90, (PB91-125419, A05, MF-A01).
- NCEER-90-0021 "Dynamic Interaction Factors for Floating Pile Groups," by G. Gazetas, K. Fan, A. Kaynia and E. Kausel, 9/10/90, (PB91-170381, A05, MF-A01).
- NCEER-90-0022 "Evaluation of Seismic Damage Indices for Reinforced Concrete Structures," by S. Rodriguez-Gomez and A.S. Cakmak, 9/30/90, PB91-171322, A06, MF-A01).
- NCEER-90-0023 "Study of Site Response at a Selected Memphis Site," by H. Desai, S. Ahmad, E.S. Gazetas and M.R. Oh, 10/11/90, (PB91-196857, A03, MF-A01).
- NCEER-90-0024 "A User's Guide to Strongmo: Version 1.0 of NCEER's Strong-Motion Data Access Tool for PCs and Terminals," by P.A. Friberg and C.A.T. Susch, 11/15/90, (PB91-171272, A03, MF-A01).
- NCEER-90-0025 "A Three-Dimensional Analytical Study of Spatial Variability of Seismic Ground Motions," by L-L. Hong and A.H.-S. Ang, 10/30/90, (PB91-170399, A09, MF-A01).
- NCEER-90-0026 "MUMOID User's Guide - A Program for the Identification of Modal Parameters," by S. Rodriguez-Gomez and E. DiPasquale, 9/30/90, (PB91-171298, A04, MF-A01).
- NCEER-90-0027 "SARCF-II User's Guide - Seismic Analysis of Reinforced Concrete Frames," by S. Rodriguez-Gomez, Y.S. Chung and C. Meyer, 9/30/90, (PB91-171280, A05, MF-A01).
- NCEER-90-0028 "Viscous Dampers: Testing, Modeling and Application in Vibration and Seismic Isolation," by N. Makris and M.C. Constantinou, 12/20/90 (PB91-190561, A06, MF-A01).
- NCEER-90-0029 "Soil Effects on Earthquake Ground Motions in the Memphis Area," by H. Hwang, C.S. Lee, K.W. Ng and T.S. Chang, 8/2/90, (PB91-190751, A05, MF-A01).

- NCEER-91-0001 "Proceedings from the Third Japan-U.S. Workshop on Earthquake Resistant Design of Lifeline Facilities and Countermeasures for Soil Liquefaction, December 17-19, 1990," edited by T.D. O'Rourke and M. Hamada, 2/1/91, (PB91-179259, A99, MF-A04).
- NCEER-91-0002 "Physical Space Solutions of Non-Proportionally Damped Systems," by M. Tong, Z. Liang and G.C. Lee, 1/15/91, (PB91-179242, A04, MF-A01).
- NCEER-91-0003 "Seismic Response of Single Piles and Pile Groups," by K. Fan and G. Gazetas, 1/10/91, (PB92-174994, A04, MF-A01).
- NCEER-91-0004 "Damping of Structures: Part 1 - Theory of Complex Damping," by Z. Liang and G. Lee, 10/10/91, (PB92-197235, A12, MF-A03).
- NCEER-91-0005 "3D-BASIS - Nonlinear Dynamic Analysis of Three Dimensional Base Isolated Structures: Part II," by S. Nagarajaiah, A.M. Reinhorn and M.C. Constantinou, 2/28/91, (PB91-190553, A07, MF-A01). This report has been replaced by NCEER-93-0011.
- NCEER-91-0006 "A Multidimensional Hysteretic Model for Plasticity Deforming Metals in Energy Absorbing Devices," by E.J. Graesser and F.A. Cozzarelli, 4/9/91, (PB92-108364, A04, MF-A01).
- NCEER-91-0007 "A Framework for Customizable Knowledge-Based Expert Systems with an Application to a KBES for Evaluating the Seismic Resistance of Existing Buildings," by E.G. Ibarra-Anaya and S.J. Fennes, 4/9/91, (PB91-210930, A08, MF-A01).
- NCEER-91-0008 "Nonlinear Analysis of Steel Frames with Semi-Rigid Connections Using the Capacity Spectrum Method," by G.G. Deierlein, S-H. Hsieh, Y-J. Shen and J.F. Abel, 7/2/91, (PB92-113828, A05, MF-A01).
- NCEER-91-0009 "Earthquake Education Materials for Grades K-12," by K.E.K. Ross, 4/30/91, (PB91-212142, A06, MF-A01). This report has been replaced by NCEER-92-0018.
- NCEER-91-0010 "Phase Wave Velocities and Displacement Phase Differences in a Harmonically Oscillating Pile," by N. Makris and G. Gazetas, 7/8/91, (PB92-108356, A04, MF-A01).
- NCEER-91-0011 "Dynamic Characteristics of a Full-Size Five-Story Steel Structure and a 2/5 Scale Model," by K.C. Chang, G.C. Yao, G.C. Lee, D.S. Hao and Y.C. Yeh," 7/2/91, (PB93-116648, A06, MF-A02).
- NCEER-91-0012 "Seismic Response of a 2/5 Scale Steel Structure with Added Viscoelastic Dampers," by K.C. Chang, T.T. Soong, S-T. Oh and M.L. Lai, 5/17/91, (PB92-110816, A05, MF-A01).
- NCEER-91-0013 "Earthquake Response of Retaining Walls; Full-Scale Testing and Computational Modeling," by S. Alampalli and A-W.M. Elgamal, 6/20/91, to be published.
- NCEER-91-0014 "3D-BASIS-M: Nonlinear Dynamic Analysis of Multiple Building Base Isolated Structures," by P.C. Tsopelas, S. Nagarajaiah, M.C. Constantinou and A.M. Reinhorn, 5/28/91, (PB92-113885, A09, MF-A02).
- NCEER-91-0015 "Evaluation of SEAOC Design Requirements for Sliding Isolated Structures," by D. Theodossiou and M.C. Constantinou, 6/10/91, (PB92-114602, A11, MF-A03).
- NCEER-91-0016 "Closed-Loop Modal Testing of a 27-Story Reinforced Concrete Flat Plate-Core Building," by H.R. Somaprasad, T. Toksoy, H. Yoshiyuki and A.E. Aktan, 7/15/91, (PB92-129980, A07, MF-A02).
- NCEER-91-0017 "Shake Table Test of a 1/6 Scale Two-Story Lightly Reinforced Concrete Building," by A.G. El-Attar, R.N. White and P. Gergely, 2/28/91, (PB92-222447, A06, MF-A02).
- NCEER-91-0018 "Shake Table Test of a 1/8 Scale Three-Story Lightly Reinforced Concrete Building," by A.G. El-Attar, R.N. White and P. Gergely, 2/28/91, (PB93-116630, A08, MF-A02).
- NCEER-91-0019 "Transfer Functions for Rigid Rectangular Foundations," by A.S. Veletsos, A.M. Prasad and W.H. Wu, 7/31/91, to be published.

- NCEER-91-0020 "Hybrid Control of Seismic-Excited Nonlinear and Inelastic Structural Systems," by J.N. Yang, Z. Li and A. Daniellians, 8/1/91, (PB92-143171, A06, MF-A02).
- NCEER-91-0021 "The NCEER-91 Earthquake Catalog: Improved Intensity-Based Magnitudes and Recurrence Relations for U.S. Earthquakes East of New Madrid," by L. Seeber and J.G. Armbruster, 8/28/91, (PB92-176742, A06, MF-A02).
- NCEER-91-0022 "Proceedings from the Implementation of Earthquake Planning and Education in Schools: The Need for Change - The Roles of the Changemakers," by K.E.K. Ross and F. Winslow, 7/23/91, (PB92-129998, A12, MF-A03).
- NCEER-91-0023 "A Study of Reliability-Based Criteria for Seismic Design of Reinforced Concrete Frame Buildings," by H.H.M. Hwang and H-M. Hsu, 8/10/91, (PB92-140235, A09, MF-A02).
- NCEER-91-0024 "Experimental Verification of a Number of Structural System Identification Algorithms," by R.G. Ghanem, H. Gavin and M. Shinozuka, 9/18/91, (PB92-176577, A18, MF-A04).
- NCEER-91-0025 "Probabilistic Evaluation of Liquefaction Potential," by H.H.M. Hwang and C.S. Lee," 11/25/91, (PB92-143429, A05, MF-A01).
- NCEER-91-0026 "Instantaneous Optimal Control for Linear, Nonlinear and Hysteretic Structures - Stable Controllers," by J.N. Yang and Z. Li, 11/15/91, (PB92-163807, A04, MF-A01).
- NCEER-91-0027 "Experimental and Theoretical Study of a Sliding Isolation System for Bridges," by M.C. Constantinou, A. Kartoum, A.M. Reinhorn and P. Bradford, 11/15/91, (PB92-176973, A10, MF-A03).
- NCEER-92-0001 "Case Studies of Liquefaction and Lifeline Performance During Past Earthquakes, Volume 1: Japanese Case Studies," Edited by M. Hamada and T. O'Rourke, 2/17/92, (PB92-197243, A18, MF-A04).
- NCEER-92-0002 "Case Studies of Liquefaction and Lifeline Performance During Past Earthquakes, Volume 2: United States Case Studies," Edited by T. O'Rourke and M. Hamada, 2/17/92, (PB92-197250, A20, MF-A04).
- NCEER-92-0003 "Issues in Earthquake Education," Edited by K. Ross, 2/3/92, (PB92-222389, A07, MF-A02).
- NCEER-92-0004 "Proceedings from the First U.S. - Japan Workshop on Earthquake Protective Systems for Bridges," Edited by I.G. Buckle, 2/4/92, (PB94-142239, A99, MF-A06).
- NCEER-92-0005 "Seismic Ground Motion from a Haskell-Type Source in a Multiple-Layered Half-Space," A.P. Theoharis, G. Deodatis and M. Shinozuka, 1/2/92, to be published.
- NCEER-92-0006 "Proceedings from the Site Effects Workshop," Edited by R. Whitman, 2/29/92, (PB92-197201, A04, MF-A01).
- NCEER-92-0007 "Engineering Evaluation of Permanent Ground Deformations Due to Seismically-Induced Liquefaction," by M.H. Baziar, R. Dobry and A-W.M. Elgamal, 3/24/92, (PB92-222421, A13, MF-A03).
- NCEER-92-0008 "A Procedure for the Seismic Evaluation of Buildings in the Central and Eastern United States," by C.D. Poland and J.O. Malley, 4/2/92, (PB92-222439, A20, MF-A04).
- NCEER-92-0009 "Experimental and Analytical Study of a Hybrid Isolation System Using Friction Controllable Sliding Bearings," by M.Q. Feng, S. Fujii and M. Shinozuka, 5/15/92, (PB93-150282, A06, MF-A02).
- NCEER-92-0010 "Seismic Resistance of Slab-Column Connections in Existing Non-Ductile Flat-Plate Buildings," by A.J. Durrani and Y. Du, 5/18/92, (PB93-116812, A06, MF-A02).
- NCEER-92-0011 "The Hysteretic and Dynamic Behavior of Brick Masonry Walls Upgraded by Ferrocement Coatings Under Cyclic Loading and Strong Simulated Ground Motion," by H. Lee and S.P. Prawel, 5/11/92, to be published.
- NCEER-92-0012 "Study of Wire Rope Systems for Seismic Protection of Equipment in Buildings," by G.F. Demetriades, M.C. Constantinou and A.M. Reinhorn, 5/20/92, (PB93-116655, A08, MF-A02).

- NCEER-92-0013 "Shape Memory Structural Dampers: Material Properties, Design and Seismic Testing," by P.R. Witting and F.A. Cozzarelli, 5/26/92, (PB93-116663, A05, MF-A01).
- NCEER-92-0014 "Longitudinal Permanent Ground Deformation Effects on Buried Continuous Pipelines," by M.J. O'Rourke, and C. Nordberg, 6/15/92, (PB93-116671, A08, MF-A02).
- NCEER-92-0015 "A Simulation Method for Stationary Gaussian Random Functions Based on the Sampling Theorem," by M. Grigoriu and S. Balopoulou, 6/11/92, (PB93-127496, A05, MF-A01).
- NCEER-92-0016 "Gravity-Load-Designed Reinforced Concrete Buildings: Seismic Evaluation of Existing Construction and Detailing Strategies for Improved Seismic Resistance," by G.W. Hoffmann, S.K. Kunnath, A.M. Reinhorn and J.B. Mander, 7/15/92, (PB94-142007, A08, MF-A02).
- NCEER-92-0017 "Observations on Water System and Pipeline Performance in the Limón Area of Costa Rica Due to the April 22, 1991 Earthquake," by M. O'Rourke and D. Ballantyne, 6/30/92, (PB93-126811, A06, MF-A02).
- NCEER-92-0018 "Fourth Edition of Earthquake Education Materials for Grades K-12," Edited by K.E.K. Ross, 8/10/92, (PB93-114023, A07, MF-A02).
- NCEER-92-0019 "Proceedings from the Fourth Japan-U.S. Workshop on Earthquake Resistant Design of Lifeline Facilities and Countermeasures for Soil Liquefaction," Edited by M. Hamada and T.D. O'Rourke, 8/12/92, (PB93-163939, A99, MF-E11).
- NCEER-92-0020 "Active Bracing System: A Full Scale Implementation of Active Control," by A.M. Reinhorn, T.T. Soong, R.C. Lin, M.A. Riley, Y.P. Wang, S. Aizawa and M. Higashino, 8/14/92, (PB93-127512, A06, MF-A02).
- NCEER-92-0021 "Empirical Analysis of Horizontal Ground Displacement Generated by Liquefaction-Induced Lateral Spreads," by S.F. Bartlett and T.L. Youd, 8/17/92, (PB93-188241, A06, MF-A02).
- NCEER-92-0022 "IDARC Version 3.0: Inelastic Damage Analysis of Reinforced Concrete Structures," by S.K. Kunnath, A.M. Reinhorn and R.F. Lobo, 8/31/92, (PB93-227502, A07, MF-A02).
- NCEER-92-0023 "A Semi-Empirical Analysis of Strong-Motion Peaks in Terms of Seismic Source, Propagation Path and Local Site Conditions, by M. Kamiyama, M.J. O'Rourke and R. Flores-Berrones, 9/9/92, (PB93-150266, A08, MF-A02).
- NCEER-92-0024 "Seismic Behavior of Reinforced Concrete Frame Structures with Nonductile Details, Part I: Summary of Experimental Findings of Full Scale Beam-Column Joint Tests," by A. Beres, R.N. White and P. Gergely, 9/30/92, (PB93-227783, A05, MF-A01).
- NCEER-92-0025 "Experimental Results of Repaired and Retrofitted Beam-Column Joint Tests in Lightly Reinforced Concrete Frame Buildings," by A. Beres, S. El-Borgi, R.N. White and P. Gergely, 10/29/92, (PB93-227791, A05, MF-A01).
- NCEER-92-0026 "A Generalization of Optimal Control Theory: Linear and Nonlinear Structures," by J.N. Yang, Z. Li and S. Vongchavalitkul, 11/2/92, (PB93-188621, A05, MF-A01).
- NCEER-92-0027 "Seismic Resistance of Reinforced Concrete Frame Structures Designed Only for Gravity Loads: Part I - Design and Properties of a One-Third Scale Model Structure," by J.M. Bracci, A.M. Reinhorn and J.B. Mander, 12/1/92, (PB94-104502, A08, MF-A02).
- NCEER-92-0028 "Seismic Resistance of Reinforced Concrete Frame Structures Designed Only for Gravity Loads: Part II - Experimental Performance of Subassemblages," by L.E. Aycaardi, J.B. Mander and A.M. Reinhorn, 12/1/92, (PB94-104510, A08, MF-A02).
- NCEER-92-0029 "Seismic Resistance of Reinforced Concrete Frame Structures Designed Only for Gravity Loads: Part III - Experimental Performance and Analytical Study of a Structural Model," by J.M. Bracci, A.M. Reinhorn and J.B. Mander, 12/1/92, (PB93-227528, A09, MF-A01).

- NCEER-92-0030 "Evaluation of Seismic Retrofit of Reinforced Concrete Frame Structures: Part I - Experimental Performance of Retrofitted Subassemblages," by D. Choudhuri, J.B. Mander and A.M. Reinhorn, 12/8/92, (PB93-198307, A07, MF-A02).
- NCEER-92-0031 "Evaluation of Seismic Retrofit of Reinforced Concrete Frame Structures: Part II - Experimental Performance and Analytical Study of a Retrofitted Structural Model," by J.M. Bracci, A.M. Reinhorn and J.B. Mander, 12/8/92, (PB93-198315, A09, MF-A03).
- NCEER-92-0032 "Experimental and Analytical Investigation of Seismic Response of Structures with Supplemental Fluid Viscous Dampers," by M.C. Constantinou and M.D. Symans, 12/21/92, (PB93-191435, A10, MF-A03). This report is available only through NTIS (see address given above).
- NCEER-92-0033 "Reconnaissance Report on the Cairo, Egypt Earthquake of October 12, 1992," by M. Khater, 12/23/92, (PB93-188621, A03, MF-A01).
- NCEER-92-0034 "Low-Level Dynamic Characteristics of Four Tall Flat-Plate Buildings in New York City," by H. Gavin, S. Yuan, J. Grossman, E. Pekelis and K. Jacob, 12/28/92, (PB93-188217, A07, MF-A02).
- NCEER-93-0001 "An Experimental Study on the Seismic Performance of Brick-Infilled Steel Frames With and Without Retrofit," by J.B. Mander, B. Nair, K. Wojtkowski and J. Ma, 1/29/93, (PB93-227510, A07, MF-A02).
- NCEER-93-0002 "Social Accounting for Disaster Preparedness and Recovery Planning," by S. Cole, E. Pantoja and V. Razak, 2/22/93, (PB94-142114, A12, MF-A03).
- NCEER-93-0003 "Assessment of 1991 NEHRP Provisions for Nonstructural Components and Recommended Revisions," by T.T. Soong, G. Chen, Z. Wu, R-H. Zhang and M. Grigoriu, 3/1/93, (PB93-188639, A06, MF-A02).
- NCEER-93-0004 "Evaluation of Static and Response Spectrum Analysis Procedures of SEAOC/UBC for Seismic Isolated Structures," by C.W. Winters and M.C. Constantinou, 3/23/93, (PB93-198299, A10, MF-A03).
- NCEER-93-0005 "Earthquakes in the Northeast - Are We Ignoring the Hazard? A Workshop on Earthquake Science and Safety for Educators," edited by K.E.K. Ross, 4/2/93, (PB94-103066, A09, MF-A02).
- NCEER-93-0006 "Inelastic Response of Reinforced Concrete Structures with Viscoelastic Braces," by R.F. Lobo, J.M. Bracci, K.L. Shen, A.M. Reinhorn and T.T. Soong, 4/5/93, (PB93-227486, A05, MF-A02).
- NCEER-93-0007 "Seismic Testing of Installation Methods for Computers and Data Processing Equipment," by K. Kosar, T.T. Soong, K.L. Shen, J.A. HoLung and Y.K. Lin, 4/12/93, (PB93-198299, A07, MF-A02).
- NCEER-93-0008 "Retrofit of Reinforced Concrete Frames Using Added Dampers," by A. Reinhorn, M. Constantinou and C. Li, to be published.
- NCEER-93-0009 "Seismic Behavior and Design Guidelines for Steel Frame Structures with Added Viscoelastic Dampers," by K.C. Chang, M.L. Lai, T.T. Soong, D.S. Hao and Y.C. Yeh, 5/1/93, (PB94-141959, A07, MF-A02).
- NCEER-93-0010 "Seismic Performance of Shear-Critical Reinforced Concrete Bridge Piers," by J.B. Mander, S.M. Waheed, M.T.A. Chaudhary and S.S. Chen, 5/12/93, (PB93-227494, A08, MF-A02).
- NCEER-93-0011 "3D-BASIS-TABS: Computer Program for Nonlinear Dynamic Analysis of Three Dimensional Base Isolated Structures," by S. Nagarajaiah, C. Li, A.M. Reinhorn and M.C. Constantinou, 8/2/93, (PB94-141819, A09, MF-A02).
- NCEER-93-0012 "Effects of Hydrocarbon Spills from an Oil Pipeline Break on Ground Water," by O.J. Helweg and H.H.M. Hwang, 8/3/93, (PB94-141942, A06, MF-A02).
- NCEER-93-0013 "Simplified Procedures for Seismic Design of Nonstructural Components and Assessment of Current Code Provisions," by M.P. Singh, L.E. Suarez, E.E. Matheu and G.O. Maldonado, 8/4/93, (PB94-141827, A09, MF-A02).
- NCEER-93-0014 "An Energy Approach to Seismic Analysis and Design of Secondary Systems," by G. Chen and T.T. Soong, 8/6/93, (PB94-142767, A11, MF-A03).

- NCEER-93-0015 "Proceedings from School Sites: Becoming Prepared for Earthquakes - Commemorating the Third Anniversary of the Loma Prieta Earthquake," Edited by F.E. Winslow and K.E.K. Ross, 8/16/93, (PB94-154275, A16, MF-A02).
- NCEER-93-0016 "Reconnaissance Report of Damage to Historic Monuments in Cairo, Egypt Following the October 12, 1992 Dahshur Earthquake," by D. Sykora, D. Look, G. Croci, E. Karaesmen and E. Karaesmen, 8/19/93, (PB94-142221, A08, MF-A02).
- NCEER-93-0017 "The Island of Guam Earthquake of August 8, 1993," by S.W. Swan and S.K. Harris, 9/30/93, (PB94-141843, A04, MF-A01).
- NCEER-93-0018 "Engineering Aspects of the October 12, 1992 Egyptian Earthquake," by A.W. Elgamal, M. Amer, K. Adalier and A. Abul-Fadl, 10/7/93, (PB94-141983, A05, MF-A01).
- NCEER-93-0019 "Development of an Earthquake Motion Simulator and its Application in Dynamic Centrifuge Testing," by I. Krstelj, Supervised by J.H. Prevost, 10/23/93, (PB94-181773, A-10, MF-A03).
- NCEER-93-0020 "NCEER-Taisei Corporation Research Program on Sliding Seismic Isolation Systems for Bridges: Experimental and Analytical Study of a Friction Pendulum System (FPS)," by M.C. Constantinou, P. Tsopelas, Y-S. Kim and S. Okamoto, 11/1/93, (PB94-142775, A08, MF-A02).
- NCEER-93-0021 "Finite Element Modeling of Elastomeric Seismic Isolation Bearings," by L.J. Billings, Supervised by R. Shepherd, 11/8/93, to be published.
- NCEER-93-0022 "Seismic Vulnerability of Equipment in Critical Facilities: Life-Safety and Operational Consequences," by K. Porter, G.S. Johnson, M.M. Zadeh, C. Scawthorn and S. Eder, 11/24/93, (PB94-181765, A16, MF-A03).
- NCEER-93-0023 "Hokkaido Nansei-oki, Japan Earthquake of July 12, 1993, by P.I. Yanev and C.R. Scawthorn, 12/23/93, (PB94-181500, A07, MF-A01).
- NCEER-94-0001 "An Evaluation of Seismic Serviceability of Water Supply Networks with Application to the San Francisco Auxiliary Water Supply System," by I. Markov, Supervised by M. Grigoriu and T. O'Rourke, 1/21/94, (PB94-204013, A07, MF-A02).
- NCEER-94-0002 "NCEER-Taisei Corporation Research Program on Sliding Seismic Isolation Systems for Bridges: Experimental and Analytical Study of Systems Consisting of Sliding Bearings, Rubber Restoring Force Devices and Fluid Dampers," Volumes I and II, by P. Tsopelas, S. Okamoto, M.C. Constantinou, D. Ozaki and S. Fujii, 2/4/94, (PB94-181740, A09, MF-A02 and PB94-181757, A12, MF-A03).
- NCEER-94-0003 "A Markov Model for Local and Global Damage Indices in Seismic Analysis," by S. Rahman and M. Grigoriu, 2/18/94, (PB94-206000, A12, MF-A03).
- NCEER-94-0004 "Proceedings from the NCEER Workshop on Seismic Response of Masonry Infills," edited by D.P. Abrams, 3/1/94, (PB94-180783, A07, MF-A02).
- NCEER-94-0005 "The Northridge, California Earthquake of January 17, 1994: General Reconnaissance Report," edited by J.D. Goltz, 3/11/94, (PB94-193943, A10, MF-A03).
- NCEER-94-0006 "Seismic Energy Based Fatigue Damage Analysis of Bridge Columns: Part I - Evaluation of Seismic Capacity," by G.A. Chang and J.B. Mander, 3/14/94, (PB94-219185, A11, MF-A03).
- NCEER-94-0007 "Seismic Isolation of Multi-Story Frame Structures Using Spherical Sliding Isolation Systems," by T.M. Al-Hussaini, V.A. Zayas and M.C. Constantinou, 3/17/94, (PB94-193745, A09, MF-A02).
- NCEER-94-0008 "The Northridge, California Earthquake of January 17, 1994: Performance of Highway Bridges," edited by I.G. Buckle, 3/24/94, (PB94-193851, A06, MF-A02).
- NCEER-94-0009 "Proceedings of the Third U.S.-Japan Workshop on Earthquake Protective Systems for Bridges," edited by I.G. Buckle and I. Friedland, 3/31/94, (PB94-195815, A99, MF-A06).

- NCEER-94-0010 "3D-BASIS-ME: Computer Program for Nonlinear Dynamic Analysis of Seismically Isolated Single and Multiple Structures and Liquid Storage Tanks," by P.C. Tsopelas, M.C. Constantinou and A.M. Reinhorn, 4/12/94, (PB94-204922, A09, MF-A02).
- NCEER-94-0011 "The Northridge, California Earthquake of January 17, 1994: Performance of Gas Transmission Pipelines," by T.D. O'Rourke and M.C. Palmer, 5/16/94, (PB94-204989, A05, MF-A01).
- NCEER-94-0012 "Feasibility Study of Replacement Procedures and Earthquake Performance Related to Gas Transmission Pipelines," by T.D. O'Rourke and M.C. Palmer, 5/25/94, (PB94-206638, A09, MF-A02).
- NCEER-94-0013 "Seismic Energy Based Fatigue Damage Analysis of Bridge Columns: Part II - Evaluation of Seismic Demand," by G.A. Chang and J.B. Mander, 6/1/94, (PB95-18106, A08, MF-A02).
- NCEER-94-0014 "NCEER-Taisei Corporation Research Program on Sliding Seismic Isolation Systems for Bridges: Experimental and Analytical Study of a System Consisting of Sliding Bearings and Fluid Restoring Force/Damping Devices," by P. Tsopelas and M.C. Constantinou, 6/13/94, (PB94-219144, A10, MF-A03).
- NCEER-94-0015 "Generation of Hazard-Consistent Fragility Curves for Seismic Loss Estimation Studies," by H. Hwang and J-R. Huo, 6/14/94, (PB95-181996, A09, MF-A02).
- NCEER-94-0016 "Seismic Study of Building Frames with Added Energy-Absorbing Devices," by W.S. Pong, C.S. Tsai and G.C. Lee, 6/20/94, (PB94-219136, A10, A03).
- NCEER-94-0017 "Sliding Mode Control for Seismic-Excited Linear and Nonlinear Civil Engineering Structures," by J. Yang, J. Wu, A. Agrawal and Z. Li, 6/21/94, (PB95-138483, A06, MF-A02).
- NCEER-94-0018 "3D-BASIS-TABS Version 2.0: Computer Program for Nonlinear Dynamic Analysis of Three Dimensional Base Isolated Structures," by A.M. Reinhorn, S. Nagarajaiah, M.C. Constantinou, P. Tsopelas and R. Li, 6/22/94, (PB95-182176, A08, MF-A02).
- NCEER-94-0019 "Proceedings of the International Workshop on Civil Infrastructure Systems: Application of Intelligent Systems and Advanced Materials on Bridge Systems," Edited by G.C. Lee and K.C. Chang, 7/18/94, (PB95-252474, A20, MF-A04).
- NCEER-94-0020 "Study of Seismic Isolation Systems for Computer Floors," by V. Lambrou and M.C. Constantinou, 7/19/94, (PB95-138533, A10, MF-A03).
- NCEER-94-0021 "Proceedings of the U.S.-Italian Workshop on Guidelines for Seismic Evaluation and Rehabilitation of Unreinforced Masonry Buildings," Edited by D.P. Abrams and G.M. Calvi, 7/20/94, (PB95-138749, A13, MF-A03).
- NCEER-94-0022 "NCEER-Taisei Corporation Research Program on Sliding Seismic Isolation Systems for Bridges: Experimental and Analytical Study of a System Consisting of Lubricated PTFE Sliding Bearings and Mild Steel Dampers," by P. Tsopelas and M.C. Constantinou, 7/22/94, (PB95-182184, A08, MF-A02).
- NCEER-94-0023 "Development of Reliability-Based Design Criteria for Buildings Under Seismic Load," by Y.K. Wen, H. Hwang and M. Shinozuka, 8/1/94, (PB95-211934, A08, MF-A02).
- NCEER-94-0024 "Experimental Verification of Acceleration Feedback Control Strategies for an Active Tendon System," by S.J. Dyke, B.F. Spencer, Jr., P. Quast, M.K. Sain, D.C. Kaspari, Jr. and T.T. Soong, 8/29/94, (PB95-212320, A05, MF-A01).
- NCEER-94-0025 "Seismic Retrofitting Manual for Highway Bridges," Edited by I.G. Buckle and I.F. Friedland, published by the Federal Highway Administration (PB95-212676, A15, MF-A03).
- NCEER-94-0026 "Proceedings from the Fifth U.S.-Japan Workshop on Earthquake Resistant Design of Lifeline Facilities and Countermeasures Against Soil Liquefaction," Edited by T.D. O'Rourke and M. Hamada, 11/7/94, (PB95-220802, A99, MF-E08).

- NCEER-95-0001 “Experimental and Analytical Investigation of Seismic Retrofit of Structures with Supplemental Damping: Part 1 - Fluid Viscous Damping Devices,” by A.M. Reinhorn, C. Li and M.C. Constantinou, 1/3/95, (PB95-266599, A09, MF-A02).
- NCEER-95-0002 “Experimental and Analytical Study of Low-Cycle Fatigue Behavior of Semi-Rigid Top-And-Seat Angle Connections,” by G. Pekcan, J.B. Mander and S.S. Chen, 1/5/95, (PB95-220042, A07, MF-A02).
- NCEER-95-0003 “NCEER-ATC Joint Study on Fragility of Buildings,” by T. Anagnos, C. Rojahn and A.S. Kiremidjian, 1/20/95, (PB95-220026, A06, MF-A02).
- NCEER-95-0004 “Nonlinear Control Algorithms for Peak Response Reduction,” by Z. Wu, T.T. Soong, V. Gattulli and R.C. Lin, 2/16/95, (PB95-220349, A05, MF-A01).
- NCEER-95-0005 “Pipeline Replacement Feasibility Study: A Methodology for Minimizing Seismic and Corrosion Risks to Underground Natural Gas Pipelines,” by R.T. Eguchi, H.A. Seligson and D.G. Honegger, 3/2/95, (PB95-252326, A06, MF-A02).
- NCEER-95-0006 “Evaluation of Seismic Performance of an 11-Story Frame Building During the 1994 Northridge Earthquake,” by F. Naeim, R. DiSulio, K. Benuska, A. Reinhorn and C. Li, to be published.
- NCEER-95-0007 “Prioritization of Bridges for Seismic Retrofitting,” by N. Basöz and A.S. Kiremidjian, 4/24/95, (PB95-252300, A08, MF-A02).
- NCEER-95-0008 “Method for Developing Motion Damage Relationships for Reinforced Concrete Frames,” by A. Singhal and A.S. Kiremidjian, 5/11/95, (PB95-266607, A06, MF-A02).
- NCEER-95-0009 “Experimental and Analytical Investigation of Seismic Retrofit of Structures with Supplemental Damping: Part II - Friction Devices,” by C. Li and A.M. Reinhorn, 7/6/95, (PB96-128087, A11, MF-A03).
- NCEER-95-0010 “Experimental Performance and Analytical Study of a Non-Ductile Reinforced Concrete Frame Structure Retrofitted with Elastomeric Spring Dampers,” by G. Pekcan, J.B. Mander and S.S. Chen, 7/14/95, (PB96-137161, A08, MF-A02).
- NCEER-95-0011 “Development and Experimental Study of Semi-Active Fluid Damping Devices for Seismic Protection of Structures,” by M.D. Symans and M.C. Constantinou, 8/3/95, (PB96-136940, A23, MF-A04).
- NCEER-95-0012 “Real-Time Structural Parameter Modification (RSPM): Development of Innervated Structures,” by Z. Liang, M. Tong and G.C. Lee, 4/11/95, (PB96-137153, A06, MF-A01).
- NCEER-95-0013 “Experimental and Analytical Investigation of Seismic Retrofit of Structures with Supplemental Damping: Part III - Viscous Damping Walls,” by A.M. Reinhorn and C. Li, 10/1/95, (PB96-176409, A11, MF-A03).
- NCEER-95-0014 “Seismic Fragility Analysis of Equipment and Structures in a Memphis Electric Substation,” by J-R. Huo and H.H.M. Hwang, 8/10/95, (PB96-128087, A09, MF-A02).
- NCEER-95-0015 “The Hanshin-Awaji Earthquake of January 17, 1995: Performance of Lifelines,” Edited by M. Shinozuka, 11/3/95, (PB96-176383, A15, MF-A03).
- NCEER-95-0016 “Highway Culvert Performance During Earthquakes,” by T.L. Youd and C.J. Beckman, available as NCEER-96-0015.
- NCEER-95-0017 “The Hanshin-Awaji Earthquake of January 17, 1995: Performance of Highway Bridges,” Edited by I.G. Buckle, 12/1/95, to be published.
- NCEER-95-0018 “Modeling of Masonry Infill Panels for Structural Analysis,” by A.M. Reinhorn, A. Madan, R.E. Valles, Y. Reichmann and J.B. Mander, 12/8/95, (PB97-110886, MF-A01, A06).
- NCEER-95-0019 “Optimal Polynomial Control for Linear and Nonlinear Structures,” by A.K. Agrawal and J.N. Yang, 12/11/95, (PB96-168737, A07, MF-A02).

- NCEER-95-0020 "Retrofit of Non-Ductile Reinforced Concrete Frames Using Friction Dampers," by R.S. Rao, P. Gergely and R.N. White, 12/22/95, (PB97-133508, A10, MF-A02).
- NCEER-95-0021 "Parametric Results for Seismic Response of Pile-Supported Bridge Bents," by G. Mylonakis, A. Nikolaou and G. Gazetas, 12/22/95, (PB97-100242, A12, MF-A03).
- NCEER-95-0022 "Kinematic Bending Moments in Seismically Stressed Piles," by A. Nikolaou, G. Mylonakis and G. Gazetas, 12/23/95, (PB97-113914, MF-A03, A13).
- NCEER-96-0001 "Dynamic Response of Unreinforced Masonry Buildings with Flexible Diaphragms," by A.C. Costley and D.P. Abrams, 10/10/96, (PB97-133573, MF-A03, A15).
- NCEER-96-0002 "State of the Art Review: Foundations and Retaining Structures," by I. Po Lam, to be published.
- NCEER-96-0003 "Ductility of Rectangular Reinforced Concrete Bridge Columns with Moderate Confinement," by N. Wehbe, M. Saiidi, D. Sanders and B. Douglas, 11/7/96, (PB97-133557, A06, MF-A02).
- NCEER-96-0004 "Proceedings of the Long-Span Bridge Seismic Research Workshop," edited by I.G. Buckle and I.M. Friedland, to be published.
- NCEER-96-0005 "Establish Representative Pier Types for Comprehensive Study: Eastern United States," by J. Kulicki and Z. Prucz, 5/28/96, (PB98-119217, A07, MF-A02).
- NCEER-96-0006 "Establish Representative Pier Types for Comprehensive Study: Western United States," by R. Imbsen, R.A. Schamber and T.A. Osterkamp, 5/28/96, (PB98-118607, A07, MF-A02).
- NCEER-96-0007 "Nonlinear Control Techniques for Dynamical Systems with Uncertain Parameters," by R.G. Ghanem and M.I. Bujakov, 5/27/96, (PB97-100259, A17, MF-A03).
- NCEER-96-0008 "Seismic Evaluation of a 30-Year Old Non-Ductile Highway Bridge Pier and Its Retrofit," by J.B. Mander, B. Mahmoodzadegan, S. Bhadra and S.S. Chen, 5/31/96, (PB97-110902, MF-A03, A10).
- NCEER-96-0009 "Seismic Performance of a Model Reinforced Concrete Bridge Pier Before and After Retrofit," by J.B. Mander, J.H. Kim and C.A. Ligozio, 5/31/96, (PB97-110910, MF-A02, A10).
- NCEER-96-0010 "IDARC2D Version 4.0: A Computer Program for the Inelastic Damage Analysis of Buildings," by R.E. Valles, A.M. Reinhorn, S.K. Kunnath, C. Li and A. Madan, 6/3/96, (PB97-100234, A17, MF-A03).
- NCEER-96-0011 "Estimation of the Economic Impact of Multiple Lifeline Disruption: Memphis Light, Gas and Water Division Case Study," by S.E. Chang, H.A. Seligson and R.T. Eguchi, 8/16/96, (PB97-133490, A11, MF-A03).
- NCEER-96-0012 "Proceedings from the Sixth Japan-U.S. Workshop on Earthquake Resistant Design of Lifeline Facilities and Countermeasures Against Soil Liquefaction, Edited by M. Hamada and T. O'Rourke, 9/11/96, (PB97-133581, A99, MF-A06).
- NCEER-96-0013 "Chemical Hazards, Mitigation and Preparedness in Areas of High Seismic Risk: A Methodology for Estimating the Risk of Post-Earthquake Hazardous Materials Release," by H.A. Seligson, R.T. Eguchi, K.J. Tierney and K. Richmond, 11/7/96, (PB97-133565, MF-A02, A08).
- NCEER-96-0014 "Response of Steel Bridge Bearings to Reversed Cyclic Loading," by J.B. Mander, D-K. Kim, S.S. Chen and G.J. Premus, 11/13/96, (PB97-140735, A12, MF-A03).
- NCEER-96-0015 "Highway Culvert Performance During Past Earthquakes," by T.L. Youd and C.J. Beckman, 11/25/96, (PB97-133532, A06, MF-A01).
- NCEER-97-0001 "Evaluation, Prevention and Mitigation of Pounding Effects in Building Structures," by R.E. Valles and A.M. Reinhorn, 2/20/97, (PB97-159552, A14, MF-A03).
- NCEER-97-0002 "Seismic Design Criteria for Bridges and Other Highway Structures," by C. Rojahn, R. Mayes, D.G. Anderson, J. Clark, J.H. Hom, R.V. Nutt and M.J. O'Rourke, 4/30/97, (PB97-194658, A06, MF-A03).

- NCEER-97-0003 "Proceedings of the U.S.-Italian Workshop on Seismic Evaluation and Retrofit," Edited by D.P. Abrams and G.M. Calvi, 3/19/97, (PB97-194666, A13, MF-A03).
- NCEER-97-0004 "Investigation of Seismic Response of Buildings with Linear and Nonlinear Fluid Viscous Dampers," by A.A. Seleemah and M.C. Constantinou, 5/21/97, (PB98-109002, A15, MF-A03).
- NCEER-97-0005 "Proceedings of the Workshop on Earthquake Engineering Frontiers in Transportation Facilities," edited by G.C. Lee and I.M. Friedland, 8/29/97, (PB98-128911, A25, MR-A04).
- NCEER-97-0006 "Cumulative Seismic Damage of Reinforced Concrete Bridge Piers," by S.K. Kunnath, A. El-Bahy, A. Taylor and W. Stone, 9/2/97, (PB98-108814, A11, MF-A03).
- NCEER-97-0007 "Structural Details to Accommodate Seismic Movements of Highway Bridges and Retaining Walls," by R.A. Imbsen, R.A. Schamber, E. Thorkildsen, A. Kartoum, B.T. Martin, T.N. Rosser and J.M. Kulicki, 9/3/97, (PB98-108996, A09, MF-A02).
- NCEER-97-0008 "A Method for Earthquake Motion-Damage Relationships with Application to Reinforced Concrete Frames," by A. Singhal and A.S. Kiremidjian, 9/10/97, (PB98-108988, A13, MF-A03).
- NCEER-97-0009 "Seismic Analysis and Design of Bridge Abutments Considering Sliding and Rotation," by K. Fishman and R. Richards, Jr., 9/15/97, (PB98-108897, A06, MF-A02).
- NCEER-97-0010 "Proceedings of the FHWA/NCEER Workshop on the National Representation of Seismic Ground Motion for New and Existing Highway Facilities," edited by I.M. Friedland, M.S. Power and R.L. Mayes, 9/22/97, (PB98-128903, A21, MF-A04).
- NCEER-97-0011 "Seismic Analysis for Design or Retrofit of Gravity Bridge Abutments," by K.L. Fishman, R. Richards, Jr. and R.C. Divito, 10/2/97, (PB98-128937, A08, MF-A02).
- NCEER-97-0012 "Evaluation of Simplified Methods of Analysis for Yielding Structures," by P. Tsopelas, M.C. Constantinou, C.A. Kircher and A.S. Whittaker, 10/31/97, (PB98-128929, A10, MF-A03).
- NCEER-97-0013 "Seismic Design of Bridge Columns Based on Control and Repairability of Damage," by C-T. Cheng and J.B. Mander, 12/8/97, (PB98-144249, A11, MF-A03).
- NCEER-97-0014 "Seismic Resistance of Bridge Piers Based on Damage Avoidance Design," by J.B. Mander and C-T. Cheng, 12/10/97, (PB98-144223, A09, MF-A02).
- NCEER-97-0015 "Seismic Response of Nominally Symmetric Systems with Strength Uncertainty," by S. Balopoulou and M. Grigoriu, 12/23/97, (PB98-153422, A11, MF-A03).
- NCEER-97-0016 "Evaluation of Seismic Retrofit Methods for Reinforced Concrete Bridge Columns," by T.J. Wipf, F.W. Klaiber and F.M. Russo, 12/28/97, (PB98-144215, A12, MF-A03).
- NCEER-97-0017 "Seismic Fragility of Existing Conventional Reinforced Concrete Highway Bridges," by C.L. Mullen and A.S. Cakmak, 12/30/97, (PB98-153406, A08, MF-A02).
- NCEER-97-0018 "Loss Assessment of Memphis Buildings," edited by D.P. Abrams and M. Shinozuka, 12/31/97, (PB98-144231, A13, MF-A03).
- NCEER-97-0019 "Seismic Evaluation of Frames with Infill Walls Using Quasi-static Experiments," by K.M. Mosalam, R.N. White and P. Gergely, 12/31/97, (PB98-153455, A07, MF-A02).
- NCEER-97-0020 "Seismic Evaluation of Frames with Infill Walls Using Pseudo-dynamic Experiments," by K.M. Mosalam, R.N. White and P. Gergely, 12/31/97, (PB98-153430, A07, MF-A02).
- NCEER-97-0021 "Computational Strategies for Frames with Infill Walls: Discrete and Smeared Crack Analyses and Seismic Fragility," by K.M. Mosalam, R.N. White and P. Gergely, 12/31/97, (PB98-153414, A10, MF-A02).

- NCEER-97-0022 "Proceedings of the NCEER Workshop on Evaluation of Liquefaction Resistance of Soils," edited by T.L. Youd and I.M. Idriss, 12/31/97, (PB98-155617, A15, MF-A03).
- MCEER-98-0001 "Extraction of Nonlinear Hysteretic Properties of Seismically Isolated Bridges from Quick-Release Field Tests," by Q. Chen, B.M. Douglas, E.M. Maragakis and I.G. Buckle, 5/26/98, (PB99-118838, A06, MF-A01).
- MCEER-98-0002 "Methodologies for Evaluating the Importance of Highway Bridges," by A. Thomas, S. Eshenaur and J. Kulicki, 5/29/98, (PB99-118846, A10, MF-A02).
- MCEER-98-0003 "Capacity Design of Bridge Piers and the Analysis of Overstrength," by J.B. Mander, A. Dutta and P. Goel, 6/1/98, (PB99-118853, A09, MF-A02).
- MCEER-98-0004 "Evaluation of Bridge Damage Data from the Loma Prieta and Northridge, California Earthquakes," by N. Basoz and A. Kiremidjian, 6/2/98, (PB99-118861, A15, MF-A03).
- MCEER-98-0005 "Screening Guide for Rapid Assessment of Liquefaction Hazard at Highway Bridge Sites," by T. L. Youd, 6/16/98, (PB99-118879, A06, not available on microfiche).
- MCEER-98-0006 "Structural Steel and Steel/Concrete Interface Details for Bridges," by P. Ritchie, N. Kaulh and J. Kulicki, 7/13/98, (PB99-118945, A06, MF-A01).
- MCEER-98-0007 "Capacity Design and Fatigue Analysis of Confined Concrete Columns," by A. Dutta and J.B. Mander, 7/14/98, (PB99-118960, A14, MF-A03).
- MCEER-98-0008 "Proceedings of the Workshop on Performance Criteria for Telecommunication Services Under Earthquake Conditions," edited by A.J. Schiff, 7/15/98, (PB99-118952, A08, MF-A02).
- MCEER-98-0009 "Fatigue Analysis of Unconfined Concrete Columns," by J.B. Mander, A. Dutta and J.H. Kim, 9/12/98, (PB99-123655, A10, MF-A02).
- MCEER-98-0010 "Centrifuge Modeling of Cyclic Lateral Response of Pile-Cap Systems and Seat-Type Abutments in Dry Sands," by A.D. Gadre and R. Dobry, 10/2/98, (PB99-123606, A13, MF-A03).
- MCEER-98-0011 "IDARC-BRIDGE: A Computational Platform for Seismic Damage Assessment of Bridge Structures," by A.M. Reinhorn, V. Simeonov, G. Mylonakis and Y. Reichman, 10/2/98, (PB99-162919, A15, MF-A03).
- MCEER-98-0012 "Experimental Investigation of the Dynamic Response of Two Bridges Before and After Retrofitting with Elastomeric Bearings," by D.A. Wendichansky, S.S. Chen and J.B. Mander, 10/2/98, (PB99-162927, A15, MF-A03).
- MCEER-98-0013 "Design Procedures for Hinge Restrainers and Hinge Sear Width for Multiple-Frame Bridges," by R. Des Roches and G.L. Fenves, 11/3/98, (PB99-140477, A13, MF-A03).
- MCEER-98-0014 "Response Modification Factors for Seismically Isolated Bridges," by M.C. Constantinou and J.K. Quarshie, 11/3/98, (PB99-140485, A14, MF-A03).
- MCEER-98-0015 "Proceedings of the U.S.-Italy Workshop on Seismic Protective Systems for Bridges," edited by I.M. Friedland and M.C. Constantinou, 11/3/98, (PB2000-101711, A22, MF-A04).
- MCEER-98-0016 "Appropriate Seismic Reliability for Critical Equipment Systems: Recommendations Based on Regional Analysis of Financial and Life Loss," by K. Porter, C. Scawthorn, C. Taylor and N. Blais, 11/10/98, (PB99-157265, A08, MF-A02).
- MCEER-98-0017 "Proceedings of the U.S. Japan Joint Seminar on Civil Infrastructure Systems Research," edited by M. Shinozuka and A. Rose, 11/12/98, (PB99-156713, A16, MF-A03).
- MCEER-98-0018 "Modeling of Pile Footings and Drilled Shafts for Seismic Design," by I. PoLam, M. Kapuskar and D. Chaudhuri, 12/21/98, (PB99-157257, A09, MF-A02).

- MCEER-99-0001 "Seismic Evaluation of a Masonry Infilled Reinforced Concrete Frame by Pseudodynamic Testing," by S.G. Buonopane and R.N. White, 2/16/99, (PB99-162851, A09, MF-A02).
- MCEER-99-0002 "Response History Analysis of Structures with Seismic Isolation and Energy Dissipation Systems: Verification Examples for Program SAP2000," by J. Scheller and M.C. Constantinou, 2/22/99, (PB99-162869, A08, MF-A02).
- MCEER-99-0003 "Experimental Study on the Seismic Design and Retrofit of Bridge Columns Including Axial Load Effects," by A. Dutta, T. Kokorina and J.B. Mander, 2/22/99, (PB99-162877, A09, MF-A02).
- MCEER-99-0004 "Experimental Study of Bridge Elastomeric and Other Isolation and Energy Dissipation Systems with Emphasis on Uplift Prevention and High Velocity Near-source Seismic Excitation," by A. Kasalanati and M. C. Constantinou, 2/26/99, (PB99-162885, A12, MF-A03).
- MCEER-99-0005 "Truss Modeling of Reinforced Concrete Shear-flexure Behavior," by J.H. Kim and J.B. Mander, 3/8/99, (PB99-163693, A12, MF-A03).
- MCEER-99-0006 "Experimental Investigation and Computational Modeling of Seismic Response of a 1:4 Scale Model Steel Structure with a Load Balancing Supplemental Damping System," by G. Pekcan, J.B. Mander and S.S. Chen, 4/2/99, (PB99-162893, A11, MF-A03).
- MCEER-99-0007 "Effect of Vertical Ground Motions on the Structural Response of Highway Bridges," by M.R. Button, C.J. Cronin and R.L. Mayes, 4/10/99, (PB2000-101411, A10, MF-A03).
- MCEER-99-0008 "Seismic Reliability Assessment of Critical Facilities: A Handbook, Supporting Documentation, and Model Code Provisions," by G.S. Johnson, R.E. Sheppard, M.D. Quilici, S.J. Eder and C.R. Scawthorn, 4/12/99, (PB2000-101701, A18, MF-A04).
- MCEER-99-0009 "Impact Assessment of Selected MCEER Highway Project Research on the Seismic Design of Highway Structures," by C. Rojahn, R. Mayes, D.G. Anderson, J.H. Clark, D'Appolonia Engineering, S. Gloyd and R.V. Nutt, 4/14/99, (PB99-162901, A10, MF-A02).
- MCEER-99-0010 "Site Factors and Site Categories in Seismic Codes," by R. Dobry, R. Ramos and M.S. Power, 7/19/99, (PB2000-101705, A08, MF-A02).
- MCEER-99-0011 "Restrainer Design Procedures for Multi-Span Simply-Supported Bridges," by M.J. Randall, M. Saiidi, E. Maragakis and T. Isakovic, 7/20/99, (PB2000-101702, A10, MF-A02).
- MCEER-99-0012 "Property Modification Factors for Seismic Isolation Bearings," by M.C. Constantinou, P. Tsopelas, A. Kasalanati and E. Wolff, 7/20/99, (PB2000-103387, A11, MF-A03).
- MCEER-99-0013 "Critical Seismic Issues for Existing Steel Bridges," by P. Ritchie, N. Kauh and J. Kulicki, 7/20/99, (PB2000-101697, A09, MF-A02).
- MCEER-99-0014 "Nonstructural Damage Database," by A. Kao, T.T. Soong and A. Vender, 7/24/99, (PB2000-101407, A06, MF-A01).
- MCEER-99-0015 "Guide to Remedial Measures for Liquefaction Mitigation at Existing Highway Bridge Sites," by H.G. Cooke and J. K. Mitchell, 7/26/99, (PB2000-101703, A11, MF-A03).
- MCEER-99-0016 "Proceedings of the MCEER Workshop on Ground Motion Methodologies for the Eastern United States," edited by N. Abrahamson and A. Becker, 8/11/99, (PB2000-103385, A07, MF-A02).
- MCEER-99-0017 "Quindío, Colombia Earthquake of January 25, 1999: Reconnaissance Report," by A.P. Asfura and P.J. Flores, 10/4/99, (PB2000-106893, A06, MF-A01).
- MCEER-99-0018 "Hysteretic Models for Cyclic Behavior of Deteriorating Inelastic Structures," by M.V. Sivaselvan and A.M. Reinhorn, 11/5/99, (PB2000-103386, A08, MF-A02).

- MCEER-99-0019 "Proceedings of the 7th U.S.- Japan Workshop on Earthquake Resistant Design of Lifeline Facilities and Countermeasures Against Soil Liquefaction," edited by T.D. O'Rourke, J.P. Bardet and M. Hamada, 11/19/99, (PB2000-103354, A99, MF-A06).
- MCEER-99-0020 "Development of Measurement Capability for Micro-Vibration Evaluations with Application to Chip Fabrication Facilities," by G.C. Lee, Z. Liang, J.W. Song, J.D. Shen and W.C. Liu, 12/1/99, (PB2000-105993, A08, MF-A02).
- MCEER-99-0021 "Design and Retrofit Methodology for Building Structures with Supplemental Energy Dissipating Systems," by G. Pekcan, J.B. Mander and S.S. Chen, 12/31/99, (PB2000-105994, A11, MF-A03).
- MCEER-00-0001 "The Marmara, Turkey Earthquake of August 17, 1999: Reconnaissance Report," edited by C. Scawthorn; with major contributions by M. Bruneau, R. Eguchi, T. Holzer, G. Johnson, J. Mander, J. Mitchell, W. Mitchell, A. Papageorgiou, C. Scaethorn, and G. Webb, 3/23/00, (PB2000-106200, A11, MF-A03).
- MCEER-00-0002 "Proceedings of the MCEER Workshop for Seismic Hazard Mitigation of Health Care Facilities," edited by G.C. Lee, M. Ettouney, M. Grigoriu, J. Hauer and J. Nigg, 3/29/00, (PB2000-106892, A08, MF-A02).
- MCEER-00-0003 "The Chi-Chi, Taiwan Earthquake of September 21, 1999: Reconnaissance Report," edited by G.C. Lee and C.H. Loh, with major contributions by G.C. Lee, M. Bruneau, I.G. Buckle, S.E. Chang, P.J. Flores, T.D. O'Rourke, M. Shinozuka, T.T. Soong, C-H. Loh, K-C. Chang, Z-J. Chen, J-S. Hwang, M-L. Lin, G-Y. Liu, K-C. Tsai, G.C. Yao and C-L. Yen, 4/30/00, (PB2001-100980, A10, MF-A02).
- MCEER-00-0004 "Seismic Retrofit of End-Sway Frames of Steel Deck-Truss Bridges with a Supplemental Tendon System: Experimental and Analytical Investigation," by G. Pekcan, J.B. Mander and S.S. Chen, 7/1/00, (PB2001-100982, A10, MF-A02).
- MCEER-00-0005 "Sliding Fragility of Unrestrained Equipment in Critical Facilities," by W.H. Chong and T.T. Soong, 7/5/00, (PB2001-100983, A08, MF-A02).
- MCEER-00-0006 "Seismic Response of Reinforced Concrete Bridge Pier Walls in the Weak Direction," by N. Abo-Shadi, M. Saiidi and D. Sanders, 7/17/00, (PB2001-100981, A17, MF-A03).
- MCEER-00-0007 "Low-Cycle Fatigue Behavior of Longitudinal Reinforcement in Reinforced Concrete Bridge Columns," by J. Brown and S.K. Kunnath, 7/23/00, (PB2001-104392, A08, MF-A02).
- MCEER-00-0008 "Soil Structure Interaction of Bridges for Seismic Analysis," I. PoLam and H. Law, 9/25/00, (PB2001-105397, A08, MF-A02).
- MCEER-00-0009 "Proceedings of the First MCEER Workshop on Mitigation of Earthquake Disaster by Advanced Technologies (MEDAT-1), edited by M. Shinozuka, D.J. Inman and T.D. O'Rourke, 11/10/00, (PB2001-105399, A14, MF-A03).
- MCEER-00-0010 "Development and Evaluation of Simplified Procedures for Analysis and Design of Buildings with Passive Energy Dissipation Systems, Revision 01," by O.M. Ramirez, M.C. Constantinou, C.A. Kircher, A.S. Whittaker, M.W. Johnson, J.D. Gomez and C. Chrysostomou, 11/16/01, (PB2001-105523, A23, MF-A04).